



University of CAGLIARI  
Faculty of Biology and Pharmacy

Corso di Laurea in Farmacia  
DIPARTIMENTO DI SCIENZE DELLA VITA E DELL'AMBIENTE  
Sezione Scienze del Farmaco  
Direttore: Prof. Angelo Cau

**“Synthesis of different series of small  
molecules targeting HIV-1 RT, Candida  
*albicans*, MAO and G-Quadruplex”**

Dr. Rita Meleddu

*Supervisor*

Prof. Dr. Elias Maccioni

Prof. Dr. Péter Mátyus



*To Mommy&Daddy  
Carla&Fabio, Raffaella&Marco and  
Padrino  
always and forever with love...  
Rita*

*This report would not have been possible without the collaboration and contribution of my supervisor. He is not only a great scientist but also a symbol of humanity and simplicity. He has always been a referring point in my experimental work. Professor Elias Maccioni. Thank you very much!*

*I would like to thank Professor Péter Mátyus, model of great skill and reliability, that guided me with patience and care during my research period in Budapest.*

*A special thank goes to Professor Antonio Maccioni interlocutor of very interesting scientific discussions, who fascinated me with his great science and a life-model to imitate.*

*A special thank is addressed to Dr. Simona Distinto, a very important presence in my working life by means of her valuable suggestions and teachings and her constant presence every time.*

*Special thanks to Dr. Antonella Arridu and Dr. Giulia Bianco for having always been close and for their friendship especially in this period.*

*Finally thanks to Paolo Bonsignore for his help and his support in the lab, since the 2003...*

*With love Rita*



## **Preface**

*My PhD work has been focused towards four different targets: HIV-1 RT, Candida albicans, Monoamine oxidase, and G-Quadruplex.*

*Thus in order to give the reader a clearer exposition this report has been divided in four different chapters.*

*Each of the chapters has his own numbering for pages, figures, schemes, tables and references.*

*The main part of my work has been dedicated to HIV-1 RT, thus this chapter is the major and first one.*



## **I Part:**

**Synthesis and biological activity evaluation of new  
dual inhibitors of both associated functions of HIV-1  
RT**



## CONTENTS

1	<i>Introduction</i>	
1.1	<i>Historical overview</i>	3
1.2	<i>HIV Pathogenesis and prevention</i>	4
1.3	<i>Virus structure</i>	7
1.4	<i>Organization of viral genome</i>	9
1.5	<i>HIV structural proteins</i>	10
	1.5.1 <i>Gag</i>	
	1.5.2 <i>Gag-Pol precursor</i>	
	1.5.3 <i>Pro</i>	
	1.5.4 <i>RT</i>	
	1.5.5 <i>Integrase</i>	
	1.5.6 <i>Env</i>	
1.6	<i>Regulatory proteins</i>	14
	1.6.1 <i>Tat</i>	
	1.6.2 <i>Rev</i>	
1.7	<i>Accessory proteins</i>	16
	1.7.1 <i>Nef</i>	
	1.7.2 <i>Vpr</i>	
	1.7.3 <i>Vpu</i>	
	1.7.4 <i>Vif</i>	
1.8	<i>HIV-1 life cycle</i>	21
1.9	<i>Reverse transcription</i>	22
1.10	<i>Reverse transcriptase inhibitors</i>	27
	1.10.1 <i>Inhibitors of the RDDP function</i>	
	1.10.2 <i>Inhibitors of the RNase H function</i>	
	1.10.3 <i>Dual inhibitor</i>	
2	<i>Results and discussion</i>	40
3	<i>Materials and methods</i>	69
	3.1 <i>Chemistry</i>	
	3.2 <i>Biology</i>	
4	<i>Acknowledgments</i>	173
5	<i>References and notes</i>	175



# **1 INTRODUCTION**

## **1.1 Historical overview**

In 1980, Michael Gottlieb, an immunologist of the Los Angeles UCLA Medical Center analysed three cases of young homosexual men presenting clinical signs such as weight loss, mycosis, fever, oral Candida, and pneumonia.

In early May 1981, local clinicians and the Epidemic Intelligence Service (EIS) Officer stationed at the Los Angeles County Department of Public Health, prepared a report of five cases of Pneumocystis carinii pneumonia (PCP) among previously healthy young men in Los Angeles and submitted it for Morbidity and Mortality Weekly Report (MMWR) publication. [1]

All of the men were described as homosexuals; two had died.

The editorial note, that accompanied the published report, stated that the case histories suggested a cellular-immune dysfunction related to a common exposure and a disease acquired through sexual contact.

In June 1981, the Centers for Disease Control (CDC) developed a team to identify risk factors and to develop a case definition for national surveillance. In March 1983, CDC issued recommendations for prevention of a sexual, drug related, and occupational transmission based infection on these early epidemiologic studies and before the cause of the new, unexplained illness was known.

In 1983, Montagnier and colleagues isolated a T-lymphotropic retrovirus, named lymphadenopathy-associated virus (LAV) and, almost simultaneously, Robert Gallo published on the frequent detection and isolation of cytopathic retroviruses from patients with AIDS or at risk for AIDS. [2, 3] The same year Levy and colleagues isolated from AIDS patients in S.Francisco a retrovirus that was named Aids Related Virus (ARV). [4]

The three viruses were then cloned and characterised and are now known as Human Immunodeficiency Virus type 1 (HIV-1). [5]

1985 is an important year for the proceeding of the AIDS related knowledge

- Tests to identify the virus are marketed
- First clinical trials in USA aimed to the identification of drugs to fight the virus
- First ever conference on AIDS was held in Atlanta (USA), where interaction between scientific groups from all the world began.

In 1987, the Food and Drugs Administration (FDA) approved Azidovudine (AZT), the first molecule to treat the HIV infection.

Between 1995 and 1997, David Ho findings on viral dynamics provide, not only a kinetic picture of HIV-1 pathogenesis, but also theoretical principles to guide the development of treatment strategies. [6, 7]

There are more than 20 antiretroviral drugs approved for the clinical treatment of HIV infected patients targeting different steps of the HIV replication cycle. [8] These drugs can be efficiently associated for the so called *highly active antiretroviral therapy* (HAART). [9]

Currently we have at our disposal a rich armamentarium of drugs that change the prognosis of HIV infected patients from high probability of mortality to a chronic infection.

## **1.2 HIV Pathogenesis and Prevention**

Despite rigorous and multifaceted approaches to the prevention of HIV infection, ~39.000 new infections occur annually in the United States, a number that has not changed significantly in the last years. [10]

Prevention methods that have been successful in certain populations need to be adapted in order to target other groups and must be provided to more people.

In particular it is important to pursue prevention approaches that are based on our growing understanding of the pathogenic mechanisms of HIV disease.

Such strategies include the identification and treatment of coinfections, including sexually transmitted infections; the use of topical microbicides; the circumcision of men; the use of antiretroviral drugs for preexposure prophylaxis; the reduction of the viral load in order to decrease transmission rates; and the development of vaccines.

All these modalities focus on the pathogenesis of HIV disease, in the sense that they involve preventing the initial entry of HIV into the body, blocking the spread of infection, or slowing the progression of disease once infection is established.

The early events in HIV disease take place rapidly, and once they occur, infection is permanently established. [11] The events associated with primary HIV infection are likely critical determinants of the subsequent course of HIV disease.

So far, preventing or interfering with these early events is an important goal of all prevention efforts that focus on pathogenic events.

When HIV is transmitted during sexual activity, dendritic cells at or near the mucosal surface of the involved sites play an important role in the initiation of HIV infection. [12]

These cells bind with high affinity to the HIV envelope glycoprotein gp120 and can retain infectious particles for days, thus facilitating the presentation of the virus to susceptible cells.

The replication cycle of HIV in its target cell begins with the binding of viral gp120 to the CD4 molecule, its receptor on the host-cell surface.

Once gp120 binds to CD4, fusion with the host cell membrane follows, and infection is established. An early burst of viremia and rapid dissemination of virus to lymphoid organs, particularly the gut-associated lymphoid tissue, are major factors in the establishment of the chronic and persistent infection that is a hallmark of HIV disease. [13–15]

Despite the vigorous cellular and humoral immune responses seen during primary HIV infection, the virus succeeds in escaping immune-mediated clearance. Hence, once infection is established, it is never eliminated completely from the body.

Paradoxically, HIV seems to thrive on immune activation. Chronic immune activation results in increased viral replication and immune cell depletion, immune cell dysfunction, and aberrant lymphocyte turnover. [13]

Treating coinfections that potentially increase immune activation and provide a permissive environment for HIV replication is a promising, pathogenesis-associated approach to preventing HIV disease.

There is considerable epidemiologic evidence for a link between the presence of other sexually transmitted diseases, particularly genital-ulcer diseases, and the risk of HIV transmission. [16]

Recent studies have strengthened the evidence for this association. It has been reported that patients with recent or incident syphilis had a >4-fold increased risk for HIV acquisition. [17]

The same authors found that recent incidents of herpes simplex virus–2 (HSV-2) infection was associated with a ~4-fold increased risk of HIV acquisition. [18]

It had been assumed that the biologic mechanism for an increased risk of HIV infection in individuals with sexually transmitted diseases (STDs) was the impaired integrity of the mucosa, but, it has been reported that [18] the risk of HIV infection was increased for individuals who were asymptomatic for HSV-2 infection (i.e., persons who did not have clinically apparent or self-reported genital ulcers), as well as for individuals with symptomatic HSV-2 infection.

This and other studies suggest that additional mechanisms, such as immune activation, also may play a role. So far, the prevention and treatment of STDs, both

ulcerative and nonulcerative, offers promise as a strategy for preventing HIV infection. [16]

There is an increasing evidence on other infections such as helminthic infections, tuberculosis, and malaria increasing susceptibility to HIV infection or worsening progression of HIV disease. [19-25]

Concerning the sexual transmission of HIV, the use of topical microbicides could represent a valid approach for HIV infection prevention, in particular for women that are subjected to male-controlled modalities of protection.

These compounds have varying mechanisms of action, but the activities of all of the compounds focus on early mucosal events in pathogenesis.

In this respect, it has been recently reported that medically performed adult male circumcision significantly reduced a man's risk of acquiring HIV through heterosexual intercourse. [26, 27]

Male circumcision could protect against HIV acquisition by several mechanisms. [26, 27]

- The highly vascularised inner foreskin tissue contains a high density of Langerhans' cells as well as increased numbers of CD4+ T cells, macrophages, and other cellular targets for HIV.
- In contrast to the dry environment of the keratinized area on the outer surface of the foreskin, the moist environment under the foreskin may promote the presence or persistence of microbial flora, which, via inflammatory modification, may lead to even higher concentrations of target cells for HIV in the foreskin and a higher density of HIV-susceptible cells.
- The inner mucosa of the foreskin is more susceptible to microabrasion, providing a portal of entry for HIV, and the higher rates of ulcerative STDs in uncircumcised men may also increase susceptibility to HIV infection.

Hence, eliminating the foreskin diminishes some of the targets for the virus, and allows a more protective skin surface barrier against HIV. [28, 29]

Preexposure and postexposure chemoprophylaxis represent another important area of prevention research. It has been reported that tenofovir and emtricitabine have good safety profiles. Moreover they exhibit long half-life and, so far, may exert protection even if some doses are missed.

The most direct approach is the treatment of infected individuals with combination antiretroviral treatment, which, in a majority of individuals, can reduce plasma levels of virus to undetectable levels. [30]

In an analysis of transmission rates in the Women and Infants Transmission Study, the rate of maternal-fetal transmission was 23.4% when the viral load of the mother was  $\geq 30,000$  RNA copies/mL, compared with only 1% when her viral load was  $< 400$  RNA copies/mL. [31]

Thus, although not considered to be “prevention research,” studies of the pathogenesis of HIV disease could provide us with important opportunities to develop novel preventive measures.

### 1.3 Virus Structure

The genome and proteins of HIV (human immunodeficiency virus) have been the subject of extensive research since the discovery of the virus in 1983. [2, 3] Each virion comprises a viral envelope and associated matrix enclosing a capsid, which itself encloses two copies of the single-stranded RNA genome and several enzymes. The discovery of the virus itself was not until two years after the first major cases of AIDS associated illnesses were reported in 1981. [1]

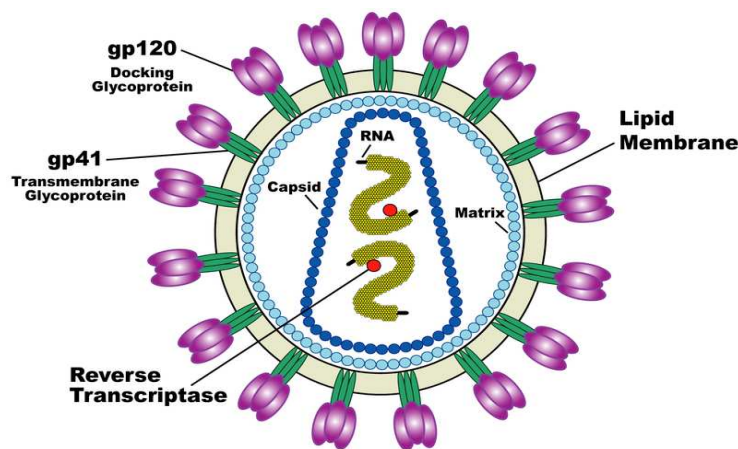


Figure 1. Schematic illustration of HIV structure

HIV structure is different from other retroviruses. It has a icosahedral shape with 120 nm in diameter (around 60 times smaller than a red blood cell).

HIV-1 is composed of two copies of single-stranded RNA enclosed by a conical capsid comprising the viral protein p24, typical of lentiviruses (Figure 1). The RNA component is 9749 nucleotides long. [32, 33]

This is in turn surrounded by an envelope originating from the host-cell. The single-strand RNA is tightly bound to the nucleocapsid proteins, p6, p7 and enzymes that are indispensable for the development of the virion, such as reverse transcriptase and integrase.

The nucleocapsid (p7 and p6) associates with the genomic RNA (one molecule per hexamer) and protects the RNA from digestion by nucleases.

A matrix, composed of an association of the viral protein p17, surrounds the capsid, ensuring the integrity of the virion particle.

Also enclosed within the virion particle are Vif, Vpr, Nef, p7 and viral Protease (Figure 1).



The envelope is formed when the capsid buds from the host cell, taking some of the host-cell membrane with it. The envelope includes the glycoproteins gp120 and gp41.

As a result of its role in virus-cell attachment, the structure of the virus envelope spike, consisting of gp120 and gp41, is of particular importance.

The first model of its structure was compiled in 2006 using cryo-electron tomography and suggested that each spike consists of a trimer of three gp120–gp41 heterodimers. [34]

However, evidence for a single-stalk “mushroom” model, with a head consisting of a trimer gp120 and gp41 stem, which appear as a compact structure with no obvious separation between the three monomers, anchoring it to the envelope was published shortly after. [35]

There are various possibilities as to the source of this difference, as it is unlikely that the viruses imaged by the two groups were structurally different.[36]

More recently, further evidence backing up the heterodimer trimer-based model has been found. [37]

## 1.4 Organisation of the Viral genome

The integrated form of HIV-1, also known as the provirus, is approximately 9.8 kilobases in length. [38]

The provirus genome is flanked by a repeated sequence known as the long terminal repeats (LTRs) on each side. The genes of HIV are located in the central region of the proviral DNA and encode at least nine proteins (Figure 2). [39]

These proteins are divided into three classes:

1. HIV structural proteins, Gag, Pol, and Env
2. The regulatory proteins, Tat and Rev
3. The accessory proteins, Vpu, Vpr, Vif, and Nef

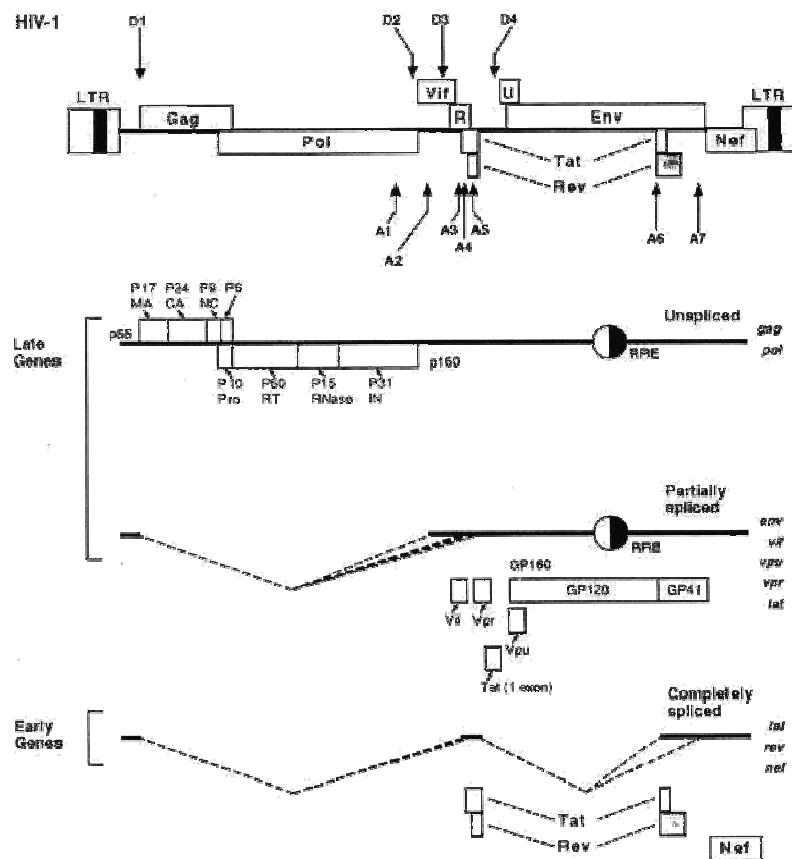


Figure 2. Schematic illustration of HIV genome

## **1.5 HIV structural Proteins**

### **1.5.1 Gag**

The gag gene gives rise to the 55-kilodalton (kD) Gag precursor protein, also called p55, which is expressed from the unspliced viral mRNA.

During translation, the N terminus of p55 is myristoylated, [40] triggering its association with the cytoplasmic aspect of cell membranes.

The membrane-associated Gag polyprotein recruits two copies of the viral genomic RNA along with other viral and cellular proteins that triggers the budding of the viral particle from the surface of an infected cell.

After budding, p55 is cleaved by the virally encoded protease (a product of the pol gene) during the process of viral maturation into four smaller proteins designated MA (matrix [p17]), CA (capsid [p24]), NC (nucleocapsid [p9]), and p6. [41]

The MA polypeptide is derived from the N-terminal, myristoylated end of p55. Most MA molecules remain attached to the inner surface of the virion lipid bilayer, stabilizing the particle.

A subset of MA is recruited inside the deeper layers of the virion where it becomes part of the complex which escorts the viral DNA to the nucleus. [42]

These MA molecules facilitate the nuclear transport of the viral genome because a karyophilic signal on MA is recognized by the cellular nuclear import machinery. This phenomenon allows HIV to infect nondividing cells, an unusual property for a retrovirus. [43]

The p24 (CA) protein forms the conical core of viral particles. Cyclophilin A has been demonstrated to interact with the p24 region of p55 leading to its incorporation into HIV particles. [44, 45]

The interaction between Gag and cyclophilin A is essential because the disruption of this interaction by cyclosporine A inhibits viral replication. [46]

The NC region of Gag is responsible for specifically recognizing the so-called packaging signal of HIV. [47]

The packaging signal consists of four stem loop structures located near the 5' end of the viral RNA, and is sufficient to mediate the incorporation of a heterologous RNA into HIV-1 virions. [48]

NC binds to the packaging signal through interactions mediated by two zinc-finger motifs. NC also facilitates reverse transcription. [49]

The p6 polypeptide region mediates interactions between p55 Gag and the accessory protein Vpr, leading to the incorporation of Vpr into assembling virions. [50]

The p6 region also contains a so-called late domain which is required for the efficient release of budding virions from an infected cell.

### **1.5.2 Gag-Pol Precursor**

The viral protease (Pro), integrase (IN), and reverse transcriptase (RT) are always expressed within the context of a Gag-Pol fusion protein. [51]

The Gag-Pol precursor (p160) is generated by a ribosomal frame shifting event, which is triggered by a specific cis-acting RNA motif [52] (a heptanucleotide sequence followed by a short stem loop in the distal region of the Gag RNA).

When ribosomes encounter this motif, they shift approximately 5% of the time to the pol reading frame without interrupting translation.

The frequency of ribosomal frameshifting explains why the Gag and the Gag-Pol precursor are produced at a ratio of approximately 20:1.

During viral maturation, the virally encoded protease cleaves the Pol polypeptide away from Gag and further digests it to separate the protease (p10), RT (p50), RNase H (p15), and integrase (p31) activities.

These cleavages do not all occur efficiently, for example, roughly 50% of the RT protein remains linked to RNase H as a single polypeptide (p66).

### **1.5.3 Pro**

The HIV-1 protease is an aspartyl protease [53] that acts as a dimer. Protease activity is required for cleavage of the Gag and Gag-Pol polyprotein precursors during virion maturation as described previously.

The three-dimensional structure of the protease dimer has been determined. [54, 55]

Knowledge of this structure has led to a class of drugs directed toward inhibiting the HIV protease function. These antiviral compounds have greatly improved treatment for HIV-infected individuals.

### **1.5.4 RT**

The pol gene encodes reverse transcriptase. Pol has RNA-dependent and DNA-dependent polymerase activities.

During the process of reverse transcription, the polymerase makes a double-stranded DNA copy of the dimer of single-stranded genomic RNA present in the virion.

RNase H removes the original RNA template from the first DNA strand, allowing synthesis of the complementary strand of DNA.

Viral DNA can be completely synthesized within 6 hours after viral entry, although the DNA may remain unintegrated for prolonged periods. [59]

Many cis-acting elements in the viral RNA are required for the generation of viral DNA.

For example, the TAR element, a small RNA stem-loop structure located at the 5' end of viral RNAs and containing the binding site for Tat, is required for the initiation of reverse transcription. [57]

The predominant functional species of the polymerase is a heterodimer of p66 and p51.

All of the pol gene products can be found within the capsid of free HIV-1 virions. Because the polymerase does not contain a proof-reading activity, replication is error-prone and introduces several point mutations into each new copy of the viral genome.

The crystal structure of HIV-1 RT has been determined. [58]

### **1.5.5 Integrase (IN)**

The IN protein mediates the insertion of the HIV proviral DNA into the genomic DNA of an infected cell. This process is mediated by three distinct functions of IN. [59]

First, an exonuclease activity trims two nucleotides from each 3' end of the linear viral DNA duplex.

Then, a double-stranded endonuclease activity cleaves the host DNA at the integration site.

Finally, a ligase activity generates a single covalent linkage at each end of the proviral DNA.

It is believed that cellular enzymes then repair the integration site. No exogenous energy source, such as ATP, is required for this reaction.

The accessibility of the chromosomal DNA within chromatin, rather than specific DNA sequences, seems to influence the choice of integration sites. [60]

Sites of DNA kinking within chromatin are thus "hot-spots" for integration, at least *in vitro*. [61]

It is possible to promote integration within specific DNA regions by fusing integrase to sequence-specific DNA binding proteins. [62]

Preferential integration into regions of open, transcriptionally active, chromatin may facilitate the expression of the provirus. Viral genes are not efficiently expressed from nonintegrated proviral DNA. [63]

### **1.5.6 Env**

The 160 kD Env (gp160) is expressed from singly spliced mRNA.

First synthesized in the endoplasmic reticulum, Env migrates through the Golgi complex where it undergoes glycosylation with the addition of 25 to 30 complex N-linked carbohydrate side chains that are added at asparagine residues.

Env glycosylation is required for infectivity. [64]

A cellular protease cleaves gp160 to generate gp41 and gp120.

The gp41 moiety contains the transmembrane domain of Env, while gp120 is located on the surface of the infected cell and of the virion through noncovalent interactions with gp41.

Env exists as a trimer on the surface of infected cells and virions. [65]

Interactions between HIV and the virion receptor, CD4, are mediated through specific domains of gp120. [66]

The structure of gp120 has recently been determined. [67] The gp120 moiety has nine highly conserved intrachain disulfide bonds.

In gp120 are also present five hypervariable regions, designated V1 through V5, whose amino acid sequences can vary greatly among HIV-1 isolates.

One of these regions, called the V3 loop, is not involved in CD4 binding, but is rather an important determinant of the preferential tropism of HIV-1 for either T lymphoid cell lines or primary macrophages. [68]

Sequences within the V3 loop interact with the HIV co-receptors CXCR4 and CCR5, which belong to the family of chemokine receptors and partially determine the susceptibility of cell types to given viral strains. [69, 70]

The V3 loop is also the principal target for neutralizing antibodies that block HIV-1 infectivity. [71]

The gp120 moiety also interacts with the protein DC-SIGN (Dendritic Cell-Specific Intercellular adhesion molecule-3-Grabbing Non-integrin) which is expressed on the surface of dendritic cells. Interaction with DC-SIGN increases the efficiency of infection of CD4 positive T cells. [72]

Further, it is believed that DC-SIGN can facilitate mucosal transmission by transporting HIV to lymphoid tissues.

The gp41 moiety contains an N-terminal fusogenic domain that mediates the fusion of the viral and cellular membranes, thereby allowing the delivery of the virion's inner components into the cytoplasm of the newly infected cell. [73]

A new class of antiviral therapeutics, which prevent membrane fusion, are showing promise in clinical trials.

## 1.6 Regulatory Proteins

### 1.6.1 Tat

Tat is a transcriptional transactivator that is essential for HIV-1 replication. [74] The 72 and 101 amino acid long forms of Tat are expressed by early fully spliced mRNAs or late incompletely spliced HIV mRNAs, respectively. Both forms function as transcriptional activators and are found within the nuclei and nucleoli of infected cells.

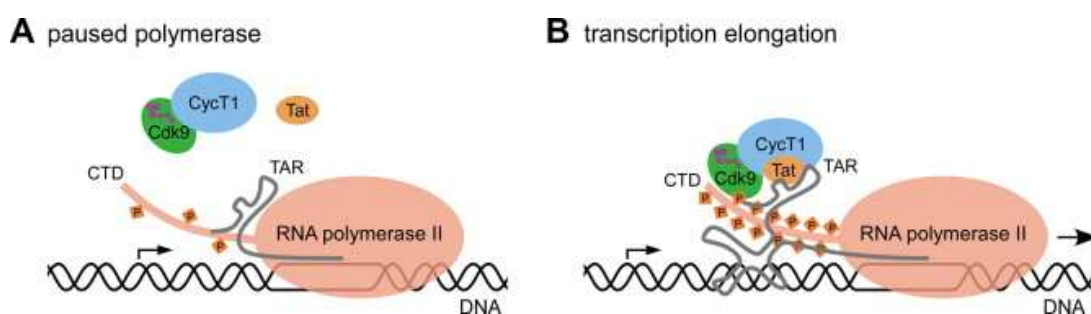
Tat is an RNA binding protein, unlike conventional transcription factors that interact with DNA. [75, 76] Tat binds to a short-stem loop structure, known as the transactivation response element (TAR), that is located at the 5' terminus of HIV RNAs. Tat binding occurs in conjunction with cellular proteins that contribute to the effects of Tat. The binding of Tat to TAR activates transcription from the HIV LTR at least 1000-fold.

The mechanism of Tat function has recently been elucidated. It acts principally to promote the elongation phase of HIV-1 transcription, so that full-length transcripts can be produced. [77, 78] In the absence of Tat expression, HIV generates primarily short (>100 nucleotides) transcripts.

Stimulation of polymerase elongation is accomplished by the recruitment of a serine kinase which phosphorylates the carboxylterminal domain (CTD) of RNA polymerase II (Figure 3).

This kinase, which is known as CDK9, is part of a complex which binds directly to Tat. [79]

Tat function requires a cellular co-factor, known as Cyclin T, which facilitates the recognition of the TAR loop region by the Cyclin T-Tat complex. [80]



**Figure 3.** Stimulation of polymerase elongation

The cellular uptake of Tat released by infected cells has been observed, [78] although the impact of this phenomenon on pathogenesis is unknown.

On the other hand, Tat has been shown to activate the expression of a number of cellular genes including tumor necrosis factor beta [81] and transforming growth factor beta (TNF- $\beta$ ), [82] and to downregulate the expression of other cellular genes including bcl-2 [83] and the chemokine MIP-1 alpha. [84]

### 1.6.2 Rev

Rev is a 13-kD sequence-specific RNA binding protein. [85] It is produced from fully spliced mRNAs, and acts to induce the transition from the early to the late phase of HIV gene expression. [86]

Rev, which is encoded by two exons, accumulates within the nuclei and nucleoli of infected cells. It binds to a 240-base region of complex RNA secondary structure, called the Rev response element (RRE), that lies within the second intron of HIV. [87]

Rev binds to a "bubble" within a double-stranded RNA helix containing a non-Watson-Crick G-G basepair. [88]

This structure, known as the Rev high affinity binding site, is located in a region of the RRE known as stem loop 2.

The binding of Rev to the RRE facilitates the export of unspliced and incompletely spliced viral RNAs from the nucleus to the cytoplasm. Normally, RNAs that contain introns (ie, unspliced or incompletely spliced RNA) are retained in the nucleus.

High levels of Rev expression can lead to the export of so much intron containing viral RNA that the amount of RNA available for complete splicing is decreased, which, in turn, reduces the levels of Rev expression.

Therefore, this ability of Rev to decrease the rate of splicing of viral RNA generates a negative feedback loop whereby Rev expression levels are tightly regulated. [89])

Rev has been shown to contain at least three functional domains. [90]



**Figure 4.** Rev high affinity binding site



An arginine-rich RNA binding mediates interactions with the RRE. A multimerization domain is required for Rev to function. [91]

Rev is believed to exist as a homo-tetramer in solution. [92] It also contains an effector domain, which is a specific nuclear export signal (NES). [93, 94]

The export of the viral RNA by Rev is through a pathway typically used by the small nuclear RNAs (snRNAs) and the ribosomal 5s RNA rather than the normal pathway for cellular mRNAs. [94] Rev Export is mediated through interactions with the NES receptor known as CRM1. NES mutants of Rev are dominant negative. [90]

Inhibition is caused by the formation of non-functional multimers between NES-mutant and wild type Rev monomers. [95]

Rev is absolutely required for HIV-1 replication: proviruses that lack Rev function are transcriptionally active but do not express viral late genes and thus do not produce virions.

## **1.7 Accessory Proteins**

In addition to the gag, pol, and env genes, contained in all retroviruses, and the tat and rev regulatory genes, HIV-1 contains four additional genes: nef, vif, vpr and vpu, encoding the so-called accessory proteins.

HIV-2 does not contain vpu, but instead harbors another gene, vpx.

The accessory proteins are not absolutely required for viral replication in all *in vitro* systems, but represent critical virulence factors *in vivo*.

Nef is expressed from a multiply spliced mRNA and is therefore Rev independent. In contrast, Vpr, Vpu, and Vif are the product of incompletely spliced mRNA, and thus are expressed only during the late Rev-dependent phase of infection from singly spliced mRNAs.

Most of the small accessory proteins of HIV have multiple functions as described below.

### **1.7.1 Nef**

Nef (an acronym for negative factor) is a 27-kD myristoylated protein that is encoded by a single exon that extends into the 3' LTR. Nef, an early gene of HIV, is the first viral protein to accumulate in detectable levels in a cell following HIV-1 infection. [86]

Its name is a consequence of early reports, claiming that Nef downregulated transcriptional activity of the HIV-1 LTR.

However, it is no longer believed that Nef has a direct effect on HIV gene expression.

Nef has been shown to have multiple activities, including the downregulation of the cell surface expression of CD4, the perturbation of T cell activation, and the stimulation of HIV infectivity.

Nef acts post-translationally to decrease the cell-surface expression of CD4, the primary receptor for HIV. [96]

It increases the rate of CD4 endocytosis and lysosomal degradation. [97]

The cytoplasmic tail of CD4, and in particular a dileucine repeat sequence contained in its membrane proximal region, is key for the effect of Nef on CD4. [90]

CD4 downregulation appears to be advantageous to viral production because an excess of CD4 on the cell surface has been found to inhibit Env incorporation and virion budding. [98, 99]

Nef also downregulates the cell surface expression of Class I major histocompatibility complex (MHC), albeit to a lesser degree. [100]

The downregulation of Class I MHC decreases the efficiency of the killing of HIV infected cells by cytotoxic T cells.

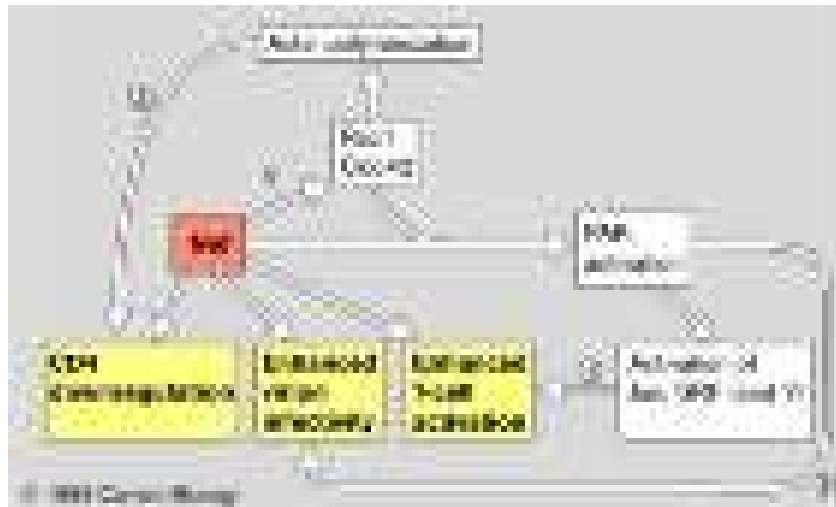
Nef perturbs T cell activation. Studies in the Jurkat T cell line indicated that Nef expression has a negative effect on induction of the transcription factor NF-kappa B and on IL-2 expression. [101]

In contrast, results obtained in Nef transgenic mice revealed that Nef led to elevated T cell signalling. [102]

The expression of a CD8-Nef chimeric molecule in Jurkat cells had either positive or negative effects depending on the cellular localization of the hybrid Nef molecule. [103]

When the CD8-Nef protein accumulated in the cytoplasm, there was a block in normal signaling through the T cell receptor.

When the CD8-Nef chimera was expressed at high levels on the cell surface, however, spontaneous activation followed by apoptosis was detected.



**Figure 5.** Nef activity network

Together, these observations suggest that Nef can exert pleiomorphic effects on T cell activation depending on the context of expression.

Consistent with this model, Nef has been found to associate with several different cellular kinases that are present in helper T lymphocytes.

Nef also stimulates the infectivity of HIV virions. [104]

HIV-1 particles produced in the presence of Nef can be up to ten times more infectious than virions produced in the absence of Nef.

Nef is packaged into virions, where it is cleaved by the viral protease during virion maturation. [105]

The importance of this event, however, is not clear. Virions produced in the absence of Nef are less efficient for proviral DNA synthesis, although Nef does not appear to influence directly the process of reverse transcription. [106]

The downregulation of CD4 and the effect on virion infectivity by Nef are genetically distinct as demonstrated by certain mutations that affect only one of these two activities. [107]

There is compelling genetic evidence that the Nef protein of simian immunodeficiency virus is absolutely required for high-titer growth and the typical development of disease in adult animals. [108]

It is possible, however, for Nef-defective mutants of SIV to cause disease in newborn animals. [109]

Further, Nef-defective virions do cause an AIDS-like disease in infected animals although onset is delayed. [110]

### **1.7.2 Vpr**

The Vpr protein is incorporated into viral particles. Approximately 100 copies of Vpr are associated with each virion. [111]

Incorporation of Vpr into virions is mediated through specific interactions with the carboxyl-terminal region of p55 Gag, [56] which corresponds to p6 in the proteolytically processed protein.

Vpr plays a role in the ability of HIV to infect non dividing cells by facilitating the nuclear localization of the preintegration complex (PIC). [112] Vpr is present in the PIC.

However, rather than tethering additional nuclear localization signals to the PIC, Vpr may act as a nucleocytoplasmic transport factor by directly tethering the viral genome to the nuclear pore.

Consistent with this model, Vpr expressed in cells is found associated with the nuclear pore and can be biochemically demonstrated to bind to components of the nuclear pore complex. [113] Vpr can also block cell division. [114]

Cells expressing Vpr accumulate in the G2 phase of the cell cycle. [115]

The expression of Vpr has been shown to prevent the activation of the p34cdc2/cyclin B complex, which is a regulator of the cell cycle important for entry into mitosis. [116, 117]

Accordingly, expression of a constitutively active mutant of p34cdc2 prevents the Vpr-induced accumulation of cells in the G2 phase of the cell cycle.

Vpr has also been shown to interact with the cellular protein uracil-DNA glycosylase (UNG). [118]

The biological consequences of this phenomenon have yet to be determined.

Another enzyme involved in the modification of deoxyuracil (dUTP), deoxyuracil phosphatase (dUTPase), is expressed by two lentiviruses that do not contain a vpr gene: equine infectious anemia virus and feline immunodeficiency virus.

It is believed that the dUTPase depletes the dUTP within the cell thus preventing the deleterious consequences of dUTP incorporation into viral DNA. [119]

### **1.7.3 Vpu**

The 16-kD Vpu polypeptide is an integral membrane phosphoprotein that is primarily localized in the internal membranes of the cell. [120]

It is expressed from the mRNA that also encodes env. Vpu is translated from this mRNA at levels tenfold lower than that of Env because the Vpu translation initiation codon is not as efficient. [121]

The two functions of Vpu, the down-modulation of CD4 and the enhancement of virion release, can be genetically separated. [122]

In HIV-infected cells, complexes formed between the viral receptor, CD4, and the viral envelope protein (Env) in the endoplasmic reticulum cause the trapping of both proteins in this compartment.

Thus, the formation of intracellular Env-CD4 complexes interferes with virion assembly.

Vpu liberates the viral envelope by triggering the ubiquitin-mediated degradation of CD4 molecules complexed with Env. [123]

Vpu also increases the release of HIV from the surface of an infected cell. In the absence of Vpu, large numbers of virions can be seen attached to the surface of infected cells. [124]

#### **1.7.4 Vif**

Vif is a 23-kD polypeptide that is essential for the replication of HIV in peripheral blood lymphocytes, macrophages, and certain cell lines. [125]

In most cell lines, Vif is not required, suggesting that these cells may express a protein that can complement Vif function.

These cell lines are called permissive for Vif mutants of HIV.

Virions generated in permissive cells can infect non permissive cells but the virus subsequently produced is non infectious.

Complementation studies indicate that it is possible to restore the infectivity of HIV Vif mutants by expression of Vif in producer cells but not in target cells. [126]

These results indicate that Vif must be present during virion assembly. Thus, Vif is incorporated into virions of HIV. [127]

This phenomenon, however, might be nonspecific because Vif is also incorporated into heterologous retroviruses such as murine leukemia viruses. [128]

Studies producing HIV from heterokaryons generated by the fusion of permissive and non-permissive cells revealed that non-permissive cells contain a naturally occurring antiviral factor that is overcome by Vif. [129]

Further support for a model that Vif is counteracting an antiviral cellular factor comes from the observation that Vif proteins from different lentiviruses are species specific. [130]

For instance, HIV Vif can modulate the infectivity of HIV-2 and SIV in human cells while SIV Vif protein does not function in human cells.

This observation suggests that cellular factors, rather than viral components, are the target of Vif action.

Vif-defective HIV strains can enter cells but cannot efficiently synthesize the proviral DNA. [126]

It is not clear whether the Vif defect affects reverse transcription *per se*, viral uncoating, or the overall stability of the viral nucleoprotein complex. Vif mutant virions have improperly packed nucleoprotein cores as revealed by electron microscopic analyses. [131]

## 1.8 HIV life cycle

The HIV life cycle consist of several steps, starting from the attachment of the virus to the host cell membrane and finishing with the release of progeny virions from the cell, as summarized in Figure 6.

It starts with a specific interaction of the viral glycoprotein gp120 sited on the outer membrane and the CD4 receptor on the host cell surface.

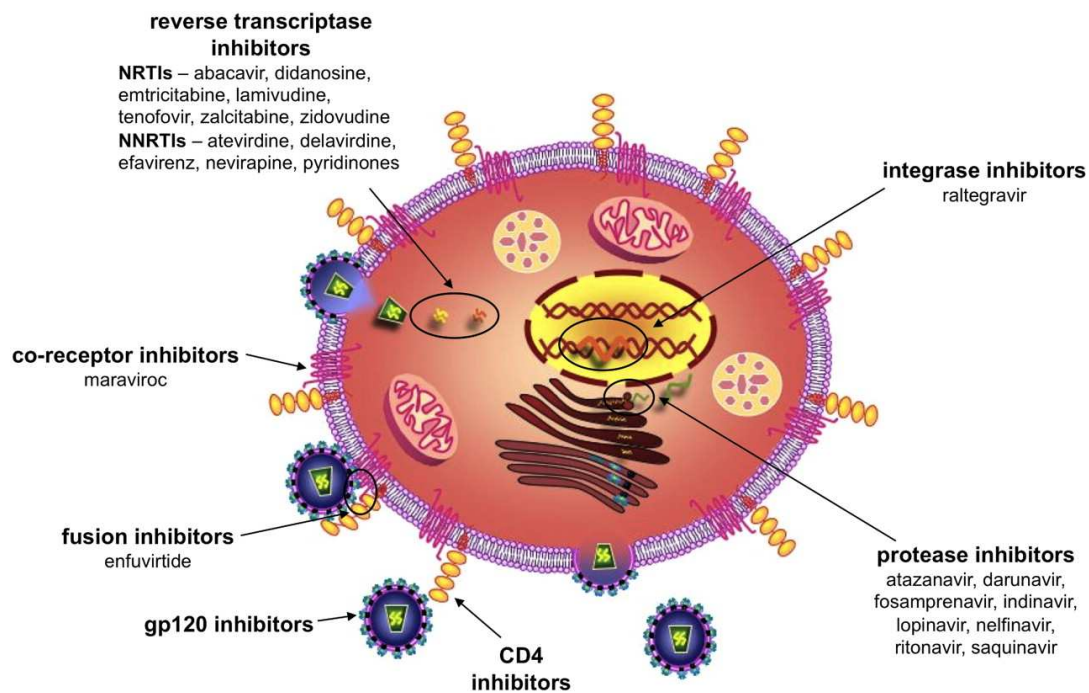


Figure 6. HIV life cycle

This reaction leads to a conformational change allowing the interaction of gp120 with the chemokine co-receptors CXCR4 and CCR5.

This step is then followed by further conformational changes that expose a fusogenic peptide, which anchors into the host cell membrane.

Once the viral envelope and cell membrane have fused, the virion is decapsidated releasing the viral RNA into the host cell's cytoplasm.

Through the reverse transcription, the viral RNA is transcribed to viral double-stranded DNA.

This process is catalyzed by an RNA-dependent DNA polymerase, known as reverse transcriptase (RT), which is encoded by the viral genome.

Then, the viral DNA is integrated into the host chromosome, and after transcription and translation into viral proteins using the cells' machinery, the assembly of the Gag and Gag-Pol polyproteins occurs near the cell membrane.

During viral assembly, two copies of single-stranded viral RNA are incorporated into the virion, which then buds off from the cell, taking with it part of the host cell membrane.

Soon after budding, viral protease cleaves the Gag-Pol polyprotein to generate a mature, functional virion.

Generally, antiviral drugs could, in principle, be targeted at either viral proteins or cellular proteins.

The first approach is likely to yield more specific, less toxic compounds, with a narrow spectrum of activity, but a higher likelihood of virus drug resistance development.

However, the second approach might afford anti-HIV drugs with a broader activity spectrum and less chance of resistance but higher likelihood of toxicity. [132-134]

From the Medicinal Chemistry point of view, each of these steps is a possible druggable target to combat the HIV infection (Figure 6).

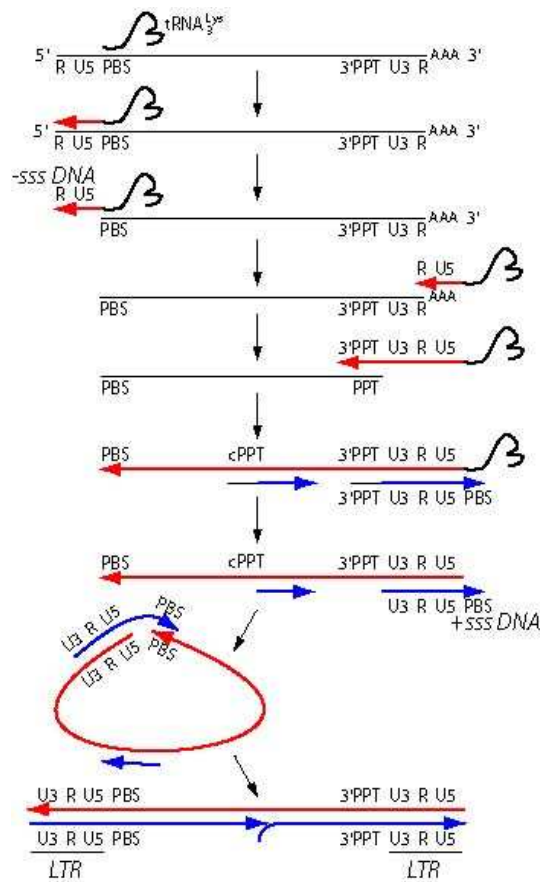
In this project I have focused my attention on the design and synthesis of unconventional Reverse Transcriptase inhibitors (RTis).

## **1.9 Reverse Transcription**

The retrotranscription process is a key step in the early phases of HIV infection. It consists of the conversion of the viral ssRNA genome into integration-competent dsDNA, and requires both viral and cellular elements, among which the most important is the virus-coded RT protein.

In each viral particle two copies of (+)ssRNA are enclosed coding both structural and non structural proteins and having, in the 5'- and 3'-ends, two identical sequences. [135]

Proximal to the 5'-end of the viral genome there is a 18 nucleotides long segment, termed primer binding site (PBS), which is complementary to the 3'-end 18 nucleotides of the human tRNA<sup>Lys3</sup> (Figure 7).



**Figure 7.** Schematic illustration of the retrotranscription process

Once the cellular tRNA is hybridized to the PBS, it serves as RNA primer and the RT associated DNA polymerase function can initiate the first (-)strand DNA synthesis using the viral RNA genome as a template.

Then, when tRNA elongation reaches the ssRNA 5'-end a first (-)strand strong-stop DNA is encountered.

The synthesis of the (-)strand DNA generates an RNA:DNA hybrid that is selectively degraded by the RT-associated ribonuclease H (RNase H) function.

Therefore the hydrolysis of the RNA strand of the RNA:DNA hybrid [136] leaves the nascent (-)strand DNA free to hybridize with the complementary sequence at the 3'-end of one of the two viral genomic ssRNAs.

A strand transfer therefore occurs from the R region at the 5'-end of the genome to the equivalent R region at the 3'-end.

Once (-)strand transfer has occurred, (-)strand synthesis can continue along the viral RNA starting from its 3'-end, while the RNase H function cleaves the RNA strand of the RNA:DNA at numerous points.



Although most of the RNase H cleavages do not appear to be sequence specific, there are two specific purine-rich sequences, known as the polypurine tracts (PPTs), that are resistant to the RNase H hydrolysis and remain annealed to the nascent (-)strand DNA.

These two well-defined sites are located in the central part of the HIV-1 genome. In particular, the 3'-end PPT defines the 5'-end of the viral coding (+)strand DNA synthesis since this PPT serves as primer. [137, 138]

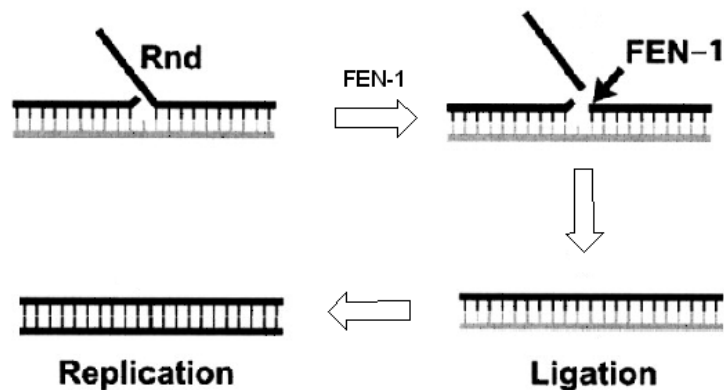
The (+)strand DNA synthesis continues until it reaches the 5'-end of the (-)strand DNA, and also uses the 18 nucleotides PBS sequence of the tRNA as a template.

Noteworthy, the 19th base from the 3'-end of tRNA<sup>Lys3</sup> is a methyl-A, and the presence of such modified base blocks the RT, generating a (+)strand strong-stop DNA.

Subsequently, the RNase H function cleaves the RNA segment of the tRNA:DNA hybrid, freeing the PBS sequence of the (+)strand DNA and allowing it to anneal to the complementary site near the 3'-end of the extended (-)strand DNA. [139]

After this key step, a bidirectional synthesis occurs to complete a viral dsDNA that has a 90 nucleotides single-stranded flap at the center.

In all probability a host mechanism occurs to solve this unusual situation and, most likely the flap removal is operated by the flap endonuclease-1 (FEN-1) (Figure 8). [138]



**Figure 8.** Flap removal operated by the flap endonuclease-1 (FEN-1)

The process is terminated by a specific cleavage that removes the PPT primers and exposes the integration sequence to ease the insertion of the viral dsDNA into the cell chromosome.

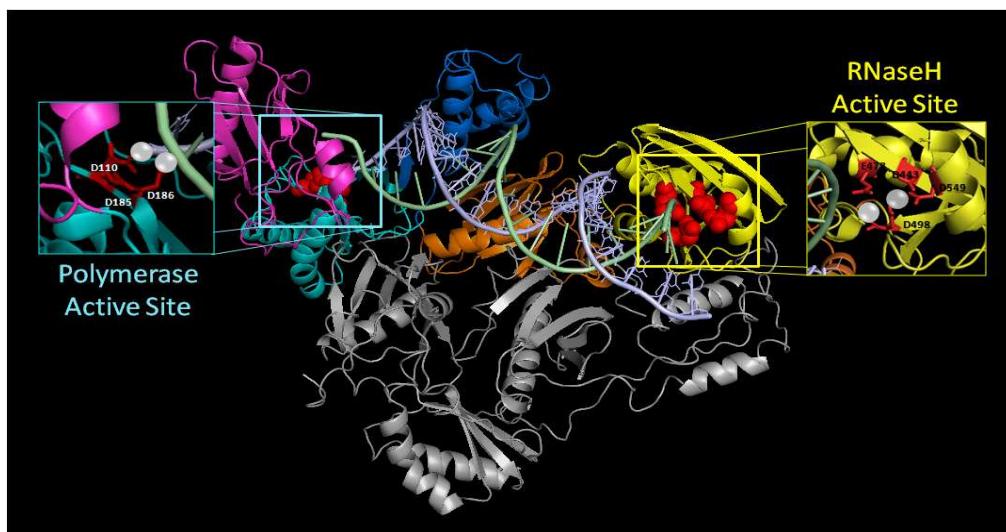
On this basis RT has been considered to be a major target for HIV chemotherapy and indeed it has been the subject of extensive research through crystal structures determinations, biochemical assays and single-molecule analyses.

RT consists of two subunits of different length, p66 and p51, generated by a viral protease cleavage of a virus-coded polyprotein.

p66 and p51 share a common amino terminus and are combined in a stable asymmetric heterodimer. [140]

Analysis of the crystal structure of RT reveals that p66 is composed of two spatially distinct catalytic domains, polymerase domain and RNase H domain (Figure 9).

In more detail p66 is composed of the polymerase domain (residues 1-318), the connection domain (residues 319-426), and the RNase H domain (residues 427-560). [141, 142]



**Figure 9.** Reverse transcriptase catalytic sites

The polymerase domain shows a characteristic highly conserved structure that resembles a right hand, consisting of fingers domain (residues 1-85 and 118-155), palm domain (residues 86-117 and 156-237), and thumb domain (residues 238-318).

Regarding the p51 subunit a different folding is observed, due to the lack of the RNase H domain.

Although with different relative positions, all the other subdomains are identical to those of p66, however no enzymatic activity is associated with the p51 subunit which performs a merely structural function, keeping the p66 subunit in the proper folding to perform all the catalytic functions.

Several distinct activities, all indispensable for the retrotranscription process, are associated to RT: RNA- and DNA-dependent DNA synthesis, RNase H activity, strand transfer and strand displacement synthesis. [143]

The synthesis of the viral DNA is catalyzed by both RT associated RNA- and DNA dependent DNA polymerase activities (RDDP and DDDP, respectively) with a mechanism similar to that of all others polymerases. [144]

The polymerase active site is located in the middle of palm, fingers and thumb subdomains. Noteworthy is the palm subdomain which plays a key role for the substrate binding since its  $\beta 12$ – $\beta 13$  sheets extensively interact with the phosphate backbone and are termed the “primer grip”. [145] Moreover three aspartic acid residues (D110, D185 and D186), located in the palm subdomain of p66, bind the divalent ion co-factor ( $Mg^{2+}$ ) through their catalytic carboxylates groups, and are essential for catalysis Fig. (1). [146]

Firstly RT binds to the template primer on the priming binding site; this interaction is stabilized by a change of the conformation of the p66 thumb (from closed to open) and is an essential step in DNA synthesis. Afterwards, the dNTP binds at the nucleotide binding site to form an RT:DNA:dNTP ternary complex. [147]

Then the dNTP is trapped by a conformational change of the fingers which precisely aligns the  $\alpha$ -phosphate of the dNTP to the 3'-OH of the primer inside the polymerase active site (this is actually the rate limiting step).

The enzyme is then ready to catalyze the formation of a phosphodiester bond between the primer 3'-OH and the dNMP with the release of a pyrophosphate which is free to exit from the catalytic site.

Finally either a translocation of the elongated DNA primer frees the nucleotide-binding site for the next incoming dNTP or RT can dissociate from the complex.

The RNase H domain is located on the other side of the p66 subunit, 60 Å from the polymerase active site (Figure 9) equivalent to 17 nucleotides of a DNA:DNA hybrid and/or 18 nucleotides of a RNA:DNA hybrid. [148]

RT is able to degrade selectively the RNA portion of an RNA:DNA hybrid and to remove the priming tRNA and PPT. This RNase H function is essential for virus replication since RNase H deficient viruses are non-infectious. [149]

It is worthy of note that the strand transfer process is a crucial step in the reverse transcription and consists of the annellation of two ssNAs to permit the continuation of the DNA synthesis. In both (-) and (+)strand transfers the ssNA develops secondary structures: the R region consists of a strong-structured motif TAR hairpin and a poly(A) hairpin. [150]

Furthermore a stable hairpin structure can be formed by the PBS sequence at the 3'-end of the (-)strand DNA.

In this respect, the viral-coded nucleocapsid (NC) protein plays a crucial role in helping the RT to perform this step and could be considered as a promising target for drug design. [151, 152]

Common to most DNA polymerases, RT can perform the retroreaction of the dNTP incorporation.

This reaction termed pyrophosphorolysis requires either a pyrophosphate (PPi) or an NTP (ie ATP) as acceptor [153, 154] and leads to the formation of a dinucleotide tetraphosphate (formed by the excised dNMP and the acceptor ATP substrate) and a free 3'-OH end as reaction products.

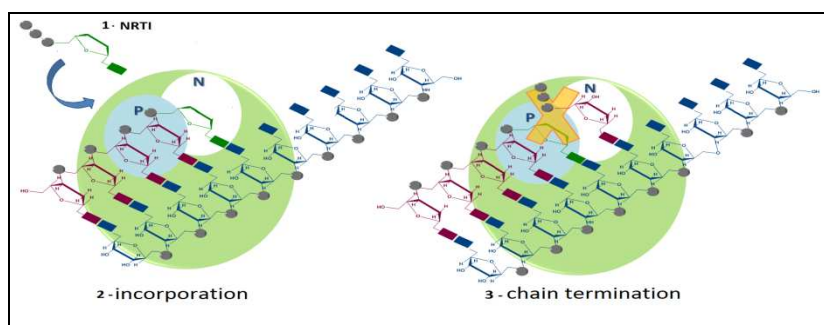
## 1.10 Reverse Transcriptase Inhibitors

### 1.10.1 Inhibitors of the RDDP Function

Two classes of RTIs, that target the viral enzyme with two different mechanisms of action, are included in the approved combination treatments used for HIV-1 handling.

The first class comprises compounds known as Nucleoside/Nucleotide RT Inhibitors (NRTIs/NtRTIs), while the second class comprises compounds known as Non-Nucleoside RT Inhibitors (NNRTIs). NRTIs are analogs of the natural substrate (dNTP) and inhibit RDDP function by a competitive mechanism at the active site.

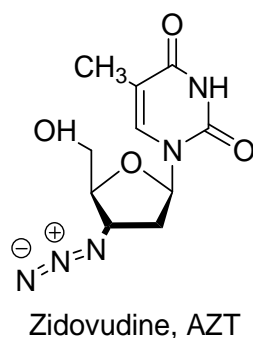
To act on such a mechanism, these inhibitors must necessarily lack a free OH group in 3' position (Figure 10).



**Figure 10.** Mechanism of action of NRTIs

Zidovudine (AZT, 3'-azidothymidine) was identified as the first NRTI acting as pro-drug. It requires successive phosphorylation steps and operates through its triphosphate metabolite. [156]

The active form of the drug is used as a false substrate during reverse transcription of viral RNA (Figure 11).

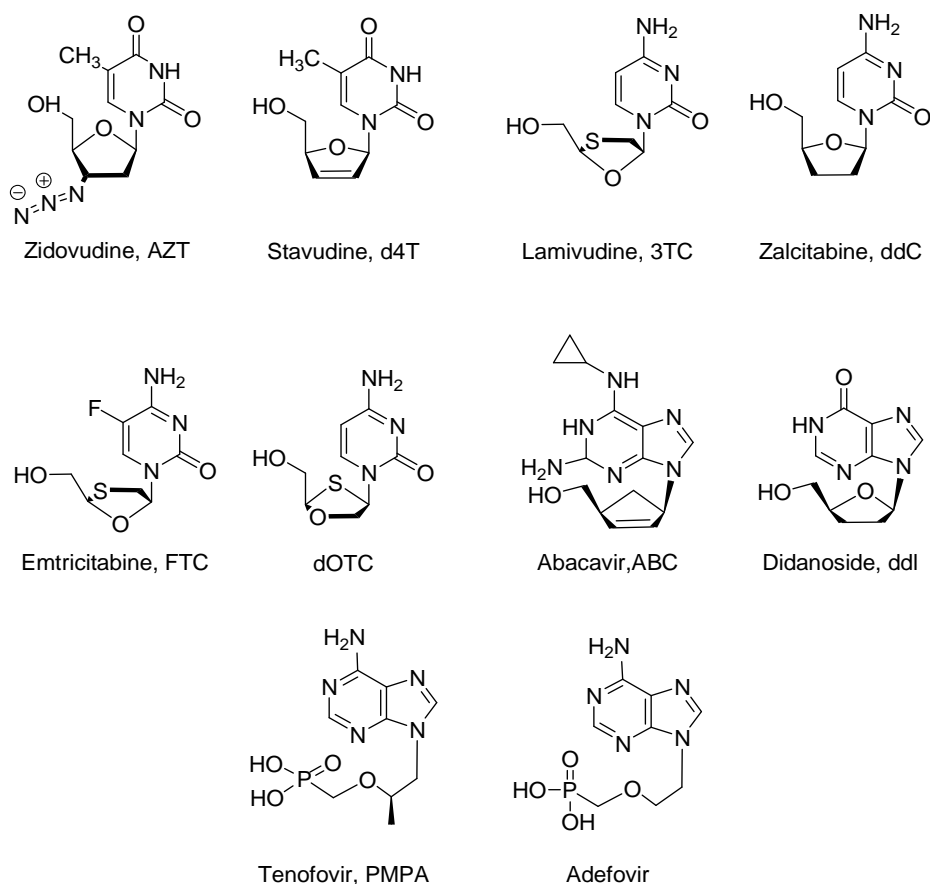


**Figure 11.** Zidovudine structure

Currently eight NRTIs are clinically available, structurally resembling either pyrimidine or purine analogues.

In the pyrimidine nucleoside analogues both thymine and cytosine analogues are included.

Between the most representative thymine analogues 3'-azido-2',3'-dideoxythymidine (zidovudine, AZT) and 2',3'-didehydro-2',3'-dideoxythymidine (stavudine, d4T) are worth noting while cytosine analogues are (-)-2',3'-dideoxy-3'-thiacytidine (lamivudine, 3TC), 2',3'-dideoxycytidine (zalcitabine, ddC) which, however, is no longer recommended due to its peripheral neuropathy, (-)-2',3'-dideoxy-5-fluoro-3'-thiacytidine (emtricitabine, FTC) and [(-)-2'-deoxy-3'-oxa-4'-thiacytidine) (dOTC) (Figure 12).



**Figure 12.** Clinically available NRTIs and NtRTIs

Purine nucleoside analogues include (1S-4R)-4-[2-amino-6-(cyclo-propylamino)-9H-purin-9-yl]-2-cyclopentane-1-methanol (abacavir, ABC) and 2',3'-dideoxyinosine (didanosine, ddl) as guanine and adenine analogues.

Unfortunately drug resistant viral mutants can gain a competitive advantage over wt virus under selective drug pressure, almost becoming the dominant species.

Generally two different mechanisms lead to HIV-1 resistance to NRTIs.

The first consists of NRTI discrimination leading to a reduction of the incorporation rate, the second consists of NRTI excision that unblocks NRTI-terminated primers.

Typically, discrimination occurs due to steric hindrance leading to a selective alteration of the NRTI binding and/or incorporation rate.

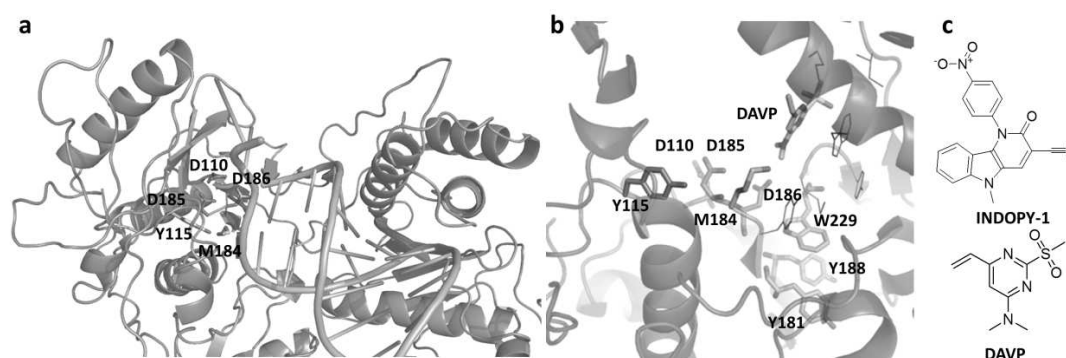
Regarding NRTI excision it is mostly increased through mutations, located around the dNTP binding pocket and also in termed thymidine analogs mutations (TAMs).

NRTI resistance could also be conferred by mutations in the connection and RNase H domains. [158-162]

The NtRTIs, such as adefovir [9-(2-phosphonylmethoxyethyl) adenine (PMEA)] and tenofovir [(R)-9-(2-phosphonylmethoxypropyl) adenine (PMPA)] are acyclic phosphonate analogues of adenine, and, therefore, only need two phosphorylation steps to be converted into the active drug. Like the NRTIs they act as obligatory chain terminators. [163]

Along with exploration of the NRTI binding pocket to obtain analogous molecules with improved drug-like properties and effective against many NRTI drug-resistant RT variants [164], recently, two families of compounds have been reported as new classes of “nucleotide-competing RT inhibitors” (NcRTIs).

The first is represented by indolopyridones (INDOPY) derivatives. Although structurally different from classic NRTI it seems that this series can occupy the active site of the enzyme (or a site in close proximity) and compete with natural dNTP substrates.

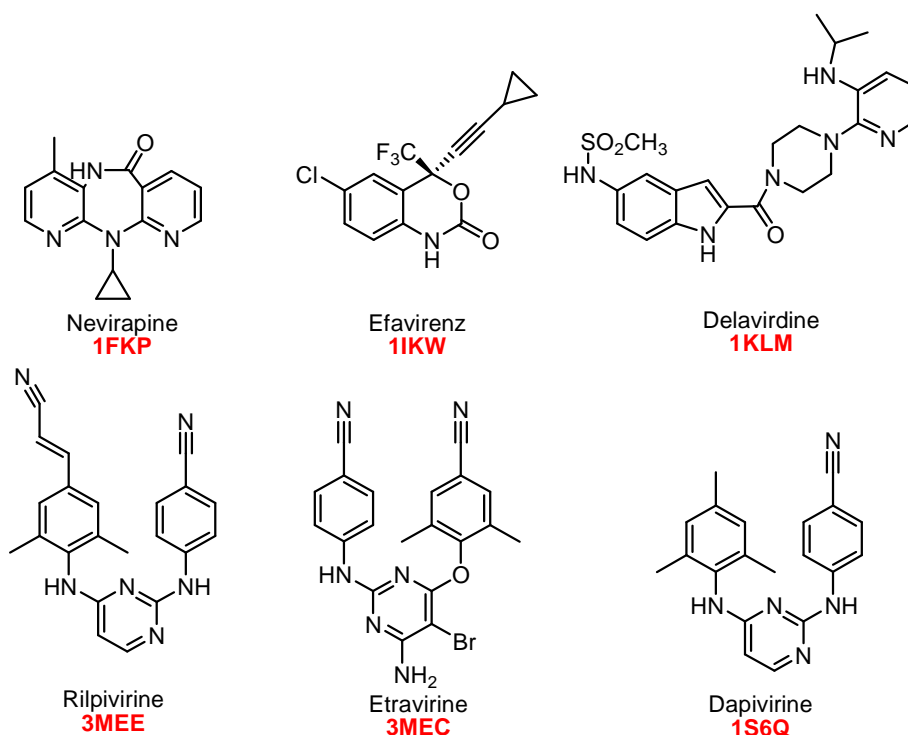


**Figure 13.** NcRTI: a) INDOPY binding site: mutational studies suggested that the INDOPY binding site is close to M184 and Y115. The DNA template is represented in cartoon and the aspartate catalytic triad in sticks (pdb code 1rtd [166]); b) DAVP-1 binding mode (pdbcode 3isn [167] ); c) Chemical structures of INDOPY-1 and DAVP.

The observed resistance associated to mutation of Y115 + M184 give support to this hypothesis (Figure 13a). [165, 166]

The second class includes 4-dimethylamino-6-vinylpyrimidine derivatives (DAVP) whose binding site is close to the polymerase active site as illustrated in Figure 13b. [167]

In contrast to the NRTI class, NNRTIs are a family of compounds characterized by a high variety of structures (Figure 14).



**Figure 14.** NNRTIs approved for therapy (PDB codes are reported in red)

They act as noncompetitive inhibitors against the substrate and bind close to the polymerase active site provoking a distortion of the protein structure and inhibiting the polymerase activity.

Worthnoting they do not need intracellular activation.

Many different classes of NNRTIs could be distinguished and 5 drugs, acting as NNRTIs, have been approved for HIV-1 treatment so far.

It should be mentioned that, while in the case of first generation NNRTIs, like delavirdine and nevirapine, single mutations (Y181C, K103N and Y188C) could lead to drug resistance; in the case of the more bulky second generation NNRTIs, like efavirenz and dapivirine, more than one mutation is generally required to induce drug resistance.

Although resistance and toxicity are some of the most important drawbacks of NNRTIs, an intense research activity is focused on this class of compounds and more than 30 different classes of NNRTIs have been reported. [169, 170]

More recently molecules with a higher flexibility, although less favored by a thermodynamic point of view, have been proposed as NNRTIs. [171, 172]

Molecules like etravirine and rilpivirine are successful examples of this new approach as well as dapivirine which is currently under clinical evaluation.



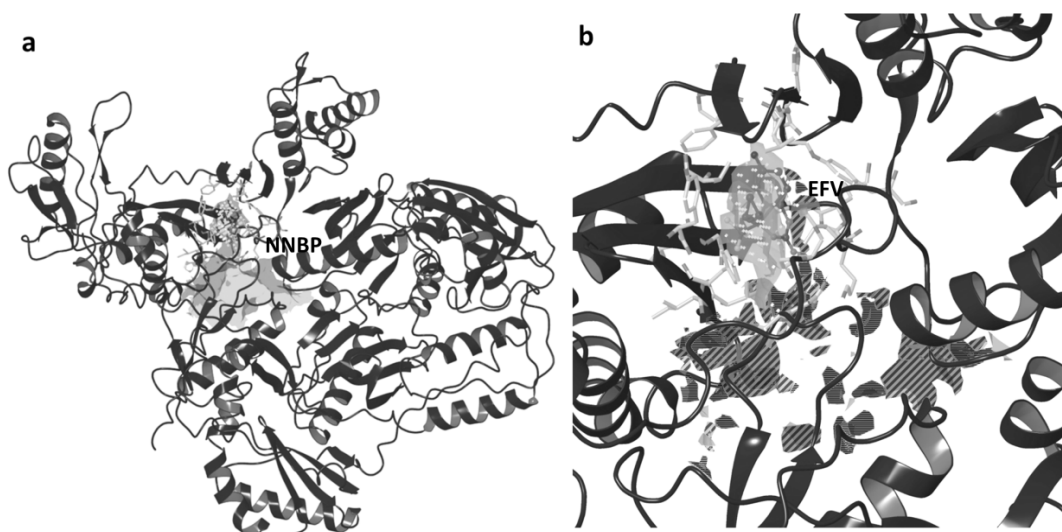
NNRTIs inhibit RT by binding to the enzyme in a hydrophobic pocket (NNIBP) located in the palm domain of the p66 subunit of the heterodimeric RT, approximately 10 Å from the catalytic site of the enzyme.

This pocket contains the side chains of aromatic and hydrophobic amino acid residues Y181, Y188, F227, W229, Y318, P95, L100, V106, V108, V179, L234, and P236 from the p66 subunit.

The NNIBP is flexible and its conformation depends on the size, shape, and binding mode of the different NNRTI.

It can accommodate a space of about 620-720 Å<sup>3</sup>, which is approximately more than twice the volume occupied by most of the present NNRTIs. (Figure 15). [173]

This explains the large variety of chemical scaffolds of this class of inhibitors whose shapes inspired authors to create imaginative names to describe them (e. g “butterfly” [174], “horseshoe” [171], and “dragon” [175]).



**Figure 15.** NNBP: a) surface map size and shape of the space available visualized with SiteMap [176]; b) hydrophobic (light grey), donor (diagonal stripes), and acceptor (dark grey fine stripes) maps. Efavirenz (EFV) is shown in ball and stick and interacting residues in the NNIBP in stick (pdbcode 1ikw)

The NNIBP is not present in structures of HIV-1 RT that do not have a bound NNRTI (closed pocket form).

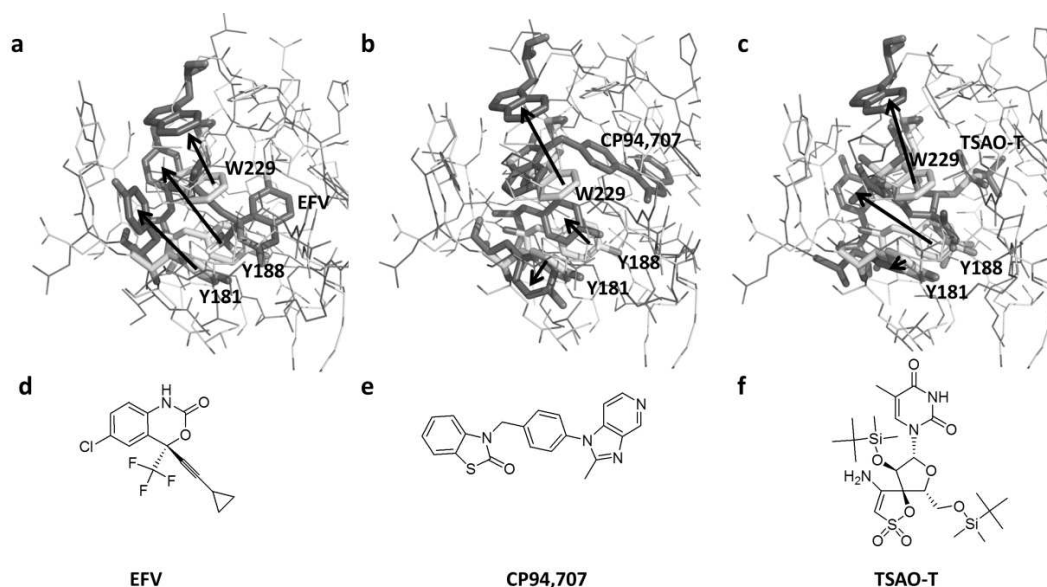
Upon binding of ligands its opening is observed. In most cases the flipping of the aromatic side chains of Y181 and Y188 (e. g efavirenz pdbcode1ikw (Figure 16a) [177], or etravirine pdbcode 1suq [178] is a binding key feature.

For other ligands it is possible to notice the expansion of the pocket (e.g CP94,707 pdbname 1tv6 [179]) but not the flipping of tyrosines (Figure 16b) or the flipping of only one tyrosine as in the complex RT-TSAO-T (Figure 16c) (pdbcode 3qo9. [175])

The binding of NNRTI causes the dislocation of the  $\beta$ 12-  $\beta$ 13-  $\beta$ 14 sheets that results in a movement of the primer grip away from the polymerization site sheet. [180]

TSAO series also act by destabilizing heterodimeric p66/p51 HIV-1 RT. [181]

Commonly observed resistance mutations in NNRTI-treated patients include L100I, K103N, V106A, Y181C, Y188L, and G190A.



**Figure 16.** NNRTI binding mode and comparison of NNIBP residues with unbound enzyme (pdb code 1dlo[182]). a) Efavirenz; b) CP94,707; c) TSAO-T. Y181, Y188 and W229 are visualized in sticks for the comparison. d-e-f) Chemical structure of inhibitors co-crystallized in the complexes examined

These mutations occur alone or in combination and cause clinically relevant drug resistance, directly, by altering the size, shape, and polarity of different parts of the NNIBP or, indirectly, by affecting access to the pocket.

To overcome this problem several attempts have been made either to optimize interactions between drug candidates and highly conserved amino acid residues in the NNIBP, such as W229 [183] or to design more flexible drug candidate, as in the case of diarylpyrimidine (DAPY). [171]

In fact, etravirine has the ability to bind in multiple modes and this would permit the NNRTI to retain activity evading drug-resistant mutations.

Another possibility is to look for structures able to enter the NNIBP but that show less hydrophobic interaction and different key contacts.

A promising example is calanolide A and its derivatives that exhibit enhanced activity against HIV-1 isolates most commonly with Y181C and K103N mutations.

The putative binding mode reported and the biological study support this hypothesis. [184]

### ***1.10.2 Inhibitors of the RNase H Function***

As reported above RNase H function is essential for the reverse transcription but, until now no inhibitors, specific for this enzymatic activity have been introduced in therapy.

Nevertheless, quite recently, some RNase H inhibitors (RNase HI) have been designed and studied.

Generally they act by chelating the  $Mg^{2+}$  ions within the active site. Unfortunately this mechanism of action is quite unspecific, due to the possible interaction with other divalent ions in cellular enzymes.

Moreover the RNase H active site is an open pocket that gives very few hints for the design of specific inhibitors.

However several studies have demonstrated that the abolition of the HIV-1 RNase H activity stops viral replication. [185, 186]

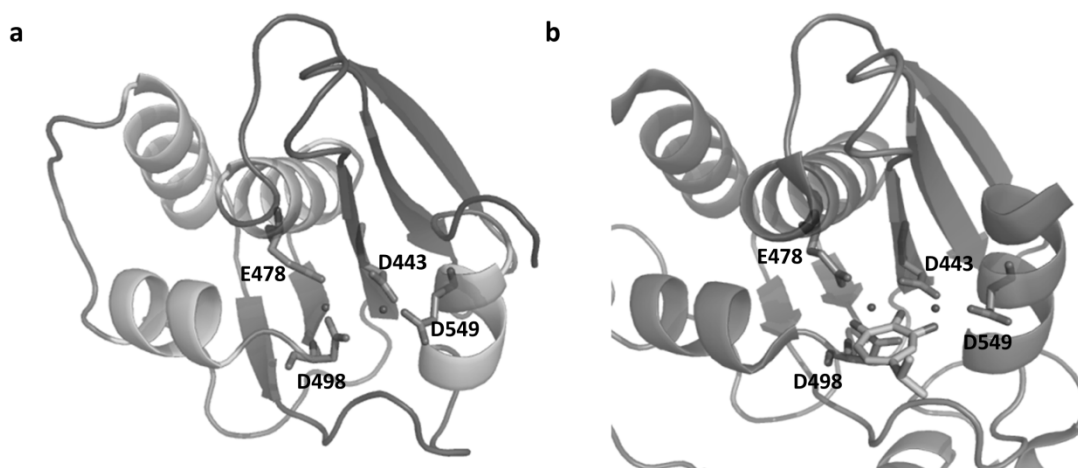
The three dimensional (3D) structure of HIV-1 RT including the RNase H domain is currently available providing a solid basis for rational drug design and the development of inhibitors.

RNase H fold has a characteristic central beta-sheet which contains five strands. The central beta-sheet 4 is flanked by four alpha-helices, three on one side (1-2-3) and one on the other.

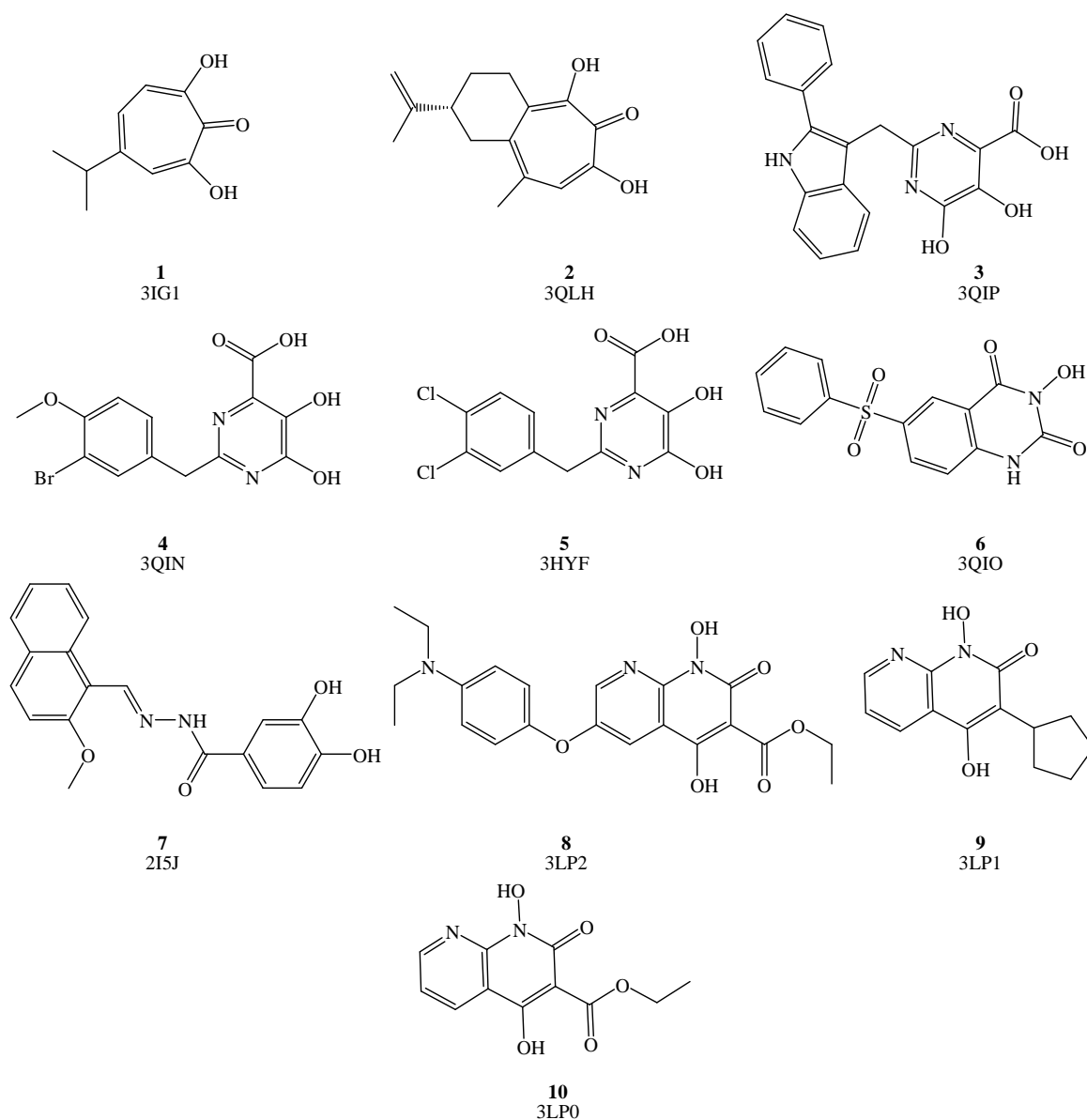
Noteworthy, strand 2 is anti-parallel to the others.

The active site of the RNase H domain is composed of four carboxylate residues forming a DEDD motif which binds catalytic  $Mg^{2+}$  ions (Figure 17).

Most of inhibitors block the active site from binding hybrid DNA:RNA chelating the divalent metal ions ( $Mg^{2+}$ ) which are coordinated by the catalytic pattern D443, E478, D498 and D549.



**Figure 17.** RNase H domain a) unbound (pdbcode 1DLO) and b) bound with b-thujaplicinol (pdbcode 3IG1)



**Figure 18.** RNase H inhibitors co-crystallized and relative pdb code

$\beta$ -thujaplicinol **1** [187] and  $\alpha$ -hydroxytropolone **2** [188] are RNase inhibitors acting by coordinating the two metal ions in the active site, also pyrimidinol carboxylic acid derivatives **3,4,5** and N-hydroxyquinazolidinone **6** show this mechanism (Figure 18). [189, 190]

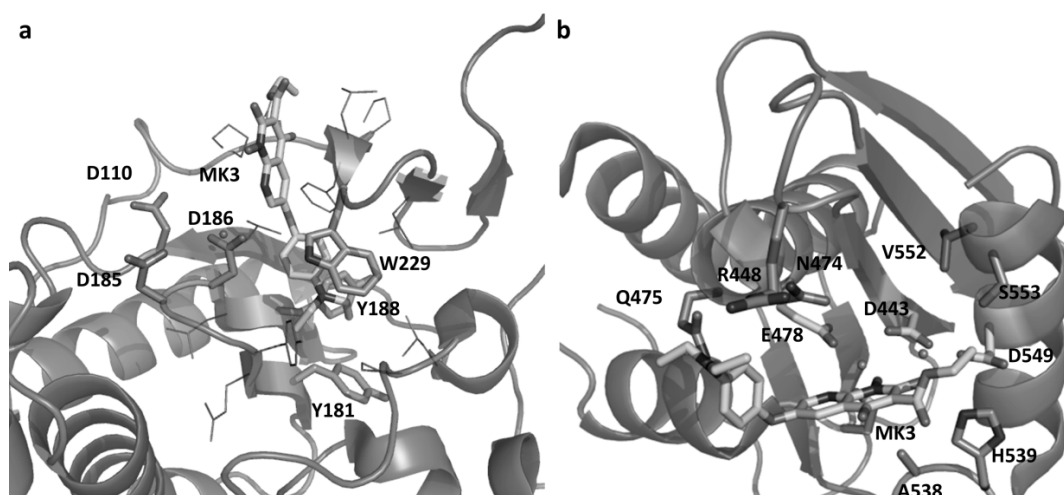
Others scaffolds such as N-hydroxyimides derivatives [191] and diketo acids provide an alternative pharmacophoric solution to chelate the two metal ions in the active binding site. [192, 193]

Interestingly some RNase H inhibitors bind the RT in an allosteric pocket to avoid duplication of site located between polymerase catalytic region and NNIBP 50 Å from the RNase H catalytic site.

Both hydrazone **7** [194] and naphthyridinone derivative (MK3) **8** are accommodated in this site.

Moreover, MK3 and other analogous (**9-10**) were co-crystallized also in the catalytic site where in addition to the classic interaction with two Mn<sup>2+</sup> ions other residues are involved in stabilizing of the complex R448, N474, Q475, S499, A538, H539, V552, and S553 (Figure 19). [195]

It may conceivably be that occupancy of the allosteric pocket would not allow the correct anchorage of the RNA:DNA hybrid and its direction toward RNase H domain would be modified leading, indirectly, to the RNase H inhibition. [194]



**Figure 19.** MK3 binding mode a) in the allosteric binding site (pdbcode 3LP2) and b) in the catalytic pocket (pdbcode 3LP3)

Moreover, other RT regions proximal to the RNase H domain could represent a novel and attractive target for allosteric inhibitory activity.

Hence there is great attention to the development of vinylogous ureas [196] and inhibitors able to bind the area close to residue Q507.

The binding to an allosteric pocket could cause a conformational change at the interface between the RNase H domain and the p51 domain.

This would modify the orientation of the active site and influence its availability to act on the DNA:RNA substrate. [197]

In addition, the binding of the catalytic pocket requires species able to chelate bivalent ions usually characterized by high toxicity.

For this reason the development of chelating compounds raises some worries.

### **1.10.3 Dual Inhibitors**

Until now we have analyzed classes of compounds selective towards one of the RT associated activities.

It is easy to understand what advantage there would be in the development of compounds inhibiting both RDDP and RNase H activity.

Indeed dual inhibitors may completely block RT activities and show a new favorable drug resistance profile by binding to unexplored protein pockets.

All known compounds with dual inhibitory activity have the same binding pocket in common.

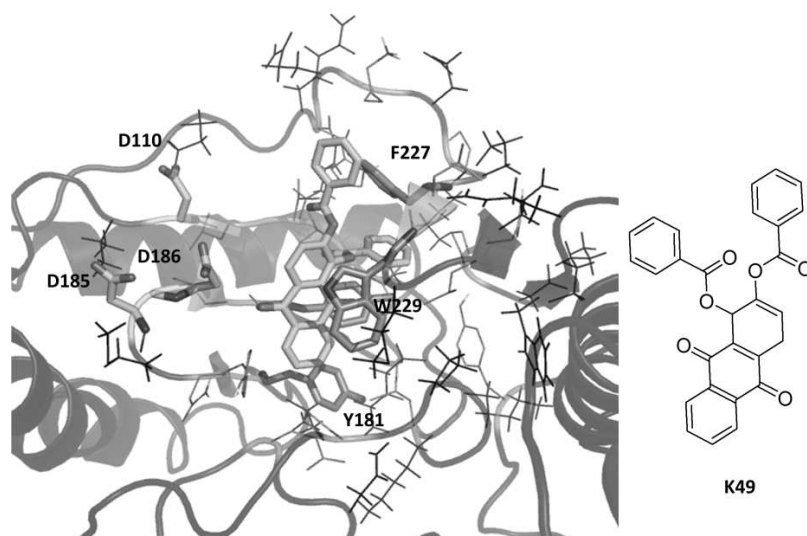
The allosteric pocket of RNase H is located in a strategic point close to the pocket where most of known polymerase inhibitors bind. As it was suggested by Himmel, this pocket communicates directly with the NNRTI pocket. [194]

By binding to this allosteric pocket and to NNIBP residues these compounds seem to acquire dual activity.

Sluis-Cremer was the first who reported the dual inhibitory activity of N-acyl hydrazone derivative. [198] A similar compound **7** was later co-crystallized by Himmel, confirming the hypothesis of an allosteric pocket. The same author reported that analogues of compound **7**, bearing bulkier substituent in place of the 3,4-dihydroxyphenile exhibit dual inhibitory activity. [194]

However none of these compounds have been co-crystallized.

Recently, activity data of a series of alizarine derivatives showing dual activity in the low micromolar range and also towards mutated RTs, commonly resistant to NNRTI has been published. [199]



**Figure 20.** Putative binding mode of K49, best compound of alizarine derivatives serie

The most active alizarine derivatives studied have bulky substituents and are able to go right through the allosteric pocket and interact with NNIBP (Figure 20).

This study confirms the possibility of inhibiting both activities. However the rigidity of the scaffold presents some limitation as it does not offer a wide margin of improvement.



## **2 Results and Discussion**

My research work is focused on the design of new HIV RT inhibitors of the two associated functions of the enzyme, RNA and DNA polymerase function and RNase H function.

With the aim of finding new RNaseH inhibitors the medicinal chemistry research group of the department of life and environmental sciences, performed a successful ligand based virtual screening (VS) [200]: out of 69 compounds selected 26 are active towards RNase H and many of them are dual inhibitors.

In particular hydrazoneindolin-2-one derivative (**46**, numbered as in the paper) was found to be active on RNase H ( $IC_{50} \sim 2 \mu M$ ) and RDDP ( $IC_{50} \sim 1.4 \mu M$ ). [200]

Furthermore, compound **46** represents a remarkable new scaffold.

Moreover it is not mutually exclusive if associated with both NNRTIs and RNase HIs, indicating that, in all probability, it does not bind either in the NNIBP or in the RNase HI pocket. [200]

Molecular modeling analysis of the putative binding mode, combined with biochemical studies was useful to rationalize the activity.

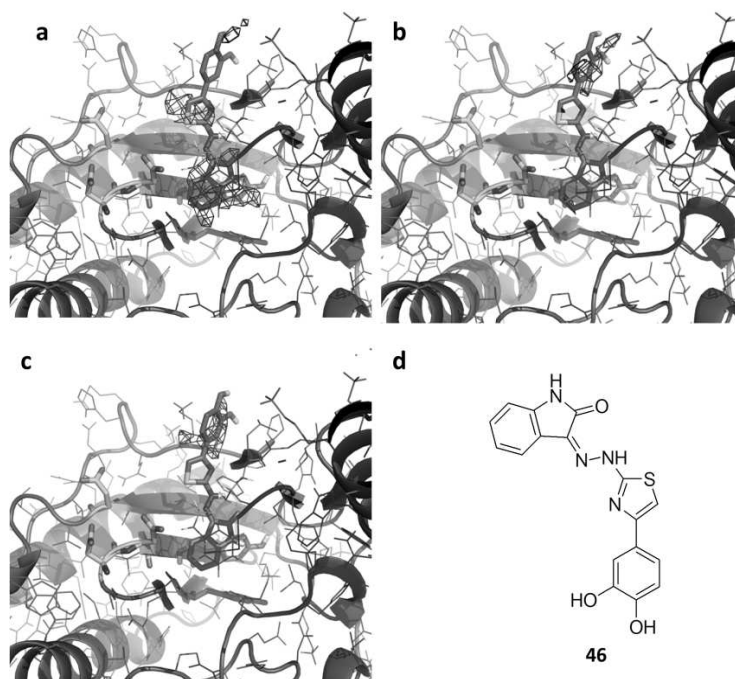
Such studies confirmed that the compound binds in an allosteric pocket.

From the analysis of the binding mode along with its Grid Base Pharmacophore Model (GBPM) (Figure 21) [200, 201], the importance of hydrophobic portions corresponding to indolinone and thiazole moieties can be highlighted.

These portions positively interact with hydrophobic residues V208, F227, Y188, W229.

However the wide hydrophobic area suggests that the indolinone moiety could be substituted by bulkier groups, in the region exposed to the solvent both donors and acceptors are favored.

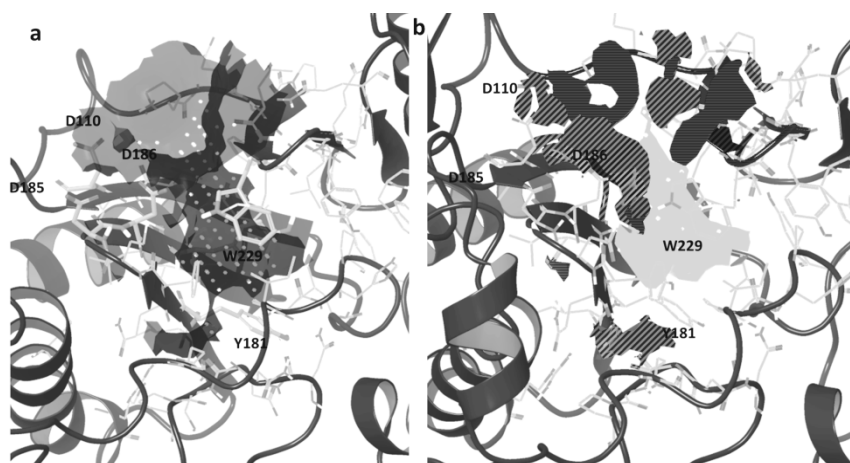
The analysis of the pocket with SiteMap [202] allows for a better understanding of the degree of complementarities to the receptor and the visualization of unexplored regions.



**Figure 21.** GBPM maps and binding mode of compound 46: a) DRY probe, b) N1 probe, c) O probe

Therefore it could be observed that there is space in the left and right bottom portions of the pocket (Figure 22).

Furthermore the flexibility of side chains of NNIBP residues could increase the space available.



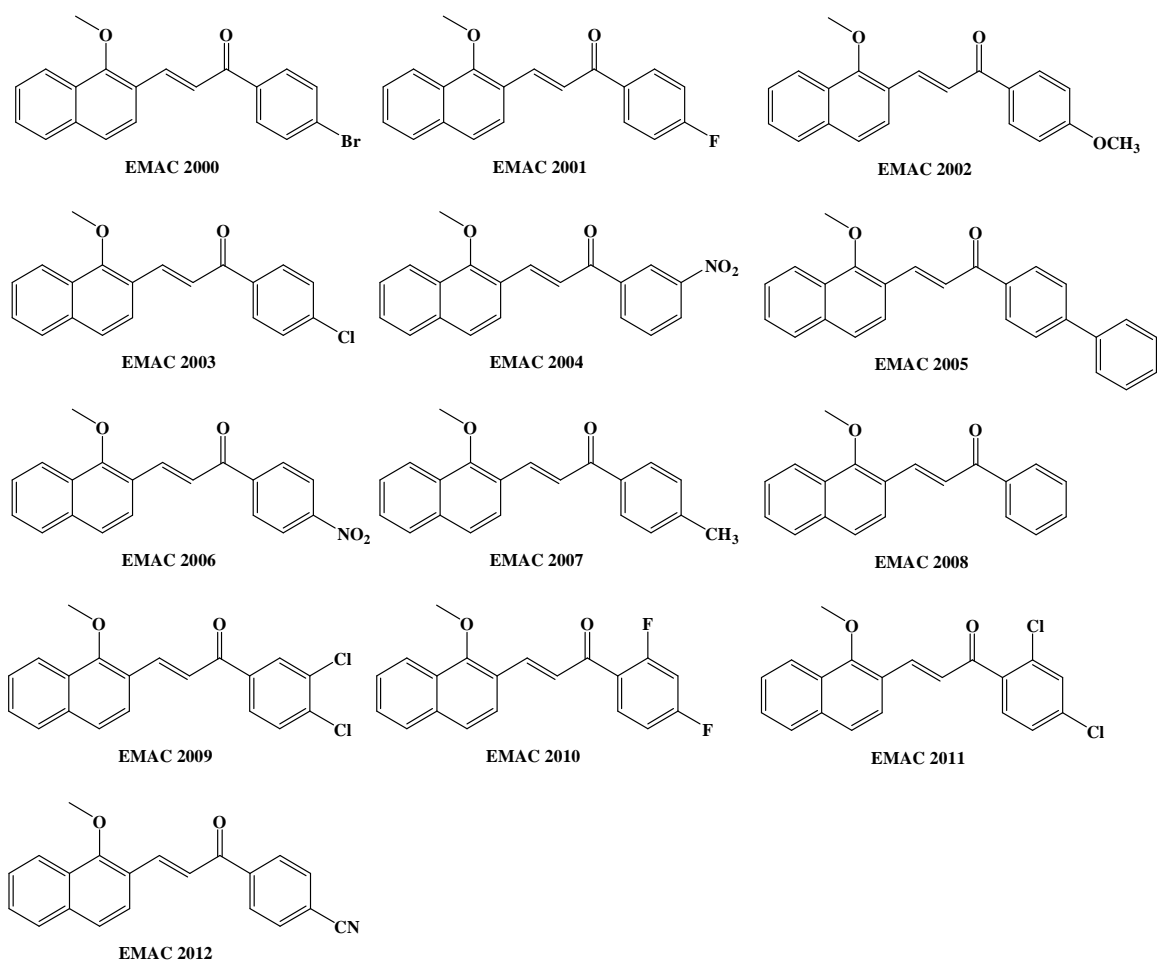
**Figure 22.** Surface map: a) size and shape of the space of the pocket available visualized with SiteMap; b) hydrophobic (light grey), donor (diagonal stripes), and acceptor (dark grey fine stripes) favourable maps (pdbcode 3lp2)

In addition to spatial requirements evaluation, the examination of the distribution of hydrophobic, acceptor and donor maps is useful to understand a worthwhile strategy of lead optimization.

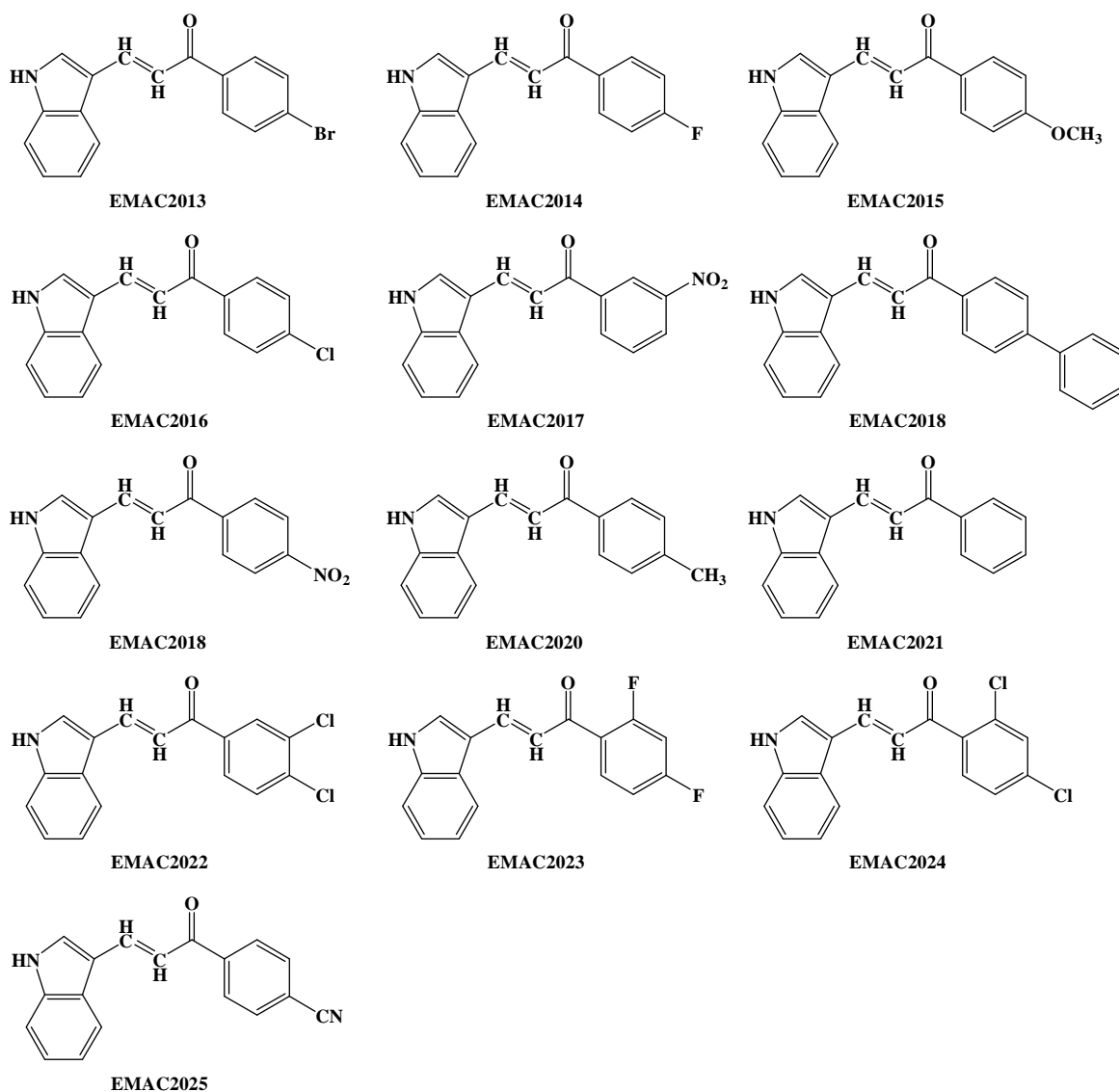
It was noticed that there is a wide area where donor groups could have room. The donor map is located in the area facing the polymerase catalytic triad, while two acceptor maps are at the left and right part of it. This information, together with the pharmacophore model, should lead to the design of compounds with increased activity. The optimization procedure should be carried out also considering most common NNRTI induced mutations. Hence flexibility and care in avoiding key interactions with these residues may help the drug optimization process. Furthermore, besides compound **46**, there are other promising scaffolds coming from VS study which show a similar behavior and can be better characterized and optimized.

Starting from this observation we synthesised new series of compounds (**EMAC 2000-2096**) in order to obtain further information on the SARs of these derivatives and to identify other possible scaffolds.

Firstly we synthesised a new series of chalcones (**EMAC 2000-2012, EMAC 2013-2025**) whose structures are illustrated in Figure 23, 24.



**Figure 23.** Structure of compounds 2000-2012



**Figure 24.** Structure of compounds 2013-2025

All compounds were synthesised according to literature methods. [203, 204]

Compounds **EMAC 2000-2012** were synthesised by reaction of 1-methoxy-2-naphthaldehyde with the appropriate methylarylketone in ethanol and 10% NaOH water solution.

In the case of compounds **EMAC 2013-2025**, different synthetic pathway was followed; 1H-indole-3-carboxyaldehyde was reacted with the appropriate methylarylketone in ethanol/piperidine solution.

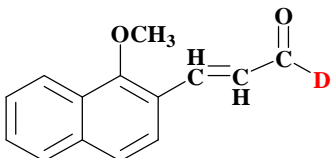


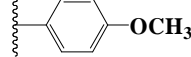
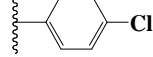
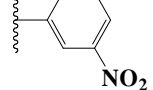
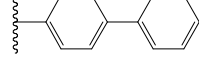
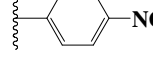
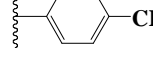
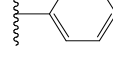
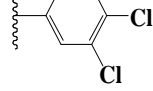
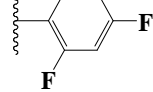
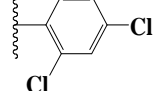
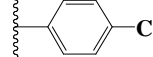
In both series the expected “E” configuration was obtained as suggested by the CH=CH double bond coupling constants that ranges from 15 to 16 Hz.

To evaluate their capability to inhibit both functions of HIV RT the RNase H polymerase-independent cleavage assay was measured [192] using Poly(dC)-[3H]Poly(rG) hybrid as reaction substrate.

Moreover the RDDP activity of HIV-1 RT was measured according to the procedure previously described. [207]

Regarding compounds **EMAC 2000-2012** an interesting activity could be observed (Table 1).

**Table 1.** EMAC 2000-2012 activity

			
"D"-ring		HIV-1 RDDP <sup>a</sup> IC <sub>50</sub> (μM)*	HIV-1 RNase H <sup>b</sup> IC <sub>50</sub> (μM)*
	EMAC 2000	6	47
	EMAC 2001	5	23
	EMAC 2002	6	9
	EMAC 2003	5	76
	EMAC 2004	5	31
	EMAC 2005	4	6
	EMAC 2006		
	EMAC 2007		
	EMAC 2008		
	EMAC 2009		Test in progress
	EMAC 2010		
	EMAC 2011		
	EMAC 2012		
RDS 1643		> 100	13
Efavirenz		0,003	> 10

<sup>a</sup>Compound concentration required to reduce the HIV-1 RT-associated RNase H activity by 50%. <sup>b</sup>Compound concentration required to reduce the HIV-1 RT-associated RNA-dependent DNA-polymerase activity by 50%. The activity was measured together with two known inhibitors of the RDDP and RNase H functions, respectively Efavirenz and RDS 1643. \* Results are means of 3 experiments.

Some of the compounds exhibit comparable activity towards the two associated functions of HIV-1 RT.

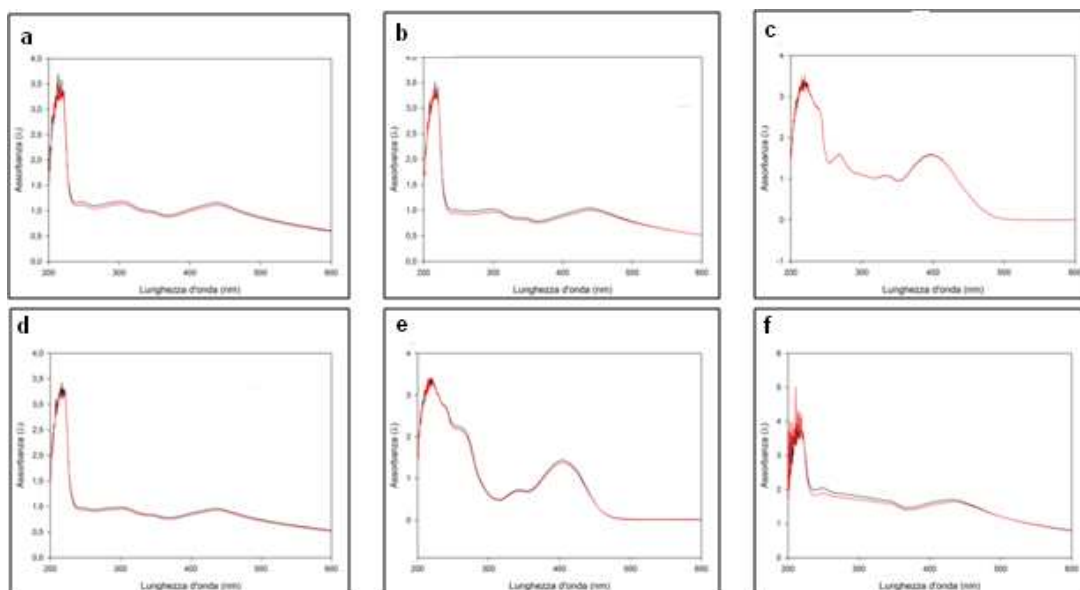
In particular, **EMAC 2002** and **2005** have an  $IC_{50}$  value in the low  $\mu M$  range.

To gain a better comprehension of the mechanism of action and to identify the binding site of these new compounds we have performed some biochemical and computational investigation.

All the known RNase H inhibitors that binds to the RNase H active site are  $Mg^{2+}$  chelating agents.

Thus to verify if our compounds bind either in the RNase H active site or in an allosteric pocket we measured the effect of  $MgCl_2$  on the compounds **EMAC 2000-2005** UV spectrum.

Results showed that  $MgCl_2$  does not significantly change the compounds maximum of absorbance, suggesting that these compounds do not act by chelating the magnesium ion in the RNase H catalytic site (Figure 25).



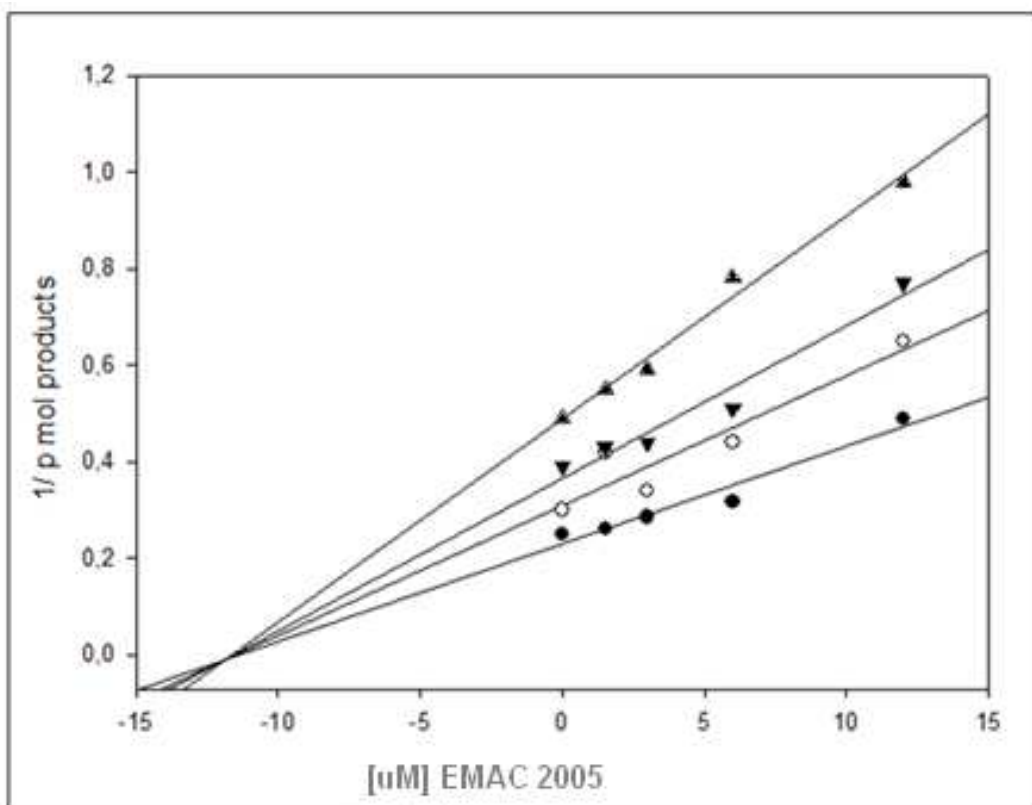
**Figure 25.** Magnesium chelating assay (in black: absence of  $Mg^{2+}$ , in red presence of 6 mM  $MgCl_2$ ; a) EMAC 2000, b) EMAC 2001, c) EMAC 2002, d) EMAC 2003, e) EMAC 2004, f) EMAC 2005.

To further confirm that our compounds do not bind to the RNase active site we measured the interference between the most active **EMAC 2005** and a known inhibitor at the RNase H catalytic site (**RDS1643**) by the Yonetani Theorell plot. [208]

This is a graphical method to analyze the multiple inhibition of an enzyme by two competing inhibitors.



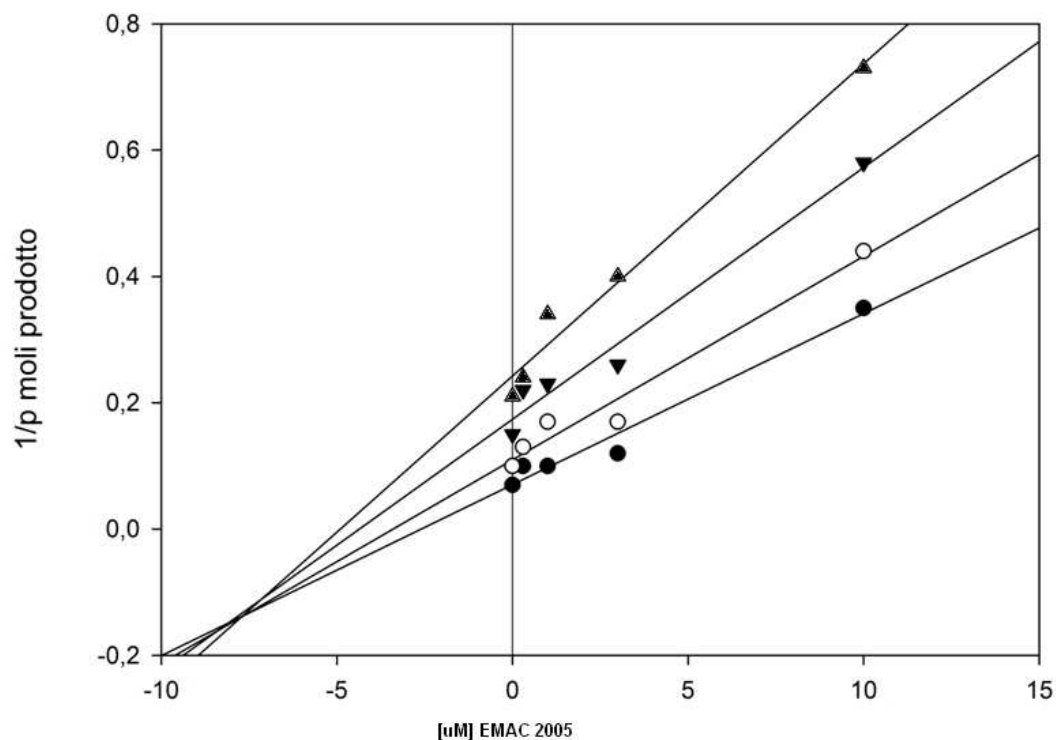
This method not only distinguishes whether two inhibitors interact with the same site or different sites of the enzyme, but also gives an interaction constant ( $\alpha$ ) between two inhibitors in the enzyme-inhibitor complex.



**Figure 26.** Yonetani Theorell plot of increasing concentrations of EMAC 2005 vs RDS 1643; ●[EMAC 2005] = 0, ○[EMAC 2005] = 2,5µM, ▼[EMAC 2005] = 5µM, ▲[EMAC 2005] = 10µM.

This kinetic analysis quantitatively reconfirmed our previous finding that EMAC 2005 and RDS 1642 interact independently with different sites of the enzyme and are not mutually exclusive.

To investigate if **EMAC 2005** binds to the NNRTIs binding pocket active site we performed the same kinetic experiment (Figure 27) with increasing concentrations of **EMAC 2005** and a known NNRTI (**Efavirenz**).



**Figure 27.** Yonetani Theorell plot of increasing concentrations of EMAC 2005 vs Efavirenz; ●[EMAC 2005] = 0, ○[EMAC 2005] = 1,5 $\mu$ M, ▼[EMAC 2005] = 3,5 $\mu$ M, ▲[EMAC 2005] = 10 $\mu$ M.

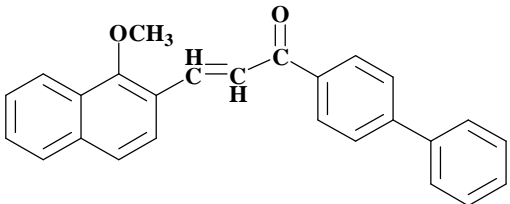
According to the kinetic analysis **EMAC 2005** and Efavirenz are not mutually exclusive.

Thus we can affirm that **EMAC 2005** binds neither at the NNRTI binding pocket, nor at the RNase active site.

In order to verify if compound **EMAC 2005** binds in the allosteric site close to the NNRTIs binding pocket we tested its activity towards both associated activities of K103Nsn and Y181C RTs, two NNRTI resistant mutant enzymes, since derivatives which have been proposed to interact with the drug pocket, close to both NNRTI binding pocket and DNA polymerase active site, have shown a degree of cross resistance with NNRTI resistant RTs.

The results are summarized in Table 2.

**Table 2.** EMAC 2005 activity on mutants

EMAC 2005 activity on mutants (K103N and Y181C)						
						
Compound	<i>wt RT a IC<sub>50</sub></i> (μM)		<i>K103N RT IC<sub>50</sub></i> (μM)		<i>Y181C RT IC<sub>50</sub></i> (μM)	
	RNase H	RDDP	RNase H	RDDP	RNase H	RDDP
<b>EMAC 2005</b>	6 ± 2	4 ± 1	59 ± 8	3 ± 1	>100 (79%)	8 ± 5
<b>EFV</b>	> 10	0,013 ± 0.008	ND	0,68	ND	0,40

Results showed that when tested on the K103N RT compound **EMAC 2005** was 10 fold less potent on the RNase H and almost the same active towards RT-associated RDDP.

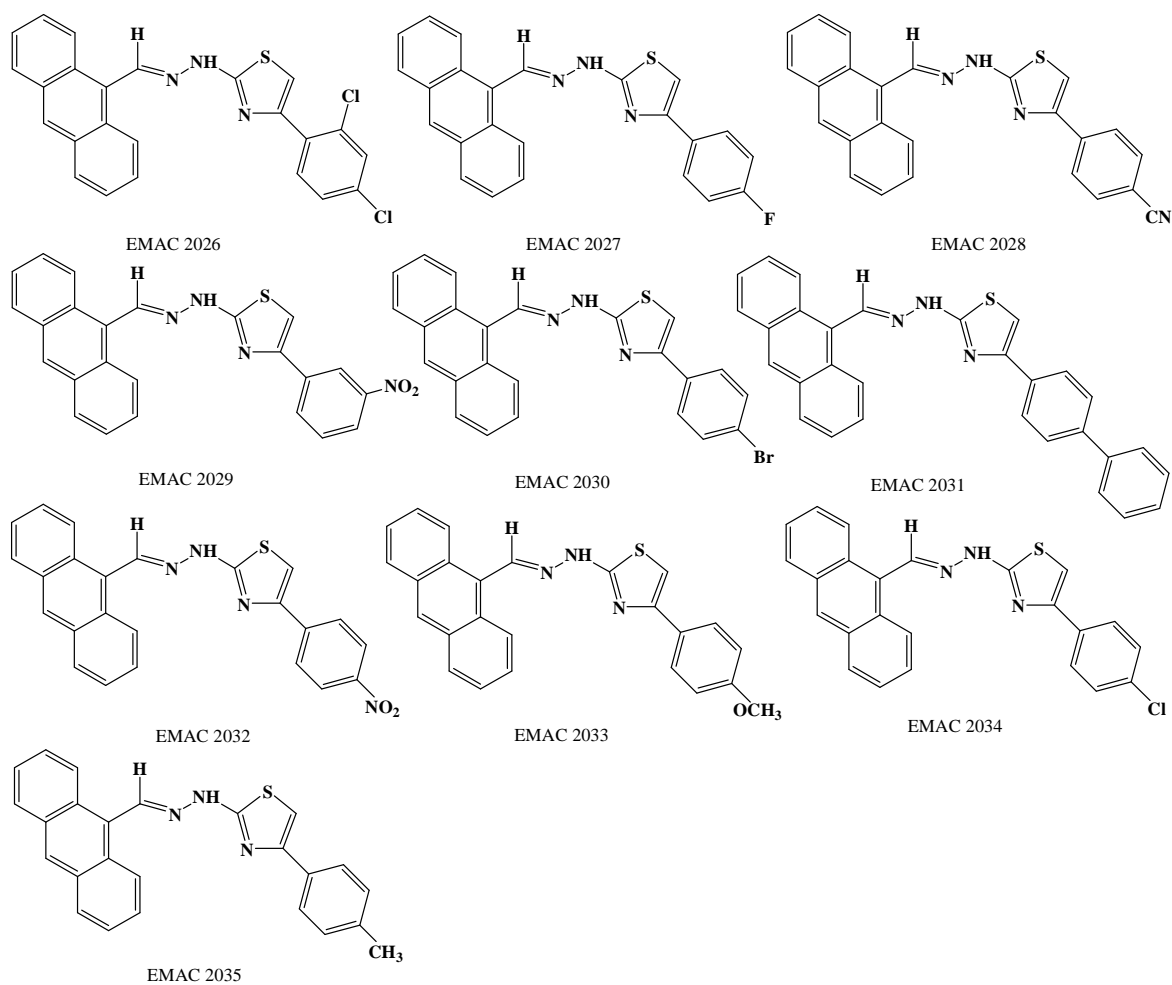
As it was expected, this result indicates that EMAC 2005 activity on RNase H activity is most likely associated to its binding close to the NNRTI binding pocket.

On the contrary, no influence of K103N mutation on the RDDP activity was observed.

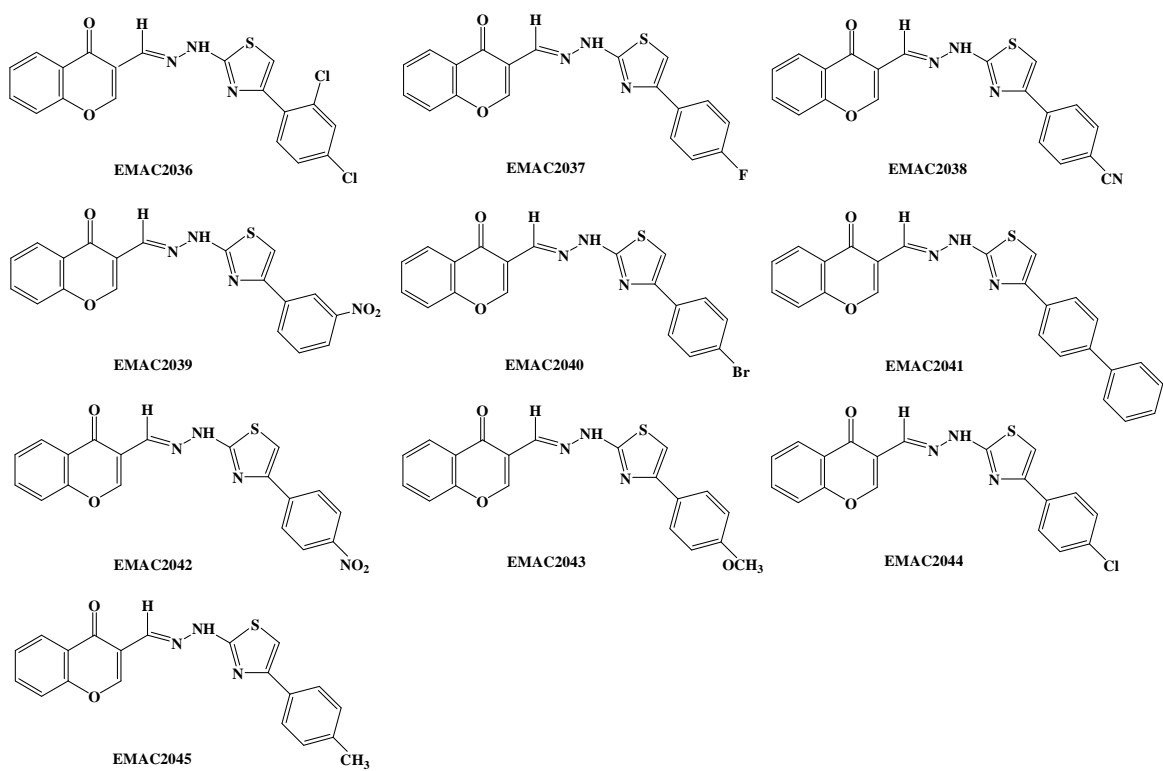
In the case of Y181C mutation a more dramatic effect, with respect to K103N, can be observed. The activity towards RNase H activity is almost suppressed indicating that this residue is essential for exerting the inhibition of this function.

Also in this case the activity towards the RT-associated RDDP is almost not affected, indicating that Y181 is not essential for the binding but only for the inhibition of the RNase H function. This behavior might be explained either by two different poses in the hydrazones pocket, or by the interaction with an other pocket close to the RNase H site, whose structure is affected by the Y181C mutation.

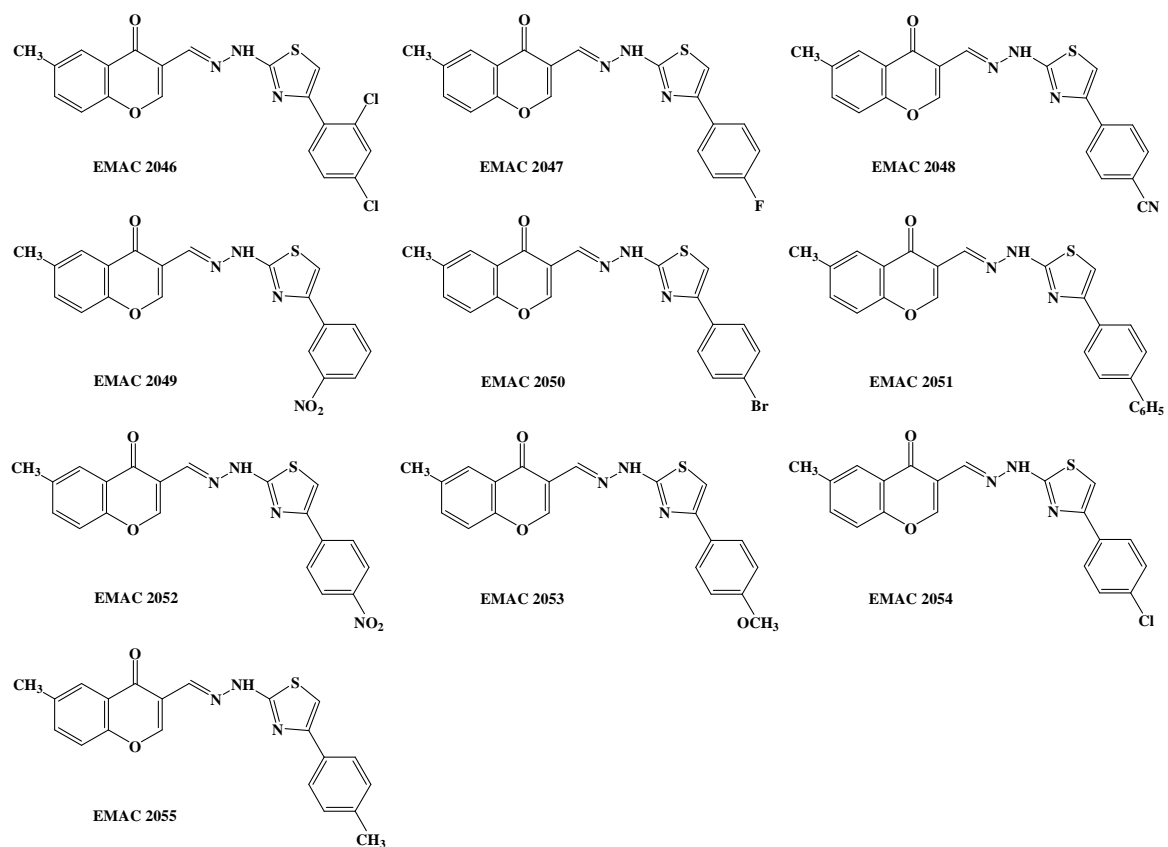
Prompted by these results we synthesized other series of compounds **EMAC 2026-2096** reported in the figures 28-34.



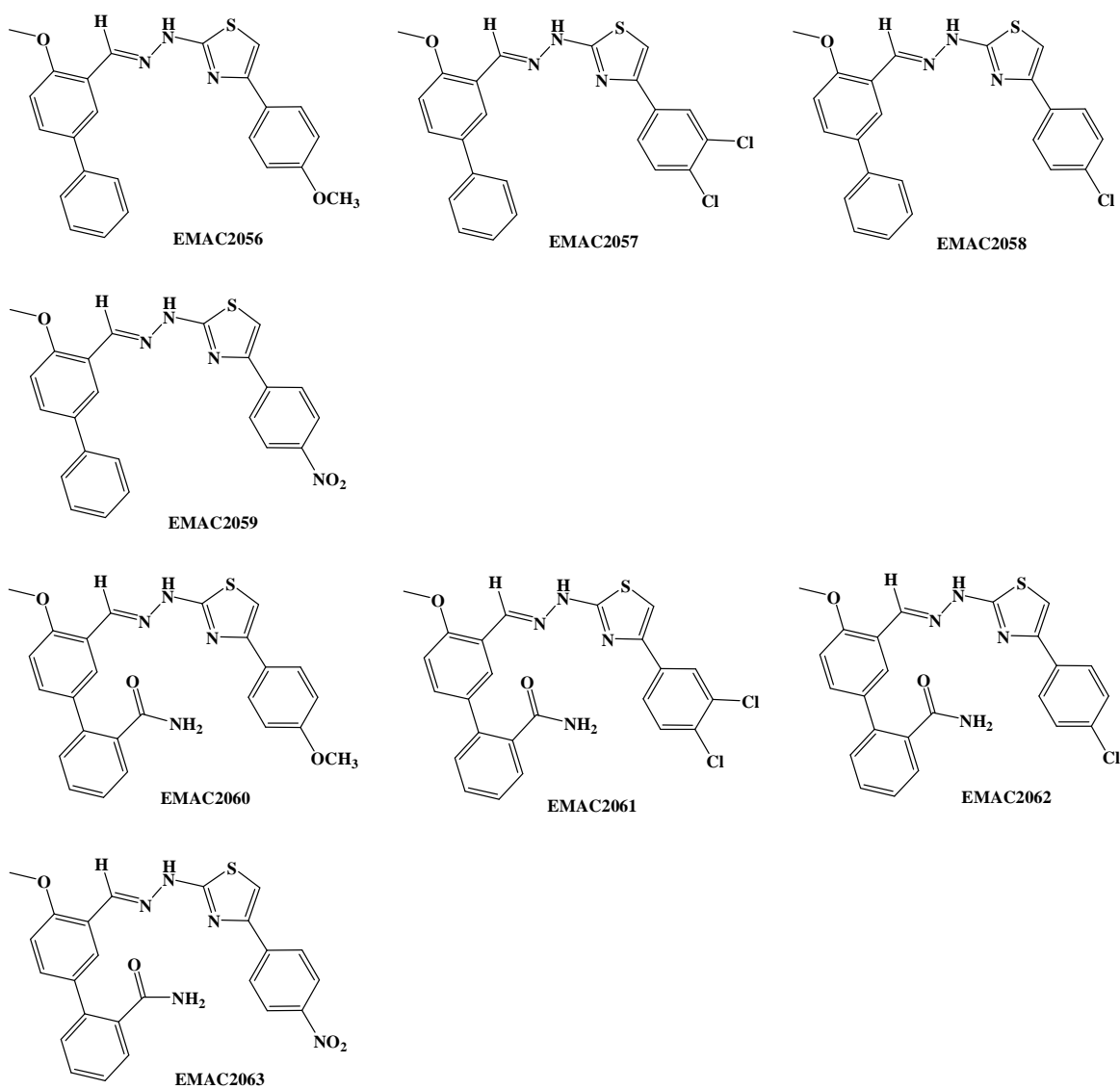
**Figure 28.** Structure of compounds 2026-2035



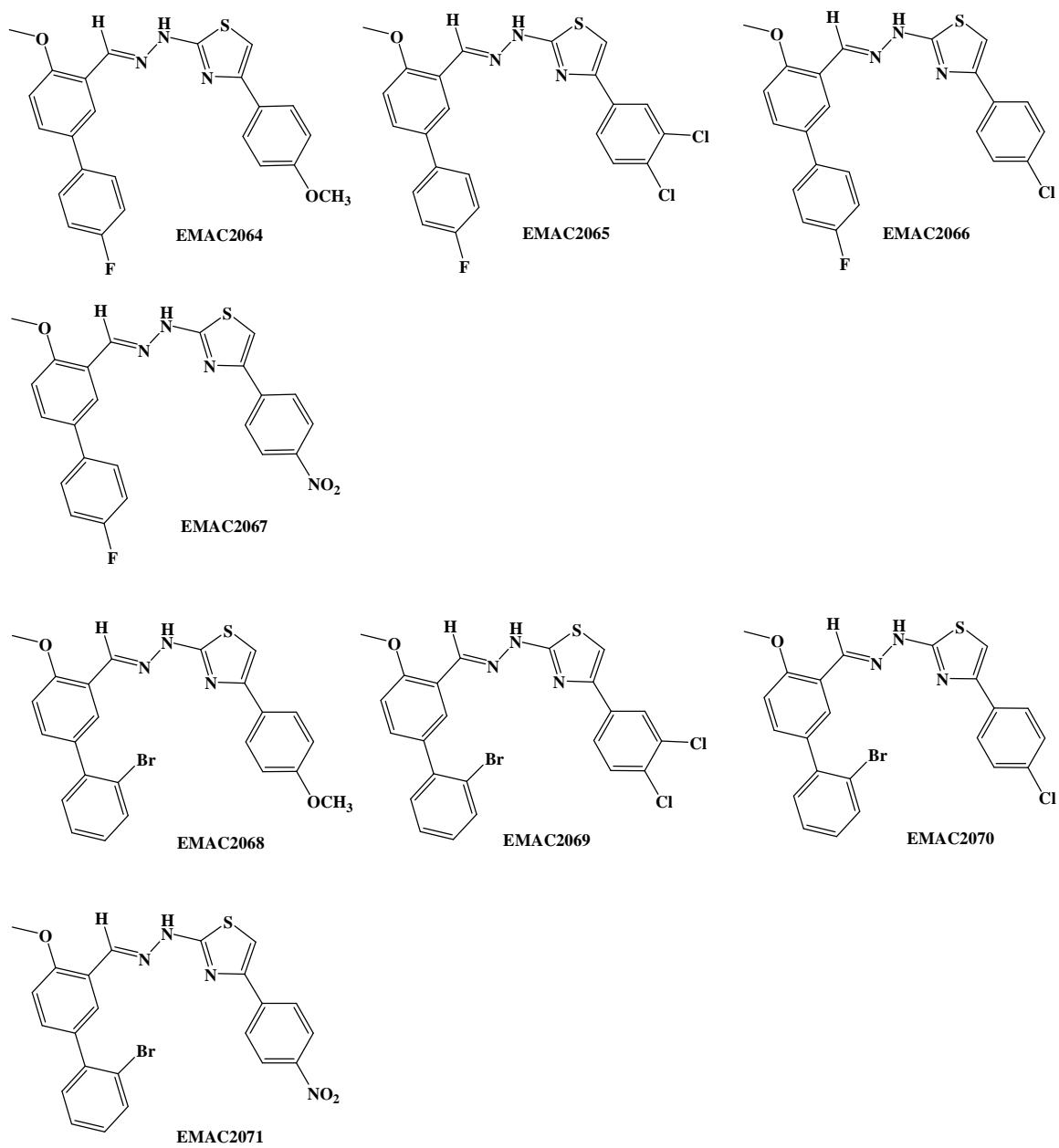
**Figure 29.** Structure of compounds 2036-2045



**Figure 30.** Structure of compounds 2046-2055

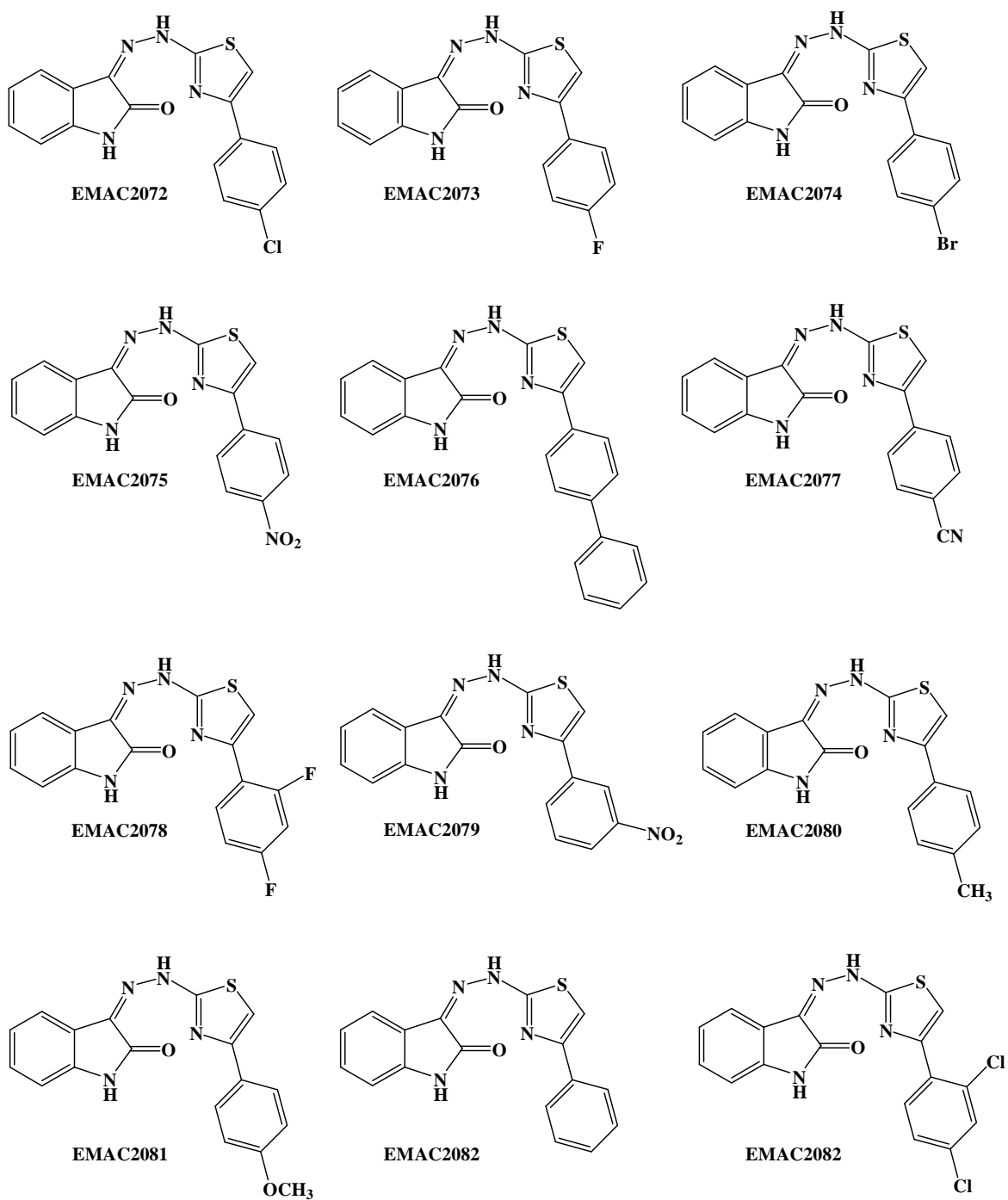


**Figure 31.** Structure of compounds EMAC 2056-2063

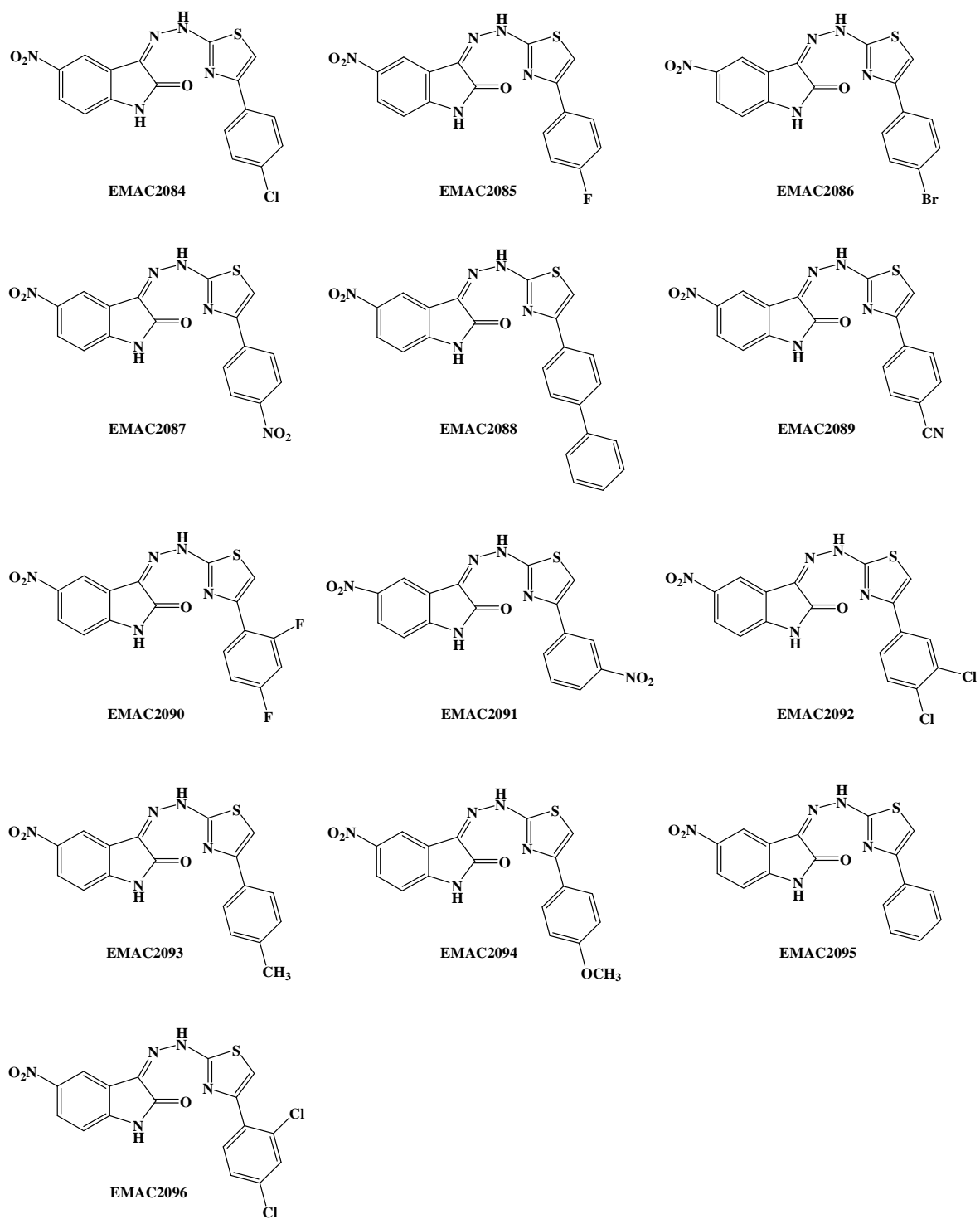


**Figure 32.** Structure of compounds EMAC 2064-2071





**Figure 33.** Structure of compounds EMAC 2072-2082



**Figure 34.** Structure of compounds EMAC 2084-2096

The synthetic pathway to compounds **EMAC 2026-2096** is reported in materials and methods (chemistry).

Generally the appropriate aldehyde, either purchased or synthesized by Suzuki coupling reaction (**EMAC 2056-2071**), was reacted with thiosemicarbazide in isopropyl alcohol in the presence of catalytic amounts of acetic acid.

The obtained thiosemicarbazone is then suspended in isopropyl alcohol in the presence of the appropriate  $\alpha$ -halogenoarylketone to give the desired thiazole derivative.

All the compounds were obtained as free bases as revealed by halogen ions test with 1M solution of  $\text{AgNO}_3$ .

Most of the compounds were submitted for biological evaluations and the results are summarized in tables 3-7.

In some cases it has been possible to evaluate the activity in HIV infected cells, thanks to the group of Prof. Cheng at the University of Yale.

In table 3 the activity of compounds **EMAC 2026-2035** is reported.

Interestingly the biphenyl substituents in the position 4 of the thiazole ring (**EMAC 2031**) leads to a complete loss of activity while a similar substitution in the chalcone series led to the best activity (**EMAC 2005**).

However, compounds **EMAC 2028**, **EMAC 2034**, and **EMAC 2035** exhibit a promising activity towards HIV infected cells with an  $\text{EC}_{50}$  of <5, 8 and <5  $\mu\text{M}$  respectively.

These data are comparable with the activity exhibited in the enzymatic assay towards RNase H function.

Moreover these compounds are relatively not toxic and further biological experiments are in progress.

In particular their activity towards the RT associated RDDP function will be evaluated and the mechanism and site of action investigated.

**Table 3.** EMAC 2026-2035 activity

"D"-ring	HIV-1 RNase H <sup>b</sup> IC <sub>50</sub> (μM)*	HIV-1 RDDP <sup>a</sup> IC <sub>50</sub> (μM)*	TZM-bl <sup>c</sup> CC <sub>50</sub> (μM)	HIV-1 <sup>d</sup> EC <sub>50</sub> (μM)
	> 100	35		Test in progress
	97	11		
	16	7	7	< 5
	48	15		Test in progress
	24	4	> 50	15
	51	9		Test in progress
	13	10	14	> 30
	42	10	> 50	> 30
	14	7	50	8
	28	8	50	< 5
<b>Efavirenz</b>	> 100	0,003		

<sup>a</sup>Compound concentration required to reduce the HIV-1 RT-associated RNA-dependent DNA-polymerase activity by 50%. <sup>b</sup>Compound concentration required to reduce the HIV-1 RT-associated RNase H activity by 50%.

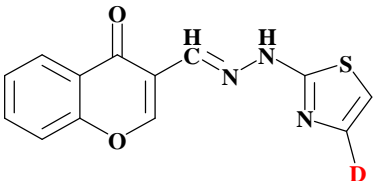
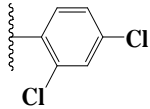

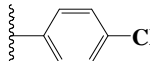
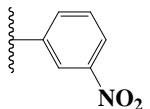
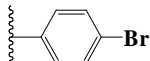
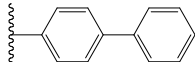

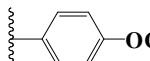
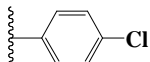
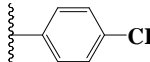
<sup>c</sup>Compound concentration required to reduce MT-2 cell replication by 50% after 4 days incubation.

<sup>d</sup>Compound concentration required to reduce the HIV-1 replication by 50% in TZM-bl cells after 1 day incubation.

\* Results are means of 3 experiments.

Also in the case of compounds **EMAC 2044** and **EMAC 2045** a promising activity towards the HIV-1 replication was observed and a deeper investigation on their mode of action will be pursued (Table 4).

**Table 4.** EMAC 2036-2045 activity

				
"D"-ring	HIV-1 RNase H <sup>b</sup> IC <sub>50</sub> (μM)	HIV-1 RDDP <sup>a</sup> IC <sub>50</sub> (μM)	TZM-bl <sup>c</sup> CC <sub>50</sub> (μM)	HIV-1 <sup>d</sup> EC <sub>50</sub> (μM)
	34	31		
	46	21	Test in progress	
	60	100		
	28	28	> 50	> 30
	>100 (58%)	>100		
	22	19	Test in progress	
	>100	97		
	100	98		
	28	33	> 50	2,5
	29	22	32	>30
<b>Efavirenz</b>	> 100	0,003		

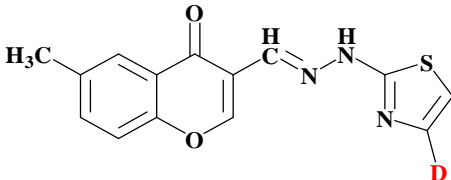
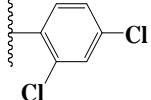


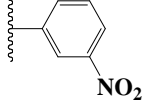
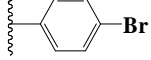
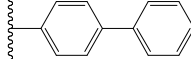
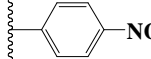
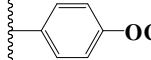
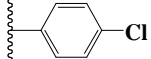
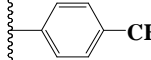
<sup>a</sup>Compound concentration required to reduce the HIV-1 RT-associated RNase H activity by 50%. <sup>b</sup>Compound concentration required to reduce the HIV-1 RT-associated RNA-dependent DNA-polymerase activity by 50%.

<sup>c</sup>Compound concentration required to reduce MT-2 cell replication by 50% after 4 days incubation.

<sup>d</sup>Compound concentration required to reduce the HIV-1 replication by 50% in TZM-bl cells after 1 day incubation. \* Results are means of 3 experiments.

A similar behavior was observed for the analogous compounds **EMAC 2046** and **EMAC 2050**, but introduction of different substituents with respect to previous compounds, lead to the best performing compounds (Table 5).

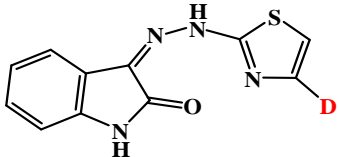
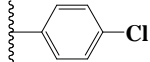

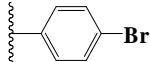
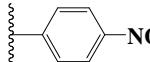
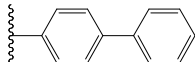
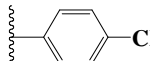
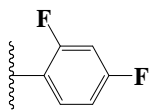
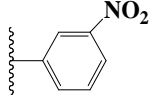

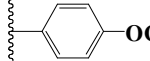
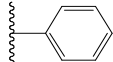
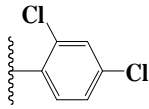
**Table 5.** EMAC 2046-2055 activity

 <b>"D"-ring</b>	HIV-1 RNase H	HIV-1 RDDP	TZM-bl	HIV-1
	<sup>b</sup> IC <sub>50</sub> (μM)*	<sup>a</sup> IC <sub>50</sub> (μM)*	<sup>c</sup> CC <sub>50</sub> (μM)	<sup>d</sup> EC <sub>50</sub> (μM)
	17	23	35	3
	24	13		
	64	56	Test in progress	
	55	33		
	13	40	> 50	2,5
	23	10	Test in progress	
	40	26		
	10	6	<2	23
	20	17	Test in progress	
	17	17	35	> 30
<b>Efavirenz</b>	> 100	0,003		

<sup>a</sup>Compound concentration required to reduce the HIV-1 RT-associated RNase H activity by 50%. <sup>b</sup>Compound concentration required to reduce the HIV-1 RT-associated RNA-dependent DNA-polymerase activity by 50%. <sup>c</sup>Compound concentration required to reduce MT-2 cell replication by 50% after 4 days incubation. <sup>d</sup>Compound concentration required to reduce the HIV-1 replication by 50% in TZM-bl cells after 1 day incubation. \* Results are means of 3 experiments.

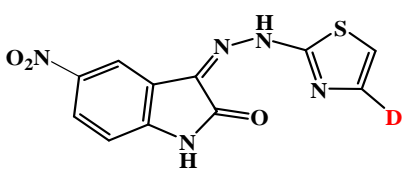
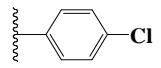
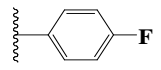
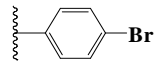
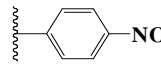
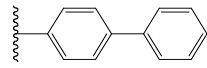
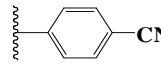
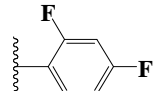
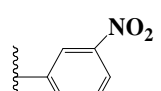
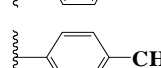
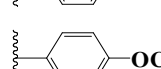
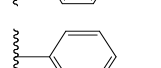
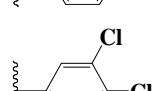
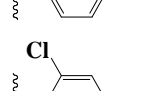
These data needs further investigation to rationalize the SARs of this scaffold and more data are needed in order to explain such discontinuous SARs.

**Table 6.** EMAC 2072-2083 activity

				
	"D"-ring	HIV-1 RNase H <sup>b</sup> IC <sub>50</sub> (μM)*	HIV-1 RDDP <sup>a</sup> IC <sub>50</sub> (μM)*	TZM-bl <sup>c</sup> CC <sub>50</sub> (μM)
	11.2	3.3	>50	>50
	8.2	2.0	>50	>50
	13	4.0	>50	>50
	3.8	0.8	>50	>50
	3.5	0.8	>50	>50
	2.1	5.3	>50	>50
	6.2	1.4	>50	>50
	4.7	0.8	>50	>50
	10.6	1.0	>50	>50
	23.0	3.0	>50	>50
	> 30	11	>50	>50
	3.9	2.7	>50	>50

<sup>a</sup>Compound concentration required to reduce the HIV-1 RT-associated RNase H activity by 50%. <sup>b</sup>Compound concentration required to reduce the HIV-1 RT-associated RNA-dependent DNA-polymerase activity by 50%. <sup>c</sup>Compound concentration required to reduce MT-2 cell replication by 50% after 4 days incubation. <sup>d</sup>Compound concentration required to reduce the HIV-1 replication by 50% in TZM-bl cells after 1 day incubation. \* Results are means of 3 experiments.

**Table 7.** EMAC 2084-2096 activity

 <b>"D"-ring</b>	HIV-1 RNase H <sup>b</sup> IC <sub>50</sub> (μM)*	HIV-1 RDDP <sup>a</sup> IC <sub>50</sub> (μM)*	TZM-bI <sup>c</sup> CC <sub>50</sub> (μM)	HIV-1 <sup>d</sup> EC <sub>50</sub> (μM)
	4,6	10,5		
	5,1	9,5		
	4,3	8,5		
	7,6	21,0		
	7,1	12,0		
	6,0	9,3		
	6,0	11,5		
	6,5	18,5		
	8,5	18,5		
	8,5	14,5		
	6,0	13,0		
	6,5	11,5		
	3,5	10,5		

Test in progress

<sup>a</sup>Compound concentration required to reduce the HIV-1 RT-associated RNase H activity by 50%. <sup>b</sup>Compound concentration required to reduce the HIV-1 RT-associated RNA-dependent DNA-polymerase activity by 50%.

\* Results are means of 3 experiments.



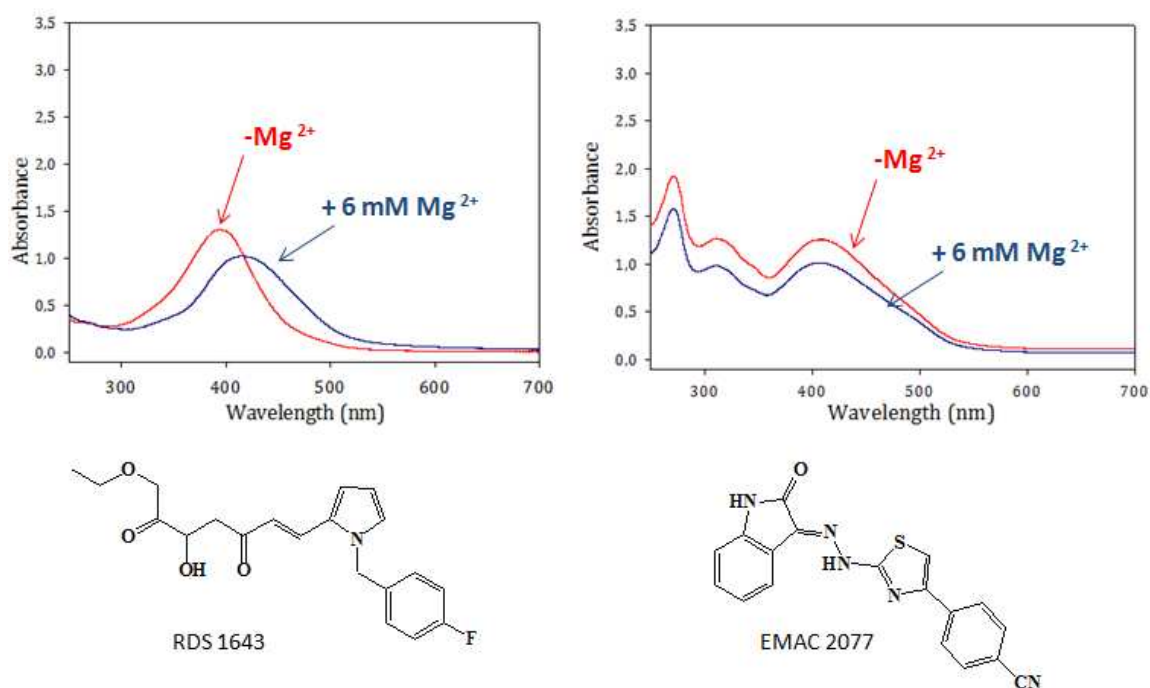
Compounds **EMAC 2072-2083** exhibit potent activity in the enzymatic assay almost all substitutions are well tolerated and moreover most of the compounds exhibit dual activity towards the two associated functions of HIV RT (Table 6).

These results indicate that the combination of the indolinone ring together with the hydrazine spacer and the 4-substituted thiazole may constitute the best performing scaffold for dual inhibition.

Prompted by these encouraging findings we performed a deeper characterization of these compounds.

We selected compound **EMAC 2077** for mode of action biochemical studies and computational investigation.

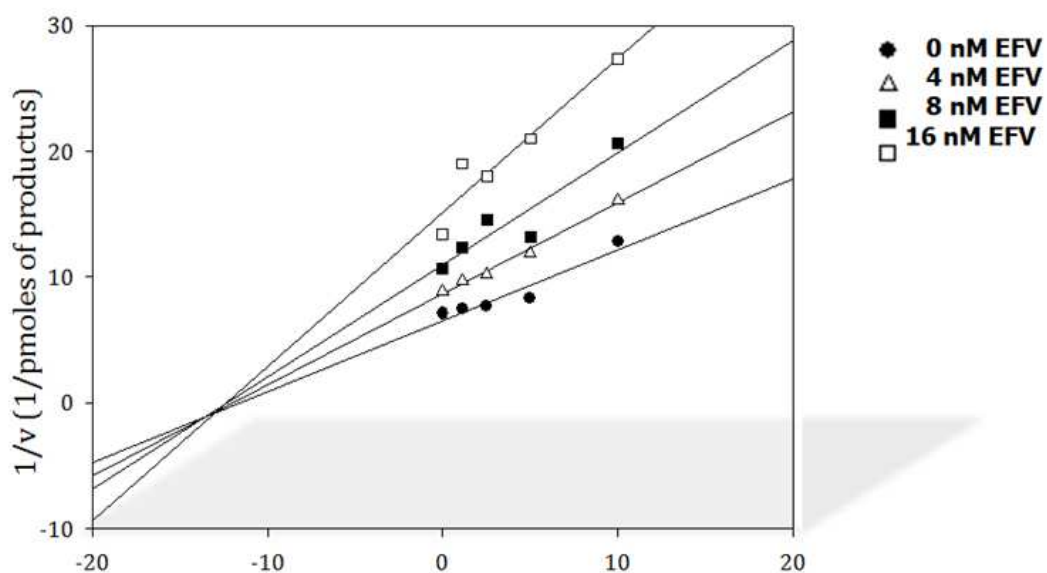
Firstly we measured the effect of  $MgCl_2$  on **EMAC 2077** Uv spectrum in comparison with a known inhibitor at the RNase active site that acts by chelating the  $Mg^{2+}$  cofactor (Figure 34).



**Figure 35.** EMAC 2077 interaction with the  $Mg^{2+}$  RT cofactor: in red absence of  $Mg^{2+}$  and in blue presence of 6 mM  $Mg^{2+}$

As previously observed for compounds EMAC 2000-2005, the addition of 6 mM of  $MgCl_2$  to the solution of **EMAC 2077** does not significantly shift the maximum of absorbance indicating that this compound does not act by chelating the magnesium ion in the RNase H catalytic site.

Moreover, we performed kinetic analysis of **EMAC 2077** in the presence of known inhibitors of both associated functions, RDDP and RNase H, Efavirenz and RDS 1643 respectively.



Figure

36. EMAC 2077 kinetic analysis in the presence of Efavirenz

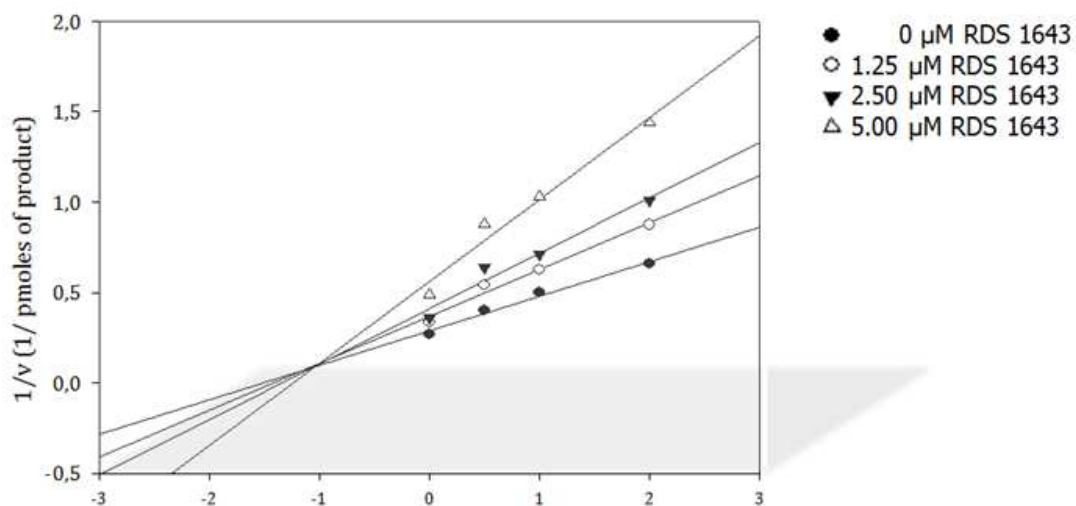


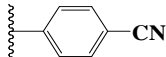
Figure 37. EMAC 2077 kinetic analysis in the presence of RDS 1643

In both cases no interaction was observed. Thus we can assume that **EMAC 2077** neither binds in the same site of Efavirenz nor of RDS1643.

The activity towards RT mutants K103N and Y181C was also measured, in order to verify if **EMAC 2077** binds in the allosteric site close to the NNRTIs binding pocket.

The results are summarized in Table 8.

**Table 8.** EMAC 2077 activity on mutants (K103N and Y181C)

"D"-ring	K103N RT IC <sub>50</sub> (μM)		Y181C RT IC <sub>50</sub> (μM)	
	RNase H	RDDP	RNase H	RDDP
	20.16±2.5	4.08±1.4	23.4±0.6	2 ±1
<b>EFV</b>	ND	0,68	ND	0,40

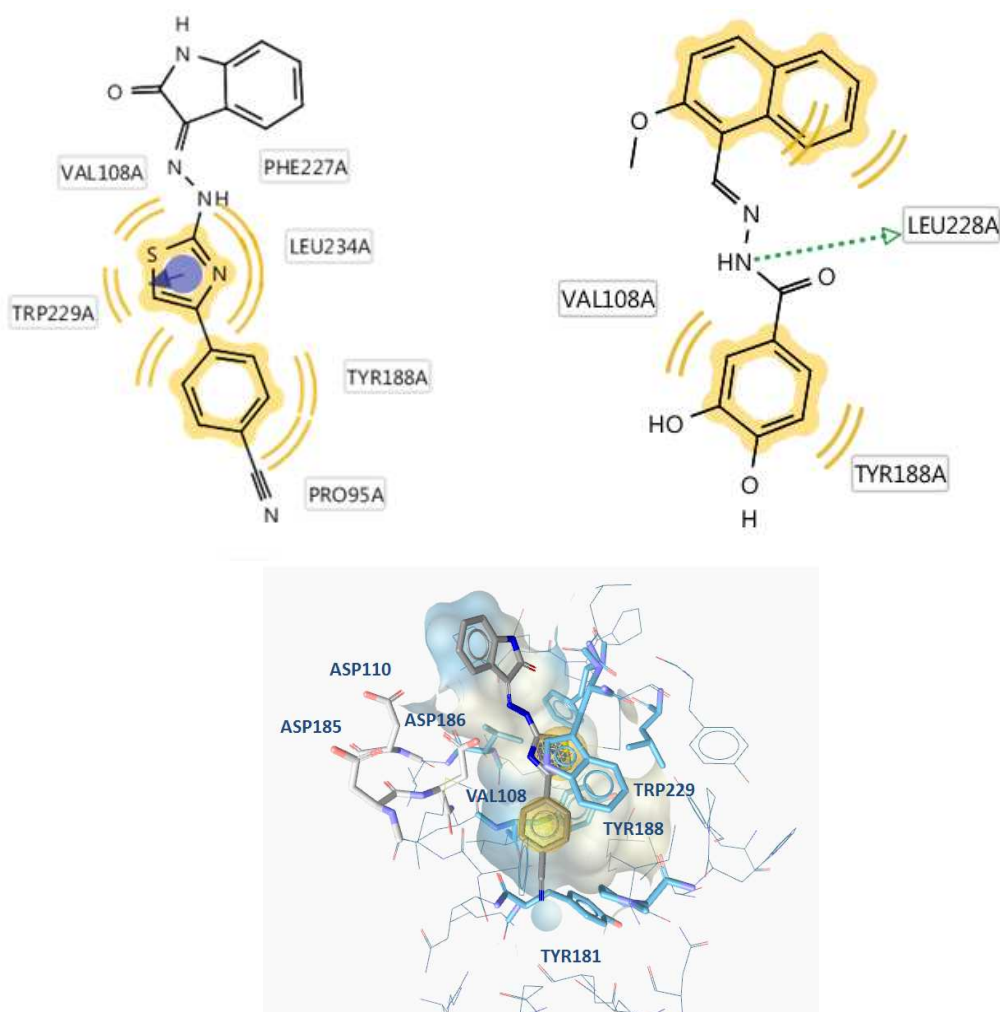
Compound **EMAC 2077** activity towards RNase H function is only slightly affected by mutations, while almost no influence of mutation on the RT RDDP function is observed.

These data are more than encouraging suggesting that this compound could be a valid hit compound for the development of new dual inhibitors of both RT associated functions.

Docking experiments also confirmed that the most probable binding site of compound **EMAC 2077** is the allosteric pocket between the NNRTIs binding pocket and the polymerase active site. [194]

In Figure 38 the most favoured binding mode of compound **EMAC 2077** is reported, in comparison with DHBNH. [194]

Both compounds, although with small differences, bind to the same lipophilic pocket.



**Figure 38.** Compound EMAC 2077 interactions with RT were analyzed using LigandScout [209]: the yellow spheres show hydrophobic contacts, green arrows (HB acceptor) violet circle (aromatic interaction)

In the case of compound **EMAC 2077**, with respect to DHBNH, a deeper contact with important residues of the NNRTIs binding pocket is observed.

This may be the explanation for the dual activity of **EMAC 2077** in comparison to DHBNH that only inhibit the RNase H function. Moreover, an aromatic interaction between the thiazole ring of compound EMAC2077 and TRP229 is observed. This interaction is particularly interesting considering that TRP229 is a highly conserve residue of HIV-1 RT.

Indeed more investigation are needed to better clarify the mode of action of such compounds and further synthetic effort should be dedicated to the achievement of more selective and less toxic derivatives.

Nevertheless the results of this research suggest that the allosteric site, between the NNRTIs binding pocket and the polymerase active site, is a druggable target to achieve a complete block of RT enzymatic activity.

## **3 Materials and methods**

### **3.1 Chemistry**

Unless otherwise noted, starting materials and reagents were obtained from commercial suppliers and were used without purification.

All melting points were determined by the capillary method on a Stuart SMP11 melting point apparatus or on a Büchi-540 capillary melting points apparatus and are uncorrected.

All samples were measured in DMSO-*d*<sub>6</sub> solvent, DMF-*d*<sub>7</sub> solvent and CDCl<sub>3</sub> at 278.1 K temperature on a Varian Unity 500 or with a Varian Unity 300 spectrometer. In the signal assignments the proton chemical shifts are referred to the solvent (1H:  $\delta$  = 7.24 ppm,). Coupling constants *J* are expressed in hertz (Hz).

Elemental analyses were obtained on a Perkin–Elmer 240 B microanalyser. Analytical data of the synthesised compounds are in agreement with the theoretical data.

HPLC-MS/MS analysis was performed using an HPLC-MS/MS Varian (Varian Palo Alto, CA, USA) system fitted with a 1200 L triple quadrupole mass spectrometer equipped with an electrospray ionization source (ESI). A Varian MS workstation version 6.8 software was used for data acquisition and processing. Rapid identification was achieved with direct infusion of the purified molecule, dissolved in methanol, on the mass spectrometer source.

TLC chromatography was performed using silica gel plates (Merck F 254), spots were visualised by UV light

## COMPOUNDS EMAC 2000-2025

In all investigated molecules the NMR analysis supports the “E” configuration (Figure 39).

According the double bond protons coupling constants that ranges from 15 to 16 Hz.

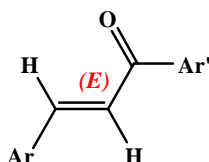
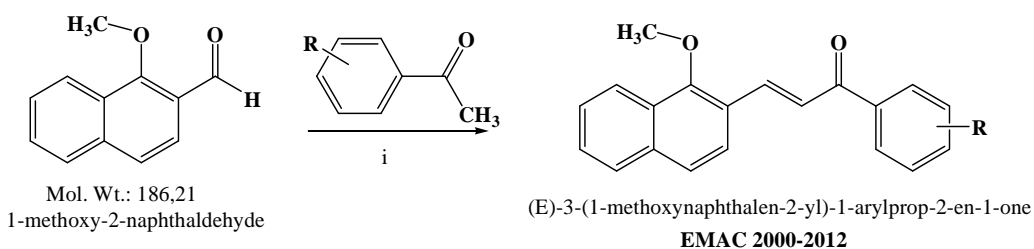


Figure 39. (E)-3-aryl-1-arylprop-2-en-1-one

### First series: (E)-3-(1-methoxynaphthalen-2-yl)-1-arylprop-2-en-1-one

#### General synthetic scheme:



R= 4-Br, 4-F, 4-OCH<sub>3</sub>, 4-Cl, 3-NO<sub>2</sub>, 4-C<sub>6</sub>H<sub>5</sub>, 4-NO<sub>2</sub>, 4-CH<sub>3</sub>, H, 3,4-Cl, 2,4-F, 2,4-Cl, 4-CN

**Scheme 1.** Synthesis of (E)-3-(1-methoxynaphthalen-2-yl)-1-arylprop-2-en-1-one derivatives EMAC 2000-2012. Reagents: (i) ethanol, NaOH 10 %.

#### General procedure for (E)-3-(1-methoxynaphthalen-2-yl)-1-arylprop-2-en-1-one

Chalcones were synthesized via Claisen-Schmidt condensation of substituted acetophenone with substituted benzaldehyde under basic conditions in ethanol.

Crude chalcones were purified by recrystallization from a suitable solvent. [203, 204]

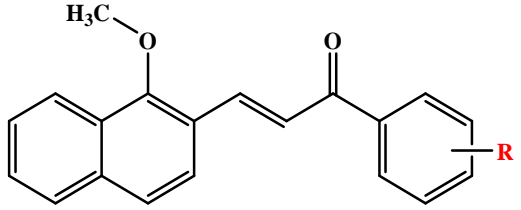
All synthesized compounds were characterised by analytical and spectral data as listed in Table 9 and 10.

**Table 9.** Chemical and physical data of derivatives EMAC 2000-2012

Compound	R	M.W.	Mp (C°)	% Yield
EMAC 2000	4-Br	367.24	110-112	67
EMAC 2001	4-F	306.33	93-95	81
EMAC 2002	4-OCH <sub>3</sub>	318.37	137-139	83
EMAC 2003	4-Cl	322.78	108-109	53
EMAC 2004	3-NO <sub>2</sub>	333.34	143-145	64
EMAC 2005	4-C <sub>6</sub> H <sub>5</sub>	364.44	104-105	87
EMAC 2006	4-NO <sub>2</sub>	334.34	133-135	63
EMAC 2007	4-CH <sub>3</sub>	302.37	91-93	76
EMAC 2008	H	288.34	108-110	79
EMAC 2009	3,4-Cl	357.23	135-137	79
EMAC 2010	2,4-F	324.32	94-96	67
EMAC 2011	2,4-Cl	357.23	112-114	70
EMAC 2012	4-CN	313.35	150-152	64



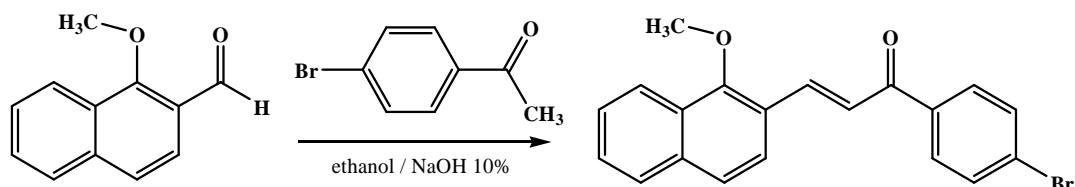
**Table 10.** Analytical data of derivatives EMAC 2000-2012

					
Compound	R	Reaction solvent	Crystallisation solvent	Aspect	Reaction time (h)
EMAC 2000	4-Br	Ethanol/NaOH 10%	Water/Ethanol	Crystalline yellow solid	24
EMAC 2001	4-F	Ethanol/NaOH 10% I	Water/Ethanol	Crystalline yellow solid	24
EMAC 2002	4-OCH <sub>3</sub>	Ethanol/NaOH 10%	Water/Ethanol	Crystalline yellow solid	24
EMAC 2003	4-Cl	Ethanol/NaOH 10%	Water/Ethanol	Crystalline yellow solid	24
EMAC 2004	3-NO <sub>2</sub>	Ethanol/NaOH 10%	Water/Ethanol	Crystalline pale orange solid	24
EMAC 2005	4-C <sub>6</sub> H <sub>5</sub>	Ethanol/NaOH 10%	Water/Ethanol	Crystalline yellow solid	24
EMAC 2006	4-NO <sub>2</sub>	Ethanol/NaOH 10%	Water/Ethanol	Crystalline yellow solid	24
EMAC 2007	4-CH <sub>3</sub>	Ethanol/NaOH 10%	Water/Ethanol	Crystalline yellow solid	24
EMAC 2008	H	Ethanol/NaOH 10%	Water/Ethanol	Crystalline yellow solid	24
EMAC 2009	3,4-Cl	Ethanol/NaOH 10%	Water/Ethanol	Crystalline yellow solid	24
EMAC 2010	2,4-F	Ethanol/NaOH 10%	Water/Ethanol	Crystalline yellow solid	24
EMAC 2011	2,4-Cl	Ethanol/NaOH 10%	Water/Ethanol	Crystalline yellow solid	24
EMAC 2012	4-CN	Ethanol/NaOH 10%	Water/Ethanol	Crystalline yellow solid	24

According to this procedure the following compounds have been synthesised:

#### EMAC 2000

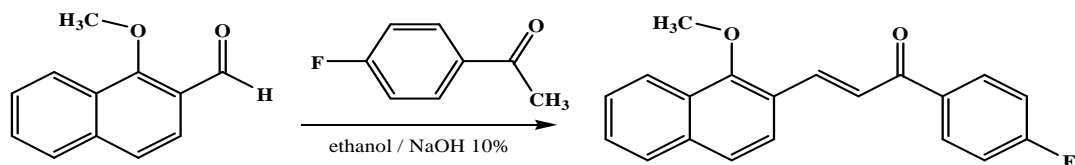
##### *(E)*-1-(4-bromophenyl)-3-(1-methoxynaphthalen-2-yl)prop-2-en-1-one



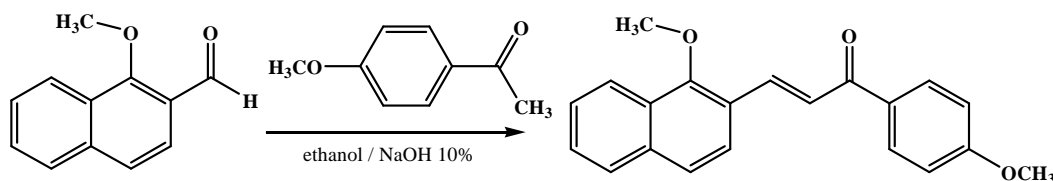
$^1\text{H-NMR}$  (300 MHz, DMSO)  $\delta$ H 4.06 (s, 3H,  $\text{OCH}_3$ ), 7.33 (d, 1H,  $J$ : 9.15, Ar-CH), 7.41 (t, 1H,  $J$ : 7.5, Ar-CH), 7.55 (t, 1H,  $J$ : 7.5, Ar-CH), 7.65 (d, 2H,  $J$ : 8.3, Ar-CH), 7.82 (d, 1H,  $J$ : 7.5, Ar-CH), 7.85 (d, 1H,  $J$ : 15.6, -CH=), 7.9 (d, 1H,  $J$ : 9, Ar-CH), 7.93 (d, 2H,  $J$ : 8.32, Ar-CH), 8.25 (d, 1H,  $J$ : 8.65, Ar-CH), 8.51 (d, 1H,  $J$ : 15.6, -CH=)

#### EMAC 2001

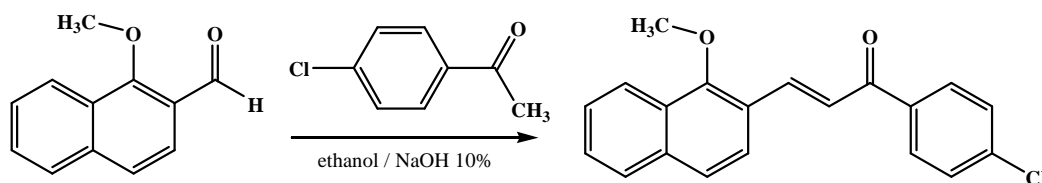
##### *(E)*-1-(4-fluorophenyl)-3-(1-methoxynaphthalen-2-yl)prop-2-en-1-one



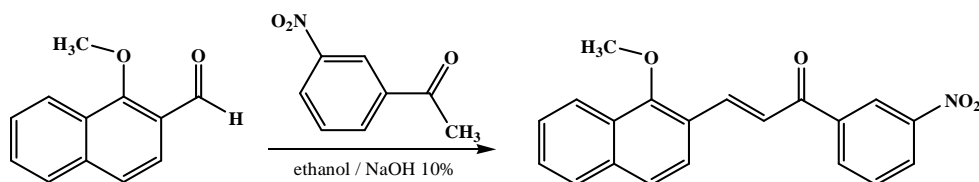
$^1\text{H-NMR}$  (300 MHz, DMSO)  $\delta$ H 4.07 (s, 3H,  $\text{OCH}_3$ ), 7.11 (t, 1H,  $J$ : 8.65,  $J$ : 8.49, Ar-CH), 7.26 (d, 2H,  $J$ : 9, Ar-CH), 7.42 (d, 1H,  $J$ : 7.15, Ar-CH), 7.50 (t, 1H,  $J$ : 8.49, Ar-CH), 7.57 (d, 1H,  $J$ : 7.15, Ar-CH), 7.78 (d, 1H,  $J$ : 15.9, -CH=), 7.93 (d, 1H,  $J$ : 8.65, Ar-CH), 8.09 (d, 2H,  $J$ : 9, Ar-CH), 8.18 (d, 1H,  $J$ : 8.49, Ar-CH), 8.43 (d, 1H,  $J$ : 15.9, -CH=)

**EMAC 2002*****(E)*-3-(1-methoxynaphthalen-2-yl)-1-(4-methoxyphenyl)prop-2-en-1-one**

$^1\text{H-NMR}$  (300 MHz, DMSO)  $\delta\text{H}$  3.9 (s, 3H,  $\text{OCH}_3$ ), 4.05 (s, 3H,  $\text{OCH}_3$ ), 7.00 (d, 1H,  $J$ : 8.99, Ar-CH), 7.33 (d, 2H,  $J$ : 9, Ar-CH), 7.70 (t, 1H,  $J$ : 8, Ar-CH), 7.47 (d, 1H,  $J$ : 16, -CH=), 7.55 (t, 1H,  $J$ : 8, Ar-CH), 7.82 (d, 1H,  $J$ : 8, Ar-CH), 7.89 (d, 1H,  $J$ : 9, Ar-CH), 8.08 (d, 1H,  $J$ : 9, Ar-CH), 8.28 (d, 2H,  $J$ : 9, Ar-CH), 8.45 (d, 1H, -CH=)

**EMAC 2003*****(E)*-1-(4-chlorophenyl)-3-(1-methoxynaphthalen-2-yl)prop-2-en-1-one**

$^1\text{H-NMR}$  (300 MHz, DMSO)  $\delta\text{H}$  4.06 (s, 3H,  $\text{OCH}_3$ ), 7.33 (d, 1H,  $J$ : 9.16, Ar-CH), 7.41 (t, 1H,  $J$ : 7.83, Ar-CH), 7.49 (d, 2H,  $J$ : 8.48, Ar-CH), 7.53 (d, 1H,  $J$ : 15.65, -CH=), 7.55 (t, 1H,  $J$ : 7.82, Ar-CH), 7.74 (d, 1H,  $J$ : 8.16, Ar-CH), 7.90 (d, 1H,  $J$ : 9.65, Ar-CH), 8.01 (d, 2H,  $J$ : 8.32, Ar-CH), 8.25 (d, 1H,  $J$ : 8.66, Ar-CH), 8.51 (d, 1H,  $J$ : 15.65, -CH=)

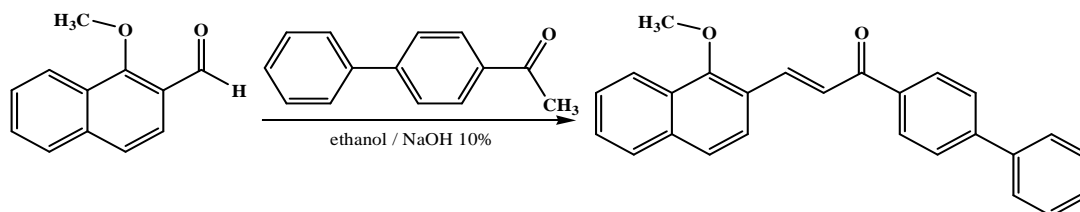
**EMAC 2004*****(E)*-3-(1-methoxynaphthalen-2-yl)-1-(3-nitrophenyl)prop-2-en-1-one**

$^1\text{H-NMR}$  (300 MHz, DMSO)  $\delta\text{H}$  4.10 (s, 3H,  $\text{OCH}_3$ ), 7.35 (d, 1H,  $J$ : 8.98, Ar-CH), 7.42 (t, 1H,  $J$ : 7.82, Ar-CH), 7.58 (t, 1H,  $J$ : 8.5, Ar-CH), 7.72 (t, 1H,  $J$ : 7.82, Ar-CH), 7.83 (d, 1H,  $J$ : 8, Ar-CH),

7.93 (d, 1H,  $J$ :8.5, Ar-CH), 7.94 (d, 1H,  $J$ : 15.6, -CH=), 8.25 (d, 1H,  $J$ : 8.5, Ar-CH), 8.39 (d, 1H,  $J$ : 8.5, Ar-CH), 8.44 (d, 1H,  $J$ : 8, Ar-CH), 8.60 (d, 1H,  $J$ : 15.6, -CH=), 8.89 (s, 1H, Ar-CH)

#### EMAC 2005

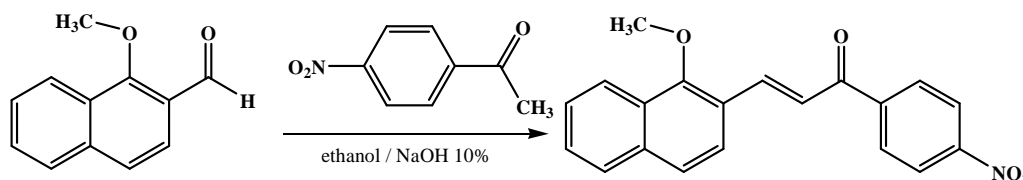
##### *(E)-3-(1-methoxynaphthalen-2-yl)-1-(4-biphenyl)prop-2-en-1-one*



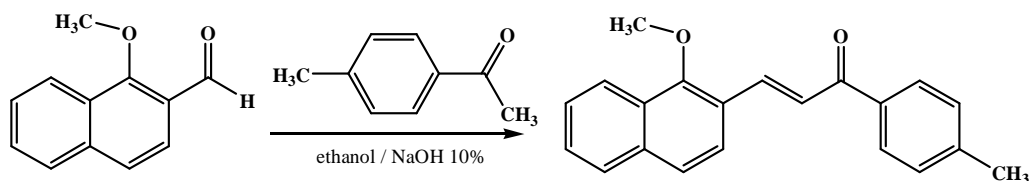
$^1\text{H-NMR}$  (300 MHz, DMSO)  $\delta\text{H}$  4.07 (s, 3H, OCH<sub>3</sub>), 7.34- 7.50 (m, 2H, Ar-CH), 7.56 (t, 1H,  $J$ : 8.1, Ar-CH), 7.69 (d, 2H,  $J$ : 7.8, Ar-CH), 7.75 (d, 2H,  $J$ : 7.8, Ar-CH), 7.83(d, 1H,  $J$ : 8.8, Ar-CH), 7.88 (d, 1H,  $J$ : 8.0, Ar-CH), 7.91 (d, 2H,  $J$ : 8.2, Ar-CH), 7.95 (d, 1H,  $J$ : 15.9, -CH=), 8.04 (d, 2H,  $J$ : 8.2, Ar-CH), 8.19 (d, 1H,  $J$ : 8.8, Ar-CH), 8.29 (d, 1H,  $J$ : 8.1, Ar-CH), 8.54 (d, 1H,  $J$ : 15.9, -CH=)

#### EMAC 2006

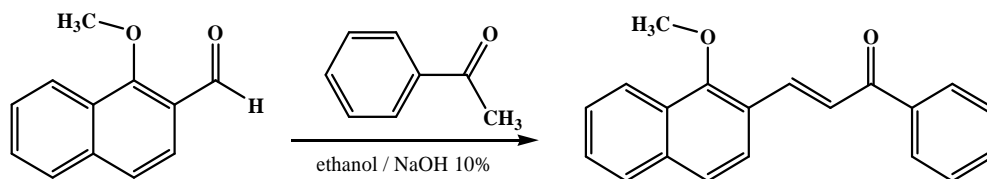
##### *(E)-3-(1-methoxynaphthalen-2-yl)-1-(4-nitrophenyl)prop-2-en-1-one*



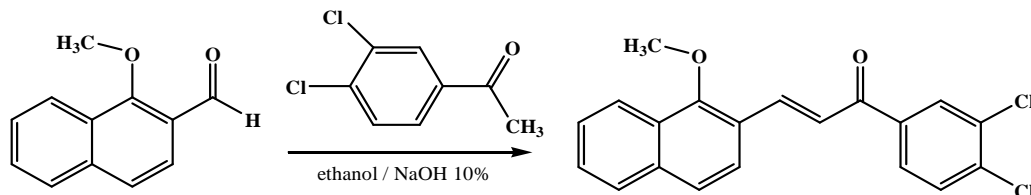
$^1\text{H-NMR}$  (500 MHz, DMSO)  $\delta\text{H}$  3.55 (s, 3H, OCH<sub>3</sub>) 7.34 (d, 1H,  $J$ : 9, Ar-CH) 7.42 (t, 1H,  $J$ : 7.5, Ar-CH), 7.57 (t, 1H,  $J$ : 7.5, Ar-CH), 7.89 (d, 1H,  $J$ : 15.5, -CH=), 7.93 (d, 1H,  $J$ : 9.5, Ar-CH), 8.18 (d, 2H,  $J$ : 9 Ar-CH), 8.23 (d, 1H,  $J$ : 9, Ar-CH), 8.36 (d, 2H,  $J$ : 8.5, Ar-CH), 8.42 (d, 1H,  $J$ : 9, Ar-CH), 8.57 (d, 1H,  $J$ : 16, -CH=)

**EMAC 2007****(E)-3-(1-methoxynaphthalen-2-yl)-1-p-tolylprop-2-en-1-one**

$^1\text{H-NMR}$  (500 MHz, DMSO)  $\delta\text{H}$  2.44 (s, 3H,  $\text{CH}_3$ ), 4.05 (s, 3H,  $\text{OCH}_3$ ), 7.31 (d, 2H,  $J$ : 8.5, Ar-CH, Ar-CH), 7.33 (d, 1H,  $J$ : 9, Ar-CH), 7.39 (t, 1H,  $J$ : 7.5, Ar-CH), 7.53 (t, 1H,  $J$ : 8, Ar-CH), 7.81 (d, 1H,  $J$ : 8.5, Ar-CH), 7.87 (d, 1H,  $J$ : 15.5,  $-\text{CH}=\text{}$ ), 7.88 (d, 1H,  $J$ : 9, Ar-CH), 7.98 d, 2H,  $J$ : 8, Ar-CH), 8.26 (d, 1H,  $J$ : 8.5, Ar-CH), 8.47 (d, 1H,  $J$ : 16,  $-\text{CH}=\text{}$ )

**EMAC 2008****(E)-3-(1-methoxynaphthalen-2-yl)-1-phenylprop-2-en-1-one**

$^1\text{H-NMR}$  (500 MHz, DMSO)  $\delta\text{H}$  4.06 (s, 3H,  $\text{OCH}_3$ ), 7.33 (d, 1H,  $J$ : 8.5, Ar-CH), 7.4 (t, 1H,  $J$ : 8, Ar-CH), 7.52 (d, 2H,  $J$ : 7, Ar-CH), 7.54 (t, 1H,  $J$ : 8, Ar-CH), 7.58 (t, 1H,  $J$ : 7.5, Ar-CH), 7.81 (d, 1H,  $J$ : 8, Ar-CH), 7.88 (d, 1H,  $J$ : 7.5, Ar-CH), 7.89 (d, 1H,  $J$ : 15.5,  $-\text{CH}=\text{}$ ), 8.07 (d, 2H,  $J$ : 7.5, Ar-CH), 8.26 (d, 1H,  $J$ : 8.5, Ar-CH), 8.49 (d, 1H,  $J$ : 15.5,  $-\text{CH}=\text{}$ )

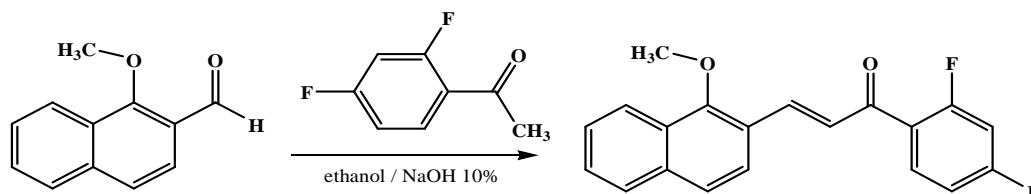
**EMAC 2009****(E)-1-(4-bromophenyl)-3-(1-methoxynaphthalen-2-yl)prop-2-en-1-one**

$^1\text{H-NMR}$  (500 MHz, DMSO)  $\delta\text{H}$  4.07 (s, 3H,  $\text{OCH}_3$ ), 7.33 (d, 1H,  $J_m$ : 2,  $J_p$ : 1,  $J_o$ : 8, Ar-CH), 7.41 (t, 1H,  $J_m$ : 1,  $J_o$ : 8.5, Ar-CH), 7.56 (t, 1H,  $J_m$ : 1,  $J_o$ : 8.5, Ar-CH), 7.59 (d, 1H,  $J$ : 8, Ar-CH), 7.81

(d, 1H,  $J$ : 8.5, Ar-CH), 7.81 (d, 1H,  $J$ : 16, -CH=), 7.88 (d, 1H,  $J_o$ : 8,  $J_m$ : 2, Ar-CH), 7.91 (d, 1H,  $J$ : 9), 8.14 (s, 1H,  $J_m$ : 2), 8.23 (d, 1H,  $J$ : 9, Ar-CH), 8.52 (d, 1H,  $J$ : 16, -CH=)

#### EMAC 2010

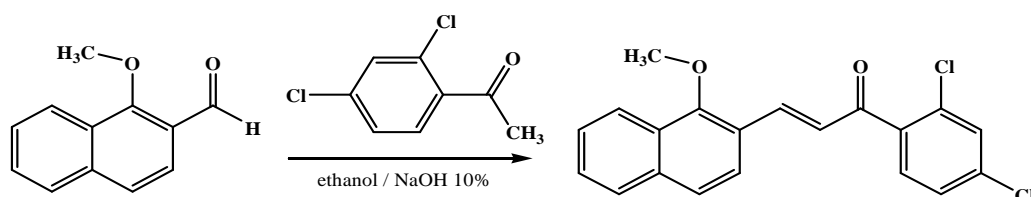
##### *(E)*-1-(2,4-difluorophenyl)-3-(1-methoxynaphthalen-2-yl)prop-2-en-1-one



$^1\text{H-NMR}$  (500 MHz, DMSO)  $\delta$ H 4.04 (s, 3H, OCH<sub>3</sub>), 7.34 (d, 1H,  $J$ : 8.5, Ar-CH), 7.44 (t, 1H,  $J$ : 8.5, Ar-CH), 7.55 (t, 1H,  $J$ : 8.5, Ar-CH), 7.70 (d, 1H,  $J$ : 9, Ar-CH), 7.71 (d, 1H,  $J$ : 7.5, Ar-CH), 7.76 (d, 1H,  $J$ : 16, -CH=), 7.81 (d, 1H,  $J$ : 8.5, Ar-CH), 7.81 (s, 1H, Ar-CH), 7.89 (d, 1H,  $J$ : 9.5, Ar-CH), 8.24 (d, 1H,  $J$ : 8.5, Ar-CH), 8.48 (d, 1H,  $J$ : 15.5, -CH=)

#### EMAC 2011

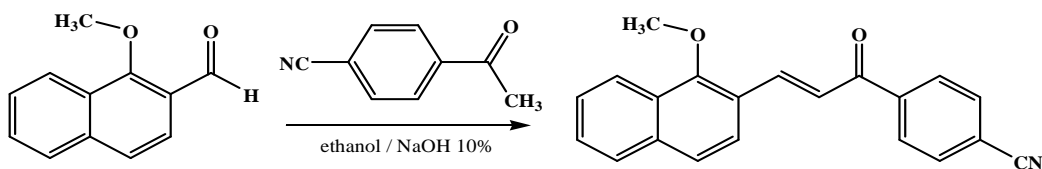
##### *(E)*-1-(2,4-dichlorophenyl)-3-(1-methoxynaphthalen-2-yl)prop-2-en-1-one



$^1\text{H-NMR}$  (500 MHz, DMSO)  $\delta$ H 4.05 (s, 3H, OCH<sub>3</sub>), 7.34 (d, 1H,  $J$ : 8.5, Ar-CH), 7.44 (t, 1H, Ar-CH), 7.54 (t, 1H, Ar-CH), 7.6 (d, 1H,  $J$ : 9, Ar-CH), 7.73 (d, 1H,  $J$ : 9.5, Ar-CH), 7.8 (d, 1H, Ar-CH), 7.87 (s, 1H, Ar-CH), 7.94 (d, 1H,  $J$ : 8, Ar-CH), 8.17 (d, 1H,  $J$ : 16.5, -CH=), 8.28 (d, 1H,  $J$ : 8.5, Ar-CH), 8.44 (d, 1H,  $J$ : 16.5, -CH=)

EMAC 2012

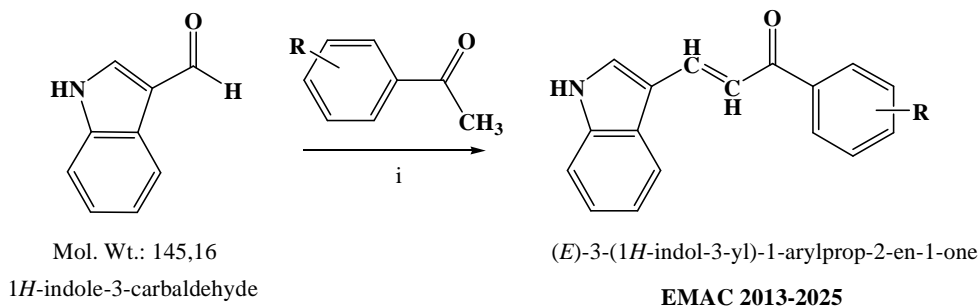
*(E)*-4-(3-(1-methoxynaphthalen-2-yl)acryloyl)benzonitrile



$^1\text{H-NMR}$  (500 MHz, DMSO)  $\delta$  4.07 (s, 3H,  $\text{OCH}_3$ ), 7.33 (d, 1H,  $J$ : 8.5, Ar-CH), 7.42 (t, 1H,  $J$ : 7.5, Ar-CH), 7.56 (t, 1H,  $J$ : 7.5, Ar-CH), 7.70 (d, 2H,  $J$ : 9, Ar-CH), 7.82 (d, 1H,  $J$ : 8.5, Ar-CH), 7.87 (d, 1H,  $J$ : 15.5, -CH=), 7.93 (d, 2H,  $J$ : 9, Ar-CH), 8.12 (d, 1H,  $J$ : 8.5, Ar-CH), 8.23 (d, 1H,  $J$ : 8.5, Ar-CH), 8.56 (d, 1H,  $J$ : 15.5, -CH=)

## Second series: (E)-3-indol-3-yl-1-arylprop-2-en-1-one derivatives

### General synthetic scheme:



R= 4-Br, 4-F, 4-OCH<sub>3</sub>, 4-Cl, 3-NO<sub>2</sub>, 4-C<sub>6</sub>H<sub>5</sub>, 4-NO<sub>2</sub>, 4-CH<sub>3</sub>, H, 3,4-Cl, 2,4-F, 2,4-Cl, 4-CN

**Scheme 2.** Synthesis of (*E*)-3-indol-3-yl-1-arylprop-2-en-1-one derivatives EMAC 2013-2025.  
Reagents: (i) ethanol, piperidine.

### General procedure for (*E*)-3-indol-3-yl-1-arylprop-2-en-1-one derivatives

According to literature method, [205, 206] 3.45 mmol of indol-3-carboxaldehyde and 3.45 mmol of suitable acetophenone, in the presence of 2 mmol of piperidine added dropwise, were dissolved in 20 ml of ethanol and stirring for 24 h. The reaction mixture was neutralized with diluted HCl 10%; the solid was filtered and crystallised from appropriate solvent (Scheme 2).

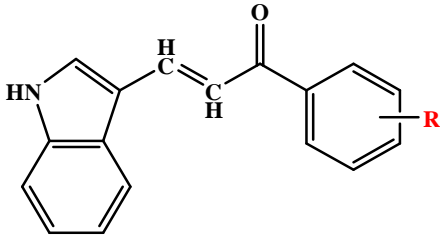
All synthesized compounds were characterised by analytical and spectral data as listed in Table 11 and 12



**Table 11.** Chemical and physical data of derivatives EMAC 2013-2025

Compound	R	M.W.	Mp (C°)	% Yield
EMAC 2013	4-Br	326.19	194-195	47
EMAC 2014	4-F	265.28	173-174	30
EMAC 2015	4-OCH <sub>3</sub>	277.32	159-160	20
EMAC 2016	4-Cl	281.74	188-190	52
EMAC 2017	3-NO <sub>2</sub>	292.29	194-196	80
EMAC 2018	4-C <sub>6</sub> H <sub>5</sub>	323.39	250-253	82
EMAC 2019	4-NO <sub>2</sub>	292.29	227-229	78
EMAC 2020	4-CH <sub>3</sub>	261.32	140-144	71
EMAC 2021	H	247.29	154-156	68
EMAC 2022	3,4-Cl	316.18	212-214	80
EMAC 2024	2,4-Cl	316.18	186-188	69
EMAC 2025	4-CN	272.3	183-185	64

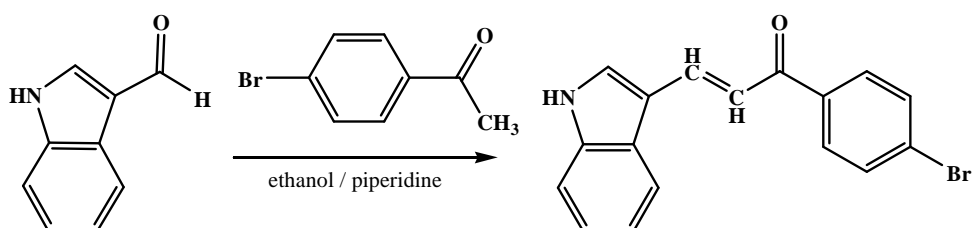
**Table 12.** Analytical data of derivatives EMAC 2013-2025

Compound	R					Reaction time (h)
		Reaction solvent	Crystallisation solvent	Aspect		
EMAC 2013	4-Br	Ethanol/ Piperidine	Ethanol	Crystalline orange solid	24	
EMAC 2014	4-F	Ethanol/ Piperidine	Ethanol	Crystalline off-white solid	24	
EMAC 2015	4-OCH <sub>3</sub>	Ethanol/ Piperidine	Ethanol	Crystalline yellow solid	24	
EMAC 2016	4-Cl	Ethanol/ Piperidine	Ethanol	Crystalline orange solid	24	
EMAC 2017	3-NO <sub>2</sub>	Ethanol/ Piperidine	Ethanol	Crystalline orange solid	24	
EMAC 2018	4-C <sub>6</sub> H <sub>5</sub>	Ethanol/ Piperidine	Ethanol	Crystalline yellow solid	24	
EMAC 2019	4-NO <sub>2</sub>	Ethanol/ Piperidine	Ethanol	Crystalline red solid	24	
EMAC 2020	4-CH <sub>3</sub>	Ethanol/ Piperidine	Ethanol	Crystalline pale orange solid	24	
EMAC 2021	H	Ethanol/ Piperidine	Ethanol	Crystalline yellow solid	24	
EMAC 2022	3,4-Cl	Ethanol/ Piperidine	Ethanol	Crystalline orange solid	24	
EMAC 2024	2,4-Ck	Ethanol/ Piperidine	Ethanol	Crystalline yellow solid	24	
EMAC 2025	4-CN	Ethanol/ Piperidine	Ethanol	Crystalline orange solid	24	

According to this procedure the following compounds have been synthesised:

#### EMAC 2013

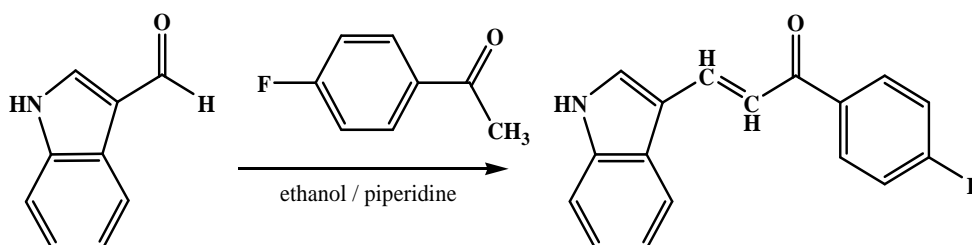
##### *(E)*-1-(4-bromophenyl)-3-(1H-indol-3-yl)prop-2-en-1-one



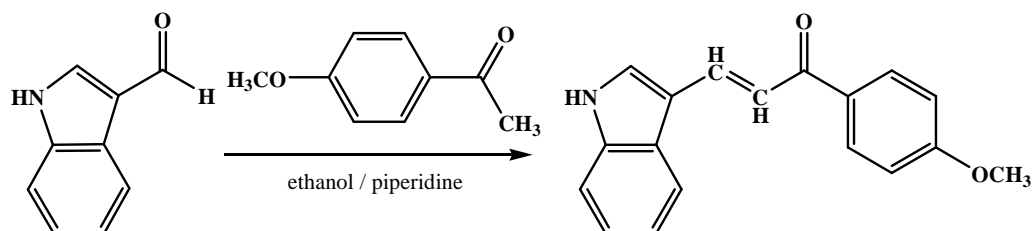
$^1\text{H-NMR}$  (500 MHz, DMSO)  $\delta$  H 7.32 (m, 2H, Ar-CH), 7.46 (m, 1H, Ar-CH), 7.53 (d, 1H,  $J$ : 15, -CH=), 7.63 (d, 1H,  $J_m$ : 2.5, Ar-CH), 7.65 (d, 2H,  $J$ : 8.5, Ar-CH), 7.92 (d, 2H,  $J$ : 8.5, Ar-CH), 8.01 (m, 1H, Ar-CH), 8.10 (d, 1H,  $J$ :15, -CH=), 8.59 (br.s, 1H, NH)

#### EMAC 2014

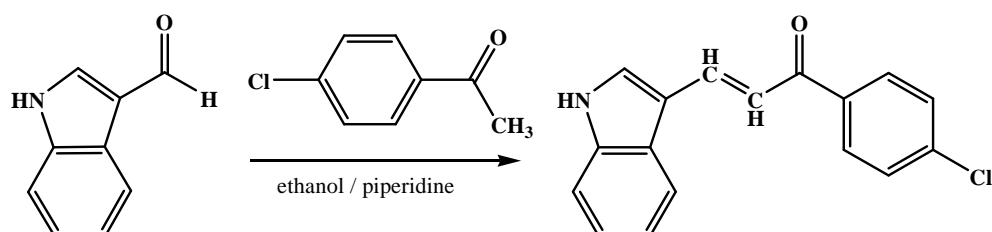
##### *(E)*-1-(4-fluorophenyl)-3-(1H-indol-3-yl)prop-2-en-1-one



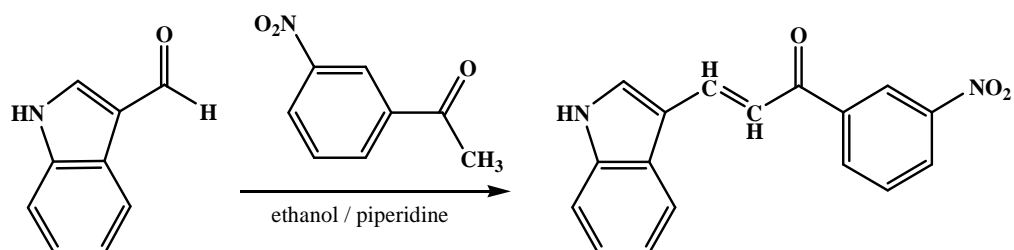
$^1\text{H-NMR}$  (500 MHz, DMSO)  $\delta$  H 7.18 (t, 1H,  $J$ : 8.5, Ar-CH), 7.32 (m, 2H, Ar-CH), 7.46 (m, 1H, Ar-CH), 7.49 (d, 2H,  $J$ : 8,  $J_{H-F}$ : 6, Ar-CH), 7.54 (d, 1H,  $J$ : 15.5, Ar-CH), 7.63 (s, 1H,  $J_m$ : 2.5, Ar-CH), 8.00 (d, 2H,  $J$ : 8.5,  $J_{H-F}$ : 6.5, Ar-CH), 8.11 (d, 1H,  $J$ : 15.5, -CH=), 8.57 (br.s, 1H, NH)

**EMAC 2015*****(E)*-3-(1*H*-indol-3-yl)-1-(4-methoxyphenyl)prop-2-en-1-one**

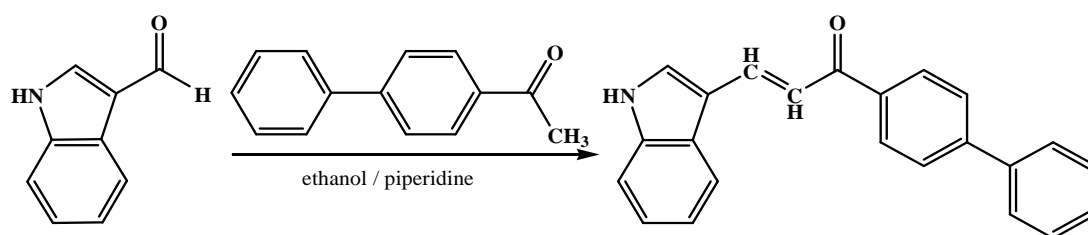
$^1\text{H-NMR}$  (500 MHz, DMSO)  $\delta$ H 3.09 (s, 3H, OCH<sub>3</sub>), 7.18 (m, 1H, Ar-CH), 7.32 (m, 2H, Ar-CH), 7.46 (m, 1H, Ar-CH), 7.47 (m, 1H, Ar-CH), 7.53 (d, 1H, *J*: 15, -CH=), 7.63 (d, 1H, *J*<sub>m</sub>: 2.5, Ar-CH), 8.08 (m, 3H, Ar-CH), 8.11 (d, 1H, *J*: 15, -CH=), 8.57 (br.s, 1H, NH)

**EMAC 2016*****(E)*-1-(4-chlorophenyl)-3-(1*H*-indol-3-yl)prop-2-en-1-one**

$^1\text{H-NMR}$  (500 MHz, DMSO)  $\delta$ H 7.32 (m, 2H, Ar-CH), 7.46 (m, 1H, Ar-CH), 7.48 (d, 2H, *J*: 8, Ar-CH), 7.55 (d, 1H, *J*: 15.5, -CH=), 7.62 (d, 1H, *J*<sub>m</sub>: 1.5, Ar-CH), 8.00 (m, 3H, *J*: 8, Ar-CH), 8.11 (d, 1H, *J*: 15.5, -CH=), 8.66 (br.s, 1H, NH)

**EMAC 2017*****(E)*-3-(1*H*-indol-3-yl)-1-(3-nitrophenyl)prop-2-en-1-one**

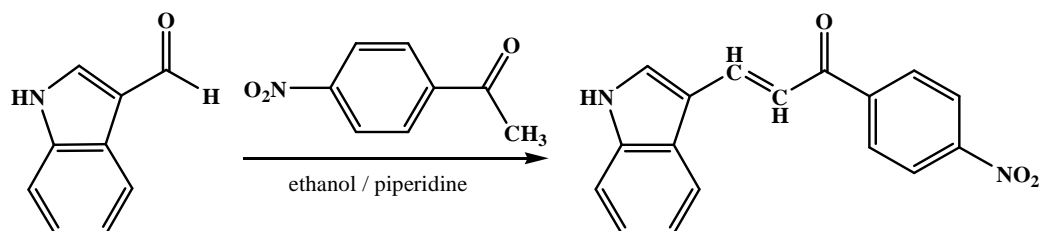
$^1\text{H-NMR}$  (500 MHz, DMSO)  $\delta\text{H}$  7.35 (m, 2H, Ar-CH), 7.47 (m, 1H,  $J$ : 9, Ar-CH), 7.56 (d, 1H,  $J$ : 15.5, -CH=), 7.89 (d, 1H,  $J_m$ : 2.5, Ar-CH), 7.71 (t, 1H,  $J$ : 8, Ar-CH), 8.03 (m, 1H,  $J$ : 8, Ar-CH), 8.19 (d, 1H,  $J$ : 15.5, Ar-CH), 8.37 (d, 1H,  $J$ : 7.5, Ar-CH), 8.42 (d, 1H,  $J$ : 8, Ar-CH), 8.59 (br.s, 1H, NH), 8.87 (s, 1H, Ar-CH)

**EMAC 2018*****(E)*-3-(1*H*-indol-3-yl)-1-(4-phenylphenyl)prop-2-en-1-one**

$^1\text{H-NMR}$  (500 MHz, DMSO)  $\delta\text{H}$  7.33 (m, 2H, Ar-CH), 7.40 (m, 1H, Ar-CH), 7.48 (m, 3H,  $J$ : 7.5, Ar-CH), 7.64 (s, 1H, Ar-CH), 7.65 (d, 1H,  $J$ : 15.5, -CH=), 7.78 (d, 2H,  $J$ : 7.5, Ar-CH), 7.74 (d, 2H,  $J$ : 8, Ar-CH), 8.06 (m, 1H, Ar-CH), 8.15 (d, 2H,  $J$ : 7, Ar-CH), 8.14 (d, 1H,  $J$ : 15.5, Ar-CH), 8.5 (br.s, 1H, NH)

**EMAC 2019**

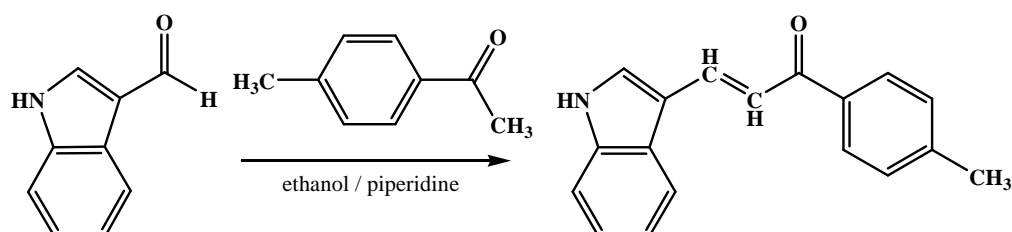
**(E)-3-(1H-indol-3-yl)-1-(4-nitrophenyl)prop-2-en-1-one**



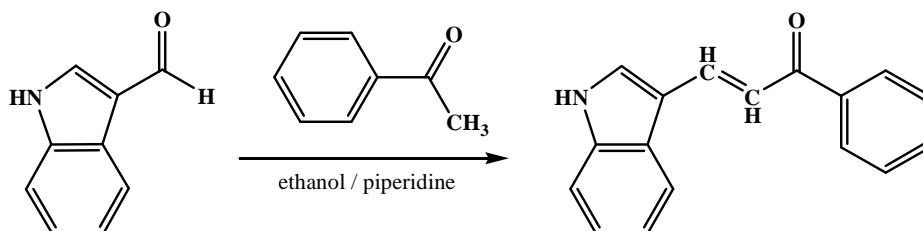
$^1\text{H-NMR}$  (500 MHz, DMSO)  $\delta\text{H}$  7.34 (m, 2H, Ar-CH), 7.47 (m, 1H, Ar-CH), 7.53 (d, 1H,  $J$ : 15.5, -CH=), 7.67 (d, 1H,  $J_m$ : 2.5, Ar-CH), 8.01 (m, 1H, Ar-CH), 8.14 (d, 1H,  $J$ : 15.5, -CH=), 8.17 (d, 2H,  $J$ : 8.5, Ar-CH), 8.36 (d, 2H,  $J$ : 8.5, Ar-CH), 8.59 (br.s, 1H, NH)

**EMAC 2020**

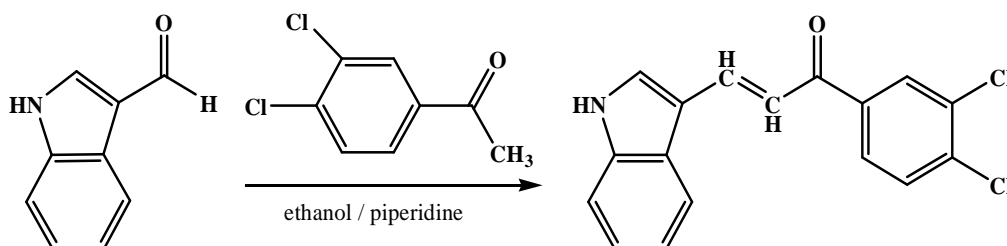
**(E)-3-(1H-indol-3-yl)-1-p-tolylprop-2-en-1-one**



$^1\text{H-NMR}$  (500 MHz, DMSO)  $\delta\text{H}$  2.44 (s, 3H,  $\text{CH}_3$ ), 7.31 (m, 4H,  $J$ : 8, Ar-CH), 7.46 (m, 1H, Ar-CH), 7.60 (d, 1H,  $J$ : 15, -CH=), 7.61 (s, 1H, Ar-CH), 7.97 (d, 2H,  $J$ : 8, Ar-CH), 8.01 (m, 1H, Ar-CH), 8.1 (d, 1H,  $J$ : 15.5, -CH=), 8.9 (br.s, 1H, NH)

**EMAC 2021****(E)-3-(1H-indol-3-yl)-1-phenylprop-2-en-1-one**

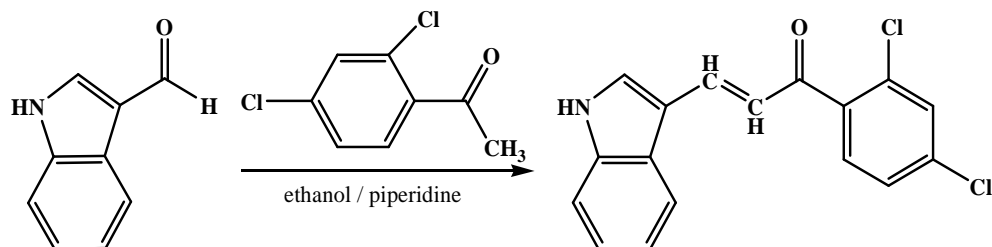
$^1\text{H-NMR}$  (500 MHz, DMSO)  $\delta$ H 7.31 (m, 2H, Ar-CH), 7.45 (m, 1H, Ar-CH), 7.52 (t, 2H,  $J$ : 7.5,  $J$ : 7 Ar-CH), 7.57 (t, 1H,  $J$ : 7.5, Ar-CH), 7.61 (d, 1H,  $J_m$ : 2.5, Ar-CH), 7.6 (d, 1H,  $J$ : 15.5, -CH=), 8.03 (m, 1H, Ar-CH), 8.06 (d, 2H,  $J$ : 7, Ar-CH), 8.11 (d, 1H,  $J$ : 15.5, -CH=), 8.74 (br.s, 1H, NH)

**EMAC 2022****(E)-1-(3,4-dichlorophenyl)-3-(1H-indol-3-yl)prop-2-en-1-one**

$^1\text{H-NMR}$  (500 MHz, DMSO)  $\delta$ H 7.34 (m, 2H, Ar-CH), 7.46 (t, 1H,  $J$ : 8.5, Ar-CH), 7.48 (d, 1H,  $J$ : 15.5, -CH=), 7.59 (d, 1H,  $J$ : 8.5, Ar-CH), 7.65 (d, 1H,  $J_m$ : 2.5, Ar-CH), 7.87 (d, 1H,  $J_o$ : 8.5,  $J_m$ : 2, Ar-CH), 8.01 (m, 1H, Ar-CH), 8.13 (d, 1H,  $J_m$ : 2, Ar-CH), 8.12 (d, 1H,  $J$ : 15.5, -CH=), 8.57 (br.s, 1H, NH)

#### EMAC 2024

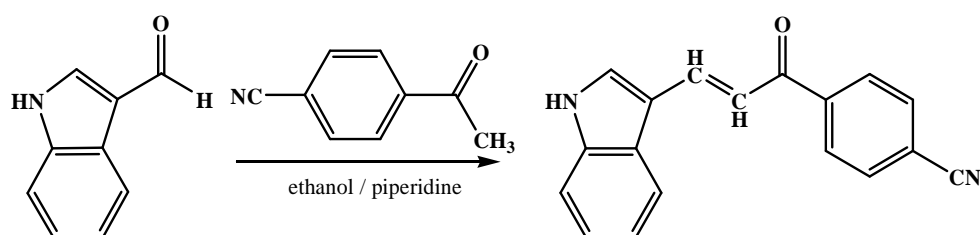
##### *(E)*-1-(2,4-dichlorophenyl)-3-(1H-indol-3-yl)prop-2-en-1-one



$^1\text{H-NMR}$  (500 MHz, DMSO)  $\delta\text{H}$  7.18 (d, 1H,  $J$ : 15.5, -CH=), 7.3 (m, 2H,  $J_m$ : 2,  $J_o$ : 7.5, Ar-CH), 7.35 (d, 1H,  $J_m$ : 2,  $J_o$ : 8, Ar-CH), 7.43 (d, 1H,  $J_m$ : 2,  $J_o$ : 8.5, Ar-CH), 7.46 (d, 1H,  $J$ : 8, Ar-CH), 7.49 (d, 1H,  $J_m$ : 2, Ar-CH) 7.55 (d, 1H,  $J_m$ : 3, Ar-CH), 7.72 (d, 1H,  $J$ : 15.5, -CH=), 7.95 (d, 1H,  $J$ : 8.5, Ar-CH), 8.64 (br.s, 1H, NH)

#### EMAC 2025

##### *(E)*-4-(3-(1H-indol-3-yl)acryloyl)benzonitrile

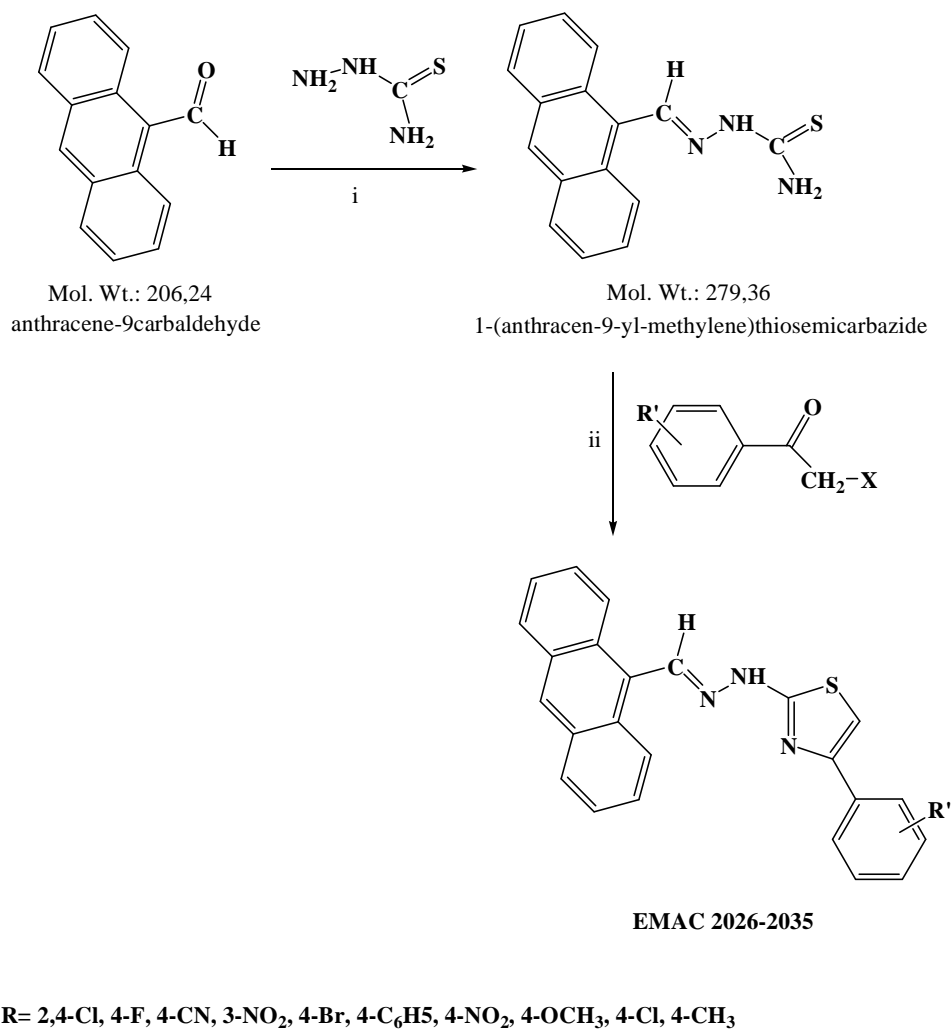


$^1\text{H-NMR}$  (500 MHz, DMSO)  $\delta\text{H}$  7.33 (m, 2H, Ar-CH), 7.47 (m, 1H, Ar-CH), 7.51 (d, 1H,  $J$ : 15.5, -CH=), 7.65 (d, 1H,  $J_m$ : 2.5, Ar-CH), 7.8 (d, 2H,  $J$ : 8.5, Ar-CH), 8.00 (m, 1H, Ar-CH), 8.13 (d, 1H,  $J$ : 15, -CH=), 8.11 (d, 2H,  $J$ : 8, Ar-CH), 8.71 (br.s, 1H, NH)



## COMPOUNDS EMAC 2026-2035

### General synthetic scheme:



**Scheme 3.** Synthesis of 1-(anthracen-9-yl-methylene)-2-(4-arylthiazol-2-yl)hydrazine derivatives EMAC 2026-2035. Reagents: (i) 2-propanol, AcOH; (ii) 2-propanol, reflux condition.

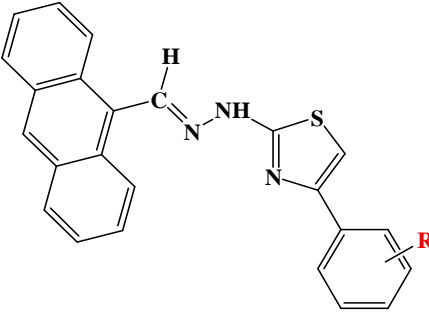
**General procedure for 1-(anthracen-9-yl-methylene)-2-(4-arylthiazol-2-yl)hydrazine derivatives**

Anthracene derivative were synthesized by a multi step reaction.

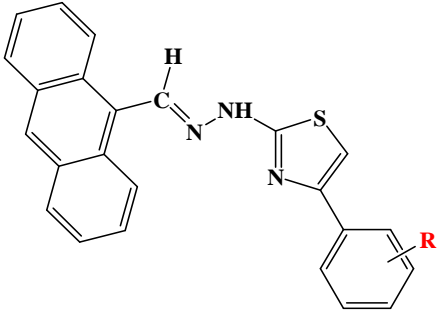
The first synthetic step leads to the formation of 1-(anthracen-9-yl-methylene)thiosemicarbazide by reacting anthracene-9-carbaldehyde and thiosemicarbazide in 2-propanol and acid acetic as catalyst.

In the second step, the thiazole ring is formed by reaction between 1-(anthracen-9-yl-methylene)thiosemicarbazide and differently substituted  $\alpha$ -halogen-acetophenones as outlined in the Scheme 3.

All synthesized compounds were characterised by analytical and spectral data as listed in Table 13 and 14.

**Table 13.** Chemical and physical data of derivatives EMAC 2026-2035

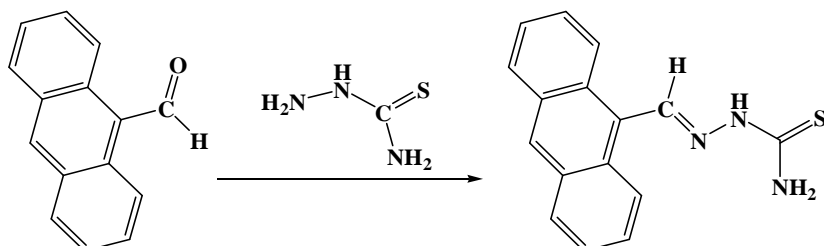
Compound	R	M.W.	Mp (C°)	% Yield
EMAC 2026	2,4-Cl	448.37	190	92
EMAC 2027	4-F	397.47	228	80
EMAC 2028	4-CN	404.49	243	85
EMAC 2029	3-NO <sub>2</sub>	424.7	245	97
EMAC 2030	4-Br	458.37	250	89
EMAC 2031	4-C <sub>6</sub> H <sub>5</sub>	455.57	246-248	95
EMAC 2032	4-NO <sub>2</sub>	424.47	253	99
EMAC 2033	4-OCH <sub>3</sub>	409.5	233	83
EMAC 2034	4-Cl	413.92	260-262	97
EMAC 2035	4-CH <sub>3</sub>	393.5	225	70

**Table 14.** Analytical data of derivatives EMAC 2026-2035


Compound	R	Reaction solvent	Crystallisation solvent	Aspect	Reaction time (h)
EMAC 2026	2,4-Cl	2-propanol	Ethanol	Pale solid yellow	10
EMAC 2027	4-F	2-propanol	Ethanol	Pale solid orange	10
EMAC 2028	4-CN	2-propanol	Ethanol	Pale solid orange	10
EMAC 2029	3-NO <sub>2</sub>	2-propanol	Ethanol	Pale solid orange	12
EMAC 2030	4-Br	2-propanol	Ethanol	Crystalline pale orange	10
EMAC 2031	4-C <sub>6</sub> H <sub>5</sub>	2-propanol	Ethanol	Crystalline yellow solid	10
EMAC 2032	4-NO <sub>2</sub>	2-propanol	Ethanol	Crystalline bright orange solid	10
EMAC 2033	4-OCH <sub>3</sub>	2-propanol	Ethanol	Crystalline orange solid	12
EMAC 2034	4-Cl	2-propanol	Ethanol	Crystalline yellow solid	9
EMAC 2035	4-CH <sub>3</sub>	2-propanol	Ethanol	Crystalline orange solid	10

According to this procedure the following compounds have been synthesised:

**1-(anthracen-9-yl-methylene)thiosemicarbazide**

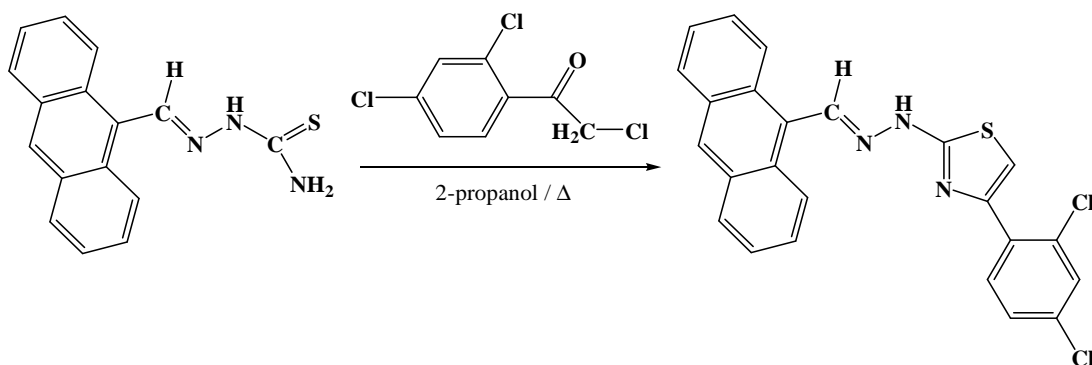


M.W.: 279.36 g/mol; R.f.: 0.81 (eluent: DCM:methanol 20:1); M.P.: 200°C; Yield: 90,31%

<sup>1</sup>H-NMR: (300 MHz, DMSO)  $\delta$ H 11.76 (s, 1H, NH) 9.44 (s, 1H, CH=N), 8.83 (s, 1H, Ar-CH), 8.68 (d, 2H, *J*: 8.68, Ar-CH), 8.44 (br.s, 1H, NH<sub>2</sub>), 8.26 (d, 2H, *J*: 8.18, Ar-CH), 7.84 (br.s, 1H, NH<sub>2</sub>), 7.72 (m, 4H, Ar-CH)

**EMAC 2026**

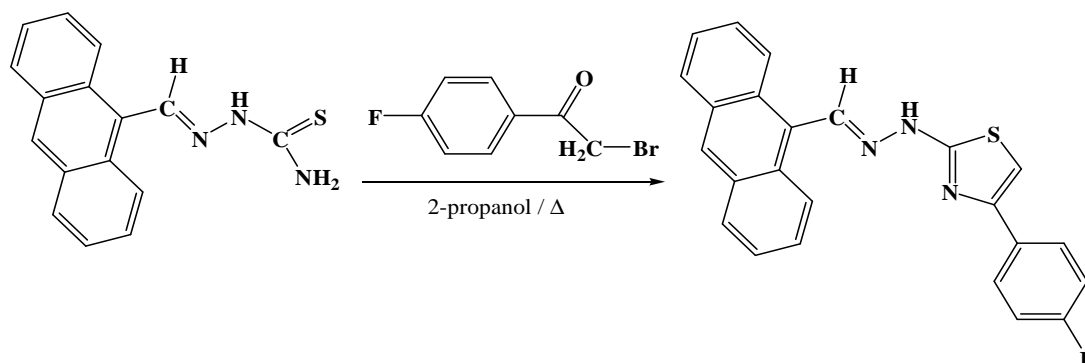
**1-(anthracen-9-yl-methylene)-2-(4-(2,4-dichlorophenyl)thiazol-2-yl)hydrazine**



<sup>1</sup>H-NMR: (300 MHz, DMSO)  $\delta$ H 12.49 (br.s, 1H, NH), 9.29 (s, 1H, CH=N), 8.7 (d+s, 3H, Ar-CH), 8.17 (d, 2H, *J*: 8.34, Ar-CH), 7.95 (d, 1H, *J*: 8.01, Ar-CH), 7.73 (s, 1H, Ar-CH), 7.65 (m, 4H, Ar-CH), 7.55 (d, 1H, *J*: 8.01, Ar-CH), 7.44 (s, 1H, thiazole)

## EMAC 2027

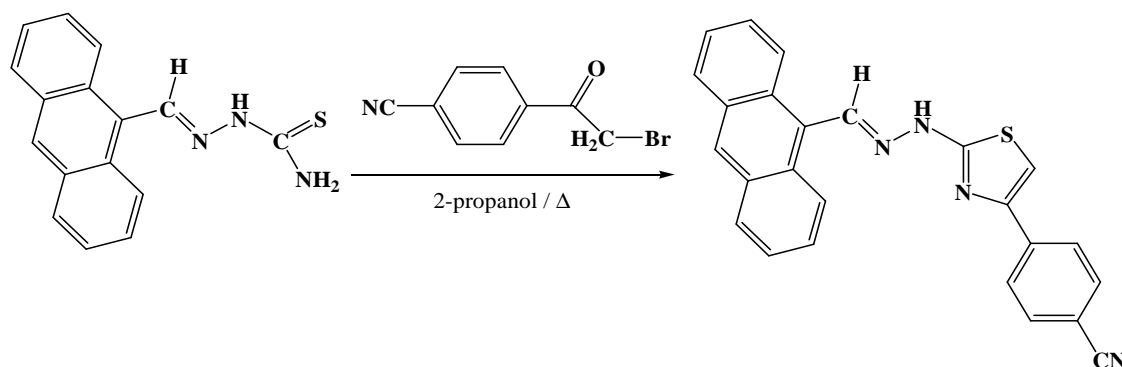
### 1-(anthracen-9-yl-methylene)-2-(4-(4-fluorophenyl)thiazol-2-yl)hydrazine



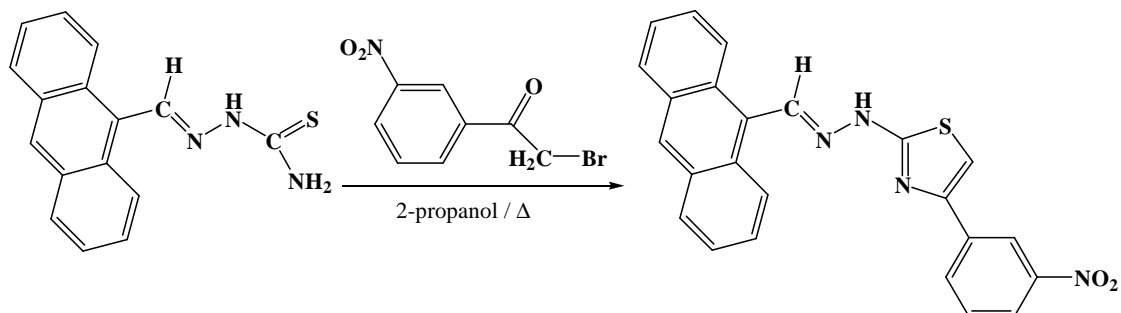
$^1\text{H-NMR}$ : (300 MHz, DMSO)  $\delta$ H 12.51 (brs, 1H, NH), 9.29 (s, 1H, CH=N), 8.7 (d+s, 3H, Ar-CH), 8.18 (d, 2H,  $J$ : 8.34, Ar-CH), 7.95 (t, 2H, Ar-CH), 7.64 (m, 4H, Ar-CH), 7.36 (s, 1H, thiazole), 7.28 (t, 2H, Ar-CH)

## EMAC 2028

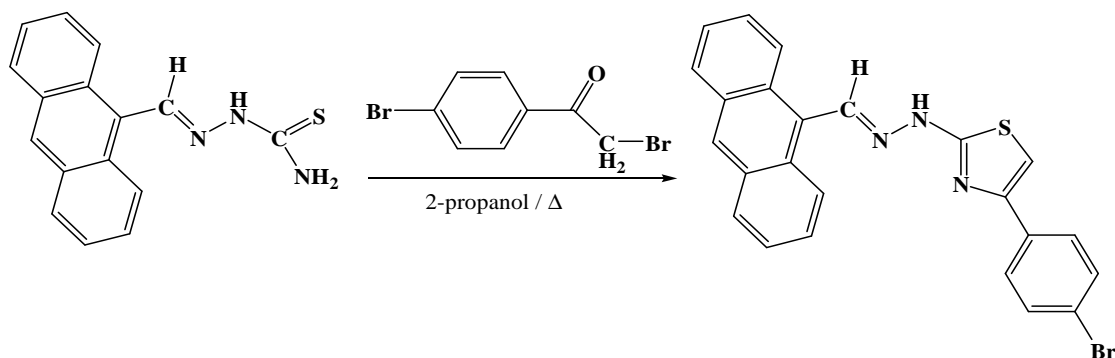
### 1-(anthracen-9-yl-methylene)-2-(4-(4-cyanophenyl)thiazol-2-yl) hydrazine



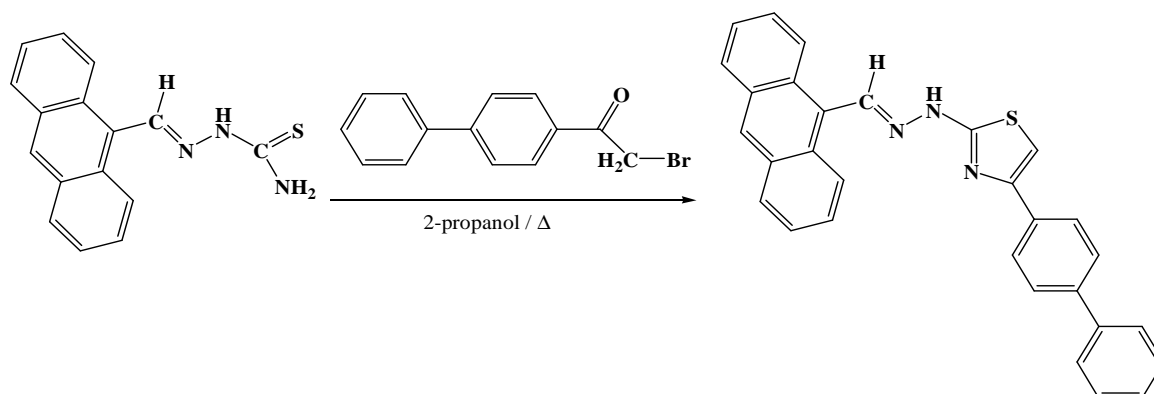
$^1\text{H-NMR}$ : (300 MHz, DMSO)  $\delta$ H 12.52 (brs, 1H, NH), 9.3 (s, 1H, CH=N); 8.71 (d+s, 3H, Ar-CH), 8.18 (d, 2H,  $J$ : 8.17, Ar-CH), 8.10 (d, 2H,  $J$ : 8.16, Ar-CH), 7.92 (d, 2H,  $J$ : 8.03, Ar-CH), 7.7 (s, 1H, thiazole), 7.64 (m, 4H, Ar-CH)

**EMAC 2029****1-(anthracen-9-yl-methylene)-2-(4-(3-nitrophenyl)thiazol-2-yl)hydrazine**

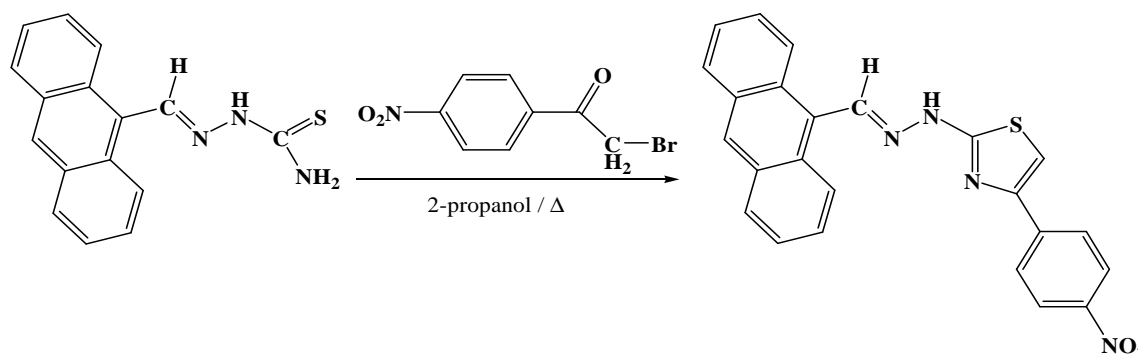
$^1\text{H-NMR}$ : (300 MHz, DMSO)  $\delta$ H 12.58 (brs, 1H, NH), 9.29 (s, 1H, CH=N), 8.71(d+s, 3H, Ar-CH), 8.37 (d, 1H,  $J$ : 7.84, Ar-CH), 8.19 (d, 2H,  $J$ : 8.01, Ar-CH), 7.68 (m, 8H, Ar-CH)

**EMAC 2030****1-(anthracen-9-yl-methylene)-2-(4-(4-bromophenyl)thiazol-2-yl)hydrazine**

$^1\text{H-NMR}$ : (300 MHz, DMSO)  $\delta$ H 12.46 (s, 1H, NH), 9.29 (s, 1H, CH=N), 8.71 (d+s, 3H,  $J$ : 8.34, Ar-CH), 8.18 (d, 2H,  $J$ : 8.35, Ar-CH), 8.42 (d, 2H,  $J$ : 8.51, Ar-CH), 7.58 (m, 6H, Ar-CH), 7.46 (s, 1H, thiazole)

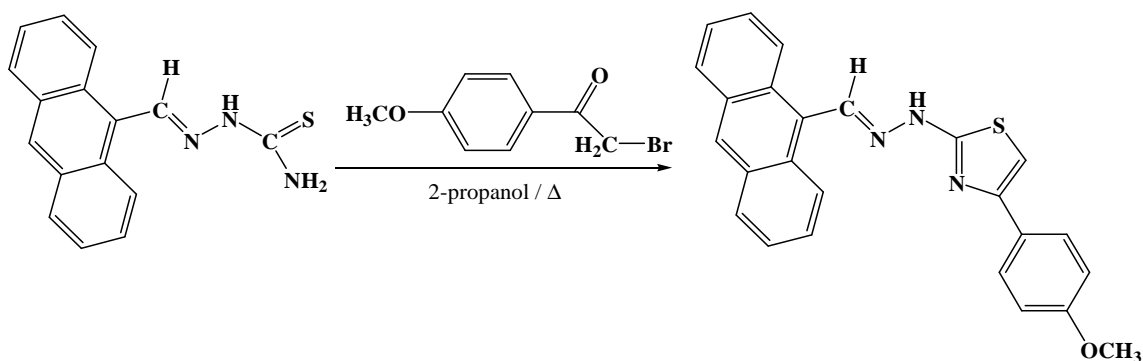
**EMAC 2031****1-(anthracen-9-yl-methylene)-2-(4-(4-phenylphenyl)thiazol-2-yl)hydrazine**

$^1\text{H-NMR}$ : (300 MHz, DMSO)  $\delta$ H 12.58 (s, 1H, NH), 9.31 (s, 1H, CH=N), 8.70 (d, 2H,  $J$ : 8.18, Ar-CH), 8.72 (s, 1H, Ar-CH), 8.18 (d, 2H,  $J$ : 8.35, Ar-CH), 8.01 (d, 2H, Ar-CH), 7.75 (m, 4H, Ar-CH), 7.64 (m, 4H, Ar-CH), 7.5 (t, 2H, Ar-CH), 7.44 (s, 1H, thiazole), 7.39 (t, 1H, Ar-CH)

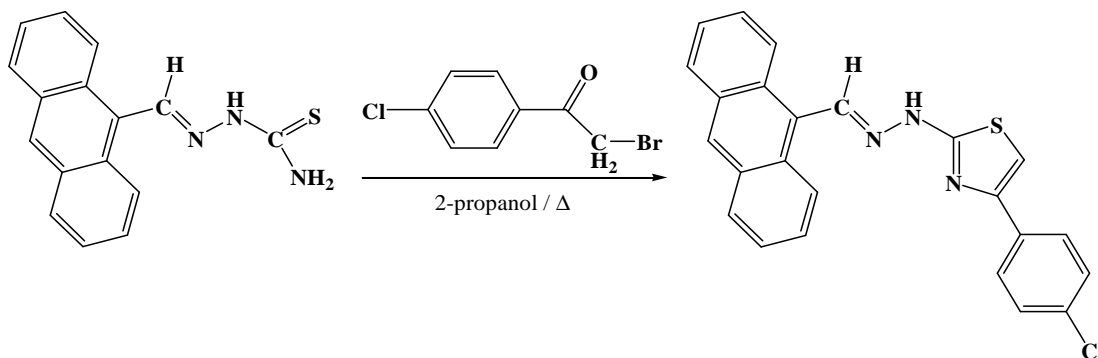
**EMAC 2032****1-(anthracen-9-yl-methylene)-2-(4-(4-nitrophenyl)thiazol-2-yl)hydrazine**

$^1\text{H-NMR}$ : (300 MHz, DMSO)  $\delta$ H 12.56 (brs, 1H, NH), 9.3 (s, 1H, CH=N), 8.7 (d+s, 3H, Ar-CH), 8.31 (d, 2H,  $J$ : 8.72, Ar-CH), 8.17 (d, 4H,  $J$ : 6.5, Ar-CH), 7.77 (s, 1H, thiazole), 7.63 (m, 4H, Ar-CH)



**EMAC 2033****1-(anthracen-9-yl-methylene)-2-(4-(4-methoxyphenyl)thiazol-2-yl)hydrazine**

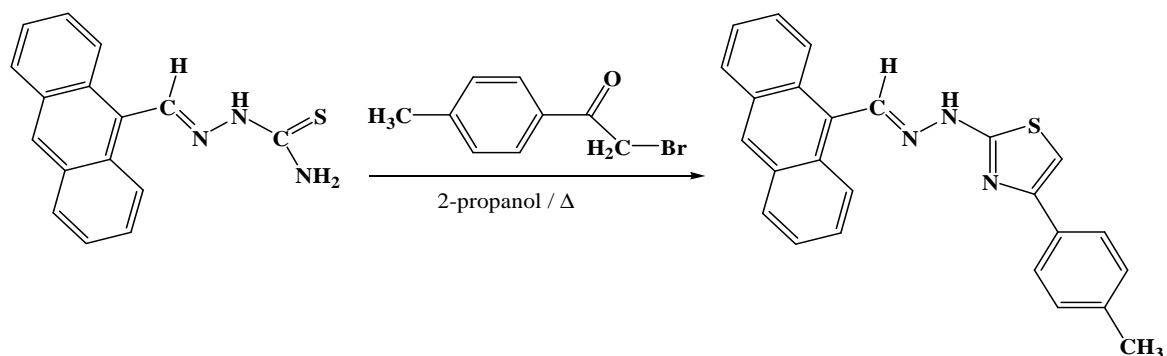
$^1\text{H-NMR}$ : (300 MHz, DMSO)  $\delta$ H 9.31 (s, 1H, CH=N), 8.72 (d+s, 3H,  $J$ : 8.18, Ar-CH), 8.18 (d, 2H,  $J$ : 8.01, Ar-CH), 7.84 (d, 2H,  $J$ : 8.68, Ar-CH), 7.65 (m, 4H, Ar-CH), 7.21 (s, 1H, thiazole), 7.01 (d, 2H,  $J$ : 8.68, Ar-CH), 3.82 (s, 1H,  $\text{OCH}_3$ )

**EMAC 2034****1-(anthracen-9-yl-methylene)-2-(4-(4-chlorophenyl)thiazol-2-yl)hydrazine**

$^1\text{H-NMR}$ : (300 MHz, DMSO)  $\delta$ H 12.45 (s, 1H, NH), 9.28 (s, 1H, CH=N), 8.7 (d+s, 3H, Ar-CH), 8.17 (d, 2H,  $J$ : 8.51, Ar-CH), 7.93 (d, 2H,  $J$ : 8.68, Ar-CH), 7.63 (m, 4H, Ar-CH), 7.50 (d, 2H,  $J$ : 6.68, Ar-CH), 7.44 (s, 1H, thiazole)

EMAC 2035

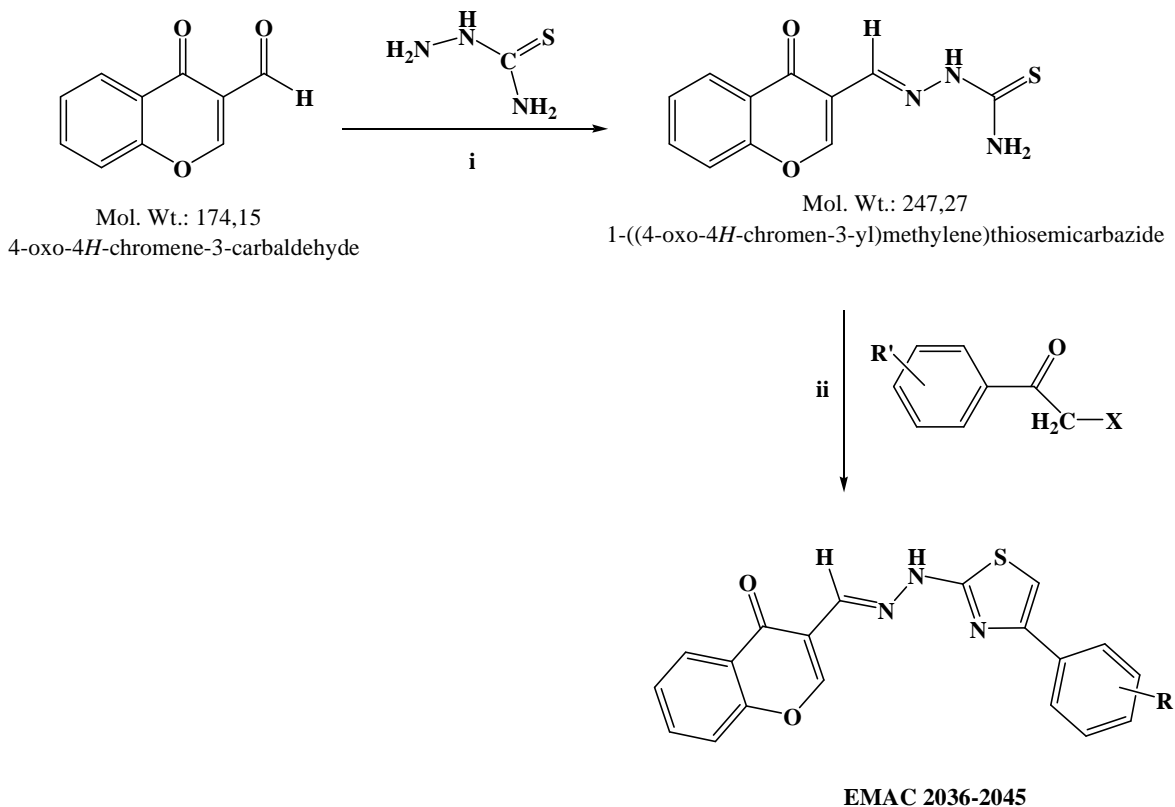
**1-(anthracen-9-yl-methylene)-2-(4-p-tolylthiazol-2-yl)hydrazine**



$^1\text{H-NMR}$ : (300 MHz, DMSO)  $\delta$ H 9.28 (s, 1H, CH=N), 8.7 (d+s, 3H, Ar-CH), 8.17 (d, 2H,  $J$ : 8.34, Ar-CH), 7.78, (d, 2H,  $J$ : 8.01, Ar-CH), 7.7 (m, 4H, Ar-CH), 7.29 (s, 1H, thiazole), 7.25 (d, 2H,  $J$ : 8.17, Ar-CH), 2.35 (s, 1H, CH<sub>3</sub>)

## COMPOUNDS EMAC 2036-2045

### General synthetic scheme:



R= 2,4-Cl, 4-F, 4-CN, 3-NO<sub>2</sub>, 4-Br, 4-C<sub>6</sub>H<sub>5</sub>, 4-NO<sub>2</sub>, 4-OCH<sub>3</sub>, 4-Cl, 4-CH<sub>3</sub>

**Scheme 4.** Synthesis of 3-[[2-[4-aryl-1,3-thiazol-2-yl]hydrazin-1-ylidene]methyl]-4H-chromen-4-one derivatives EMAC 2036-2045. Reagents: (i) 2-propanol, AcOH; (ii) 2-propanol, reflux condition.

### General procedure for 3-[[2-[4-aryl-1,3-thiazol-2-yl]hydrazin-1-ylidene]methyl]-4H-chromen-4-one derivatives

Chromone derivative were synthesized by a multi step reaction.

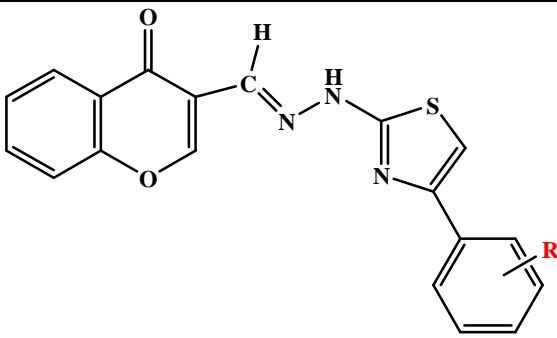
The first synthetic step leads to the formation of 1-[(4-oxo-4H-chromen-3-yl)methylidene]amino]thiourea by reacting 4-oxo-4H-chromene-3-carbaldehyde and thiosemicarbazide in 2-propanol and acid acetic as catalyst.

In the second step, the thiazole ring is formed by reaction between [(4-oxo-4H-chromen-3-yl)methylidene]amino]thiourea and differently substituted  $\alpha$ -halogen-acetophenones

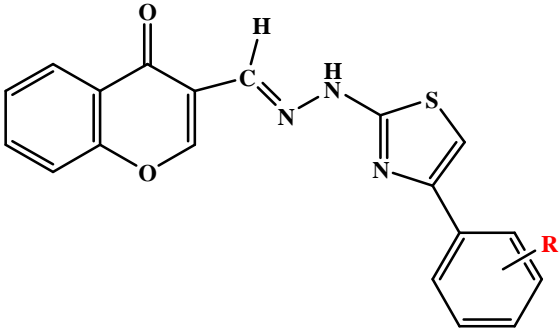
as outlined in the Scheme 4.

All synthesized compounds were characterised by analytical and spectral data as listed in Table 15 and 16.

**Table 15.** Chemical and physical data of derivatives EMAC 2036-2045

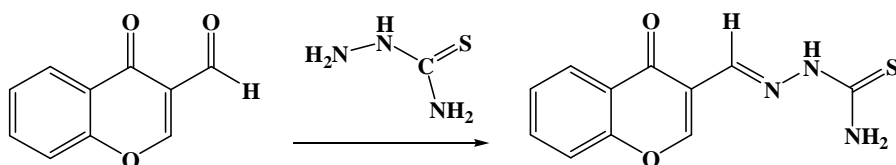
				
Compound	R	M.W.	Mp (C°)	% Yield
EMAC 2036	2,4-Cl	416.28	260	75
EMAC 2037	4-F	365.38	212-215	75
EMAC 2038	4-CN	372.4	275	95
EMAC 2039	3-NO <sub>2</sub>	392.39	260	90
EMAC 2040	4-Br	426.29	270	91
EMAC 2041	4-C <sub>6</sub> H <sub>5</sub>	423.49	237-239	83
EMAC 2042	4-NO <sub>2</sub>	392.39	282-284	99
EMAC 2043	4-OCH <sub>3</sub>	377.42	230	30
EMAC 2044	4-Cl	381.84	270	38
EMAC 2045	4-CH <sub>3</sub>	361.42	245	74

**Table 16.** Analytical data of derivatives EMAC 2036-2045

						
Compound	R	Reaction solvent	Crystallisation solvent	Aspect		Reaction time (h)
EMAC 2036	2,4-Cl	2-propanol	Acetonitrile/ Water	Crystalline solid	yellow	10
EMAC 2037	4-F	2-propanol	Acetonitrile/ Water	Crystalline solid	yellow	12
EMAC 2038	4-CN <sub>3</sub>	2-propanol	Acetonitrile/ Water	Crystalline solid	yellow	12
EMAC 2039	3-NO <sub>2</sub>	2-propanol	Acetonitrile/ Water	Crystalline solid	pale orange	24
EMAC 2040	4-Br	2-propanol	Acetonitrile/ Water	Crystalline solid	pale yellow	12
EMAC 2041	4-C <sub>6</sub> H <sub>5</sub>	2-propanol	Acetonitrile/ Water	Crystalline solid	pale pink	24
EMAC 2042	4-NO <sub>2</sub>	2-propanol	Acetonitrile/ Water	Crystalline solid	pale yellow	24
EMAC 2043	4-OCH <sub>3</sub>	2-propanol	Acetonitrile/ Water	Crystalline solid	pale yellow	24
EMAC 2044	4-Cl	2-propanol	Acetonitrile/ Water	Crystalline solid	white	24
EMAC 2045	4-CH <sub>3</sub>	2-propanol	Acetonitrile/ Water	Crystalline solid	pale yellow	24

According to this procedure the following compounds have been synthesised:

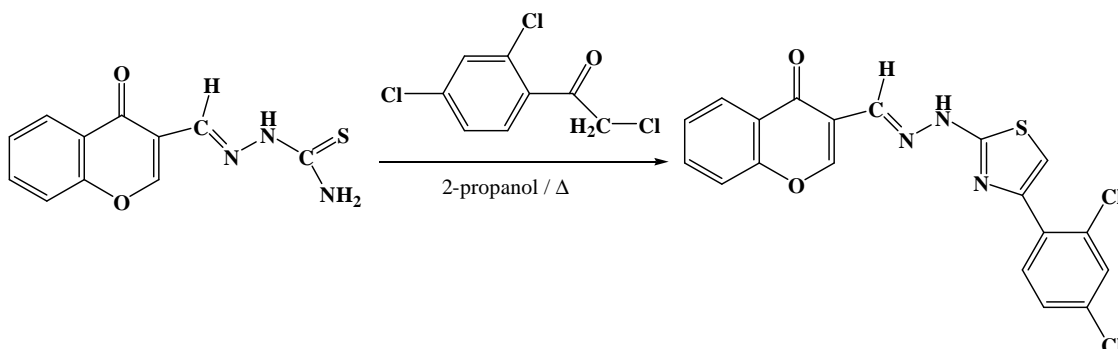
**1-((4-oxo-4H-chromen-3-yl)methylene)thiosemicarbazide**



M.W.: 247.27 g/mol; R.f.: 0.3 (DCM: methanol 20:1); M.P.: 235 °C; Yield: 97.42%  
MS (ESI+): 248.04 ([M+H]<sup>+</sup>)

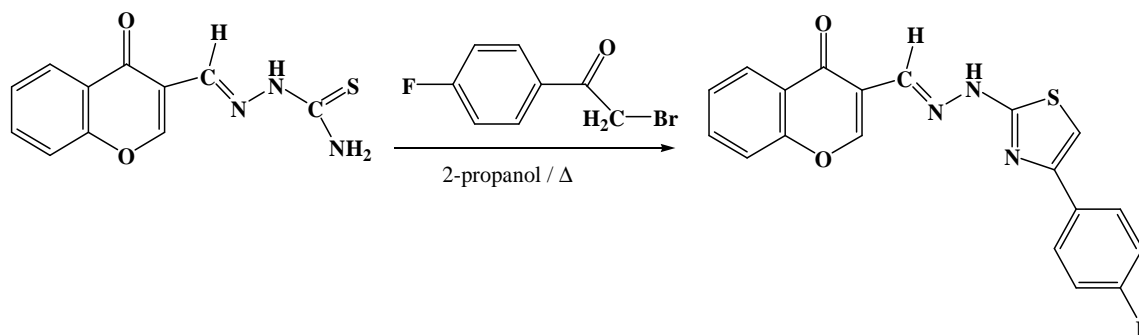
**EMAC 2036**

**3-[[2-[4-(2,4-dichlorophenyl)-1,3-thiazol-2-yl]hydrazin-1-ylidene]methyl]-4H-chromen-4-one**



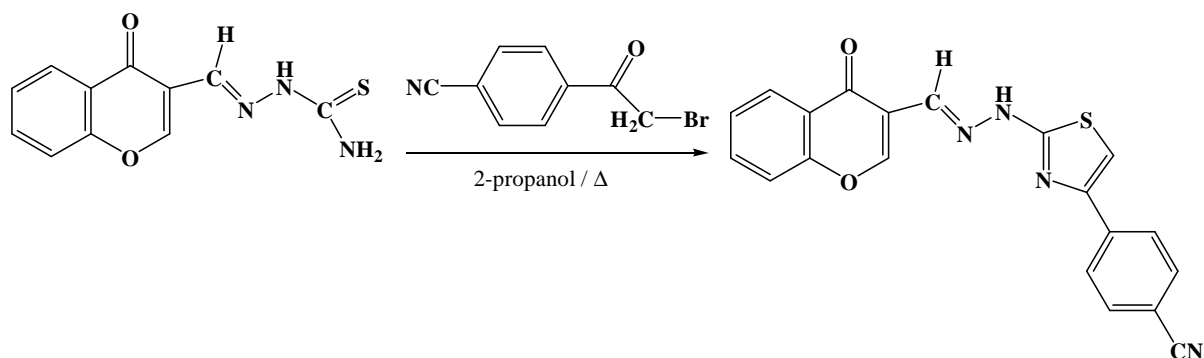
MS (ESI+): 416.00 ([M+H]<sup>+</sup>)

*The NMR analyses are in progress.*

**EMAC 2037****3-[[2-[4-(4-fluorophenyl)-1,3-thiazol-2-yl]hydrazin-1-ylidene]methyl]-4H-chromen-4-one**

MS (ESI+): 366.07 ( $[M+H]^+$ )

The NMR analyses are in progress.

**EMAC 2038****3-[[2-[4-(4-cyanophenyl)-1,3-thiazol-2-yl]hydrazin-1-ylidene]methyl]-4H-chromen-4-one**

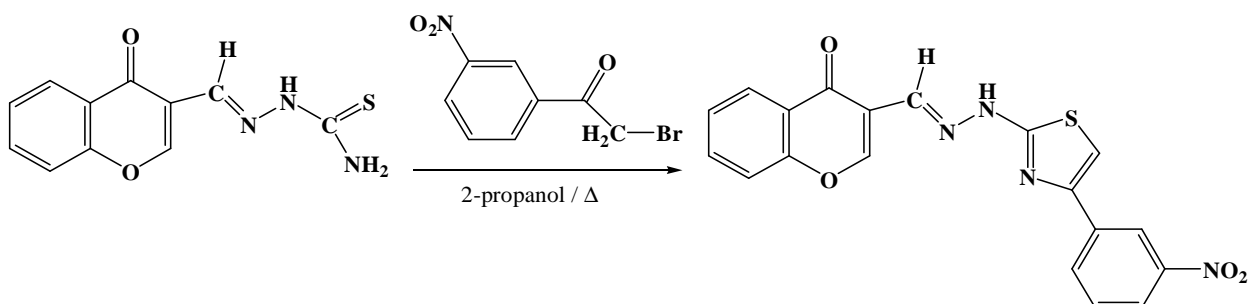
MS (ESI+): 373.07 ( $[M+H]^+$ )

The NMR analyses are in progress.



**EMAC 2039**

**3-[[2-[4-(3-nitrophenyl)-1,3-thiazol-2-yl]hydrazin-1-ylidene]methyl]-4H-chromen-4-one**

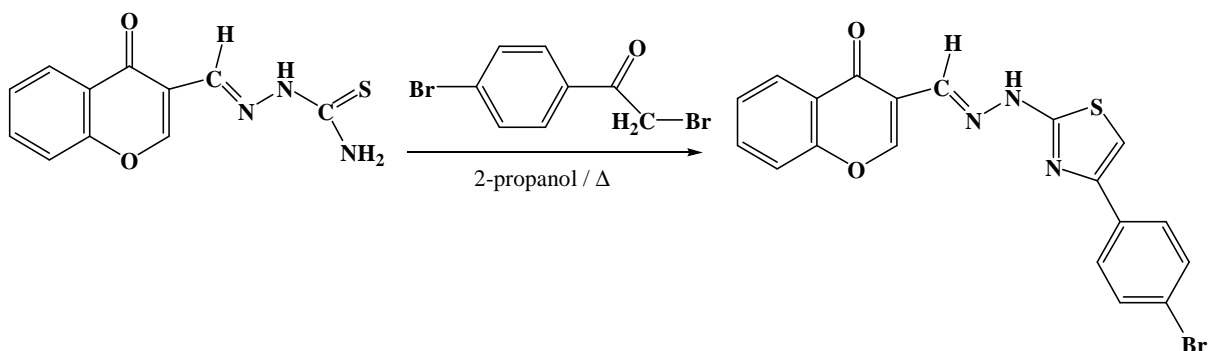


MS (ESI+): 393.06 ( $[M+H]^+$ )

The NMR analyses are in progress.

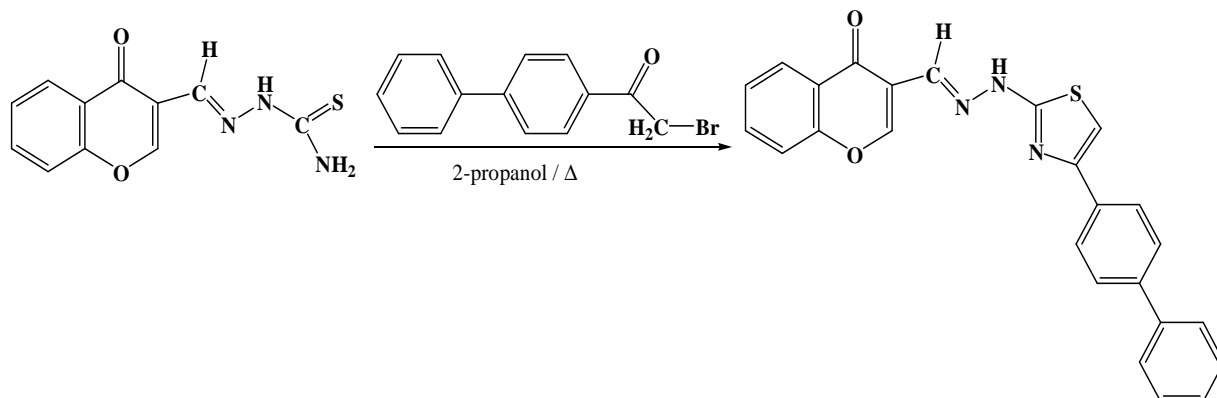
**EMAC 2040**

**3-[[2-[4-(4-bromophenyl)-1,3-thiazol-2-yl]hydrazin-1-ylidene]methyl]-4H-chromen-4-one**



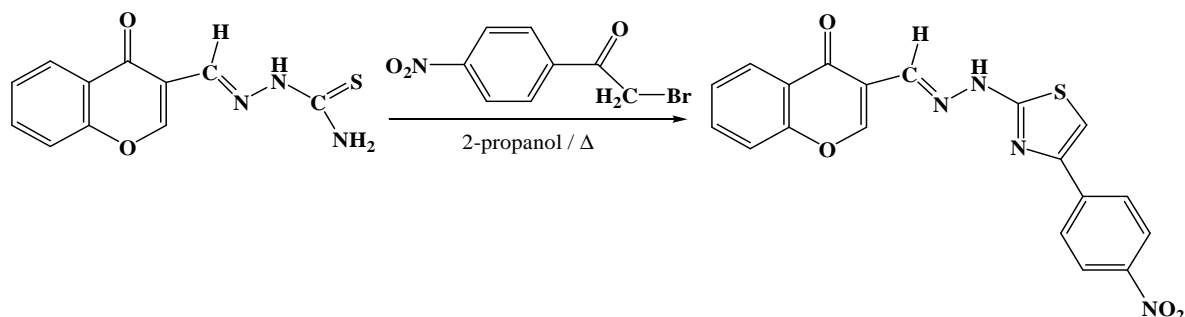
MS (ESI+): 424.98 - 426.98 ( $[M+H]^+$ )

The NMR analyses are in progress.

**EMAC 2041****3-[[2-[4-(4-phenylphenyl)-1,3-thiazol-2-yl]hydrazin-1-ylidene]methyl]-4H-chromen-4-one**

MS (ESI+): 424.11 ([M+H]<sup>+</sup>)

The NMR analyses are in progress.

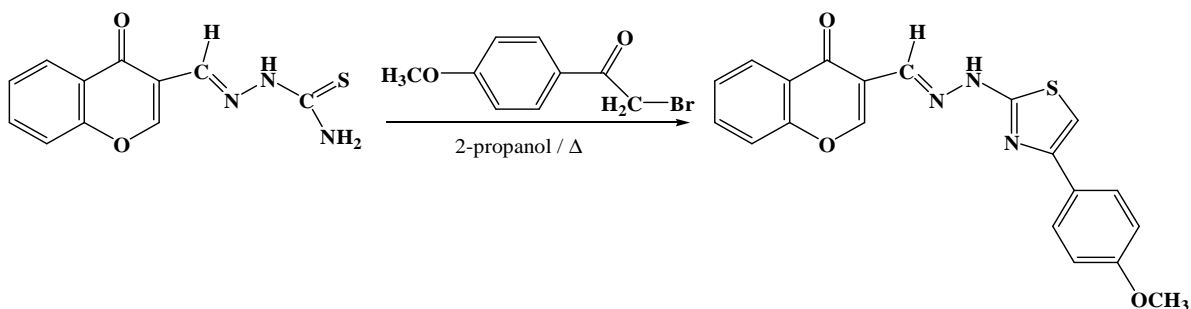
**EMAC 2042****3-[[2-[4-(4-nitrophenyl)-1,3-thiazol-2-yl]hydrazin-1-ylidene]methyl]-4H-chromen-4-one**

MS (ESI+): 393.06 ([M+H]<sup>+</sup>)

The NMR analyses are in progress.

MAC 2043

**3-[[2-[4-(4-methoxyphenyl)-1,3-thiazol-2-yl]hydrazin-1-ylidene]methyl]-4H-chromen-4-one**

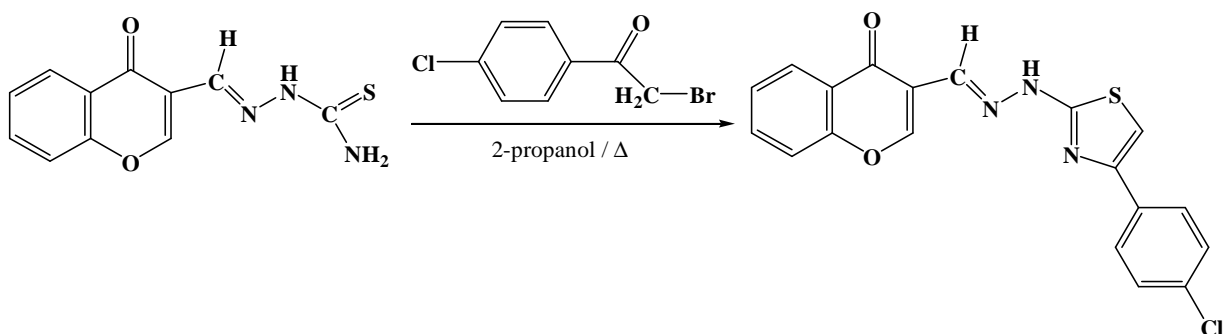


MS (ESI+): 378.09 ( $[M+H]^+$ )

The NMR analyses are in progress.

EMAC 2044

**3-[[2-[4-(4-chlorophenyl)-1,3-thiazol-2-yl]hydrazin-1-ylidene]methyl]-4H-chromen-4-one**

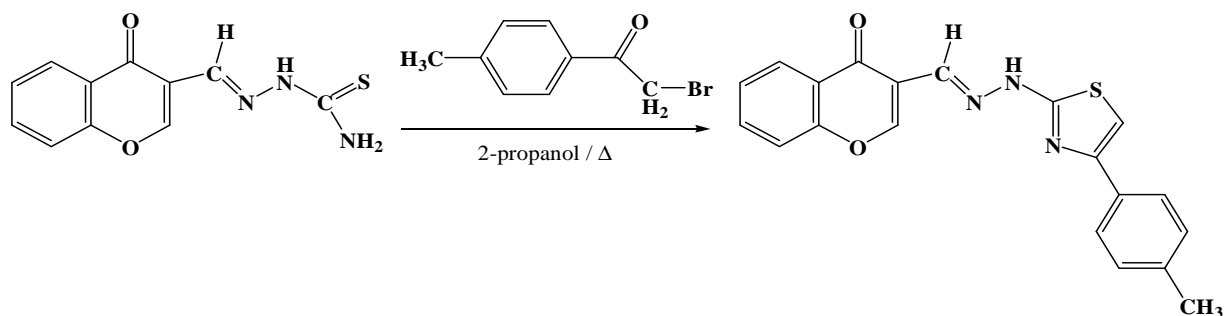


MS (ESI+): 383.03 ( $[M+H]^+$ )

The NMR analyses are in progress.

EMAC 2045

**3-[[2-[4-(4-methylphenyl)-1,3-thiazol-2-yl]hydrazin-1-ylidene]methyl]-4H-chromen-4-one**

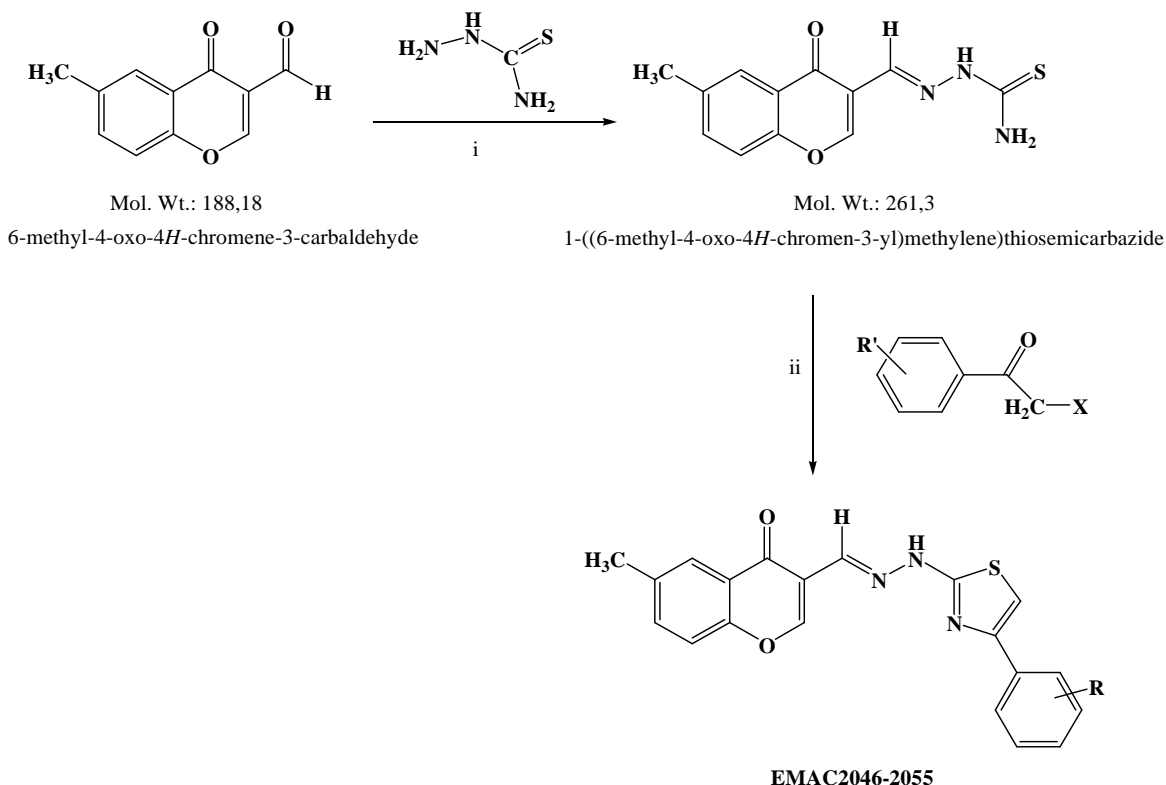


MS (ESI+): 362.9 ( $[M+H]^+$ )

*The NMR analyses are in progress.*

## COMPOUNDS EMAC 2046-2055

### General synthetic scheme:



R= 2,4-Cl, 4-F, 4-CN, 3-NO<sub>2</sub>, 4-Br, 4-C<sub>6</sub>H<sub>5</sub>, 4-NO<sub>2</sub>, 4-OCH<sub>3</sub>, 4-Cl, 4-CH<sub>3</sub>

**Scheme 5.** Synthesis of 3-[[2-[4-aryl-1,3-thiazol-2-yl]hydrazin-1-ylidene]methyl]-6-methyl-4H-chromen-4-one derivatives EMAC 2046-2055. Reagents: (i) 2-propanol, AcOH; (ii) 2-propanol, reflux condition.

### General procedure for 3-[[2-[4-aryl-1,3-thiazol-2-yl]hydrazin-1-ylidene]methyl]-6-methyl-4H-chromen-4-one derivatives

6-methyl-chromone derivative were synthesized by a multi step reaction.

The first synthetic step leads to the formation of 1-((6-methyl-4-oxo-4H-chromen-3-yl) methylene) thiosemicarbazide by reacting 4-oxo-4H-chromene-6-methyl-3-carbaldehyde and thiosemicarbazide in 2-propanol and acid acetic as catalyst.

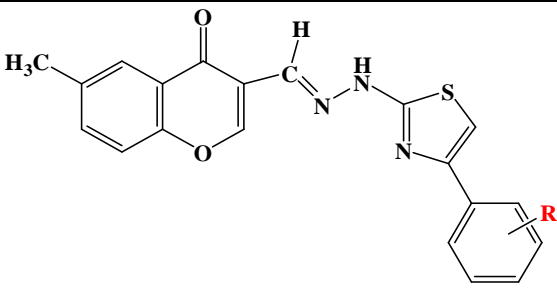
In the second step, the thiazole ring is formed by reaction between (E)-1-((6-methyl-4-oxo-4H-chromen-3-yl) methylene) thiosemicarbazide and differently substituted  $\alpha$ -halogenoacetophenones as outlined in the Scheme 5.

All synthesized compounds were characterised by analytical and spectral data as listed in Table 17 and 18.

**Table 17.** Chemical and physical data of derivatives EMAC 2046-2055

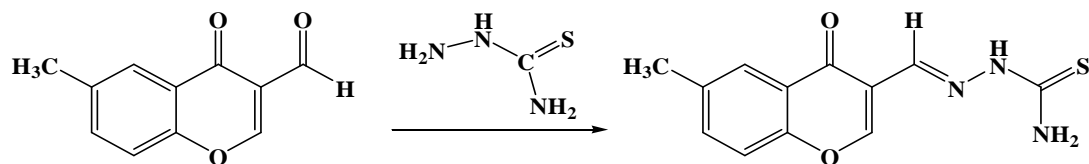
Compound	R	M.W.	Mp (C°)	% Yield
EMAC 2046	2,4-Cl	430.31	260	58
EMAC 2047	4-F	379.41	232	74
EMAC 2048	4-CN <sub>3</sub>	386.43	275	62
EMAC 2049	3-NO <sub>2</sub>	406.41	273-275	68
EMAC 2050	4-Br	440.31	244-245	76
EMAC 2051	4-C <sub>6</sub> H <sub>5</sub>	437.51	246-248	95
EMAC 2052	4-NO <sub>2</sub>	406.41	265-267	69
EMAC 2053	4-OCH <sub>3</sub>	391.44	235	63
EMAC 2054	4-Cl	395.86	237	74
EMAC 2055	4-CH <sub>3</sub>	375.44	249	79

**Table 18.** Analytical data of derivatives EMAC 2046-2055



Compound	R	Reaction solvent	Crystallisation solvent	Aspect	Reaction time (h)
EMAC 2036	2,4-Cl	2-propanol	Acetonitrile/ Water	Crystalline bright yellow solid	24
EMAC 2037	4-F	2-propanol	Acetonitrile/ Water	Crystalline pale pink solid	24
EMAC 2038	4-CN <sub>3</sub>	2-propanol	Acetonitrile/ Water	Crystalline pale yellow solid	24
EMAC 2039	3-NO <sub>2</sub>	2-propanol	Acetonitrile/ Water	Crystalline bright yellow solid	24
EMAC 2040	4-Br	2-propanol	Acetonitrile/ Water	Crystalline pale yellow solid	24
EMAC 2041	4-C <sub>6</sub> H <sub>5</sub>	2-propanol	Acetonitrile/ Water	Crystalline paleyellow solid	24
EMAC 2042	4-NO <sub>2</sub>	2-propanol	Acetonitrile/ Water	Crystalline bright yellow solid	24
EMAC 2043	4-OCH <sub>3</sub>	2-propanol	Acetonitrile/ Water	Crystalline white solid	24
EMAC 2044	4-Cl	2-propanol	Acetonitrile/ Water	Crystalline pale yellow solid	24
EMAC 2045	4-CH <sub>3</sub>	2-propanol	Acetonitrile/ Water	Crystalline pale pink solid	24

**1-((6-methyl-4-oxo-4H-chromen-3-yl)methylene)thiosemicarbazide**



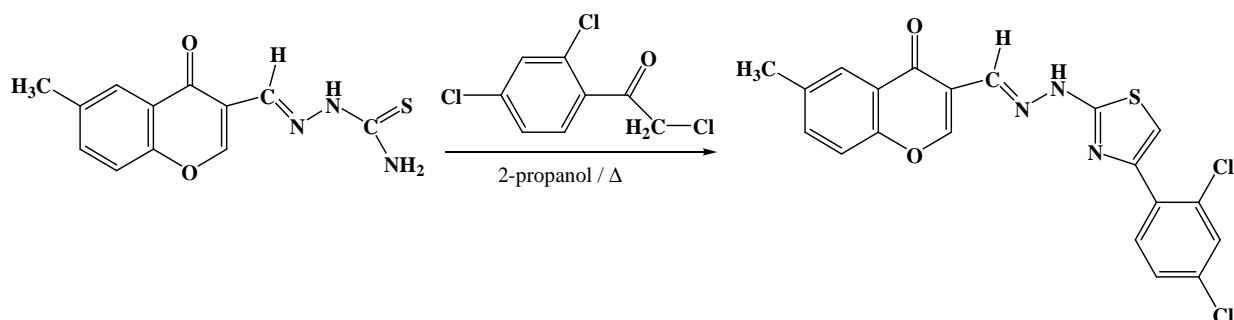
M.W.: 261.3 g/mol; R.f.: 0.26 (DCM: methanol 20:1); M.P.: 234 °C; Yield: 80 %

MS (ESI+): 262.06 ([M+H]<sup>+</sup>)

*The NMR analyses are in progress.*

**EMAC 2046**

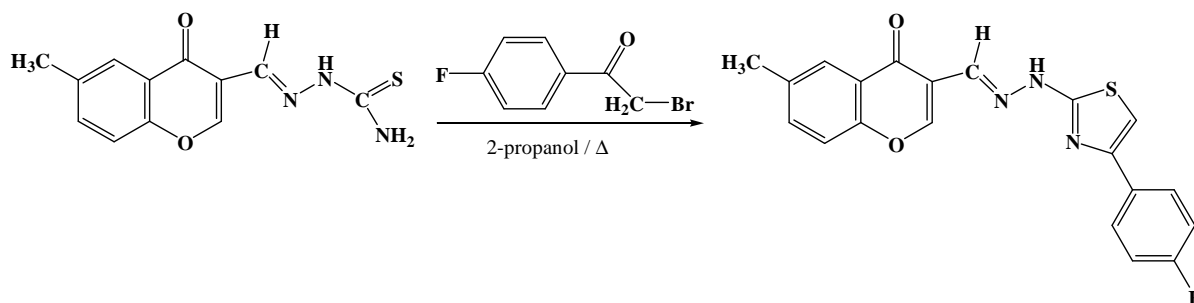
**3-[[2-[4-(2,4-dichlorophenyl)-1,3-thiazol-2-yl]hydrazin-1-ylidene]methyl]-6-methyl-4H-chromen-4-one**



MS (ESI+): 430.01 ([M+H]<sup>+</sup>)

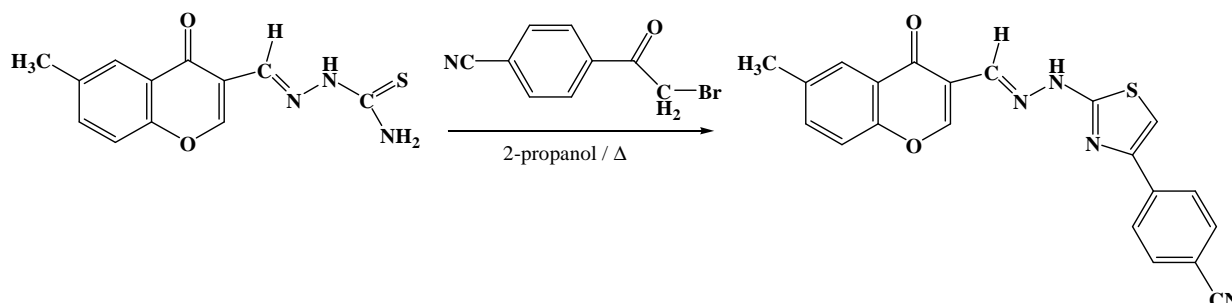
*The NMR analyses are in progress.*



**EMAC 2047****3-[[2-[4-(4-fluorophenyl)-1,3-thiazol-2-yl]hydrazin-1-ylidene]methyl]-6-methyl-4H-chromen-4-one**

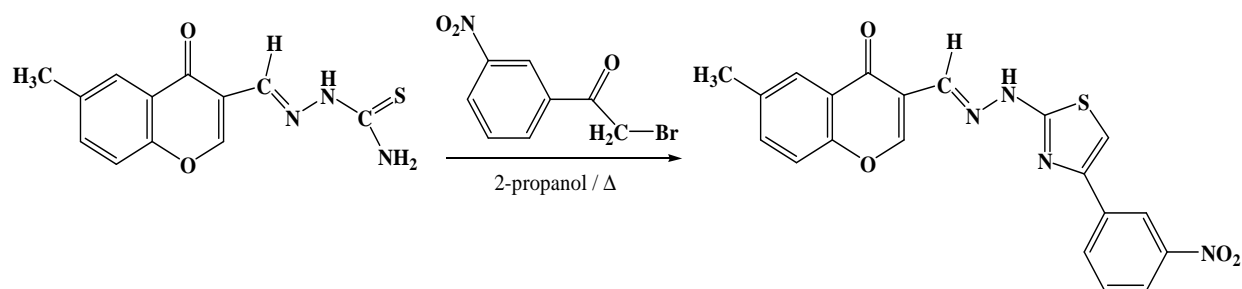
MS (ESI+): 380.08 ( $[M+H]^+$ )

The NMR analyses are in progress.

**EMAC 2048****3-[[2-[4-(4-cyanophenyl)-1,3-thiazol-2-yl]hydrazin-1-ylidene]methyl]-6-methyl-4H-chromen-4-one**

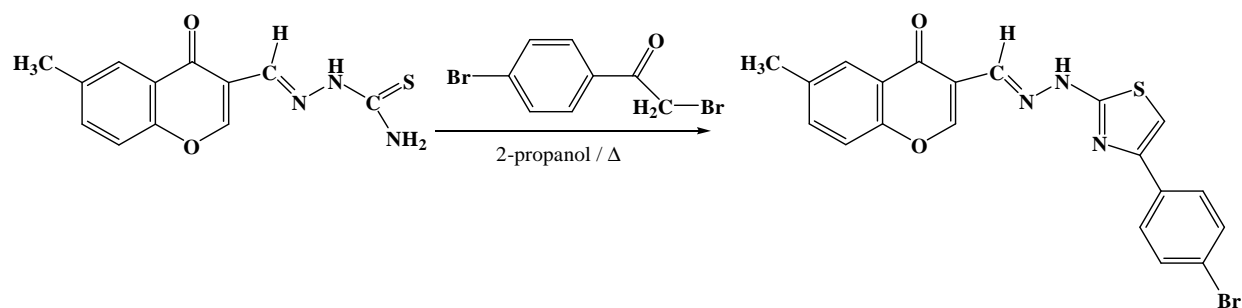
MS (ESI+): 387.09 ( $[M+H]^+$ )

The NMR analyses are in progress.

**EMAC 2049****3-[[2-[4-(3-nitrophenyl)-1,3-thiazol-2-yl]hydrazin-1-ylidene]methyl]-6-methyl-4H-chromen-4-one**

MS (ESI+): 407.08 ( $[M+H]^+$ )

The NMR analyses are in progress.

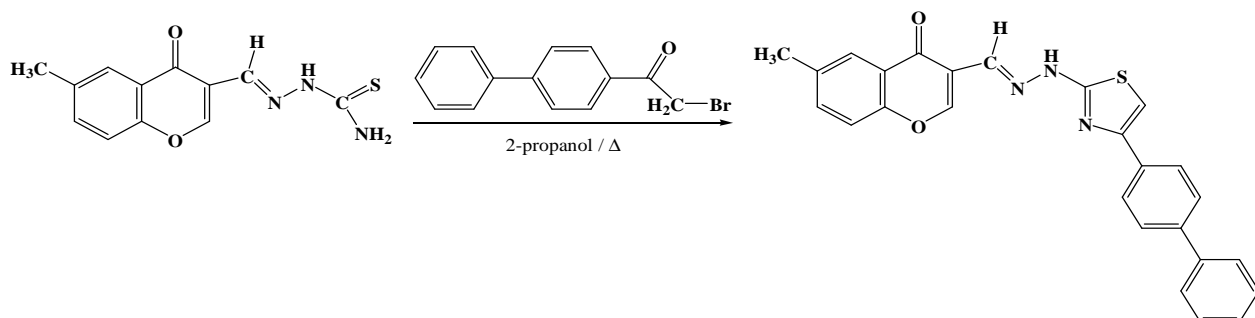
**EMAC 2050****3-[[2-[4-(4-bromophenyl)-1,3-thiazol-2-yl]hydrazin-1-ylidene]methyl]-6-methyl-4H-chromen-4-one**

MS (ESI+): 439.00 - 441.00 ( $[M+H]^+$ )

The NMR analyses are in progress.

**EMAC 2051**

**3-[[2-[4-(4-phenylphenyl)-1,3-thiazol-2-yl]hydrazin-1-ylidene]methyl]-6-methyl-4H-chromen-4-one**

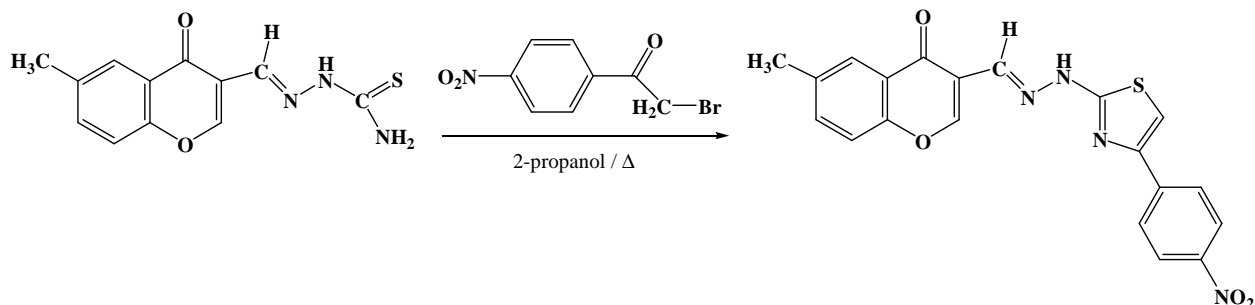


MS (ESI+): 438.13 ( $[M+H]^+$ )

The NMR analyses are in progress.

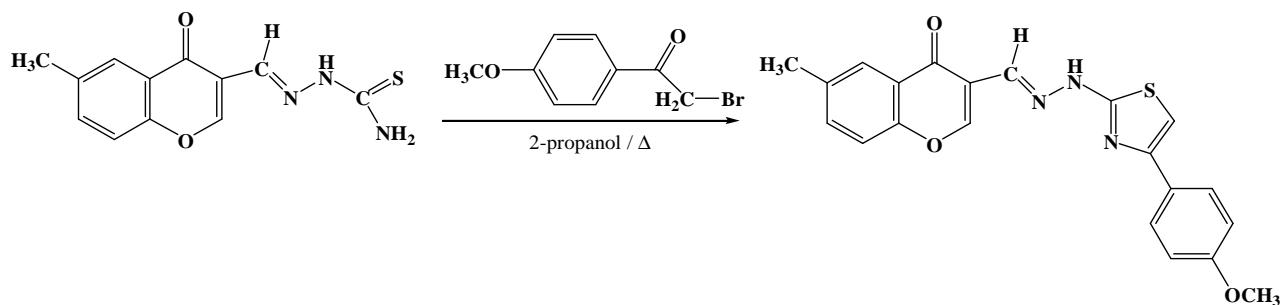
**EMAC 2052**

**3-[[2-[4-(4-nitrophenyl)-1,3-thiazol-2-yl]hydrazin-1-ylidene]methyl]-6-methyl-4H-chromen-4-one**



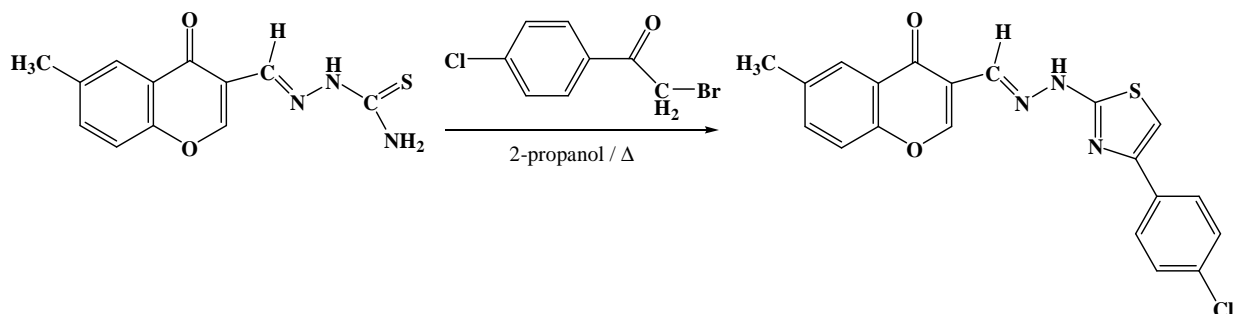
MS (ESI+): 407.08 ( $[M+H]^+$ )

The NMR analyses are in progress.

**EMAC 2053****3-{{2-[4-(4-methoxyphenyl)-1,3-thiazol-2-yl]hydrazin-1-ylidene}methyl]-6-methyl-4H-chromen-4-one**

MS (ESI+): 392.10 ( $[M+H]^+$ )

The NMR analyses are in progress.

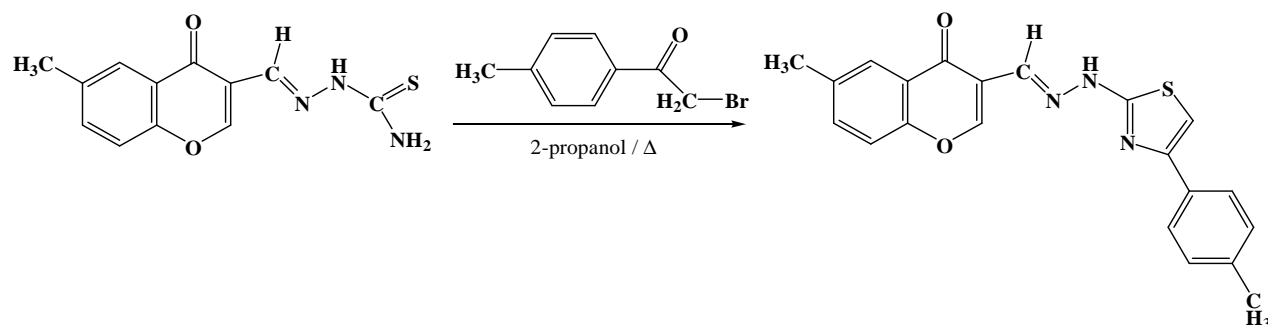
**EMAC 2054****3-{{2-[4-(4-chlorophenyl)-1,3-thiazol-2-yl]hydrazin-1-ylidene}methyl]-6-methyl-4H-chromen-4-one**

MS (ESI+): 396.05( $[M+H]^+$ )

The NMR analyses are in progress.

EMAC 2055

**3-[[2-[4-(4-methylphenyl)-1,3-thiazol-2-yl]hydrazin-1-ylidene]methyl]-6-methyl-4H-chromen-4-one**

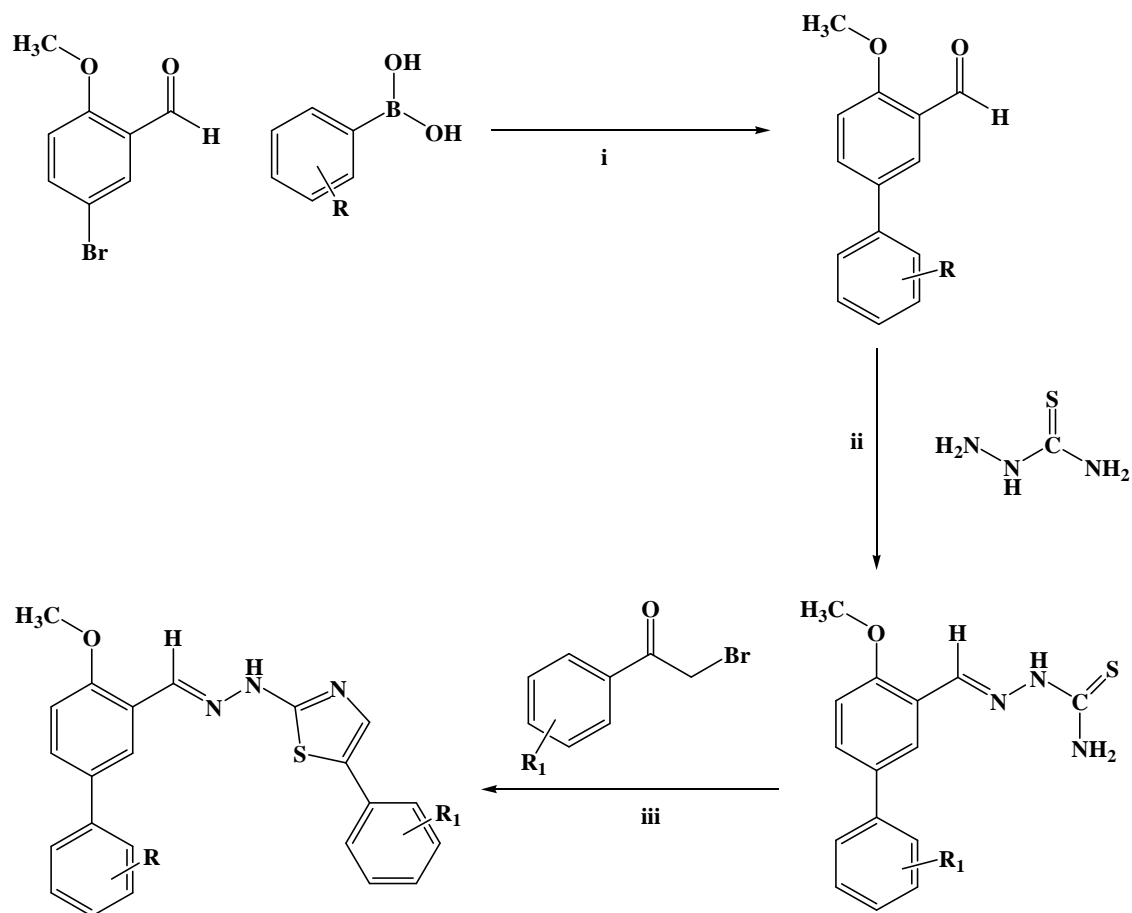


MS (ESI+): 376.10 ( $[M+H]^+$ )

*The NMR analyses are in progress.*

## COMPOUNDS EMAC 2056-2071

### General synthetic scheme:



EMAC 2056- 2071

R: H, 2-CN, 4-F, 2-Br

R': 4-OCH<sub>3</sub>, 3,4-Cl, 4-Cl, 4-NO<sub>2</sub>

**Scheme 6.** Synthesis of 3-[[2-[4-aryl-1,3-thiazol-2-yl]hydrazin-1-ylidene]methyl]-6-methyl-4H-chromen-4-one derivatives EMAC 2056-2071. Reagents: (i) Dimethoxyethane / argon flow, Pd(PPh<sub>3</sub>)<sub>4</sub>, Na<sub>2</sub>CO<sub>3</sub> 2M, 110°C; (ii) n-propanol, AcOH, R.T.; (iii) n-propanol, R.T.

Compounds EMAC 2056-2071 were synthesized by a multi step reaction.

The first synthetic step leads to the formation of 5-aryl-2-methoxybenzaldehyde by reacting 5-bromo-2-methoxybenzaldehyde with differently substituted phenylboronic acids according to slightly modified Suzuki coupling reaction condition. [210]

In the second step, thiosemicarbazones are formed by reaction between 5-aryl-2-methoxybenzaldehyde, thiosemicarbazide and catalytic amount of  $\text{CH}_3\text{COOH}$  in n-propanol at room temperature. Finally, in the third step the thiazole ring is formed by reaction of the appropriate thiosemicarbazones with substituted  $\alpha$ -halogenacetophenones, as outlined in the Scheme 6.

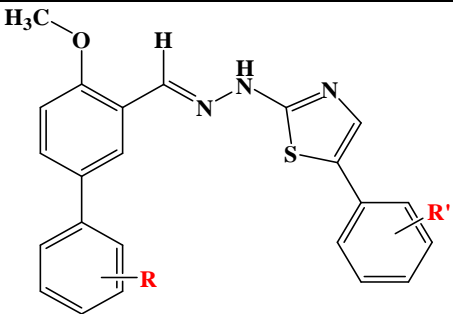
All samples were measured in  $\text{DMSO-}d_6$  solvent at 278.1 K temperature on a Bruker AVANCE III spectrometer.

In the signal assignments the proton and carbon chemical shifts are referred to the solvent ( $^1\text{H}$ :  $\delta = 2.49$  ppm,  $^{13}\text{C}$  dowfield methyl signal:  $\delta=34.89$  ppm respectively).

Melting points were determined on a Büchi-540 capillary melting points apparatus and are uncorrected.

*These compounds were synthesised and analysed during my research period in Budapest under the supervision of Prof. Peter Matyus.*

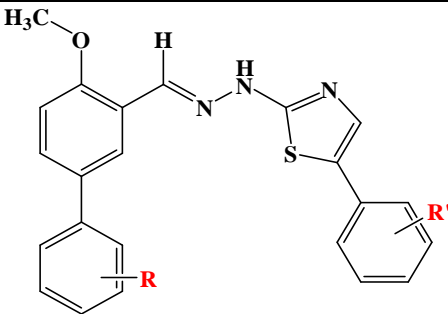
All synthesized compounds were characterised by analytical and spectral data as listed in Table 19 and 20.

**Table 19.** Chemical and physical data of derivatives EMAC 2056-2071


Compound	R	R'	M.W.	Mp (C°)	% Yield
EMAC 2056	H	4-OCH <sub>3</sub>	415.51	209 decomposition	81.5
EMAC 2057	H	3,4-Cl	454.37	213 decomposition	92
EMAC 2058	H	4-Cl	419.93	215 decomposition	91.3
EMAC 2059	H	4-NO <sub>2</sub>	430.48	208 decomposition	89.4
EMAC 2060	2-CONH <sub>2</sub>	4-OCH <sub>3</sub>	458.53	203 decomposition	70.5
EMAC 2061	2-CONH <sub>2</sub>	3,4-Cl	497.4	221 decomposition	77.7
EMAC 2062	2-CONH <sub>2</sub>	4-Cl	462.95	222 decomposition	84.7
EMAC 2063	2-CONH <sub>2</sub>	4-NO <sub>2</sub>	473.5	208 decomposition	89.4
EMAC 2064	4-F	4-OCH <sub>3</sub>	433.5	193 decomposition	83.65
EMAC 2065	4-F	3,4-Cl	472.36	220 decomposition	91.4
EMAC 2066	4-F	4-Cl	437.92	218 decomposition	98
EMAC 2067	4-F	4-NO <sub>2</sub>	448.47	233 decomposition	91
EMAC 2068	2-Br	4-OCH <sub>3</sub>	494.4	186 decomposition	82.3
EMAC 2069	2-Br	3,4-Cl	533.27	225 decomposition	88
EMAC 2070	2-Br	4-Cl	498.82	235 decomposition	87
EMAC 2071	2-Br	4-NO <sub>2</sub>	509.38	237 decomposition	94



**Table 20.** Analytical data of derivatives EMAC 2056-2071

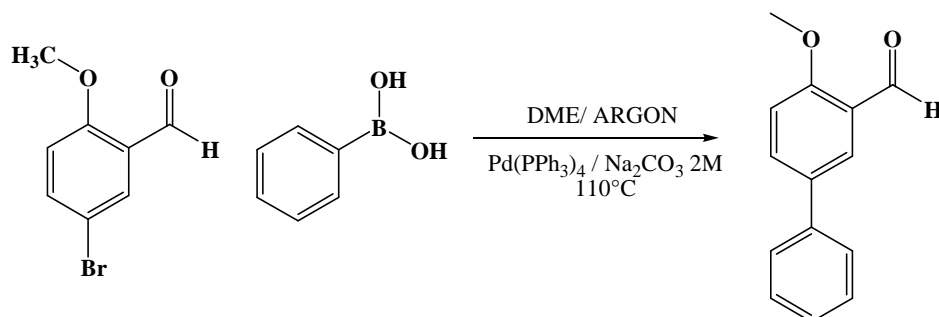
Compound			Reaction solvent	Crystallisation solvent	Aspect	Reaction time (h)
	R	R'				
EMAC 2056	H	4-OCH <sub>3</sub>	n-propanol	Ethanol	Fluffy yellow solid	4
EMAC 2057	H	3,4-Cl	n-propanol	Water/Ethanol	Pale yellow solid	8
EMAC 2058	H	4-Cl	n-propanol	Water/Ethanol	Pale yellow solid	7
EMAC 2059	H	4-NO <sub>2</sub>	n-propanol	Water/Ethanol	Orange solid	5
EMAC 2060	2-CONH <sub>2</sub>	4-OCH <sub>3</sub>	n-propanol	Ethanol	Yellow solid	15
EMAC 2061	2-CONH <sub>2</sub>	3,4-Cl	n-propanol	Ethanol	Pale pink solid	18
EMAC 2062	2-CONH <sub>2</sub>	4-Cl	n-propanol	Ethanol	Yellow solid	18
EMAC 2063	2-CONH <sub>2</sub>	4-NO <sub>2</sub>	n-propanol	Water/Ethanol	Orange solid	18
EMAC 2064	4-F	4-OCH <sub>3</sub>	n-propanol	Water/Ethanol	Pale yellow solid	4
EMAC 2065	4-F	3,4-Cl	n-propanol	Water/Ethanol	Pale yellow powder	4
EMAC 2066	4-F	4-Cl	n-propanol	Ethanol	Pale yellow solid	4
EMAC 2067	4-F	4-NO <sub>2</sub>	n-propanol	Water/Ethanol	Gold solid	8
EMAC 2068	2-Br	4-OCH <sub>3</sub>	n-propanol	Ethanol	Pale yellow solid	8
EMAC 2069	2-Br	3,4-Cl	n-propanol	Ethanol	Pale yellow solid	4
EMAC 2070	2-Br	4-Cl	n-propanol	Water/Ethanol	Pale yellow solid	10
EMAC 2071	2-Br	4-NO <sub>2</sub>	n-propanol	Water/Ethanol	Yellow-orange solid	4

### General procedure for Suzuki cross-coupling reaction.

The ortho-halogen compound (10 mmol) was dissolved in dimethoxyethane (15 mL), and Pd(PPh<sub>3</sub>)<sub>4</sub> (577.8 mg, 0.50 mmol,) was added to the solution at room temperature under argon flow. After stirring the mixture at room temperature for 10 min, 2-formylphenylboronic acid (2.249 g, 15 mmol,) and aq 2M Na<sub>2</sub>CO<sub>3</sub> solution (10.6 mL) were added and the reaction mixture was refluxed at 110 °C (oil temperature). When the reaction was complete (monitored by TLC, eluent: n-hexane - ethyl acetate 4:1), the reaction mixture was cooled and poured onto ice (100 g). The solution was filtered on Celite and washed with ethyl acetate (100 mL). The aqueous phase was extracted with ethyl acetate (3×40 mL). The combined organic layers were washed with water (1×20 mL), dried over MgSO<sub>4</sub>, evaporated under reduced pressure. The oily residue was purified by flash column chromatography on silica gel (eluent: n-hexane - ethyl acetate 5:1). [210]

According to this procedure the following compounds have been synthesised:

#### 2-methoxy-5-phenylbenzaldehyde

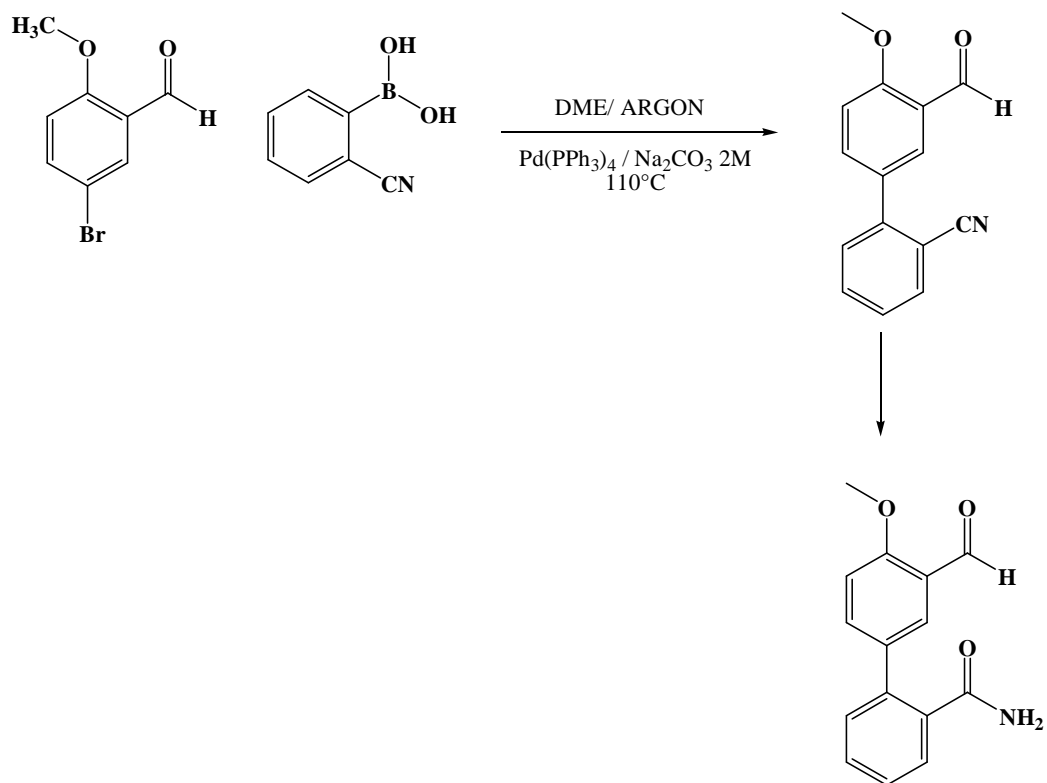


M.W.: 212.24 g/mol; R.f.: 0.82 (exane-ethylacetate 1;1); HPLC: 97.336%; M.P.: 77°C-78°C; Yield:98.8%

NMR: <sup>1</sup>H-NMR (500 MHz, DMSO) δH 3.97 ( s, 3H, OCH<sub>3</sub>), 7.34 ( d, 1H, Ar-CH, J: 8.5), 7.36 ( m, 1H, J: 8, Ar-CH) 7.46 ( t, 2H, J: 8, Ar-CH) 7.65 ( d, 2H, J: 8, Ar-CH), 7.93 ( s, 1H, J: 2.5, Ar-CH), 7.98 ( d, 1H, J: 8, J: 2.5, Ar-CH) 10.4 ( s,1H, CHO).

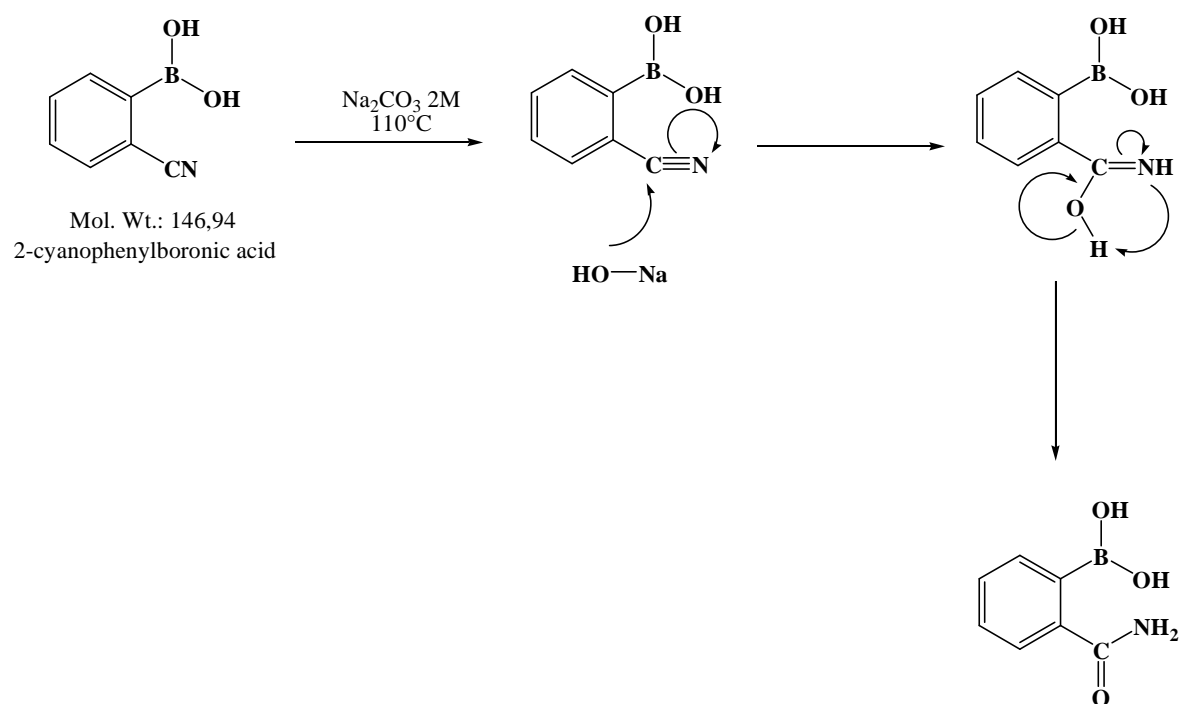
<sup>13</sup>C-NMR (500 MHz, DMSO) δ 56.2 ( 1C, OCH<sub>3</sub> ), 113.5 ( 1C, phenyl), 124.3, ( 1C, phenyl), 125.6 ( 1C, phenyl), 126.3 ( 2C, phenyl), 127.4 ( 1C, phenyl), 129.0 ( 2C, phenyl), 132.6 ( 1C, phenyl), 134.5 ( 1C, phenyl), 138.7 ( 1C, phenyl), 161.0 ( 1C, phenyl), 189.1 ( 1C, aldehyde).

### 2-(3-formyl-4-methoxyphenyl)benzamide



In this particular case, the hydrolysis of CN group into CONH<sub>2</sub> group is observed.

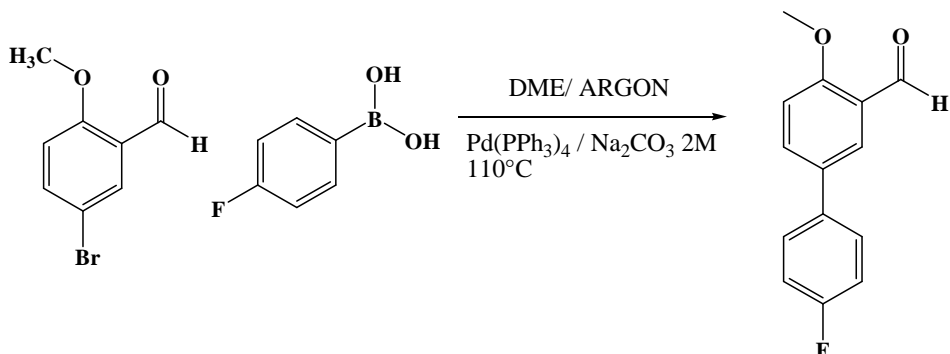
This is probably due to an hydrolysis reaction mediated by the basic reaction media according to the following mechanism:



M.W.: 255.28 g/mol; R.f.: 0.29 (exane-ethylacetate 1:7); HPLC: 98,00%; M.P.:  $140^\circ\text{C}$ ; Yield: 87.2%

$^1\text{H-NMR}$  (500 MHz, DMSO)  $\delta_{\text{H}}$  3.96 (s, 1H,  $\text{OCH}_3$ ), 7.34 (bs, 2H,  $\text{NH}_2$ ), 7.29 (d, 1H, J: 8.5, Ar-CH), 7.37 (m, 1H, Ar-CH), 7.40 (m, 1H, Ar-CH), 7.45 (m, 1H, Ar-CH), 7.48 (m, 1H, Ar-CH), 7.70 (m, 1H, J: 8.5, J: 2.5, Ar-CH), 7.71 (bs, 2H,  $\text{NH}_2$ ), 7.74 (d, 1H, J: 2.5, Ar-CH), 10.39 (s, 1H, COH).

**5-(4-fluorophenyl)-2-methoxybenzaldehyde**

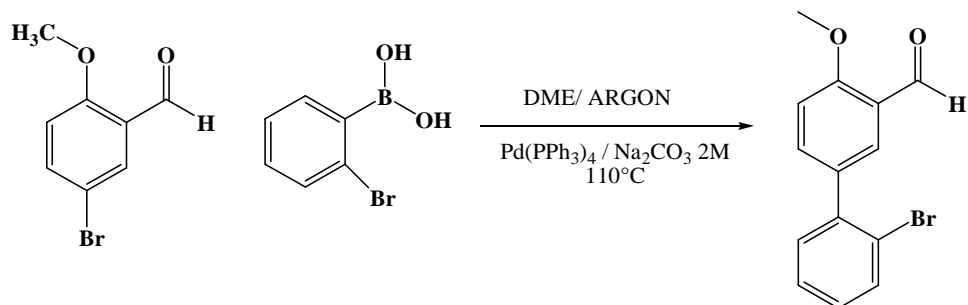


M.W.: 230.23 g/mol; R.f.: 0.41 (exane-ethylacetate 2,5:1); HPLC: 99.038%; M.P.: 81°C;  
Yield: 88.60%

<sup>1</sup>H-NMR (500 MHz, DMSO) δH 3.96 (s, 3H, OCH<sub>3</sub>), 7.28 (m, 2H, J: 9, Ar-CH), 7.33 (d, 1H, J: 8.5, Ar-CH), 7.70 (m, 2H, Ar-CH), 7.90 (d, 1H, J:2.5, Ar-CH), 7.96 (dd, 1H, J: 8.5, J: 2.5, Ar-CH), 10.39 (s, 1H, CHO).

<sup>13</sup>C-NMR (500 MHz, DMSO) δ 56.2 (1C, OCH<sub>3</sub>), 113.5 (1C, phenyl), 115.8 (2C, phenyl), 124.3 (1C, phenyl), 125.6 (1C, phenyl), 128.3 (2C, phenyl), 131.6 (1C, phenyl), 134.4 (1C, phenyl), 135.2 (1C, phenyl), 160.9 (1C, phenyl), 162.7 (1C, phenyl), 189.1 (1C, CHO).

### 5-(2-bromophenyl)-2-methoxybenzaldehyde



M.W.: 291.14 g/mol; R.f.: 0.43 (exane-ethylacetate 4:1); HPLC: 94.15%; M.P.: 106°C-107°C; Yield: 23.36%

NMR: <sup>1</sup>H-NMR (500 MHz, DMSO) δH 3.98 (s, 3H, OCH<sub>3</sub>), 7.32 (m, 1H, J: 8, Ar-CH), 7.33 (d, 1H, J: 8.5, Ar-CH), 7.40 (m, 1H, J: 8, J: 2, J: 6, Ar-CH), 7.47 (m, 1H, J: 2, Ar-CH), 7.69 (d, 1H, J: 2, Ar-CH), 7.71 (dd, 1H, J: 8.5, J: 2, Ar-CH), 7.74 (m, 1H, Ar-CH), 10.39 (s, 1H, COH).

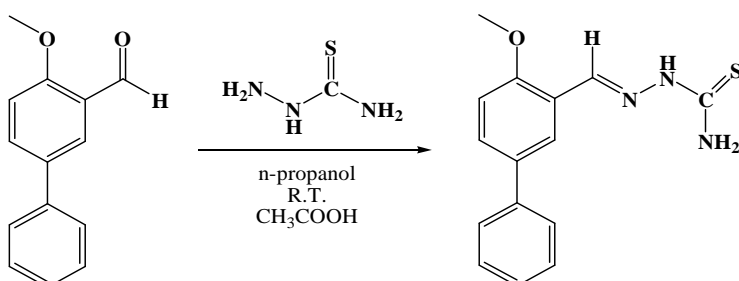
<sup>13</sup>C-NMR (500 MHz, DMSO) δ 56.2 (1C, OCH<sub>3</sub>), 112.7 (1C, phenyl), 121.8 (1C, phenyl), 123.6 (1C, phenyl), 128.2 (1C, phenyl), 128.3 (1C, phenyl), 129.6 (1C, phenyl), 131.4 (1C, phenyl), 132.7 (2C, phenyl), 133.1 (1C, phenyl), 140.4 (1C, phenyl), 161.0 (1C, phenyl), 188.9 (1C, COH).

**General method for the synthesis of thiosemicarbazones.**

In a flask equipped with a reflux condenser, equimolar amounts of thiosemicarbazide and of the appropriate ketone are reacted in n-propanol in the presence of a catalytic amount of AcOH. The mixture is allowed to react overnight, and the obtain solid is filtered and used without further purification.

According to this procedure the following compounds have been synthesised:

**[(2-methoxy-5-phenylphenyl)methylidene]amino]thiourea**

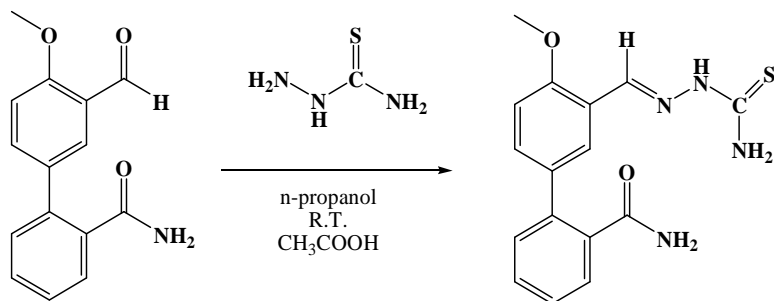


M.W.: 285.36 g/mol; R.f.: 0.71 (exane-ethylacetate 1:1); HPLC: 95.933%; M.P.: 223.3°-223.8°C; Yield: 97%

NMR: <sup>1</sup>H-NMR (500 MHz, DMSO) δH 3.87 ( s, 3H, OCH<sub>3</sub>), 7.15 ( d, 1H, J: 8.5, Ar-CH), 7.32 ( m, 1H, Ar-CH), 7.44 ( m, 2H, Ar-CH), 7.68 ( dd, 1H, J: 8.15, Ar-CH), 7.72 ( m, 2H, J: 8.5, Ar-CH) 8.18-8.19 ( brs, 2H, NH<sub>2</sub>), 8.37 ( d, 1H, Ar-CH), 8.45 ( s, 1H, CH=N), 11.45 ( s, 1H, NH).

<sup>13</sup>C-NMR (500 MHz, DMSO) δ 55.9 ( 1C, OCH<sub>3</sub>), 112.2 ( 1C, phenyl), 122.5 ( 1C, phenyl), 123.8 ( 1C, phenyl), 126.5 ( 2C, phenyl), 126.9 ( 1C, phenyl), 128.7 ( 2C, phenyl), 129.4 ( 1C, phenyl), 132.7 ( 1C, phenyl), 137.8 ( 1C, CH=N), 139.4 ( 1C, phenyl), 157.3 ( 1C, phenyl), 177.8 ( 1C, NH-CSNH<sub>2</sub>)

**2-{3-[(carbamothioylamino)imino]methyl}-4-methoxyphenyl} benzamide**

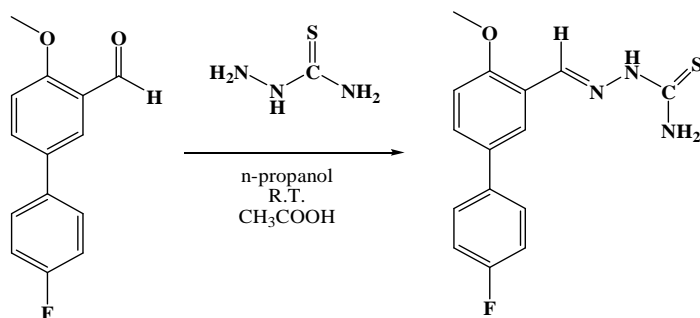


M.W.: 328.39 g/mol; R.f.: 0.26 (exane-ethylacetate 1:4); HPLC: 88.22%; M.P.: 234°-235°C;  
Yield: 82.48%

$^1\text{H-NMR}$  (500 MHz, DMSO)  $\delta$  3.86 (s, 3H,  $\text{OCH}_3$ ), 7.09 (d, 1H,  $J$ :8.5, Ar-CH), 7.33 (bs, 1H,  $\text{NH}_2$ ), 7.40 (dd, 1H, Ar-CH), 7.40 (m, 1H, Ar-CH), 7.41 (m, 2H, Ar-CH), 7.46 (m, 1H, Ar-CH), 7.66 (bs, 1H,  $\text{NH}_2$ ), 7.88 (bs, 1H,  $\text{NH}_2$ ), 8.15 (d, 1H,  $J$ : 2.5), 8.18 (bs, 1H,  $\text{NH}_2$ ), 8.43 (s, 1H,  $\text{CH}=\text{N}$ ), 11.46 (s, 1H,  $\text{NH-CSNH}_2$ ).

$^{13}\text{C-NMR}$  (500 MHz, DMSO)  $\delta$  55.8 (1C,  $\text{OCH}_3$ ), 111.4 (1C, phenyl), 121.9 (1C, phenyl), 125.8 (1C, phenyl), 126.7 (1C, phenyl), 127.3 (1C, phenyl), 129.0 (1C, phenyl), 130.0 (1C, phenyl), 131.2 (2C, phenyl), 137.5 (1C, phenyl), 137.8 (1C,  $\text{CH}=\text{N}$ ), 138.2 (1C, phenyl), 157.1 (1C, phenyl), 171.3 (1C,  $\text{CONH}_2$ ), 177.8 (1C,  $\text{NH-CSNH}_2$ )

**{[5-(4-fluorophenyl)-2-methoxyphenyl]methylidene}amino]thiourea**



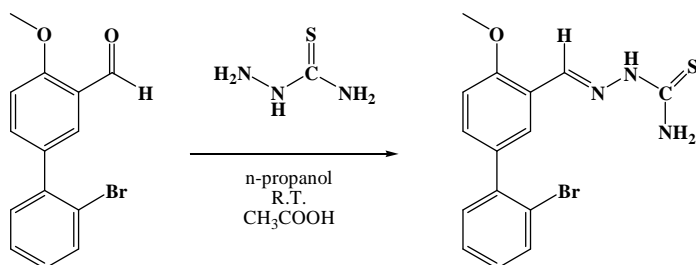
M.W.: 303.35 g/mol; R.f.: 0.63 (exane-ethylacetate 1:1); HPLC: 99.98%; M.P.: 217-218°C;  
Yield: 84%



NMR:  $^1\text{H-NMR}$  (500 MHz, DMSO)  $\delta$  3.87 (s, 3H,  $\text{OCH}_3$ ), 7.14 (d, 1H, J: 9, Ar-CH), 7.26 (m, 2H, J: 8.5, Ar-CH), 7.67 (dd, 1H, J: 8.5, J: 2, Ar-CH), 7.76 (m, 2H, J: 8.5, J:2, Ar-CH), 8.21-8.18 (brd, 2H,  $\text{NH}_2$ ), 8.35 (d, 1H, J: 2.5, Ar-CH), 8.44 (s, 1H, CHN), 11.46 (s, 1H, NH).

$^{13}\text{C-NMR}$  (500 MHz, DMSO)  $\delta$  55.9 (1C,  $\text{OCH}_3$ ), 112.2 (1C, phenyl), 115.4 (1C, phenyl), 115.5 (1C, phenyl), 122.5 (1C, phenyl), 123.7 (1C, phenyl), 128.4 (1C, phenyl), 128.5 (1C, phenyl), 129.3 (1C, phenyl), 131.7 (1C, phenyl), 135.8 (1C, phenyl), 137.6 (1C, CH=N), 157.3 (1C, phenyl), 161.6 (1C, phenyl), 177.8 (1C, NH- $\text{CSNH}_2$ ).

**(2-methoxy-5-(2-bromo)phenylphenyl)methylidene]amino] thiourea**



M.W.: 364.26 g/mol; R.f.: 0.725 (exane-ethylacetate 1:1); HPLC: 93.98%; M.P.: 219-220°C; Yield: 62.45%

$^1\text{H-NMR}$  (500 MHz, DMSO)  $\delta$  3.88 (s, 3H,  $\text{OCH}_3$ ), 7.13 (d, 1H, J: 9), 7.39 (m, 1H, J: 1.5), 7.39 (m, 2H), 7.45 (m, 1H, J: 1), 7.72 (m, 1H, J: 8, J: 1.5), 8.10-8.06 (brs, 2H, NH), 8.14 (d, 1H, J: 2), 8.44 (s, 1H, CH=N), 11.43 (s, 1H, NH).

$^{13}\text{C-NMR}$  (500 MHz, DMSO)  $\delta$  55.9 (1C,  $\text{OCH}_3$ ), 111.2 (1C, phenyl), 121.9 (1C, phenyl), 122.2 (1C, phenyl), 126.6 (1C, phenyl), 127.8 (1C, phenyl), 129.1 (1C, phenyl), 131.6 (1C, phenyl), 132.0 (1C, phenyl), 132.8 (1C, phenyl), 133.2 (1C, phenyl), 137.5 (1C, CH=N), 141.4 (1C, phenyl), 157.2 (1C, phenyl), 177.8 (1C, NH- $\text{CSNH}_2$ )

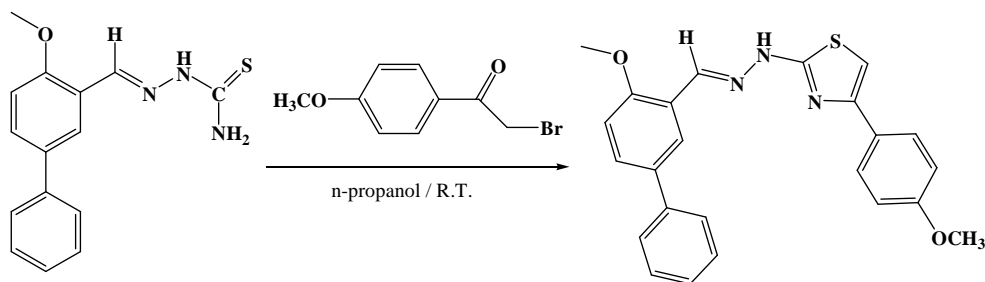
### General method for the synthesis of compound EMAC 2056-2071

Equimolar amounts of thiosemicarbazone and  $\alpha$ -halogen keton are reacted at RT n-propanol. The mixture is stirred for 4 to 24 hours. Then the formation of a precipitate is observed which is filtered. The obtained solid is washed with ethyl ether and crystallised from ethanol, water/ethanol.

According to this method, the following listed compounds have been synthesised.

#### EMAC 2056

#### 2-[2-[(2-methoxy-5-phenylphenyl)methylidene]hydrazin-1-yl]-4-(4-methoxyphenyl)-1,3-thiazole

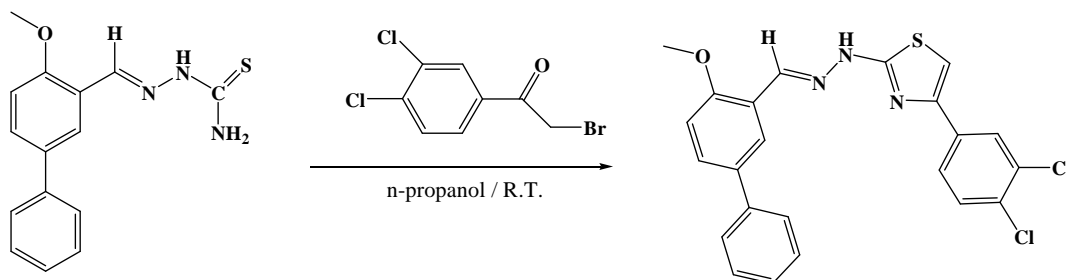


$^1\text{H-NMR}$  (500 MHz, DMSO)  $\delta$  3.78 (s, 3H,  $\text{OCH}_3$ ), 3.90 (s, 3H,  $\text{OCH}_3$ ), 6.97 (m, 2H, J: 9), 7.15 (s, 1H, CH thiazole), 7.19 (d, 1H, J: 9), 7.36 (m, 1H, Ar-CH), 7.48 (m, 2H, Ar-CH), 7.62 (m, 2H, J: 7.5, Ar-CH), 7.67 (d, 1H, J: 8.5, J: 2.5, Ar-CH), 7.78 (m, 2H, J: 9, Ar-CH), 8.03 (d, 1H, J: 2.5), 8.42 (s, 1H, CHN), 11.45 (brs, 1H, NH)

$^{13}\text{C-NMR}$  (500 MHz, DMSO)  $\delta$  55.9 (2C,  $\text{OCH}_3$ ), 101.7 (1C, thiazole), 114.0 (3C, phenyl), 122.6 (1C, phenyl), 122.8 (1C, phenyl), 126.2 (2C, phenyl), 127.0 (3C, phenyl), 127.1 (1C, phenyl), 129.1 (3C, phenyl), 132.8 (1C, phenyl), 137.2 (1C, CH=N), 139.6 (1C, phenyl), 149.4 (1C, thiazole), 156.7 (1C, phenyl), 158.9 (1C, phenyl), 168.2 (1C, thiazole).

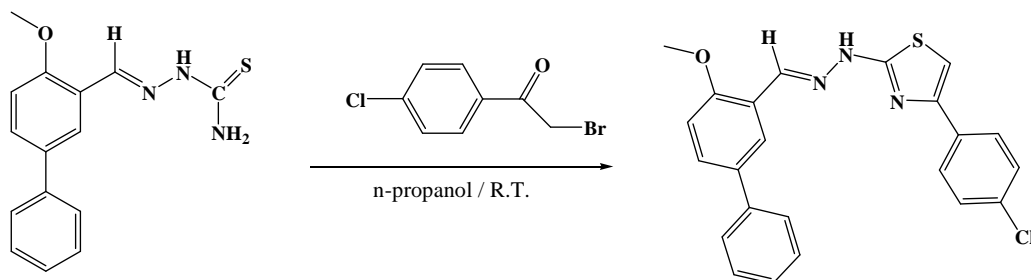
**EMAC 2057**

**4-(3,4-dichlorophenyl)-2-[2-[(2-methoxy-5-phenylphenyl)methylidene]hydrazin-1-yl]-1,3-thiazole**



$^1\text{H-NMR}$  (500 MHz, DMSO)  $\delta$  3.90 (s, 3H,  $\text{OCH}_3$ ), 7.19 (d, 1H,  $J$ : 8.5, Ar-CH), 7.35 (m, 2H, Ar-CH), 7.48 (m, 2H, Ar-CH), 7.55 (s, 1H, CH thiazole), 7.62 (m, 1H, Ar-CH), 7.66 (d, 1H,  $J$ : 8.5), 7.67 (dd, 1H, 8.5), 7.84 (dd, 1H,  $J$ : 8.5,  $J$ : 2), 8.01 (d, 1H,  $J$ : 2.5), 8.08 (d, 1H,  $J$ : 2), 8.40 (s, 1H,  $\text{CH}=\text{N}$ ), 12.2 (brs, 1H, NH).

$^{13}\text{C-NMR}$  (500 MHz, DMSO)  $\delta$  55.9 (1C,  $\text{OCH}_3$ ), 106.0 (1C, thiazole), 112.5 (1C, phenyl), 122.6 (1C, phenyl), 122.7 (1C, phenyl), 125.6 (1C, phenyl), 126.2 (2C, phenyl), 127.1 (1C, phenyl), 127.2 (1C, phenyl), 129.0 (2C, phenyl), 129.1 (1C, phenyl), 129.7 (1C, phenyl), 130.9 (1C, phenyl), 131.4 (1C, phenyl), 132.8 (1C, phenyl), 135.2 (1C, phenyl), 136.9 (1C,  $\text{CH}=\text{N}$ ), 139.6 (1C, phenyl), 147.9 (1C, thiazole), 156.7 (1C, phenyl), 168.5 (1C, thiazole).

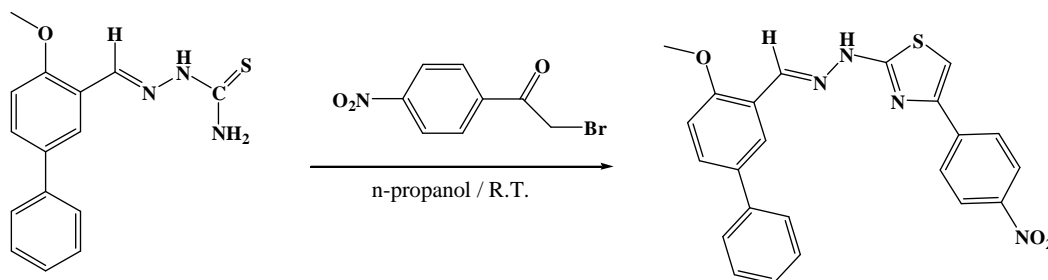
**EMAC 2058****4-(3-chlorophenyl)-2-[2-[(2-methoxy-5-phenylphenyl)methylidene]hydrazin-1-yl]-1,3-thiazole**

$^1\text{H-NMR}$  (500 MHz, DMSO)  $\delta$  3.90 (s, 3H,  $\text{OCH}_3$ ), 7.19 (d, 1H, J: 8.5, Ar-CH), 7.36 (m, 1H, Ar-CH), 7.39 (s, 1H, CH thiazole), 7.46 (m, 2H, Ar-CH), 7.48 (m, 2H, Ar-CH), 7.62 (m, 2H, J: 7.5, Ar-CH), 7.67 (dd, 1H, J: 8.5, J: 2.5, Ar-CH), 7.87 (m, 2H, J: 8.5, Ar-CH), 8.02 (d, 1H, J: 2.5, Ar-CH), 8.40 (s, 1H,  $\text{CH}=\text{N}$ , Ar-CH), 12.24 (brs, 1H, NH, Ar-CH).

$^{13}\text{C-NMR}$  (500 MHz, DMSO)  $\delta$  55.9 (1C,  $\text{OCH}_3$ ), 104.5 (1C, thiazole), 112.5 (1C, phenyl), 122.7 (1C, phenyl), 122.7 (1C, phenyl), 126.3 (2C, phenyl), 127.1 (1C, phenyl), 127.3 (2C, phenyl), 128.6 (2C, phenyl), 129.0 (2C, phenyl), 129.1 (1C, phenyl), 131.9 (1C, phenyl), 132.8 (1C, phenyl), 133.4 (1C, phenyl), 136.8 (1C,  $\text{CH}=\text{N}$ ), 139.6 (1C, phenyl), 149.1 (1C, thiazole), 156.7 (1C, phenyl), 168.4 (1C, thiazole).

**EMAC 2059**

**4-(4-nitrophenyl)-2-[2-[(2-methoxy-5-phenylphenyl)methylidene]hydrazin-1-yl]-1,3-thiazole**

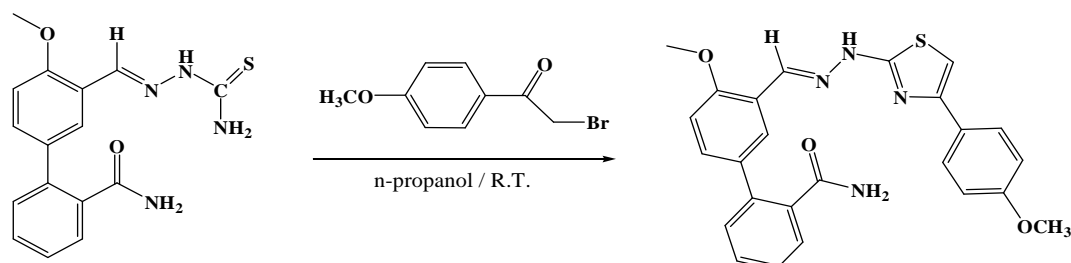


<sup>1</sup>H-NMR (500 MHz, DMSO)  $\delta$  3.90 (s, 3H, OCH<sub>3</sub>), 7.19 (d, 1H, J: 8.5, Ar-CH), 7.36 (m, 1H, Ar-CH), 7.48 (m, 2H, Ar-CH), 7.63 (m, 2H, J: 7.5, Ar-CH), 7.67 (dd, 1H, J: 8.5, J: 2.5, Ar-CH), 7.71 (s, 1H, thiazole), 8.02 (d, 1H, J: 2.5, Ar-CH), 8.11 (d, 2H, J: 9, Ar-CH), 8.27 (d, 2H, J: 9, Ar-CH), 8.41 (s, 1H, CH=N), 12.32 (brs, 1H, NH).

<sup>13</sup>C-NMR (500 MHz, DMSO)  $\delta$  55.9 (1C, OCH<sub>3</sub>), 108.6 (1C, thiazole), 112.5 (1C, phenyl), 122.6 (1C, phenyl), 122.8 (1C, phenyl), 124.1 (2C, phenyl), 126.3 (2C, phenyl), 126.3 (2C, phenyl), 127.1 (1C, phenyl), 129.0 (2C, phenyl), 129.2 (1C, phenyl), 132.8 (1C, phenyl), 137.1 (1C, CH=N), 139.6 (1C, phenyl), 140.6 (1C, phenyl), 146.2 (1C, phenyl), 148.5 (1C, thiazole), 156.7 (1C, phenyl), 168.7 (1C, thiazole).

## EMAC 2060

### 2-{4-methoxy-3-[(1E)-{2-[4-(4-methoxyphenyl)-1,3-thiazol-2-yl]hydrazin-1-ylidene}methyl] phenyl}benzamide

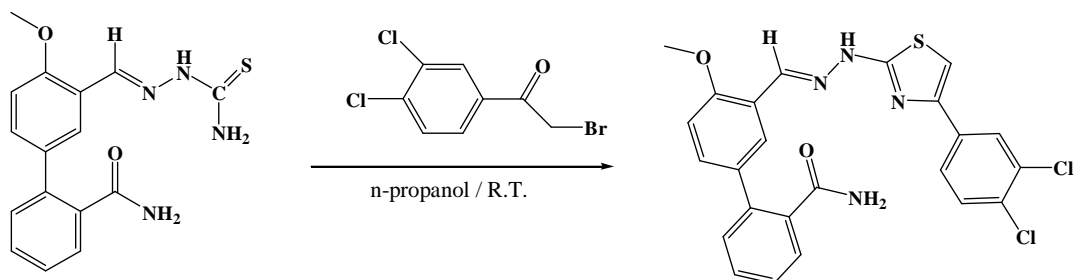


$^1\text{H-NMR}$  (500 MHz, DMSO)  $\delta$  3.78 (s, 3H,  $\text{OCH}_3$ ), 3.90 (s, 3H,  $\text{OCH}_3$ ), 6.50 (bs, 1H,  $\text{CONH}_2$ ), 6.96 (d, 2H, J: 9, Ar-CH), 7.13 (s + d, 2H, thiazole + Ar-CH), 7.30-7.50 (m, 8H, Ar-CH), 7.72 (bs, 1H,  $\text{CONH}_2$ ), 7.86 (d, 1H, J: 2.5), 12.19 (bs, 1H, NH).

$^{13}\text{C-NMR}$  (500 MHz, DMSO)  $\delta$  55.2 (1C,  $\text{OCH}_3$ ), 55.8 (1C,  $\text{OCH}_3$ ), 106.0 (1C, thiazole), 111.6 (1C, phenyl), 122.0 (1C, phenyl), 124.8 (1C, phenyl), 126.8 (1C, phenyl), 127.3 (2C, phenyl), 127.6 (1C, phenyl), 128.6 (2C, phenyl), 129.3 (1C, phenyl), 129.7 (1C, phenyl), 130.7 (1C, phenyl), 131.9 (1C, phenyl), 133.1 (1C, phenyl), 133.4 (1C, phenyl), 136.9 (1C,  $\text{CH}=\text{N}$ ), 137.3 (1C, phenyl), 138.3 (1C, phenyl), 149.1 (1C, thiazole), 156.4 (1C, phenyl), 168.4 (1C, thiazole), 171.1 (1C,  $\text{CONH}_2$ ).

**EMAC 2061**

**2-{3-[[2-[4-(3,4-dichlorophenyl)-1,3-thiazol-2-yl]hydrazin-1-ylidene)methyl]-4-methoxyphenyl}benzamide**

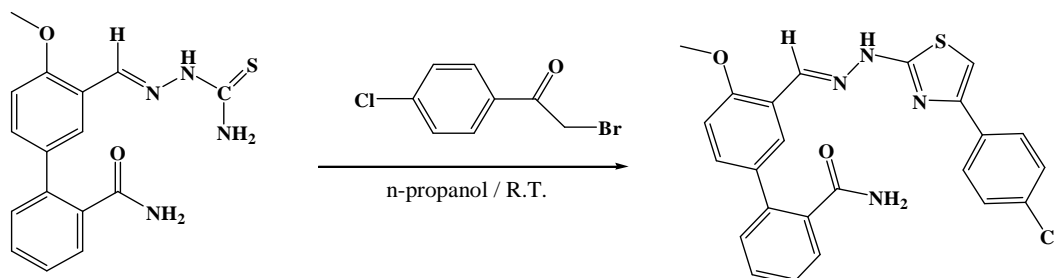


$^1\text{H-NMR}$  (500 MHz, DMSO)  $\delta$  3.89 (s, 3H,  $\text{OCH}_3$ ), 7.13 (d, 1H, J: 9, Ar-CH), 7.32 (bs, 1H,  $\text{NH}_2$ ), 7.37 (m, 1H, Ar-CH), 7.39 (m, 1H, Ar-CH), 7.41 (m, 1H, Ar-CH), 7.49 (m, 2H, Ar-CH), 7.53 (s, 1H, thiazole), 7.66 (d, 1H, J: 8.5, Ar-CH), 7.72 (bs, 1H,  $\text{NH}_2$ ), 7.83 (dd, 1H, J: 8.5, J: 2, Ar-CH), 7.87 (d, 1H, J: 2.5, Ar-CH), 8.08 (d, 1H, J: 2, Ar-CH), 8.38 (s, 1H,  $\text{CH}=\text{N}$ ), 12.21 (bs, 1H, NH).

$^{13}\text{C-NMR}$  (500 MHz, DMSO)  $\delta$  55.8 (1C,  $\text{OCH}_3$ ), 106.0 (1C, thiazole), 111.6 (1C, phenyl), 122.0 (1C, phenyl), 124.8 (1C, phenyl), 125.6 (1C, phenyl), 126.8 (1C, phenyl), 127.1 (1C, phenyl), 127.6 (1C, phenyl), 129.3 (1C, phenyl), 129.6 (1C, phenyl), 129.7 (1C, phenyl), 130.7 (1C, phenyl), 130.9 (1C, phenyl), 131.4 (1C, phenyl), 133.1 (1C, phenyl), 135.2 (1C, phenyl), 136.9 (1C,  $\text{CH}=\text{N}$ ), 137.3 (1C, phenyl), 138.3 (1C, phenyl), 147.9 (1C, thiazole), 156.4 (1C, phenyl), 168.5 (1C, thiazole), 171.1 (1C,  $\text{CONH}_2$ ).

**EMAC 2062**

**2-{3-[[2-[4-(4-chlorophenyl)-1,3-thiazol-2-yl]hydrazin-1-ylidene]methyl]-4-methoxyphenyl}benzamide**



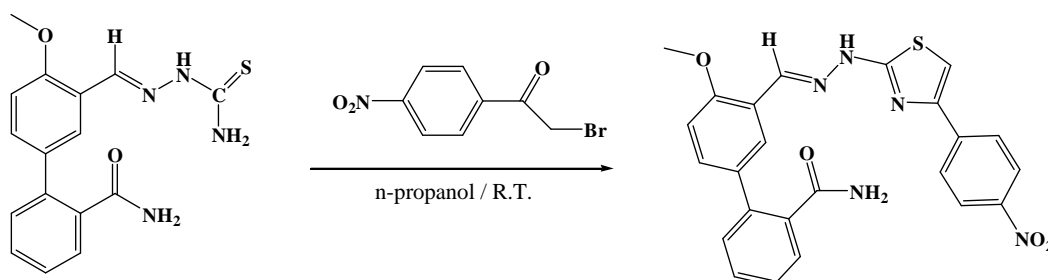
$^1\text{H-NMR}$  (500 MHz, DMSO)  $\delta$  3.89 (s, 3H,  $\text{OCH}_3$ ), 7.13 (d, 1H,  $J$ : 9, Ar-CH), 7.32 (bs, 1H,  $\text{CONH}_2$ ), 7.37 (s, 1H, thiazole), 7.37 (m, 1H, Ar-CH), 7.40 (m, 1H, Ar-CH), 7.41 (dd, 1H, Ar-CH), 7.44 (m, 1H, Ar-CH), 7.46 (m, 2H, Ar-CH), 7.49 (m, 2H, Ar-CH), 7.72 (bs, 1H,  $\text{CONH}_2$ ), 7.86 (m, 2H, Ar-CH), 7.87 (d, 1H, Ar-CH), 12.19 (bs, 1H, NH).

$^{13}\text{C-NMR}$  (500 MHz, DMSO)  $\delta$  55.8 (1C,  $\text{OCH}_3$ ), 106.0 (1C, thiazole), 111.6 (1C, phenyl), 122.0 (1C, phenyl), 124.8 (1C, phenyl), 126.8 (1C, phenyl), 127.3 (2C, phenyl), 127.6 (1C, phenyl), 128.6 (2C, phenyl), 129.3 (1C, phenyl), 129.7 (1C, phenyl), 130.7 (1C, phenyl), 131.9 (1C, phenyl), 133.1 (1C, phenyl), 133.4 (1C, phenyl), 136.9 (1C, CH=N), 137.3 (1C, phenyl), 138.3 (1C, phenyl), 149.1 (1C, thiazole), 156.4 (1C, phenyl), 168.4 (1C, thiazole), 171.1 (1C,  $\text{CONH}_2$ ).



**EMAC 2063**

**2-{3-[(2-{4-[4-(hydroxynitroso)phenyl]-1,3-thiazol-2-yl}hydrazin-1-ylidene)methyl]-4-methoxyphenyl}benzamide**

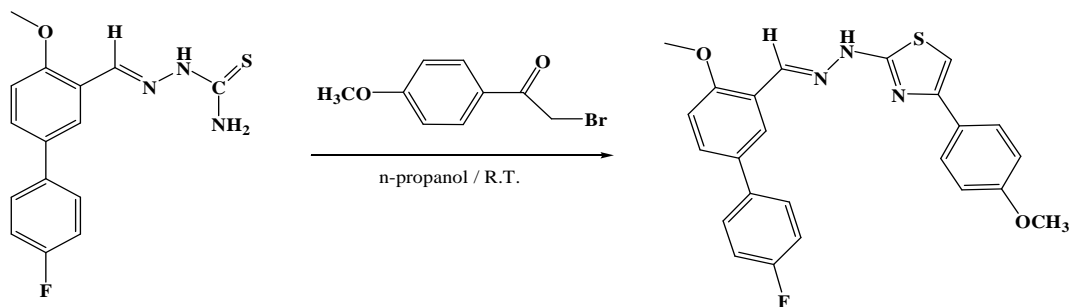


<sup>1</sup>H-NMR (500 MHz, DMSO)  $\delta$  3.89 (s, 3H, OCH<sub>3</sub>), 7.13 (d, 1H, J: 9, Ar-CH), 7.32 (bs, 1H, CONH<sub>2</sub>), 7.38 (m, 1H, Ar-CH), 7.40 (m, 1H, Ar-CH), 7.41 (dd, 1H, Ar-CH), 7.44 (m, 1H, Ar-CH), 7.49 (m, 1H, Ar-CH), 7.70 (s, 1H, thiazole), 7.73 (bs, 1H, CONH<sub>2</sub>), 7.88 (d, 1H, J: 2.5, Ar-CH), 8.11 (m, 2H, J: 9, Ar-CH), 8.27 (m, 2H, J: 8.5, Ar-CH), 8.39 (s, 1H, CH=N), 12.28 (bs, 1H, NH).

<sup>13</sup>C-NMR (500 MHz, DMSO)  $\delta$  55.9 (1C, OCH<sub>3</sub>), 108.6 (1C, thiazole), 111.7 (1C, phenyl), 121.9 (1C, phenyl), 124.1 (2C, phenyl), 124.8 (1C, phenyl), 126.3 (2C, phenyl), 126.8 (1C, phenyl), 127.6 (1C, phenyl), 129.3 (1C, phenyl), 129.7 (1C, phenyl), 130.8 (1C, phenyl), 133.1 (1C, phenyl), 137.1 (1C, CH=N), 137.3 (1C, phenyl), 138.3 (1C, phenyl), 140.7 (1C, phenyl), 146.2 (1C, phenyl), 148.5 (1C, thiazole), 156.5 (1C, phenyl), 168.7 (1C, thiazole), 171.1 (1C, CONH<sub>2</sub>).

**EMAC 2064**

**2-[2-{{[5-(4-fluorophenyl)-2-methoxyphenyl]methylidene}hydrazin-1-yl]-4-(4-methoxyphenyl)-1,3-thiazole**

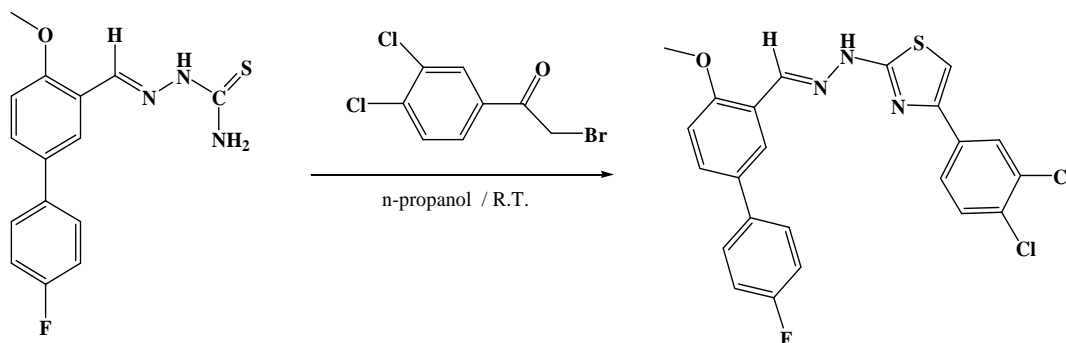


NMR:  $^1\text{H-NMR}$  (500 MHz, DMSO)  $\delta$  3.78 (s, 3H,  $\text{OCH}_3$ ), 3.90 (s, 3H,  $\text{OCH}_3$ ), 6.97 (m, 2H, J: 8.5, Ar-CH), 7.16 (s, 1H, thiazole), 7.18 (d, 2H, J: 8.5, Ar-CH), 7.30 (m, 2H, Ar-CH), 7.64 (dd, 2H, J: 8.5, J: 2.5, Ar-CH), 7.77 (m, 2H, J: 8.5, Ar-CH), 7.98 (d, 1H, J: 2, Ar-CH), 8.41 (s, 1H,  $\text{CH}=\text{N}$ ), 12.28 (brs, 1H, NH).

$^{13}\text{C-NMR}$  (500 MHz, DMSO)  $\delta$  55.2 (1C,  $\text{OCH}_3$ ), 55.9 (1C,  $\text{OCH}_3$ ), 101.7 (1C, thiazole), 112.5 (1C, phenyl), 114.0 (2C, phenyl), 115.7 (1C, phenyl), 115.9 (1C, phenyl), 122.7 (1C, phenyl), 122.7 (1C, phenyl), 126.9 (1C, phenyl), 127.0 (2C, phenyl), 128.2 (1C, phenyl), 128.3 (1C, phenyl), 129.1 (1C, phenyl), 131.8 (1C, phenyl), 136.1 (1C, phenyl), 137.1 (1C,  $\text{CH}=\text{N}$ ), 149.4 (1C, thiazole), 156.7 (1C, phenyl), 158.9 (1C, phenyl), 161.6 (1C, phenyl), 168.2 (1C, thiazole).

**EMAC 2065**

**4-(3,4-dichlorophenyl)-2-[2-[[5-(4-fluorophenyl)-2-methoxyphenyl]methylidene}hydrazin-1-yl]-1,3-thiazole**

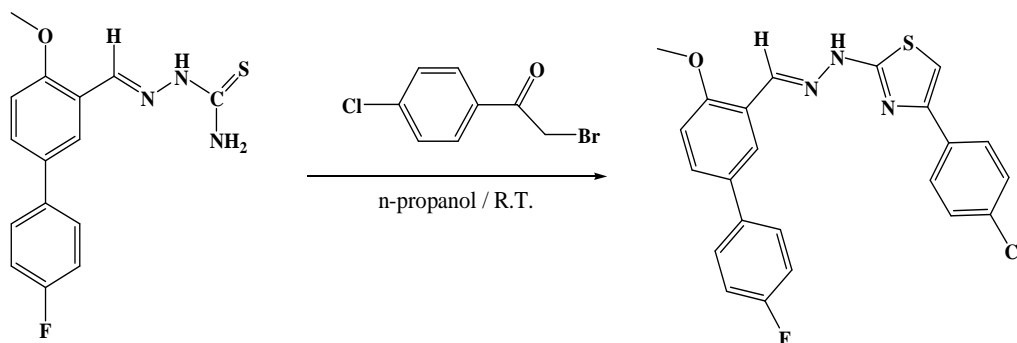


<sup>1</sup>H-NMR (500 MHz, DMSO)  $\delta$  3.90 (s, 3H, OCH<sub>3</sub>), 7.18 (d, 1H, J: 9, Ar-CH), 7.30 (m, 2H, Ar-CH), 7.55 (s, 1H, thiazole), 7.64 (dd, 1H, Ar-CH), 7.65 (m, 2H, Ar-CH), 7.66 (d, 1H, Ar-CH), 7.83 (dd, 1H, J: 8.5, J: 2, Ar-CH), 7.97 (d, 1H, J: 2, Ar-CH), 8.08 (d, 1H, J: 2, Ar-CH), 8.39 (s, 1H, CHN), 12.26 (brs, 1H, NH).

<sup>13</sup>C-NMR (500 MHz, DMSO)  $\delta$  55.9 (1C, OCH<sub>3</sub>), 106.0 (1C, thiazole), 112.5 (1C, phenyl), 115.7 (1C, phenyl), 115.9 (1C, phenyl), 122.6 (1C, phenyl), 122.7 (1C, phenyl), 127.2 (2C, phenyl), 128.2 (2C, phenyl), 129.7 (2C, phenyl), 130.9 (1C, phenyl), 131.4 (1C, phenyl), 131.8 (1C, phenyl), 135.2 (1C, phenyl), 136.1 (1C, phenyl), 136.9 (1C, CH=N), 147.9 (1C, thiazole), 156.7 (1C, phenyl), 161.6 (1C, phenyl), 168.5 (1C, thiazole).

**EMAC 2066**

**4-(4-chlorophenyl)-2-[2-{[5-(4-fluorophenyl)-2-methoxyphenyl]methylidene}hydrazin-1-yl]-1,3-thiazole**

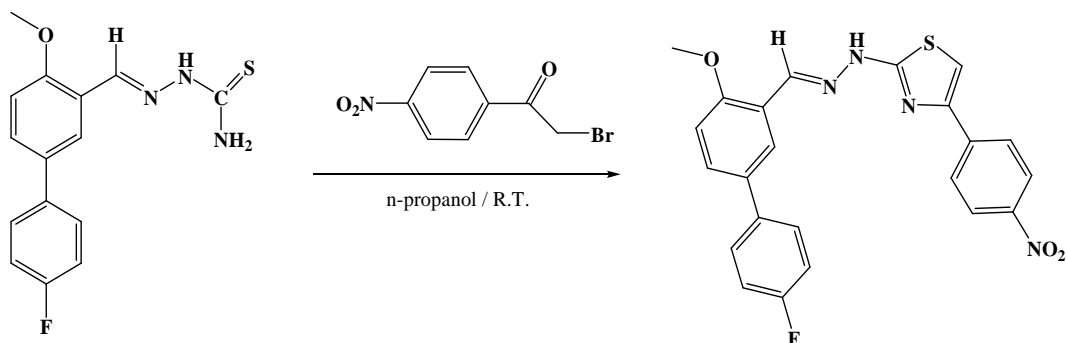


$^1\text{H-NMR}$  (500 MHz, DMSO)  $\delta$  3.90 (s, 3H,  $\text{OCH}_3$ ), 7.18 (d, 1H, J: 8.5, Ar-CH), 7.30 (m, 2H, J: 8.5, Ar-CH), 7.39 (s, 1H, thiazole), 7.46 (m, 2H, J: 9, Ar-CH), 7.64 (dd, 1H, Ar-CH), 7.65 (m, 2H, Ar-CH), 7.87 (m, 2H, J: 8.5, Ar-CH), 7.97 (d, 1H, J: 2, Ar-CH), 8.40 (s, 1H, CHN), 12.25 (brs, 1H, NH).

$^{13}\text{C-NMR}$  (500 MHz, DMSO)  $\delta$  55.9 (1C,  $\text{OCH}_3$ ), 104.6 (1C, thiazole), 112.5 (1C, phenyl), 115.7 (1C, phenyl), 115.9 (1C, phenyl), 122.7 (2C, phenyl), 127.3 (2C, phenyl), 128.2 (2C, phenyl), 128.6 (2C, phenyl), 129.1 (2C, phenyl), 131.8 (1C, phenyl), 132.0 (1C, phenyl), 136.1 (1C, phenyl), 136.8 (1C, CH=N), 149.1 (1C, thiazole), 156.7 (1C, phenyl), 161.6 (1C, phenyl), 168.4 (1C, thiazole).

EMAC 2067)

**[(4-{2-[2-{[5-(4-fluorophenyl)-2-methoxyphenyl]methylidene}hydrazin-1-yl]-1,3-thiazol-4-yl}phenyl)nitroso]oxidanol**

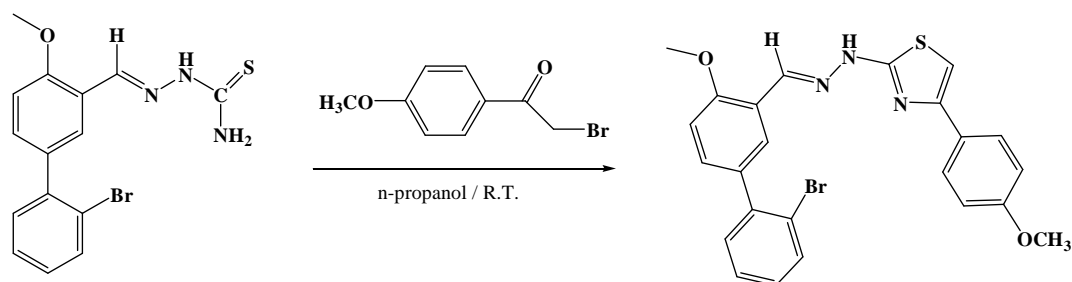


<sup>1</sup>H-NMR (500 MHz, DMSO)  $\delta$  3.90 (s, 3H, OCH<sub>3</sub>), 7.18 (d, 1H, J: 8.5, Ar-CH), 7.30 (m, 2H, Ar-CH), 7.65 (m, 3H, Ar-CH), 7.72 (s, 1H, thiazole), 7.97 (d, 1H, J: 2.5, Ar-CH), 8.11 (m, 2H, J: 9, Ar-CH), 8.27 (m, 2H, J: 9, Ar-CH), 8.40 (s, 1H, CHN), 12.32 (brs, 1H, NH).

<sup>13</sup>C-NMR (500 MHz, DMSO)  $\delta$  55.9 (1C, OCH<sub>3</sub>), 108.7 (1C, thiazole), 112.5 (1C, phenyl), 115.7 (1C, phenyl), 115.9 (1C, phenyl), 122.6 (1C, phenyl), 122.7 (1C, phenyl), 124.1 (2C, phenyl), 126.4 (2C, phenyl), 128.2 (1C, phenyl), 128.3 (1C, phenyl), 129.1 (1C, phenyl), 131.8 (1C, phenyl), 136.1 (1C, phenyl), 137.0 (1C, CH=N), 140.6 (1C, phenyl), 146.2 (1C, phenyl), 148.5 (1C, thiazole), 156.7 (1C, phenyl), 161.7 (1C, phenyl), 168.6 (1C, thiazole).

EMAC 2068

**2-[[5-(2-bromophenyl)-2-methoxyphenyl]methylidene]hydrazin-1-yl]-4-(4-methoxyphenyl)-1,3-thiazole**

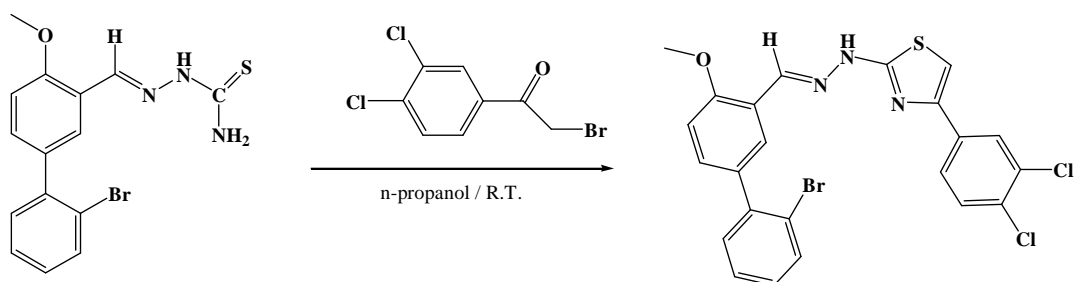


$^1\text{H-NMR}$  (500 MHz, DMSO)  $\delta$  3.77 (s, 3H,  $\text{OCH}_3$ ), 3.91 (s, 3H,  $\text{OCH}_3$ ), 6.96 (m, 2H, J: 9, Ar-CH), 7.11 (s, 1H, thiazole), 7.18 (d, 1H, J: 8.5, Ar-CH), 7.32 (m, 1H, Ar-CH), 7.40 (dd, 1H, J: 9, Ar-CH), 7.42 (m, 1H, J: 9.5, Ar-CH), 7.48 (m, 2H, Ar-CH), 7.75 (m, 1H, Ar-CH), 7.76 (m, 1H, Ar-CH), 7.81 (d, 1H, J: 2.5), 8.41 (s, 1H,  $\text{CH}=\text{N}$ ), 12.25 (brs, 1H, NH).

$^{13}\text{C-NMR}$  (500 MHz, DMSO)  $\delta$  55.1 (1C,  $\text{OCH}_3$ ), 55.9 (1C,  $\text{OCH}_3$ ), 101.6 (1C, thiazole), 111.7 (1C, phenyl), 114.0 (1C, phenyl), 121.9 (1C, phenyl), 122.0 (1C, phenyl), 124.8 (1C, phenyl), 125.5 (1C, phenyl), 127.0 (2C, phenyl), 127.6 (1C, phenyl), 128.1 (1C, phenyl), 129.3 (1C, phenyl), 131.4 (1C, phenyl), 131.5 (1C, phenyl), 132.9 (1C, phenyl), 133.1 (1C, phenyl), 136.8 (1C,  $\text{CH}=\text{N}$ ), 141.2 (1C, phenyl), 149.5 (1C, thiazole), 156.6 (1C, phenyl), 158.9 (1C, phenyl), 168.1 (1C, thiazole).

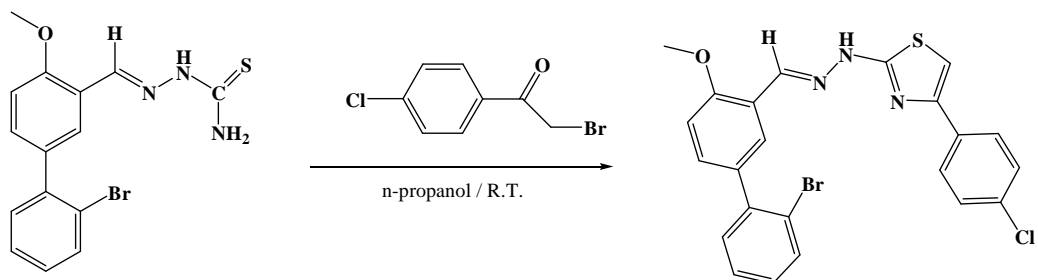
EMAC 2069

**2-[[5-(2-bromophenyl)-2-methoxyphenyl]methylidene]hydrazin-1-yl]-4-(3,4-dichlorophenyl)-1,3-thiazole**



$^1\text{H-NMR}$  (500 MHz, DMSO)  $\delta$  3.91 (s, 3H,  $\text{OCH}_3$ ), 7.18 (d, 1H, J: 9, Ar-CH), 7.32 (m, 1H, Ar-CH), 7.40 (dd, 1H, J: 9, J: 2.5, Ar-CH), 7.42 (m, 1H, J: 7.5, J: 2, Ar-CH), 7.47 (m, 1H, Ar-CH), 7.51 (s, 1H, thiazole), 7.56 (d, 1H, J: 8.5, Ar-CH), 7.75 (m, 1H, J: 6.5, J: 1.5, Ar-CH), 7.80 (d, 1H, J: 2.5, Ar-CH), 7.82 (dd, 1H, J: 6.5, J: 2, Ar-CH), 8.07 (d, 1H, J: 2, Ar-CH), 8.39 (s, 1H,  $\text{CH}=\text{N}$ ), 12.24 (bs, 1H, NH).

$^{13}\text{C-NMR}$  (500 MHz, DMSO)  $\delta$  55.9 (1C,  $\text{OCH}_3$ ), 106.0 (1C, thiazole), 111.7 (1C, phenyl), 121.9 (1C, phenyl), 122.0 (1C, phenyl), 125.5 (1C, phenyl), 125.6 (1C, phenyl), 127.1 (1C, phenyl), 128.1 (1C, phenyl), 129.3 (1C, phenyl), 129.7 (1C, phenyl), 130.9 (1C, phenyl), 131.4 (1C, phenyl), 131.4 (1C, phenyl), 131.5 (1C, phenyl), 132.9 (1C, phenyl), 133.1 (1C, phenyl), 135.2 (1C, phenyl), 136.7 (1C,  $\text{CH}=\text{N}$ ), 141.2 (1C, phenyl), 147.9 (1C, thiazole), 156.6 (1C, phenyl), 168.4 (1C, thiazole).

**EMAC 2070****2-[[5-(2-bromophenyl)-2-methoxyphenyl]methylidene]hydrazin-1-yl]-4-(4-chlorophenyl)-1,3-thiazole**

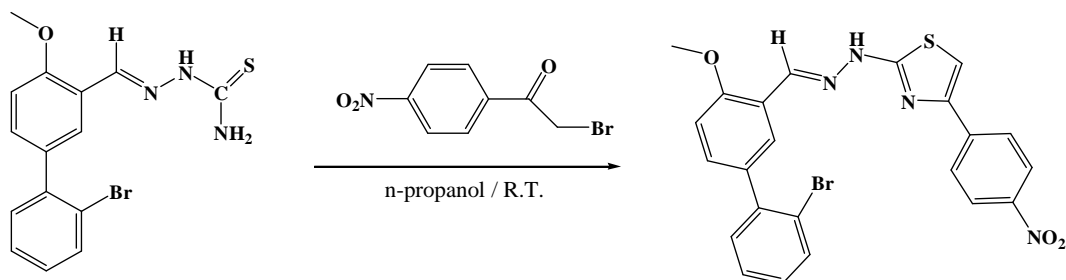
$^1\text{H-NMR}$  (500 MHz, DMSO)  $\delta$  3.91 (s, 3H,  $\text{OCH}_3$ ), 7.18 (d, 1H, J: 8.5, Ar-CH), 7.32 (m, 1H, Ar-CH), 7.35 (s, 1H, thiazole), 7.40 (dd, 1H, J: 8.5, J: 2.5, Ar-CH), 7.42 (m, 1H, Ar-CH), 7.45 (m, 2H, J: 8.5, Ar-CH), 7.48 (m, 1H, J: 1.5, Ar-CH), 7.75 (m, 1H, J: 8, J: 2, Ar-CH), 7.8 (d, 1H, J: 2, Ar-CH), 7.85 (m, 2H, J: 8.5, J: 2, Ar-CH), 8.4 (s, 1H,  $\text{CH}=\text{N}$ ), 12.21 (bs, 1H, NH).

$^{13}\text{C-NMR}$  (500 MHz, DMSO)  $\delta$  55.9 (1C,  $\text{OCH}_3$ ), 104.5 (1C, thiazole), 111.7 (1C, phenyl), 121.9 (1C, phenyl), 122.0 (1C, phenyl), 125.5 (1C, phenyl), 127.2 (2C, phenyl), 128.1 (1C, phenyl), 128.6 (2C, phenyl), 129.3 (1C, phenyl), 131.4 (1C, phenyl), 131.5 (1C, phenyl), 131.9 (1C, phenyl), 131.9 (1C, phenyl), 133.1 (1C, phenyl), 133.4 (1C, phenyl), 136.6 (1C,  $\text{CH}=\text{N}$ ), 141.2 (1C, phenyl), 149.1 (1C, thiazole), 156.6 (1C, phenyl), 168.3 (1C, thiazole).



EMAC 2071

**2-[[5-(2-bromophenyl)-2-methoxyphenyl]methylidene]hydrazin-1-yl]-4-(4-nitrophenyl)-1,3-thiazole**

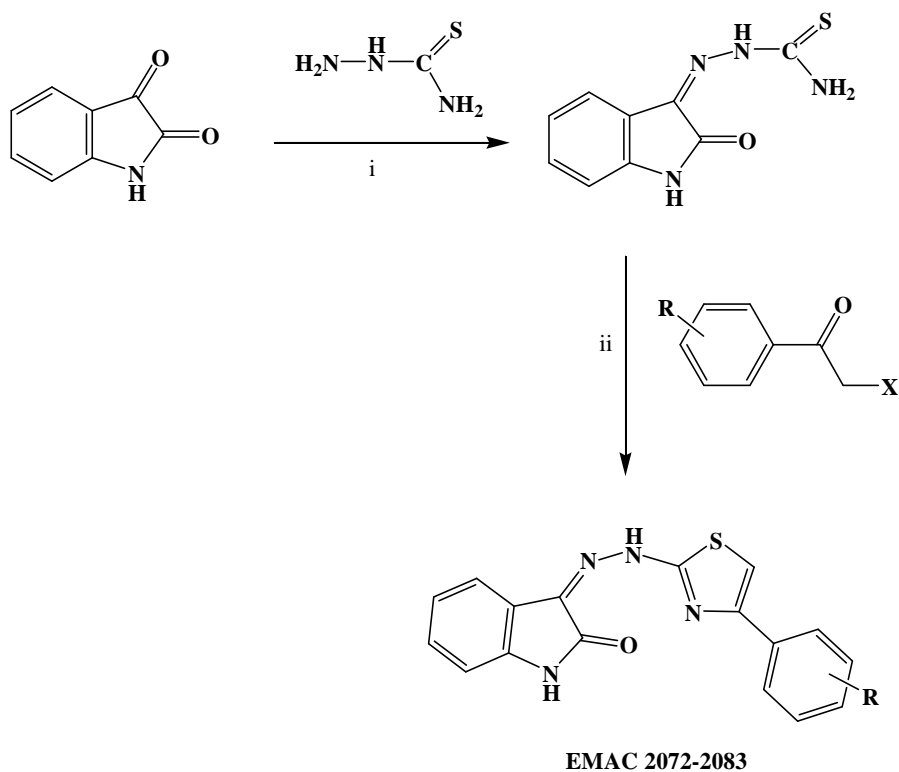


<sup>1</sup>H-NMR (500 MHz, DMSO)  $\delta$  3.91 (s, 3H, OCH<sub>3</sub>), 7.18 (d, 1H, J: 8.5, Ar-CH), 7.32 (m, 1H, Ar-CH), 7.40 (dd, 1H, J: 8.5, J: 2.5, Ar-CH), 7.42 (m, 1H, Ar-CH), 7.48 (m, 1H, Ar-CH), 7.68 (s, 1H, thiazole), 7.75 (m, 1H, J: 8, J: 1, Ar-CH), 7.81 (d, 1H, J: 2.5, Ar-CH), 8.10 (m, 2H, J: 9, Ar-CH), 8.26 (m, 2H, J: 8.5, Ar-CH), 8.40 (s, 1H, CH=N), 12.32 (bs, 1H, NH).

<sup>13</sup>C-NMR (500 MHz, DMSO)  $\delta$  55.9 (1C, OCH<sub>3</sub>), 108.6 (1C, thiazole), 111.7 (1C, phenyl), 121.9 (1C, phenyl), 122.0 (1C, phenyl), 124.1 (2C, phenyl), 125.5 (1C, phenyl), 126.3 (2C, phenyl), 128.1 (1C, phenyl), 129.3 (2C, phenyl), 131.4 (1C, phenyl), 132.9 (1C, phenyl), 133.1 (1C, phenyl), 136.8 (1C, CH=N), 140.6 (1C, phenyl), 141.2 (1C, phenyl), 146.2 (1C, phenyl), 148.5 (1C, thiazole), 156.6 (1C, phenyl), 168.6 (1C, thiazole)

## COMPOUNDS 2072-2083

### General synthetic scheme:



R: 4-Cl, 4-F, 4-Br, 4-NO<sub>2</sub>, 4-C<sub>6</sub>H<sub>5</sub>, 4-CN, 2,4-F, 3-NO<sub>2</sub>, 4-CH<sub>3</sub>, 4-OCH<sub>3</sub>, H, 2,4-Cl

**Scheme 7.** Synthesis of (Z)-3-(2-(4-arylthiazol-2-yl)hydrazono)indolin-2-one derivatives EMAC 2072-2083. Reagents: (i) 2-propanol, AcOH; (iii) 2-propanol, R.T.

Indolinone derivative were synthesized by a multi step reaction.

The first synthetic step leads to the formation of 1-(2-oxoindolin-3-ylidene)thiosemicarbazide by reacting isatin and thiosemicarbazide in 2-propanol and acid acetic as catalyst.

In the second step, the thiazole ring is formed by reaction between 1-(2-oxoindolin-3-ylidene)thiosemicarbazide and differently substituted α-haloacetophenones as outlined in the scheme.

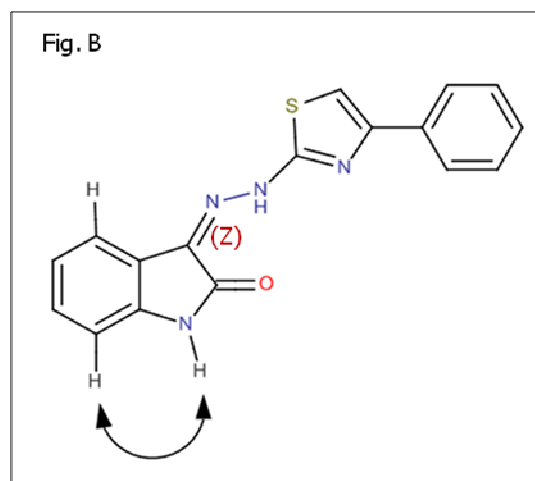
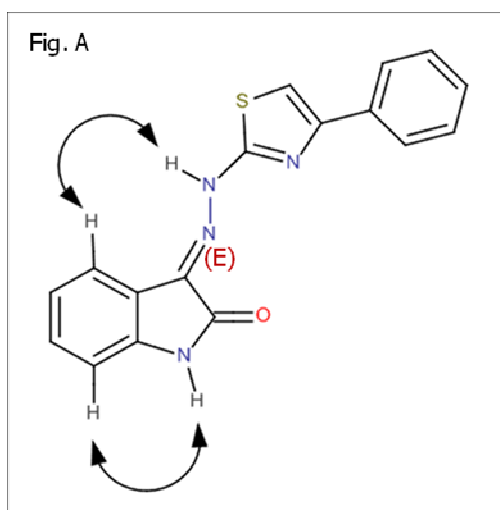
*NMR spectra were measured during my research period at the Semmelweis University in Budapest under the supervision of Prof. Peter Matyus.*

All samples were measured in DMF-d7 solvent at 278.1 K temperature on a Bruker AVANCE III spectrometer. In the signal assignments the proton and carbon chemical shifts are referred to the solvent (1H:  $\delta = 8.03$  ppm, 13C dowfield methyl signal:  $\delta=34.89$  ppm respectively). In the  $^{15}\text{N}$  chemical shift assignments we applied the spectrometer's digital reference which is calibrated to liq.  $\text{NH}_3$   $\delta= 0$  ppm.

For all investigated compound Z configuration was supported by NMR.

This was based on the selective NOE experiments, where we observed NOE interaction between the indole NH and CH protons, while no correlation was seen between the indole CH and =N-NH- hydrogens.

The geometry of the C=N double bond was defined by NOE experiments. In the case of the "E" diastereoisomer two NOE effects should be measured as indicated in figure A:



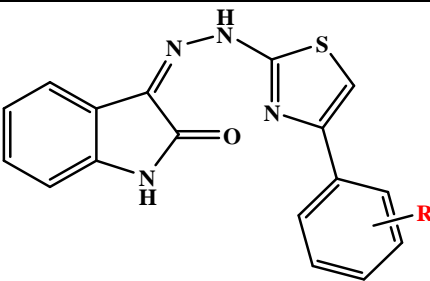
In our compounds only the NOE effect related to the indolinone protons was measured indicating that the proton in the position 4 of the indolinone ring and the hydrazine proton are too far to interact.

This distance is only possible if the configuration is "Z". (figure B)

All synthesized compounds were characterised by analytical and spectral data as listed in Table 21 and 22.

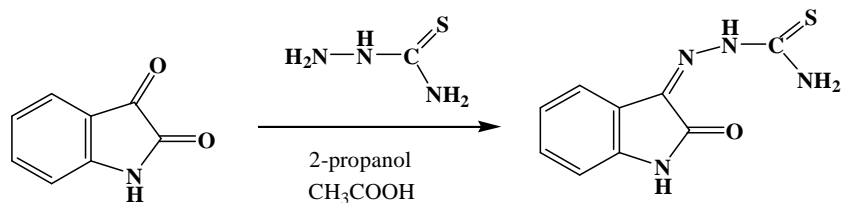
**Table 21.** Chemical and physical data of derivatives EMAC 2072-2083

Compound	R	M.W.	Mp (C°)	% Yield
EMAC 2072	4-Cl	354.81	>250	73
EMAC 2073	4-F	338.36	>250	57
EMAC 2074	4-Br	399.26	>250	95
EMAC 2075	4-NO <sub>2</sub>	365.37	>250	84
EMAC 2076	4-C <sub>6</sub> H <sub>5</sub>	396.46	>250	96
EMAC 2077	4-CN	345.38	>250	99
EMAC 2078	2,4-F	356.35	>250	66
EMAC 2079	3-NO <sub>2</sub>	365.37	>250	86
EMAC 2080	4-CH <sub>3</sub>	334.39	>250	72
EMAC 2081	4-OCH <sub>3</sub>	350.39	>250	84
EMAC 2082	H	320.37	250	92
EMAC 2083	2,4-Cl	389.26	>250	90

**Table 22.** Analytical data of derivatives EMAC 2072-2083


Compound	R	Reaction solvent	Crystallisation solvent	Aspect	Reaction time (h)
EMAC 2072	4-Cl	2-propanol	Water/Ethanol	Yellow-orange solid	24
EMAC 2073	4-F	2-propanol	Water/Ethanol	Yellow-orange solid	12
EMAC 2074	4-Br	2-propanol	Water/Ethanol	Yellow-orange solid	24
EMAC 2075	4-NO <sub>2</sub>	2-propanol	Water/Ethanol	Yellow-orange solid	24
EMAC 2076	4-C <sub>6</sub> H <sub>5</sub>	2-propanol	Water/Ethanol	Yellow-orange solid	12
EMAC 2077	4-CN	2-propanol	Water/Ethanol	Yellow-orange solid	24
EMAC 2078	2,4-F	2-propanol	Water/Ethanol	Yellow-orange solid	24
EMAC 2079	3-NO <sub>2</sub>	2-propanol	Water/Ethanol	Yellow-orange solid	12
EMAC 2080	4-CH <sub>3</sub>	2-propanol	Water/Ethanol	Yellow-orange solid	12
EMAC 2081	4-OCH <sub>3</sub>	2-propanol	Water/Ethanol	Yellow-orange solid	24
EMAC 2082	H	2-propanol	Water/Ethanol	Yellow-orange solid	12
EMAC 2083	2,4-Cl	2-propanol	Water/Ethanol	Yellow-orange solid	12

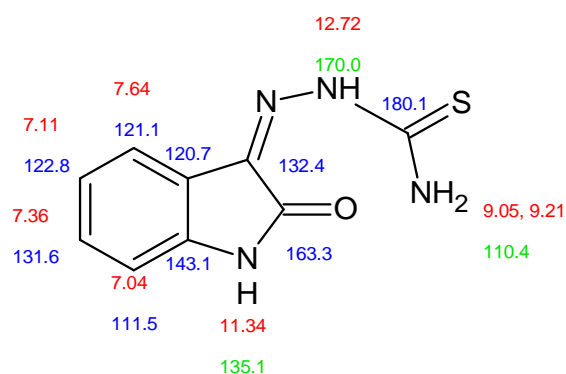
**1-(2-oxoindolin-3-ylidene)thiosemicarbazide**



$^1\text{H}$  NMR (DMF)  $\delta$ (ppm): 12.72 (s; 1H); 11.34 (s; 1H); 9.21 (s; 1H); 9.05 (s; 1H); 7.66-7.64 (m; 1H); 7.42-7.34 (m; 1H); 7.17-7.10 (m; 1H); 7.06-7.02 (m; 1H)

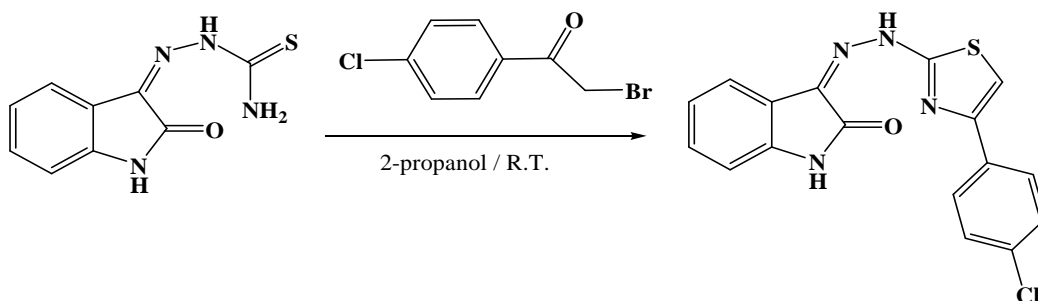
$^{13}\text{C}$  NMR (DMF)  $\delta$ (ppm): 180.1; 163.3; 143.1; 132.4; 131.6; 122.8; 121.1; 120.7; 111.5

$^{15}\text{N}$  NMR (DMF)  $\delta$ (ppm): 170.0; 135.6; 110.4



EMAC 2072

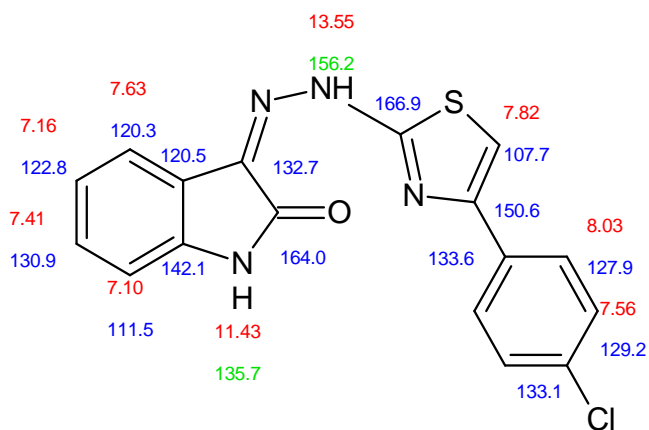
*(Z)*-3-(2-(4-(4-chlorophenyl)thiazol-2-yl)hydrazono)indolin-2-one



$^1\text{H}$  NMR (DMF)  $\delta$ (ppm): 13.55 (s, 1H); 11.43 (s, 1H); 8.07-8.02 (m, 2H); 7.82 (s, 1H); 7.63 (dm;  $J=7.6$  Hz; 1H); 7.58-7.53 (m; 2H); 7.41 (td;  $J=7.6$  Hz; 1.1 Hz; 1H); 7.16 (td;  $J=7.6$  Hz; 1.0 Hz; 1H); 7.10 (dm;  $J=7.6$  Hz; 1H)

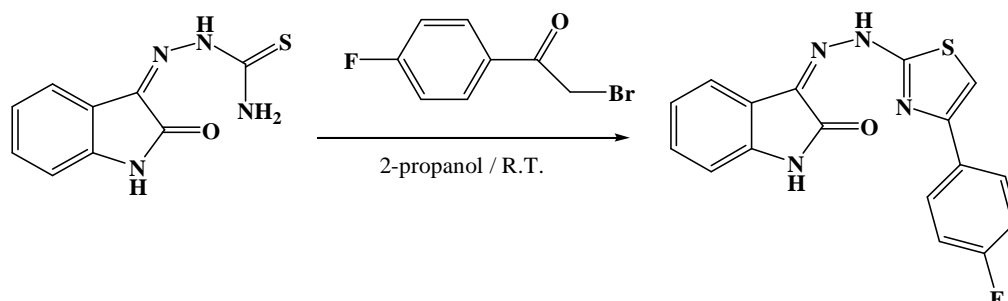
$^{13}\text{C}$  NMR (DMF)  $\delta$ (ppm): 166.9; 164.0; 150.6; 142.1; 133.6; 133.1; 132.7; 130.9; 129.2; 127.9; 122.8; 120.5; 120.3; 111.5; 107.7

$^{15}\text{N}$  NMR (DMF)  $\delta$ (ppm): 156.2; 135.7



## EMAC 2073

### *(Z)*-3-(2-(4-(4-fluorophenyl)thiazol-2-yl)hydrazono)indolin-2-one



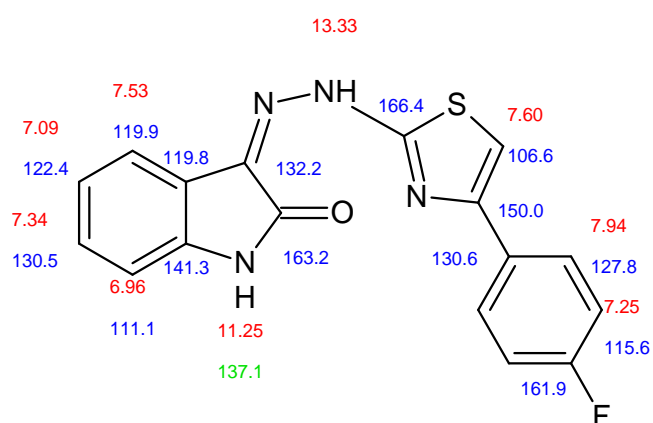
The NMR analysis supports a mixture of two tautomers:

The major compound is:

$^1\text{H}$  NMR (DMSO)  $\delta$ (ppm): 13.33 (s; 1H); 11.25 (s; 1H); 7.97-7.90 (m; 2H); 7.60 (s; 1H); 7.53 (dm;  $J$ : 7.5 Hz; 1H); 7.34 (tm;  $J$ : 7.5 Hz; 1H); 7.29-7.17 (m; 2H); 7.09 (tm;  $J$ : 7.5 Hz; 1H); 6.99-6.92 (m; 1H)

$^{13}\text{C}$  NMR (DMSO)  $\delta$ (ppm): 166.4; 163.2; 161.9 (d;  $J$ = 244.6 Hz); 150.0; 141.3; 132.2; 130.6; 130.5; 127.8 (d;  $J$ = 8.3 Hz) 122.4; 119.9; 119.8; 115.6 (d;  $J$ = 21.6 Hz); 111.1; 106.6

$^{15}\text{N}$  NMR (DMSO)  $\delta$ (ppm): 137.1



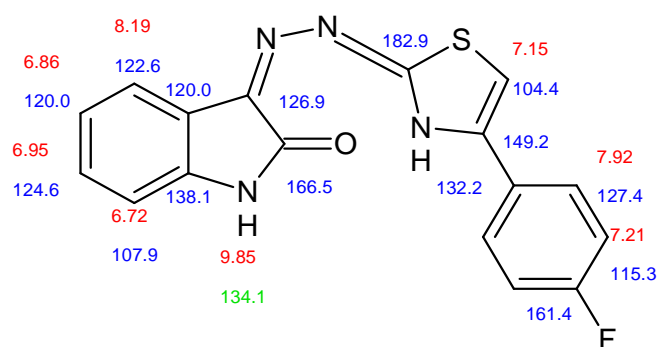


The minor compound is:

$^1\text{H}$  NMR (DMSO)  $\delta$ (ppm): 9.85 (s; 1H); 8.19 (dm;  $J$ : 7.4 Hz; 1H); 7.97-7.90 (m; 2H); 7.29-7.17 (m; 2H); 7.15 (s; 1H); 6.99-6.92 (m; 1H); 6.86 (td;  $J$ : 7.5 Hz; 1.0 Hz; 1H); 6.72 (dm;  $J$ : 7.5 Hz; 1H)

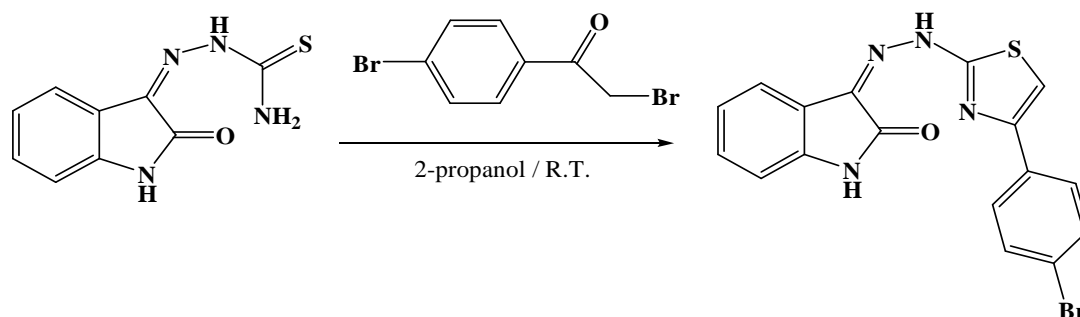
$^{13}\text{C}$  NMR (DMSO)  $\delta$ (ppm): 182.9; 166.5; 161.4 (d;  $J$ : 244.0 Hz); 149.2; 138.1; 132.2; 127.4 (d;  $J$ : 8.0 Hz); 126.9; 124.6; 122.6; 120.0; 120.0; 115.3 (d;  $J$ : 21.3 Hz); 107.9; 104.4

$^{15}\text{N}$  NMR (DMSO)  $\delta$ (ppm): 134.1



EMAC 2074

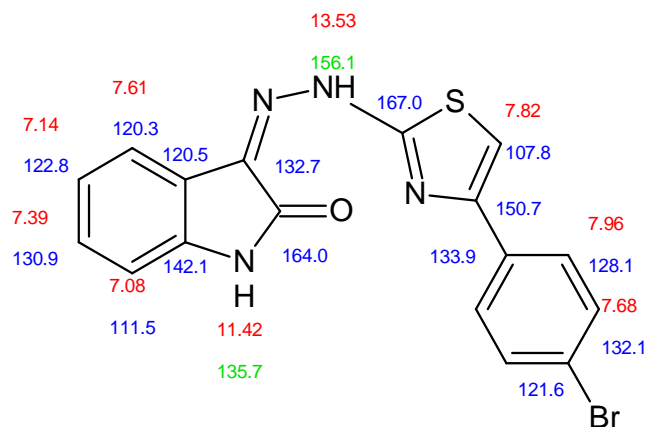
*(Z)*-3-(2-(4-(4-bromophenyl)thiazol-2-yl)hydrazono)indolin-2-one



$^1\text{H}$  NMR (DMF)  $\delta$ (ppm): 13.53 (s; 1H); 11.42 (s; 1H); 7.99-7.93 (m; 2H); 7.82 (s; 1H); 7.71-7.65 (m; 2H); 7.61 (dm;  $J$ : 7.6 Hz; 1H); 7.39 (tm;  $J$ : 7.6 Hz; 1H); 7.14 (tm;  $J$ : 7.6 Hz; 1H); 7.08 (dm;  $J$ : 7.6 Hz; 1H)

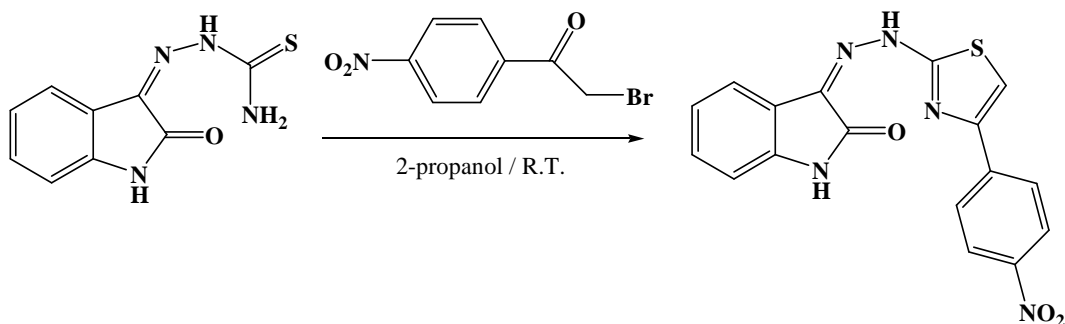
$^{13}\text{C}$  NMR (DMF)  $\delta$ (ppm): 167.0; 164.0; 150.7; 142.1; 133.9; 132.7; 132.1; 130.9; 128.1; 122.8; 121.6; 120.5; 120.3; 111.5; 107.8

$^{15}\text{N}$  NMR (DMF)  $\delta$ (ppm): 156.1; 135.7



EMAC 2075

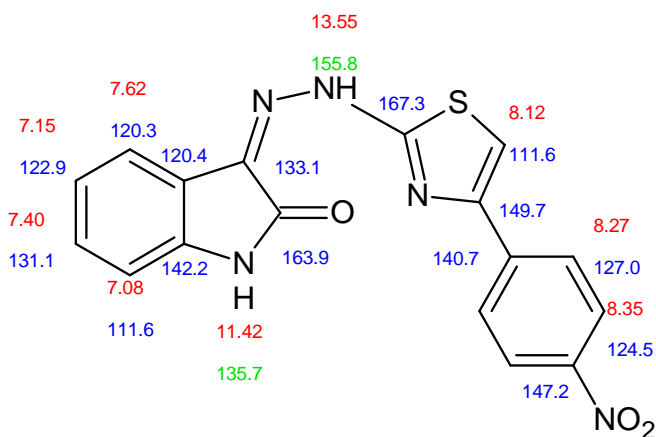
*(Z)*-3-(2-(4-(4-nitrophenyl)thiazol-2-yl)hydrazono)indolin-2-one



$^1\text{H}$  NMR (DMF)  $\delta$ (ppm): 13.55 (s; 1H); 11.42 (s; 1H); 8.38-8.32 (m; 2H); 8.30-8.24 (m; 2H); 8.12 (s; 1H); 7.62 (dm;  $J$ : 7.7 Hz; 1H); 7.40 (td;  $J$ : 7.7 Hz; 1.2 Hz; 1H); 7.15 (td;  $J$ : 7.7 Hz; 0.7 Hz; 1H); 7.08 (dm;  $J$ : 7.7 Hz; 1H)

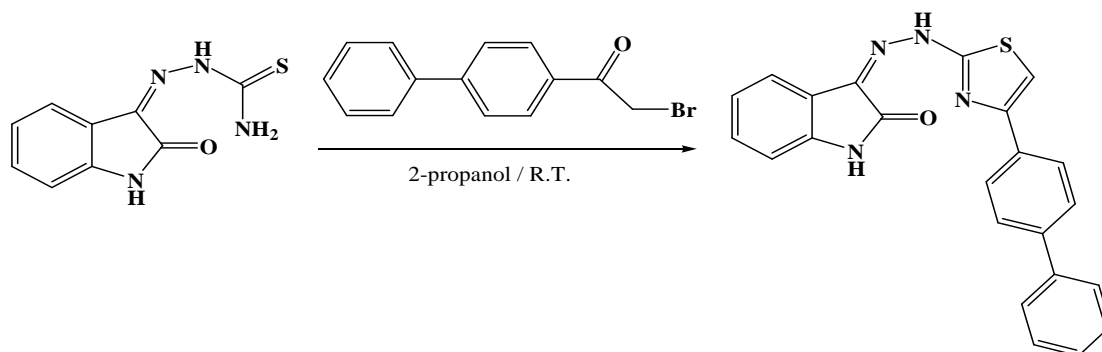
$^{13}\text{C}$  NMR (DMF)  $\delta$ (ppm): 167.3; 163.9; 149.7; 147.2; 142.2; 140.7; 133.1; 131.1; 127.0; 124.5; 122.9; 120.4; 120.3; 111.6; 111.6

$^{15}\text{N}$  NMR (DMF)  $\delta$ (ppm): 155.8; 135.7



EMAC 2076

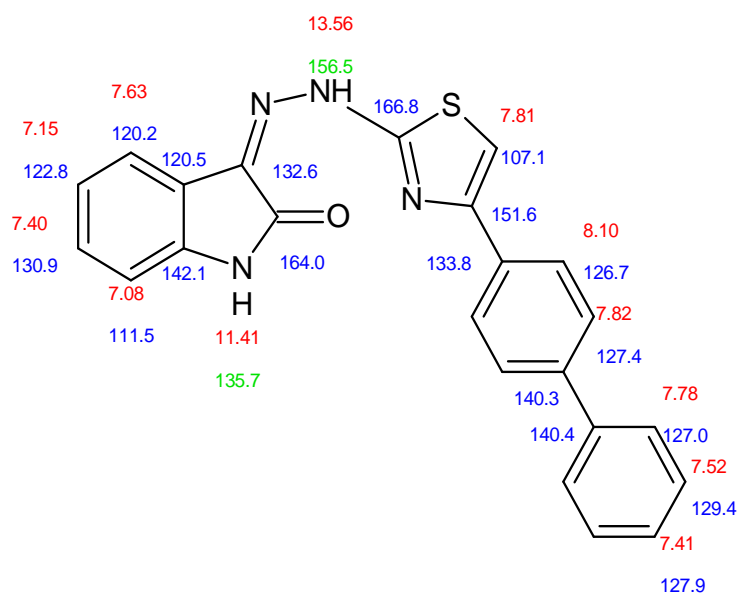
**(Z)-3-{2-[4-(4-phenylphenyl)-1,3-thiazol-2-yl]hydrazin-1-ylidene}-2,3-dihydro-1H-indol-2-one**



$^1\text{H}$  NMR (DMF)  $\delta$ (ppm): 13.56 (s; 1H); 11.41 (s; 1H); 8.13-8.08 (m; 2H); 7.85-7.75 (m; 5H); 7.63 (d;  $J$ : 7.6 Hz; 1H); 7.55-7.49 (m; 2H); 7.44-7.36 (m; 2H); 7.15 (tm;  $J$ : 7.6 Hz; 1H); 7.08 (dm;  $J$ : 7.6 Hz; 1H)

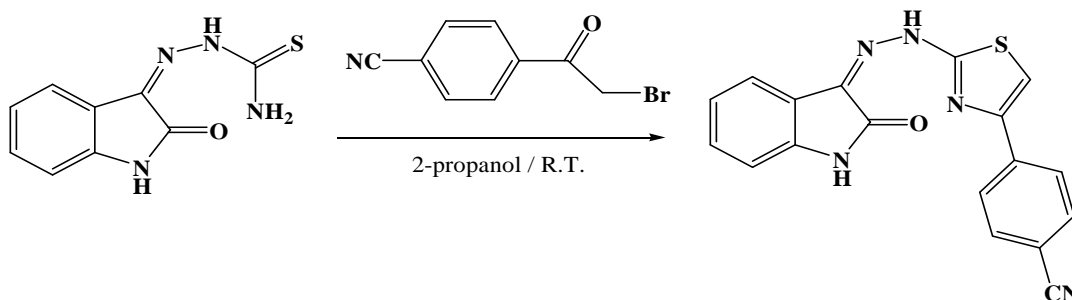
$^{13}\text{C}$  NMR (DMF)  $\delta$ (ppm): 166.8; 164.0; 151.6; 142.1; 140.4; 140.3; 133.8; 132.6; 130.9; 129.4; 127.9; 127.4; 127.0; 126.7; 122.8; 120.5; 120.2; 111.5; 107.1

$^{15}\text{N}$  NMR (DMF)  $\delta$ (ppm): 156.5; 135.7



EMAC 2077

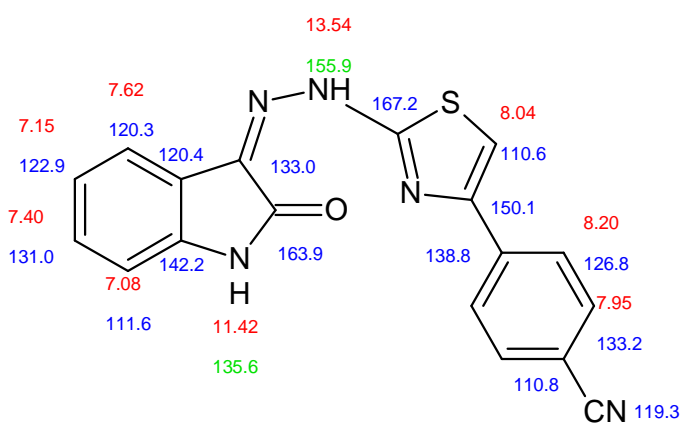
4-(2-{2-[(3Z)-2-oxo-2,3-dihydro-1H-indol-3-ylidene]hydrazin-1-yl}-1,3-thiazol-4-yl)benzonitrile

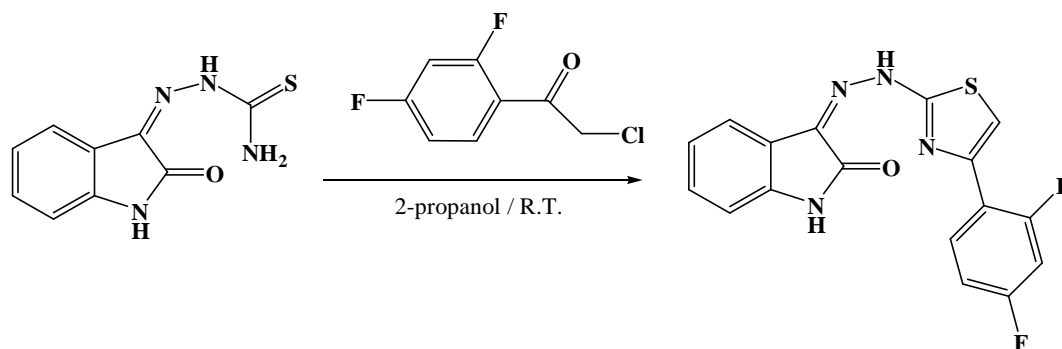


$^1\text{H}$  NMR (DMF)  $\delta$ (ppm): 13.54 (s; 1H); 11.42 (s; 1H); 8.23-8.17 (m; 2H); 8.04 (s; 1H); 7.97-7.93 (m; 2H); 7.62 (d;  $J$ : 7.6 Hz; 1H); 7.40 (tm;  $J$ : 7.6 Hz; 1H); 7.15 (tm;  $J$ : 7.6 Hz; 1H); 7.08 (d;  $J$ : 7.6 Hz; 1H)

$^{13}\text{C}$  NMR (DMF)  $\delta$ (ppm): 167.2; 163.9; 150.1; 142.2; 138.8; 133.2; 133.0; 131.0; 126.8; 122.9; 120.4; 120.3; 119.3; 111.6; 110.8; 110.6

$^{15}\text{N}$  NMR (DMF)  $\delta$ (ppm): 155.9; 135.6



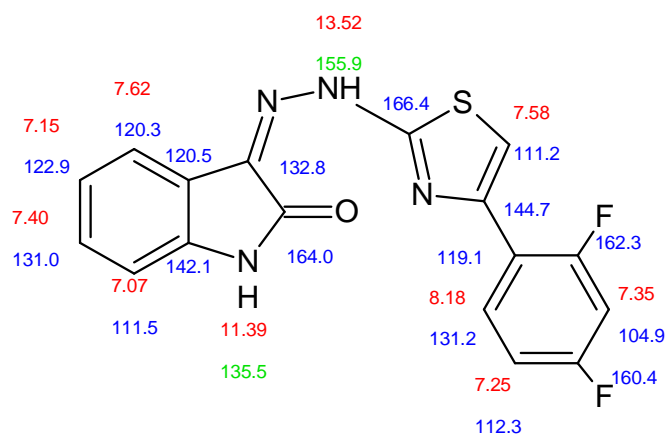
**EMAC 2078****(Z)-3-(2-(4-(2,4-difluorophenyl)thiazol-2-yl)hydrazono)indolin-2-one**

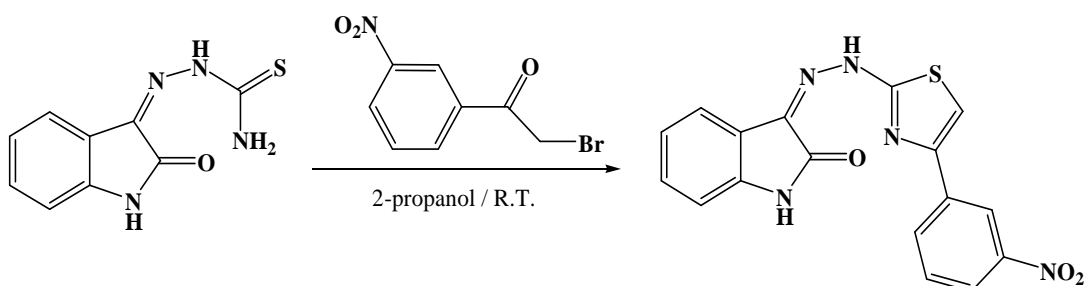
$^1\text{H}$  NMR (DMF)  $\delta$ (ppm): 13.52 (s; 1H); 11.39 (s; 1H); 8.23-8.14 (m; 1H); 7.62 (d;  $J$ : 7.6 Hz; 1H); 7.58(d;  $J$ : 2.4 Hz; 1H); 7.45-7.36 (m; 2H); 7.25 (td;  $J$ : 8.5 Hz; 2.5 Hz; 1H); 7.15 (td;  $J$ : 7.6 Hz; 0.7 Hz; 1H); 7.07 (dm;  $J$ : 7.6 Hz; 1H)

$^{13}\text{C}$  NMR (DMF)  $\delta$ (ppm): 166.4; 164.0; 162.3 (dd;  $J$ : 248.0 Hz; 12.4 Hz); 160.4 (dd;  $J$ : 251.9 Hz; 12.3 Hz); 144.7 (dd;  $J$ : 2.6 Hz; 0.9 Hz); 142.1; 132.8; 131.2 (dd;  $J$ : 9.6Hz; 4.8 Hz); 131.0; 122.9; 120.5; 120.3; 119.1 (dd;  $J$ : 11.3Hz; 3.7 Hz); 112.3 (dd;  $J$ : 21.4Hz; 3.4 Hz); 111.5; 111.2 (d;  $J$ : 15.0 Hz); 104.9 (t;  $J$ : 26.5 Hz)

$^{15}\text{N}$  NMR (DMF)  $\delta$ (ppm): 155.9; 135.5

$^{19}\text{F}$  NMR (DMF)  $\delta$ (ppm): -110.85; -111.77

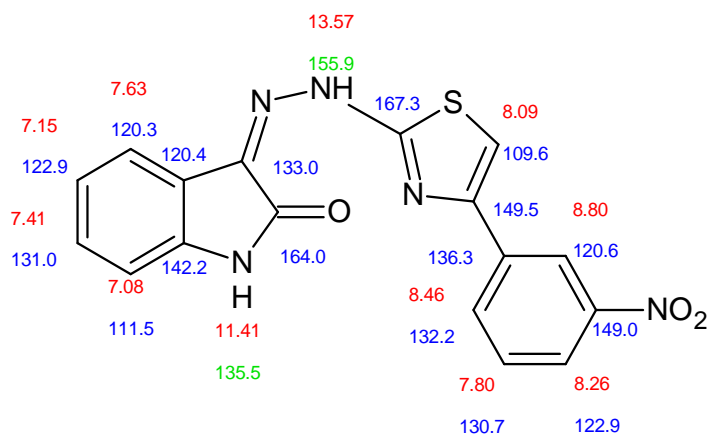


**EMAC 2079****(Z)-3-(2-(4-(3-nitrophenyl)thiazol-2-yl)hydrazono)indolin-2-one**

$^1\text{H}$  NMR (DMF)  $\delta$ (ppm): 13.57 (s; 1H); 11.41 (s; 1H); 8.84-8.76 (m; 1H); 8.46 (dm;  $J$ : 8.1 Hz; 1H); 8.26 (dm;  $J$ : 8.1 Hz; 1H); 8.09 (s; 1H); 7.80 (t;  $J$ : 8.1 Hz; 1H); 7.63 (d;  $J$ : 7.6 Hz; 1H); 7.41 (tm;  $J$ : 7.6 Hz; 1H); 7.15 (tm;  $J$ : 7.6 Hz; 1H); 7.08 (dm;  $J$ : 7.6 Hz; 1H)

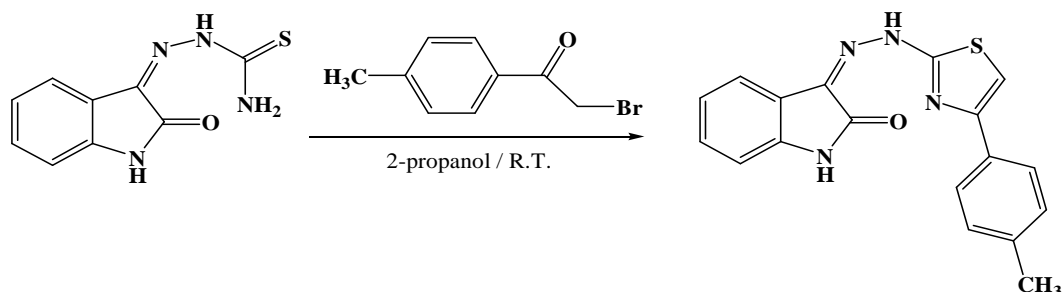
$^{13}\text{C}$  NMR (DMF)  $\delta$ (ppm): 167.3; 164.0; 149.5; 149.0; 142.2; 136.3; 133.0; 132.2; 131.0; 130.7; 122.9; 122.9; 120.6; 120.4; 120.3; 111.5; 109.6

$^{15}\text{N}$  NMR (DMF)  $\delta$ (ppm): 155.9; 135.5



## EMAC 2080

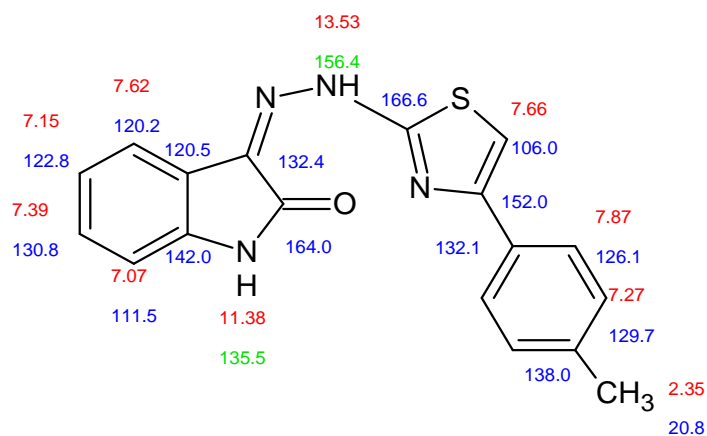
### (Z)-3-(2-(4-p-tolylthiazol-2-yl)hydrazono)indolin-2-one



<sup>1</sup>H NMR (DMF) δ(ppm): 13.53 (s; 1H); 11.38 (s; 1H); 7.91-7.86 (m; 2H); 7.66 (s; 1H); 7.62 (d; *J*: 7.6 Hz; 1H); 7.39 (td; *J*: 7.6 Hz; 1.2 Hz; 1H); 7.30-7.25 (m; 2H); 7.15 (td; *J*: 7.6 Hz; 0.8 Hz; 1H); 7.07 (dm; *J*: 7.6 Hz; 1H); 2.35 (s; 3H)

<sup>13</sup>C NMR (DMF) δ(ppm): 166.6; 164.0; 152.0; 142.0; 138.0; 132.4; 132.1; 130.8; 129.7; 126.1; 122.8; 120.5; 120.2; 111.5; 106.0; 20.8

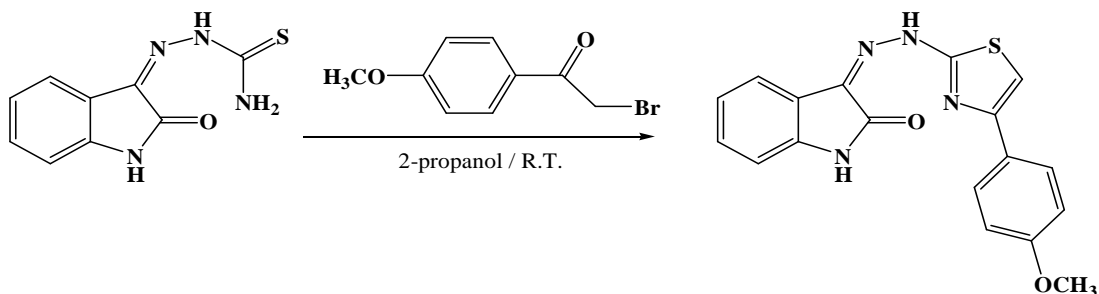
<sup>15</sup>N NMR (DMF) δ(ppm): 156.4; 135.5





EMAC 2081

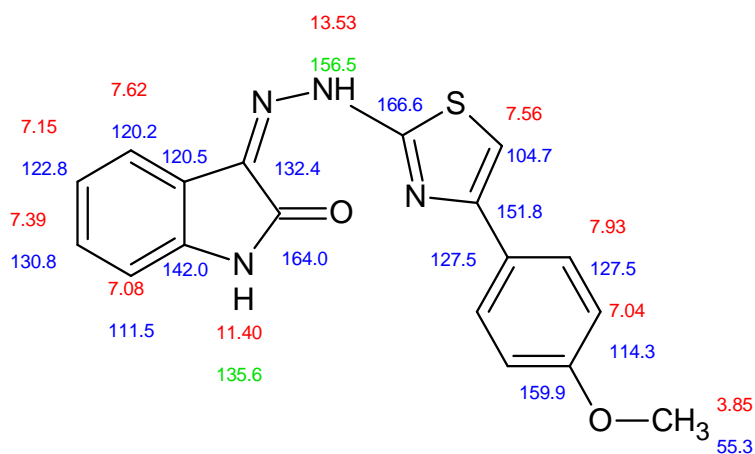
*(Z)*-3-(2-(4-(4-methoxyphenyl)thiazol-2-yl)hydrazono)indolin-2-one



<sup>1</sup>H NMR (DMF) δ(ppm): 13.53 (s; 1H); 11.40 (s; 1H); 7.95-7.91 (m; 2H); 7.63-7.59 (dm; *J*: 7.7 Hz; 1H); 7.56 (s; 1H); 7.39 (td; *J*: 7.7 Hz; 1.1 Hz; 1H); 7.15 (td; *J*: 7.7 Hz; 1.0 Hz; 1H); 7.08 (dm; *J*: 7.7 Hz; 1H); 7.06-7.02 (m, 2H); 3.85 (s; 3H)

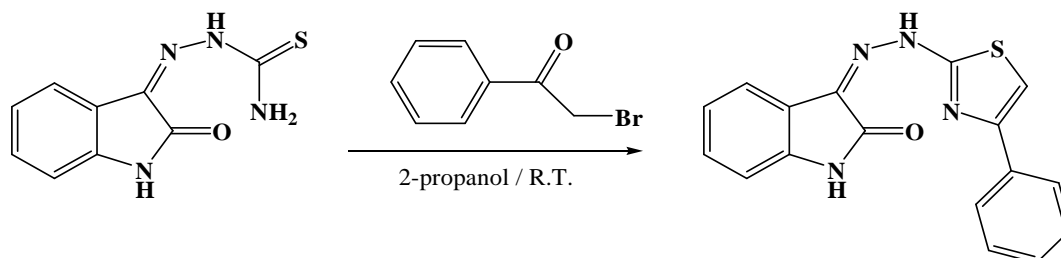
<sup>13</sup>C NMR (DMF) δ(ppm): 166.6; 164.0; 159.9; 151.8; 142.0; 132.4; 130.8; 127.5; 127.5; 122.8; 120.5; 120.2; 114.3; 111.5; 104.7; 55.3

<sup>15</sup>N NMR (DMF) δ(ppm): 156.6; 135.6



EMAC 2082

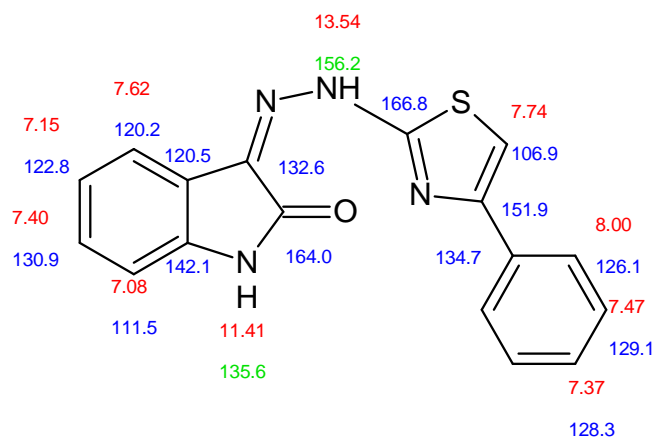
*(Z)*-3-(2-(4-phenylthiazol-2-yl)hydrazono)indolin-2-one



$^1\text{H}$  NMR (DMF)  $\delta$ (ppm): 13.54 (s; 1H); 11.41 (s; 1H); 8.01-7.97 (m; 2H); 7.74 (s; 1H); 7.62 (dm;  $J$ : 7.7 Hz; 1H); 7.49-7.44 (m; 2H); 7.42-7.34 (m; 2H); 7.17-7.10 (m; 1H); 7.08 (dm;  $J$ : 7.7 Hz; 1H)

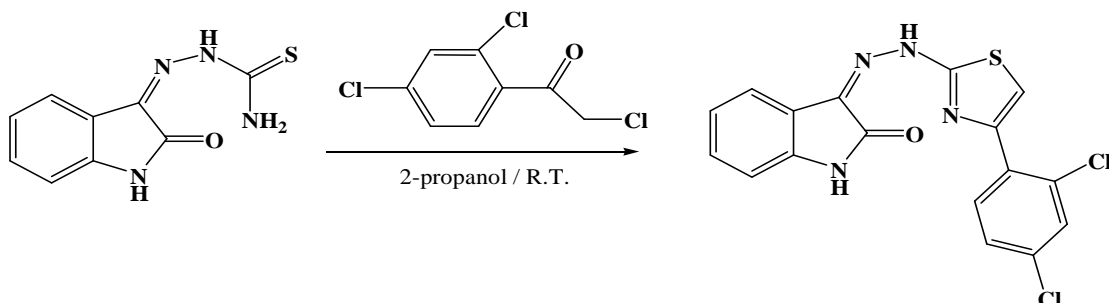
$^{13}\text{C}$  NMR (DMF)  $\delta$ (ppm): 166.8; 164.0; 151.9; 142.1; 134.7; 132.6; 130.9; 129.1; 128.3; 126.1; 122.8; 120.5; 120.2; 111.5; 106.9

$^{15}\text{N}$  NMR (DMF)  $\delta$ (ppm): 156.2; 135.6



EMAC 2083

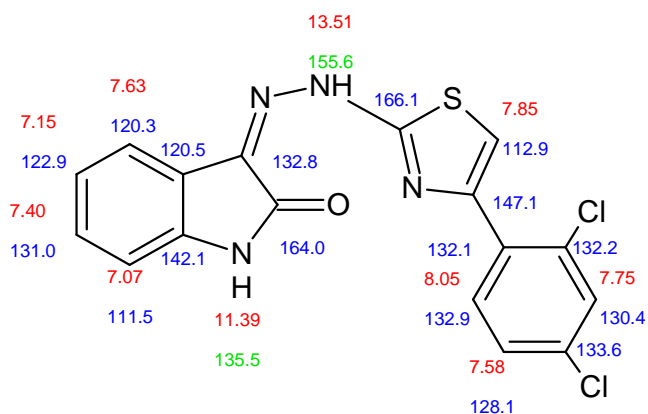
*(Z)*-3-(2-(4-(2,4-dichlorophenyl)thiazol-2-yl)hydrazono)indolin-2-one



$^1\text{H}$  NMR (DMF)  $\delta$ (ppm): 13.51 (s; 1H); 11.39 (s; 1H); 8.05 (d;  $J$ : 8.5 Hz; 1H); 7.85 (s; 1H); 7.75 (d;  $J$ : 2.2 Hz; 1H); 7.63 (dm;  $J$ : 7.6 Hz; 1H); 7.58 (dd;  $J$ : 8.5 Hz; 2.2 Hz; 1H); 7.40 (td;  $J$ : 7.6 Hz; 1.2 Hz; 1H); 7.15 (td;  $J$ : 7.6 Hz; 1.0 Hz; 1H); 7.07 (dm;  $J$ : 7.6 Hz; 1H)

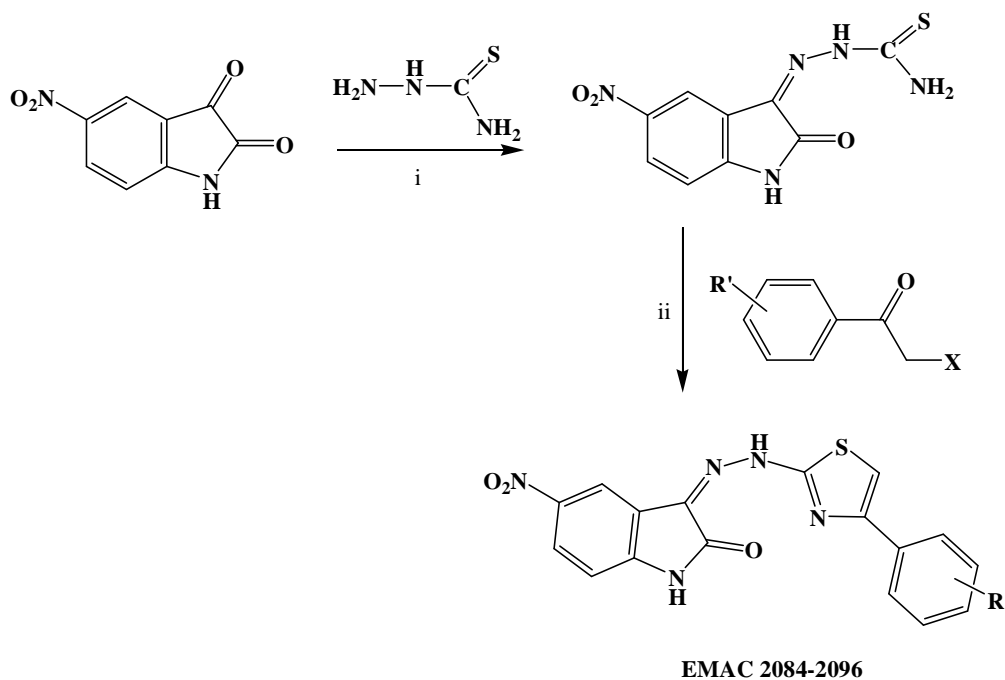
$^{13}\text{C}$  NMR (DMF)  $\delta$ (ppm): 166.1; 164.0; 147.1; 142.1; 133.6; 132.6; 132.9; 132.2; 132.1; 131.0; 130.4; 128.1; 122.9; 120.5; 120.3; 112.9; 111.5

$^{15}\text{N}$  NMR (DMF)  $\delta$ (ppm): 155.6; 135.5



## COMPOUNDS EMAC 2084-2096

### General synthetic scheme:



R: 4-Cl, 4-F, 4-Br, 4-NO<sub>2</sub>, 4-C<sub>6</sub>H<sub>5</sub>, 4-CN, 2,4-F, 3-NO<sub>2</sub>, 3,4-Cl, 4-CH<sub>3</sub>, 4-OCH<sub>3</sub>, H, 2,4-Cl

**Scheme 8.** Synthesis of 3-(2-(4-arylthiazol-2-yl)hydrazono)5-nitroindolin-2-one derivatives EMAC 2084-2096. Reagents: (i) 2-propanol, AcOH; (iii) 2-propanol, R.T.

5-nitroindolinone derivative were synthesized by a multi step reaction.

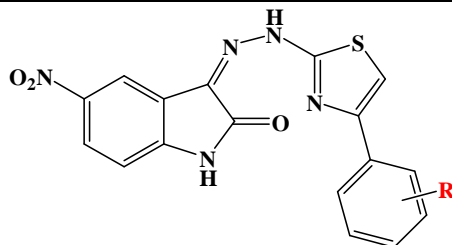
The first synthetic step leads to the formation of 1-(5-nitro-2-oxoindolin-3-ylidene)thiosemicarbazide by reacting 5-nitroisatin with thiosemicarbazide in 2-propanol and catalytic amount of AcOH.

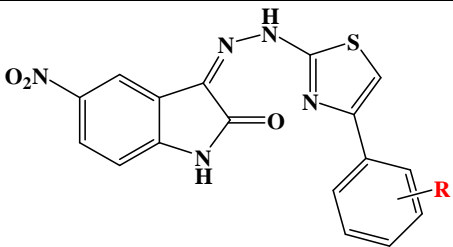
In the second step, the thiazole ring is formed by reaction between 1-(5-nitro-2-oxoindolin-3-ylidene)thiosemicarbazide and differently substituted  $\alpha$ -halogenacetophenones as outlined in Scheme 8.

All synthesized compounds were characterised by analytical and spectral data as listed in Table 23 and 24.

**Table 23.** Chemical and physical data of derivatives EMAC 2084-2096

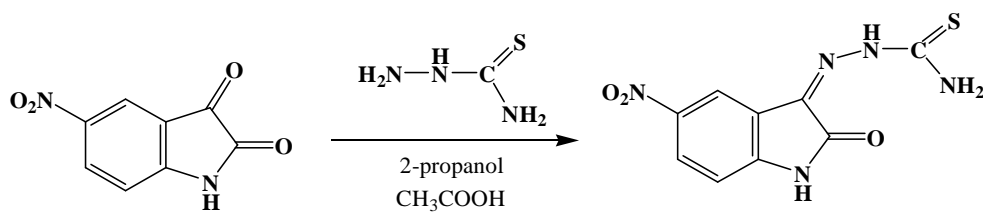
Compound	R	M.W.	Mp (C°)	% Yield
EMAC 2084	4-Cl	399.81	>250	63
EMAC 2085	4-F	383.36	>250	56
EMAC 2086	4-Br	444.26	>250	61
EMAC 2087	4-NO <sub>2</sub>	410.36	>250	67.5
EMAC 2088	4-C <sub>6</sub> H <sub>5</sub>	441.46	>250	69.5
EMAC 2089	4-CN	390.38	>250	69.3
EMAC 2090	2,4-F	401.35	>250	66
EMAC 2091	3-NO <sub>2</sub>	410.36	>250	43
EMAC 2092	3,4-Cl	434.26	>250	50
EMAC 2093	4-CH <sub>3</sub>	379.39	>250	69
EMAC 2094	4-OCH <sub>3</sub>	395.39	>250	72
EMAC 2095	H	365.37	>250	63
EMAC 2096	2,4-Cl	434.26	>250	54



**Table 24.** Analytical data of derivatives EMAC 2084-2096


Compound	R	Reaction solvent	Crystallisation solvent	Aspect	Reaction time (h)
EMAC 2084	4-Cl	2-propanol	Water/Ethanol	Crystalline orange solid	24
EMAC 2085	4-F	2-propanol	Water/Ethanol	Crystalline yellow solid	12
EMAC 2086	4-Br	2-propanol	Water/Ethanol	Crystalline yellow solid	12
EMAC 2087	4-NO <sub>2</sub>	2-propanol	Water/Ethanol	Yellow-orange solid	24
EMAC 2088	4-C <sub>6</sub> H <sub>5</sub>	2-propanol	Water/Ethanol	Yellow-orange solid	12
EMAC 2089	4-CN	2-propanol	Water/Ethanol	Yellow-orange solid	24
EMAC 2090	2,4-F	2-propanol	Water/Ethanol	Yellow-brown solid	24
EMAC 2091	3-NO <sub>2</sub>	2-propanol	Water/Ethanol	Yellow-orange solid	12
EMAC 2092	3,4-Cl	2-propanol	Water/Ethanol	Yellow solid	24
EMAC 2093	4-CH <sub>3</sub>	2-propanol	Water/Ethanol	Yellow-orange solid	24
EMAC 2094	4-OCH <sub>3</sub>	2-propanol	Water/Ethanol	Red-orange solid	24
EMAC 2095	H	2-propanol	Water/Ethanol	Yellow-orange solid	12
EMAC 2096	2,4-Cl	2-propanol	Water/Ethanol	Yellow solid	12

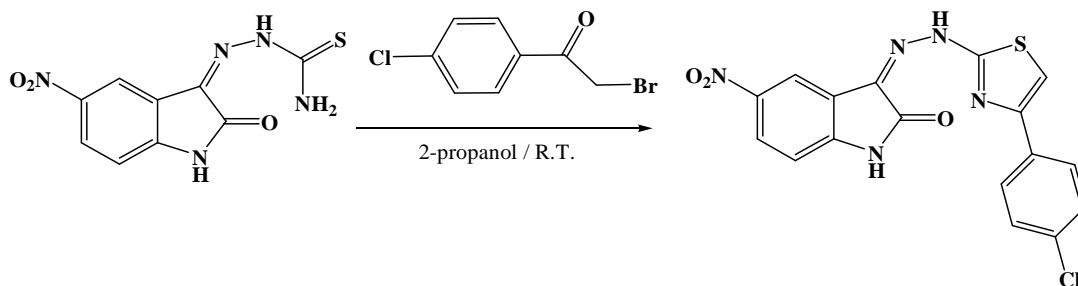
**1-(5-nitro-2-oxoindolin-3-ylidene)thiosemicarbazide**



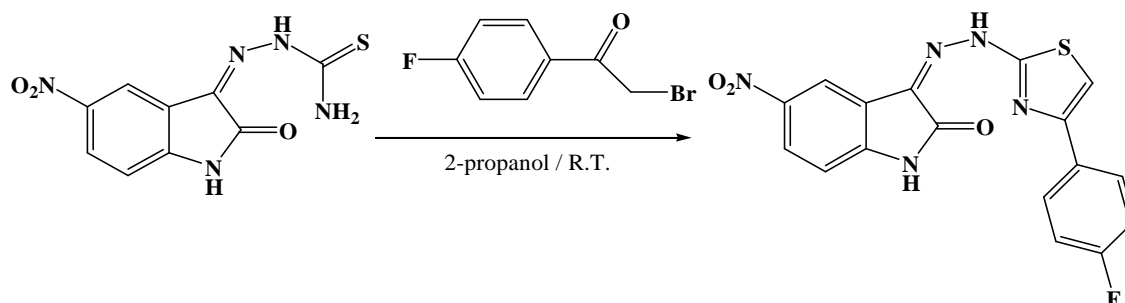
M.W.: 265.25 g/mol; R.f.: 0.28 (exane-ethylacetate 1:1); M.P.: >250°C; Yield: 97%  
MS (ESI+): 266.03 ([M+H]<sup>+</sup>)

**EMAC 2084**

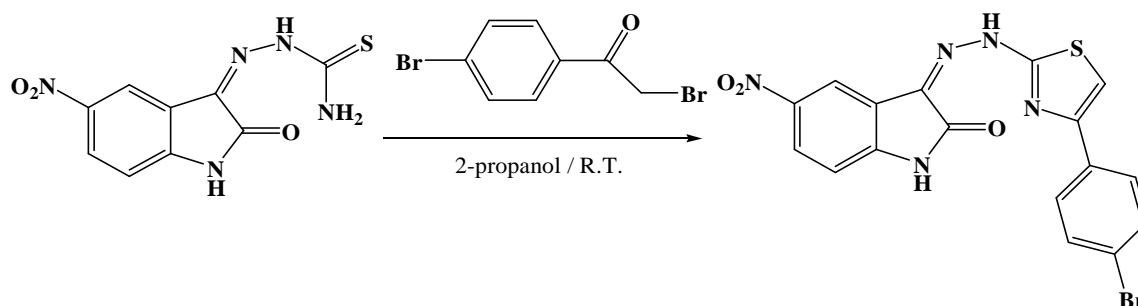
**3-(2-(4-(4-chlorophenyl)thiazol-2-yl)hydrazono)-5-nitroindolin-2-one**



<sup>1</sup>H-NMR (500 MHz, DMSO) δH 7.11 (d, 1H, J: 8.5, Ar-CH), 7.48 (d, 1H, J: 8.5, Ar-CH), 7.76 (s, 1H, thiazole), 7.87 (d, 2H, J: 9, Ar-CH), 7.92 (d, 2H, J: 9, Ar-CH), 8.6 (s, 1H, Ar-CH), 12.22 (s, 1H, NH), 13.25 (brs, 1H, NH)

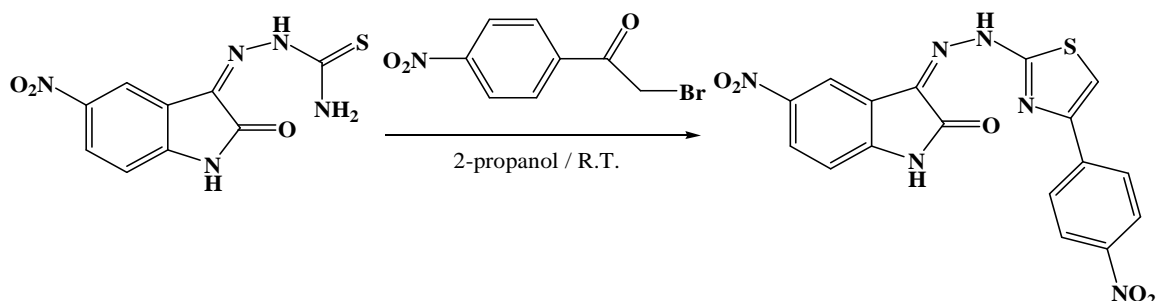
**EMAC 2085****3-(2-(4-(4-fluorophenyl)thiazol-2-yl)hydrazono)-5-nitroindolin-2-one**

$^1\text{H-NMR}$  (500 MHz, DMSO)  $\delta$ H 7.11 (d, 1H,  $J$ : 8.5, Ar-CH), 7.48 (d, 1H,  $J$ : 8.5, Ar-CH), 7.35 (d, 2H,  $J$ : 9, Ar-CH), 7.69 (s, 1H, thiazole), 8.25 (d, 2H,  $J$ : 9, Ar-CH), 8.6 (s, 1H, Ar-CH), 12.22 (s, 1H, NH), 13.23 (brs, 1H, NH)

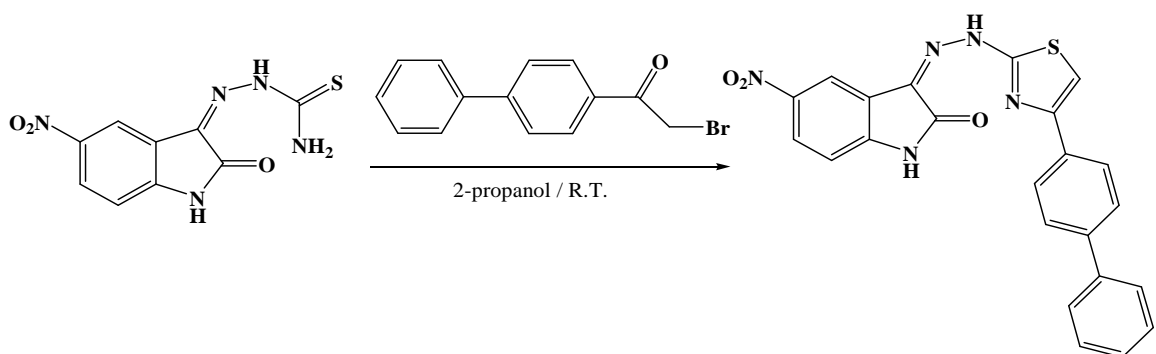
**EMAC 2086****3-(2-(4-(4-bromophenyl)thiazol-2-yl)hydrazono)-5-nitroindolin-2-one**

$^1\text{H-NMR}$  (500 MHz, DMSO)  $\delta$ H 7.12 (d, 1H,  $J$ : 8.5, Ar-CH), 7.50 (d, 1H,  $J$ : 8.5, Ar-CH), 7.77 (s, 1H, thiazole), 7.86 (d, 2H,  $J$ : 9, Ar-CH), 8.22 (d, 2H,  $J$ : 9, Ar-CH), 8.6 (s, 1H, Ar-CH), 12.22 (s, 1H, NH), 13.25 (brs, 1H, NH)

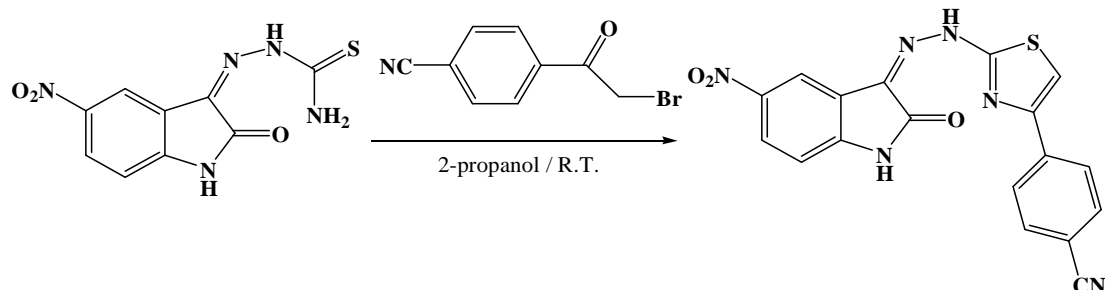


**EMAC 2087****5-nitro-3-(2-(4-(4-nitrophenyl)thiazol-2-yl)hydrazono)indolin-2-one**

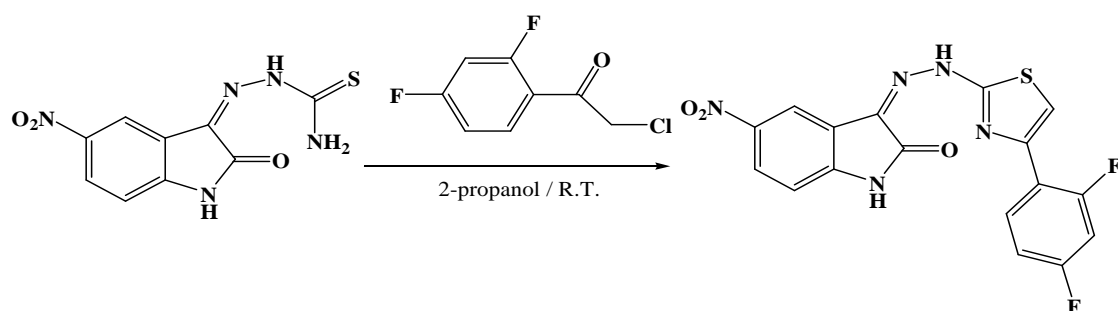
$^1\text{H-NMR}$  (500 MHz, DMSO)  $\delta$ H 7.2 (d, 1H,  $J$ : 8.5, Ar-CH), 7.52 (d, 1H,  $J$ : 8.5, Ar-CH), 8.15 (s, 1H, thiazole), 8.37 (d, 2H,  $J$ : 9; Ar-CH), 8.45 (d, 2H,  $J$ : 9, Ar-CH), 8.62 (s, 1H, Ar-CH), 12.25 (s, 1H, NH), 13.55 (brs, 1H, NH)

**EMAC 2088****3-(2-(4-(4-difluorophenyl)thiazol-2-yl)hydrazono)-5-nitroindolin-2-one**

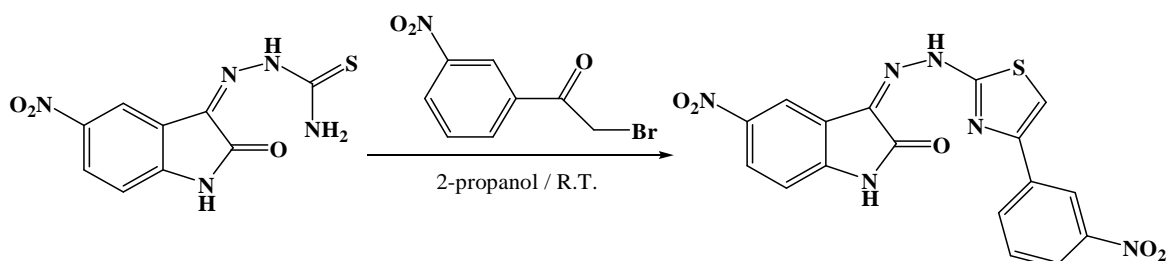
$^1\text{H-NMR}$  (500 MHz, DMSO)  $\delta$ H 7.21 (d, 1H,  $J$ : 8.5, Ar-CH), 7.22 (t, 1H, Ar-CH), 7.32 (d, 2H, Ar-CH), 7.48 (m, 3H, Ar-CH), 7.54 (m, 4H, Ar-CH), 7.77 (s, 1H, thiazole), 8.6 (s, 1H, Ar-CH), 12.25 (s, 1H, NH), 13.55 (brs, 1H, NH)

**EMAC 2089****3-(2-(4-(4-cyanophenyl)thiazol-2-yl)hydrazono)-5-nitroindolin-2-one**

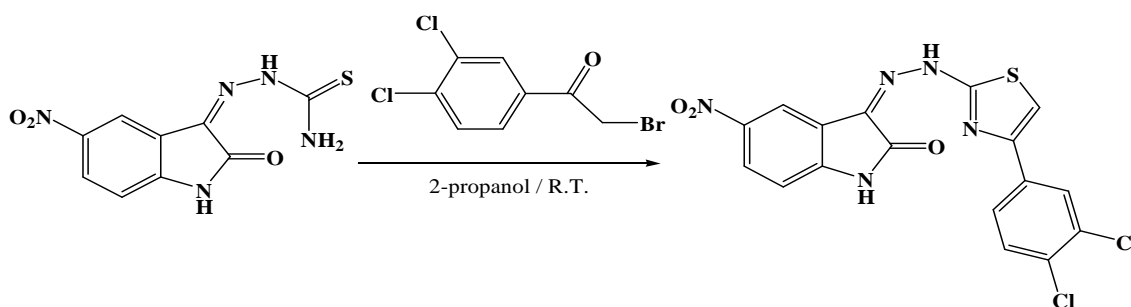
$^1\text{H-NMR}$  (500 MHz, DMSO)  $\delta$ H 7.11 (d, 1H,  $J$ : 8.5, Ar-CH), 7.48 (d, 1H,  $J$ : 8.5, Ar-CH), 8.05 (s, 1H, thiazole), 8.00 (d, 2H,  $J$ : 9, Ar-CH), 8.22 (d, 2H,  $J$ : 9, Ar-CH), 8.06 (s, 1H, Ar-CH), 12.22 (s, 1H, NH), 13.55 (brs, 1H, NH)

**EMAC 2090****3-(2-(4-(2,4-difluorophenyl)thiazol-2-yl)hydrazono)-5-nitroindolin-2-one**

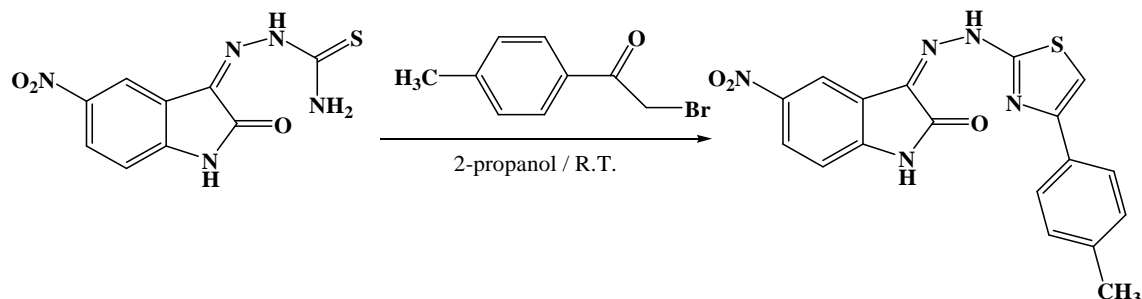
$^1\text{H-NMR}$  (500 MHz, DMSO)  $\delta$ H 7.11 (d, 1H,  $J$ : 8.5, Ar-CH), 7.35 (d, 1H,  $J$ : 8.5, Ar-CH), 7.45 (s, 1H, Ar-CH), 7.48 (d, 1H,  $J$ : 8.5, Ar-CH), 7.6 (s, 1H, thiazole), 8.28 (d, 1H,  $J$ : 8.5, Ar-CH), 8.6 (s, 1H, Ar-CH), 12.22 (s, 1H, NH), 13.55 (brs, 1H, NH)

**EMAC 2091****5-nitro-3-(2-(4-(3-nitrophenyl)thiazol-2-yl)hydrazono)indolin-2-one**

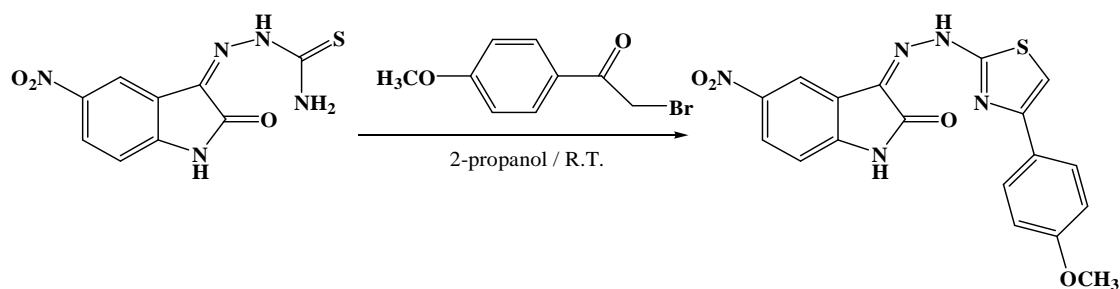
$^1\text{H-NMR}$  (500 MHz, DMSO)  $\delta\text{H}$  7.11 (d, 1H,  $J$ : 8.5, Ar-CH), 7.48 (d, 1H,  $J$ : 8.5, Ar-CH), 7.90 (t, 1H,  $J$ : 8, Ar-CH), 8.1 (s, 1H, thiazole), 8.36 (d, 1H,  $J$ : 8, Ar-CH), 8.56 (d, 1H,  $J$ : 8, Ar-CH), 8.6 (s, 1H, Ar-CH), 12.22 (s, 1H, NH), 13.55 (brs, 1H, NH)

**EMAC 2092****3-(2-(4-(3,4-dichlorophenyl)thiazol-2-yl)hydrazono)-5-nitroindolin-2-one**

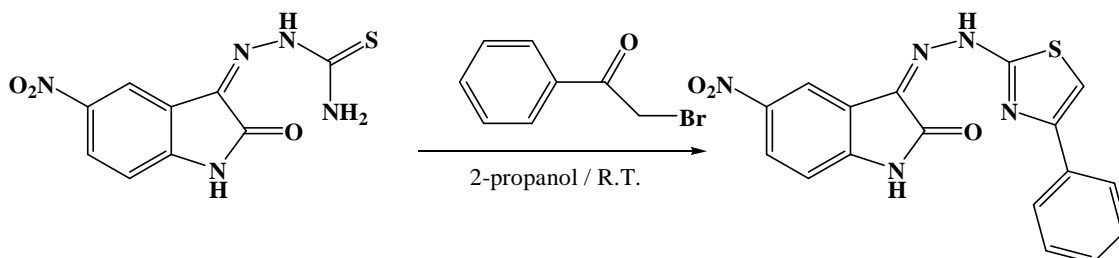
$^1\text{H-NMR}$  (500 MHz, DMSO)  $\delta\text{H}$  7.11 (d, 1H,  $J$ : 8.5, Ar-CH), 7.48 (d, 1H,  $J$ : 8.5, Ar-CH), 7.67 (d, 1H,  $J$ : 8, Ar-CH), 7.72 (s, 1H, thiazole), 8.15 (d, 1H,  $J$ : 8, Ar-CH), 8.4 (s, 1H, Ar-CH), 8.6 (s, 1H, Ar-CH), 12.22 (s, 1H, NH), 13.55 (brs, 1H, NH)

**EMAC 2093****5-nitro-3-(2-(4-p-tolylthiazol-2-yl)hydrazono)indolin-2-one**

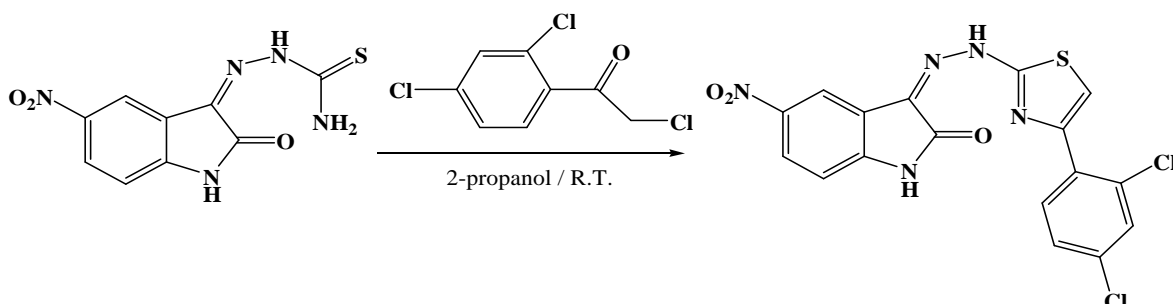
$^1\text{H-NMR}$  (500 MHz, DMSO)  $\delta\text{H}$  2.35 (s, 3H,  $\text{CH}_3$ ), 7.11 (d, 1H,  $J$ : 8.5, Ar-CH), 7.37 (d, 2H,  $J$ : 9, Ar-CH), 7.48 (d, 1H,  $J$ : 8.5, Ar-CH), 7.76 (s, 1H, thiazole), 7.94 (d, 2H,  $J$ : 9, Ar-CH), 8.6 (s, 1H, Ar-CH), 12.22 (s, 1H, NH), 13.55 (brs, 1H, NH)

**EMAC 2094****3-(2-(4-(4-methoxyphenyl)thiazol-2-yl)hydrazono)-5-nitroindolin-2-one**

$^1\text{H-NMR}$  (500 MHz, DMSO)  $\delta\text{H}$  3.85 (s, 3H,  $\text{OCH}_3$ ), 7.11 (d, 1H,  $J$ : 8.5, Ar-CH), 7.14 (d, 2H,  $J$ : 8.5, Ar-CH), 7.48 (d, 1H,  $J$ : 8.5, Ar-CH), 7.66 (s, 1H, thiazole), 8.03 (d, 2H,  $J$ : 8.5, Ar-CH), 8.6 (s, 1H, Ar-CH), 12.22 (s, 1H, NH), 13.55 (brs, 1H, NH)

**EMAC 2095****5-nitro-3-(2-(4-phenylthiazol-2-yl)hydrazono)indolin-2-one**

$^1\text{H-NMR}$  (500 MHz, DMSO)  $\delta\text{H}$  7.11 (d, 1H,  $J$ : 8.5, Ar-CH), 7.47 (t, 1H,  $J$ : 8.5, Ar-CH), 7.48 (d, 1H,  $J$ : 8.5, Ar-CH), 7.57 (d, 2H,  $J$ : 9, Ar-CH), 7.84 (s, 1H, thiazole), 8.1 (d, 2H,  $J$ : 9, Ar-CH), 8.6 (s, 1H, Ar-CH), 12.22 (s, 1H, NH), 13.55 (brs, 1H, NH)

**EMAC 2096****3-(2-(4-(2,4-dichlorophenyl)thiazol-2-yl)hydrazono)-5-nitroindolin-2-one**

$^1\text{H-NMR}$  (500 MHz, DMSO)  $\delta\text{H}$  7.11 (d, 1H,  $J$ : 8.5, Ar-CH), 7.48 (d, 1H,  $J$ : 8.5, Ar-CH), 7.68 (d, 1H,  $J$ : 8.5, Ar-CH), 7.85 (s, 1H, Ar-CH), 7.86 (s, 1H, thiazolo), 8.15 (d, 1H,  $J$ : 8.5, Ar-CH), 8.6 (s, 1H, Ar-CH), 12.22 (s, 1H, NH), 13.55 (brs, 1H, NH)

## **3.2 Biology**

### ***Protein expression and purification***

The recombinant HIV-1 RT protein, whose coding gene was subcloned in the p6HRT\_prot plasmid, was expressed in E. coli strain M15. [207, 210]

The bacteria cells were grown up to an optical density (OD<sub>600</sub>) of 0.8 and induced with 1.7 mM isopropyl β-D-1-thiogalactopyranoside (IPTG) for 5 hrs.

HIV-1 RT purification was carried out as described [211]. Briefly, cell pellets were resuspended in Lyses Buffer (20 mM 4-(2-hydroxyethyl)-1-piperazineethanesulfonic acid (Hepes) pH 7.5, 0.5 M NaCl, 5 mM β-mercaptoethanol, 5 mM imidazole, 0.4 mg/mL lysozyme), incubated on ice for 20 min, sonicated and centrifuged at 30,000 x g for 1 hr.

The supernatant was applied to a His-binding resin column and washed thoroughly with wash buffer (20 mM Hepes pH 7.5, 0.3 M NaCl, 5 mM β-mercaptoethanol, 60 mM imidazole, 10% glycerol).

RT was eluted by imidazole gradient and the enzyme-containing fractions were pooled, dialyzed and aliquots were stored at -80 °C.

### ***RNase H polymerase-independent cleavage assay***

The HIV-1 RT associated RNase H activity was measured as described [200] in 100 μL reaction volume containing 50 mM Tris-HCl pH 7.8, 6 mM MgCl<sub>2</sub>, 1 mM dithiothreitol (DTT), 80 mM KCl, hybrid RNA/DNA (5'-GTTTTCTTTTCCCCCTGA C-3'-Fluorescein, 5'-CAAAAGAAAAGG GGGGACUG-3'-Dabcyl) and 3.8 nM RT. The reaction mixture was incubated for 1 hr at 37 °C. The enzymatic reaction is stopped with the addition to EDTA and measured with Victor3 (Perkin) at 490/528 nm.

### ***DNA polymerase assay***

The HIV-1 RT associated (RDDP) activity was measured using Invitrogen EnzCheck Reverse Transcriptase Assay Kit, in 50 μL volume containing 60 mM Tris-HCl pH 8.1, 8 mM MgCl<sub>2</sub>, 60 mM KCl, 13 mM Dithiothreitol, 100 μM dTTP, 2 nM HIV-1 RT and poly(A)-oligo(dT). The reaction mixture was incubated for 30 minutes at 37°C. The enzymatic reaction is stopped with the addition to EDTA and measured with Victor3 (Perkin) at 502/523 nm after the addition to picogreen.

## **4 Acknowledgments**

*This work was supported by Regione Autonoma della Sardegna.*

*I wish to thank Fondazione Banco di Sardegna for founding my Phd grant.*

*I acknowledge Prof. Enzo Tramontano and his group from the University of Cagliari for the biological investigation; Prof. Stefano Alcaro and his group from University of Magna Graecia, for their help in computational studies; Prof. Cheng from Yale University and Prof. Cristina Parolin from University of Padua for the antiviral activity investigation in infected cells.*







## 5 References

- [1] CDC. Pneumocystis pneumonia — Los Angeles. *MMWR*; **30** (1981) 250–252.
- [2] Barre-Sinoussi, F.; Chermann, J.C.; Rey, F.; Nugeyre, M.T.; Chamaret, S.; Gruest, J.; Dauguet, C.; Axler-Blin, C.; Vèzinet-Brun, F.; Rouzioux, C.; Rozenbaum, W.; Montagnier, L. Isolation of a T-lymphotropic retrovirus from a patient at risk for acquired immune deficiency syndrome (AIDS). *Science*, **220**, (1983), 868-871.
- [3] Gallo, R.C.; Salahuddin, S.Z.; Popovic, M.; Shearer, G.M.; Kaplan, M.; Haynes, B.F.; Palker, T.J.; Redfield, R.; Oleske, J.; Safai, B. Frequent detection and isolation of cytopathic retroviruses (HTLV-III) from patients with AIDS and at risk for AIDS. *Science*, **224**(4648), (1984), 500-503.
- [4] Levy, J.A.; Hoffman, A.D.; Kramer, S.M.; Landis, J.A.; Shimabukuro, J.M.; Oshiro, L.S. Isolation of lymphocytopathic retroviruses from San Francisco patients with AIDS. *Science*, **225**, (1984), 840-842.
- [5] Shaw, G.M.; Hahn, B.H.; Arya, S.K.; Gropman, J.E.; Gallo, R.C.; Wong-Staal, F. Molecular characterization of human T-cell leukaemia (lymphotropic) virus type III in the acquired immune deficiency syndrome. *Science*, **226**, (1984), 1165-1171.
- [6] Ho, D. Time to hit HIV, early and hard. *The New England Journal of Medicine*, **333**, (1995), 450–451.
- [7] Perelson, A.S.; Essunger, P.; Cao, Y.; Vesanen, M.; Hurley, A.; Saksela, K.; Markowitz, M.; Ho, D.D. Decay characteristics of HIV-1-infected compartments during combination therapy. *Nature*, **387**, (1997), 188-191.
- [8] Mehellou, Y.; De Clercq, E. Twenty-six years of anti-HIV drug discovery: Where do we stand and where do we go? *Journal of Medicinal Chemistry*, **53**, (2009), 521-38.
- [9] Chen, L.F.; Hoy, J.; Lewin, S.R. Ten years of highly active antiretroviral therapy for HIV infection. *Med J Aust*, **186**, (2007), 146-51.
- [10] Centers for Disease Control and Prevention (CDC). CDC’s HIV Surveillance Report: Diagnoses of HIV Infection and AIDS in the United States and Dependent Areas, **22**, (2010).
- [11] Pope, M.; Haase, A.T. Transmission, acute HIV-1 infection and the quest for strategies to prevent infection. *Nat Med*, **9**, (2003), 847–52.
- [12] Lederman, M.M.; Offord, R.E.; Hartley, O. Microbicides and other topical strategies to prevent vaginal transmission of HIV. *Nat Rev Immunol*, **6**, (2006), 371–82.
- [13] Fauci, A.S.; Lane, H.C. Human immunodeficiency virus (HIV) disease: AIDS and related disorders. In: Kasper, D.L.; Braunwald, E.; Fauci, A.S.; Hauser, S.L.; Longo, D.L.; Jameson, J.L.; eds. *Harrison’s principles of internal medicine*. 16th ed. New York, NY: McGraw Hill, (2005), 1076–1139.

- [14] Fauci, A.S.; Pantaleo, G.; Stanley, S.; Weissman, D. Immunopathogenic mechanisms of HIV infection. *Ann Intern Med*, **124**, (1996), 654–663.
- [15] Brenchley, J.M.; Price, D.A.; Douek, D.C. HIV disease: fallout from a mucosal catastrophe? *Nat Immunol*, **7**, (2006), 235–239.
- [16] Galvin, S.R.; Cohen, M.S. The role of sexually transmitted diseases in HIV transmission. *Nat Rev Microbiol*, **2**, (2004), 33–42.
- [17] Reynolds, S.J.; Risbud, A.R.; Shepherd, M.E.; Rompalo, A. M.; Ghate, M. V.; Godbole, S. V.; Joshi, S. N.; Divekar, A. D.; Gangakhedkar, R. R.; Bollinger, R. C.; Mehendale, S. M. High rates of syphilis among STI patients are contributing to the spread of HIV-1 in India. *Sex Transm Infect*, **82**, (2006), 121–26.
- [18] Reynolds, S.J.; Risbud, A.R.; Shepherd, M.E.; Zenilman, J. M.; Brookmeyer, R.S.; Paranjape, R. S.; Divekar, A. D.; Gangakhedkar, R. R.; Ghate, M. V.; Bollinger, R. C.; Mehendale, S. M. Recent herpes simplex virus type 2 infection and the risk of human immunodeficiency virus type 1 acquisition in India. *J Infect Dis*, **187**, (2003), 1513–1521.
- [19] Hotez, P.J.; Molyneux, D.H.; Stillwaggon, E.; Bentwich, Z.; Kumaresan, J. Neglected tropical diseases and HIV/AIDS. *Lancet*, **368**, (2006), 1865–1866.
- [20] Bentwich, Z.; Maartens, G.; Torten, D.; Lal, A.A.; Lal, R.B. Concurrent infections and HIV pathogenesis. *AIDS*, **14**, (2000), 2071–2081.
- [21] Borkow, G.; Bentwich, Z. HIV and helminth co-infection: is deworming necessary? *Parasite Immunol*, **28**, (2006) 605–612.
- [22] Gopinath, R.; Ostrowski, M.; Justement, S.J.; Fauci, A.S.; Nutman, T.B. Filarial infections increase susceptibility to human immunodeficiency virus infection in peripheral blood mononuclear cells in vitro. *J Infect Dis*, **182**, (2000), 1804–1808.
- [23] Modjarrad, K.; Zulu, I.; Redden, D.T.; Njobvu, L.; Lane, H.C.; Bentwich, Z.; Vermund, S.H. Treatment of intestinal helminths does not reduce plasma concentrations of HIV-1 RNA in coinfecting Zambian adults. *J Infect Dis*, **192**, (2005), 1277–1283.
- [24] Collins, K.R.; Quinones-Mateu, M.E.; Toossi, Z.; Arts, E.J. Impact of tuberculosis on HIV-1 replication, diversity, and disease progression. *AIDS Rev*, **4**, (2002), 165–176.
- [25] Goletti, D.; Weissman, D.; Jackson, R.W.; Graham, N. M.; Vlahov, D.; Klein, R. S.; Munsiff, S. S.; Ortona, L.; Cauda, R.; Fauci, A. S. Effect of Mycobacterium tuberculosis on HIV replication: role of immune activation. *J. Immunol*, **157**, (1996), 1271–1278.
- [26] Bailey, R.C.; Moses, S.; Parker, C.B.; Agot, K.; Maclean, I.; Krieger, J. N.; Williams, C. FM; Campbell, R. T.; Ndinya-Achola, J. O.; MBchBh. Male circumcision for HIV prevention in young men in Kisumu, Kenya: a randomized controlled trial. *Lancet*, **369**, (2007), 643–56
- [27] Gray, R.H.; Kigozi, G.; Serwadda, D.; et al. Male circumcision for HIV prevention in men in Rakai, Uganda: a randomized trial. *Lancet*, **369**, (2007), 657–66.

- [28] Szabo, R.; Short, R.V. How does male circumcision protect against HIV infection? *B.M.J.*, **320**, (2000), 1592–4.
- [29] Centers for Disease Control and Prevention (CDC). Male circumcision and risk for HIV transmission: implications for the United States. Atlanta, GA: US Department of Health and Human Services, *CDC*, (2007) Available at: <http://www.cdc.gov/hiv/>
- [30] US Department of Health and Human Services Panel on Antiretroviral Guidelines for Adults and Adolescents. Guidelines for the use of antiretroviral agents in HIV-1–infected adults and adolescents. 10 October 2006. Available at: <http://aidsinfo.nih.gov/contentfiles/AdultandAdolescentGL.pdf>
- [31] Cooper, E.R.; Charurat, M.; Mofenson, L.; et al. Combination antiretroviral strategies for the treatment of pregnant HIV-1–infected women and prevention of perinatal HIV-1 transmission. Women and Infants’ Transmission Study Group. *J Acquir Immune Defic Syndr*, **29**, (2002), 484–494.
- [32] Wain-Hobson, S.; Sonigo, P.; Danos, O.; Stewart, C.; Alizon, M. Nucleotide sequence of the AIDS virus, LAV. *Cell*, **40**, (1985), 9–17.
- [33] Ratner, L.; Haseltine, W.; Patarca, R.; Livak, K.J.; Starcich, B.; Josephs, S.F.; Doran, E.R.; Rafalsk, J.A.; Whitehorn, E.A.; Baumeister, K.; Ivanoff, L.; Petteway S.R. Jr; Pearson, M.L.; Lautenberger, J.A.; Papas, T.S.; Ghayeb, J.; Chang, N.T.; Gallo, R.C.; Wong-Staal, F. Complete nucleotide sequence of the AIDS virus, HTLV-III. *Nature*, **313**, (1985), 277-284.
- [34] Zhu, P.; Liu, J.; Bess, J. Jr; Chertova, E.; Lifson, J.D.; Grisé, H.; Ofek, G.A.; Taylor, K.A.; Roux, K.H. Distribution and three-dimensional structure of AIDS virus envelope spikes. *Nature*, **441**, (2006), 847-852 .
- [35] Zanetti, G.; Briggs, J.A.G.; Grünwald, K.; Sattentau, Q.J.; Fuller, S.D. Cryo-Electron Tomographic Structure of an Immunodeficiency Virus Envelope Complex In Situ. *PLoS Pathog.*, **2**, (2006), 790-797.
- [36] Subramaniam, S. The SIV Surface Spike Imaged by Electron Tomography: One Leg or Three? *PLoS Pathog.*, **2**, (2006), 727-730.
- [37] Zhu, P.; Winkler, H.; Chertova, E.; Taylor, K.A.; Roux, K.H. Cryoelectron Tomography of HIV-1 Envelope Spikes: Further Evidence for Tripod-Like Legs. *PLoS Pathog.*, **4**, (2008), 1-9.
- [38] Muesing, M.A.; Smith, D.H.; Cabradilla, C.D.; Benton, C. V.; Lasky, L. A.; Capon, D.J. Nucleic acid structure and expression of the human AIDS/lymphadenopathy retrovirus. *Nature*, **313**(6002), (1985), 450-458.
- [39] Gallo, R.; Wong-Staal, F.; Montagnier, L.; Haseltine, W.A.; Yoshida, M.. HIV/HTLV gene nomenclature. *Nature*, **333**(6173), (1988), 333-504.
- [40] Bryant, M.; Ratner, L. Myristoylation-dependent replication and assembly of human immunodeficiency virus 1. *Proc Natl Acad Sci USA*, **87**, (1990), 523-527.

- [41] Gottlinger, H.G.; Sodroski, J.G.; Haseltine, W.A. Role of capsid precursor processing and myristoylation in morphogenesis and infectivity of human immunodeficiency virus type 1. *Proc Natl Acad Sci USA*, **86**, (1989), 5781-5785.
- [42] Galloway, P.; Swingle, S.; Song, J.; Bushman, F.; Trono, D. HIV nuclear import is governed by the phosphotyrosine-mediated binding of matrix to the core domain of integrase. *Cell*, **83**(4), (1995), 569-576.
- [43] Lewis, P.; Hensel, M.; Emerman, M. Human immunodeficiency virus infection of cells arrested in the cell cycle. *EMBO J*, **11**, (1992), 3053-3058.
- [44] Franke, E.K.; Yuan, H.E.; Luban, J. Specific incorporation of cyclophilin A into HIV-1 virions. *Nature*, **372**, (1994), 359-362.
- [45] Thali, M.; Bukovsky, A.; Kondo, E.; Rosenwirth, B.; Walsh, C.T.; Sodroski, J.; Göttinger, H.G. Functional association of cyclophilin A with HIV-1 virions. *Nature*, **372**(6504), (1994), 363-365.
- [46] Franke, E.K.; Luban, J. Inhibition of HIV-1 replication by cyclosporine A or related compounds correlates with the ability to disrupt the Gag-cyclophilin A interaction. *J Virol*, **222**, (1996), 279-282.
- [47] Harrison, G.P.; Lever, A.M. The human immunodeficiency virus type 1 packaging signal and major splice donor region have a conserved stable secondary structure. *J Virol*, **66**, (1992), 4144-4153.
- [48] Poznansky, M.; Lever, A.; Bergeron, L.; Haseltine, W.; Sodroski, J. Gene transfer into human lymphocytes by a defective human immunodeficiency virus type 1 vector. *J Virol*, **65**(1), (1991), 532-536.
- [49] Lapadat-Tapolsky, M.; De Rocquigny, H.; Van Gent, D.; Roques, B.; Plasterk, R.; Darlix, J.-L. Interactions between HIV-1 nucleocapsid protein and viral DNA may have important functions in the viral life cycle. *Nucleic Acids Res*, **21**(4), (1993), 831-839.
- [50] Paxton, W.; Connor, R.I.; Landau, N.R. Incorporation of Vpr into human immunodeficiency virus type 1 virions: Requirement for the p6 region of gag and mutational analysis. *J Virol*, **67**, (1993), 7229-7237.
- [51] Jacks, T.; Power, M. D.; Masiarz, F. R.; Luciw, P. A.; Barr, P. J.; Varmus, H. E. Characterization of ribosomal frameshifting in HIV-1 Gag-Pol expression. *Nature*, **331**(6153), (1988), 280-283.
- [52] Parkin, N.T.; Chamorro, M.; Varmus, H.E. Human immunodeficiency virus type 1 gag-pol frameshifting is dependent on mRNA secondary structure: Demonstration by expression in vivo. *J Virol*, **66**, (1992), 5147-5151.
- [53] Ashorn, P.; McQuade, T.J.; Thaisrivongs, S.; Tomasselli, A. G.; Tarpley, W. G.; Moss, B. An inhibitor of the protease blocks maturation of human and simian immunodeficiency viruses and spread of infection. *Proc Natl Acad Sci USA*, **87**(19), (1990), 7472-7476.

- [54] Miller, M.; Jaskolski, M.; Rao, J.K.; LEIS, J.; WLODAWER A. Crystal structure of a retroviral protease proves relationship to aspartic protease family. *Nature*, **337**, (1989), 576-579.
- [55] Navia, M.A.; Fitzgerald, P.M.; McKeever, B.M.; Leu, C. T.; Heimbach, J. C.; Herber, W. K.; Sigal, I. S.; Darke, P. L.; Springer, J. P. Three-dimensional structure of aspartyl protease from human immunodeficiency virus HIV-1. *Nature*, **337**(6208), (1989), 615-620.
- [56] Zack, J.A.; Arrigo, S.J., Weitsman, S.R.; Go, A. S.; Haislip, A.; Chen, I. S. HIV-1 entry into quiescent primary lymphocytes: Molecular analysis reveals a labile, latent viral structure. *Cell*, **61**(2), (1990), 213-222.
- [57] Harrich, D.; Ulich, C.; Gaynor, R.B. A critical role for the TAR element in promoting efficient human immunodeficiency virus type 1 reverse transcription. *J Virol*, **70**, (1996), 4017-4127.
- [58] Kohlstaedt, L.A.; Wang, J.; Friedman, J.M.; Rice, P.A.; Steitz, T.A. Crystal structure at 3.5 Å resolution of HIV-1 reverse transcriptase complexed with an inhibitor. *Science*, **256**(5065), (1992), 1783-1790.
- [59] Bushman, F.D., Fujiwara, T., Craigie, R. Retroviral DNA integration directed by HIV integration protein in vitro. *Science*, **249**, (1990), 1555-1558.
- [60] Pryciak, P.M.; Varmus, H.E. Nucleosomes, DNA-binding proteins, and DNA sequence modulate retroviral integration target site selection. *Cell*, **69**, (1992), 769-780.
- [61] Pruss, D.; Bushman, F.D.; Wolffe, A.P. Human immunodeficiency virus integrase directs integration to sites of severe DNA distortion within the nucleosome core. *Proc Natl Acad Sci USA*, **91**, (1994), 5913-5917.
- [62] Bushman, F.D. Tethering human immunodeficiency virus 1 integrase to a DNA site directs integration to nearby sequences. *Proc Natl Acad Sci USA*, **91**, (1994), 9233-9237.
- [63] Wiskerchen, M.; Muesing, M.A. Human immunodeficiency virus type 1 integrase: Effects of mutations on viral ability to integrate, direct viral gene expression from unintegrated viral DNA templates, and sustain viral propagation in primary cells. *J Virol*, **69**, (1995), 376-386.
- [64] Capon, D.J.; Ward, R.H. The CD4-gp120 interaction and AIDS pathogenesis. *Annu Rev Immunol*, **9**, (1991), 649-678.
- [65] Bernstein, H.B., Tucker, S.P.; Kar, S.R.; et. al. Oligomerization of the hydrophobic heptad repeat of gp41. *J Virol*, **69**, (1995), 2745-2750.
- [66] Landau, N.R., Warton, M.; Littman, D.R. The envelope glycoprotein of the human immunodeficiency virus binds to the immunoglobulin-like domain of CD4. *Nature*, **334**, (1988), 159-162.

- [67] Kwong, P.D.; Wyatt, R.; Robinson, J.; Sweet, R.W.; Sodroski, J.; Hendrickson, W.A. Structure of an HIV gp120 envelope glycoprotein in complex with the CD4 receptor and a neutralizing human antibody. *Nature*, **393**, (1998), 648-59.
- [68] Hwang, S.S.; Boyle, T.J.; Lyerly, H.K.; Cullen, B.R. Identification of the envelope V3 loop as the primary determinant of cell tropism in HIV-1. *Science*, **253**, (1991), 71-74.
- [69] Feng, Y.; Broder, C.C.; Kennedy, P.E.; Berger, E. A. HIV-1 entry cofactor: Functional cDNA cloning of a seven-transmembrane, G protein-coupled receptor. *Science*, **272**, (1996), 872-877.
- [70] Deng, H.; Liu, R.; Ellmeier, W.; CHOE, S.; UNUTMAZ, D.; BURKHART, M.; DI MARZIO, P.; MARMON, S.; SUTTON, R. E.; HILL, C. M.; DAVIS, C. B.; PEIPER, S. C.; SCHALL, T. J.; LITTMAN, D. R.; LANDAU, N.R. Identification of a major co-receptor for primary isolates of HIV-1. *Nature*, **381**, (1996), 661-666.
- [71] Goudsmit, J.; Debouck, C.; Meloen, R.H.; Smit, L.; Bakker, M.; Asher, D. M.; Wolff, A. V.; Gibbs, C. J. Jr.; Gajdusek D. C. Human immunodeficiency virus type 1 neutralization epitope with conserved architecture elicits early type-specific antibodies in experimentally infected chimpanzees. *Proc Natl Acad Sci USA*, **85**(12), (1988), 4478-4482.
- [72] Geijtenbeek, T.B.; Kwon, D.S.; Torensma, R.; Van Vliet, S.J.; Van Duijnhoven, G.C.; Middel, J.; Cornelissen, I.L.; Nottet, H.S.; KewalRamani, V.N.; Littman, D.R.; Figdor, C.G.; Van Kooyk, Y. DC-SIGN, a dendritic cell-specific HIV-1-binding protein that enhances trans-infection of T cells. *Cell*, **100**, (2000), 587-97.
- [73] Camerini, D.; Seed, B. A CD4 domain important for HIV-mediated syncytium formation lies outside the virus binding site. *Cell*, **60**, (1990), 747-754.
- [74] Ruben, S.; Perkins, A.; Purcell, R.; Joung, K.; Sia, R.; Burghoff, R.; Haseltine, W. A.; Rosen C. A. Structural and functional characterization of human immunodeficiency virus tat protein. *J Virol*, **63**(1), (1989), 1-8.
- [75] Feng, S.; Holland, E.C. HIV-1 tat trans-activation requires the loop sequence within tar. *Nature*, **334**, (1988), 165-167.
- [76] Roy, S.; Delling, U.; Chen, C.H.; Rosen C. A.; Sonenberg, N. A bulge structure in HIV-1 TAR RNA is required for Tat binding and Tat-mediated trans-activation. *Genes Dev*, **4**(8), (1990), 1365-73.
- [77] Kao, S.Y.; Calman, A.F.; Luciw, P.A.; Peterlin B.M. Anti-termination of transcription within the long terminal repeat of HIV-1 by tat gene product. *Nature*, **330**(6147), (1987), 489-493.
- [78] Feinberg, M.B.; Baltimore, D.; Frankel, A.D. The role of Tat in the human immunodeficiency virus life cycle indicates a primary effect on transcriptional elongation. *Proc Natl Acad Sci USA*, **88**, (1991), 4045-4049.

- [79] Zhu, Y.; Pe'ery, T.; Peng, J.; Ramanathan, Y.; Marshall, N.; Marshall, T.; Amendt, B.; Mathews, M.B.; Price, D.H. Transcription elongation factor P-TEFb is required for HIV-1 tat transactivation in vitro. *Genes Dev.*, **11**, (1997), 2622-32.
- [80] Wei, P.; Garber, M.E.; Fang, S.M.; Fischer, W.H.; Jones, K.A. A novel CDK9-associated C-type cyclin interacts directly with HIV-1 Tat and mediates its high-affinity, loop-specific binding to TAR RNA. *Cell*, **92**, (1998), 451-62.
- [81] Brother, M.B.; Chang, H.K.; Lisziewicz, J.; Su, D.; Murty, L. C.; Ensoli, B. Block of Tat-mediated transactivation of tumor necrosis factor beta gene expression by polymeric-TAR decoys. *Virology*, **222**(1), (1996), 252-256.
- [82] Rasty, S.; Thatikunta, P.; Gordon, J.; Khalili K, Amini S, Glorioso JC. Human immunodeficiency virus tat gene transfer to the murine central nervous system using a replication-defective herpes simplex virus vector stimulates transforming growth factor beta 1 gene expression. *Proc Natl Acad Sci USA*, **93**(12), (1996), 6073-78.
- [83] Sastry, K. J.; Marin, M. C.; Nehete, P. N.; McConnell, K.; El-Naggar, A. K.; McDonnell, T. J. Expression of human immunodeficiency virus type I tat results in down-regulation of bcl-2 and induction of apoptosis in hematopoietic cells. *Oncogene*, **13**(3), (1996), 487-493.
- [84] Sharma, V.; Xu, M.; Ritter, L.M. HIV-1 tat induces the expression of a new hematopoietic cell-specific transcription factor and downregulates MIP-1 alpha gene expression in activated T cells. *Biochem Biophys Res Commun*, **223**, (1996), 526-533.
- [85] Zapp, M.L.; Green, M.R. Sequence-specific RNA binding by the HIV-1 Rev protein. *Nature*, **342**, (1989), 714-716.
- [86] Kim, S.Y.; Byrn, R., Groopman, J.; Baltimore D. Temporal aspects of DNA and RNA synthesis during human immunodeficiency virus infection: Evidence for differential gene expression. *J Virol*, **63**(9), (1989), 3708-3713.
- [87] Malim, M.H.; Hauber, J.; Le, S.Y.; Maizel, J. V.; Cullen, B. R. The HIV-1 rev transactivator acts through a structured target sequence to activate nuclear export of unspliced viral mRNA. *Nature*, **338**(6212), (1989), 254-257.
- [88] Bartel, D. P.; Zapp, M. L.; Green, M. R.; Szostak, J. W. HIV-1 Rev regulation involves recognition of non-Watson-Crick base pairs in viral RNA. *Cell*, **67**(3), (1991), 529-536.
- [89] Felber, B.K.; Drysdale, C.M.; Pavlakis, G.N. Feedback regulation of human immunodeficiency virus type 1 expression by the Rev protein. *J Virol*, **64**, (1990), 3734-3741.
- [90] Malim, M.H.; Bohnlein, S.; Hauber, J.; Cullen, B. R. Functional dissection of the HIV-1 Rev trans-activator" derivation of a trans-dominant repressor of Rev function. *Cell*, **58**(1), (1989), 205-214.
- [91] Hope, T.J.; McDonald, D.; Huang, X.J.; Low, J.; Parslow, T. G. Mutational analysis of the human immunodeficiency virus type 1 Rev transactivator: Essential residues near the amino terminus. *J Virol*, **64**(11), (1990), 5360-5366.



- [92] Zapp, M.L.; Hope, T.J.; Parslow, T.G.; Green, M. R. Oligomerization and RNA binding domains of the type 1 human immunodeficiency virus Rev protein: A dual function for an arginine-rich binding motif. *Proc Natl Acad Sci USA*, **88**, (1991), 7734-7738.
- [93] Wen, W.; Meinkoth, J.L.; Tsien, R.Y.; Taylor, S. S. Identification of a signal for rapid export of proteins from the nucleus. *Cell*, **82**(3), (1995), 463-473.
- [94] Fischer, U.; Huber, J.; Boelens, W. C.; Mattajt, L. W.; Lührmann, R. The HIV-1 Rev activation domain is a nuclear export signal that accesses an export pathway used by specific cellular RNAs. *Cell*, **82**(3), (1995), 475-483.
- [95] Hope, T.J.; Klein, N.P.; Elder, M.E.; Parslow, T.G. Trans-dominant inhibition of human immunodeficiency virus type 1 Rev occurs through formation of inactive protein complexes. *J Virol*, **66**, (1992), 1849-55.
- [96] Garcia, J.V.; Miller, A.D. Downregulation of cell surface CD4 by nef. *Res Virol*, **143**, (1992), 52-55.
- [97] Aiken, C., Konner, J.; Landau, N.R.; Lenburg, M. E.; Trono, D. Nef induces CD4 endocytosis: Requirement for a critical dileucine motif in the membrane-proximal CD4 cytoplasmic domain. *Cell*, **76**(5), (1994), 853-64.
- [98] Lama, J.; Mangasarian, A.; Trono, D. Cell-surface expression of CD4 reduces HIV-1 infectivity by blocking Env incorporation in a Nef- and Vpu-inhibitable manner. *Curr Biol*, **9**, (1999), 622-31.
- [99] Ross, T.M.; Oran, A.E.; Cullen, B.R. Inhibition of HIV-1 progeny virion release by cell-surface CD4 is relieved by expression of the viral Nef protein. *Curr Biol* **9**, (1999), 613-21.
- [100] Schwartz, O.; Marechal, V.; Le Gall, S.; Lemonnier, F.; Heard, J.-M. Endocytosis of major histocompatibility complex class I molecules is induced by the HIV-1 Nef protein. *Nature Medicine*, **2**, (1996), 338-342.
- [101] Luria, S.; Chambers, I.; Berg, P. Expression of the type 1 human immunodeficiency virus Nef protein in T cells prevents antigen receptor-mediated induction of interleukin 2 mRNA. *Proc Natl Acad Sci USA*, **88**, (1991), 5326-5330.
- [102] Skowronski, J.; Parks, D.; Mariani, R. Altered T cell activation and development in transgenic mice expressing the HIV-1 nef gene. *EMBO J*, **12**, (1993), 703-713.
- [103] Baur, A.S.; Sawai, E.T.; Dazin, P.; Fantl, W. J.; Cheng-Mayer, C.; Peterlin B. M. HIV-1 Nef leads to inhibition or activation of T cells depending on its intracellular localization. *Immunity*, **1**(5), (1994), 373-384.
- [104] Miller, M.D.; Warmerdam, M.T.; Gaston, I.; Greene, W. C.; Feinberg, M.B. The human immunodeficiency virus-1 nef gene product: A positive factor for viral infection and replication in primary lymphocytes and macrophages. *J Exp Med*, **179**(1), (1994), 101-113.

- [105] Pandori, M.W.; Fitch, N.J.; Craig, H.M.; Richman, D. D.; Spina, C. A.; Guatelli, J. C. Producer-cell modification of human immunodeficiency virus type 1: Nef is a virion protein. *J Virol*, **70**(7), (1996), 4283-90.
- [106] Schwartz, O.; Marechal, V.; Danos, O.; Heard, J. M. Human immunodeficiency virus type 1 Nef increases the efficiency of reverse transcription in the infected cell. *J Virol*, **69**(7), (1995), 4053-4059.
- [107] Goldsmith, M.A.; Warmerdam, M.T.; Atchison, R.E.; Miller, M. D.; Greene, W. C. Dissociation of the CD4 downregulation and viral infectivity enhancement functions of human immunodeficiency virus type 1 Nef. *J Virol*, **69**(7), (1995), 4112-4121.
- [108] Kestler, H.W. 3rd; Ringler, D.J.; Mori, K.; Panicali, D.L.; Sehgal, P. K.; Daniel, M. D.; Desrosiers, R.C. Importance of the nef gene for maintenance of high virus loads and for development of AIDS. *Cell*, **65**(4), (1991), 651-662.
- [109] Baba, T.W.; Jeong, Y.S.; Pennick, D.; Bronson, R.; Greene, M. F.; Ruprecht, R. M. Pathogenicity of live, attenuated SIV after mucosal infection of neonatal macaques. *Science*, **267**(5205), (1995), 1820-1825.
- [110] Collins, K.L.; Nabel, G.J. Naturally attenuated HIV--lessons for AIDS vaccines and treatment. *N Engl J Med*, **340**, (1999), 1756-7.
- [111] Cohen, E.A.; Dehni, G.; Sodroski, J.G.; Haseltine, W. A. Human immunodeficiency virus vpr product is a virion-associated regulatory protein. *J Virol*, **64**(6), (1990), 3097-3099.
- [112] Heinzinger, N.K.; Bukinsky, M.I.; Haggerty, S.A.; Ragland, A. M.; Kewalramani, V.; Lee, M. A.; Gendelman, H. E.; Ratner, L.; Stevenson, M.; Emerman, M. The Vpr protein of human immunodeficiency virus type 1 influences nuclear localization of viral nucleic acids in nondividing host cells. *Proc Natl Acad Sci USA*, **91**(15), (1994), 7311-15.
- [113] Vodicka, M.A.; Koepp, D.M.; Silver, P.A.; Emerman, M. HIV-1 Vpr interacts with the nuclear transport pathway to promote macrophage infection. *Genes Dev*, **12**(2), (1998), 175-85.
- [114] Rogel, M.E.; Wu, L.I.; Emerman, M. The human immunodeficiency virus type 1 vpr gene prevents cell proliferation during chronic infection. *J Virol*, **69**, (1995), 882-888.
- [115] Jowett, J.B.; Planelles, V.; Poon, B.; Shah, N. P.; Chen, M. L.; Chen, I. S. The human immunodeficiency virus type 1 vpr gene arrests infected T cells in the G2 + M phase of the cell cycle. *J Virol*, **69**(10), (1995), 6304-13.
- [116] Braaten, D.; Franke, E.K.; Luban, J. Human immunodeficiency virus type 1 Vpr arrests the cell cycle in G2 by inhibiting the activation of p34cdc2-cyclin B. *J Virol*, **69**, (1995), 6859-64.
- [117] He, J.; Choe, S.; Walker, R.; Di Marzio, P.; Morgan, D. O.; Landau, N. R. Human immunodeficiency virus type 1 viral protein R (Vpr) arrests cells in the G2 phase of the cell cycle by inhibiting p34cdc2 activity. *J Virol*, **69**(11), (1995), 6705-11.

- [118] Bouhamdan, M.; Benichou, S.; Rey, F.; Navarro, J. M.; Agostini, I.; Spire, B.; Camonis, J.; Slupphaug, G.; Vigne, R.; Benarous, R.; Sire, J. Human immunodeficiency virus type 1 Vpr protein binds to the uracil DNA glycosylase DNA repair enzyme. *J Virol*, **70**(2), (1996), 697-704.
- [119] Steagall, W.K.; Robek, M.D.; Perry, S.T.; Fuller, F. J.; Payne, S. L. Incorporation of uracil into viral DNA correlates with reduced replication of EIAV in macrophages. *Virology*, **210**(2), (1995), 302-313.
- [120] Sato, A.; Igarashi, H.; Adachi, A.; Hayami, M. Identification and localization of vpr gene product of human immunodeficiency virus type 1. *Virus Genes*, **4**, (1990), 303-312.
- [121] Schwartz, S.; Felber, B.K.; Fenyo, E.M.; Pavlakis, G. N. Env and Vpu proteins of human immunodeficiency virus type 1 are produced from multiple bicistronic mRNAs. *J Virol*, **64**(11), (1990), 5448-5456.
- [122] Schubert, U.; Bour, S.; Ferrer-Montiel, A.V.; Montal, M.; Maldarell, F.; Strebel, K. The two biological activities of human immunodeficiency virus type 1 Vpu protein involve two separable structural domains. *J Virol*, **70**(2), (1996), 809-819.
- [123] Willey, R.L.; Maldarelli, F.; Martin, M.A.; Strebel, K. Human immunodeficiency virus type 1 Vpu protein induces rapid degradation of CD4. *J Virol*, **66**(12), (1992), 7193-7200.
- [124] Klimkait, T.; Strebel, K.; Hoggan, M. D.; Martin, M. A.; Orenstein, J. M. The human immunodeficiency virus type 1-specific protein vpu is required for efficient virus maturation and release. *J Virol*, **64**(2), (1990), 621-29.
- [125] Strebel, K.; Daugherty, D.; Clouse, K.; Cohen, D.; Folks, T.; Martin, M. A. The HIV 'A' (sor) gene product is essential for virus infectivity. *Nature*, **328**(6132), (1987), 728-730.
- [126] Von Schwedler, U.; Song, J.; Aiken, C.; Trono, D. Vif is crucial for human immunodeficiency virus type 1 proviral DNA synthesis in infected cells. *J Virol*, **67**(8), (1993), 4945-4955.
- [127] Liu, H.; Wu, X.; Newman, M.; Shaw, G. M.; Hahn, B. H.; Kappes, J. C. The Vif protein of human and simian immunodeficiency viruses is packaged into virions and associates with viral core structures. *J Virol*, **69**(12), (1995), 7630-7638.
- [128] Camaur, D.; Trono, D. Characterization of human immunodeficiency virus type 1 Vif particle incorporation. *J Virol*, **70**, (1996), 6106-6111.
- [129] Simon, J.H.; Gaddis, N.C.; Fouchier, R.A.; Malim, M.H. Evidence for a newly discovered cellular anti-HIV-1 phenotype. *Nat Med*, **4**, (1998), 1397-400.
- [130] Simon, J.H.; Miller, D.L.; Fouchier, R.A.; Soares, M.A.; Peden, K.W.; Malim, M.H. The regulation of primate immunodeficiency virus infectivity by Vif is cell species restricted: a role for Vif in determining virus host range and cross-species transmission. *EMBO J*, **17**, (1998), 1259-67.

- [131] Hoglund, S.; Ohagen, A.; Lawrence, K.; Gabuzda, D. Role of vif during packing of the core of HIV-1. *Virology*, **201**(2), (1994), 349-355.
- [132] De Clercq, E. Strategies in the design of antiviral drugs. *Nat. Rev. Drug Discovery*, **1**, (2002), 13-25.
- [133] Meadows, D.C.; Gervay-Hague, J. Current developments in HIV chemotherapy. *ChemBioChem*, **1**, (2006), 16-29.
- [134] Mitsuya, H.; Broder, S. Strategies for antiviral therapy of AIDS. *Nature*, **325**, (1997), 773-778.
- [135] Ratner, L.; Haseltine, W.; Patarca, R.; Livak, K. J.; Starcich, B.; Josephs, S. F.; Doran, E. R.; Rafalski, J. A.; Whitehorn, E. A.; Baumeister, K.; Ivanoff, L.; Petteway, S. R. Jr; Pearson, M. L.; Lautenberger, J. A.; Papas, T. S.; Ghrayeb, J.; Chang, N. T.; Gallo, R. C.; Wong-Staal, F. Complete Nucleotide Sequence Of The AIDS virus, HTLV-III. *Nature*, **313**(6000), (1985), 277-84.
- [136] Hughes, S.; Arnold, E.; Hostomsky, Z. RNase H of retroviral reverse transcriptases. In: H CR, Toulmé JJ., Eds. Ribonucleases. Les Editions Inserm: Paris, (1998), 195-224.
- [137] Huber, H.E.; Richardson, C.C. Processing of the primer for plus strand DNA synthesis by human immunodeficiency virus 1 reverse transcriptase. *J Biol Chem*, **265**(18), (1990), 10565-73.
- [138] Rausch, J.W.; Le Grice, S.F.J. 'Binding, bending and bonding': polypurine tract-primed initiation of plus-strand DNA synthesis in human immunodeficiency virus. *Int J Biochem Cell Biol*, **36**(9), (2004), 1752-66.
- [139] Basu, V.P.; Song, M.; Gao, L.; Rigby, S.T.; Hanson, M.N.; Bambara, R.A. Strand transfer events during HIV-1 reverse transcription. *Virus Res*, **134**(1-2), (2008), 19-38.
- [140] Divita, G.; Rittinger, K.; Geourjon, C.; Deléage, G.; Goody, R.S. Dimerization kinetics of HIV-1 and HIV-2 Reverse Transcriptase: A two step process. *J Mol Biol*, **245**(5), (1995), 508-21.
- [141] Jacobo-Molina, A.; Ding, J.; Nanni, R.G.; Clark, A. D. Jr; Lu, X.; Tantillo, C.; Williams, R. L.; Kamer, G.; Ferris, A. L.; Clark, P. Crystal structure of human immunodeficiency virus type 1 reverse transcriptase complexed with double-stranded DNA at 3.0 Å resolution shows bent DNA. *Proc Natl Acad Sci USA*, **90**(13), (1993), 6320-4.
- [142] Kohlstaedt, L.; Wang, J.; Friedman, J.; Rice, P.; Steitz, T. Crystal structure at 3.5 Å resolution of HIV-1 reverse transcriptase complexed with an inhibitor. *Science*, **256**(5065), (1992), 1783-90.
- [143] Liu, S.; Abbondanzieri, E.A.; Rausch, J.W.; Le Grice, S.F.; Zhuang, X. Slide into action: Dynamic shuttling of HIV Reverse Transcriptase on nucleic acid substrates. *Science*, **322**(5904), (2008), 1092-7.
- [144] Steitz, T.A. Structural biology: A mechanism for all polymerases. *Nature*, **391**(6664), (1998), 231-2.

- [145] Dash, C.; Scarth, B.J.; Badorrek, C.; Götte, M.; Le Grice, S.F. Examining the ribonuclease H primer grip of HIV-1 reverse transcriptase by charge neutralization of RNA/DNA hybrids. *Nucleic Acids Res*, **36**(20), (2008), 6363-71.
- [146] Sarafianos, S.G.; Marchand, B.; Das, K.; Himmel, D. M.; Parniak, M. A.; Hughes, S. H.; Arnold, E. Structure and function of HIV-1 Reverse Transcriptase: Molecular mechanisms of polymerization and Inhibition. *J Mol Biol*, **385**(3), (2009), 693-713.
- [147] Kellinger, M.W.; Johnson, K.A. Nucleotide-dependent conformational change governs specificity and analog discrimination by HIV reverse transcriptase. *Proc Natl Acad Sci USA*, **107**(17), (2010), 7734-7739.
- [148] Tramontano, E.; Di Santo, R. HIV-1 RT-associated RNase H function inhibitors: Recent advances in drug development. *Curr Med Chem*, **17**(26), (2010), 2837-53.
- [149] Nowotny, M.; Gaidamakov, S.A.; Crouch, R.J.; Yang, W. Crystal structures of RNase H bound to an RNA/DNA hybrid: Substrate specificity and metal-dependent catalysis. *Cell*, **121**(7), (2005), 1005-16.
- [150] Telesnitsky, A.; Goff, S. Reverse transcriptase and the generation of retroviral DNA. In: Coffin JM HS, Varmus HE., Eds. *Retroviruses*. Cold Spring Harbor Laboratory Press: NY, (1997), 121-60.
- [151] Grohmann, D.; Godet, J.; Mély, Y.; Darlix, J-L.; Restle, T. HIV-1 nucleocapsid traps Reverse Transcriptase on nucleic acid substrates. *Biochemistry*, **47**(46), (2008), 12230-40.
- [152] Ji, X.; Klarmann, G.J.; Preston, B.D. Effect of Human Immunodeficiency Virus Type 1 (HIV-1) nucleocapsid protein on HIV-1 reverse transcriptase activity in vitro. *Biochemistry*, **35**(1), (1996), 132-43.
- [153] Meyer, P.R.; Matsuura, S.E.; So, A.G.; Scott, W.A. Unblocking of chainterminated primer by HIV-1 reverse transcriptase through a nucleotide-dependent mechanism. *Proc Natl Acad Sci USA*, **95**(23), (1998), 13471-6.
- [154] Arion, D.; Kaushik, N.; McCormick, S.; Borkow, G.; Parniak, M.A. Phenotypic mechanism of HIV-1 resistance to 3'-Azido-3'-deoxythymidine (AZT): increased polymerization processivity and enhanced sensitivity to pyrophosphate of the mutant viral Reverse Transcriptase. *Biochemistry*, **37**(45), (1998), 15908-17.
- [155] Aguiar, R.S.; Peterlin, B.M. APOBEC3 proteins and reverse transcription. *Virus Res*, **134**(1-2), (2008), 74-85.
- [156] Cihlar, T.; Chen, M.S. Incorporation of selected nucleoside phosphonates and anti-human immunodeficiency virus nucleotide analogues into DNA by human DNA polymerases  $\alpha$ ,  $\beta$  and  $\gamma$ . *Antivir Chem Chemother*, **8**(3), (1997), 187-95.
- [157] Das, K.; Martinez, S.E.; Bauman, J.D.; Arnold, E. HIV-1 reverse transcriptase complex with DNA and nevirapine reveals non-nucleoside inhibition mechanism. *Nat Struct Mol Biol*, **19**(2), (2012), 253-9.

- [158] Hachiya, A.; Kodama, E.N.; Sarafianos, S.G.; Schuckmann, M.M.; Sakagami, Y.; Matsuoka, M.; Takiguchi, M.; Gatanaga, H.; Oka, S. Amino acid mutation N348I in the connection subdomain of human immunodeficiency virus type 1 reverse transcriptase confers multiclass resistance to nucleoside and nonnucleoside reverse transcriptase inhibitors. *J Virol*, **82**(7), (2008), 3261-70.
- [159] Brehm, J.H.; Koontz, D.; Meteer, J.D.; Pathak, V.; Sluis-Cremer, N.; Mellors, J.W. Selection of mutations in the connection and RNase H domains of human immunodeficiency virus type 1 reverse transcriptase that increase resistance to 3'-azido-3'-dideoxythymidine. *J Virol*, **81**(15), (2007), 7852-9.
- [160] Delviks-Frankenberry, K.A.; Nikolenko, G.N.; Barr, R.; Pathak, V.K. Mutations in human immunodeficiency virus type 1 RNase H primer grip enhance 3-Azido-3'-dideoxythymidine resistance. *J Virol*, **81**(13), (2007), 6837-45.
- [161] Yap, S-H.; Sheen, C-W.; Fahey, J.; Zanin, M.; Tyssen, D.; Lima, V.D.; Wynhoven, B.; Kuiper, M.; Sluis-Cremer, N.; Harrigan, P.R.; Tachedjian, G. N348I in the connection domain of HIV-1 Reverse Transcriptase confers Zidovudine and Nevirapine resistance. *PLoS Med*, **4**(12), (2007) 335.
- [162] Nikolenko, G.N.; Delviks-Frankenberry, K.A.; Palmer, S.; Maldarelli, F.; Fivash, M.J. Jr.; Coffin, J.M.; Pathak, V.K. Mutations in the connection domain of HIV-1 reverse transcriptase increase 3'-azido-3'-dideoxythymidine resistance. *Proc Natl Acad Sci USA*, **104**(1), (2007), 317-22.
- [163] Balzarini, J.; Naesens, L.; Aquaro, S.; Knispel, T.; Perno, C.F.; De Clercq, E.; Meier, C. Intracellular metabolism of CycloSaligenyl 3'-azido-2',3'-dideoxythymidine monophosphate, a prodrug of 3'-azido-2',3'-dideoxythymidine (zidovudine). *Mol Pharmacol*, **56**(6), (1999), 1354-61.
- [164] Cihlar, T.; Ray, A.S. Nucleoside and nucleotide HIV reverse transcriptase inhibitors: 25 years after zidovudine. *Antivir Res*, **85**(1), (2010), 39-58.
- [165] Ehteshami, M.; Scarth, B.J.; Tchesnokov, E.P.; Dash, C.; Le Grice, S.F.; Hallenberger, S.; Jochmans, D.; Goette, M. Mutations M184V and Y115F in HIV-1 Reverse Transcriptase discriminate against "Nucleotide-competing Reverse Transcriptase inhibitors". *J Biol Chem*, **283**(44), (2008), 29904-11.
- [166] Jochmans, D.; Deval, J.; Kesteleyn, B.; Van Marck, H.; Bettens, E.; De Baere, I.; Dehertogh, P.; Ivens, T.; Van Ginderen, M.; Van Schoubroeck, B.; Ehteshami, M.; Wigerinck, P.; Götte, M.; Hertogs, K. Indolopyridones inhibit Human Immunodeficiency Virus Reverse Transcriptase with a novel mechanism of action. *J Virol*, **80**(24), (2006), 12283-92.
- [167] Freisz, S.; Bec, G.; Radi, M.; Wolff, P.; Crespan, E.; Angeli, L.; Dumas, P.; Maga, G.; Botta, M.; Ennifar, E. Crystal structure of HIV-1 Reverse Transcriptase bound to a non-nucleoside inhibitor with a novel mechanism of action. *Angew Chem, Int Ed*, **49**(10), (2010), 1805-8.

- [168] Huang, H.F.; Chopra, R.; Verdine, G.L.; Harrison, S.C. Structure of a covalently trapped catalytic complex of HIV-I reverse transcriptase: Implications for drug resistance. *Science*, **282**(5394), (1998), 1669-75.
- [169] Sluis-Cremer, N.; Tachedjian, G. Mechanisms of inhibition of HIV replication by non-nucleoside reverse transcriptase inhibitors. *Virus Res*, **134**(1-2), (2008), 147-56.
- [170] Zhan, P.; Chen, X.; Li, D.; Fang, Z.; De Clercq, E.; Liu, X. HIV-1 NNRTIs: Structural diversity, pharmacophore similarity, and implications for drug design. *Med Res Rev*, (2011) DOI: 10.1002/med.20241.
- [171] Das, K.; Lewi, P.J.; Hughes, S.H.; Arnold, E. Crystallography and the design of anti-AIDS drugs: conformational flexibility and positional adaptability are important in the design of non-nucleoside HIV-1 reverse transcriptase inhibitors. *Prog Biophys Mol Biol*, **88**(2), (2005), 209-31.
- [172] Zhan, P.; Liu, X.; Li, Z.; Pannecouque C, De Clercq E. Design strategies of novel NNRTIs to overcome drug resistance. *Curr Med Chem*, **16**(29), (2009), 3903-17.
- [173] Sahlberg, C.; Zhou, X-X. Development of non-nucleoside Reverse Transcriptase inhibitors for anti-HIV therapy. *Anti-Infect Agents Med Chem*, **7**(2), (2008), 101-17.
- [174] Ding, J.P.; Das, K.; Moereels, H.; Koymans, L.; Andries, K.; Janssen, P.A.J.; Hughes, S.H.; Arnold, E. Structure of HIV-1 RT/TIBO R 86183 complex reveals similarity in the binding of diverse nonnucleoside inhibitors. *Nat Struct Biol*, **2**(5), (1995), 407-15.
- [175] Das, K.; Bauman, J.D.; Rim, A.S.; Dharia, C.; Clark, A.D.; Camarasa, Ma-J.; Balzarini, J.; Arnold, E. Crystal structure of tert-Butyldimethylsilyl-spiroaminoxathioledioxide-thymine (TSAO-T) in Complex with HIV-1 Reverse Transcriptase (RT) redefines the elastic limits of the non-nucleoside inhibitor-binding pocket. *J Med Chem*, **54**(8), (2011), 2727-37.
- [176] Halgren, T.A. Identifying and characterizing binding sites and assessing druggability. *J Chem Inf Model*, **49**(2), (2009), 377-89.
- [177] Lindberg, J.; Sigurðsson, S.; Löwgren, S.; Andersson H.O.; Sahlberg, C.; Noréen, R.; Fridborg, K.; Zhang, H.; Unge, T. Structural basis for the inhibitory efficacy of efavirenz (DMP-266), MSC194 and PNU142721 towards the HIV-1 RT K103N mutant. *Eur J Biochem*, **269**(6), (2002), 1670-7.
- [178] Das, K.; Clark, A.D.; Lewi, P.J.; Heeres, J.; de Jonge, M.R.; Koymans, L.M.H.; Vinkers, H.M.; Daeyaert, F.; Ludovici, D.W.; Kukla, M.J.; De Corte, B.; Kavash, R.W.; Ho, C.Y.; Ye, H.; Lichtenstein, M.A.; Andries, K.; Pauwels, R.; de Béthune, M-P.; Boyer, P.L.; Clark, P.; Hughes, S.H.; Janssen, P.A.J.; Arnold, E. Roles of conformational and positional adaptability in structure-based design of TMC125-R165335 (Etravirine) and related non-nucleoside Reverse Transcriptase inhibitors that are highly potent and effective against wild-type and drug-resistant HIV-1 variants. *J Med Chem*, **47**(10), (2004), 2550-60.

- [179] Pata, J.D.; Stirtan, W.G.; Goldstein, S.W.; Steitz, T.A. Structure of HIV-1 reverse transcriptase bound to an inhibitor active against mutant reverse transcriptases resistant to other nonnucleoside inhibitors. *Proc Natl Acad Sci USA*, **101**(29), (2004), 10548-53.
- [180] Das, K.; Ding, J.; Hsiou, Y.; Clark, A.D. Jr.; Moereels, H.; Koymans, L.; Andries, K.; Pauwels, R.; Janssen, P.A.J.; Boyer, P.L.; Clark, P.; Smith, R.H. Jr.; Kroeger Smith, M.B.; Michejda, C.J.; Hughes, S.H.; Arnold, E. Crystal structures of 8-Cl and 9-Cl TIBO complexed with wild-type HIV-1 RT and 8-Cl TIBO complexed with the Tyr181Cys HIV-1 RT drug-resistant mutant. *J Mol Biol*, **264**(5), (1996), 1085-100.
- [181] Camarasa, M.-J.; Velazquez, S.; San-Felix, A.; Perez-Perez, M.-J. TSAO derivatives the first non-peptide inhibitors of HIV-1 RT dimerization. *Antivir Chem Chemother*, **16**(3), (2005), 147-53.
- [182] Hsiou, Y.; Ding, J.; Das, K.; Clark, J.A.D.; Hughes, S.H.; Arnold, E. Structure of unliganded HIV-1 reverse transcriptase at 2.7 Å resolution: implications of conformational changes for polymerization and inhibition mechanisms. *Structure*, **4**(7), (1996), 853-60.
- [183] Pelemans, H.; Esnouf, R.; De Clercq, E.; Balzarini, J. Mutational analysis of Trp-229 of Human Immunodeficiency Virus Type 1 Reverse Transcriptase (RT) identifies this amino acid residue as a prime target for the rational design of new non-nucleoside RT inhibitors. *Mol Pharmacol*, **57**(5), (2000), 954-60.
- [184] Lu, X.; Liu, L.; Zhang, X.; Lau, T.C.K.; Tsui, S.K.W.; Kang, Y.; Zheng, P.; Zheng, B.; Liu, G.; Chen, Z. F18, a novel small-molecule nonnucleoside Reverse Transcriptase inhibitor, inhibits HIV-1 replication using distinct binding motifs as demonstrated by resistance selection and docking analysis. *Antimicrob Agents Chemother*, **56**(1), (2012), 341-51.
- [185] Tramontano, E. HIV-1 RNase H: Recent progress in an exciting, yet little explored, drug target. *Mini-Rev Med Chem*, **6**(6), (2006), 727-37.
- [186] Klumpp, K.; Mirzadegan, T. Recent progress in the design of small molecule inhibitors of HIV RNase H. *Curr Pharm Des*, **12**(15), (2006), 1909-22.
- [187] Himmel, D.M.; Maegley, K.A.; Pauly, T.A.; Bauman, J.D.; Das, K.; Dharia, C.; Clark, A.D. Jr.; Ryan, K.; Hickey, M.J.; Love, R.A.; Hughes, S.H.; Bergqvist, S.; Arnold, E. Structure of HIV-1 Reverse Transcriptase with the inhibitor  $\beta$ -Thujaplicinol bound at the RNase H active site. *Structure*, **17**(12), (2009), 1625-35.
- [188] Chung, S.; Himmel, D.M.; Jiang, J.-K.; Wojtak, K.; Bauman, J.D.; Rausch, J.W.; Wilson, J.A.; Beutler, J.A.; Thomas, C.J.; Arnold, E.; Le Grice, S.F. Synthesis, activity, and structural analysis of novel  $\alpha$ -Hydroxytropolone inhibitors of Human Immunodeficiency Virus Reverse Transcriptase-associated Ribonuclease H. *J Med Chem*, **54**(13), (2011), 4462-73.



- [189] Kirschberg, T.A.; Balakrishnan, M.; Squires, N.H.; Barnes, T.; Brenda, K.M.; Chen, X.; Eisenberg, E.J.; Jin, W.; Kutty, N.; Leavitt, S.; Liclican, A.; Liu, Q.; Liu, X.; Mak, J.; Perry, J.K.; Wang, M.; Watkins, W.J.; Lansdon, E.B. RNase H active site inhibitors of Human Immunodeficiency Virus Type 1 Reverse Transcriptase: Design, biochemical activity, and structural information. *J Med Chem*, **52**(19), (2009), 5781-4.
- [190] Lansdon, E.B.; Liu, Q.; Leavitt, S.A.; Balakrishnan, M.; Perry, J.K.; Lancaster-Moyer, C.; Kutty, N.; Liu, X.; Squires, N.H.; Watkins, W.J.; Kirschberg, T.A. Structural and binding analysis of pyrimidinol carboxylic acid and N-hydroxy quinazolinedione HIV-1 RNase H inhibitors. *Antimicrob Agents Chemother*, **55**(6), (2011), 2905-15.
- [191] Hang, J.Q.; Rajendran, S.; Yang, Y.; Li, Y.; Wong Kai In, P.; Overton, H.; Parkes, K.E.B.; Cammack, N.; Martin, J.A.; Klumpp, K. Activity of the isolated HIV RNase H domain and specific inhibition by N-hydroxyimides. *Biochem Biophys Res Commun*, **317**(2), (2004), 321-9.
- [192] Tramontano, E.; Esposito, F.; Badas, R.; Di Santo, R.; Costi, R.; La Colla, P. 6-[1-(4-Fluorophenyl)methyl-1H-pyrrol-2-yl]-2,4-dioxo-5-hexenoic acid ethyl ester a novel diketo acid derivative which selectively inhibits the HIV-1 viral replication in cell culture and the ribonuclease H activity in vitro. *Antivir Res*, **65**(2), (2005), 117-24.
- [193] Artico, M.; Massa, S.; Mai, A.; Marongiu, M.E.; Piras, G.; Tramontano, E.; La Colla, P. 3,4-Dihydro-2-Alkoxy-6-Benzyl-4-Oxopyrimidines (DABOs) - A new class of specific inhibitors of Human-Immunodeficiency-Virus type-1. *Antivir Chem Chemother*, **4**(6), (1993), 361-8.
- [194] Himmel, D.M.; Sarafianos, S.G.; Dharmasena, S.; Hossain, M.M.; McCoy-Simandle, K.; Ilina, T.; Clark, A.D.; Knight, J.L.; Julias, J.G.; Clark, P.K.; Krogh-Jespersen, K.; Levy, R.M.; Hughes, S.H.; Parniak, M.A.; Arnold, E. HIV-1 Reverse Transcriptase structure with RNase H inhibitor dihydroxy benzoyl naphthyl hydrazone Bound at a novel site. *ACS Chem Biol*, **1**(11), (2006), 702-12.
- [195] Su, H-P.; Yan, Y.; Prasad, G.S.; Smith, R.F.; Daniels, C.L.; Abeywickrema, P.D.; Reid, J.C.; Loughran, H.M.; Kornienko, M.; Sharma, S.; Grobler, J.A.; Xu, B.; Sardana, V.; Allison, T.J.; Williams, P.D.; Darke, P.L.; Hazuda, D.J.; Munshi, S. Structural basis for the inhibition of RNase H activity of HIV-1 Reverse Transcriptase by RNase H active site-directed inhibitors. *J Virol*, **84**(15), (2010), 7625-33.
- [196] Wendeler, M.; Lee, H-F.; Bermingham, A.; Miller, J.T.; Chertov, O.; Bona, M.K.; Baichoo, N.S.; Ehteshami, M.; Beutler, J.; O'Keefe, B.R.; Götte, M.; Kvaratskhelia, M.; Le Grice, S. Vinylogous ureas as a novel class of inhibitors of Reverse Transcriptase-associated ribonuclease H activity. *ACS Chem Biol*, **3**(10), (2008), 635-44.
- [197] Felts, A.K.; LaBarge, K.; Bauman, J.D.; Patel, D.V.; Himmel, D.M.; Arnold, E.; Parniak, M.A.; Levy, R.M. Identification of alternative binding sites for inhibitors of HIV-1 Ribonuclease H through comparative analysis of virtual enrichment studies. *J Chem Inf Model*, **51**(8), (2011), 1986-98.

- [198] Sluis-Cremer, N.; Arion, D.; Parniak, M.A. Destabilization of the HIV-1 Reverse Transcriptase dimer upon interaction with N-acyl hydrazone inhibitors. *Mol Pharmacol*, **62**(2), (2002), 398-405.
- [199] Esposito, F.; Kharlamova, T.; Distinto, S.; Zinzula, L.; Cheng, Y-C.; Dutschman, G.; Floris, G.; Markt, P.; Corona, A.; Tramontano, E. Alizarine derivatives as new dual inhibitors of the HIV-1 reverse transcriptase-associated DNA polymerase and RNase H activities effective also on the RNase H activity of non-nucleoside resistant reverse transcriptases. *FEBS J*, **278**(9), (2011), 1444-57.
- [200] Distinto, S.; Esposito, F.; Kirchmair, J.; Cardia, M.C.; Gaspari, M.; Maccioni, E.; Alcaro, S.; Markt, P.; Wolber, G.; Zinzula, L.; Tramontano, E. Identification of HIV-1 reverse transcriptase dual inhibitors by a combined shape-, 2D-fingerprint- and pharmacophore-based virtual screening approach. *Eur J Med Chem*, **50**(0), (2012), 216-29.
- [201] Ortuso, F.; Langer, T.; Alcaro, S. GBPM: GRID-based pharmacophore model: concept and application studies to protein–protein recognition. *Bioinformatics*, **22**(12), (2006), 1449-55.
- [202] SiteMap. Schrodinger Suite, 2010, Portland, OR
- [203] Claisen, L.; Claparède, A. Condensationen von Ketonen mit Aldehyden". *Berichte der Deutschen Chemischen Gesellschaft* **14** (1), (1881), 2460–2468.
- [204] Schmidt, J. G. Ueber die Einwirkung von Aceton auf Furfurol und auf Bittermandelöl in Gegenwart von Alkalilauge. *Berichte der Deutschen Chemischen Gesellschaft* **1**, **4** (1), (1881), 1459–1461.
- [205] Stroba, A.; Froehner, W.; Hartmann, R. W.; Engel, M.; Schaeffer, F.; Hindie, V.; Lopez-Garcia, L.; Adrian, I.; Biondi, R. M. *Journal of Medicinal Chemistry*, **52**(15), (2009), 4683–4693.
- [206] Kumar, D.; Kumar, N. M.; Akamatsu, K.; Kusaka, E.; Harada, H.; Ito, T. Synthesis and biological evaluation of indolyl chalcones as antitumor agents. *Bioorganic & Medicinal Chemistry Letters*, **20**, (2010), 3916–3919.
- [207] Tramontano, E.; Cheng, Y.C.; HIV-1 reverse-transcriptase inhibition by a dipyrrodoiazepinone derivative: BI-RG-587. *Biochem. Pharmacol.* **43** (1992) 1371-1376.
- [208] Yonetani, T. Theorell H: Studies on Liver Alcohol Hydrogenase Complexes. 3. Multiple Inhibition Kinetics in the Presence of Two Competitive Inhibitors. *Arch Biochem Biophys*, **106** (1964) 243-251.
- [209] IntelLigand, LigandScout 3.0 (2009) Maria Enzersdorf, Austria.
- [210] Polonka-Bálinta, Á.; Saracenoa, C.; Ludányib, K.; Bényeic, A.; Mátyus P. Novel Extensions of the tert-Amino Effect: Formation of Phenanthridines and Diarene-Fused Azocines from ortho-ortho'-Functionalized Biaryls. *Synlett*, **18**, (2008), 2846-2850

- [210] Mellors, J.; Im, G.J.; Tramontano, E.; Winkler, S.R.; Medina, D.J.; Dutschman, G.E.; Bazmi, H.Z.; Piras, G.; Gonzales, C.J.; Cheng, Y-C. A single conservative amino acid substitution in the reverse transcriptase of human immunodeficiency virus type 1 confers resistance to (+)-(5S)-4,5,6,7-tetrahydro-5-methyl-6-(3-methyl-2butenyl)imidazo[4,5,1,jk][1,4] benzodiazepin-2(1H)-thione (TIBO R82150). *Mol Pharmacol* **43** (1993) 11-16.
- [211] Suchaud, V.; Bailly, F.; Lion, C.; Tramontano, E.; Esposito, F.; Corona, A.; Christ, F.; Debyser, Z.; Cotelle, P. Development of a series of 3-hydroxyquinolin-2(1H)-ones as selective inhibitors of HIV-1 reverse transcriptase associated RNase H activity. *Bioorg. Med. Chem. Lett.* **22** (2012) 3988-3992.

## **II PART:**

**Cycloalkylidenhydrazo-4-aryl-thiazoles: synthesis and biological activity against CANDIDA albicans.**

## CONTENTS

1	<i>Introduction</i>	
	1.1 <i>Historical overview</i>	3
2	<i>Epidemiology</i>	4
3	<i>Current therapy</i>	5
4	<i>Result and discussion</i>	8
5	<i>Materials and methods</i>	17
	5.1 <i>Chemistry</i>	17
	5.2 <i>Microbiology</i>	50
	5.2.1 <i>Antifungal agents</i>	
	5.2.2 <i>Antifungal susceptibility studies</i>	
6	<i>Acknowledgments</i>	52
7	<i>References and notes</i>	53

## **1 Introduction**

### **1.1 Historical overview**

The range of human infections caused by the yeast *C. albicans* and several related species (spp.) is considerable.

They range from relatively trivial conditions such as oral and genital thrush to fatal, systemic infections in patients who are already seriously ill with other diseases. In recent years there has been an increasing interest in Candida infections and in *C. albicans* in particular because fatal infections have become more prevalent and new Candida associated disorders have been recognized.

The medical importance of Candida infections and the scientific value of *C. albicans* as a model for fungal cellular development have stimulated advances in our understanding of the epidemiology of candidosis, the pathogenesis of the disease and the genetics and biochemistry of *C. albicans*.

Oral candidal infections appear to have been described as early as the 2<sup>nd</sup> century AD by GALEN, who described as *apthas albus*.

It was not until the mid-19th century that the clinical nature of oral candidosis (syn. oral candidiasis) was defined and the etiologic agent identified. [1]

There have been a wide variety of synonyms used for members of the genus Candida, 166 synonyms being recognized for *C. albicans* worldwide. [2]

The genus Candida is within the class Deuteromycetes and has been described as a "taxonomic pit" into which yeasts without a known sexual stage or other remarkable phenotypic character have been thrown. [3] Its members are biologically diverse and include yeasts with ascomycetous and basidiomycetous affinities.

There are currently between 150 and 200 species recognized in the genus. [3]

The genus Candida includes characteristically white asporogenous (imperfect) yeasts capable of forming pseudohyphae.

Within the genus, species are characterized primarily by colonial morphology, carbon utilization, and fermentation. [4]

There are seven Candida spp. of major medical importance, the most important being *C. albicans*, the one most frequently isolated. It is believed to be the most virulent in man.

The other Candida spp. encountered in human infections are *C. tropicalis*, *C. glabrata*, *C. parapsilosis*, *C. stellatoidea*, *C. krusei*, and *C. kyfer*. [1]

Due to the relatively high DNA homology between *C. albicans* and *C. stellatoidea*, the latter has been reclassified as a sucrose-negative variant of *C. albicans*. [5]

A study has shown that there are two distinct types of sucrose-negative *C. albicans*, identified as *C. stellatoidea* types I and II. [6]

In a more detailed analysis, these authors have concluded that type II is a sucrose-negative mutant of *C. albicans*, whereas type I is indistinguishable from *C. albicans*. [7]

*C. albicans* is a dimorphic yeast and is believed to be an obligate associate of warm-blooded animals.

In a review of the biology and genetics of *C. albicans* [4], it was shown that this species are an imperfect yeast having no sexual cycle. It is diploid, having lost the ability to undergo meiosis and to form a haplophase yeast.

## **2      *Epidemiology***

It has been postulated that most people usually carry a single strain of *Candida* at different body sites for a long time. [3]

However, it has been shown that a few individuals may harbour more than one strain or species of *Candida* at the same time, and that in hospitalized and immunocompromised patients this occurs more commonly. [3]

The intraoral commensal existence of *Candida* occurs in at least 50% of the population, and if sensitive enough tests were developed, possibly more than 90% of healthy individuals would be shown to carry this organism. [3]

The gastrointestinal (GI) tract is believed to be the major habitat of the commensal *Candida* spp. The wide variation in the types of patients analysed and methods used in the analysis of the carriage rate of various sites in the GI tract allows the conclusion that *Candida* spp. are very common gut commensals. [3]

It has been shown that, if present in sufficiently high numbers, *C. albicans* can spread from the human gut, causing fungaemia and funguria [8], and it is thought that the gut is the ultimate source of most forms of *Candida* infection. [3]

It has been previously reported that the prevalence and density of *C. albicans* are greater in edentulous patients who wear dentures and who have erythematous candidosis than in normal subjects, suggesting that dentures may encourage the growth of *Candida*.

However, it has been found that, although the occurrence of *C. albicans* was greater in these patients than in healthy controls, there was no difference in the concentration of *C. albicans* when present in these groups. [9]

These authors [9] showed that it was not possible to equate specific numbers of *Candida* with health and disease, as previously proposed. [10]

Oral candidosis in all groups of patients has been classified into four main categories; acute pseudomembranous, acute atrophic, chronic atrophic, and chronic hyperplastic. [11]

Candida induced angular cheilitis was included as another category when the association between this particular lesion and its infective etiology was determined. [12]

The advent of the association of oral candidosis and human immunodeficiency virus (HIV) infection has resulted in a modification of this terminology. [13,14]

In particular, the term "atrophic" has been replaced by the term "erythematous" because "erythematous" describes the clinical picture whereas "atrophic" describes the histologic picture.

Furthermore, as lesions are nearly always chronic in HIV infected patients, the terms "acute" and "chronic" seem unnecessary.

### **3      *Current Therapy***

Invasive fungal infection is a leading cause of morbidity and mortality among immunocompromised and debilitated patients, including those with hematological malignancy, solid organ or bone marrow transplantation, and neutropenia and those receiving systemic corticosteroid therapy.

Candida species and Aspergillus species are the two predominant causative fungi, with the case fatality rates being 30% and 50% among those infected with members of these two fungal genera, respectively. [15,16]

Over the past few decades, amphotericin B has been the mainstay treatment of candidiasis and aspergillosis, whereas fluconazole has been extensively used among patients with Candida albicans infection.

After randomized controlled trials showed that extended-spectrum azoles (itraconazole, voriconazole, posaconazole) and echinocandins (anidulafungin, caspofungin, micafungin) had efficacies similar to those of amphotericin B and fluconazole, these newer antifungal agents have been used more frequently for the treatment of patients with probable or proven invasive fungal infection. [17-21]

Current practice guidelines recommend amphotericin B formulations, fluconazole, and echinocandins as first-line therapy for patients with candidemia; and amphotericin B formulations or voriconazole are the drugs of choice for the primary therapy of invasive aspergillosis. [18-21]

For patients who fail the primary therapy or who have intolerable adverse reactions, the common practice is to switch to a different class of antifungal agents. [22,23]

With regard to the safety of antifungal therapies, amphotericin B desoxycholate is known for its infusion-related adverse effects and nephrotoxicity; approximately 30% of patients developed abnormal renal function, and treatment was discontinued in 5% of patients because of toxicity. [24,25]



Other amphotericin B formulations, including amphotericin B colloidal dispersion, amphotericin B lipid complex, liposomal amphotericin B (Ambisome), and other, newer antifungal agents, are associated with substantially fewer infusion-related and nephrotoxic events.

However, hepatotoxic reactions to antifungal agents were increasingly reported and ranged from mild and asymptomatic abnormalities in liver function test results to potentially fatal fulminant hepatic failure. [26-31]

While individual reviews of new antifungal agents have been published [32-43], there has been no systematic evaluation of the toxicity associated with these treatments.

Nevertheless we have a rich armamentarium of antifungal agents as schematized in Table 1.

**Table 1.** Currently available antifungal drugs

Wall/ membrane	Ergosterol inhibitors	Azoles (lanosterol 14- $\alpha$ -demethylase inhibitors)	IMIDAZOLES	TOPICAL: Bifonazole; Butoconazole; Clomidazole#; Clomitrazone; Croconazole; Econazole; Fenticonazole; Ketoconazole; Isoconazole; Miconazole#; Neticonazole; Omoconazole; Oxiconazole; Sertaconazole; Sulconazole; Tioconazole
			TRIAZOLES	TOPICAL: Fluconazole#; Fosfluconazole; Terconazole SYSTEMIC: Fluconazole; Hexaconazole; Isavuconazole; Itraconazole; Posaconazole; Voriconazole
			THIAZOLES	TOPICAL: Abafungin
		Polyene antimicotic (ergosterol binding)	TOPICAL: Hamycin; Natamycin; Nystatin# SYSTEMIC: Amphotericin B#; Hamycin	
		Allylamines (squalene monooxygenase inhibitors)	TOPICAL: Amorolfine; Butanefine; Naftifine; Terbinafine SYSTEMIC: Terbinafine	
	$\beta$ -glucan synthase inhibitors	ECHINOCANDINS: Anidafungin, Caspofungin; Micafungin		
Intracellular	Pyrimidine analogues / Thymidylate synthase inhibitors		Flucytosine#	
	Mitotic inhibitors		Griseofulvin#	
Others	Bromochlorosalicylanilide; Methylrosaniline; Tribromometacresol; Undecylenic acid; Polynoxylin; Chlorophetanol; Chlorphenesin; Ticlatone; Sulbentine; Ethylparaben; Haloprogin; Salicylic acid Selenium sulfide; Ciclopirox; Amorolfine; Dimazole; Tolnaftate; Tolciclate; Sodium thiosulfate; Whitfield's ointment; Potassium iodide#; Taurolidine; Tea tree oil; citronella oil; lemon grass; orange oil; patchouli; lemon; myrtle; PCP; Pentamidine; Dapsone; Atovaquone			

# World Health Organization Essential Medicines (WHO-EM) list.

As reported in Table 1, current fungal therapy is directed towards different cellular targets such as wall membrane construction (Ergosterol synthesis inhibitors,  $\beta$ -glucan synthase inhibitors) or nucleic acids synthesis (Thymidylate synthase inhibitors, Mitotic inhibitors). However the emergence of drug resistance, in particular in the case of

immuno-compromised patients and the lack of fungicidal agents with low toxicity, give rise to some worries.

So far there is space for a deeper investigation and for the research of new more potent and possibly less toxic compounds.

In particular the need of new agents with different mechanism/target is now days urgent.

## 4 Results and discussion

During my PhD work I have synthesised some cycloalkyden-hydrazothiazoles as anti-candida agents.

The research group of medicinal chemistry of the department of life and environmental sciences has already synthesised similar compounds that exhibit potent activity towards several species of candida. [44-48]

Thus, to achieve more information on the SARs of these compounds and to evaluate their activity towards Fluconazole resistant Candida species, we have synthesised differently substituted cycloalkydenhydrazo-4-arylthiazoles illustrated in Figure 1-5.

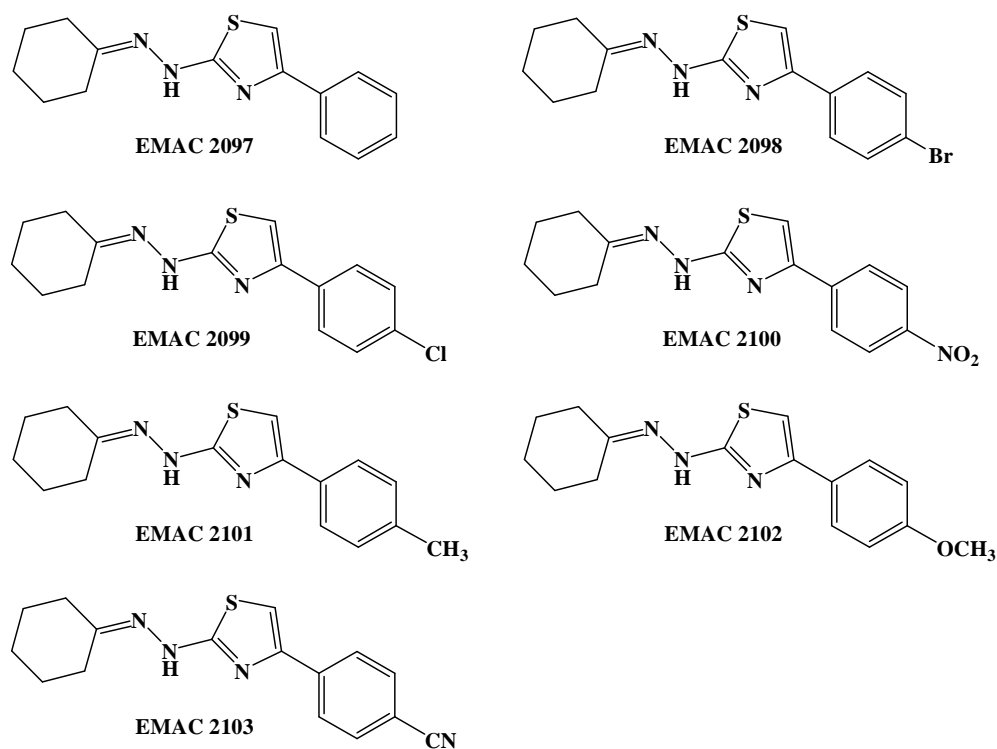
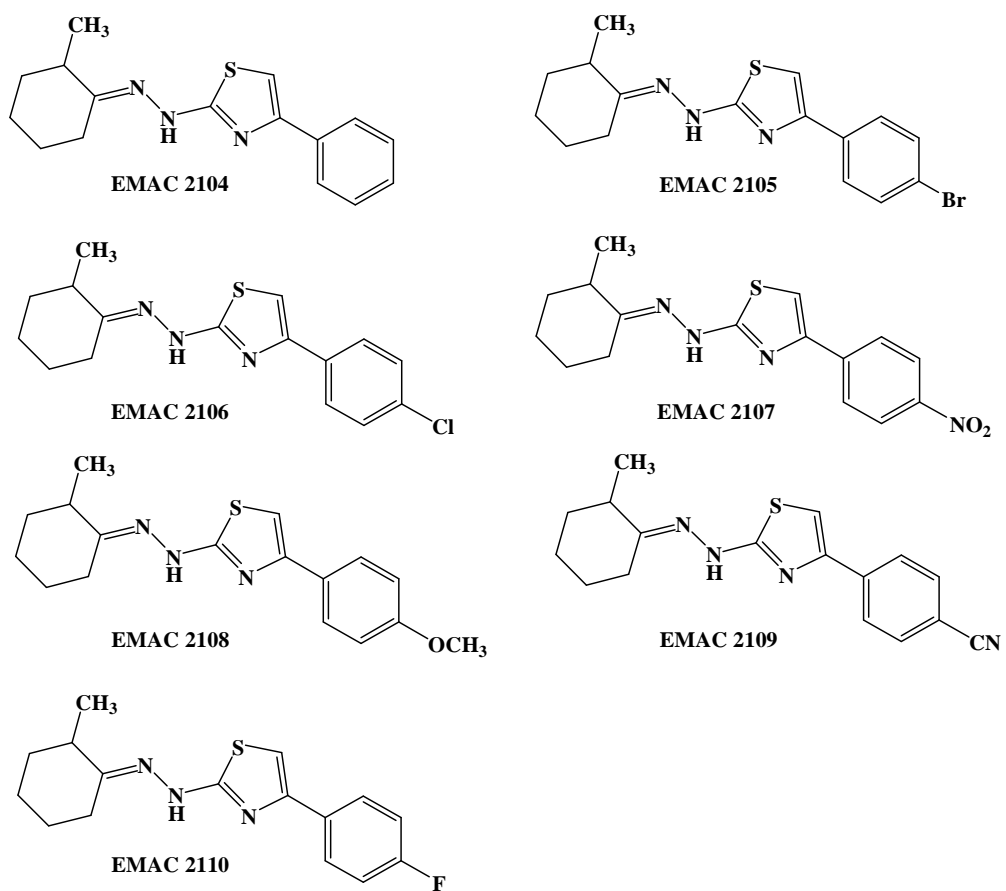
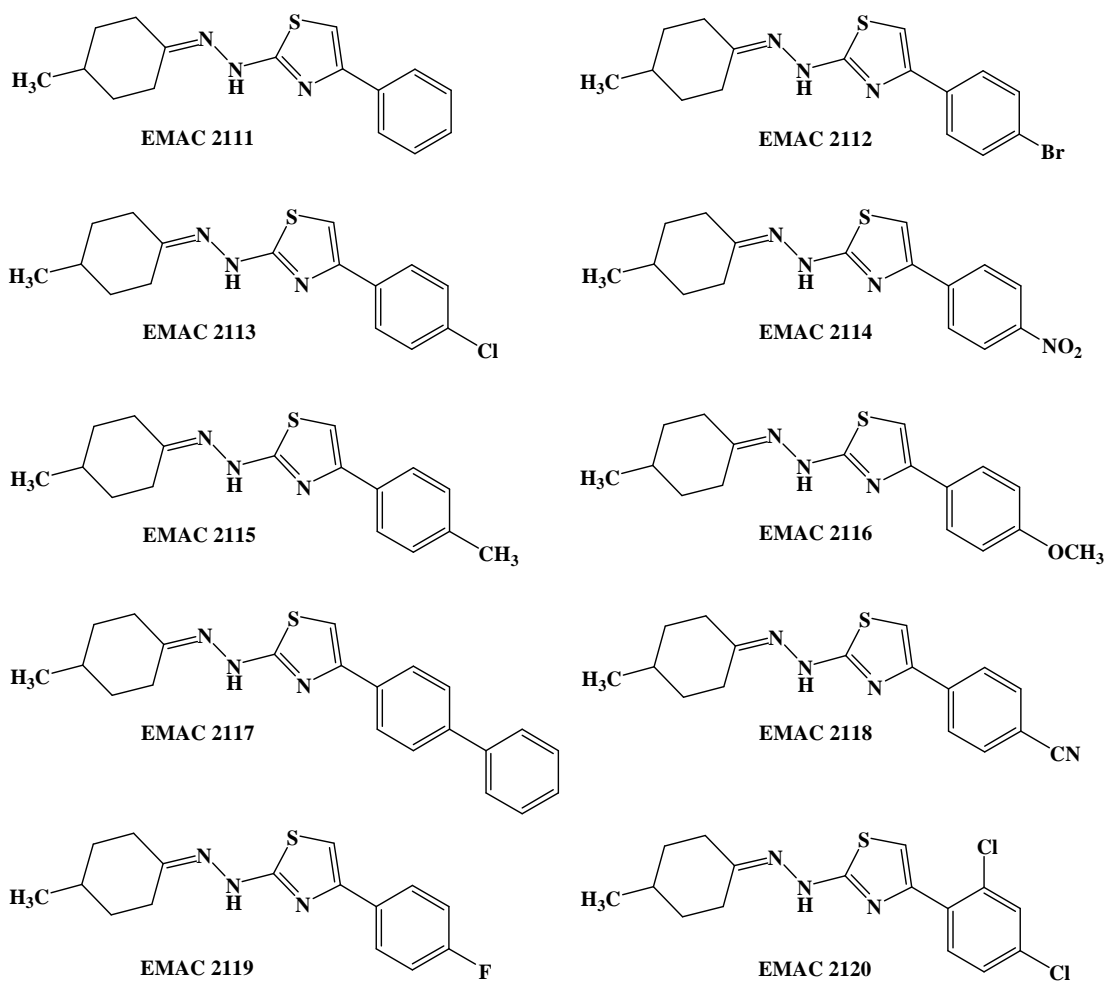


Figure 1. Structure of compounds EMAC 2097-2103



**Figure 2.** Structure of compounds EMAC 2104-2110



**Figure 3.** Structure of compounds EMAC 2111-2120

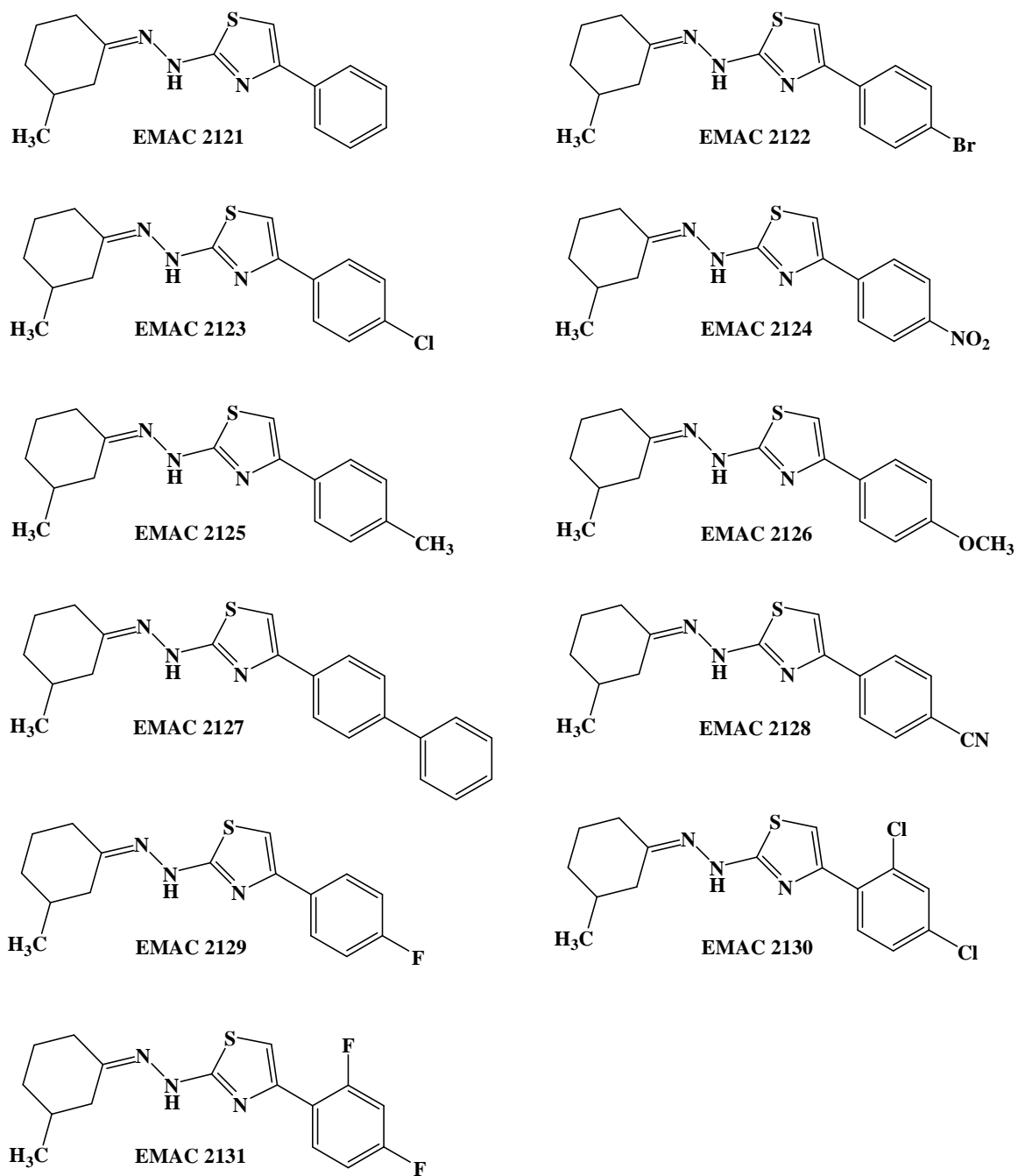
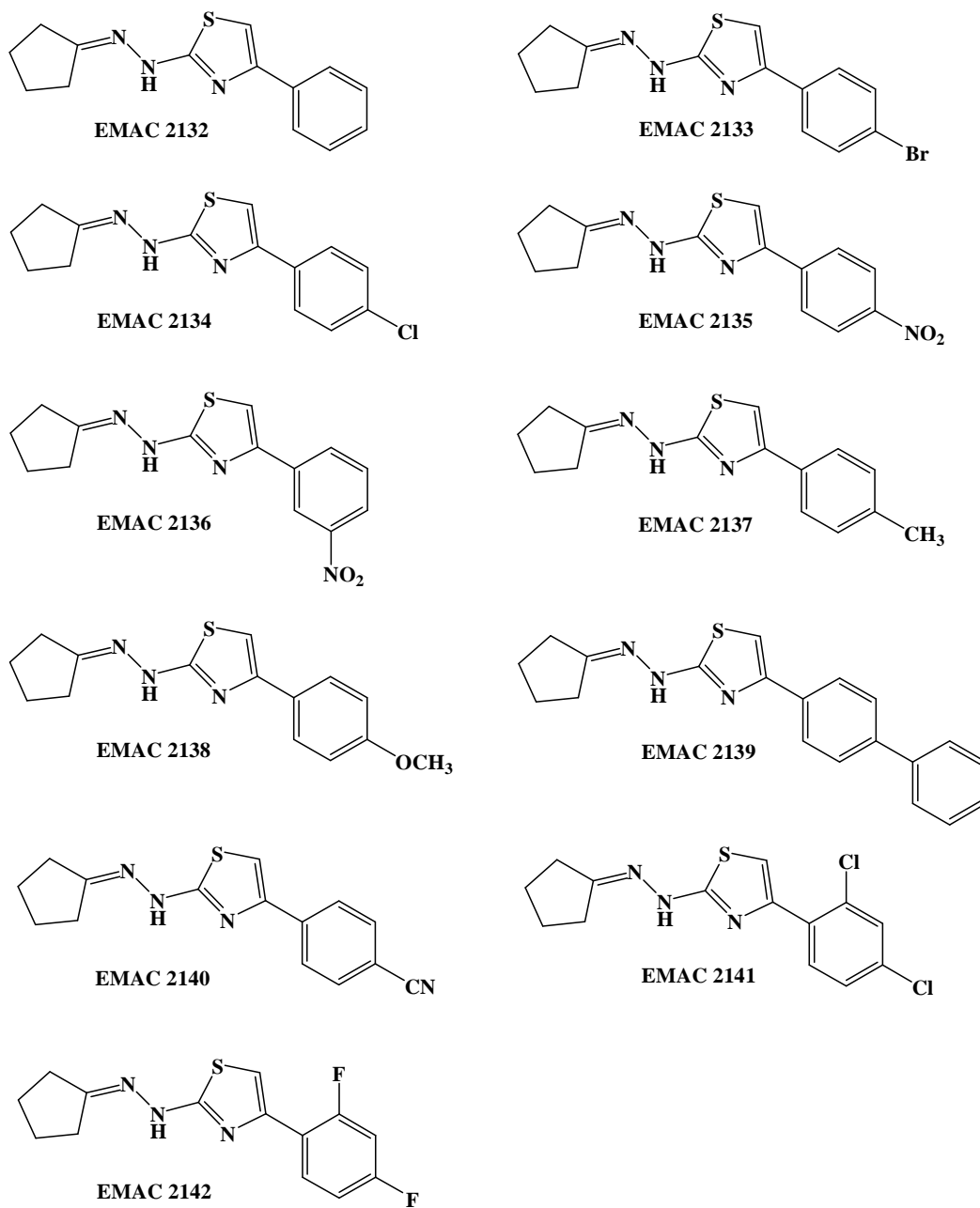
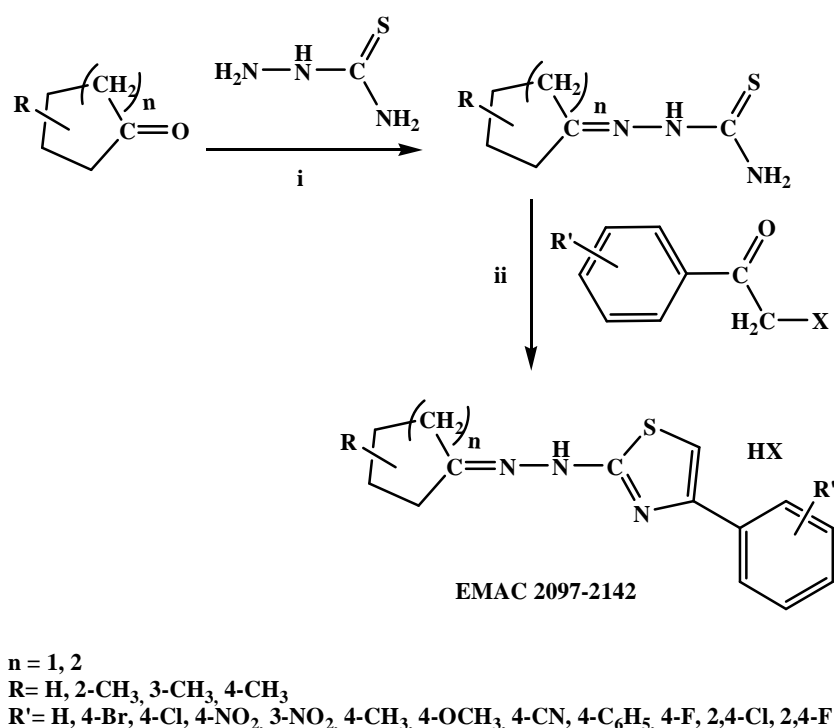


Figure 4. Structure of compounds EMAC 2121-2131



**Figure 5.** Structure of compounds EMAC 2132-2142

All the compounds were synthesised by direct reaction of the cyclic ketone (1.2 mol) with thiosemicarbazide (1 mol) in n-propanol with catalytic amounts of acetic acid (10 drops) at reflux condition for 12-24 hours to obtain the corresponding thiosemicarbazones that was subsequently reacted with  $\alpha$ -halogenoketones to yield the 4-substituted thiazole ring derivatives as shown in Scheme 1. In the synthesis of final compounds water proved to be a more efficient, cheaper, and *green* solvent for our purpose. As a matter of fact, the reaction products precipitate on cooling down and can be filtered and when needed purified by crystallization from the appropriate solvent.



**Scheme 1.** Synthesis of cycloalkylidenehydrazothiazole derivatives EMAC 2097-2142. Reagents: (i) n-propanol, AcOH; (ii) H<sub>2</sub>O or n-propanol

All synthesized compounds were characterised by analytical and spectral data as listed in Table 4 and 5.

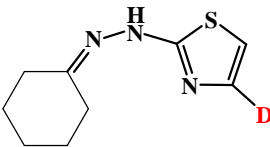
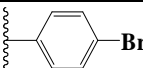
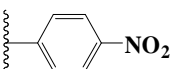
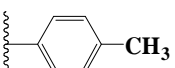
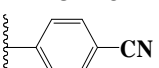
By this procedure derivatives **EMAC 2097-2142** were prepared and submitted to biological tests.

In particular, our aim was to identify those compounds that were active towards Fluconazole resistant *C.albicans*.

The preliminary biological results are reported in Table 2 and 3.



**Table 2.** EMAC 2098-2100-2101-2103 activity

EMAC 2098-2100-2101-2103 activity				
				
"D"-ring	CANDIDA <i>albicans</i> ATCC 10231		CANDIDA <i>albicans</i> 25 Fluconazole resistant	
	MIC	MCF	MIC	MCF
 EMAC 2098	0.19	0.39	0.39	50
 EMAC 2100	0.78	100	0.78	100
 EMAC 2101	0.39	12.5	>25	>25
 EMAC 2103	3.12	25	>25	>25
Fluconazole	0.78	>100	>100	>100

In the cyclohexylidene series all tested compounds exhibit a remarkable activity towards *C.albicans* ATCC 10231. MIC values range from 0.19 to 3.12 µg/ml.

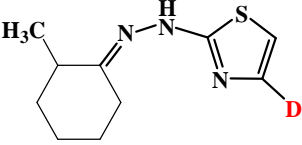
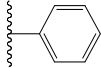
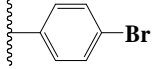
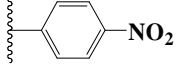
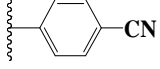
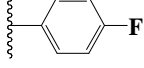
Noteworthy all compounds, with the exception of **EMAC 2100**, exhibit fungicidal activity when tested on *C.albicans* ATCC 10231.

A different behavior is observed when compounds were tested against "*C.albicans* 25 Fluconazole resistant". In this case only compound **EMAC 2098** and **EMAC 2100** show remarkable MIC values (0.39 and 0.78 µg/ml respectively), while almost no activity is observed for **EMAC 2101** and **EMAC 2103**. Unfortunately, none of the tested compounds have interesting fungicidal activity when tested on "*C.albicans* 25 Fluconazole resistant".

Nevertheless these data are more than encouraging with respect to the activity exhibited by Fluconazole (Table 1 and 2).

The introduction of a methyl substituent in the position 2 of the cyclohexylidene moiety leads to a different behavior (Table 2).

**Table 3.** EMAC 2104-2105-2107-2109-2110 activity

<b>EMAC 2104-2105-2107-2109-2110 activity</b>				
				
"D"-ring	<b>CANDIDA <i>albicans</i> ATCC 10231</b>		<b>CANDIDA <i>albicans</i> 25 Fluconazole resistant</b>	
	<b>MIC</b>	<b>MCF</b>	<b>MIC</b>	<b>MCF</b>
 EMAC 2104	0.19	25	0.19	1.56
 EMAC 2105	0.78	25	>25	>25
 EMAC 2107	0.78	>100	3.12	50
 EMAC 2109	1.56	>25	>25	>25
 EMAC 2110	0.78	3.12	1.56	3.12
Fluconazole	0.78	>100	>100	>100

Compound **EMAC 2105**, bearing a 4-bromophenyl moiety in the position 4 of the thiazole ring is active only towards *C. albicans* ATCC 10231, and its activity is comparable with that of Fluconazole but less potent than its homologous **EMAC 2098**.

It has neither fungicidal activity, nor efficacy against *C. albicans* 25 Fluconazole resistant.

On the contrary, the 4-nitro-substituted derivative **EMAC 2107** exhibits a similar activity profile with respect to its homologous **EMAC 2100**.

Both compounds only exhibit fungistatic activity on both candida species.

On the contrary, compounds **EMAC 2104** and **EMAC 2110** exhibit a very potent activity with respect to Fluconazole (Table 2).

The 4-phenylthiazole derivative **EMAC 2104** is particularly active against *C.albicans* 25 Fluconazole resistant (MIC 0.19 µg/ml; MFC 1.56 µg/ml).

Although slightly less potent, compound **EMAC 2110** is active towards both candida species. Moreover its fungicidal activity is comparable to that of **EMAC 2104**.

These data are preliminary and more experiments are needed to rationalize the SARs of this class of compounds.

In some cases cross-resistance with Fluconazole has been observed indicating that a similar mechanism of action might be postulated for **EMAC** derivatives.

Nevertheless 5 compounds out of 9 are active against candida and in some cases the activity is conserved also against *C. albicans* 25 Fluconazole resistant. Thus although the mechanism of action might be the similar a different specific target is probably involved.

Further studies on the mechanism of action, toxicity, and in vivo efficacy are needed. However, these preliminary data indicate the potential of **EMAC** derivatives as a template for the development of new antifungal agents.

## **5 Materials and methods**

### **5.1 Chemistry**

#### **COMPOUNDS EMAC 2097-2142**

All compounds are characterised by a cycloalkylidenehydrazothiazole core.

The synthetic pathway is divided in two different step (Scheme 1).

Unless otherwise noted, starting materials and reagents were obtains from commercial suppliers and were used without purification.

All melting point were determined by the capillary method on a Stuart SMP11 melting point apparatus and are uncorrected.

All samples were measured in CDCl<sub>3</sub> solvent at 278.1 K temperature on a Varian Unity 500 spectrometer. In the signal assignments the proton chemical shifts are referred to the solvent (1H:  $\delta$  = 7.24 ppm,). Coupling constants *J* are expressed in hertz (Hz).

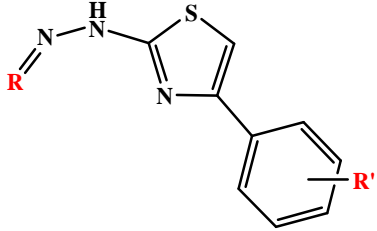
Elemental analyses were obtained on a Perkin–Elmer 240 B microanalyser.

Analytical data of the synthesised compounds are in agreement with the theoretical data.

HPLC-MS/MS analysis was performed using an HPLC-MS/MS Varian (Varian Palo Alto, CA, USA) system fitted with a 1200 L triple quadrupole mass spectrometer equipped with an electrospray ionization source (ESI). A Varian MS workstation version 6.8 software was used for data acquisition and processing. Rapid identification was achieved with direct infusion of the purified molecule, dissolved in methanol, on the mass spectrometer source.

TLC chromatography was performed using silica gel plates (Merck F 254), spots were visualised by UV light.

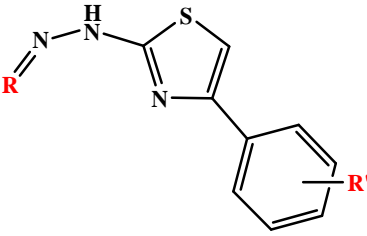
All synthesized compounds were characterised by analytical and spectral data as listed in Table 3 and 4

**Table 4.** Chemical and physical data of derivatives **EMAC 2097-2142**

Compound	R	R'	M.W.	Mp (C°)	% Yield
EMAC 2097	Cyclohexyl [	H	271.38	189-190 [46-47]	79
EMAC 2098	Cyclohexyl	4-Br	431.19	179-180	79
EMAC 2099	Cyclohexyl	4-Cl	305.83	121-122	73
EMAC 2100	Cyclohexyl	4-NO <sub>2</sub>	316.38	172-173 [48]	83
EMAC 2101	Cyclohexyl	4-CH <sub>3</sub>	285.41	183-185 [48]	76
EMAC 2102	Cyclohexyl	4-OCH <sub>3</sub>	301.41	152	77
EMAC 2103	Cyclohexyl	4-CN	296.39	206-207 [48]	83
EMAC 2104	Cyclohexyl-2-CH <sub>3</sub>	H	285.41	162-164 [46-47]	79
EMAC 2105	Cyclohexyl-2-CH <sub>3</sub>	4-Br	364.3	130-131 [48]	77
EMAC 2106	Cyclohexyl-2-CH <sub>3</sub>	4-Cl	319.85	187-188 [45]	71
EMAC 2107	Cyclohexyl-2-CH <sub>3</sub>	4-NO <sub>2</sub>	330.4	163-164 [45]	85
EMAC 2108	Cyclohexyl-2-CH <sub>3</sub>	4-OCH <sub>3</sub>	315.43	128-129 [45]	82
EMAC 2109	Cyclohexyl-2-CH <sub>3</sub>	4-CN	391.33	200-201 [45]	79
EMAC 2110	Cyclohexyl-2-CH <sub>3</sub>	4-F	303.4	178-180 [45]	79
EMAC 2111	Cyclohexyl-4-CH <sub>3</sub>	H	285.41	191-192 [47]	66
EMAC 2112	Cyclohexyl-4-CH <sub>3</sub>	4-Br	364.3	158-159	80

EMAC 2113	Cyclohexyl-4-CH <sub>3</sub>	4-Cl	319.85	177-179 [44]	74
EMAC 2114	Cyclohexyl-4-CH <sub>3</sub>	4-NO <sub>2</sub>	330.4	175-177 [48]	75
EMAC 2115	Cyclohexyl-4-CH <sub>3</sub>	4-CH <sub>3</sub>	299.43	158-160 [48]	83
EMAC 2116	Cyclohexyl-4-CH <sub>3</sub>	4-OCH <sub>3</sub>	315.43	96-97	73
EMAC 2117	Cyclohexyl-4-CH <sub>3</sub>	4-C <sub>6</sub> H <sub>5</sub>	361.5	181-182	70
EMAC 2118	Cyclohexyl-4-CH <sub>3</sub>	4-CN	310.42	196-197 [48]	78
EMAC 2119	Cyclohexyl-4-CH <sub>3</sub>	4-F	303.4	163-164 [48]	20
EMAC 2120	Cyclohexyl-4-CH <sub>3</sub>	2,4-Cl	345.3	135-136 [48]	20
EMAC 2121	Cyclohexyl-3-CH <sub>3</sub>	H	285.41	121-123	68
EMAC 2122	Cyclohexyl-3-CH <sub>3</sub>	4-Br	364.3	168-169	41
EMAC 2123	Cyclohexyl-3-CH <sub>3</sub>	4-Cl	319.85	195-199 [44]	44
EMAC 2124	Cyclohexyl-3-CH <sub>3</sub>	4-NO <sub>2</sub>	303.04	164-165	76
EMAC 2125	Cyclohexyl-3-CH <sub>3</sub>	4-CH <sub>3</sub>	299.43	171-174 [44]	85
EMAC 2126	Cyclohexyl-3-CH <sub>3</sub>	4-OCH <sub>3</sub>	315.43	162-165 [44]	42
EMAC 2127	Cyclohexyl-3-CH <sub>3</sub>	4-C <sub>6</sub> H <sub>5</sub>	361.5	128-130	79
EMAC 2128	Cyclohexyl-3-CH <sub>3</sub>	4-CN	310.42	189-190 [44]	80
EMAC 2129	Cyclohexyl-3-CH <sub>3</sub>	4-F	303.4	192-195 [44]	65
EMAC 2130	Cyclohexyl-3-CH <sub>3</sub>	2,4-F	321.39	130-132	68
EMAC 2131	Cyclohexyl-3-CH <sub>3</sub>	2,4-Cl	354.3	148-151	63
EMAC 2132	Cyclopentyl	H	257.35	215 [47]	66
EMAC 2133	Cyclopentyl	4-Br	336.25	213-215 [44]	87
EMAC 2134	Cyclopentyl	4-Cl	291.8	223-225 [44]	84

EMAC 2135	Cyclopentyl	4-NO <sub>2</sub>	302.35	219-220 [44]	71
EMAC 2136	Cyclopentyl	3-NO <sub>2</sub>	302.35	187-190 [44]	74
EMAC 2137	Cyclopentyl	4-CH <sub>3</sub>	271.38	218-220 [44]	85
EMAC 2138	Cyclopentyl	4-OCH <sub>3</sub>	287.38	214-217 [44]	77
EMAC 2139	Cyclopentyl	4-CN	282.36	207-208 [44]	70
EMAC 2140	Cyclopentyl	4-C <sub>6</sub> H <sub>5</sub>	333.45	235-237 [44]	69
EMAC 2141	Cyclopentyl	2,4-F	293.33	183-185 [48]	49
EMAC 2142	Cyclopentyl	2,4-Cl	326.24	162-164[48]	60

**Table 5.** Analytical data of derivatives EMAC 2097-2142


Compound	R	R'	Reaction solvent	Crystallisation solvent	Aspect	Reaction time (h)
EMAC 2097	Cyclohexyl	H	Water	Water/ethanol	Brown solid	32
EMAC 2098	Cyclohexyl	4-Br	Water	Ethanol	Pale yellow solid	32
EMAC 2099	Cyclohexyl	4-Cl	Water	Water/ethanol	Crystalline orange solid	28
EMAC 2100	Cyclohexyl	4-NO <sub>2</sub>	Water	Ethanol	Crystalline orange solid	26
EMAC 2101	Cyclohexyl	4-CH <sub>3</sub>	Water	Ethanol	Crystalline pale brown solid	26
EMAC 2102	Cyclohexyl	4-OCH <sub>3</sub>	n-propanol	Ethanol	Crystalline white solid	5
EMAC 2103	Cyclohexyl	4-CN	Water	Ethanol	Crystalline pale red solid	26
EMAC 2104	Cyclohexyl-2-CH <sub>3</sub>	H	Water	Water/ethanol	Pale brown solid	26
EMAC 2105	Cyclohexyl-2-CH <sub>3</sub>	4-Br	Water	Hexane	Crystalline pale orange solid	48
EMAC 2106	Cyclohexyl-2-CH <sub>3</sub>	4-Cl	Water	Ethanol	Brown orange solid	48
EMAC 2107	Cyclohexyl-2-CH <sub>3</sub>	4-NO <sub>2</sub>	Water	Water/ethanol	Crystalline yellow solid	24
EMAC 2108	Cyclohexyl-2-CH <sub>3</sub>	4-OCH <sub>3</sub>	n-propanol	Ethanol	Crystalline white solid	6
EMAC 2109	Cyclohexyl-2-CH <sub>3</sub>	4-CN	Water	Water/ethanol	Red solid	28
EMAC 2110	Cyclohexyl-2-CH <sub>3</sub>	4-F	n-propanol	Ethanol	Crystalline white solid	28
EMAC 2111	Cyclohexyl-4-CH <sub>3</sub>	H	Water	Water/ethanol	Pale brown solid	26
EMAC 2112	Cyclohexyl-4-CH <sub>3</sub>	4-Br	Water	Water/ethanol	Pale red solid	26



EMAC 2113	Cyclohexyl-4-CH <sub>3</sub>	4-Cl	Water	Water/ethanol	Brown solid	26
EMAC 2114	Cyclohexyl-4-CH <sub>3</sub>	4-NO <sub>2</sub>	Water	Water/ethanol	Yellow solid	24
EMAC 2115	Cyclohexyl-4-CH <sub>3</sub>	4-CH <sub>3</sub>	Water	Water/ethanol	Pale brown solid	26
EMAC 2116	Cyclohexyl-4-CH <sub>3</sub>	4-OCH <sub>3</sub>	Water	Water/ethanol	Pale red solid	26
EMAC 2117	Cyclohexyl-4-CH <sub>3</sub>	4-C <sub>6</sub> H <sub>5</sub>	Water	Water/ethanol	Pale brown solid	26
EMAC 2118	Cyclohexyl-4-CH <sub>3</sub>	4-CN	Water	Water/ethanol	Yellow solid	26
EMAC 2119	Cyclohexyl-4-CH <sub>3</sub>	4-F	Water	Ethanol	Yellow solid	24
EMAC 2120	Cyclohexyl-4-CH <sub>3</sub>	2,4-Cl	Water	Water/ethanol	Brown solid	24
EMAC 2121	Cyclohexyl-3-CH <sub>3</sub>	H	Water	Ethanol	Pale brown solid	26
EMAC 2122	Cyclohexyl-3-CH <sub>3</sub>	4-Br	Water	Acetonitrile	Brown solid	24
EMAC 2123	Cyclohexyl-3-CH <sub>3</sub>	4-Cl	Water	Ethanol	Pale brown solid	26
EMAC 2124	Cyclohexyl-3-CH <sub>3</sub>	4-NO <sub>2</sub>	Water	Water/ethanol	Yellow solid	26
EMAC 2125	Cyclohexyl-3-CH <sub>3</sub>	4-CH <sub>3</sub>	Water	Water/ ethanol	Pale brown solid	26
EMAC 2126	Cyclohexyl-3-CH <sub>3</sub>	4-OCH <sub>3</sub>	Water	Ethanol	Pale yellow solid	26
EMAC 2127	Cyclohexyl-3-CH <sub>3</sub>	4-C <sub>6</sub> H <sub>5</sub>	Water	Water/ethanol	Pale brown solid	24
EMAC 2128	Cyclohexyl-3-CH <sub>3</sub>	4-CN	Water	Ethanol	Pale brown solid	26
EMAC 2129	Cyclohexyl-3-CH <sub>3</sub>	4-F	Water	Water/ethanol	Pale red solid	26
EMAC 2130	Cyclohexyl-3-CH <sub>3</sub>	2,4-F	Water	Water/ethanol	Pale red solid	24
EMAC 2131	Cyclohexyl-3-CH <sub>3</sub>	2,4-Cl	Water	Water/ethanol	White-brown solid	26
EMAC 2132	Cyclopentyl	H	Water	Water/ ethanol	Pale brown solid	24
EMAC 2133	Cyclopentyl	4-Br	Water	Water/ ethanol	Pale yellow solid	24
EMAC 2134	Cyclopentyl	4-Cl	Water	Water/ethanol	Pale brown solid	24

EMAC 2135	Cyclopentyl	4-NO <sub>2</sub>	Water	Water/ethanol	Crystalline orange solid	24
EMAC 2136	Cyclopentyl	3-NO <sub>2</sub>	Water	Water/ethanol	Pale yellow solid	24
EMAC 2137	Cyclopentyl	4-CH <sub>3</sub>	Water	Water/ethanol	Pale brown solid	24
EMAC 2138	Cyclopentyl	4-OCH <sub>3</sub>	Water	Water/ethanol	Pale brown solid	24
EMAC 2139	Cyclopentyl	4-CN	Water	Water/ethanol	Pale yellow solid	24
EMAC 2140	Cyclopentyl	4-C <sub>6</sub> H <sub>5</sub>	Water	Water/ethanol	Yellow solid	24
EMAC 2141	Cyclopentyl	2,4-F	Water	Water/ethanol	Pale brown solid	24
EMAC 2142	Cyclopentyl	2,4-Cl	Water	Water/ethanol	Pale brown solid	24

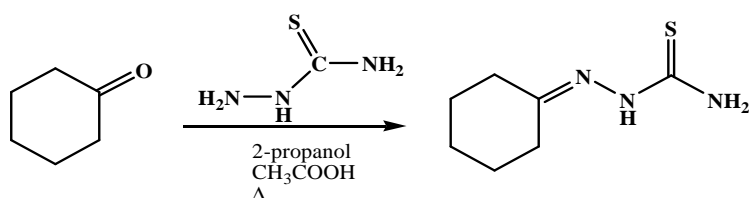
### Synthesis of starting thiosemicarbazones

The starting thiosemicarbazones have been synthesised by slightly modifying the procedures reported in the literature. [49]

In a flask equipped with a reflux condenser, equimolar amounts of thiosemicarbazide and of the appropriate ketone are reacted in n-propanol in the presence of a catalytic amount of AcOH. The mixture is then refluxed for all the night, and the obtain solid is filtered and used without further purification.

According to this procedure the following compounds have been synthesised:

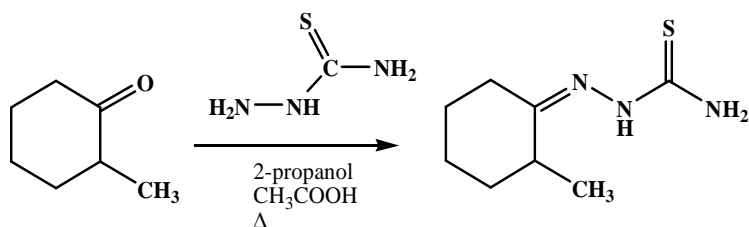
#### 1-cyclohexylidene thiosemicarbazide



M.W.: 171.26 g/mol; RF: 0.82 (eluent: ethyl acetate-hexane 20:1 ); Mp: 155°-156°C; Yield: 87%, Aspect: crystalline pale yellow solid

<sup>1</sup>H-NMR: (500 MHz, CDCl<sub>3</sub>) δH 1.55 (br s, 6H, CH<sub>2</sub>, cyclohexyl), 2.19-2.23 (m, 2H, CH<sub>2</sub>, cyclohexyl), 2.38 (br s, 2H, CH<sub>2</sub>, cyclohexyl), 7.50 (br s, 1H, NH<sub>2</sub>), 7.93 (br s, 1H, NH<sub>2</sub>), 10.13 (br s, 1H, NH).

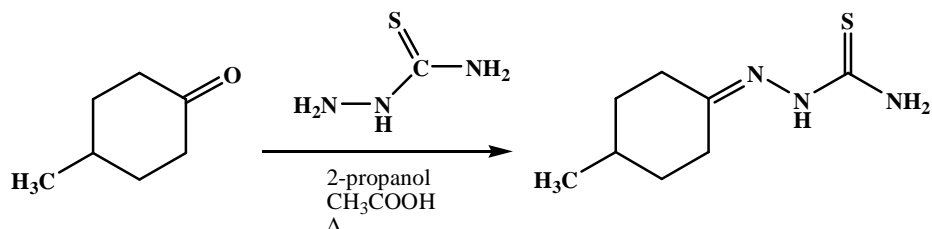
#### 1-(2-methylcyclohexylidene)thiosemicarbazide



M.W.: 185.29 g/mol; RF: 0.77 (eluent: ethyl acetate-hexane 20:1); Mp: 154°-156°C; Yield: 87%, Aspect: crystalline pale yellow solid

$^1\text{H-NMR}$ : (500 MHz,  $\text{CDCl}_3$ ) 1.08-1.10 (d,  $J$ : 6.57, 3H,  $\text{CH}_3$ ); 1.77-2.62 (m, 9H, cyclohexyl);  
6.30 (s, 2H,  $\text{NH}_2$ ,  $\text{D}_2\text{O}$  exch); 8.75 (s, 1H, NH,  $\text{D}_2\text{O}$  exch.)

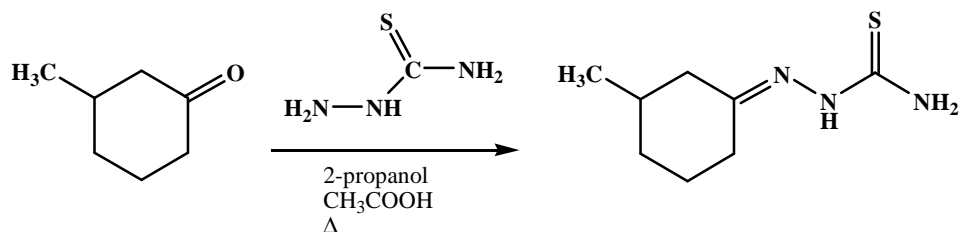
### 1-(4-methylcyclohexylidene)thiosemicarbazide



M.W.: 185.29 g/mol; RF: 0.61 (eluent: ethyl acetate-hexane 20:1); Mp: 161°-162°C; Yield: 66%, Aspect: light yellow powder

<sup>1</sup>H-NMR: (500 MHz, CDCl<sub>3</sub>) δH 0.94 (d, 3H, *J*: 6.5, CH<sub>3</sub>), 1.16 (m, 2H, CH<sub>2</sub>, cyclohexyl), 1.68 (m, 1H, CH<sub>2</sub>, cyclohexyl), 1.92 (m, 3H, CH<sub>2</sub>, cyclohexyl), 2.19 (m, 1H, CH<sub>2</sub>, cyclohexyl), 2.28 (m, 2H, CH<sub>2</sub>, cyclohexyl), 2.71 (m, 1H, CH<sub>2</sub>, cyclohexyl), 6.53 (br.s, 1H, NH<sub>2</sub>), 7.27 (br.s, 1H, NH<sub>2</sub>), 8.87 (s, 1H, NH)

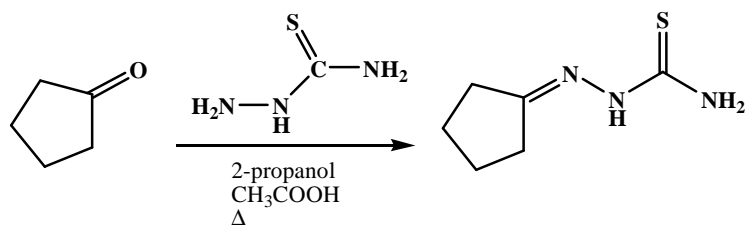
### 1-(3-methylcyclohexylidene)thiosemicarbazide



M.W.: 185.29 g/mol; RF: 0.57 (eluent: ethyl acetate: hexane 20:1); Mp: 108°-110°C; Yield: 65%, Aspect: pale yellow powder .

<sup>1</sup>H-NMR: (500 MHz, CDCl<sub>3</sub>) δH 0.92 (m, 3H, CH<sub>3</sub>), 1.13 (m, 1H, CH<sub>2</sub>, cyclohexyl), 1.35 (m, 1H, CH<sub>2</sub>, cyclohexyl), 1.57 (m, 2H, CH<sub>2</sub>, cyclohexyl), 1.69 (m, 1H, CH<sub>2</sub>, cyclohexyl), 1.81 (m, 2H, CH<sub>2</sub>, cyclohexyl), 2.28 (m, 1H, CH<sub>2</sub>, cyclohexyl), 2.91 (m, 1H, CH<sub>2</sub>, cyclohexyl), 7.48 (s, 1H, NH<sub>2</sub>), 7.93 (s, 1H, NH<sub>2</sub>), 10.13 7.48 (s, 1H, NH)

**1-cyclopentylidenethiosemicarbazide**



M.W.: 157.24 g/mol; RF: 0.60 (DCM-ethyl acetate-hexane 10:10:1); Mp: 151°-153°C; Yield: 80%, Aspect: light yellow powder .

<sup>1</sup>H-NMR: (500 MHz, CDCl<sub>3</sub>) δH 1.73 (m, 2H, *J*: 9, *J*: 17.5, CH<sub>2</sub>, cyclopropyl), 1.84 (m, 2H, *J*: 9, *J*: 17.5, CH<sub>2</sub>, cyclopropyl), 2.25 (t, 2H, *J*: 9, *J*: 9.5, CH<sub>2</sub>, cyclopropyl), 2.35 (t, 2H, *J*: 9, *J*: 9.5, CH<sub>2</sub>, cyclopropyl), 6.42 (br.s, 1H, NH<sub>2</sub>), 7.13 (br.s, 1H, NH<sub>2</sub>), 8.42 6.42 (br.s, 1H, NH)

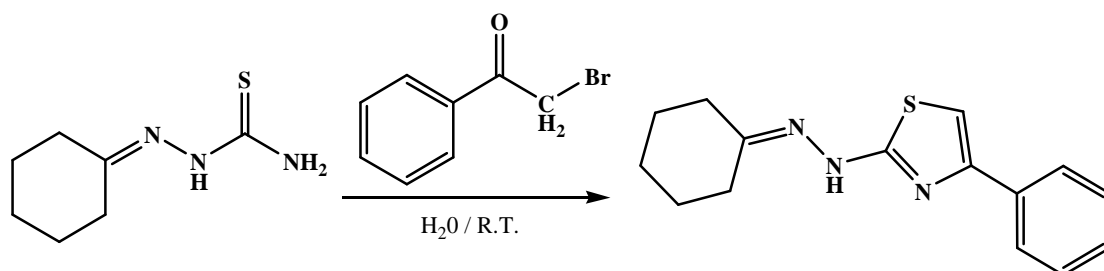
### General method for the synthesis of compound EMAC 2097-2142

Equimolar amounts of cycloalkylthiosemicarbazone and  $\alpha$ -halogen keton are reacted at RT in water or 2-propanol. The mixture was stirring for a period ranging between 24-32 hours and, a forming product was formed. The mixture was stopped and the solid filtered. The product was washed with ethyl ether and crystallised from ethanol, water/ethanol; acetonitrile or hexane.

According to this method, the following listed compounds have been synthesised.

#### EMAC 2097

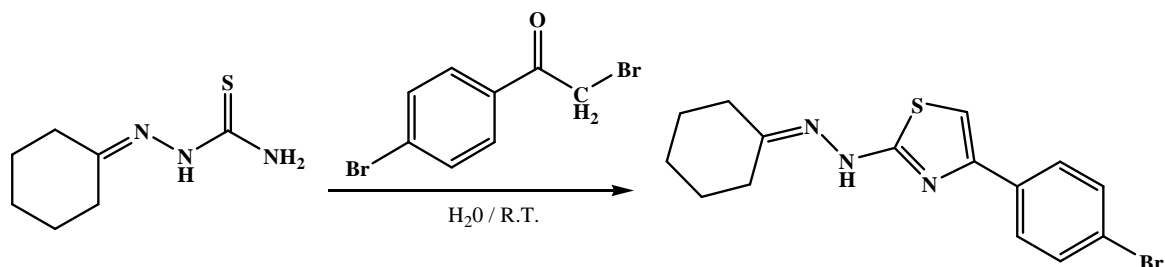
##### 1-cyclohexylidene-2-(4-phenylthiazol-2-yl)hydrazine



<sup>1</sup>H-NMR: (500 MHz, CDCl<sub>3</sub>)  $\delta$ H 1.67 (m, 2H, CH<sub>2</sub>, cyclohexyl), 1.78 (m, 4H, CH<sub>2</sub>, cyclohexyl), 2.40 (t, 2H, *J*: 6.3, CH<sub>2</sub>, cyclohexyl), 2.64 (t, 2H, *J*: 6.5, CH<sub>2</sub>, cyclohexyl), 6.68 (s, 1H, CH, thiazole), 7.48 (m, 3H, CH, Phenyl), 7.72 (m, 2H, CH, Phenyl), 12.51 (br.s, 1H, NH, D<sub>2</sub>O exch.)

#### EMAC 2098

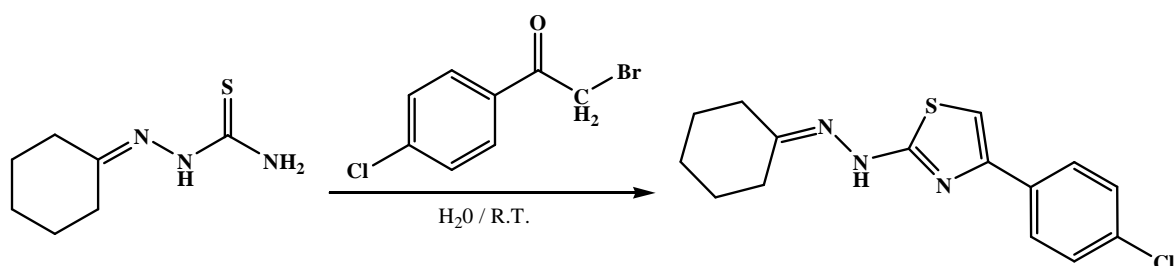
##### 1-(4-(4-bromophenyl)thiazol-2-yl)-2-cyclohexylidenehydrazine



$^1\text{H-NMR}$ : (500 MHz,  $\text{CDCl}_3$ )  $\delta\text{H}$  1.67 (m, 2H,  $\text{CH}_2$ , cyclohexyl), 1.78 (m, 4H,  $\text{CH}_2$ , cyclohexyl), 2.40 (t, 2H,  $J$ : 6.3,  $\text{CH}_2$ , cyclohexyl), 2.63 (t, 2H,  $J$ : 6.5,  $\text{CH}_2$ , cyclohexyl), 6.69 (s, 1H, CH, thiazole), 7.60 (m, 4H, CH, Phenyl), 12.45 (br.s, 1H, NH,  $\text{D}_2\text{O}$  exch.)

**EMAC 2099**

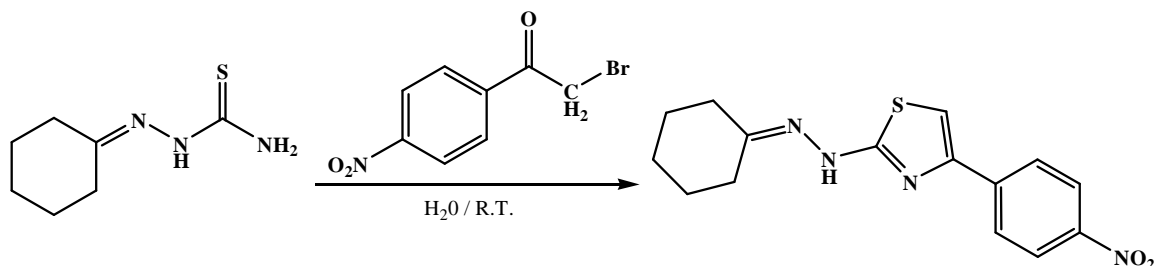
**1-(4-(4-chlorophenyl)thiazol-2-yl)-2-cyclohexylidenehydrazine**



$^1\text{H-NMR}$ : (500 MHz,  $\text{CDCl}_3$ )  $\delta\text{H}$  1.67 (m, 2H,  $\text{CH}_2$ , cyclohexyl), 1.72 (m, 4H,  $\text{CH}_2$ , cyclohexyl), 2.37 (m, 4H,  $\text{CH}_2$ , cyclohexyl), 6.79 (s, 1H, CH, thiazole), 7.36 (d, 2H,  $J$ : 8.5, CH, Phenyl), 7.70 (d, 2H,  $J$ : 8.5, CH, Phenyl), 12.55 (br.s, 1H, NH,  $\text{D}_2\text{O}$  exch.)

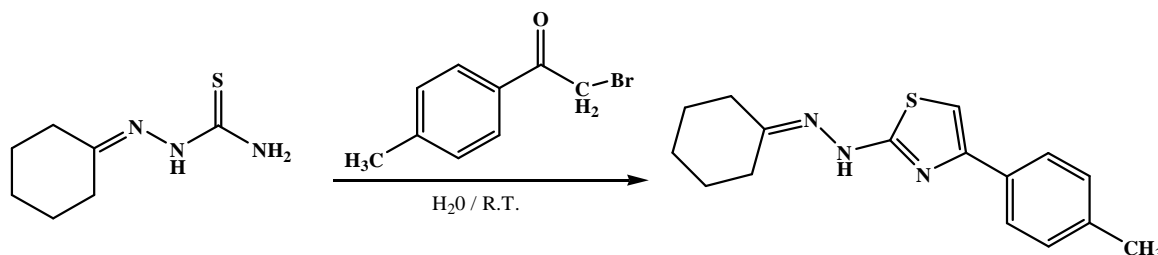
**EMAC 2100**

**1-(4-(4-nitrophenyl)thiazol-2-yl)-2-cyclohexylidenehydrazine**

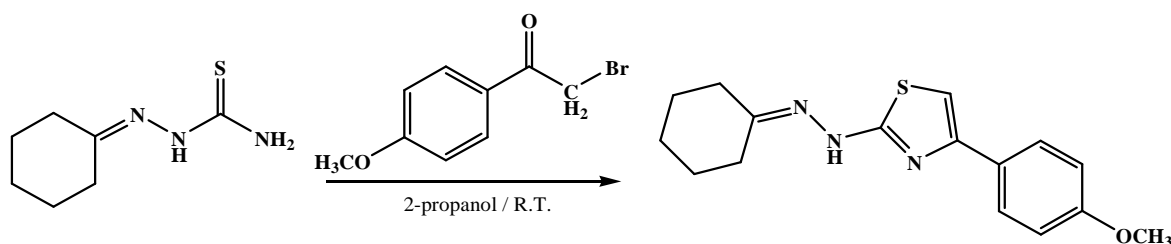


$^1\text{H-NMR}$ : (500 MHz,  $\text{CDCl}_3$ )  $\delta\text{H}$  1.70 (m, 6H,  $\text{CH}_2$ , cyclohexyl), 2.31 (m, 2H,  $\text{CH}_2$ , cyclohexyl), 2.38 (m, 2H,  $\text{CH}_2$ , cyclohexyl), 7.07 (s, 1H, CH, thiazole), 7.93 (d, 2H,  $J$ : 9.0, CH, Phenyl), 8.24 (d, 2H,  $J$ : 8.9, CH, Phenyl), 8.40 (s, 1H, NH,  $\text{D}_2\text{O}$  exch)

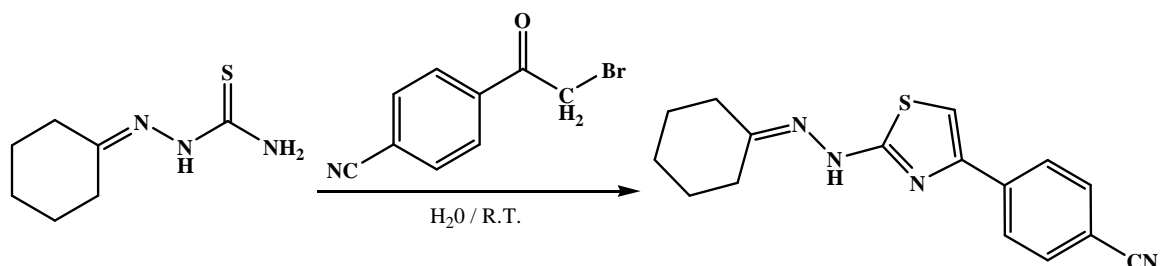


**EMAC 2101****1-(4-(4-methylphenyl)thiazol-2-yl)-2-cyclohexylidenehydrazine**

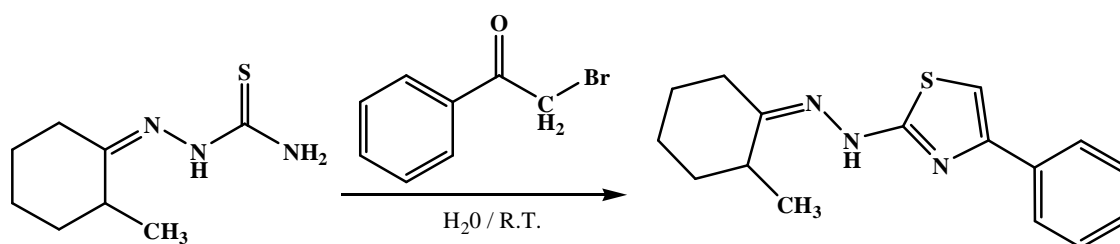
<sup>1</sup>H-NMR: (500 MHz, CDCl<sub>3</sub>) δH 1.67 (m, 2H, CH<sub>2</sub>, cyclohexyl), 1.78 (m, 4H, CH<sub>2</sub>, cyclohexyl), 2.39 (m, 5H, CH<sub>2</sub>, cyclohexyl + CH<sub>3</sub>), 2.64 (m, 2H, CH<sub>2</sub>, cyclohexyl), 6.60 (s, 1H, CH, thiazole), 7.28 (d, 2H, *J*: 7.8, CH, Phenyl), 7.60 (d, 2H, *J*: 8.2, CH, Phenyl), 12.49 (br.s, 1H, NH, D<sub>2</sub>O exch)

**EMAC 2102****1-(4-(4-methoxyphenyl)thiazol-2-yl)-2-cyclohexylidenehydrazine**

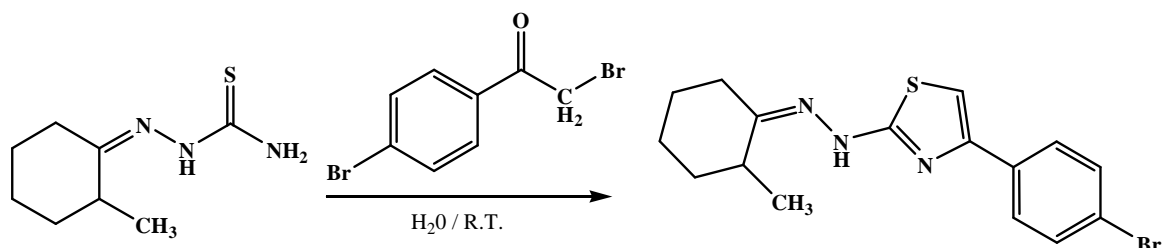
<sup>1</sup>H-NMR: (500 MHz, CDCl<sub>3</sub>) δH 1.67 (m, 2H, CH<sub>2</sub>, cyclohexyl), 1.77 (m, 4H, CH<sub>2</sub>, cyclohexyl), 2.39 (t, 2H, *J*: 6.3, CH<sub>2</sub>, cyclohexyl), 2.63 (t, 2H, *J*: 6.5, CH<sub>2</sub>, cyclohexyl), 3.85 (s, 3H, OCH<sub>3</sub>), 6.50 (s, 1H, CH, thiazole), 6.99 (d, 2H, *J*: 8.8, CH, Phenyl), 7.65 (d, 2H, *J*: 8.8, CH, Phenyl), 12.40 (br.s, 1H, NH)

**EMAC 2103****1-(4-(4-cyanophenyl)thiazol-2-yl)-2-cyclohexylidenehydrazine**

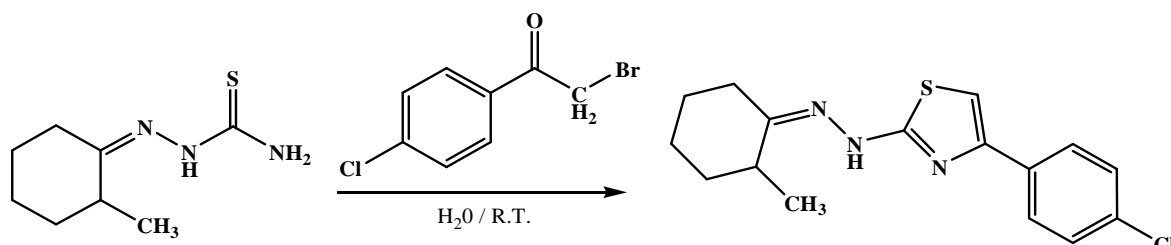
<sup>1</sup>H-NMR: (500 MHz, CDCl<sub>3</sub>) δH 1.65 (m, 4H, CH<sub>2</sub>, cyclohexyl), 1.74 (m, 2H, CH<sub>2</sub>, cyclohexyl), 2.28 (m, 2H, CH<sub>2</sub>, cyclohexyl), 2.37 (m, 2H, CH<sub>2</sub>, cyclohexyl), 7.00 (s, 1H, CH, thiazole), 7.65 (d, 2H, *J*: 8.3, CH, Phenyl), 7.87 (d, 2H, *J*: 8.4, CH, Phenyl), 8.54 (s, 1H, NH)

**EMAC 2104****1-(2-methylcyclohexylidene)-2-(4-phenylthiazol-2-yl)hydrazine**

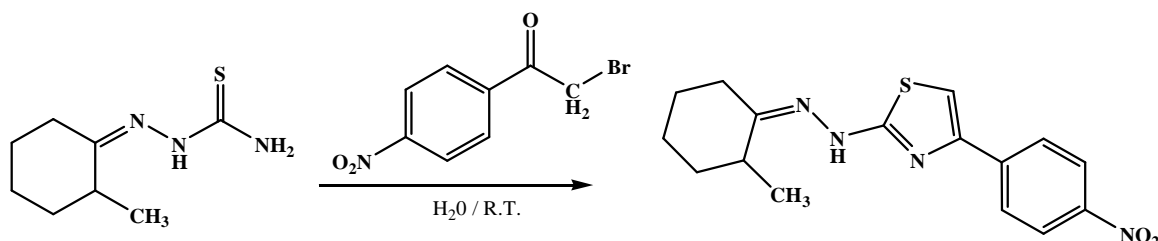
<sup>1</sup>H-NMR: (500 MHz, CDCl<sub>3</sub>) δH 1.19 (s, 3H, CH<sub>3</sub>), 1.33 (m, 1H, CH, cyclohexyl), 1.51 (m, 2H, CH<sub>2</sub>, cyclohexyl), 1.79 (m, 1H, CH, cyclohexyl), 1.86 (m, 1H, CH, cyclohexyl), 1.95 (m, 2H, CH<sub>2</sub>, cyclohexyl), 2.37 (m, 1H, CH, cyclohexyl), 2.60 (m, 1H, CH, cyclohexyl), 6.84 (s, 1H, CH, thiazole), 7.29 (m, 1H, CH, Phenyl), 7.38 (d, 2H, *J*: 7.7, CH, Phenyl), 7.79 (d, 2H, *J*: 6.6, CH, Phenyl), 8.44 (br.s, 1H, NH)

**EMAC 2105****1-(4-(4-bromophenyl)thiazol-2-yl)-2-(2-methylcyclohexylidene)hydrazine**

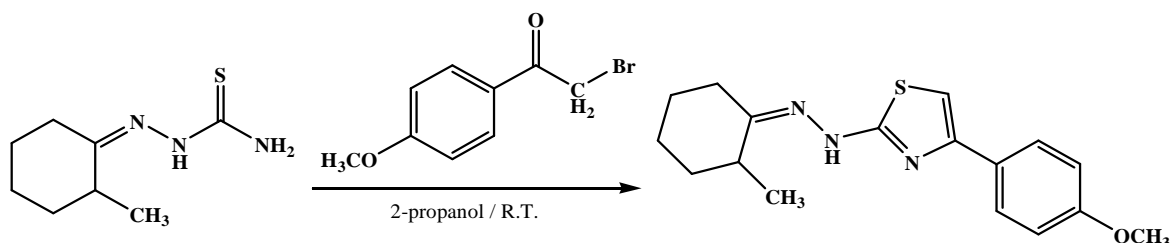
<sup>1</sup>H-NMR: (500 MHz, CDCl<sub>3</sub>) δH 1.18 (s, 3H, CH<sub>3</sub>), 1.32 (m, 1H, CH, cyclohexyl), 1.51 (m, 2H, CH<sub>2</sub>, cyclohexyl), 1.90 (m, 4H, CH<sub>2</sub>, cyclohexyl), 2.37 (m, 1H, CH, cyclohexyl), 2.58 (m, 1H, CH, cyclohexyl), 6.84 (s, 1H, CH, thiazole), 7.49 (d, 2H, *J*: 8.5, CH, Phenyl), 7.66 (d, 2H, *J*: 8.5, CH, Phenyl), 8.46 (br.s, 1H, NH, D<sub>2</sub>O exch.)

**EMAC 2106****1-(4-(4-chlorophenyl)thiazol-2-yl)-2-(2-methylcyclohexylidene)hydrazine**

<sup>1</sup>H-NMR: (500 MHz, CDCl<sub>3</sub>) δH 1.17 (s, 3H, CH<sub>3</sub>), 1.32 (m, 1H, CH, cyclohexyl), 1.54 (m, 2H, CH<sub>2</sub>, cyclohexyl), 1.80 (m, 1H, CH, cyclohexyl), 1.89 (m, 1H, CH, cyclohexyl), 1.99 (m, 2H, CH<sub>2</sub>, cyclohexyl), 2.39 (m, 1H, CH, cyclohexyl), 2.70 (m, 1H, CH, cyclohexyl), 6.79 (s, 1H, CH, thiazole), 7.37 (d, 2H, *J*: 8.5 CH, Phenyl), 7.70 (d, 2H, *J*: 8.5 CH, Phenyl), NH not detected

**EMAC 2107****1-(2-methylcyclohexylidene)-2-(4-(4-nitrophenyl)thiazol-2-yl)hydrazine**

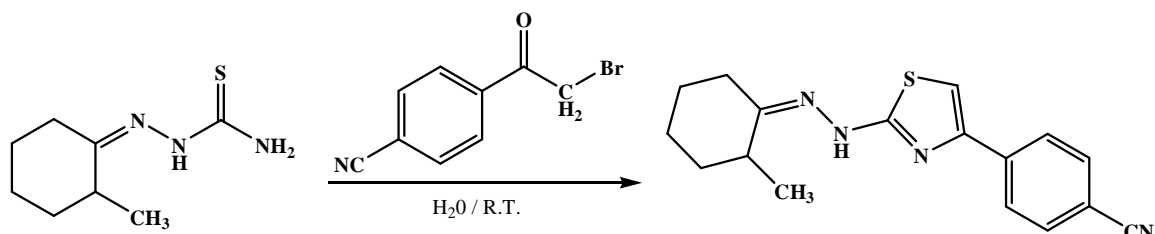
<sup>1</sup>H-NMR: (500 MHz, CDCl<sub>3</sub>) δH 1.19 (s, 3H, CH<sub>3</sub>), 1.33 (m, 1H, CH, cyclohexyl), 1.55 (m, 2H, CH<sub>2</sub>, cyclohexyl), 1.81 (m, 1H, CH, cyclohexyl), 1.91 (m, 1H, CH, cyclohexyl), 1.98 (m, 2H, CH<sub>2</sub>, cyclohexyl), 2.39 (m, 1H, CH, cyclohexyl), 2.62 (m, 1H, CH, cyclohexyl), 7.07 (s, 1H, CH, thiazole), 7.94 (d, 2H, *J*: 8.9, CH, Phenyl), 8.24 (d, 2H, *J*: 8.9, CH, Phenyl), 8.41 (br.s, 1H, NH)

**EMAC 2108****1-(4-(4-methoxyphenyl)thiazol-2-yl)-2-(2-methylcyclohexylidene)hydrazine**

<sup>1</sup>H-NMR: (500 MHz, CDCl<sub>3</sub>) δH 1.16 (s, 3H, CH<sub>3</sub>), 1.34 (m, 1H, CH, cyclohexyl), 1.55 (m, 2H, CH<sub>2</sub>, cyclohexyl), 1.80 (m, 1H, CH, cyclohexyl), 1.98 (m, 2H, CH<sub>2</sub>, cyclohexyl), 2.19 (m, 1H, CH, cyclohexyl), 2.44 (m, 1H, CH, cyclohexyl), 3.02 (m, 1H, CH, cyclohexyl), 3.85 (s, 3H, OCH<sub>3</sub>), 6.50 (s, 1H, CH, thiazole), 6.99 (d, 2H, *J*: 8.4, CH, phenyl), 7.66 (d, 2H, *J*: 8.4, CH, phenyl), 12.46 (s, 1H, NH)

### EMAC 2109

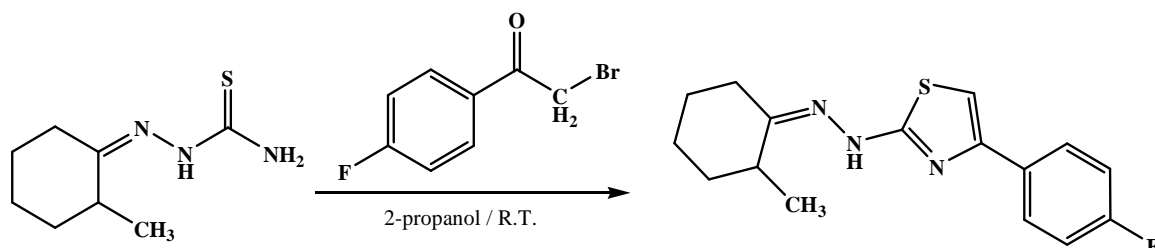
#### 1-(4-(4-cyanophenyl)thiazol-2-yl)-2-(2-methylcyclohexylidene)hydrazine



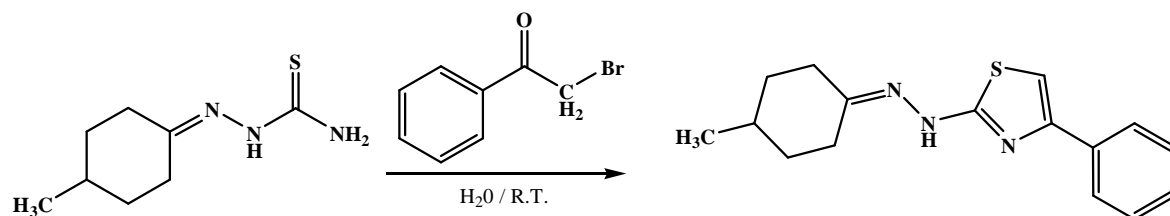
<sup>1</sup>H-NMR: (500 MHz, CDCl<sub>3</sub>) δH 1.18 (s, 3H, CH<sub>3</sub>), 1.29 (m, 1H, CH, cyclohexyl), 1.52 (m, 2H, CH<sub>2</sub>, cyclohexyl), 1.88 (m, 4H, CH<sub>2</sub>, cyclohexyl), 2.37 (m, 1H, CH, cyclohexyl), 2.60 (m, 1H, CH, cyclohexyl), 7.00 (s, 1H, CH, thiazole), 7.65 (d, 2H, *J*: 8.3, CH, phenyl), 7.88 (d, 2H, *J*: 8.3, CH, phenyl), 8.50 (br.s, 1H, NH)

### EMAC 2110

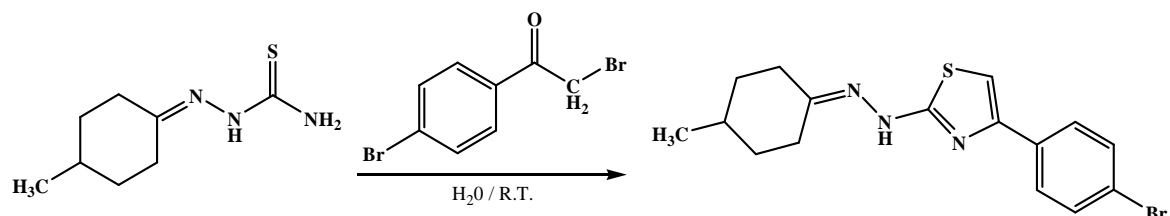
#### 1-(4-(4-fluorophenyl)thiazol-2-yl)-2-(2-methylcyclohexylidene)hydrazine



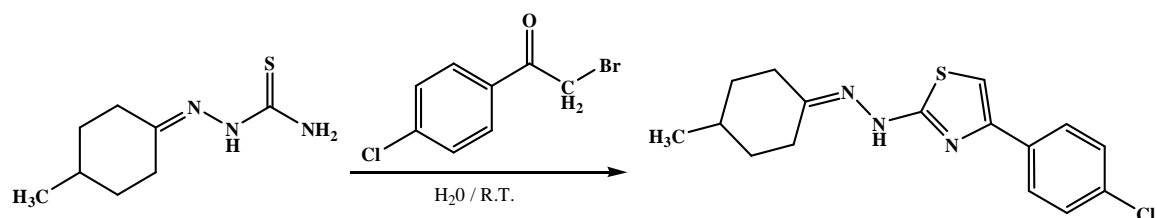
<sup>1</sup>H-NMR: (500 MHz, CDCl<sub>3</sub>) δH 1.16 (s, 3H, CH<sub>3</sub>), 1.35 (m, 1H, CH, cyclohexyl), 1.58 (m, 2H, CH<sub>2</sub>, cyclohexyl), 1.81 (m, 1H, CH, cyclohexyl), 1.99 (m, 2H, CH<sub>2</sub>, cyclohexyl), 2.20 (m, 1H, CH, cyclohexyl), 2.44 (m, 1H, CH, cyclohexyl), 3.01 (m, 1H, CH, cyclohexyl), 6.62 (s, 1H, CH, thiazole), 7.18 (m, 2H, CH, phenyl), 7.72 (dd, 2H, *J*: 4.9, *J*: 8.8, CH, phenyl), 12.45 (br.s, 1H, NH)

**EMAC 2111****1-(4-methylcyclohexylidene)-2-(4-phenylthiazol-2-yl)hydrazine**

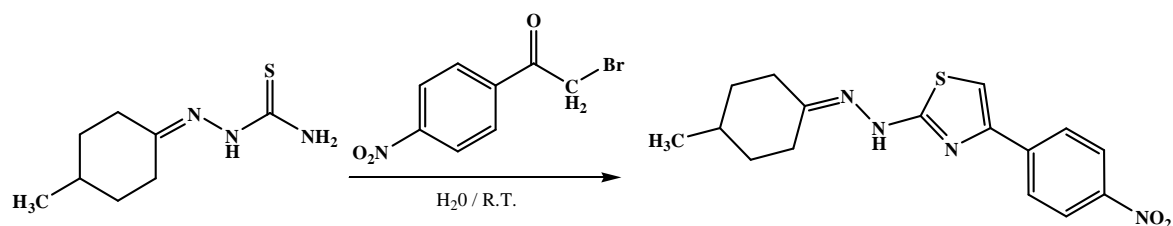
<sup>1</sup>H-NMR: (500 MHz, CDCl<sub>3</sub>) δH 0.92 (d, 3H, *J*: 6.5, CH<sub>3</sub>), 1.04 (m, 1H, CH<sub>2</sub>, cyclohexyl), 1.21 (m, 1H, CH<sub>2</sub>, cyclohexyl), 1.63 (m, 1H, CH<sub>2</sub>, cyclohexyl), 1.77 (m, 1H, CH<sub>2</sub>, cyclohexyl), 1.85 (m, 2H, CH<sub>2</sub>, cyclohexyl), 2.21 (m, 1H, CH<sub>2</sub>, cyclohexyl), 2.51 (m, 1H, CH<sub>2</sub>, cyclohexyl), 2.63 (m, 1H, CH<sub>2</sub>, cyclohexyl), 6.81 (s, 1H, thiazole), 7.27 (t, 1H, *J*: 7.5, Ar-CH), 7.36 (t, 2H, *J*: 7.5, Ar-CH), 7.75 (d, 2H, *J*: 7.5, Ar-CH), 12,22 (s, 1H, NH, D<sub>2</sub>O exch.)

**EMAC 2112****1-(4-(4-bromophenyl)thiazol-2-yl)-2-(4-methylcyclohexylidene)hydrazine**

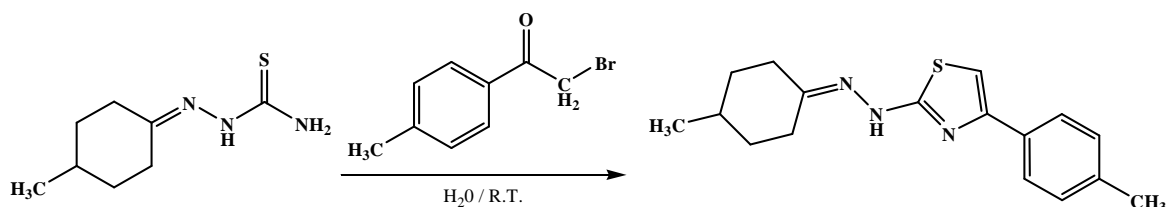
<sup>1</sup>H-NMR: (500 MHz, CDCl<sub>3</sub>) δH 0.97 (d, 3H, *J*: 7, CH<sub>3</sub>), 1.20 (m, 2H, CH<sub>2</sub>, cyclohexyl), 1.70 (m, 1H, CH<sub>2</sub>, cyclohexyl), 1.90 (m, 2H, CH<sub>2</sub>, cyclohexyl), 2.00 (m, 1H, CH<sub>2</sub>, cyclohexyl), 2.26 (m, 1H, CH<sub>2</sub>, cyclohexyl), 2.54 (m, 1H, CH<sub>2</sub>, cyclohexyl), 2.79 (m, 1H, CH<sub>2</sub>, cyclohexyl), 6.78 (s, 1H, thiazol), 7.53 (d, 2H, *J*: 8.5, Ar-CH), 7.63 (d, 2H, *J*: 8.5, Ar-CH), NH not detected

**EMAC 2113****1-(4-(4-chlorophenyl)thiazol-2-yl)-2-(4-methylcyclohexylidene)hydrazine**

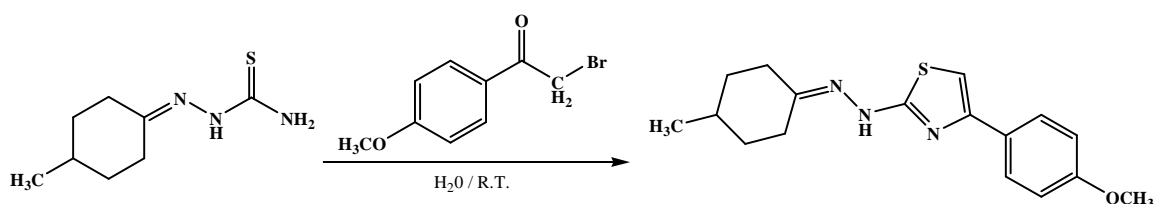
<sup>1</sup>H-NMR: (500 MHz, CDCl<sub>3</sub>) δH 0.98 (d, 3H, J: 6.5, CH<sub>3</sub>), 1.23 (m, 2H, CH<sub>2</sub>, cyclohexyl), 1.72 (m, 1H, CH<sub>2</sub>, cyclohexyl), 1.94 (m, 2H, CH<sub>2</sub>, cyclohexyl), 2.09 (m, 1H, CH<sub>2</sub>, cyclohexyl), 2.78 (m, 1H, CH<sub>2</sub>, cyclohexyl), 2.54 (m, 1H, CH<sub>2</sub>, cyclohexyl), 2.93 (m, 1H, CH<sub>2</sub>, cyclohexyl), 6.73 (s, 1H, thiazole), 7.41 (d, 2H, J: 8.5, Ar-CH), 7.67 (d, 2H, J: 8.5, Ar-CH),

**EMAC 2114****1-(4-(4-nitrophenyl)thiazol-2-yl)-2-(4-methylcyclohexylidene)hydrazine**

<sup>1</sup>H-NMR: (500 MHz, CDCl<sub>3</sub>) δH 0.97 (d, 3H, J: 6.5, CH<sub>3</sub>), 1.15 (m, 1H, CH<sub>2</sub>, cyclohexyl), 1.25 (m, 1H, CH<sub>2</sub>, cyclohexyl), 1.70 (m, 1H, CH<sub>2</sub>, cyclohexyl), 1.94 (m, 3H, CH<sub>2</sub>, cyclohexyl), 2.26 (m, 1H, CH<sub>2</sub>, cyclohexyl), 2.54 (m, 1H, CH<sub>2</sub>, cyclohexyl), 2.66 (m, 1H, CH<sub>2</sub>, cyclohexyl), 7.06 (s, 1H, thiazole), 7.93 (d, 2H, J: 8.5, Ar-CH), 8.24 (d, 2H, J: 8.5, Ar-CH), 8.59 (br.s, 1H, NH)

**EMAC 2115****1-(4-methylcyclohexylidene)-2-(4-p-tolylthiazol-2-yl)hydrazine**

<sup>1</sup>H-NMR: (500 MHz, CDCl<sub>3</sub>) δH 0.97 (d, 3H, J: 6.5, CH<sub>3</sub>), 1.21 (m, 2H, CH<sub>2</sub>, cyclohexyl), 1.71 (m, 1H, CH<sub>2</sub>, cyclohexyl), 1.92 (m, 2H, CH<sub>2</sub>, cyclohexyl), 2.05 (m, 1H, CH<sub>2</sub>, cyclohexyl), 2.27 (m, 1H, CH<sub>2</sub>, cyclohexyl), 2.37 (s, 3H, CH<sub>3</sub>), 2.54 (m, 1H, CH<sub>2</sub>, cyclohexyl), 2.90 (m, 1H, CH<sub>2</sub>, cyclohexyl), 6.69 (s, 1H, thiazole), 7.23 (d, 2H, J: 8, Ar-CH), 7.63 (d, 2H, J: 8, Ar-CH), 12.52 (br.s, 1H, NH)

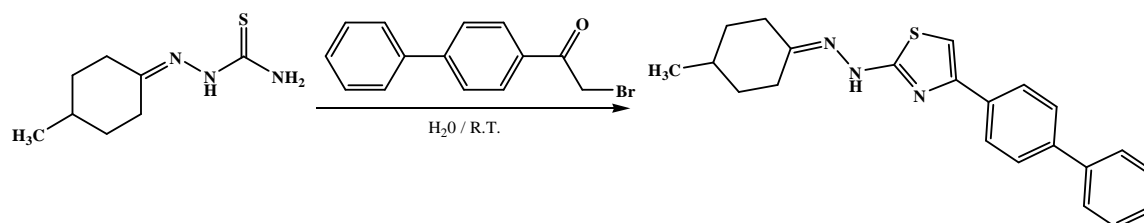
**EMAC 2116****1-(4-(4-methoxyphenyl)thiazol-2-yl)-2-(4-methylcyclohexylidene)hydrazine**

<sup>1</sup>H-NMR: (500 MHz, CDCl<sub>3</sub>) δH 0.94 (d, 3H, J: 6.5, CH<sub>3</sub>), 1.08 (m, 1H, CH<sub>2</sub>, cyclohexyl), 1.23 (m, 1H, CH<sub>2</sub>, cyclohexyl), 1.66 (m, 1H, CH<sub>2</sub>, cyclohexyl), 1.86 (m, 3H, CH<sub>2</sub>, cyclohexyl), 2.23 (m, 1H, CH<sub>2</sub>, cyclohexyl), 2.53 (m, 1H, CH<sub>2</sub>, cyclohexyl), 2.68 (m, 1H, CH<sub>2</sub>, cyclohexyl), 3.83 (s, 3H, OCH<sub>3</sub>), 6.67 (s, 1H, thiazole), 6.92 (d, 2H, J: 9, Ar-CH), 7.69 (d, 2H, J: 9, Ar-CH), NH not detected



### EMAC 2117

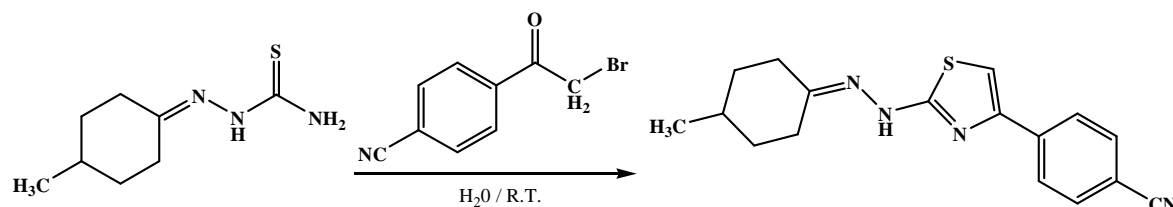
#### **1-(4-(4-biphenyl)thiazol-2-yl)-2-(4-methylcyclohexylidene)hydrazine**



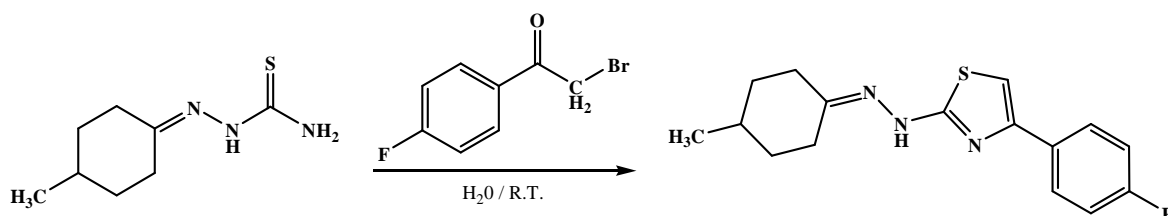
$^1\text{H-NMR}$ : (500 MHz,  $\text{CDCl}_3$ )  $\delta$ H 0.95 (d, 3H,  $J$ : 6.5,  $\text{CH}_3$ ), 1.12 (m, 1H,  $\text{CH}_2$ , cyclohexyl), 1.24 (m, 1H,  $\text{CH}_2$ , cyclohexyl), 1.67 (m, 1H,  $\text{CH}_2$ , cyclohexyl), 1.89 (m, 3H,  $\text{CH}_2$ , cyclohexyl), 2.25 (m, 1H,  $\text{CH}_2$ , cyclohexyl), 2.54 (m, 1H,  $\text{CH}_2$ , cyclohexyl), 2.69 (m, 1H,  $\text{CH}_2$ , cyclohexyl), 6.87 (s, 1H, thiazole), 7.35 (t, 1H,  $J$ : 7, Ar-CH), 7.45 (t, 2H,  $J$ : 7.5, Ar-CH), 7.63 (d, 4H,  $J$ : 8, Ar-CH), 7.85 (d, 2H,  $J$ : 8, Ar-CH), NH not detected

### EMAC 2118

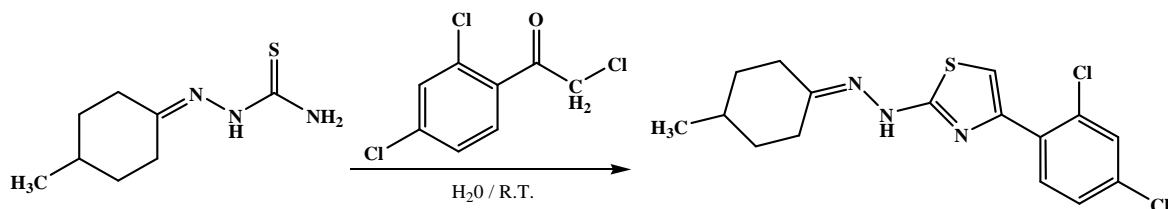
#### **1-(4-(4-cyanophenyl)thiazol-2-yl)-2-(4-methylcyclohexylidene)hydrazine (EMAC 2118)**



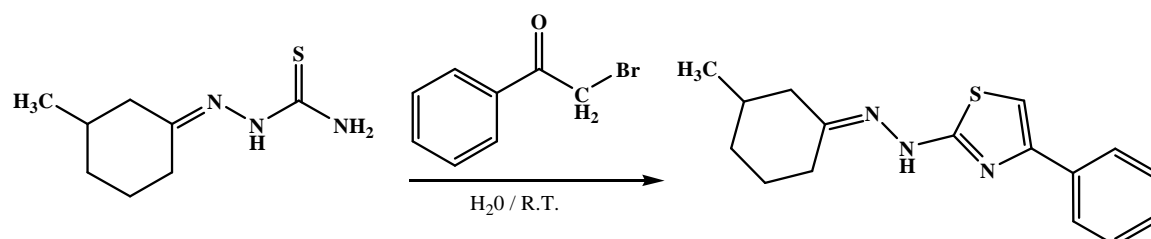
$^1\text{H-NMR}$ : (500 MHz,  $\text{CDCl}_3$ )  $\delta$ H 0.98 (d, 3H,  $J$ : 7,  $\text{CH}_3$ ), 1.23 (m, 2H,  $\text{CH}_2$ , cyclohexyl), 1.73 (m, 1H,  $\text{CH}_2$ , cyclohexyl), 1.95 (m, 2H,  $\text{CH}_2$ , cyclohexyl), 2.09 (m, 1H,  $\text{CH}_2$ , cyclohexyl), 2.28 (m, 1H,  $\text{CH}_2$ , cyclohexyl), 2.55 (m, 1H,  $\text{CH}_2$ , cyclohexyl), 2.89 (m, 1H,  $\text{CH}_2$ , cyclohexyl), 6.92 (s, 1H, thiazole), 7.72 (d, 2H,  $J$ : 8.5, Ar-CH), 7.86 (d, 2H,  $J$ : 8.5, Ar-CH), 12.45 (s, 1H, NH,  $\text{D}_2\text{O}$  exch.)

**EMAC 2119****1-(4-(4-fluorophenyl)thiazol-2-yl)-2-(4-methylcyclohexylidene)hydrazine**

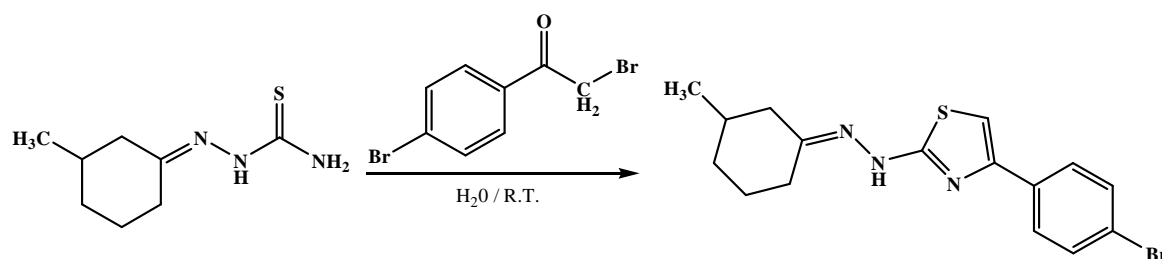
<sup>1</sup>H-NMR: (500 MHz, CDCl<sub>3</sub>) δH 0.98 (d, 3H, J: 7, CH<sub>3</sub>), 1.24 (m, 2H, CH<sub>2</sub>, cyclohexyl), 1.73 (m, 1H, CH<sub>2</sub>, cyclohexyl), 1.96 (m, 2H, CH<sub>2</sub>, cyclohexyl), 2.15 (m, 1H, CH<sub>2</sub>, cyclohexyl), 2.29 (m, 1H, CH<sub>2</sub>, cyclohexyl), 2.55 (m, 1H, CH<sub>2</sub>, cyclohexyl), 3.02 (m, 1H, CH<sub>2</sub>, cyclohexyl), 6.63 (s, 1H, thiazole), 7.17 (d, 2H, J: 8.5, Ar-CH), 7.70 (d, 2H, J: 8.5, Ar-CH), 12.75 (s, 1H, NH, D<sub>2</sub>O exch.)

**EMAC 2120****1-(4-(2,4-dichlorophenyl)thiazol-2-yl)-2-(4-methylcyclohexylidene)hydrazine**

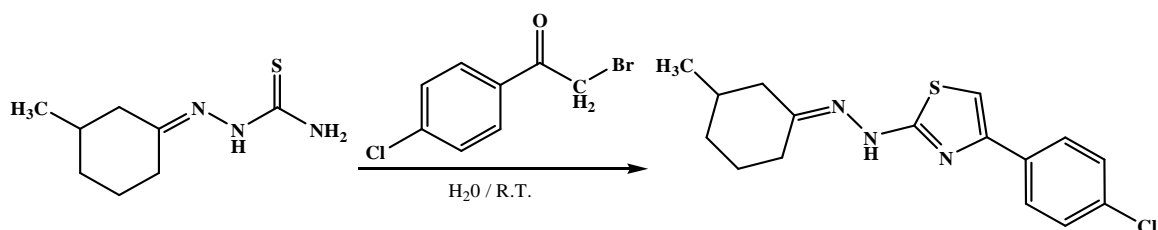
<sup>1</sup>H-NMR: (500 MHz, CDCl<sub>3</sub>) δH 0.97 (s, 3H, CH<sub>3</sub>), 1.24 (m, 2H, CH<sub>2</sub>, cyclohexyl), 1.73 (m, 1H, CH<sub>2</sub>, cyclohexyl), 1.96 (m, 2H, CH<sub>2</sub>, cyclohexyl), 2.17 (m, 1H, CH<sub>2</sub>, cyclohexyl), 2.29 (m, 1H, CH<sub>2</sub>, cyclohexyl), 2.54 (m, 1H, CH<sub>2</sub>, cyclohexyl), 3.04 (m, 1H, CH<sub>2</sub>, cyclohexyl), 6.97 (s, 1H, thiazole), 7.41 (s, 1H, Ar-CH), 7.57 (m, 2H, Ar-CH), 12.86 (s, 1H, NH, D<sub>2</sub>O exch.)

**EMAC2121****1-(3-methylcyclohexylidene)-2-(4-phenylthiazol-2-yl)hydrazine**

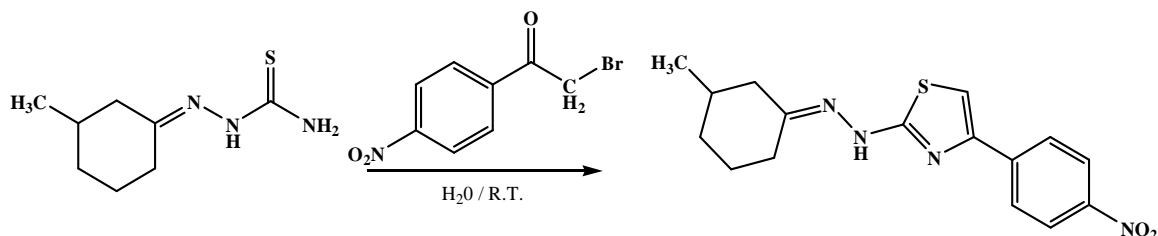
$^1\text{H-NMR}$ : (500 MHz,  $\text{CDCl}_3$ )  $\delta$  0.98 (m, 3H,  $J$ : 6.5,  $J$ : 13,  $\text{CH}_3$ ), 1.17 (m, 1H,  $\text{CH}_2$ , cyclohexyl), 1.56 (m, 2H,  $\text{CH}_2$ , cyclohexyl), 1.85 (m, 3H,  $\text{CH}_2$ , cyclohexyl), 2.15 (m, 1H,  $\text{CH}_2$ , cyclohexyl), 2.51 (m, 1H,  $\text{CH}_2$ , cyclohexyl), 2.64 (m, 1H,  $\text{CH}_2$ , cyclohexyl), 6.82 (d, 1H,  $J$ : 2.5, thiazol), 7.31 (t, 1H,  $J$ : 7.5, Ar-CH), 7.39 (t, 2H,  $J$ : 7.5, Ar-CH), 7.78 (d, 2H,  $J$ : 8,  $J$ : 2.5, Ar-CH), NH not detected

**EMAC 2122****1-(4-(4-bromophenyl)thiazol-2-yl)-2-(3-methylcyclohexylidene)hydrazine**

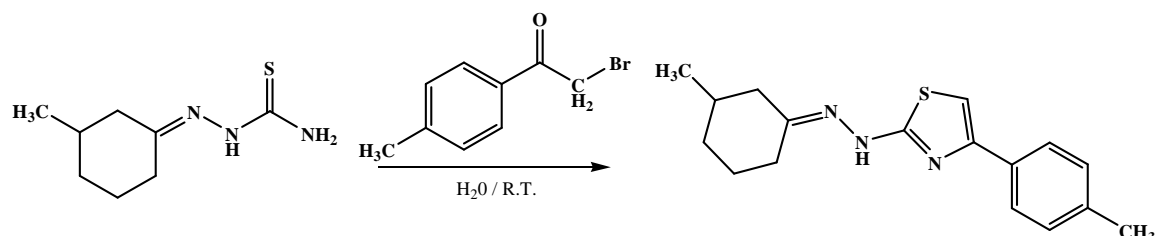
$^1\text{H-NMR}$ : (500 MHz,  $\text{CDCl}_3$ )  $\delta$  1.10 (m, 3H,  $J$ : 6,  $\text{CH}_3$ ), 1.26 (m, 1H,  $\text{CH}_2$ , cyclohexyl), 1.57 (m, 1H,  $\text{CH}_2$ , cyclohexyl), 1.83 (m, 2H,  $\text{CH}_2$ , cyclohexyl), 2.08 (m, 3H,  $\text{CH}_2$ , cyclohexyl), 2.57 (m, 1H,  $\text{CH}_2$ , cyclohexyl), 3.03 (m, 1H,  $\text{CH}_2$ , cyclohexyl), 6.70 (s, 1H, thiazole), 7.59 (d, 2H,  $J$ : 8.5, Ar-CH), 7.63 (d, 2H,  $J$ : 8.5, Ar-CH), NH not detected

**EMAC 2123****1-(4-(4-chlorophenyl)thiazol-2-yl)-2-(3-methylcyclohexylidene)hydrazine**

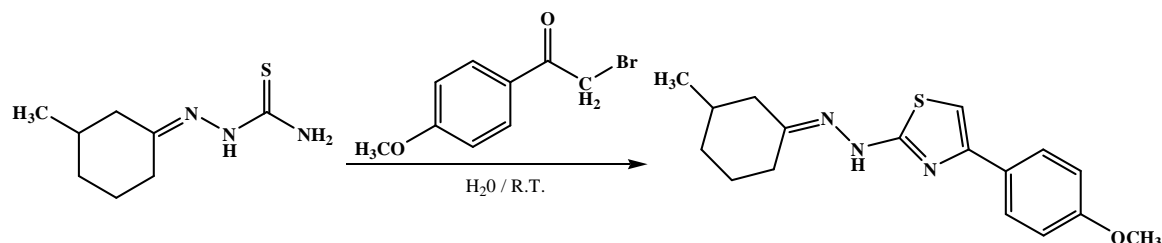
$^1\text{H-NMR}$ : (500 MHz,  $\text{CDCl}_3$ )  $\delta$ H 1.07 (m, 3H,  $J$ : 6.5,  $\text{CH}_3$ ), 1.26 (m, 1H,  $\text{CH}_2$ , cyclohexyl), 1.56 (m, 1H,  $\text{CH}_2$ , cyclohexyl), 1.82 (m, 2H,  $\text{CH}_2$ , cyclohexyl), 2.08 (m, 3H,  $\text{CH}_2$ , cyclohexyl), 2.52 (m, 1H,  $\text{CH}_2$ , cyclohexyl), 3.04 (m, 1H,  $\text{CH}_2$ , cyclohexyl), 6.69 (s, 1H, thiazole), 7.47 (d, 2H,  $J$ : 8.5, Ar-CH), 7.66 (d, 2H,  $J$ : 8.5, Ar-CH), NH not detected

**EMAC 2124****1-(4-(4-nitrophenyl)thiazol-2-yl)-2-(3-methylcyclohexylidene)hydrazine**

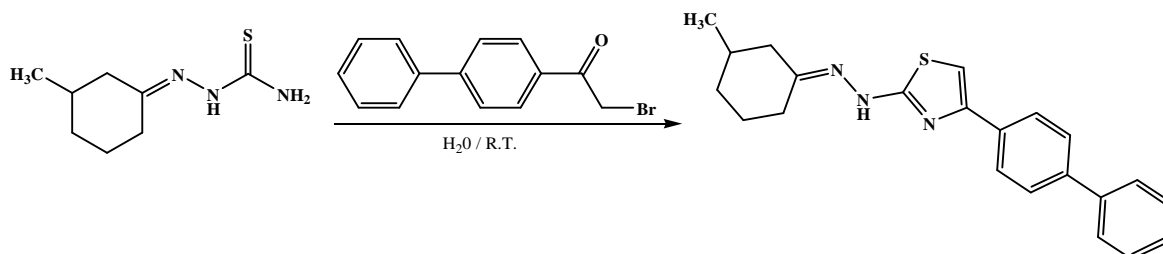
$^1\text{H-NMR}$ : (500 MHz,  $\text{CDCl}_3$ )  $\delta$ H 1.01 (m, 3H,  $J$ : 6,  $\text{CH}_3$ ), 1.21 (m, 1H,  $\text{CH}_2$ , cyclohexyl), 1.56 (m, 1H,  $\text{CH}_2$ , cyclohexyl), 1.64 (m, 2H,  $\text{CH}_2$ , cyclohexyl), 1.82 (m, 1H,  $\text{CH}_2$ , cyclohexyl), 1.93 (m, 1H,  $\text{CH}_2$ , cyclohexyl), 2.18 (m, 1H,  $\text{CH}_2$ , cyclohexyl), 2.49 (m, 1H,  $\text{CH}_2$ , cyclohexyl), 2.61 (m, 1H,  $\text{CH}_2$ , cyclohexyl), 7.07 (s, 1H, thiazole), 7.93 (d, 2H,  $J$ : 8.5, Ar-CH), 8.24 (d, 2H,  $J$ : 8.5, Ar-CH), 8.71 (br.s, 1H, NH)

**EMAC 2125****1-(3-methylcyclohexylidene)-2-(4-p-tolylthiazol-2-yl)hydrazine**

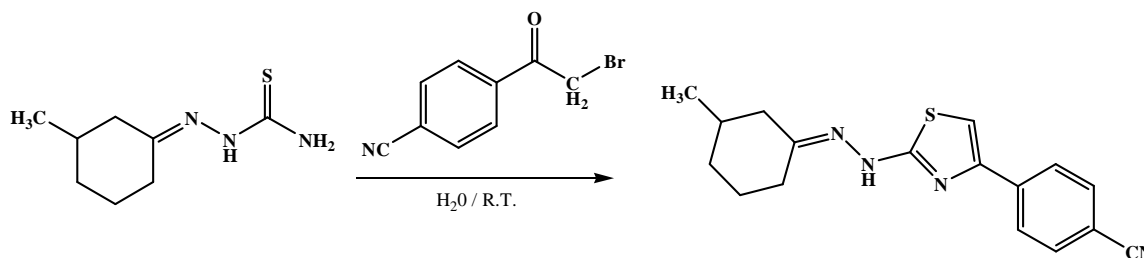
<sup>1</sup>H-NMR: (500 MHz, CDCl<sub>3</sub>) δH 1.05 (m, 3H, *J*: 6, CH<sub>3</sub>), 1.21 (m, 1H, CH<sub>2</sub>, cyclohexyl), 1.53 (m, 1H, CH<sub>2</sub>, cyclohexyl), 1.71 (m, 1H, CH<sub>2</sub>, cyclohexyl), 1.82 (m, 1H, CH<sub>2</sub>, cyclohexyl), 1.91 (m, 1H, CH<sub>2</sub>, cyclohexyl), 2.01 (m, 1H, CH<sub>2</sub>, cyclohexyl), 2.09 (m, 1H, CH<sub>2</sub>, cyclohexyl), 2.38 (s, 3H, CH<sub>3</sub>), 2.53 (m, 1H, CH<sub>2</sub>, cyclohexyl), 2.99 (m, 1H, CH<sub>2</sub>, cyclohexyl), 6.64 (s, 1H, thiazole), 7.26 (d, 2H, *J*: 8, Ar-CH), 7.61 (d, 2H, *J*: 8, Ar-CH), NH not detected

**EMAC 2126****1-(4-(4-methoxyphenyl)thiazol-2-yl)-2-(3-methylcyclohexylidene)hydrazine**

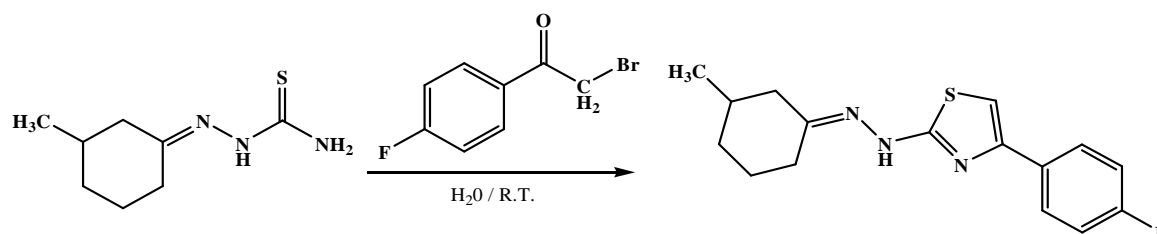
<sup>1</sup>H-NMR: (500 MHz, CDCl<sub>3</sub>) δH 1.08 (m, 3H, *J*: 6.5, CH<sub>3</sub>), 1.23 (m, 1H, CH<sub>2</sub>, cyclohexyl), 1.54 (m, 1H, CH<sub>2</sub>, cyclohexyl), 1.75 (m, 1H, CH<sub>2</sub>, cyclohexyl), 1.83 (m, 1H, CH<sub>2</sub>, cyclohexyl), 1.93 (m, 1H, CH<sub>2</sub>, cyclohexyl), 2.04 (m, 1H, CH<sub>2</sub>, cyclohexyl), 2.12 (m, 1H, CH<sub>2</sub>, cyclohexyl), 2.51 (m, 1H, CH<sub>2</sub>, cyclohexyl), 3.05 (m, 1H, CH<sub>2</sub>, cyclohexyl), 3.85 (s, 3H, OCH<sub>3</sub>), 6.52 (s, 1H, thiazole), 6.69 (d, 2H, *J*: 9, Ar-CH), 7.65 (d, 2H, *J*: 9, Ar-CH), 12.41 (br.s, 1H, NH)

**EMAC 2127****1-(4-(4-phenylphenyl)thiazol-2-yl)-2-(3-methylcyclohexylidene)hydrazine**

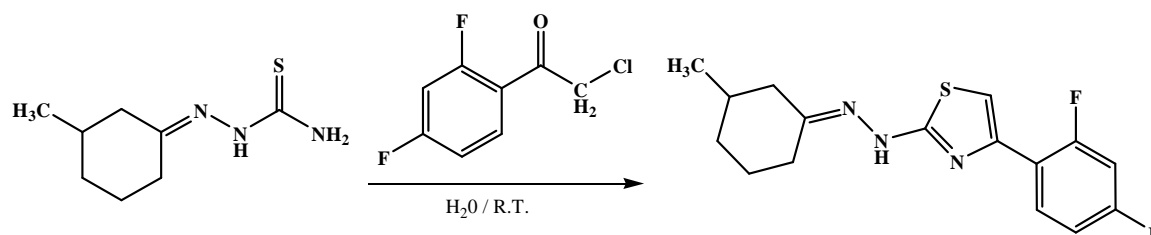
<sup>1</sup>H-NMR: (500 MHz, CDCl<sub>3</sub>) δH 1.00 (m, 3H, *J*: 6.5, CH<sub>3</sub>), 1.15 (m, 1H, CH<sub>2</sub>, cyclohexyl), 1.41 (m, 1H, CH<sub>2</sub>, cyclohexyl), 1.72 (m, 1H, CH<sub>2</sub>, cyclohexyl), 1.78 (m, 1H, CH<sub>2</sub>, cyclohexyl), 1.83 (m, 1H, CH<sub>2</sub>, cyclohexyl), 1.87 (m, 1H, CH<sub>2</sub>, cyclohexyl), 1.88 (m, 1H, CH<sub>2</sub>, cyclohexyl), 2.54 (m, 1H, CH<sub>2</sub>, cyclohexyl), 2.63 (m, 1H, CH<sub>2</sub>, cyclohexyl), 6.88 (s, 1H, thiazole), 7.36 (t, 1H, *J*: 7.5, Ar-CH), 7.45 (t, 2H, *J*: 7.5, Ar-CH), 7.63 (m, 4H, *J*: 7.5, *J*: 8.5, Ar-CH), 7.86 (d, 2H, *J*: 8.5, Ar-CH), 8.97 (br.s, 1H, NH)

**EMAC 2128****1-(4-(4-cyanophenyl)thiazol-2-yl)-2-(3-methylcyclohexylidene)hydrazine**

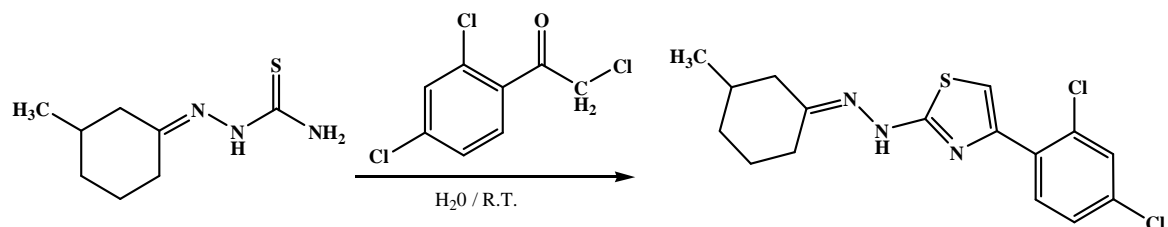
<sup>1</sup>H-NMR: (500 MHz, CDCl<sub>3</sub>) δH 1.02 (m, 3H, *J*: 6.5, CH<sub>3</sub>), 1.20 (m, 1H, CH<sub>2</sub>, cyclohexyl), 1.52 (m, 1H, CH<sub>2</sub>, cyclohexyl), 1.83 (m, 4H, CH<sub>2</sub>, cyclohexyl), 2.18 (m, 1H, CH<sub>2</sub>, cyclohexyl), 2.51 (m, 1H, CH<sub>2</sub>, cyclohexyl), 2.69 (m, 1H, CH<sub>2</sub>, cyclohexyl), 6.97 (s, 1H, thiazole), 7.69 (d, 2H, *J*: 8, Ar-CH), 7.87 (d, 2H, *J*: 8, Ar-CH), NH not detected

**EMAC 2129****1-(4-(4-fluorophenyl)thiazol-2-yl)-2-(3-methylcyclohexylidene)hydrazine**

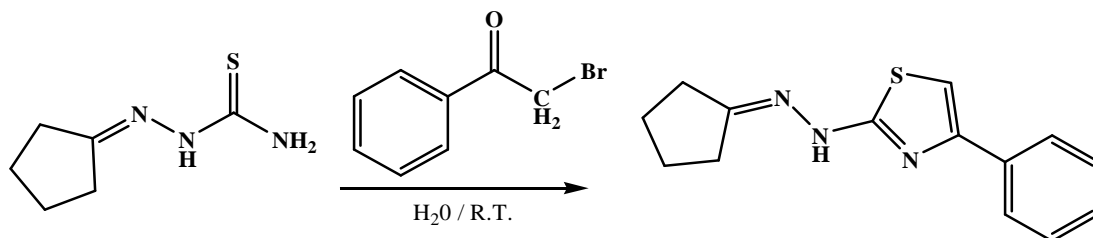
<sup>1</sup>H-NMR: (500 MHz, CDCl<sub>3</sub>) δH 1.05 (m, 3H, J: 6.5, CH<sub>3</sub>), 1.22 (m, 1H, CH<sub>2</sub>, cyclohexyl), 1.52 (m, 1H, CH<sub>2</sub>, cyclohexyl), 1.94 (m, 4H, CH<sub>2</sub>, cyclohexyl), 2.17 (m, 1H, CH<sub>2</sub>, cyclohexyl), 2.50 (m, 1H, CH<sub>2</sub>, cyclohexyl), 3.00 (m, 1H, CH<sub>2</sub>, cyclohexyl), 6.63 (s, 1H, thiazole), 7.16 (m, 2H, J: 8.5, Ar-CH), 7.71 (m, 2H, J: 8.5, Ar-CH), NH not detected

**EMAC 2130****1-(4-(2,4-fluorophenyl)thiazol-2-yl)-2-(3-methylcyclohexylidene)hydrazine**

<sup>1</sup>H-NMR: (500 MHz, CDCl<sub>3</sub>) δH 1.05 (m, 3H, J: 6.5, CH<sub>3</sub>), 1.24 (m, 1H, CH<sub>2</sub>, cyclohexyl), 1.56 (m, 1H, CH<sub>2</sub>, cyclohexyl), 1.77 (m, 1H, CH<sub>2</sub>, cyclohexyl), 1.83 (m, 1H, CH<sub>2</sub>, cyclohexyl), 1.93 (m, 1H, CH<sub>2</sub>, cyclohexyl), 2.11 (m, 2H, CH<sub>2</sub>, cyclohexyl), 2.51 (m, 1H, CH<sub>2</sub>, cyclohexyl), 2.97 (m, 1H, CH<sub>2</sub>, cyclohexyl), 6.94 (s, 1H, thiazole), 6.97 (m, 1H, Ar-CH), 7.07 (m, 1H, J: 8, Ar-CH), 7.88 (m, 1H, J: 8, Ar-CH), 12.69 (br.s, 1H, NH)

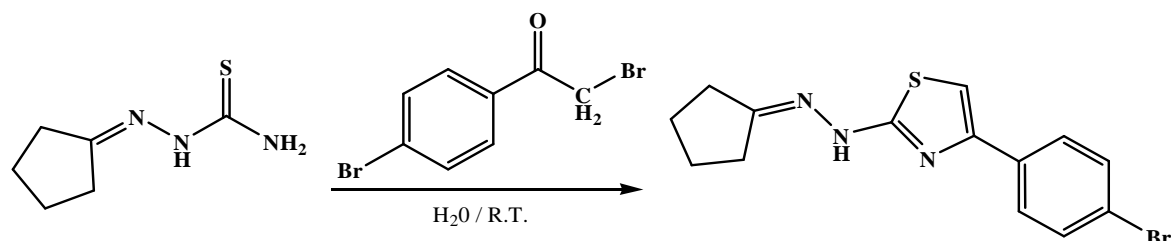
**EMAC 2131****1-(4-(2,4-chlorophenyl)thiazol-2-yl)-2-(3-methylcyclohexylidene)hydrazine**

<sup>1</sup>H-NMR: (500 MHz, CDCl<sub>3</sub>) δH 1.05 (m, 3H, *J*: 6.5, CH<sub>3</sub>), 1.23 (m, 1H, CH<sub>2</sub>, cyclohexyl), 1.54 (m, 1H, CH<sub>2</sub>, cyclohexyl), 1.75 (m, 1H, CH<sub>2</sub>, cyclohexyl), 1.82 (m, 1H, CH<sub>2</sub>, cyclohexyl), 1.92 (m, 1H, CH<sub>2</sub>, cyclohexyl), 1.99 (m, 1H, CH<sub>2</sub>, cyclohexyl), 2.15 (m, 1H, CH<sub>2</sub>, cyclohexyl), 2.50 (m, 1H, CH<sub>2</sub>, cyclohexyl), 2.98 (m, 1H, CH<sub>2</sub>, cyclohexyl), 6.98 (s, 1H, thiazole), 7.41 (d, 1H, *J*: 8.5, *J*: 2; Ar-CH), 7.53 (s, 1H, *J*: 2, Ar-CH), 7.62 (m, 1H, *J*: 8.5, Ar-CH), 12.84 (br.s, 1H, NH)

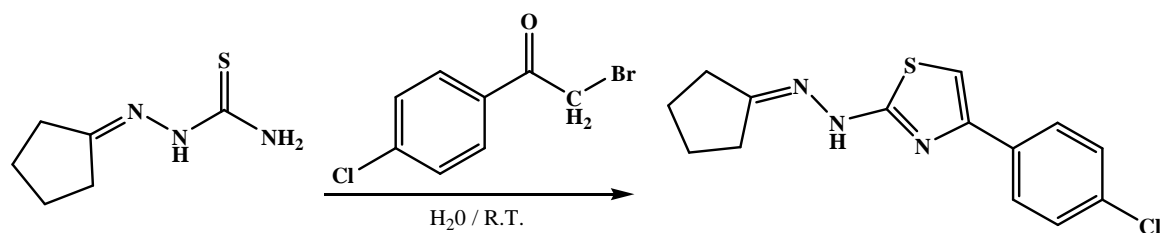
**EMAC 2132****1-cyclopentylidene-2-(4-phenylthiazol-2-yl)hydrazine**

<sup>1</sup>H-NMR: (500 MHz, CDCl<sub>3</sub>) δH 1.78 (m, 2H, *J*: 6.5, *J*: 13.5, CH<sub>2</sub>, cyclopropyl), 1.88 (m, 2H, *J*: 7, *J*: 14, CH<sub>2</sub>, cyclopropyl), 2.28 (t, 2H, *J*: 7.5, *J*: 14.5, CH<sub>2</sub>, cyclopropyl), 2.29 (t, 2H, *J*: 7, *J*: 14.5, CH<sub>2</sub>, cyclopropyl), 6.80 (s, 1H, thiazole), 7.29 (t, 1H, *J*: 7.5, *J*: 1.5 Ar-CH), 7.38 (t, 2H, *J*: 8, *J*: 7.5, *J*: 1.5 Ar-CH), 7.76 (d, 2H, *J*: 8, *J*: 1.5, Ar-CH), NH not detected

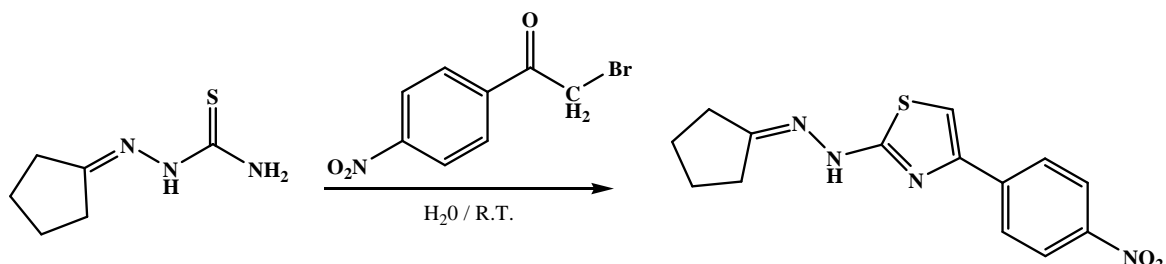


**EMAC 2133****1-(4-(4-bromophenyl)thiazol-2-yl)-2-cyclopentylidenehydrazine**

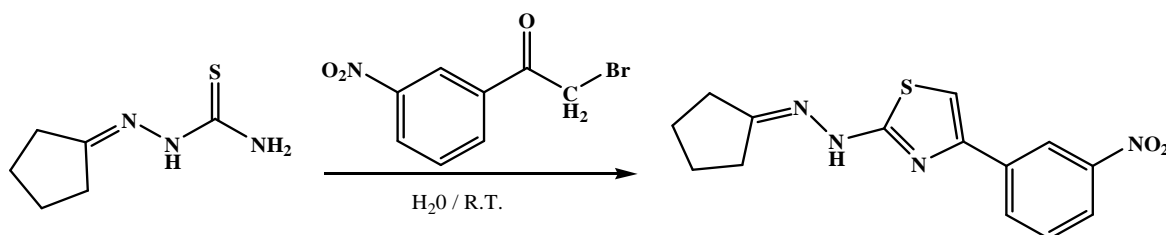
<sup>1</sup>H-NMR: (500 MHz, CDCl<sub>3</sub>) δH 1.83 (m, 2H, *J*: 6.5, *J*: 13.5, CH<sub>2</sub>, cyclopropyl), 1.92 (m, 2H, *J*: 7, *J*: 13.5, CH<sub>2</sub>, cyclopropyl), 2.47 (t, 2H, *J*: 7.5, *J*: 14.5, CH<sub>2</sub>, cyclopropyl), 2.51 (t, 2H, *J*: 7.5, *J*: 14.5, CH<sub>2</sub>, cyclopropyl), 6.76 (s, 1H, thiazole), 7.55 (d, 2H, *J*: 8.5, Ar-CH), 7.61 (t, 2H, *J*: 8, Ar-CH), NH not detected

**EMAC2134****1-(4-(4-chlorophenyl)thiazol-2-yl)-2-cyclopentylidenehydrazine**

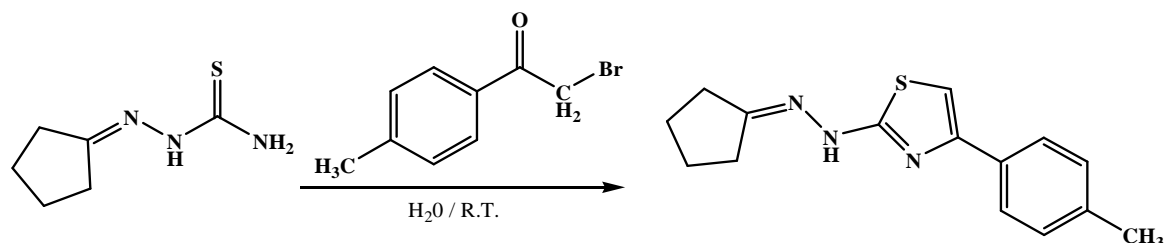
<sup>1</sup>H-NMR: (500 MHz, CDCl<sub>3</sub>) δH 1.82 (m, 2H, *J*: 6.5, *J*: 13.5, CH<sub>2</sub>, cyclopropyl), 1.92 (m, 2H, *J*: 7, *J*: 14, CH<sub>2</sub>, cyclopropyl), 2.47 (t, 2H, *J*: 7.5, *J*: 14.5, CH<sub>2</sub>, cyclopropyl), 2.51 (t, 2H, *J*: 7.5, *J*: 14.5, CH<sub>2</sub>, cyclopropyl), 6.74 (s, 1H, thiazole), 7.40 (d, 2H, *J*: 9, Ar-CH), 7.67 (t, 2H, *J*: 8.5, Ar-CH), NH not detected

**EMAC 2135****1-(4-(4-nitrophenyl)thiazol-2-yl)-2-cyclopentylidenehydrazine (EMAC 2135)**

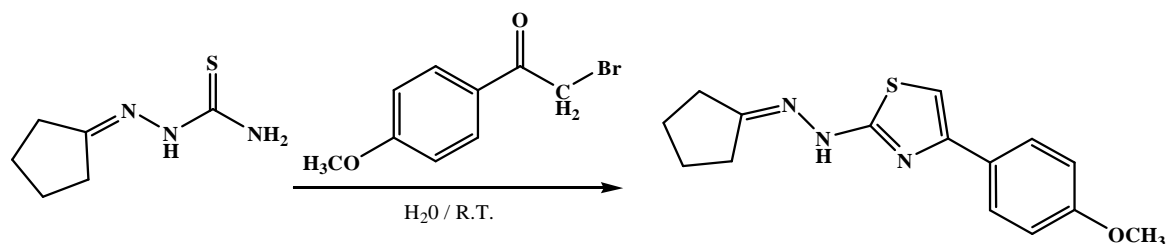
<sup>1</sup>H-NMR: (500 MHz, CDCl<sub>3</sub>) δH 1.81 (m, 2H, *J*: 7, *J*: 14, CH<sub>2</sub>, cyclopropyl), 1.92 (m, 2H, *J*: 7, *J*: 14, CH<sub>2</sub>, cyclopropyl), 2.57 (t, 2H, *J*: 7, *J*: 14, CH<sub>2</sub>, cyclopropyl), 2.50 (t, 2H, *J*: 7, *J*: 14, CH<sub>2</sub>, cyclopropyl), 7.04 (s, 1H, thiazol), 7.92 (d, 2H, *J*: 9, Ar-CH), 8.24 (t, 2H, *J*: 8.5, Ar-CH),

**EMAC 2136****1-(4-(3-nitrophenyl)thiazol-2-yl)-2-cyclopentylidenehydrazine**

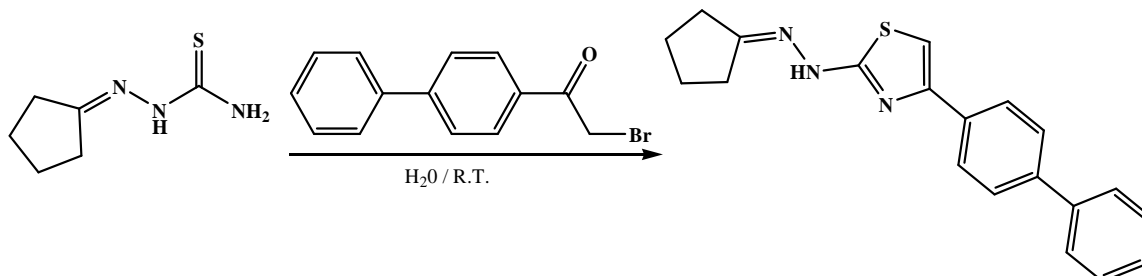
<sup>1</sup>H-NMR: (500 MHz, CDCl<sub>3</sub>) δH 1.82 (m, 2H, *J*: 7, *J*: 13.5, CH<sub>2</sub>, cyclopropyl), 1.92 (m, 2H, *J*: 7, *J*: 14, CH<sub>2</sub>, cyclopropyl), 2.35 (t, 2H, *J*: 7, *J*: 14, CH<sub>2</sub>, cyclopropyl), 2.51 (t, 2H, *J*: 7, *J*: 14, CH<sub>2</sub>, cyclopropyl), 6.98 (s, 1H, thiazole), 7.56 (t, 1H, *J*: 8, Ar-CH), 8.10 (d, 2H, *J*: 7.5, Ar-CH), 8.14 (d, 1H, *J*: 8, Ar-CH), 8.61 (s, 1H, Ar-CH), NH not detected

**EMAC 2137****1-(4-(4-methylphenyl)thiazol-2-yl)-2-cyclopentylidenehydrazine**

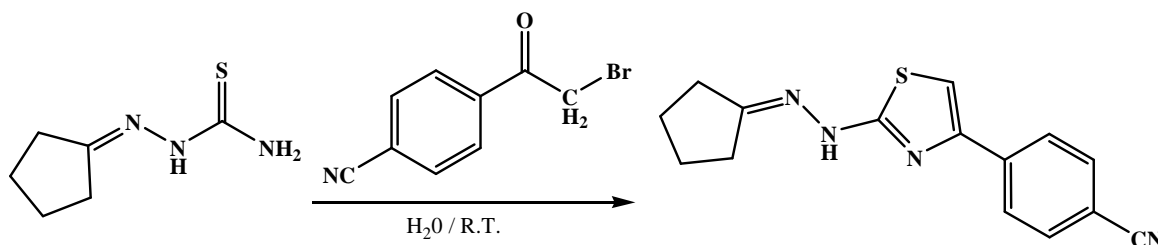
<sup>1</sup>H-NMR: (500 MHz, CDCl<sub>3</sub>) δH 1.84 (m, 2H, *J*: 7, *J*: 14, CH<sub>2</sub>, cyclopropyl), 1.93 (m, 2H, *J*: 7, *J*: 14, CH<sub>2</sub>, cyclopropyl), 2.38 (s, 3H, CH<sub>3</sub>) 2.52 (t, 2H, *J*: 7, *J*: 14, CH<sub>2</sub>, cyclopropyl), 2.56 (t, 2H, *J*: 7, *J*: 14, CH<sub>2</sub>, cyclopropyl), 6.65 (s, 1H, thiazole), 7.26 (d, 2H, *J*: 8, Ar-CH), 7.62 (d, 2H, *J*: 8, Ar-CH), 11.06 (br.s, 1H, NH)

**EMAC 2138****1-(4-(4-methoxyphenyl)thiazol-2-yl)-2-cyclopentylidenehydrazine**

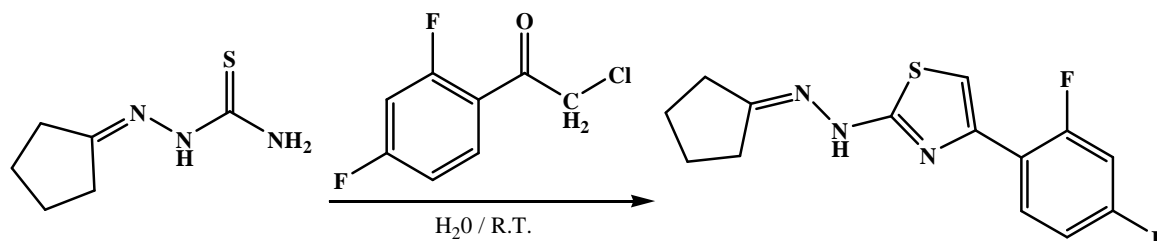
<sup>1</sup>H-NMR: (500 MHz, CDCl<sub>3</sub>) δH 1.83 (m, 2H, *J*: 7, *J*: 14, CH<sub>2</sub>, cyclopropyl), 1.93 (m, 2H, *J*: 7, *J*: 14, CH<sub>2</sub>, cyclopropyl), 2.52 (t, 2H, *J*: 7, *J*: 14, CH<sub>2</sub>, cyclopropyl), 2.57 (t, 2H, *J*: 7, *J*: 14, CH<sub>2</sub>, cyclopropyl), 3.84 (s, 3H, OCH<sub>3</sub>), 6.55 (s, 1H, thiazole), 6.97 (d, 2H, *J*: 8, Ar-CH), 7.66 (d, 2H, *J*: 8, Ar-CH), 11.00 (br.s, 1H, NH)

**EMAC 2139****1-(4-(4-phenylphenyl)thiazol-2-yl)-2-cyclopentylidenehydrazine**

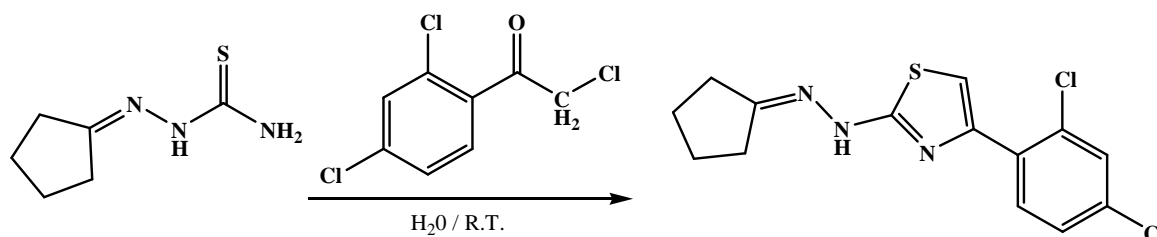
<sup>1</sup>H-NMR: (500 MHz, CDCl<sub>3</sub>) δH 1.83 (m, 2H, *J*: 7, *J*: 14, CH<sub>2</sub>, cyclopropyl), 1.93 (m, 2H, *J*: 7, *J*: 14, CH<sub>2</sub>, cyclopropyl), 2.47 (t, 2H, *J*: 7, *J*: 14, CH<sub>2</sub>, cyclopropyl), 2.52 (t, 2H, *J*: 7, *J*: 14, CH<sub>2</sub>, cyclopropyl), 6.79 (s, 1H, thiazol), 7.37 (t, 1H, *J*: 7, Ar-CH), 7.46 (t, 2H, *J*: 7.5, Ar-CH), 7.62 (d, 2H, *J*: 7, Ar-CH), 7.67 (d, 2H, *J*: 8.5, Ar-CH), 7.83 (d, 2H, *J*: 8, Ar-CH), 9.84 (br.s, 1H, NH)

**EMAC 2140****1-(4-(4-cyanophenyl)thiazol-2-yl)-2-cyclopentylidenehydrazine**

<sup>1</sup>H-NMR: (500 MHz, CDCl<sub>3</sub>) δH 1.80 (m, 2H, *J*: 7, *J*: 14, CH<sub>2</sub>, cyclopropyl), 1.90 (m, 2H, *J*: 7, *J*: 14, CH<sub>2</sub>, cyclopropyl), 2.28 (t, 2H, *J*: 7, *J*: 14, CH<sub>2</sub>, cyclopropyl), 2.50 (t, 2H, *J*: 7, *J*: 14, CH<sub>2</sub>, cyclopropyl), 6.99 (s, 1H, thiazole), 7.66 (d, 2H, *J*: 8, Ar-CH), 7.87 (d, 2H, *J*: 8.5, Ar-CH), NH not detected

**EMAC 2141****1-(4-(2,4-fluorophenyl)thiazol-2-yl)-2-cyclopentylidenehydrazine**

<sup>1</sup>H-NMR: (500 MHz, CDCl<sub>3</sub>) δH 1.85 (m, 2H, *J*: 7, *J*: 14, CH<sub>2</sub>, cyclopropyl), 1.94 (m, 2H, *J*: 7, *J*: 14, CH<sub>2</sub>, cyclopropyl), 2.53 (t, 2H, *J*: 7, *J*: 14, CH<sub>2</sub>, cyclopropyl), 2.62 (t, 2H, *J*: 7, *J*: 14, CH<sub>2</sub>, cyclopropyl), 6.94 (s, 1H, thiazole), 6.97 (m, 1H, *J*<sub>H-F</sub>: 5.5, Ar-CH), 7.06 (m, 1H, *J*: 8.5, *J*: 2.5, Ar-CH), 7.87 (m, 1H, *J*: 8.5, *J*: 2.5, Ar-CH), 12.32 (br.s, 1H, NH)

**EMAC 2142****1-(4-(2,4-chlorophenyl)thiazol-2-yl)-2-cyclopentylidenehydrazine**

<sup>1</sup>H-NMR: (500 MHz, CDCl<sub>3</sub>) δH 1.85 (m, 2H, *J*: 7, *J*: 14, CH<sub>2</sub>, cyclopropyl), 1.93 (m, 2H, *J*: 7, *J*: 14, CH<sub>2</sub>, cyclopropyl), 2.53 (t, 2H, *J*: 7, *J*: 14, CH<sub>2</sub>, cyclopropyl), 2.63 (t, 2H, *J*: 7, *J*: 14, CH<sub>2</sub>, cyclopropyl), 6.98 (s, 1H, thiazol), 7.41 (d, 1H, *J*: 8.5, *J*: 1.5, Ar-CH), 7.63 (s, 1H, *J*: 1.5, Ar-CH), 7.63 (d, 1H, *J*: 8, Ar-CH), 12.62 (br.s, 1H, NH)

## **5.2 Microbiology**

### **5.2.1 Antifungal agents**

EMAC 2097-2142 (Figure 1-5) belongs to a series of isothiosemicarbazone cyclic analogues they are obtained by the reaction of equimolar amounts of cycloalkylthiosemicarbazone and  $\alpha$ -halogenoketone in water or 2-propanol. A foaming product is formed which is filtered. The obtained solid is crystallized from water/ethanol. Amphotericin B was purchased from Sigma Chemicals Co. (St Louis, MO, USA). Fluconazole was obtained from a commercially available iv formulation (Diflucanw, Pfizer Italia S.p.A.) at 200 mg/100 mL in saline. EMAC compounds and amphotericin B were dissolved in dimethyl sulphoxide at 10 mg/mL, for antifungal susceptibility studies, and stored at 20°C. The working solution were prepared in the same medium employed for the tests. To avoid interference from the solvent, [50] the highest DMSO concentration was 1%.

### **5.2.2 Antifungal susceptibility studies**

#### **MIC assays**

MICs were determined by the broth microdilution method according to the NCCLS reference document M27-A. [51] RPMI 1640 medium (Sigma Chemicals) without sodium bicarbonate, supplemented with L-glutamine (Gibco, Invitrogen) and buffered with 0.165 M MOPS (Sigma Chemicals) at pH 7.0 was used as test medium. Two-fold dilutions of the drugs with concentrations in the range 0.008–200 mg/L were obtained in RPMI 1640 and dispensed into the wells of plastic microdilution trays. Starting inoculum suspensions were obtained by the spectrophotometric method of inoculum preparation, adjusted to  $10^6$  cfu/mL and then diluted in test medium to  $2 \times 10^4$  cells/mL. A 100 mL yeast inoculum was added to each well of the microdilution trays to obtain final concentrations of the drugs ranging between 0.004–100 mg/L and final inocula of  $10^4$  cells/mL. The inoculated plates were incubated overnight at 35°C in a humid atmosphere. After agitation, plates were read visually with the aid of a reading mirror and spectrophotometrically with an automatic plate reader (Sunrise Tecan, Grödig/Salzburg, Austria) set at 450 nm. For EM-01D2 and amphotericin B, MICs were determined at the lowest concentration at which a 100% inhibition of growth compared with drug-free control wells was observed. The MICs of fluconazole were read as the lowest concentration of drug that inhibits growth by 80%.

MICs determined either visually or by spectrophotometric evaluation showed excellent agreement.

### ***Minimum fungicidal concentration assays.***

After the MIC determination, a 100  $\mu$ L sample from each well was seeded on plates of Sabouraud dextrose agar. Plates were incubated for 72 h at 35°C. The minimum fungicidal concentration (MFC) was defined as the minimum concentration of compound that resulted in the growth of less than two colonies representing the killing of > 99% of the original inoculum.

## **7 Acknowledgments**

*This work was supported by Regione Autonoma della Sardegna.*

*I wish to thanks Fondazione Banco di Sardegna for founding my Phd grant.*

*I acknowledge Prof. Alessandro De Logu for biological investigation.*



## 8 References and notes

- [1] Samaranayake, L.P.; MacFarlane, T.W. Oral candidosis. *London: Wright*, (1990), 265.
- [2] Barnett, J.A.; Payne, R.W.; Yarrow, D. Yeasts: characteristics and identification. *Cambridge: Cambridge University Press*, (1983).
- [3] Odds, F.C. Candida infections: an overview. *Crit Rev Microbiol*, **15**, (1987), 1-5.
- [4] Shepherd, M.G.; Poulter, R.T.M.; Sullivan, P.A. Candida albicans: biology, genetics, and pathogenicity. *Ann Rev Microbiol*, **39**, (1985), 579-614.
- [5] Meyer, S. A.; Ahearn, D. G.; Yarrow, D. Genus 4. *Candida* Berkhout. In: Kreger-van Rij N J W, editor. The yeasts: a taxonomic study. 3rd ed. Amsterdam, The Netherlands: Elsevier Science Publishers B. V., (1984), 585–844
- [6] Kwon-Chung, K.J.; Wickes, B.L.; Merz, W.G. Association of electrophoretic karyotype of *Candida stellatoidea* with virulence for mice. *Infect Immun.*, **56**, (1988), 1814-19.
- [7] Kwon-Chung, K.J.; Riggsby, W.S.; Uphoff, R.A.; Hicks, J. B.; Whelan, W. L.; Reiss, E.; Magee, B. B.; Wickes, B. L. Genetic differences between type 1 and type 2 *Candida stellatoidea*. *Infect Immun.*, **57**, (1989), 527-32.
- [8] Krause, W.; Matheis, H.; Wulf, K. Fungemia and funguria after oral administration of *Candida albicans*. *Lancet*, **I**, (1969), 598-9.
- [9] Borromeo, G.L.; McCullough, M.J.; Reade, P.C. Quantitation and morphotyping of *Candida albicans* from healthy mouths and from mouths affected by erythematous candidosis. *J. Med. Vet. Mycol.*, **30**, (1992), 477-80.
- [10] Arendorf, T.M.; Walker, D.M. The prevalence and intra-oral distribution of *Candida albicans* in man. *Arch. Oral. Biol.*, **25**, (1980), 1-10.
- [11] Lehner, T. Oral candidosis. *Dent. Pract.*, **17**, (1967), 209-16.
- [12] MacFarlane, T.W.; Helnarska, S.J. The microbiology of angular cheilitis. *Br. Dent. J.*, **140**, (1976), 403-6.
- [13] Holmstrup, P.; Besserman, M. Clinical, therapeutic and pathogenic aspects of chronic oral multiple candidiasis. *Oral Surg.*, **56**, (1983), 388-95.
- [14] Samaranayake, L.E.; Yaacob, H. Classification of oral candidiasis. In: *Oral candidiasis. London: Wright*, (1990), 265.
- [15] Eggimann, P.; Garbino, J.; Pittet, D. Epidemiology of Candida species infections in critically ill non-immunosuppressed patients. *Lancet Infect. Dis*, **3**, (2003), 685–702.
- [16] Nivoix, Y.; Velten, M.; Letscher-Bru, V.; Moghaddam, A.; Natarajan-Ame, S.; Fohrer, C.; Lioure, B.; Bilger, K.; Lutun, P.; Marcellin, L.; Launoy, A.; Freys, G.; Bergerat, J.P.; Herbrecht, R. Factors associated with overall and attributable mortality in invasive aspergillosis. *Clin. Infect. Dis.*, **47**, (2008), 1176–1184.
- [17] Dismukes, W.E. Antifungal therapy: lessons learned over the past 27 years. *Clin. Infect. Dis.*, **42**, (2006), 1289–1296.
- [18] Hughes, W.T.; Armstrong, D.; Bodey, G.P.; Bow, E.J.; Brown, A.E.; Calandra, T.; Feld, R.; Pizzo, P.A.; Rolston, K.W.; Shenep, J.L.; Young, L.S. 2002 guidelines for the use of antimicrobial agents in neutropenic patients with cancer. *Clin. Infect. Dis.*, **34**, (2002), 730–751.

- [19] Pappas, P.G.; Kauffman, C.A.; Andes, D.; Benjamin, D.K. Jr.; Calandra, T.F.; Edwards, J.E. Jr.; Filler, S.G.; Fisher, J.F.; Kullberg, B.J.; Ostrosky-Zeichner, L.; Reboli, A.C.; Rex, J.H.; Walsh, T.J.; Sobel, J.D. Clinical practice guidelines for the management of candidiasis: 2009 update by the Infectious Diseases Society of America. *Clin. Infect. Dis.*, **48**, (2009), 503–535.
- [20] Patterson, T.F. Advances and challenges in management of invasive mycoses. *Lancet*, **366**, (2005), 1013–1025.
- [21] Walsh, T.J.; Anaissie, E.J.; Denning, D.W.; Herbrecht, R.; Kontoyiannis, D.P.; Marr, K.A.; Morrison, V.A.; Segal, B.H.; Steinbach, W.J.; Stevens, D.A.; Van Burik, J.A.; Wingard, J.R.; Patterson, T.F. Treatment of aspergillosis: clinical practice guidelines of the Infectious Diseases Society of America. *Clin. Infect. Dis.*, **46**, (2008), 327–360.
- [22] Patterson, T.F.; Boucher, H.W.; Herbrecht, R.; Denning, D.W.; Lortholary, O.; Ribaud, P.; Rubin, R.H.; Wingard, J.R.; DePauw, B.; Schlamm, H.T.; Troke, P.; Bennett, J.E. Strategy of following voriconazole versus amphotericin B therapy with other licensed antifungal therapy for primary treatment of invasive aspergillosis: impact of other therapies on outcome. *Clin. Infect. Dis.*, **41**, (2005), 1448–1452.
- [23] Sobel, J.D.; Revankar, S.G. Echinocandins—first-choice or firstline therapy for invasive candidiasis? *N. Engl. J. Med.*, **356**, (2007), 2525–2526.
- [24] Bates, D.W.; Su, L.; Yu, D.T.; Chertow, G.M.; Seger, D.L.; Gomes, D.R.; Dasbach, E.J.; Platt, R. Mortality and costs of acute renal failure associated with amphotericin B therapy. *Clin. Infect. Dis.*, **32**, (2001), 686–693.
- [25] Girois, S.B.; Chapuis, F.; Decullier, E.; Revol, B.G. Adverse effects of antifungal therapies in invasive fungal infections: review and meta-analysis. *Eur. J. Clin. Microbiol. Infect. Dis.*, **25**, (2006), 138–149.
- [26] Denning, D.W.; Ribaud, P.; Milpied, N.; Caillot, D.; Herbrecht, R.; Thiel, E.; Haas, A.; Ruhnke, M.; Lode, H. Efficacy and safety of voriconazole in the treatment of acute invasive aspergillosis. *Clin. Infect. Dis.*, **34**, (2002), 563–571.
- [27] Ellis, M.; Shamoan, A.; Goraka, W.; Zwaan, F.; al-Ramadi, B. Severe hepatic injury associated with lipid formulations of amphotericin B. *Clin. Infect. Dis.*, **32**, (2001), E87–E89.
- [28] Fischer, M.A.; Winkelmayr, W.C.; Rubin, R.H.; Avorn, J. The hepatotoxicity of antifungal medications in bone marrow transplant recipients. *Clin. Infect. Dis.*, **41**, (2005), 301–307.
- [29] Kim, H.; Bindslev-Jensen, C. Reported case of severe hepatotoxicity likely due to fluconazole and not desloratadine. *Acta Haematol.*, **112**, (2004), 177–178.
- [30] Song, J.C.; Deresinski, S. Hepatotoxicity of antifungal agents. *Curr. Opin. Invest. Drugs*, **6**, (2005), 170–177.
- [31] Wingard, J.R.; Leather, H. Hepatotoxicity associated with antifungal therapy after bone marrow transplantation. *Clin. Infect. Dis.*, **41**, (2005), 308–310.
- [32] Bow, E.J. Considerations in the approach to invasive fungal infection in patients with haematological malignancies. *Br. J. Haematol.*, **140**, (2008), 133–152.
- [33] Denning, D.W. Echinocandin antifungal drugs. *Lancet*, **362**, (2003) 1142–1151.

- [34] Falagas, M.E.; Ntziora, F.; Betsi, G.I.; Samonis, G. Caspofungin for the treatment of fungal infections: a systematic review of randomized controlled trials. *Int. J. Antimicrob. Agents*, **29**, (2007), 136–143.
- [35] Gafter-Gvili, A.; Vidal, L.; Goldberg, E.; Leibovici, L.; Paul, M. Treatment of invasive candidal infections: systematic review and meta-analysis. *Mayo Clin. Proc.*, **83**, (2008), 1011–1021.
- [36] Goldberg, E.; Gafter-Gvili, A.; Robenshtok, E.; Leibovici, L.; Paul, M. Empirical antifungal therapy for patients with neutropenia and persistent fever: systematic review and meta-analysis. *Eur. J. Cancer*, **44**, (2008), 2192–2203.
- [37] Jorgensen, K.J.; Gotzsche, P.C.; Johansen, H.K. Voriconazole versus amphotericin B in cancer patients with neutropenia. *Cochrane Database Systematic Review CD004707* (2006).
- [38] Leather, H.L.; Wingard, J.R. Prophylaxis, empirical therapy, or pre-emptive therapy of fungal infections in immunocompromised patients: which is better for whom? *Curr. Opin. Infect. Dis.*, **15**, (2002), 369–375.
- [39] McCormack, P.L.; Perry, C.M. Caspofungin: a review of its use in the treatment of fungal infections. *Drugs*, **65**, (2005), 2049–2068.
- [40] Mills, E.J.; Perri, D.; Cooper, C.; Nachega, J.B.; Wu, P.; Tleyjeh, I.; Phillips, P. Antifungal treatment for invasive *Candida* infections: a mixed treatment comparison meta-analysis. *Ann. Clin. Microbiol. Antimicrob.*, **8**, (2009), 23.
- [41] Robenshtok, E.; Gafter-Gvili, A.; Goldberg, E.; Weinberger, M.; Yeshurun, M.; Leibovici, L.; Paul, M. Antifungal prophylaxis in cancer patients after chemotherapy or hematopoietic stem-cell transplantation: systematic review and meta-analysis. *J. Clin. Oncol.*, **25**, (2007), 5471–5489.
- [42] Sable, C.A.; Strohmaier, K.M.; Chodakewitz, J.A. Advances in antifungal therapy. *Annu. Rev. Med.*, **59**, (2008), 361–379.
- [43] Scott, L.J.; Simpson, D. Voriconazole: a review of its use in the management of invasive fungal infections. *Drugs*, **67**, (2007), 269–298.
- [44] Chimenti, F.; Bizzarri, B.; Maccioni, E.; Secci, D.; Bolasco, A.; Fioravanti, R.; Chimenti, P.; Granese, A.; Carradori, S.; Rivanera, D.; Lilli, D.; Zicari, A.; Distinto, S. Synthesis and in vitro activity of 2-thiazolylhydrazone derivatives compared with the activity of clotrimazole against clinical isolates of *Candida* spp. *Bioorganic & Medicinal Chemistry Letters*, **17**, (2007), 4635–4640.
- [45] Chimenti, F.; Maccioni, E.; Secci, D.; Bolasco, A.; Chimenti, P.; Granese, A.; Carradori, S.; Alcaro, S.; Ortuso, F.; Yáñez, M.; Orallo, F.; Cirilli, R.; Ferretti, R.; La Torre, F. Synthesis, stereochemical identification and selective inhibitory activity against MAO-B of 2-methylcyclohexylidene-(4-arylthiazol-2-yl)hydrazones. *J. Med. Chem.*, **51**(16), (2008), 4874–4880.
- [46] De Logu, A.; Saddi, M.; Cardia, M.C.; Borgna, R.; Sanna, C.; Saddi, B.; Maccioni, E. In vitro activity of 2-cyclohexylidenhydrazo-4-phenyl-thiazole compared with those of amphotericin B and fluconazole against clinical isolates of *Candida* spp. and fluconazole-resistant *Candida albicans*, *Journal of Antimicrobial Chemotherapy*, **55**, (2005), 692–698.

- [47] Maccioni, E.; Cardia, M.C.; Bonsignore, L.; Plumitallo, A.; Pellerano, M.L.; De Logu, A. Synthesis and anti-microbial activity of isothiosemicarbazones and cyclic analogues, // *Farmaco*, **57**, (2002), 809-817.
- [48] Chimenti, F.; Secci, D.; Bolasco, A.; Chimenti, P.; Granese, A.; Carradori, S.; Maccioni, E.; Cardia, M.C.; Yáñez, M.; Orallo, F.; Bizzarri, B.; Fioravanti, R.; Alcaro, S.; Ortuso, F.; Cirilli, R.; Ferretti, R.; Distinto, S.; Kirchmair, J.; Langer, T. Synthesis, Semipreparative HPLC separation, Biological Evaluation, and 3D-QSAR of Hydrazothiazole Derivative as Human Monoamine Oxidase B Inhibitors. *Bioorganic & Medicinal Chemistry*, **18**, (2010), 5063–5070.
- [49] Dimmock, J.R.; McColl, J.M.; Wonko, S.L.; Thayer, R.S.; Hancock, D.S. Evaluation of thiosemicarbazones of some aryl alkyl ketones and related compounds for anticonvulsant activities. *J.Med.Chem.*, **26**, (1991), 529-534.
- [50] Jagannath, C.; Reddy, V.M.; Gangadharam, P.R. Enhancement of drug susceptibility of multi-drug resistant strains of *Micobacterium tuberculosis* by ethambutol and dimethyl sulfoxide. *J.Antimicrob.Chemother*, **35**, (1995), 381-390.
- [51] Reference Method for Broth Dilution Antifungal Susceptibility Testing of Yeast: Approved Standard M27-A. National Committee for Clinical Laboratory Standards. NCCLS, Villanova, PA, USA, (1997).

### **III PART:**

## **Synthesis and biological evaluation of monoamine oxidase inhibitors**

## CONTENTS

1	<i>Introduction</i>	
	1.1 <i>Historical overview</i>	3
2	<i>Results and discussion</i>	5
3	<i>Materials and methods</i>	
	3.1 <i>Chemistry</i>	15
	3.2 <i>Pharmacological studies</i>	31
	3.2.1 <i>Determination of MAO isoform activity</i>	
	3.2.2 <i>Data presentation and statistical analysis</i>	
	3.2.3 <i>Drugs and chemicals</i>	
4	<i>Acknowledgments</i>	34
5	<i>References and notes</i>	35



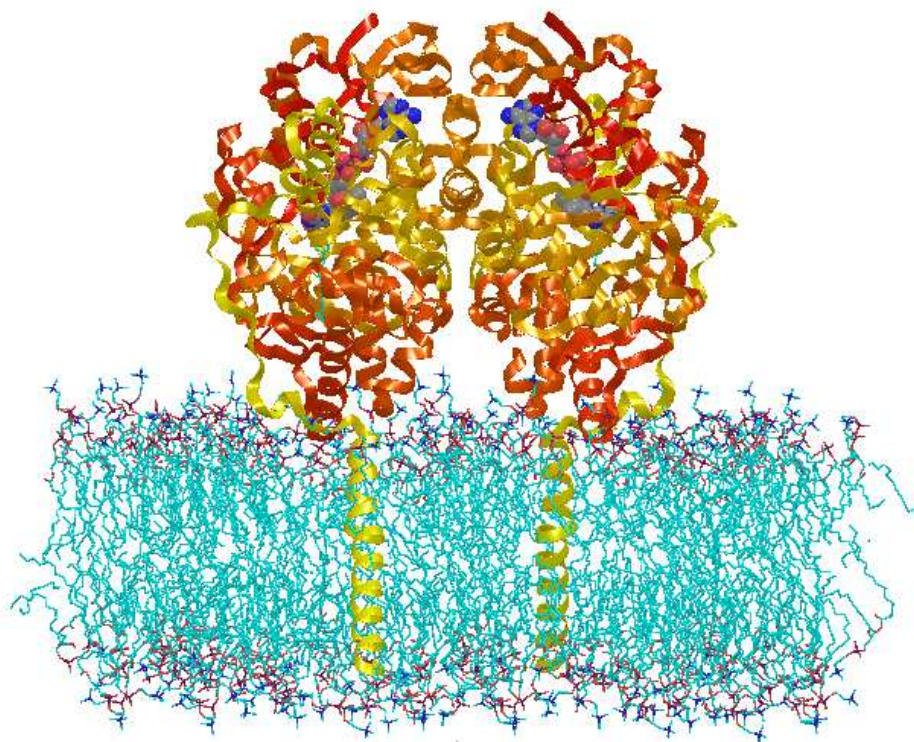




## **1 Introduction**

### **1.1 Historical overview**

Monoamine oxidase are key role enzymes in the catabolism of amines like dopamine (DA), norepinephrine (NE), epinephrine, serotonin (5HT), and 2-phenylethylamine (PEA). [1]



**Figure 1.** Representation of MAO-B homodimer bound on mitochondrial membrane

Two isoforms of the enzyme, differing for substrates and selectivity of inhibitors [2], are known, named MAO-A and MAO-B.

5HT and NE are preferentially deaminated by the A isoform, while  $\beta$ -phenylethylamine and benzylamine are MAO-B substrates.

Moreover, in mammals the inhibition of MAO-B leads to an increase of the DA and 5HT levels as well as to a neuroprotective effect. [3]

Both MAO isoforms are important in the metabolism of monoamine neurotransmitters and, as a result, MAO inhibitors (MAOi) are studied for the treatment of several psychiatric and neurological disorders.

In particular, MAO-B inhibitors are coadjuvant in the treatment of both Parkinson's (PD) [4] and Alzheimer's diseases (AD) [5], while MAO-A inhibitors are used as antidepressant and anxiolytic drugs. [6]

Furthermore, the activity of MAO-B is enhanced by aging and in AD patients. [3,5]

In addition to this, the deamination reaction, promoted by MAO-B, leads to the production of hydrogen peroxide and to other reactive oxygen species responsible for neurological damaging. [7-9]

Also, in the case of PD, a correlation between free radical production and development of the pathology has been observed. [10]

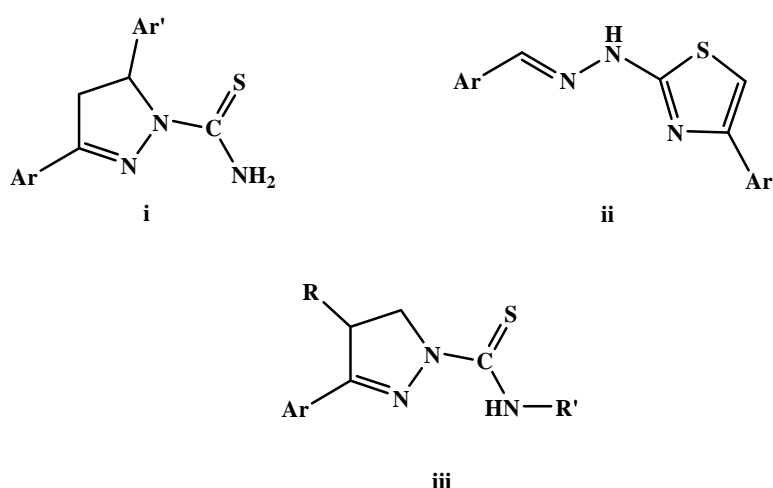
On the basis of the above we can assume that neurodegenerative disorders are associated with the production of oxidative stress, with an increased MAO-B activity, and with a decrease in the elimination rate of free radical species. [5-14]

On the contrary, MAO-A does not increase with age, suggesting that a totally independent mechanism regulates the expression of the two enzymatic isoforms. [12,14]

We have recently designed and synthesised some 1-thiocarbamoyl-3,5-diaryl-4,5-dihydro-1(H)-pyrazole (I), 2-thiazolyl hydrazones (II), and series of 1-(N-methyl)thiocarbamoyl-3-aryl-4,5-dihydro-1(H)-pyrazoles (III) and 1-thiocarbamoyl-3-aryl-4,5-dihydro-1(H)-pyrazoles both, highly active and selective towards MAO-B isoform (Figure 2). [15-17]

The synthesis, the MAO inhibition, and the pharmacophoric features of a series of 1-acetyl-3-aryl-4,5-dihydro-1(H)-pyrazoles have been reported by Chimenti and colleagues. [18]

In particular, it has been observed that the absence of substituents in position 5 of the heterocyclic ring, generally leads to a decrease of MAO-A inhibition potency. [15-18]



**Figure 2.** Previously studied MAO inhibitors

More recently we reported on the synthesis and biological assessment of novel 2-thiazolyhydrazones and the computational analysis of their recognition by monoamine oxidase B. [19]

In particular it was highlighted the importance of fluorine atom interacting with the water close to the cofactor and the influence of steric bulkiness of substituents in the arylidene moiety. Free energy perturbation (FEP) analysis confirmed experimental data.

## **2 Results and Discussion**

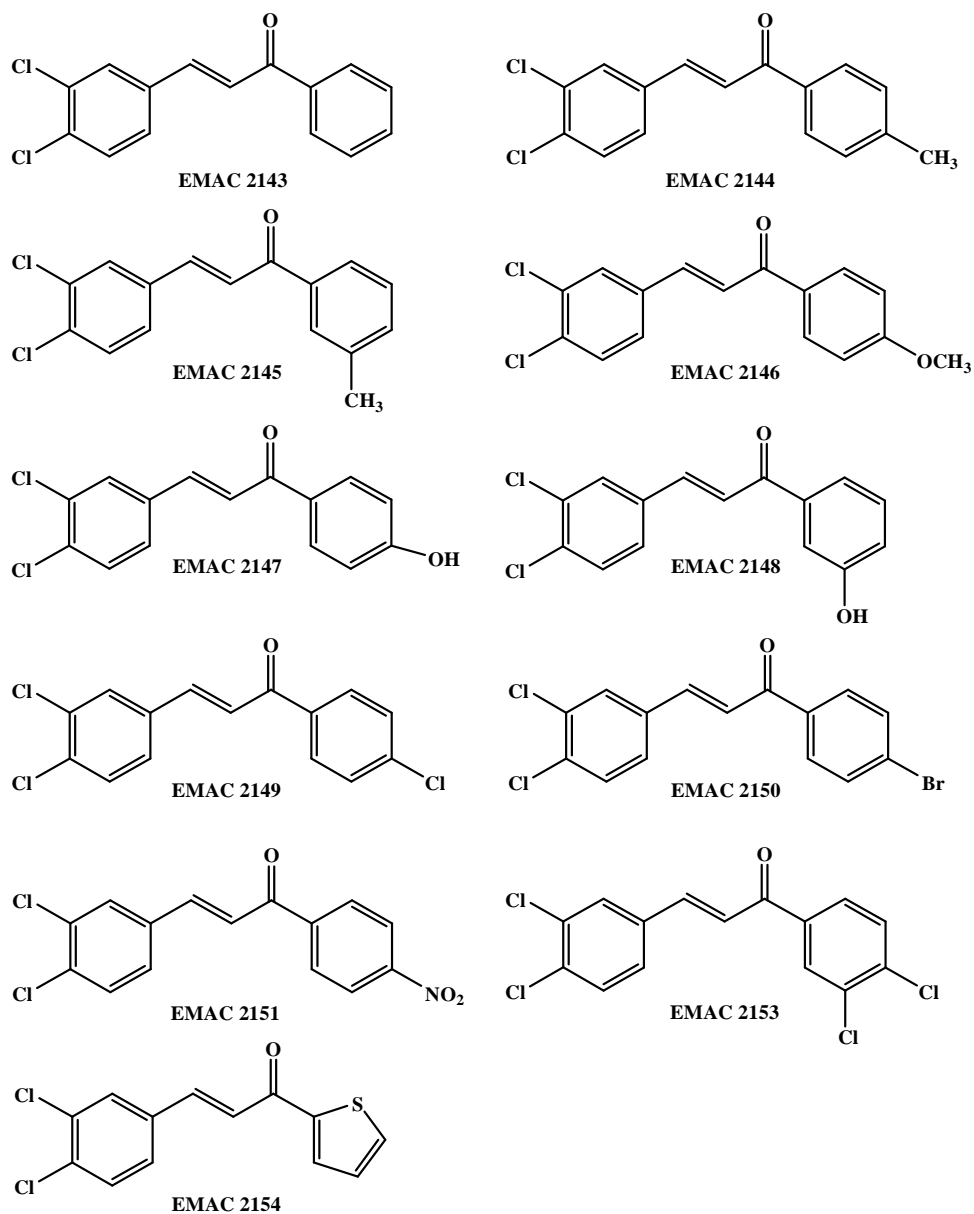
Recently, rasagiline, (N-propargyl-1-R-aminoindan, Azilect), a novel selective and irreversible MAO-B inhibitor, has been approved for PD therapy [20] while safinamide, a selective and reversible MAO-B inhibitor, is currently undergoing clinical phase III for the treatment of early stages of PD. [21]

On this basis, as part of my PhD project, I focused my interest on the synthesis of potential MAO-B inhibitors.

Firstly I have synthesized a series of chalcones EMAC 2143-2154 bearing a 3,4-dichloro moiety. This substitution demonstrated to be particularly efficient in a series of 3-Acetyl-2,5-diaryl-2,3-dihydro-1,3,4-oxadiazoles. [22]

All compounds were characterized with the usual analytic and spectroscopic methods and submitted to biochemical assay.

The structures of EMAC 2143-2154 derivatives are reported in Figure 3.

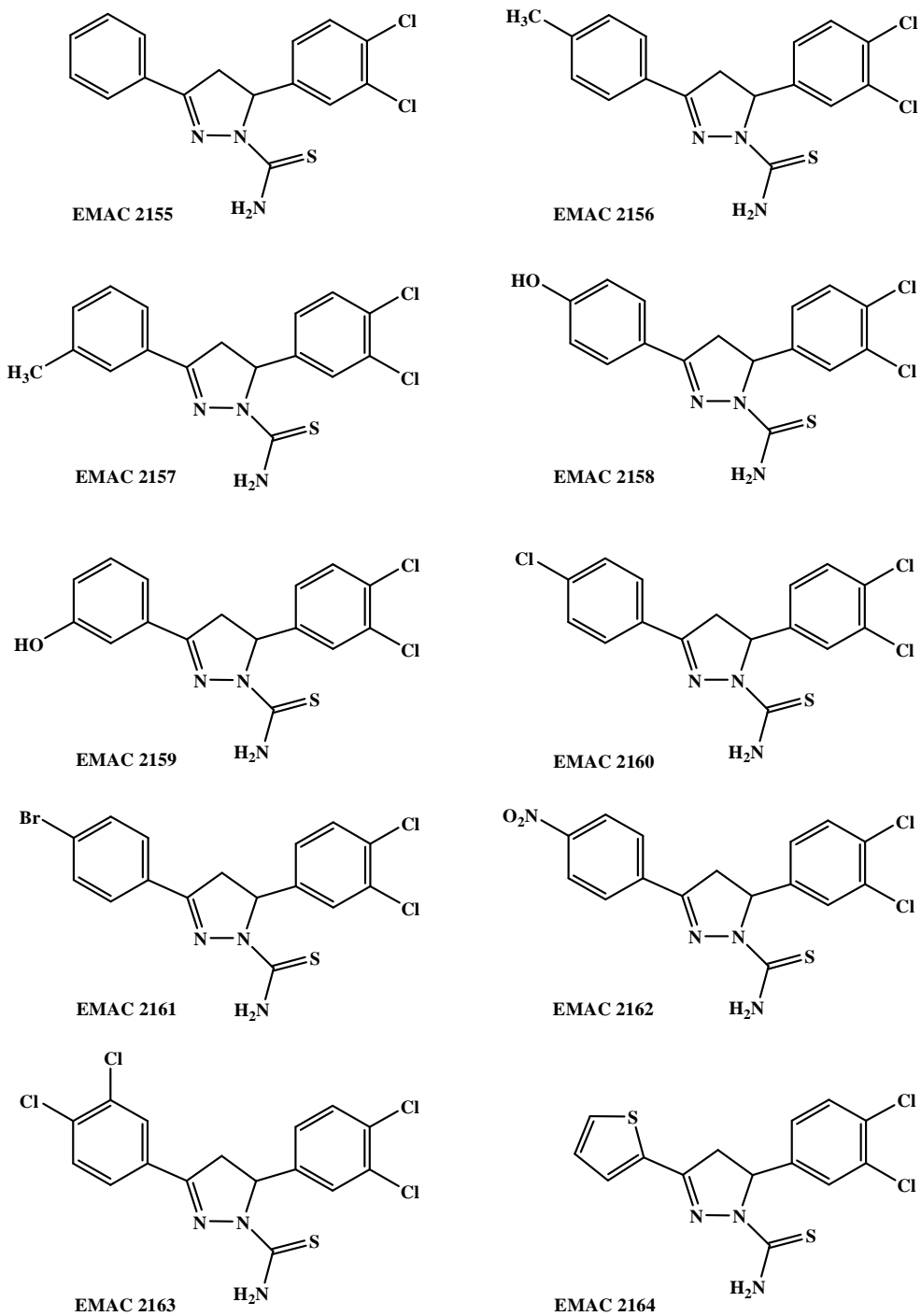


**Figure 3.** Structures of compounds EMAC 2143-2154

We have, also, synthesized a series of 3,5-dihydropyrazole-1-carbothioamide, keeping the same aryl substituents as in the chalcone series.

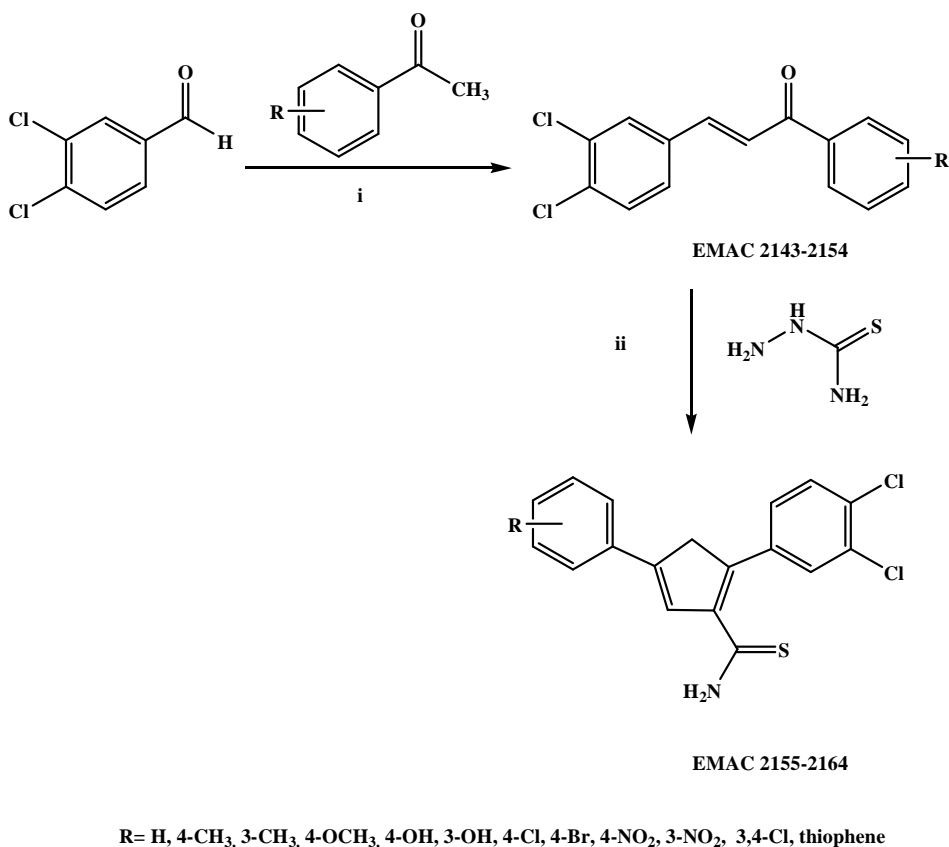
The synthesis was accomplished by reacting chalcones EMAC 2143-2154 with thiosemicarbazide in ethanol and KOH alcoholic solution.

By this method dihydropyrazoles EMAC 2155-2164 were obtained (Figure 4).



**Figure 4.** Structures of compounds EMAC 2155-2164

The synthetic pathway is divided in two different step as reported in Scheme 1



**Scheme 1.** Synthesis of (E)-3-(3,4-dichlorophenyl)-1-arylprop-2-en-1-one derivatives EMAC 2143-2154. Reagents: (i) ethanol, NaOH 10 %; Synthesis of 5-(3,4-dichlorophenyl)-3-aryl-4,5-dihydropyrazole-1-carbothioamide EMAC 2155-2164. (ii) thiosemicarbazide, ethanol, KOH EtOH 5%

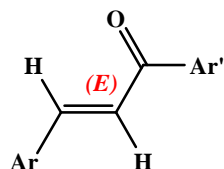
The first step consist of the formation of the chalcone derivative, synthesized via Claisen-Schmidt condensation of substituted acetophenone with 3',4'-dichlorobenzaldehyde under basic conditions in ethanol. Crude chalcones were purified by recrystallization from a suitable solvent. [23, 24].

All synthesized compounds were characterised by analytical and spectral data as listed in Table 3-6.

All samples were measured in CDCl<sub>3</sub> solvent at 278.1 K temperature on a Varian Unity 500 spectrometer and on a Varian Unity 300 spectrometer-

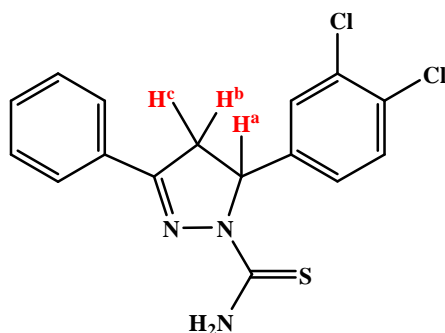
In the signal assignments the proton chemical shifts are referred to the solvent (1H:  $\delta$ = 7.24 ppm,).

In all investigated molecules the NMR analysis supports the “E” configuration (Figure 3), according to the double bond protons coupling constants that ranges from 15 to 16 Hz.



**Figure 3.** (E)-3-(3,4-dichlorophenyl)-1-arylprop-2-en-1-one

The second step of the synthetic route is the reaction of the chalcone compound with thiosemicarbazide under basic condition ( KOH 5% in ethanol) to generate the required pyrazolines (Figure 4).

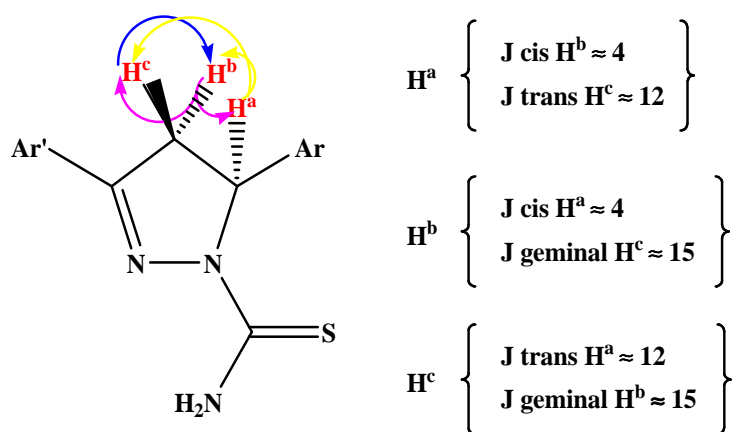


**Figure 4.** 5-(3,4-dichlorophenyl)-3-aryl-4,5-dihydropyrazole-1-carbothioamide

NMR spectroscopy was particularly efficient in the characterization of all the compounds.

In the case of pyrazolines three sets of double doublets signals, in the region of 3.00 and 6.05 ppm are diagnostic not only of the formation of the pyrazoline ring, but also of the exact position of the double bond within the dihydropyrazole nucleus.

In fact, the two protons (B and C), on the carbon 4 of the pyrazoline ring, couple in *cis* and in *trans* with different vicinal constants with the proton of carbon 5 (A) (JA-B, JA-C) and between them with a geminal characteristic constant (JB-C), giving rise to the characteristic fine structure of three double doublets in the <sup>1</sup>H-NMR spectrum (Figure 5).

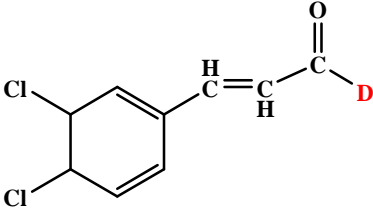
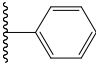
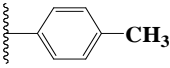
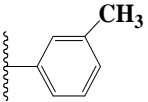
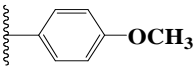
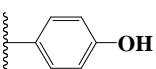
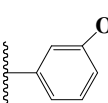
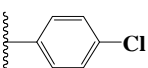
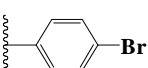
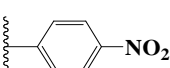
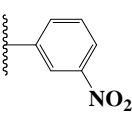
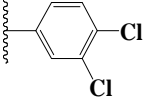
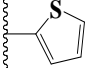


**Figure 5.** Schematic representation of the coupling network of  $H^a$ ,  $H^b$ ,  $H^c$  protons

The activity of compounds **EMAC 2143-2154** and **EMAC 2155-2164** was measured on both isoforms of the enzyme (Table 1 and 2).



**Table 1.** EMAC 2143-2154 IC<sub>50</sub> values and MAO-B selectivity ratios [IC<sub>50</sub> (MAO-A)]/[IC<sub>50</sub> (MAO-B)] for the inhibitory effects of the test drugs on the enzymatic activity of human recombinant MAO isoforms expressed in baculovirus infected BTI insect cells.

				
"D"-ring		MAO-A (IC <sub>50</sub> )	MAO-B (IC <sub>50</sub> )	RATIO
	EMAC 2143	**	44.24 ± 0.07 nM	2.260 <sup>#</sup>
	EMAC 2144	**	3.03 ± 0.04 nM	>33.003 <sup>#</sup>
	EMAC 2145	**	8.11 ± 0.17 nM	>12.330 <sup>#</sup>
	EMAC 2146	**	9.44 ± 0.32 nM	>10.593 <sup>#</sup>
	EMAC 2147	5.46 ± 0.43 μM <sup>a</sup>	1.15 ± 0.08 nM	4.748
	EMAC 2148	12.31 ± 0.73 μM <sup>a</sup>	59.98 ± 3.63 nM	205
	EMAC 2148	**	15.45 ± 1.26 nM	6.472 <sup>#</sup>
	EMAC 2150	**	9.78 ± 0.63 nM	>10.225 <sup>#</sup>
	EMAC 2151	4.48 ± 0.47 μM <sup>a</sup>	4.42 ± 0.21 nM	1.014
	EMAC 2152	**	0.93 ± 0.05 nM	107.527
	EMAC 2153	***	3.78 ± 0.24 nM	26.738
	EMAC 2154	**	60.97 ± 4.73 nM	1.640
R-(-)-deprenyl		67.25 ± 1.02 μM <sup>a</sup>	19.60 ± 0.86 nM	3431.12

All IC<sub>50</sub> values shown in this table are the mean ± S.E.M. from five experiments. Level of statistical significance:  
<sup>a</sup>P < 0.01 versus the corresponding IC<sub>50</sub> values obtained against MAO-B, as determined by ANOVA/Dunnett's.  
 \*\* Inactive at 100 μM (highest concentration tested).  
 \*\*\* 100 μM inhibits the corresponding MAO activity by approximately 40-50%. At higher concentration the

compounds precipitate.

# Values obtained under the assumption that the corresponding  $IC_{50}$  against MAO-A or MAO-B is 100  $\mu$ M.

All compounds exhibited good activity towards the B isoform of the enzyme corroborating the hypothesis that the introduction of the 3,4-dichloro moiety leads to the selectivity towards MAO B (Table 1).

According to these results also the nature of the “D” ring seems to play a key role in determining both activity and selectivity.

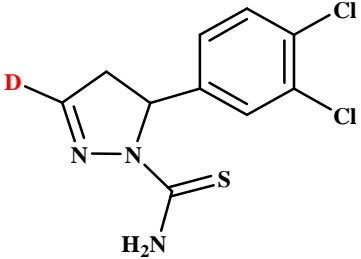
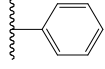
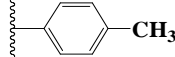
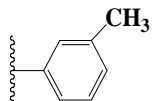
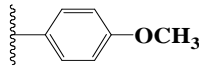
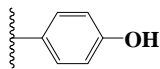
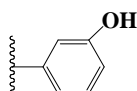
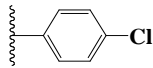
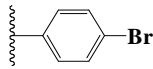
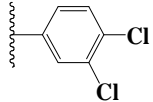
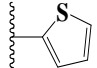
When a hydroxyl substituent is introduced, either in the position 4 or in the position 3 of the D ring, a decrease in the isoform selectivity was observed. This behavior is also observed in the case of the 4-nitro substitution.

Surprisingly when a nitro group is introduced in the position 3 of the D ring the best selectivity and activity are observed. Moreover, also the introduction of methyl or 3,4-dichloro substitution leads to active and selective compounds (ie **EMAC 2144**, **EMAC 2145**, and **EMAC 2153**).

Generally all compounds are more active and/or selective with respect to R-(-)-deprenyl that has been used as standard for the biochemical assay.

Compounds EMAC 2155-2164 were characterized and submitted to biochemical assay. Surprisingly none of the compounds exhibit activity towards MAO B.

**Table 2.** EMAC 2155-2164 IC<sub>50</sub> values and MAO-B selectivity ratios [IC<sub>50</sub> (MAO-A)]/[IC<sub>50</sub> (MAO-B)] for the inhibitory effects of the test drugs on the enzymatic activity of human recombinant MAO isoforms expressed in baculovirus infected BTI insect cells.

				
"D"-ring		MAO-A (IC <sub>50</sub> )	MAO-B (IC <sub>50</sub> )	RATIO
	EMAC 2155	**	**	
	EMAC 2156	**	**	
	EMAC 2157	**	**	
	EMAC 2158	**	**	
	EMAC 2159	31.60 ± 1.98 μM	***	<0.32 <sup>#</sup>
	EMAC 2160	**	**	**
	EMAC 2161	**	**	
	EMAC 2162	**	**	
	EMAC 2163	***	***	
	EMAC 2164	**	**	
R-(-)-deprenyl		67.25 ± 1.02 μM	19.60 ± 0.86 nM	3431.12

All IC<sub>50</sub> values shown in this table are the mean ± S.E.M. from five experiments. Level of statistical significance:  
<sup>a</sup>P < 0.01 versus the corresponding IC<sub>50</sub> values obtained against MAO-B, as determined by ANOVA/Dunnett's.  
 \*\* Inactive at 100 μM (highest concentration tested).  
 \*\*\* 100 μM inhibits the corresponding MAO activity by approximately 40-50%. At higher concentration the compounds precipitate.  
<sup>#</sup> Values obtained under the assumption that the corresponding IC<sub>50</sub> against MAO-A or MAO-B is the

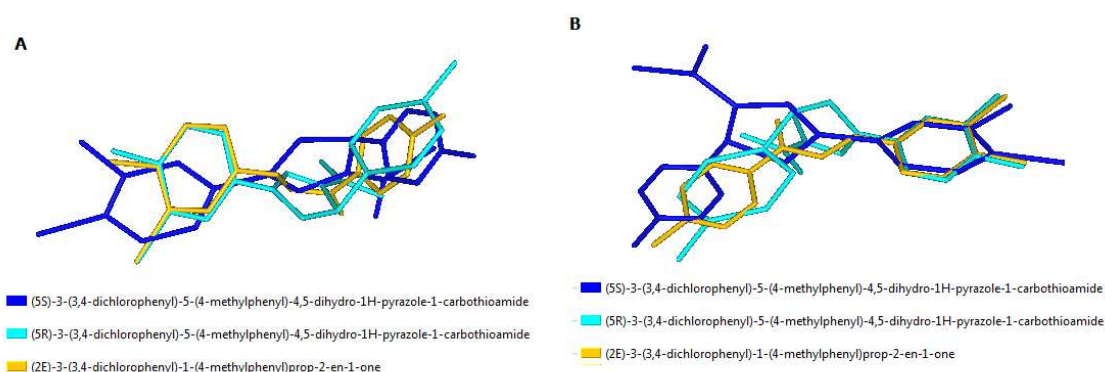
highest concentration tested (100  $\mu$ M).

Only compound EMAC 2159 is weakly active towards the A isoform of the enzyme.

It might be conceivable that the 3,4-phenyl moiety in the position 5 of the dihydropyrazole ring is constrained in an unfavourable position to interact with the enzyme with respect to previously studied analogues compounds. [22]

In all probability, in the case of derivatives EMAC 2143-2154, an optimal orientation of the two aryl substituents, with respect to the pyrazoline compounds, and a higher flexibility concur to the observed high activity and selectivity.

To achieve a better comprehension of this behaviour we performed the alignment of the lowest energy conformers of compound EMAC 2144 and of the two enantiomers of compound EMAC 2156.



**Figure 6. A** Pharmacophoric alignment of compounds EMAC 2144, (S) and (R)-EMAC 2156; **B** alignment of compounds EMAC 2144, (S) and (R)-EMAC 2156 based on 3,4-dichlorophenyl moiety superimposition

In both cases a different orientation of the 4-methylphenyl substituent is observed and, in all probability, this leads to the decrease of activity of the pyrazoline derivatives with respect to the chalcone series.

However we are performing docking experiments and dynamic simulations in order to achieve a more detailed picture of the behaviour of such compounds and to rationalise these data.

Meanwhile we are concentrating our efforts on the synthesis of other heterocyclic rings (ie dihydroisoxazoles) bearing similar substitutions with the aim of obtaining new data that might be helpful in rationalising the SARs of this class of inhibitors.

## **3 Materials and methods**

### **3.1 Chemistry**

#### **EMAC 2143-2164**

The synthetic pathway is divided in two different step (Scheme 1).

Unless otherwise noted, starting materials and reagents were obtains from commercial suppliers and were used without purification.

All melting point were determined by the capillary method on a Stuart SMP11 melting point apparatus and are uncorrected.

All samples were measured in CDCl<sub>3</sub> solvent at 278.1 K temperature on a Varian Unity 500 spectrometer and on a Variant Unity 300 spectrometer. In the signal assignments the proton chemical shifts are referred to the solvent (1H:  $\delta$  = 7.24 ppm,). Coupling constants *J* are expressed in hertz (Hz).

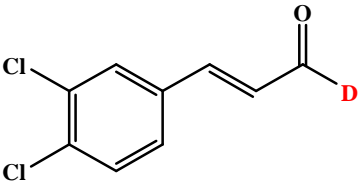
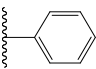
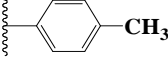
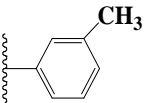
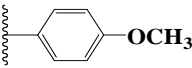
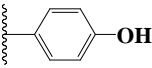
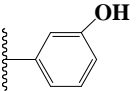
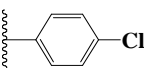
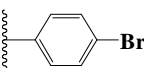
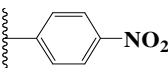
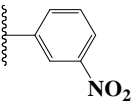
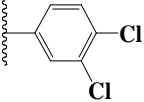
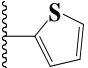
Elemental analyses were obtained on a Perkin–Elmer 240 B microanalyser. Analytical data of the synthesised compounds are in agreement with the theoretical data.

HPLC-MS/MS analysis was performed using an HPLC-MS/MS Varian (Varian Palo Alto, CA, USA) system fitted with a 1200 L triple quadrupole mass spectrometer equipped with an electrospray ionization source (ESI). A Varian MS workstation version 6.8 software was used for data acquisition and processing. Rapid identification was achieved with direct infusion of the purified molecule, dissolved in methanol, on the mass spectrometer source.

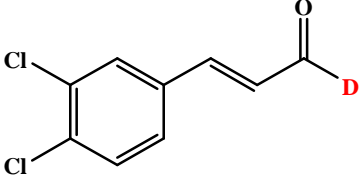
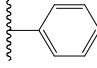
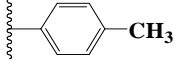
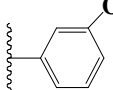
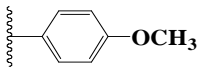
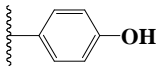
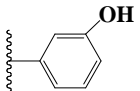
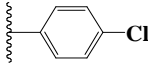
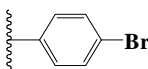
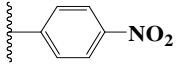
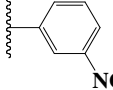
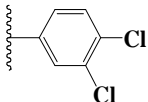
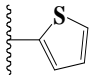
TLC chromatography was performed using silica gel plates (Merck F 254), spots were visualised by UV light.

All synthesized compounds were characterised by analytical and spectral data as listed in Table 3-6

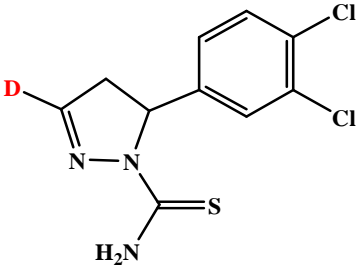
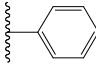
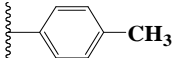
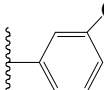
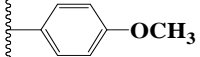
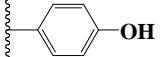
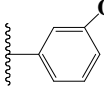
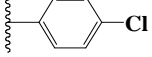
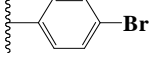
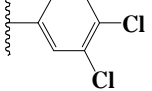
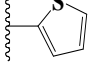
**Table 3.** Chemical and physical data of derivatives EMAC 2143-2154

				
Compound	"D" ring	M.W.	Mp (C°)	% Yield
EMAC 2143		277.15	93-95	95
EMAC 2144		291.17	127-129	93
EMAC 2145		291.17	111-113	94
EMAC 2146		307.17	125	93
EMAC 2147		293.14	196	92
EMAC 2148		293.14	135-136	92
EMAC 2149		311.59	119-120	96
EMAC 2150		356.04	143-144	97
EMAC 2151		322.14	221-222	95.5
EMAC 2152		322.14	204-205	94
EMAC 2153		346.04	157-158	94
EMAC 2154		283.17	145	94

**Table 4.** Analytical data of derivatives EMAC 2143-2154

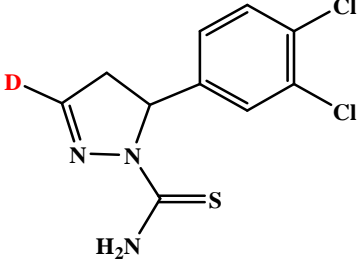
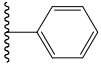
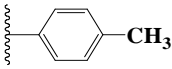
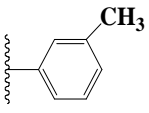
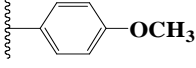
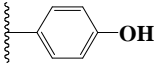
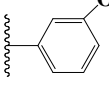
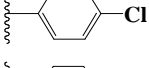
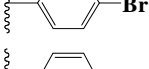
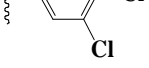
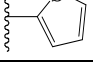
Compound	"D" ring	Reaction solvent	Crystallisation solvent	Aspect	Reaction time (h)
					
EMAC 2143		Ethanol/ NaOH 10%	Water/ethanol (1:1)	Crystalline yellow solid	24
EMAC 2144		Ethanol/ NaOH 10%	Water/ethanol (1:1)	Crystalline yellow solid	24
EMAC 2145		Ethanol/ NaOH 10%	Water/ethanol (1:1)	Crystalline yellow solid	24
EMAC 2146		Ethanol/ NaOH 10%	Water/ethanol (1:1)	Crystalline yellow solid	24
EMAC 2147		Ethanol/ NaOH 10%	Water/ethanol (1:1)	Crystalline white solid	24
EMAC 2148		Ethanol/ NaOH 10%	Water/ethanol (1:1)	Crystalline white solid	24
EMAC 2149		Ethanol/ NaOH 10%	Water/ethanol (1:1)	Crystalline pale-yellow solid	24
EMAC 2150		Ethanol/ NaOH 10%	Water/ethanol (1:1)	Crystalline pale-yellow solid	24
EMAC 2151		Ethanol/ NaOH 10%	Water/ethanol (1:1)	Crystalline orange solid	24
EMAC 2152		Ethanol/ NaOH 10%	Water/ethanol (1:1)	Crystalline pale-orange solid	24
EMAC 2153		Ethanol/ NaOH 10%	Water/ethanol (1:1)	Crystalline pale-yellow solid	24
EMAC 2154		Ethanol/ NaOH 10%	Water/ethanol (1:1)	Crystalline pale-yellow solid	24

**Table 5.** Chemical and physical data of derivatives EMAC 2155-2164

Compound	"D" ring	M.W.	Mp (C°)	% Yield
				
EMAC 2155		350.27	165-166	75
EMAC 2156		364.29	242-243	85
EMAC 2157		364.29	182-183	86
EMAC 2158		380.29	215-216	85.5
EMAC 2159		366.26	>250	85.5
EMAC 2160		366.26	229-230	85.5
EMAC 2161		384.71	242-243	87
EMAC 2162		429.16	>250	85.5
EMAC 2163		419.16	189-191	84
EMAC 2164		356.19	199-200	90



**Table 4.** Analytical data of derivatives EMAC 2155-2164

Compound	"D" ring	Reaction solvent	Crystallisation solvent	Aspect	Reaction time (h)
					
EMAC 2155		Ethanol/ KOH <sub>EtOH</sub> 5%	Water/ethanol (1:1)	Crystalline yellow solid	24
EMAC 2156		Ethanol/ KOH <sub>EtOH</sub> 5%	Water/ethanol (1:1)	Crystalline pale-yellow solid	24
EMAC 2157		Ethanol/ KOH <sub>EtOH</sub> 5%	Water/ethanol (1:1)	Crystalline yellow solid	24
EMAC 2158		Ethanol/ KOH <sub>EtOH</sub> 5%	Water/ethanol (1:1)	Crystalline pale-yellow solid	24
EMAC 2159		Ethanol/ KOH <sub>EtOH</sub> 5%	Water/ethanol (1:1)	Crystalline white solid	24
EMAC 2160		Ethanol/ KOH <sub>EtOH</sub> 5%	Water/ethanol (1:1)	Crystalline yellow solid	24
EMAC 2161		Ethanol/ KOH <sub>EtOH</sub> 5%	Water/ethanol (1:1)	Crystalline yellow solid	24
EMAC 2162		Ethanol/ KOH <sub>EtOH</sub> 5%	Water/ethanol (1:1)	Crystalline yellow solid	24
EMAC 2163		Ethanol/ KOH <sub>EtOH</sub> 5%	Water/ethanol (1:1)	Crystalline yellow solid	24
EMAC 2164		Ethanol/ KOH <sub>EtOH</sub> 5%	Water/ethanol (1:1)	Crystalline yellow solid	24

### **Synthesis of starting (E)-3-(3,4-dichlorophenyl)-1-arylprop-2-en-1-one derivatives.**

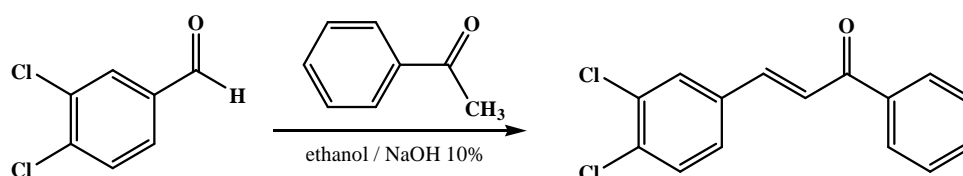
The starting (E)-3-(3,4-dichlorophenyl)-1-arylprop-2-en-1-one derivatives have been synthesised by according to the procedures reported in the literature. [23,24]

In a flask equipped with a reflux condenser, a mixture of acetophenone (1.2 mol) was dissolved in ethanol and treated with a solution of sodium hydroxide in water 10%. After stirring the mixture for 10 min, a solution of 3,4-dichlorobenzaldehyde (1 mol) was added. The mixture was stirred at room temperature for 24 h and the precipitate that formed was filtered off. The filtrate was washed with ethyl ether and recrystallized from water/ethanol (1:1) to offer pure compounds.

According to this procedure the following compounds have been synthesised:

#### **EMAC 2143**

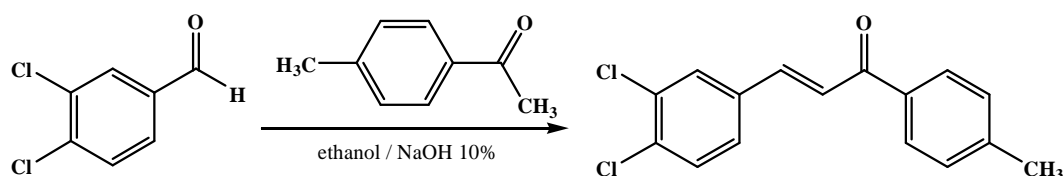
##### **(E)-3-(3,4-dichlorophenyl)-1-phenylprop-2-en-1-one**



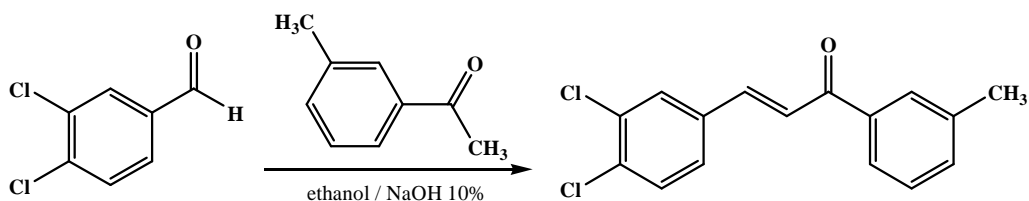
$^1\text{H-NMR}$  (500 MHz, DMSO)  $\delta\text{H}$  7.5 ( m, 5H, Ar-CH + CH=CH), 7.61 ( t, 1H, J: 7.5, Ar-CH), 7.69 ( d, 1H, J: 15.5, CH=CH), 7.73 ( s, 1H, Ar-CH), 8.02 ( d, 2H, J: 7, Ar-CH)

#### **EMAC 2144**

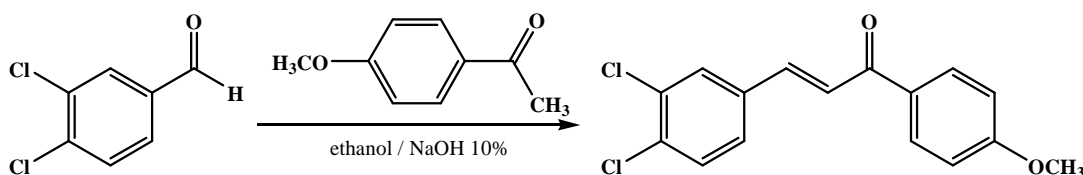
##### **(E)-3-(3,4-dichlorophenyl)-1-p-tolylprop-2-en-1-one**



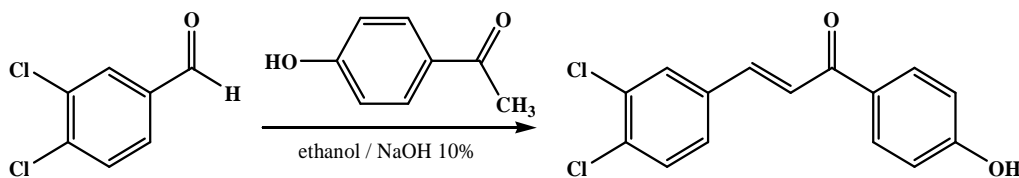
$^1\text{H-NMR}$  (500 MHz, DMSO)  $\delta\text{H}$  2.45 ( s, 3H,  $\text{CH}_3$ ), 7.31 ( d, 2H, J: 7.5, Ar-CH), 7.45 ( d, 1H, J: 8, Ar-CH), 7.49 ( d, 1H, J: 8.5, Ar-CH), 7.5 ( d, 1H, J: 16, CH=CH), 7.68 ( d, 1H, J: 16, CH=CH), 7.73 ( s, 1H, Ar-CH), 7.93 ( d, 2H, J: 8.5, Ar-CH)

**EMAC 2145*****(E)*-3-(3,4-dichlorophenyl)-1-*m*-tolylprop-2-en-1-one**

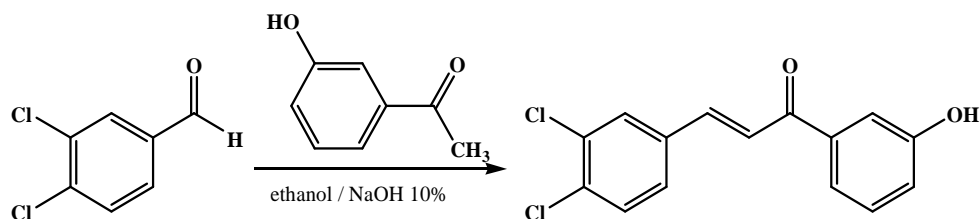
$^1\text{H-NMR}$  (500 MHz, DMSO)  $\delta$  H 2.45 (s, 3H, CH<sub>3</sub>), 7.41 (m, 2H, Ar-CH), 7.48 (m, 3H, Ar-CH + CH=CH), 7.68 (d, 1H, J: 16, CH=CH), 7.73 (s, 1H, Ar-CH), 7.81 (d, 2H, J: 8.5, Ar-CH)

**EMAC 2146*****(E)*-3-(3,4-dichlorophenyl)-1-(4-methoxyphenyl)prop-2-en-1-one**

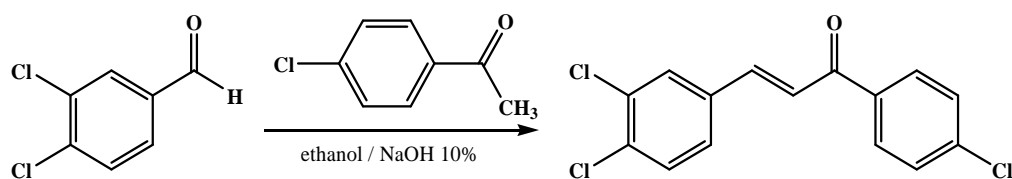
$^1\text{H-NMR}$  (500 MHz, DMSO)  $\delta$  H 3.90 (s, 3H, OCH<sub>3</sub>), 6.99 (d, 2H, J: 8.5, Ar-CH), 7.45 (d, 1H, J: 8, Ar-CH), 7.49 (d, 1H, J: 9, Ar-CH), 7.51 (d, 1H, J: 15.5, CH=CH), 7.67 (d, 1H, J: 16, CH=CH), 7.73 (s, 1H, Ar-CH), 8.03 (d, 2H, J: 9, Ar-CH)

**EMAC 2147*****(E)*-3-(3,4-dichlorophenyl)-1-(4-hydroxyphenyl)prop-2-en-1-one**

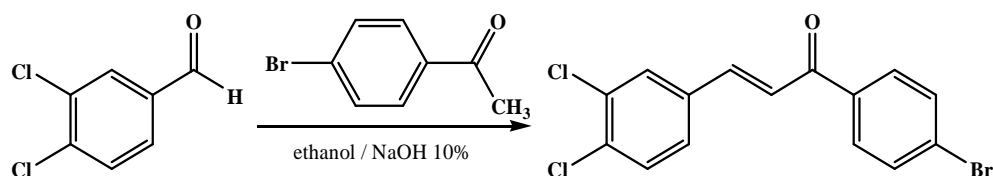
$^1\text{H-NMR}$  (500 MHz, DMSO)  $\delta$  H 6.93 (d, 2H, J: 8.5, Ar-CH), 7.27 (s, 1H, OH), 7.48 (m, 4H, Ar-CH + CH=CH), 7.23 (s, 1H, Ar-CH), 8.00 (d, 2H, J: 8.5, Ar-CH)

**EMAC 2148*****(E)*-3-(3,4-dichlorophenyl)-1-(3-hydroxyphenyl)prop-2-en-1-one**

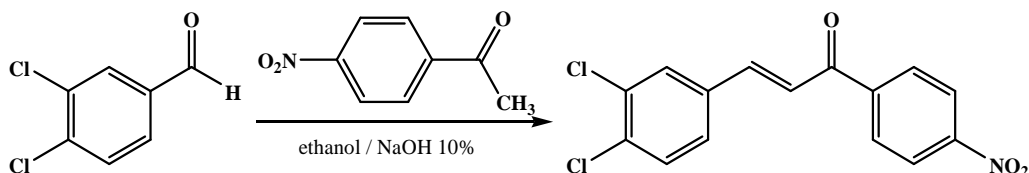
$^1\text{H-NMR}$  (500 MHz, DMSO)  $\delta\text{H}$  7.15 (d, 1H, J: 8, J: 2.5, Ar-CH), 7.41 (t, 1H, J: 8, Ar-CH), 7.58 (s, 1H, J: 2), 7.68 (m, 2H, Ar-CH), 7.73 (d, 1H, J: 15.5, CH-CH), 7.83 (d, 1H, J: 8.5, J: 2), 7.93 (d, 1H, J: 16, CH-CH), 8.12 (s, 1H, Ar-CH), 8.71 (s, 1H, OH)

**EMAC 2149*****(E)*-3-(3,4-dichlorophenyl)-1-(4-chlorophenyl)prop-2-en-1-one**

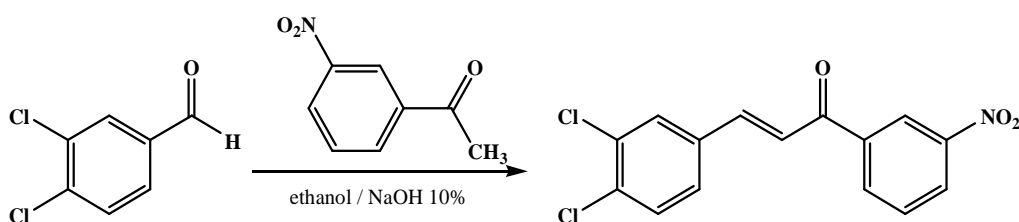
$^1\text{H-NMR}$  (500 MHz, DMSO)  $\delta\text{H}$  7.47 (m, 5H, Ar-CH + CH=CH), 7.7 (d, 1H, J: 15.5, CH=CH), 7.23 (s, 1H, Ar-CH), 7.96 (d, 2H, J: 8.5, Ar-CH)

**EMAC 2150*****(E)*-3-(3,4-dichlorophenyl)-1-(4-bromophenyl)prop-2-en-1-one**

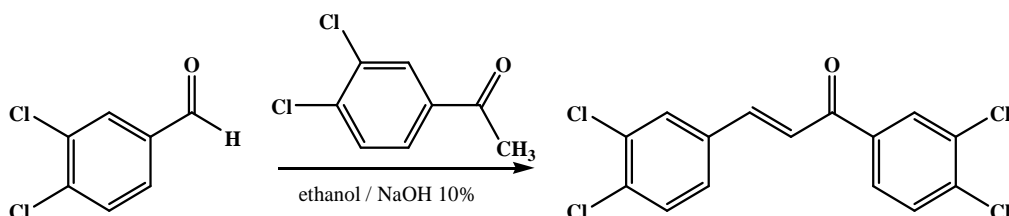
$^1\text{H-NMR}$  (500 MHz, DMSO)  $\delta\text{H}$  7.47 (m, 3H, J: 15.5, Ar-CH + CH=CH), 7.66 (d, 2H, J: 8.5, Ar-CH), 7.7 (d, 1H, J: 16, CH=CH), 7.73 (s, 1H, Ar-CH), 7.85 (d, 2H, J: 8.5, Ar-CH)

**EMAC 2151*****(E)*-3-(3,4-dichlorophenyl)-1-(4-nitrophenyl)prop-2-en-1-one**

$^1\text{H-NMR}$  (500 MHz, DMSO)  $\delta$ H 7.5 ( m, 3H, J: 15.5, Ar-CH + CH=CH), 7.76 ( m, 2H, J: 15.5, Ar-CH + CH=CH), 8.15 ( d, 2H, J: 8, Ar-CH), 8.37 ( d, 2H, J: 8, Ar-CH)

**EMAC 2152*****(E)*-3-(3,4-dichlorophenyl)-1-(3-nitrophenyl)prop-2-en-1-one**

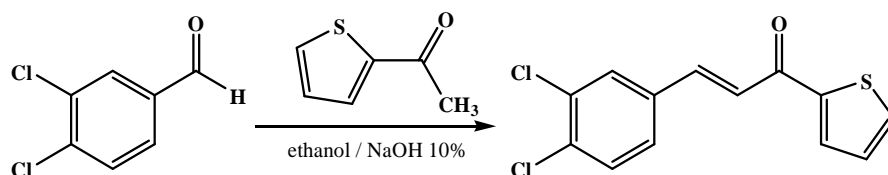
$^1\text{H-NMR}$  (500 MHz, DMSO)  $\delta$ H 7.5 ( d, 1H, J: 8, Ar-CH), 7.52 ( d, 1H, J: 8, Ar-CH), 7.53 ( d, 1H, J: 16, CH=CH), 7.74 ( t, 1H, J: 8), 7.77 ( s, 1H, Ar-CH), 7.78 ( d, 1H, J: 16, CH=CH), 8.35 ( d, 1H, J: 8, Ar-CH), 8.46 ( d, 1H, J: 8, Ar-CH), 8.83 ( s, 1H, Ar-CH)

**EMAC 2153*****(E)*-1,3-bis(3,4-dichlorophenyl)prop-2-en-1-one**

$^1\text{H-NMR}$  (500 MHz, DMSO)  $\delta$ H 7.42 ( d, 1H, J: 15.5, CH=CH), 7.47 ( d, 1H, J: 8, Ar-CH), 7.52 ( d, 1H, J: 8.5, Ar-CH), 7.6 ( d, 1H, J: 8, Ar-CH), 7.72 ( d, 1H, J: 15.5, CH=CH), 7.74 ( s, 1H, Ar-CH), 7.85 ( d, 1H, J: 8.5, Ar-CH), 8.1 ( s, 1H, Ar-CH)

**EMAC 2154**

***(E)*-3-(3,4-dichlorophenyl)-1-(thiophen-2-yl)prop-2-en-1-one**



$^1\text{H-NMR}$  (500 MHz, DMSO)  $\delta$ H 7.2 ( t, 1H, J: 4, J: 5, thiop.), 7.38 ( d, 1H, J: 15.5, CH=CH), 7.45 ( d, 1H, J: 8.5, Ar-CH), 7.5 ( d, 1H, J: 8.5, Ar-CH), 7.72 ( d, 1H, J: 5, thiop.), 7.72 ( d, 1H, J: 15.5, CH=CH), 7.73 ( s, 1H, Ar-CH), 7.87 ( d, 1H, J: 4, thiop.)

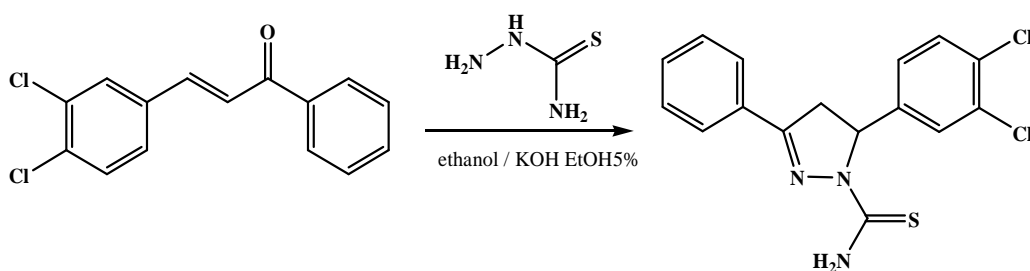
**Synthesis of 5-(3,4-dichlorophenyl)-3-aryl-4,5-dihydropyrazole-1-carbothioamide.**

5-(3,4-dichlorophenyl)-3-aryl-4,5-dihydropyrazole-1-carbothioamide was synthesised by reacting 1 mol of chalcone 1.2 mol of thiosemicarbazide and KOH in ethanol as depicted in Scheme 1. After 24 hours the precipitate that formed was filtered off. The filtrate was washed with ethyl ether and recrystallized from water/ethanol (1:1) to offer pure compounds.

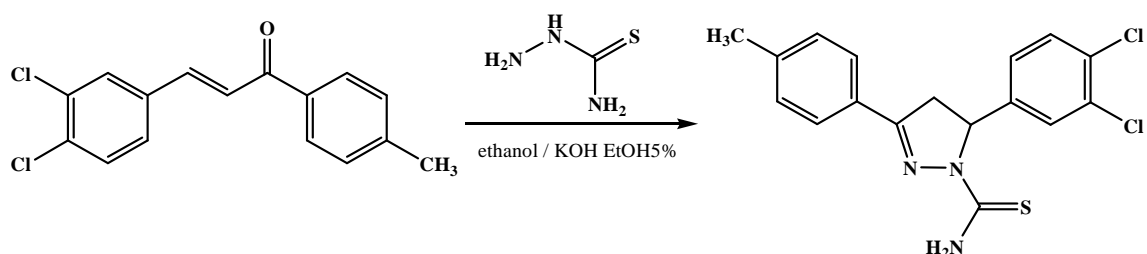
According to this procedure the following compounds have been synthesised:

**EMAC 2155**

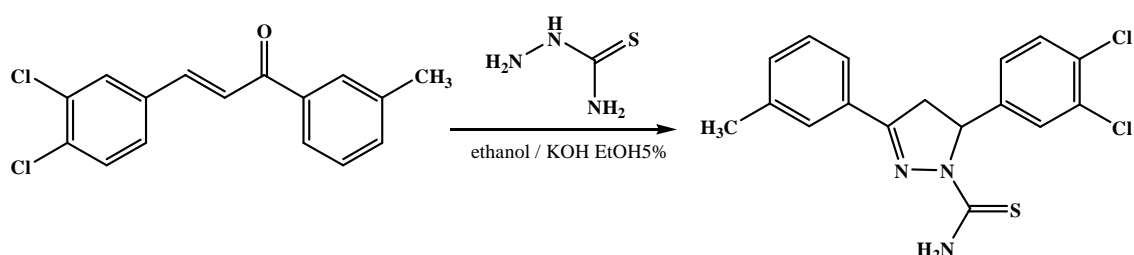
**5-(3,4-dichlorophenyl)-3-phenyl-4,5-dihydropyrazole-1-carbothioamide**



<sup>1</sup>H-NMR (300 MHz, DMSO) δH 3.17 ( dd, 1H, J: 4, J: 17.9; pyr), 3.86 ( dd, 1H, J: 12, J: 17.9, pyr), 5.99 ( dd; 1H, J: 4, J: 15, pyr), 6.08 (brs, 2H, NH<sub>2</sub>), 7.08 (d, 1H, J: 2.16, J: 8.32, Ar-CH), 7.30 (s, 1H, J: 2.16, Ar-CH), 7.40 ( d, 1H, J: 8.32, Ar-CH), 7.46 ( m, 3H, Ar-CH), 7.72 ( d, 2H, J: 2, J: 8.16, Ar-CH)

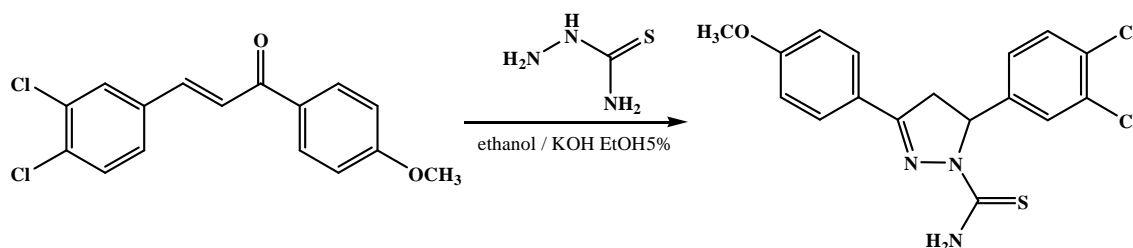
**EMAC 2156****5-(3,4-dichlorophenyl)-3-p-tolyl-4,5-dihydropyrazole-1-carbothioamide**

<sup>1</sup>H-NMR (300 MHz, DMSO) δH 2.46 ( s, 3H, CH<sub>3</sub>), 3.32 ( dd, 1H, J: 4, J: 18, pyr), 3.99 ( dd, 1H, J: 12, J: 18, pyr), 6.03 ( dd; 1H, J: 4, J: 12, pyr), 7.22 (d, 1H, J: 2, J: 8.32, Ar-CH), 7.39 ( d, 2H, J: 8.32, Ar-CH), 7.49 (s, 1H, Ar-CH), 7.70 ( d, 1H, J: 8.34, Ar-CH), 7.88 ( d, 2H, J: 8.01, Ar-CH), 8.05 ( brs, 1H, NH<sub>2</sub>), 8.23 (brs,1H, NH<sub>2</sub>)

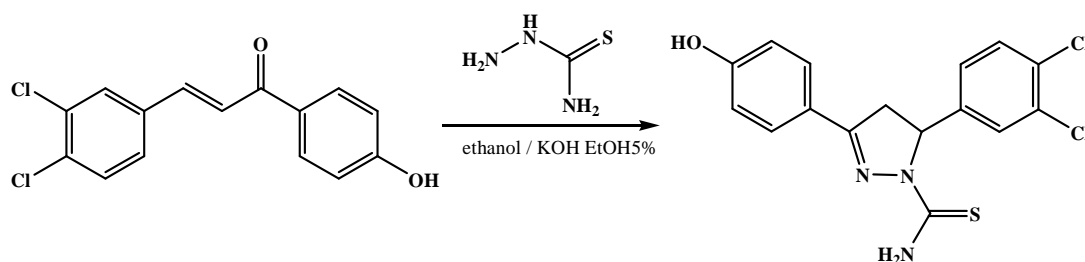
**EMAC 2157****5-(3,4-dichlorophenyl)-3-m-tolyl-4,5-dihydropyrazole-1-carbothioamide**

<sup>1</sup>H-NMR (300 MHz, DMSO) δH 2.40 ( s, 3H, CH<sub>3</sub>), 3.16 ( dd, 1H, J: 4, J: 18, pyr), 3.84 ( dd, 1H, J: 11.6, J: 18, pyr), 5.98 ( dd; 1H, J: 4, J: 11.6, pyr), 6.10 ( brs, 2H, NH<sub>2</sub>), 7.07 (d, 1H, J: 2.17, J: 8.32, Ar-CH), 7.32 (m, 3H, Ar-CH), 7.39 ( d, 1H, J: 8.32, Ar-CH), 7.5 ( m, 1H, Ar-CH), 7.54 ( s, 1H, Ar-CH)

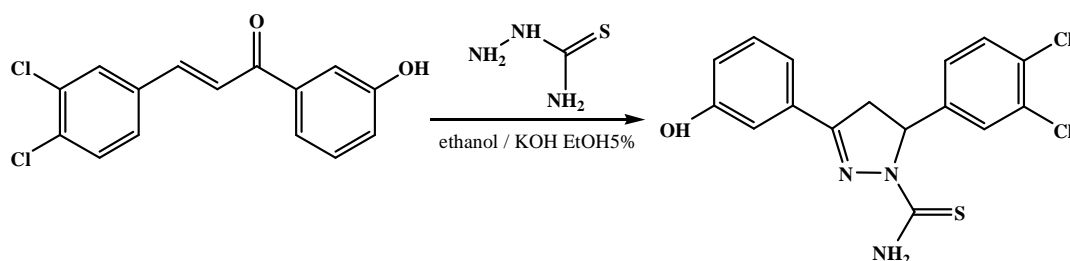


**EMAC 2158****5-(3,4-dichlorophenyl)-3-(4-methoxyphenyl)-4,5-dihydropyrazole-1-carbothioamide**

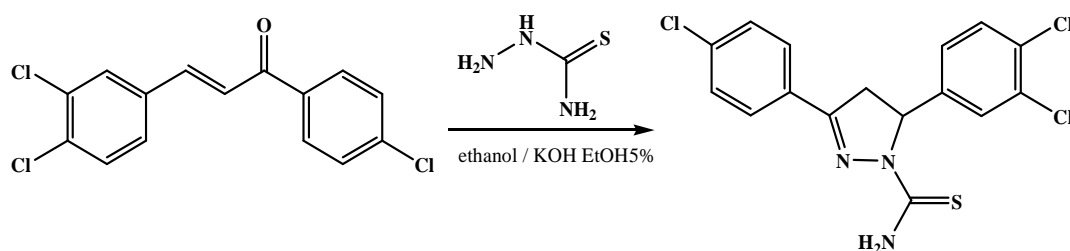
<sup>1</sup>H-NMR (300 MHz, DMSO) δH 3.31 ( dd, 1H, J: 3, J: 18, pyr), 3.92 (s, 3H, OCH<sub>3</sub>), 3.98 ( dd, 1H, J: 11.5, J: 18, pyr), 6.02 ( dd; 1H, J: 3, J: 11.5, pyr), 7.12 (d, 2H, J: 8, Ar-CH), 7.21 ( d, 1H, J: 8, Ar-CH), 7.48 (s, 1H, Ar-CH), 7.70 ( d, 1H, J: 8.6, Ar-CH), 7.93 ( d, 2H, J: 8.6, Ar-CH), 8.05 ( brs, 1H, NH<sub>2</sub>), 8.23 (brs, 1H, NH<sub>2</sub>)

**EMAC 2159****5-(3,4-dichlorophenyl)-3-(4-hydroxyphenyl)-4,5-dihydropyrazole-1-carbothioamide**

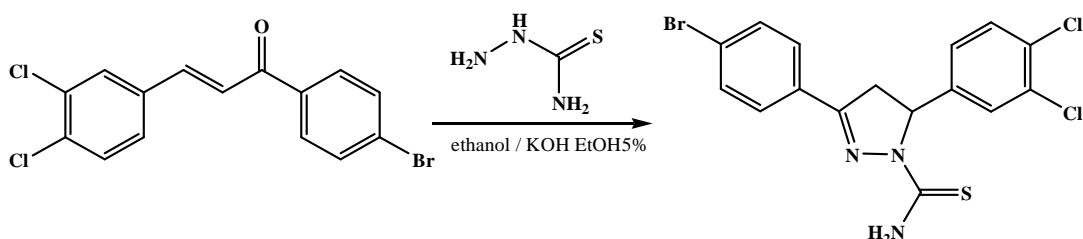
<sup>1</sup>H-NMR (300 MHz, DMSO) δH 3.26 ( dd, 1H, J: 3, J: 18, pyr), 3.45 ( dd, 1H, J: 11.2, J: 18, pyr), 6.00 ( dd; 1H, J: 3, J: 11.2, pyr), 6.93 (d, 2H, J: 8.5, Ar-CH), 7.21 (d, 1H, J: 1.8, J: 8.34, Ar-CH), 7.47 ( s, 1H, Ar-CH), 7.70 ( d, 1H, J: 8.34, Ar-CH), 7.82 ( d, 2H, J: 8.5, Ar-CH) 7.93 ( brs, 1H, NH<sub>2</sub>), 8.14 (brs, 1H, NH<sub>2</sub>), 10.16 ( s, 1H, OH)

**EMAC 2160****5-(3,4-dichlorophenyl)-3-(3-hydroxyphenyl)-4,5-dihydropyrazole-1-carbothioamide**

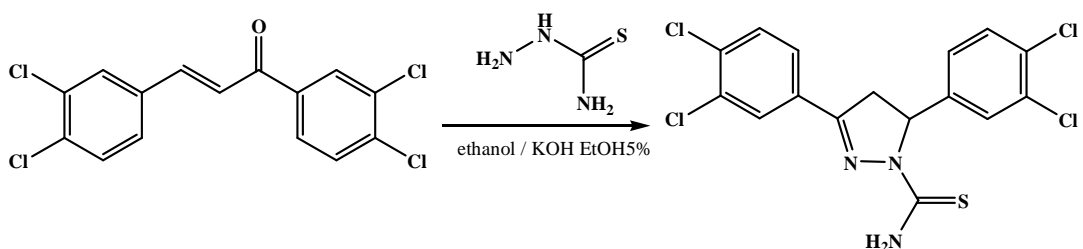
$^1\text{H-NMR}$  (300 MHz, DMSO)  $\delta\text{H}$  3.27 ( dd, 1H, J: 3, J: 18, pyr), 3.99 ( dd, 1H, J: 11.6, J: 18, pyr), 6.02 ( dd; 1H, J: 3, J: 11.6, pyr), 7.00 (d, 1H, J: 8, Ar-CH), 7.22 (d, 1H, J: 8, Ar-CH), 7.38 ( m, 3H, Ar-CH), 7.48 ( s, 1H, Ar-CH), 7.70 ( d, 1H, J: 8, Ar-CH) 8.02 ( brs, 1H,  $\text{NH}_2$ ), 8.24 (brs, 1H,  $\text{NH}_2$ ), 9.76 ( s, 1H, OH)

**EMAC 2161****5-(3,4-dichlorophenyl)-3-(4-chlorophenyl)-4,5-dihydropyrazole-1-carbothioamide**

$^1\text{H-NMR}$  (300 MHz, DMSO)  $\delta\text{H}$  3.34 ( dd, 1H, J: 4, J: 18, pyr), 4.00 ( dd, 1H, J: 11.5, J: 18, pyr), 6.04 ( dd; 1H, J: 4, J: 11.5, pyr), 7.22 (d, 1H, J: 8.5, Ar-CH), 7.49 (s, 1H, Ar-CH), 7.70 ( d, 2H, J: 8.3, Ar-CH), 7.78 ( d, 1H, J: 8.5, Ar-CH), 7.79 ( d, 2H, J: 8.3, Ar-CH), 8.16 ( brs, 1H,  $\text{NH}_2$ ), 8.30 (brs, 1H,  $\text{NH}_2$ )

**EMAC 2162****5-(3,4-dichlorophenyl)-3-(4-bromophenyl)-4,5-dihydropyrazole-1-carbothioamide**

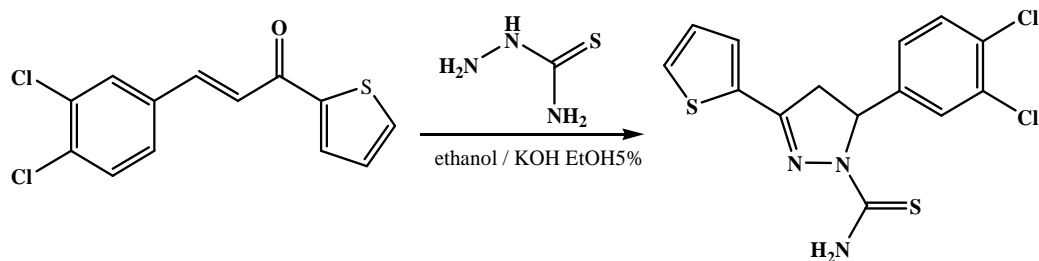
<sup>1</sup>H-NMR (300 MHz, DMSO) δH 3.34 ( dd, 1H, J: 4, J: 18, pyr), 4.00 ( dd, 1H, J: 11.5, J: 18, pyr), 6.04 ( dd; 1H, J: 4, J: 11.5, pyr), 7.22 ( d, 1H, J: 8.5, Ar-CH), 7.49 ( s, 1H, Ar-CH), 7.70 ( d, 2H, J: 8.3, Ar-CH), 7.78 ( d, 1H, J: 8.5, Ar-CH), 7.79 ( d, 2H, J: 8.3, Ar-CH), 8.16 ( brs, 1H, NH<sub>2</sub>), 8.30 ( brs, 1H, NH<sub>2</sub>)

**EMAC 2163****3,5-bis(3,4-dichlorophenyl)-4,5-dihydropyrazole-1-carbothioamide**

<sup>1</sup>H-NMR (300 MHz, DMSO) δH 3.38 ( dd, 1H, J: 4, J: 18.5, pyr), 3.99 ( dd, 1H, J: 12, J: 18.5, pyr), 6.05 ( dd; 1H, J: 4, J: 12, pyr), 7.22 ( d, 1H, J: 8.5, Ar-CH), 7.50 ( s, 1H, Ar-CH), 7.70 ( d, 1H, J: 8.34, Ar-CH), 7.84 ( d, 1H, J: 8.34, Ar-CH), 7.91 ( d, 1H, J: 8.5, Ar-CH), 8.32 ( m, 3H, NH<sub>2</sub> + Ar-CH)

**EMAC 2164**

**5-(3,4-dichlorophenyl)-3-(thiophen-2-yl)-4,5-dihydropyrazole-1-carbothioamide**



$^1\text{H-NMR}$  (300 MHz, DMSO)  $\delta$ H 3.38 ( dd, 1H, J: 4, J: 18, pyr), 4.05 ( dd, 1H, J: 11.4, J: 18, pyr), 6.07 ( dd; 1H, J: 4, J: 11.4, pyr), 7.22 ( d, 1H, J: 8.4, Ar-CH), 7.27 ( t, 1H, J: 3.8, J: 4.7, thiofene), 7.50 ( s, 1H, Ar-CH), 7.60 ( d, 1H, J: 3.8, thiofene), 7.71 ( d, 1H, J: 8.4, Ar-CH), 7.78 ( brs, 1H,  $\text{NH}_2$ ), 7.90 ( d, 1H, J: 4.7, thiofene), 8.24 ( brs, 1H,  $\text{NH}_2$ )

## **3.2 Pharmacologic studies**

### **3.2.1. Determination of MAO isoform activity**

The potential effects of the test drugs on human monoamineoxidase (hMAO) activity were investigated by measuring their effects on the production of hydrogen peroxide H<sub>2</sub>O<sub>2</sub> from p-tyramine (a common substrate for both hMAO-A and hMAO-B), using the Amplex<sup>®</sup>Red MAO assay kit (Molecular Probes, Inc., Eugene, Oregon, USA) and microsomal MAO isoforms prepared from insect cells (BTI-TN-5B1-4) infected with recombinant baculovirus containing cDNA inserts for hMAO-A or hMAO-B (SigmaAldrich Química S.A., Alcobendas, Spain). The production of H<sub>2</sub>O<sub>2</sub> catalysed by MAO isoforms can be detected using 10-acetyl-3,7-dihydroxyphenoxazine (Amplex<sup>®</sup>Red reagent), a non-fluorescent, highly sensitive and stable probe that reacts with H<sub>2</sub>O<sub>2</sub> in the presence of horseradish peroxidase to produce a fluorescent product: resorufin. In this study, hMAO activity was evaluated using the above method following the general procedure described previously by us. [25]

Briefly, 0.1 ml of sodium phosphate buffer (0.05 M, pH 7.4) containing the test drugs (new compounds or reference inhibitors) in various concentrations and adequate amounts of recombinant hMAO-A or hMAO-B required to oxidize (in the control group) 165 p mol of p-tyramine/min were incubated for 15 min at 37 °C in the corresponding wells from a 96-well flatbottom microtiter plate (BD, Franklin Lakes, NJ, USA) placed in the dark fluorimeter chamber. After this incubation period, the reaction was started by adding (final concentrations) 200 mM Amplex<sup>®</sup>Red reagent, 1 U/ml horseradish peroxidase and 1 mM p-tyramine as a common substrate for both hMAO-A and hMAO-B. The production of H<sub>2</sub>O<sub>2</sub> and, consequently, of resorufin was quantified at 37°C in a Multi-Detection microplate fluorescence reader (FLX800TM, Bio-Tek<sup>®</sup>Instruments, Inc., Winooski, VT, USA) based on the fluorescence generated (excitation 545 nm, emission 590 nm) over a 15 min period, a period in which the fluorescence increased linearly from the beginning. Control experiments were carried out simultaneously by replacing the test drugs (new compounds and reference inhibitors) with appropriate dilutions of the vehicles. In addition, the possible ability of the above test drugs to modify the fluorescence generated in the reaction mixture due to non-enzymatic inhibition (e.g., for directly reacting with Amplex<sup>®</sup>Red reagent) was determined by adding these drugs to solutions containing only the Amplex<sup>®</sup>Red reagent in a sodium phosphate buffer. The specific fluorescence emission (used to obtain the final results) was calculated after subtraction of the background activity, which was determined from vials containing all

components except the MAO isoforms, which were replaced by a sodium phosphate buffer solution.

### **3.2.2 Data presentation and statistical analysis**

Unless otherwise specified, results shown in the text and table are expressed as mean  $\pm$  standard error of the mean (S.E.M.) from  $n$  experiments. Significant differences between two means ( $P < 0.05$  or  $P < 0.01$ ) were determined by one-way analysis of variance (ANOVA) followed by the Dunnett's post-hoc test.

To study the possible effects of the test drugs (new compounds or reference inhibitors) on MAO isoform enzymatic activity, the variation of fluorescence per unit of time (fluorescence arbitrary U/min) and, indirectly, the rate of  $H_2O_2$  production and, therefore, the p mol/min of resorufin produced in the reaction between  $H_2O_2$  and Amplex<sup>®</sup>Red reagent was evaluated. For this purpose, several concentrations of resorufin were used to prepare a standard curve with  $X = p$  mol resorufin and  $Y =$  fluorescence arbitrary U. Note that the value of resorufin production is similar to the p mol of p-tyramine oxidized to p-hydroxyphenylacetaldehyde per min since the stoichiometry of the reaction (p-tyramine oxidized by MAO isoforms/resorufin produced) is 1:1.

In these experiments, the inhibitory activity of the tested drugs (new compounds and reference inhibitors) is expressed as  $IC_{50}$ , i.e. the concentration of these compounds required to reduce by 50% the control MAO isoform enzymatic activity, estimated by least-squares linear regression, using the Origin<sup>™</sup> 5.0 program (Microcal Software, Inc., Northampton, MA, USA), with  $X =$  log of tested compound molar concentration and  $Y =$  the corresponding percentage of inhibition of control resorufin production obtained with each concentration. This regression was performed using data obtained with 4-6 different concentrations of each tested compound which inhibited the control MAO isoform enzymatic activity by between 20 and 80%. In addition, the corresponding MAO-B selectivity ratios (SI A/B) [ $IC_{50}$  (MAO-A)]/[ $IC_{50}$  (MAO-B)] were calculated.

### **3.2.3 Drugs and chemicals**

The drugs used in the experiments were the new compounds, moclobemide (a generous gift from F. Hoffmann-La Roche Ltd., Basel, Switzerland), R(-)-deprenyl hydrochloride, iproniazid phosphate (purchased from SigmaAldrich, Spain), resorufin sodium salt, clorgyline hydrochloride, p-tyramine hydrochloride and horseradish peroxidase (supplied in the Amplex<sup>®</sup> Red MAO assay kit from Molecular Probes).

Appropriate dilutions of the above drugs were prepared every day immediately before use in deionized water from the following concentrated stock solutions kept at  $-20$  °C: the new compounds (0.1 M) in dimethylsulfoxide (DMSO); R(-)-deprenyl,

moclobemide, iproniazid, resorufin, clorgyline, p-tyramine and horseradish peroxidase (0.1 M) in deionized water.

Due to the photosensitivity of some chemicals (e.g., Amplex®Red reagent), all experiments were performed in the dark. In all assays, neither deionized water (Milli-Q®, Millipore Ibérica S.A., Madrid, Spain) nor appropriate dilutions of the vehicle used (DMSO) had significant pharmacological effects.

## **4 Acknowledgments**

*This work was supported by Regione Autonoma della Sardegna.*

*Fondazione Banco di Sardegna granted my PhD.*

*I acknowledge Dr Matilde Yáñez (Department of Pharmacology, University of Santiago de Compostela, Spain) for biological investigation.*



## 5 Reference and notes

- [1] Wouters, J. Structural aspects of monoamine oxidase and its reversible inhibition. *Curr. Med. Chem.*, **5**, (1998), 137-162.
- [2] Kalgutkar, S.A.; Castagnoli, J.N.; Testa, B. Selective inhibitors of monoamine oxidase (MAO-A and MAO-B) as probes of its catalytic site and mechanism. *Med. Res. Rev.*, **15**, (1995), 325-388.
- [3] Volz, H.P.; Gleiter, C.H. Monoamine oxidase inhibitors: a perspective on their use in the Elderly. *Drugs Aging*, **13**, (1998), 341-355.
- [4] Cesura, A.M.; Pletscher, A. The new generation of monoamine oxidase inhibitors. *Prog. Drug Res.*, **38**, (1992), 171-297.
- [5] Saura, J.; Luque, J.M.; Cesura, A.M.; Da Prada, M.; Chan-Palay, V.; Huber, G.; Loffler, J.; Richards, J.G. Increased monoamine oxidase B activity in plaque-associated astrocytes of Alzheimer brains revealed by quantitative enzyme radioautography. *Neuroscience*, **62**, (1994), 15-30.
- [6] Amrein, R.; Martin, J.R.; Cameron, A.M. Moclobemide in patients with dementia and depression. *Adv. Neurol.*, **80**, (1999), 509-519.
- [7] Palmer, A.M.; DeKosky, S.T. Monoamine neurons in aging and Alzheimer's disease. *J. Neural Transm.*, **91**, (1993), 135-159.
- [8] Alper, G.; Girgin, F.K.; Ozgönül, M.; Mentés, G.; Ersöz, B. MAO inhibitors and oxidant stress in aging brain tissue. *Eur. Neuropsychopharmacol.*, **9**, (1999), 247-252.
- [9] Good, P.F.; Werner, P.; Hsu, A.; Olanow, C.W.; Perl, D.P. Evidence of neuronal oxidative damage in Alzheimer's disease. *Am. J. Pathol.*, **149**, (1996), 21-28.
- [10] Drukarch, B.; Van Muiswinkel, F.L. Drug treatment of Parkinson's disease: time for phase II. *Biochem. Pharmacol.*, **59**, (2000), 1023-1031.
- [11] Cash, A.D.; Perry, G.; Smith, M.A. Therapeutic potential in Alzheimer disease. *Curr. Med. Chem.*, **9**, (2002), 1605-1610.
- [12] Sramek, J.J.; Cutler, N.R. Recent developments in the drug treatment of Alzheimer's disease. *Drugs Aging*, **14**, (1999), 359-373.
- [13] Yu, P.H. Pharmacological and clinical implications of MAO-B inhibitors. *Gen. Pharmacol. Vasc. Syst.*, **25**, (1994), 1527-1539.
- [14] Sramek, J.J.; Cutler, N.R. Ongoing trials in Alzheimer's disease. *Expert Opin. Investig. Drugs*, **9**, (2000), 899-915.
- [15] Chimenti, F.; Maccioni, E.; Secci, D.; Bolasco, A.; Chimenti, P.; Granese, A.; Befani, O.; Turini, P.; Alcaro, S.; Ortuso, F.; Cirilli, R.; La Torre, F.; Cardia, M.C.; Distinto, S. Synthesis, molecular modeling studies, and selective inhibitory activity against

- monoamine oxidase of 1-thiocarbamoyl-3,5-diaryl-4,5-dihydro-(1H)-pyrazole derivatives. *J. Med. Chem.*, **48**, (2005), 7113-7122.
- [16] Chimenti, F.; Maccioni, E.; Secci, D.; Bolasco, A.; Chimenti, P.; Granese, A.; Befani, O.; Turini, P.; Alcaro, S.; Ortuso, F.; Cardia, M.C.; Distinto, S. Selective inhibitory activity against MAO and molecular modeling studies of 2-thiazolyldiazone derivatives. *J. Med. Chem.*, **50**, (2007), 707-712.
- [17] Maccioni, E.; Alcaro, S.; Orallo, F.; Cardia, M.C.; Distinto, S.; Costa, G.; Yanez, M.; Sanna, M.L.; Vigo, S.; Meleddu, R.; Secci, D. Synthesis of new 3-aryl-4,5-dihydropyrazole-1-carbothioamide derivatives. An investigation on their ability to inhibit monoamine oxidase. *European Journal of Medicinal Chemistry*, **45**, (2010), 4490-4498.
- [18] Chimenti, F.; Bolasco, A.; Manna, F.; Secci, D.; Chimenti, P.; Granese, A.; Befani, O.; Turini, P.; Cirilli, R.; LaTorre, F.; Alcaro, S.; Ortuso, F.; Langer, T. Synthesis, biological evaluation and 3D-QSAR of 1,3,5-trisubstituted-4,5-dihydro-(1H)-pyrazole derivatives as potent and highly selective monoamine oxidase a inhibitors. *Curr. Med. Chem.*, **13**, (2006), 1411-1428.
- [19] Distinto, S.; Yáñez, M.; Alcaro, S.; Cardia, M. C.; Gaspari, M.; Sanna M. L.; Meleddu, R.; Ortuso, F.; Kirchmair, J.; Markt, P.; Bolasco, A.; Wolber, G.; Secci, D.; Maccioni, E. Synthesis and biological assessment of novel 2-thiazolyldiazones and computational analysis of their recognition by monoamine oxidase B. *European Journal of Medicinal Chemistry*, **48**, (2012), 284-295
- [20] Chen, J.J.; Swope, D.M.; Dashtipour, K. Comprehensive review of rasagiline, a second-generation monoamine oxidase inhibitor, for the treatment of Parkinson's Disease. *Clin. Ther.*, **29**, (2007), 1825-1849.
- [21] Fariello, R.G. Safinamide. *Neurotherapeutics*, **4**, (2007), 110-116.
- [22] Distinto, S.; Meleddu, R.; Arridu, A.; Bianco, G.; Yáñez, M.; Alcaro, S.; Maccioni E.; unpublished results.
- [23] Claisen, L.; Claparède, A. Condensationen von Ketonen mit Aldehyden". *Berichte der Deutschen Chemischen Gesellschaft* 14 (1), (1881), 2460–2468.
- [24] Schmidt, J. G. Ueber die Einwirkung von Aceton auf Furfurol und auf Bittermandelöl in Gegenwart von Alkalilauge. *Berichte der Deutschen Chemischen Gesellschaft* 1, 4 (1), (1881), 1459–1461.
- [25] Yáñez, M.; Fraiz, E.; Cano, E.; Orallo, F. Inhibitory effects of cis- and trans- resveratrol on noradrenaline and 5-hydroxytryptamine uptake and on monoamine oxidase activity. *Biochem. Biophys. Res. Commun.*, **344**, (2006) 688-695.

## **IV PART:**

### **Synthesis of new ligands of G-Quadruplex as potential antitumor agents**

## CONTENTS

1	<i>Introduction</i>	
	1.1 <i>Historical overview</i>	3
2	<i>Fluorenone derivatives</i>	8
3	<i>Results and discussion</i>	14
4	<i>Conclusion</i>	18
5	<i>Chemistry</i>	19
	5.1 <i>Work in progress</i>	24
6	<i>Acknowledgments</i>	32
7	<i>References and notes</i>	33





## 1 Introduction

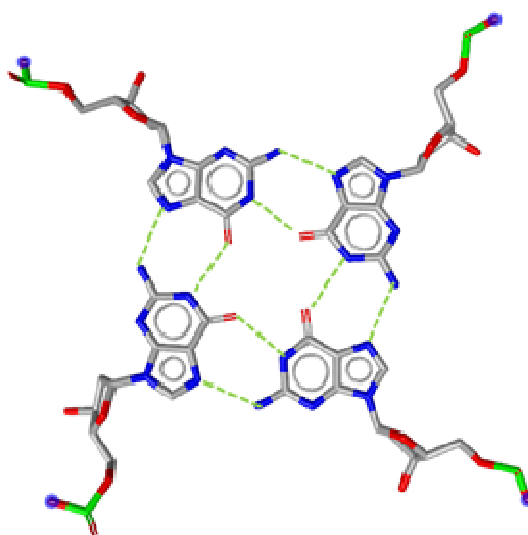
### 1.1 Historical overview

In a recent study published in Nature Chemistry a method to quantitatively visualize DNA G-quadruplex structures in human cells has been reported.

This work clear links between concentrations of four-stranded quadruplexes and the process of DNA replication, which is pivotal to cell division and production.

Furthermore, it corroborates the application of stabilizing ligands in a cellular context to target G-quadruplexes and interfere with their function. [1]

G-quadruplex structures are nucleic acid arrangements assumed by guanine-rich sequences and stabilized by the planar pairing of four guanines through eight Hoogsteen hydrogen bonds.

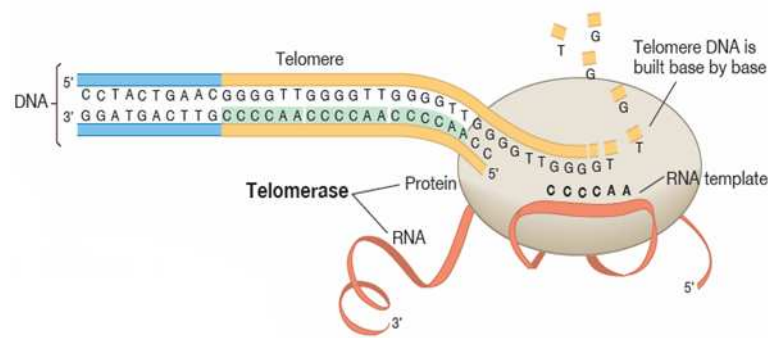


**Figure 1.** Chemical structure of the G-quartet that is formed by Hoogsteen base pairs of four guanine bases

The space between G-tetrads is well suited to coordinate monovalent cations ( $K^+$  and occasionally  $Na^+$ ) which are required to stabilize the structure through their coordination to the guanyl oxygens. The overlapping of G-quartet tetrads leads to the formation of more complex structures called G-quadruplexes. These sequences are found in crucial positions of the genome, such as telomeric ends, ribosomal DNA (rDNA), RNA or gene promoter regions (for es. *c-myc*, *bcl-2* or *c-kit*). [2]

Their composition and location is conserved through evolution and, additionally, several proteins are devoted to recognize or resolve them, [3] thus indicating regulatory roles of these structures in multiple biological processes. [4]

In normal cells the telomeric DNA is gradually shortened after each replication cycle until a critical limit is reached (“Hayflick Limit”), leading to cellular senescence and, ultimately, to apoptosis. The enzyme telomerase, which has a reverse transcriptase subunit (hTERT) and an RNA component (hTERC), adds TTAGGG repeats to telomeres providing their elongation and, subsequently, cell immortalization (Figure 2). [5]

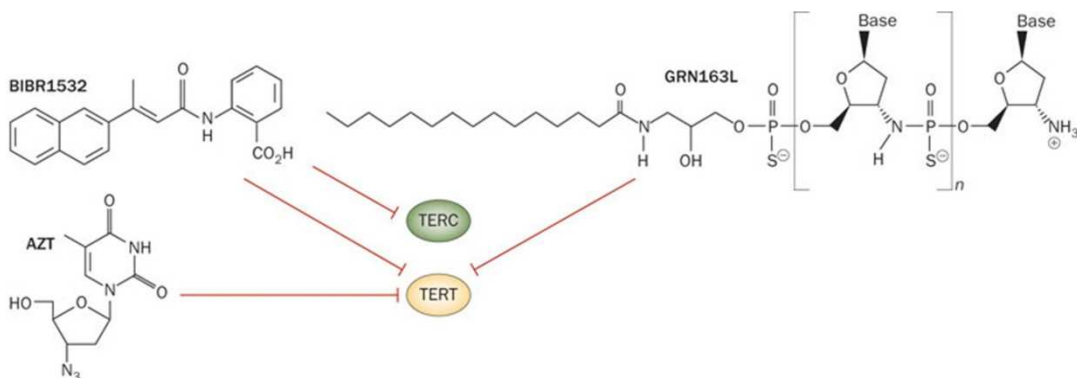


**Figure 2.** Telomerase mechanism of action

A number of studies highlighted that immortality of cancer cells is due, at least in part, to constitutive expression of telomerase, while somatic cells either entirely lack telomerase or exceptionally express low levels. Its action is detected in most primary human tumour specimens and tumour-derived cell lines, such as those of the prostate, breast, colon, lung and liver.

Hence, inhibition of this enzyme can selectively prevent cancer cells growth.

Several small molecule inhibit telomerase directly, e.g GRN163L, BIBR1532 and AZT (Figure 3). [6, 7]



**Figure 3.** Agents targeting hTERC and hTERT of telomerase enzyme



A different approach is the stabilization of G-quadruplex-DNA.

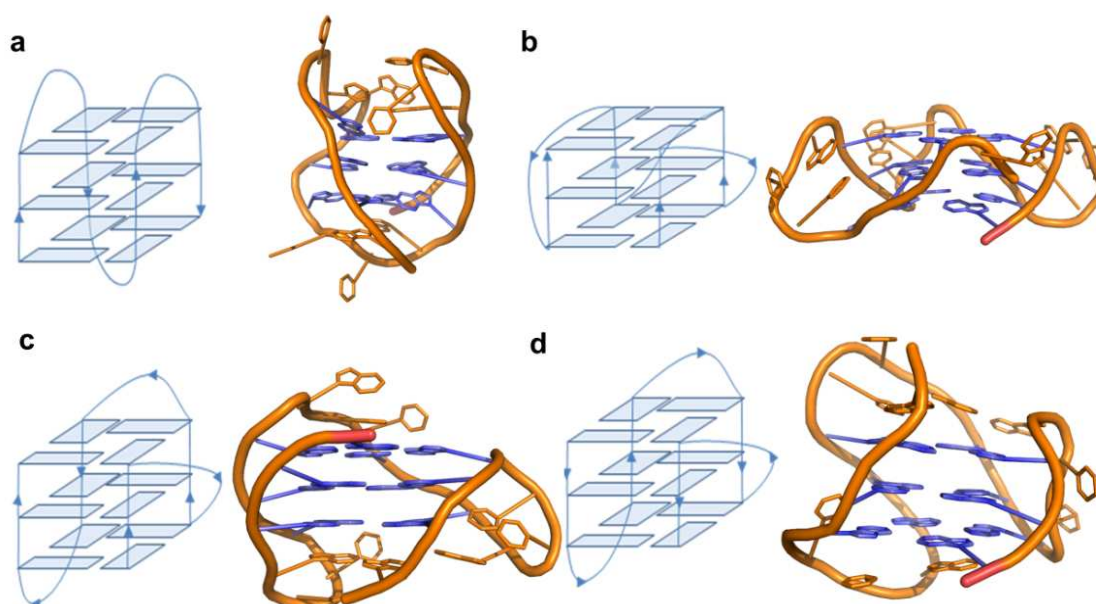
G-quadruplex-DNA stabilizers preclude the binding of telomerase and its associated proteins to telomeres and, thereby, stop the elongation process of telomerase indirectly.

Equally important is the stabilization of G-quadruplex in promoter regions or in rDNA and rRNA to achieve selective gene regulation. [8-10]

Quadruplexes can be formed from one, two or four separate strands of DNA (or RNA) and can show a wide variety of topologies, depending on combinations of strand orientation, loops size and glycoside conformation sequence.

These different arrangements are dictated not only by the nucleic acid sequence, but, as in the case of the human telomeric DNA, a given sequence can fold into a variety of different conformations according to environmental transitions. [11]

Indeed, whereas the crystal structure of the DNA G-quadruplex assumed by wild type Tel22  $AG_3[T_2AG_3]_3$  in  $K^+$  is parallel stranded, [12] multiple G-quadruplex conformations (Figure 4) have been reported in solution. [4, 11]

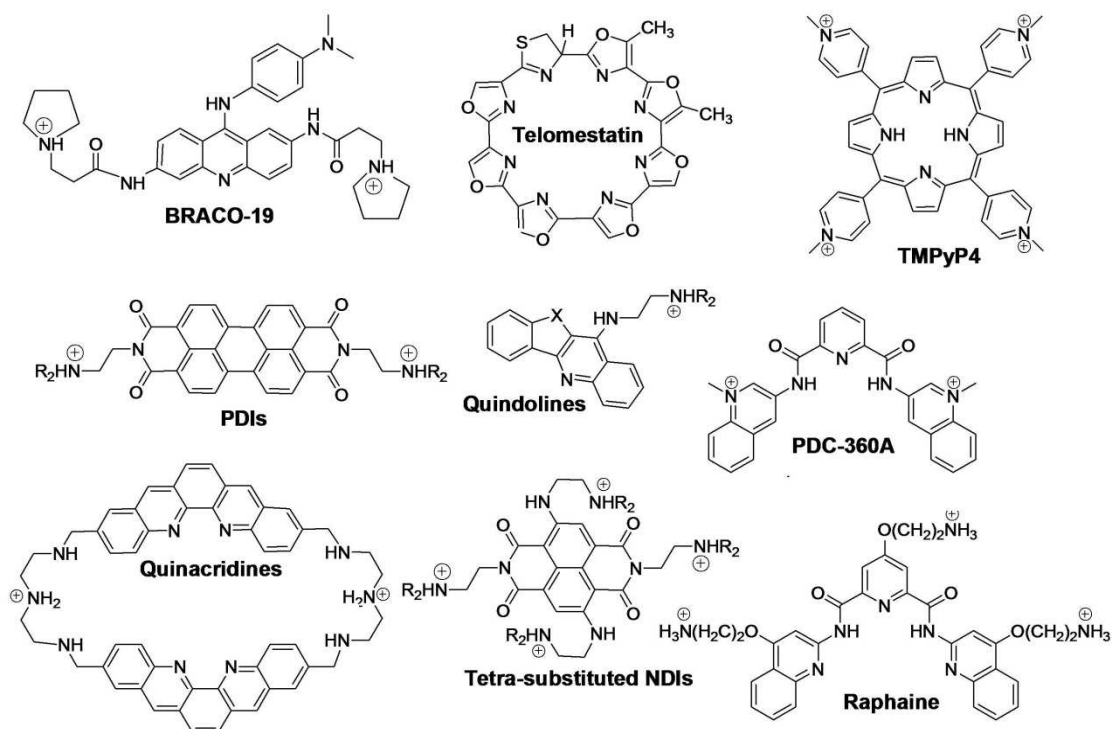


**Figure 4.** Schematic and 3D representation of the a) antiparallel or basket-type (PDB code 143D), [13] b) parallel or propeller-like (PDB code 1KF1), [12] c) hybrid type-1 (PDB code 2HY9) [14] and d) hybrid type-2 (PDB code 2JPZ) [15] DNA G-quadruplex conformations of  $d(AG_3[T_2AG_3]_3)$  sequence

Several studies have been devoted to develop novel G-quadruplex binders (Figure 5). [16]

The common structural feature of all these ligands is an extended polyaromatic (often heteroaromatic) planar chromophore, generally composed of three or four fused rings, bearing one or more positive charge(s).

The natural product telomestatine, composed of one thiazoline and seven oxazole rings, was reported to be a potent nanomolar telomerase inhibitor, with evidence indicating that its mechanism of action also involves a G-quadruplex complex. [17]

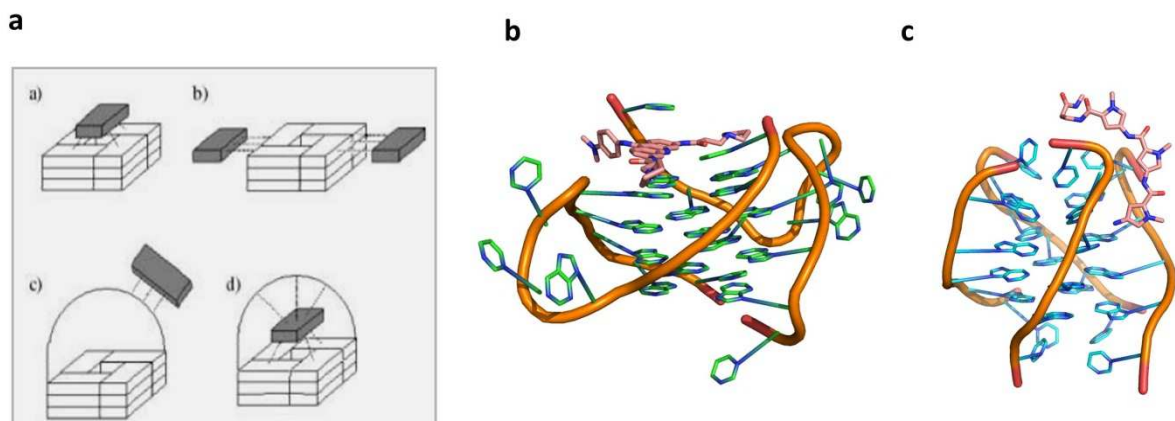


**Figure 5.** Some of the human telomeric DNA G-4 binders available in literature

An essential requirement for telomerase inhibition and antitumor effect is the low concentration of inhibitor, which needs to be below acute toxicity levels, otherwise generalized cytotoxic effect outside tumours will take place.

In some cases, it was reported that antitumor agents that bind to duplex DNA, may develop their cytotoxic activity by interfering with transcription or with the correct function of DNA topoisomerases or other enzymes involved in DNA replication.

G4-binders may be accommodated in multiple sites of the structure: mainly they can stack on the G-tetrads, but they can also be located into the grooves or can interact with the loop bases (Figure 6). [18]



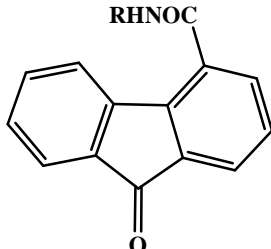
**Figure 6.** Binding modes: **a)** Schematic representation of possible ligand-quadruplex binding modes **a)** stacking or intercalation between internal tetrads **b)** groove recognition; **c)** interaction with single strand loops **d)** simultaneously end stacking and loop interaction or simultaneously end stacking and binding into the grooves **b)** stacking (BRACO-19, pdbcode 3CDM [19]); **c)** groove and loop interaction (distamycin, pdbcode 2KVY [20])

Although some of them achieved preclinical and clinical phase, none reached the market so far. The major limitations associated to their questionable biological use are the poor selectivity for quadruplex DNA, the propensity to aggregate in aqueous media, the poor water-solubility, and the chemical instability. [21]

To address this issue, a large synthetic effort have been merged to computational methods.

## 2 Fluorenone derivatives

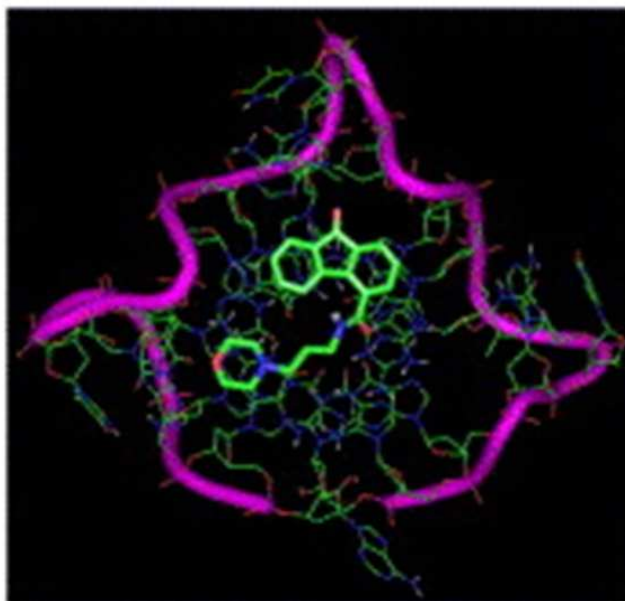
A small series of fluorenone derivatives demonstrated to selectively bind the human telomeric repeated sequence d[AG<sub>3</sub>[T<sub>2</sub>AG<sub>3</sub>]<sub>3</sub>] with respect to duplex and triplex sequences. [22]

			
compound	R	compound	R
1	-(CH <sub>2</sub> ) <sub>2</sub> OH	6	-(CH <sub>2</sub> ) <sub>2</sub> N(CH <sub>3</sub> ) <sub>2</sub>
2	-(CH <sub>2</sub> ) <sub>3</sub> OH	7	-(CH <sub>2</sub> ) <sub>3</sub> N(CH <sub>3</sub> ) <sub>2</sub>
3	-CH <sub>2</sub> CH(OH)CH <sub>3</sub>	8	-(CH <sub>2</sub> ) <sub>2</sub> N(CH <sub>2</sub> CH <sub>3</sub> ) <sub>2</sub>
4	-(CH <sub>2</sub> )OH	9	-(CH <sub>2</sub> ) <sub>2</sub> -Morph
5	-(CH <sub>2</sub> )O(CH <sub>2</sub> ) <sub>2</sub> OH	10	-(CH <sub>2</sub> ) <sub>3</sub> -Morph

**Figure 7.** Chemical structures of first series of fluorenones compounds 1–10

Among them the most interesting were the compounds 9 and 10 substituted with morpholino side-chain able to interact selectively with the DNA G-quadruplex (Figure 7).

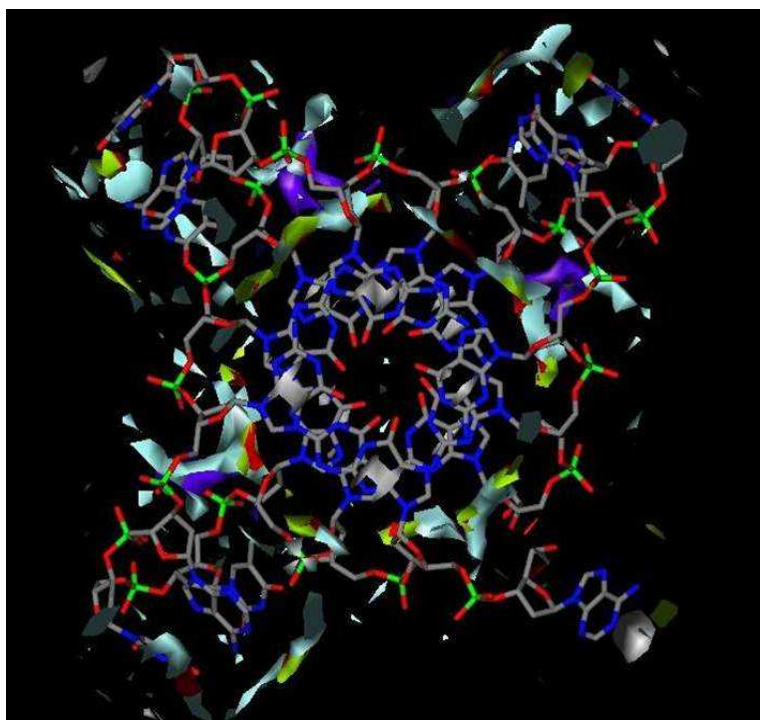
Consistent differential effects on the binding preferences of the morpholino derivatives 9 and 10 were confirmed by molecular modeling, demonstrating a major role in the length of the linker between the aromatic and heterocyclic rings (Figure 8).



**Figure 8.** Best docking pose of compound 10 into G-quadruplex with parallel conformation (pdbcode 1KF1)

Considering these preliminary interesting results, an optimization of the fluorenone analogues was performed using the GRID method. [23]

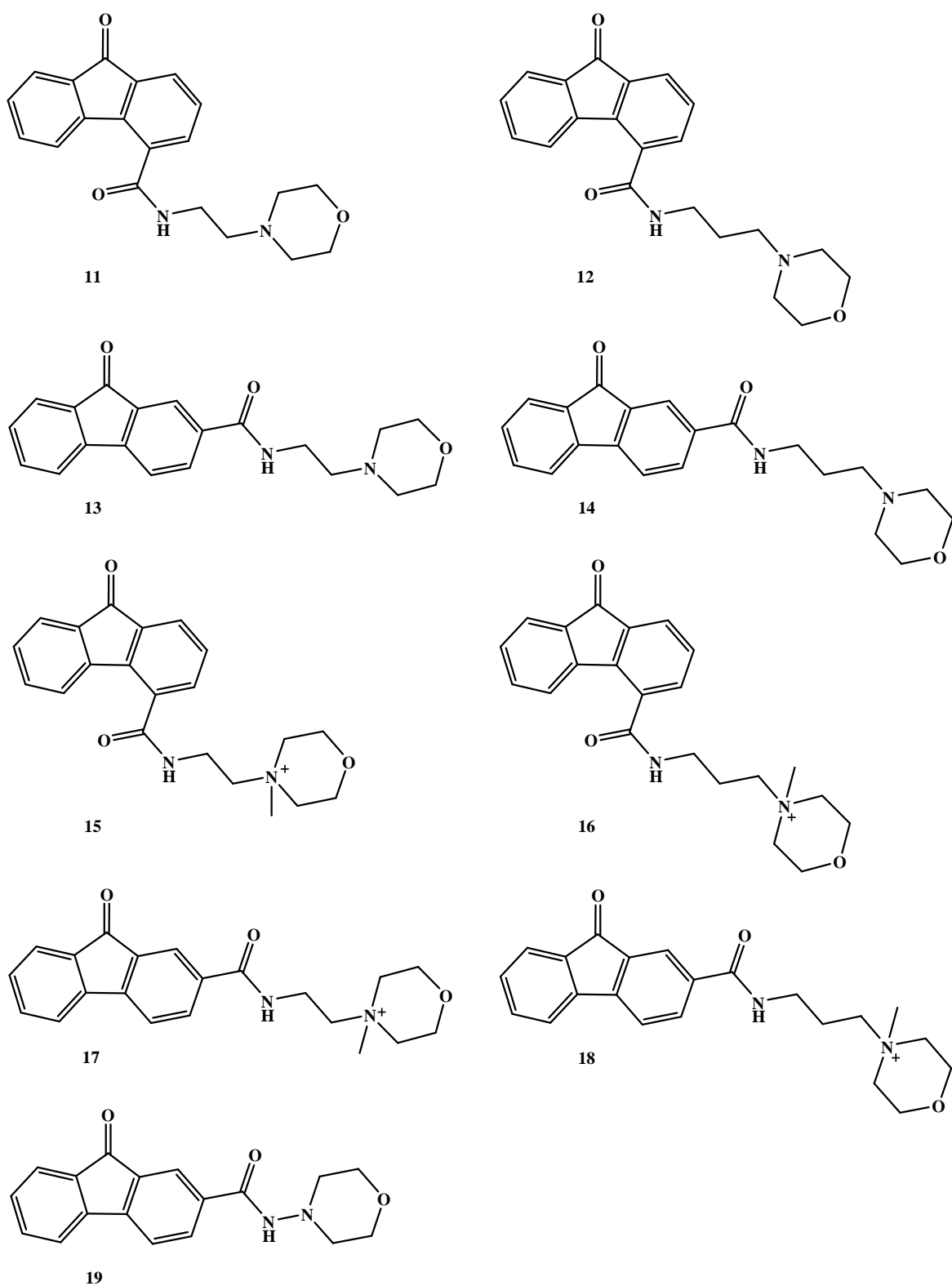
On the basis of the GRID MIFs (Molecular Interaction Fields) [24] visualization results, it was decided to insert a quaternary nitrogen at the morpholino side chain because NM3 (Trimethyl Ammonium cation) probe mapped as energetically favoured several areas in the grooves and loops of G-quadruplex.



**Figure 9.** NM3 (quaternary nitrogen) MIFs maps obtained with GRID software in the G-quadruplex with parallel conformation

A series of nine novel compounds were designed and synthesized with the following chemical features:

- quaternary nitrogen at the morpholino side chain;
- variable linker between the morpholino and fluorenone rings (from 0 to 3 methylenes);
- alternative positions 2 and 4 in the side chain substitution onto the fluorenone ring (Figure 10)



**Figure 10.** Second series of fluorenone derivatives 11-19

compound	IC <sub>50</sub> [μM]	
	M14	A549
11	>200	183±5.3
12	>200	>200
13	79.5±3.2	70.5±2.9
14	72.2±4.6	45±3.9
15	>200	123±4.8
16	>200	>200
17	145±5.5	94.16±4.5
18	105±4.9	61.5±4.9
19	>200	>200

**Table 1.** Summary of the in vitro results of compounds 11–19 against melanoma (M14) and lung (A549) cancer cell lines

Docking experiments coupling opensource AutoDock[25] with our collaborators in-house docking code MolInE [26] were performed and a good correlation with experimental data was achieved (Table 2).

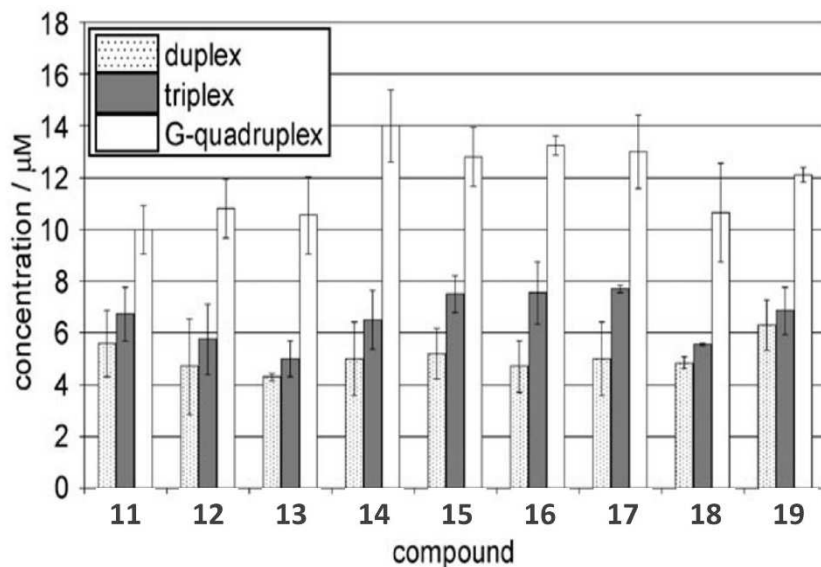
Lig	MolInE				AutoDock				Consensus			A549 IC50 (μM)
	1KF1	143D	2HY9	2JPZ	1KF1	143D	2HY9	2JPZ	MolInE	AD	Both	
<b>13</b>	-41.9	-36.2	-34.5	-40.4	-41.4	-37.1	-40.6	-43.8	-38.3	-40.7	-39.5	70.5
<b>14</b>	-46.3	-37.6	-45.5	-43.8	-41.3	-41.0	-39.6	-48.7	-43.3	-42.7	-43.0	45.0
<b>17</b>	-41.1	-36.3	-34.3	-41.0	-31.2	-33.8	-32.4	-40.6	-38.2	-34.5	-36.3	94.0
<b>18</b>	-39.6	-35.7	-39.5	-45.5	-36.0	-36.9	-41.7	-38.1	-40.1	-38.2	-39.1	61.5

**Table 2.** Docking results obtained with the X-ray (1KF1), NMR (143D) and hybrid optimized (2HY9 and 2JPZ) PDB models in complex with the most active compounds

Computational results indicated that the 2-substituted derivatives (**13**, **14**, **17**, and **18**) perform better than their 4-substituted analogues. Moreover the quaternarisation of the morpholinium nitrogen is well tolerated.

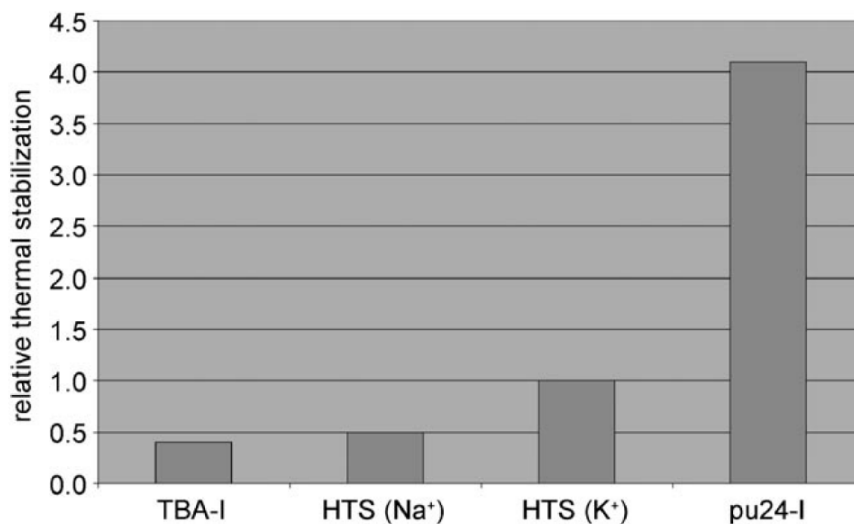


A small increment of G-quadruplex melting point was registered.



**Figure 11.** Competition dialysis results for compounds 11–19 against three polymorphs of DNA: duplex, triplex, and G-quadruplex as indicated

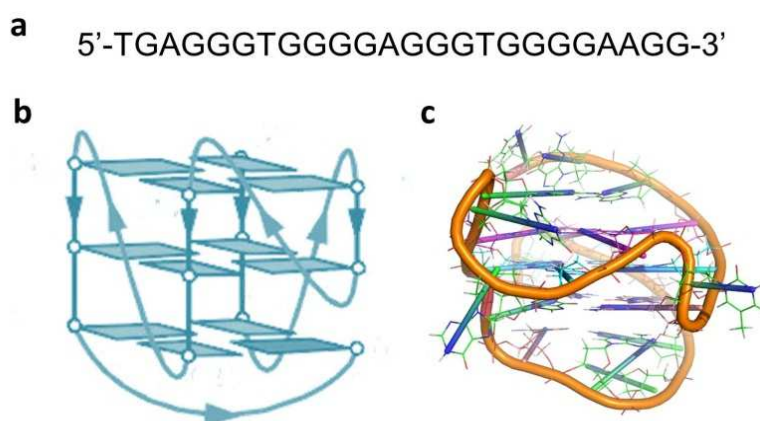
Furthermore compound **18** induced an appealing stabilization of pu24-I, a portion of the c-myc promoter that assumes a parallel arrangement in solution [27] (Figure 12).



**Figure 12.** Relative variations of G-quadruplex structure melting temperatures with reference to human telomeric sequence at K<sup>+</sup> 50 mM concentration. Data refer to 30 mM ligand concentrations of compound 18

### 3 Results and Discussion

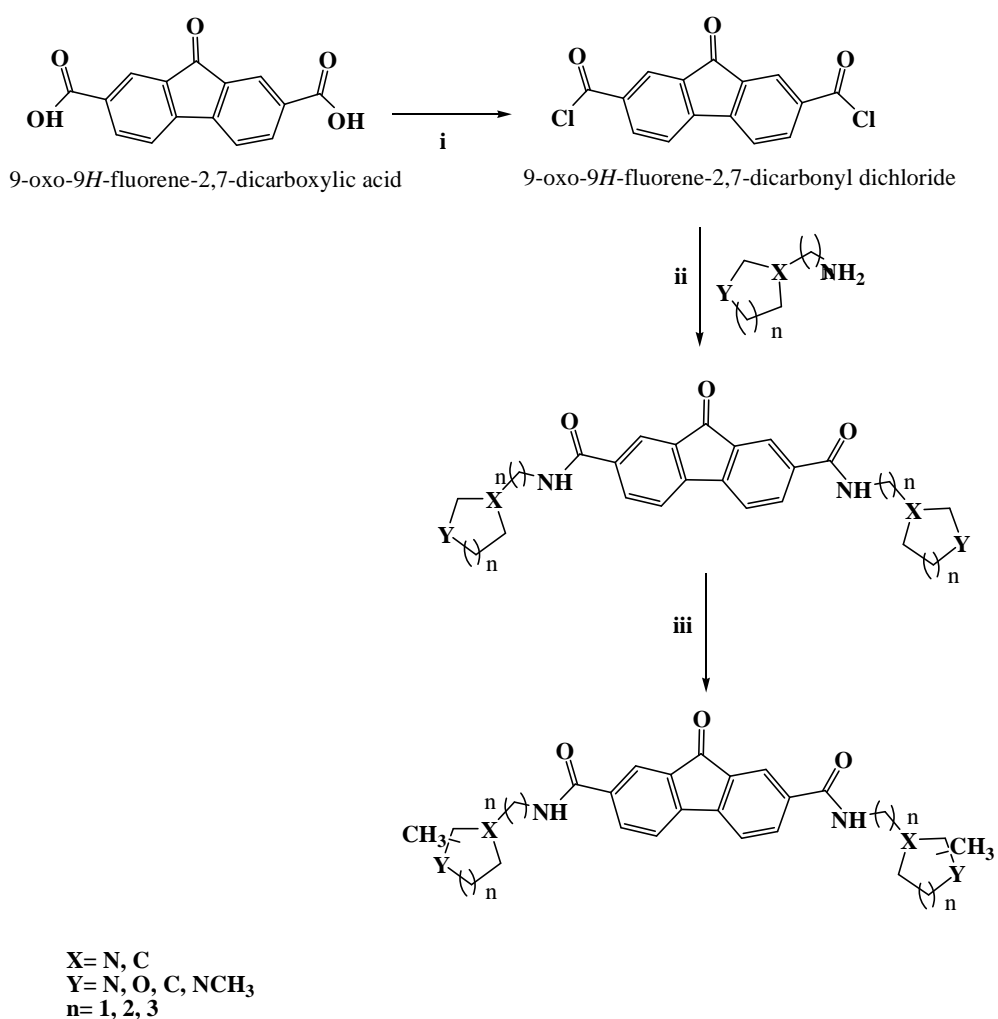
New derivatives were designed and their ability to stabilize G-quadruplex structures was simulated by carrying out docking experiments following the same protocol applied before. The DNA G-quadruplex polymorphism including parallel, anti-parallel and hybrid conformations of the human telomeric repeated sequence was considered (Figure 4). Furthermore it has been investigated also the ability of the new series to stabilize the c-myc promoter region (Figure 13).



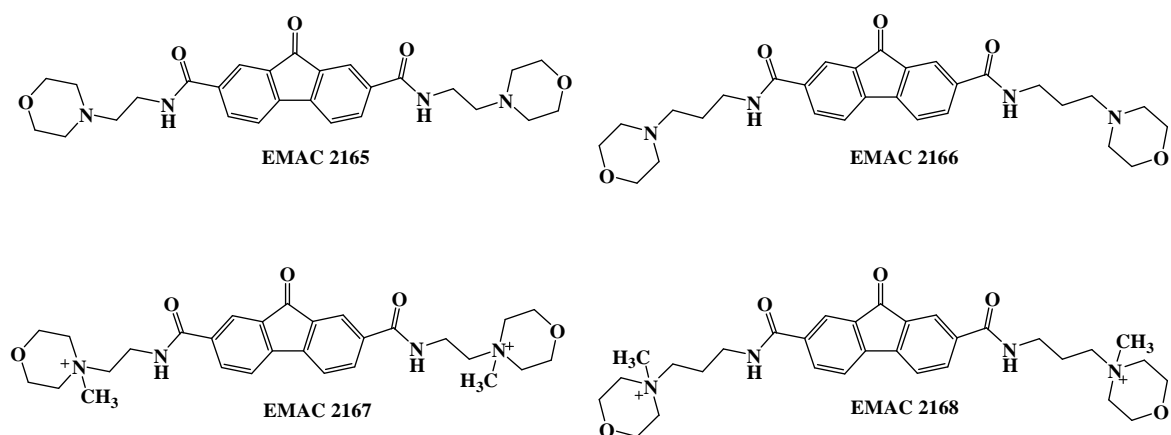
**Figure 13.** a) Sequence and b) Schematic and c) 3D representation of c-myc (1XAV[28])

All combinations of double substitution were investigated and the most promising compounds resulted to be the 2,7 substituted.

Thus a synthetic route was set (Scheme 1): the first step consists of the formation of the dichloride of the 9-oxo-9H-fluorene-2,7-dicarboxylic acid. Then the acid dichloride is reacted with the morpholinomethyleneamine side-chain to obtain compounds **EMAC 2165-2166**. The last step consists of a quaternization of morpholinium nitrogen with  $\text{CH}_3\text{I}$  and  $\text{K}_2\text{CO}_3$  in DMF to obtain the compounds **EMAC 2167-2168** (Figure 14)

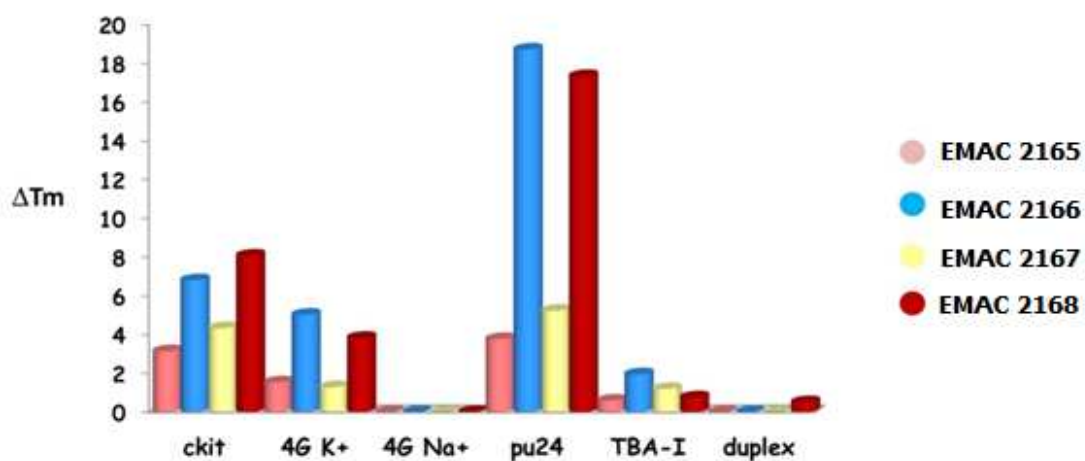


**Scheme 1.** Synthetic pathway to compounds EMAC 2165-2172. Reagents: (i)  $\text{SOCl}_2$ , reflux condition; (ii)  $\text{CHCl}_3$ , reflux condition; (iii)  $\text{CH}_3\text{I}$ ,  $\text{K}_2\text{CO}_3$ , DMF



**Figure 14.** Structure of compounds EMAC 2165-2168

The first four compounds synthesized (Figure 14) were submitted to biological tests (Figure 15).



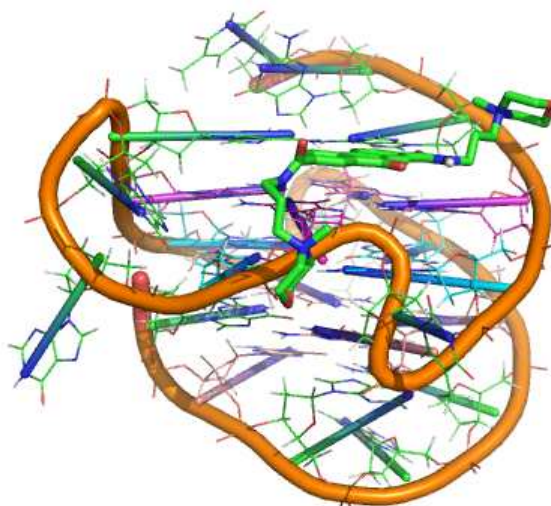
**Figure 15.** Screening of selected compounds by fluorescence melting experiment performed using different sequences of target G-quadruplex at a fixed concentration (30 $\mu$ M).

The good ability to stabilize the G-quadruplex both telomeric and promoter confirms the results obtained by the computational studies.

In particular compounds **EMAC 2166** and **EMAC 2168** show a remarkable and selective effect on the stabilization of pu24 C-myc promoter, indicating that the optimal length of the methylene spacer for this specific target is three.

Moreover, as it was previously observed, the introduction of the positive charge on the morpholine nitrogen is well tolerated and may constitute an advantage for the water-solubility of these series of ligands.

In order to understand the binding mode of these derivatives, preliminary docking experiments have been performed (Figure 16).



**Figure 16.** Best pose complex structure of the unimolecular G-quadruplex formed by the c-myc-Pu-24 in K<sup>+</sup> solution and EMAC 2168

## 4 Conclusion

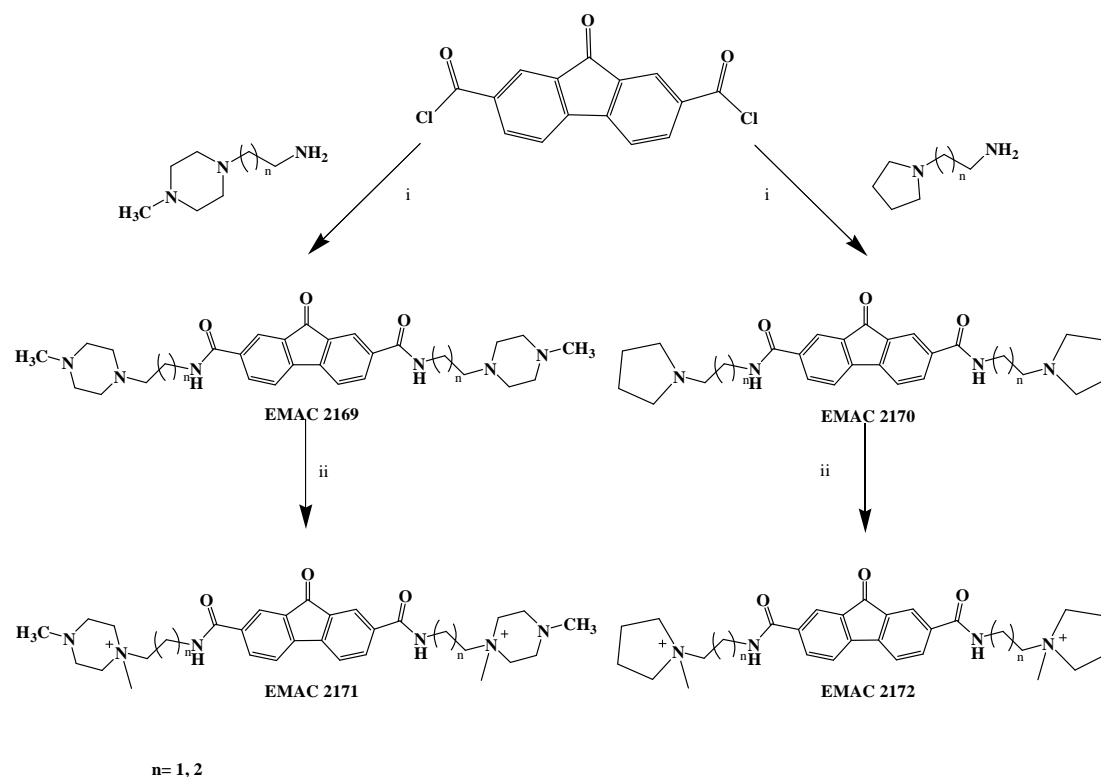
The conformational polymorphism of the G-quadruplex DNA human telomeric repeated sequence is an issue to face with in structure-based research projects.

The fluorenone scaffold has been used as starting point for lead optimization workflow. This was carried out with different computational approaches.

The new synthesized derivatives are able to induce increments not only of the DNA human telomeric sequence melting temperature but also of the c-myc promoter intramolecular G-quadruplex portion ( $\Delta T_m \sim 19^\circ\text{C}$ ).

Therefore 2,7 functionalized fluorenone could represent a promising scaffold for the development of potent stabilizers of c-myc promoter G-quadruplex as antineoplastic agents. In fact the overexpression of mutated c-myc protooncogene is often associate with a significant number of human malignancies, including colon and cervical cancers, myeloid leukemias, B and T cell lymphomas, and glioblastomas (8).

At the moment we are synthesizing new 2,7 substituted fluorenone derivatives which will be soon subjected to biological tests according to the Scheme 2.



**Scheme 2:** Synthetic pathway to new fluorenone EMAC 2169-2172. Reagents: (i)  $\text{CHCl}_3$ ,  
reflux condition; (ii)  $\text{CH}_3\text{I}$ ,  $\text{K}_2\text{CO}_3$ , DMF

## **5 Chemistry**

### **COMPOUNDS EMAC 2165-2168**

Unless otherwise noted, starting materials and reagents were obtained from commercial suppliers and were used without purification.

All melting points were determined by the capillary method on a Stuart SMP11 melting point apparatus and are uncorrected.

All samples were measured in CDCl<sub>3</sub> solvent at 278.1 K temperature on a Varian Unity 500 spectrometer. In the signal assignments the proton chemical shifts are referred to the solvent (<sup>1</sup>H: δ = 7.24 ppm). Coupling constants *J* are expressed in hertz (Hz).

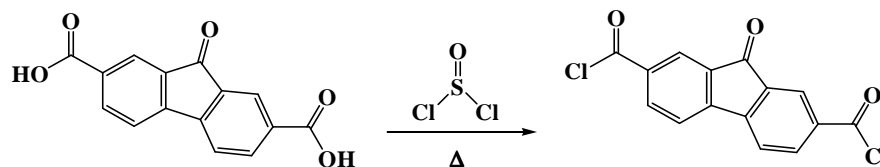
Elemental analyses were obtained on a Perkin–Elmer 240 B microanalyser. Analytical data of the synthesised compounds are in agreement with the theoretical data.

HPLC-MS/MS analysis was performed using an HPLC-MS/MS Varian (Varian Palo Alto, CA, USA) system fitted with a 1200 L triple quadrupole mass spectrometer equipped with an electrospray ionization source (ESI). A Varian MS workstation version 6.8 software was used for data acquisition and processing. Rapid identification was achieved with direct infusion of the purified molecule, dissolved in methanol, on the mass spectrometer source.

TLC chromatography was performed using silica gel plates (Merck F 254), spots were visualised by UV light.



**General method for the synthesis of 9-oxo-9H-fluorene-2,7-dicarbonyl dichloride**



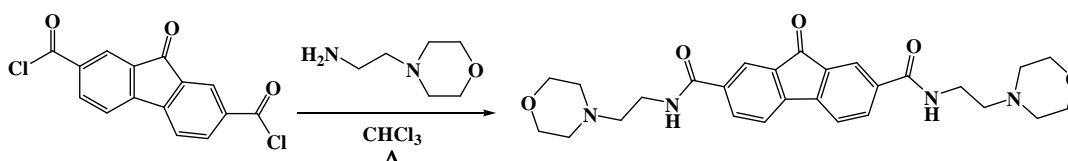
In a flask equipped with a reflux condenser 9-oxo-9H-fluorene-2,7-dicarboxylic acid ( 7.46 mmol) was dissolved in thionyl chloride that was added in excess (15 ml). The reaction was monitored with TLC (eluent ethyl acetate:hexane 1:1,5). After 24 hours under vigorous stirring at reflux condition, the precipitate that formed was filtered off. The filtrate was washed with isopropyl ether to offer pure compounds that appeared like a yellow crystalline solid.

M.W.: 305.11 g/mol; R.F.: 0.1 ( eluent: ethyl acetate:hexane 1:1,5); M.P.: >250°C; Yield: 80%

<sup>1</sup>H-NMR (500 MHz, DMSO) δH 8.04 (d, 2H, *J*: 7,5, CH-Ar), 8.07 (s, 2H, CH-Ar), 8.23 (d, 2H, *J*: 7.5)

**EMAC 2165**

***N2,N7-bis(2-morpholinoethyl)-9-oxo-9H-fluorene-2,7-dicarboxamide***



In a flask equipped with a reflux condenser 1g of 9-oxo-9H-fluorene-2,7-dicarbonyl dichloride (7.46 mmol) was dissolved in 10 ml of chloroform.

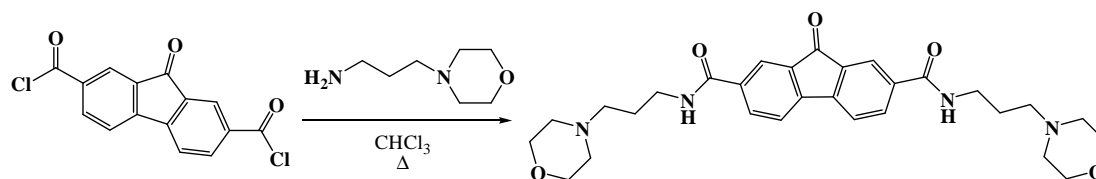
After vigorous stirring for 3 minute, 2-morpholinoethanamide was added in excess (9.84 mmol). The reaction was heated under reflux and monitored by TLC (eluent: ethyl acetate:hexane 1:1.5). After 2 hours the reaction was completed . A solid was filtered off and crystallised from ethanol. The desired pure compound appeared like a gold crystalline solid.

M.W.: 492.57 g/mol; R.F.: 0.47 ( eluent: ethyl acetate:hexane 1:1,5); M.P.: 270 °C; Yield: 60%

<sup>1</sup>H-NMR (300 MHz, CDCl<sub>3</sub>) δH 2.57 ( m, 8H, morpholino), 2.67 ( m, 4H, CH<sub>2</sub>), 3.61 ( m, 4H, CH<sub>2</sub>), 3.77 ( m, 8H, morpholino), 7.02 ( brs, 2H, NH), 7.59 ( d, 2H, J: 7.7, Ar-CH), 7.96 ( s, 2H, Ar-CH), 8.05 ( d, 2H, Ar-CH)

### EMAC 2166

#### *N2,N7-bis(2-morpholinopropyl)-9-oxo-9H-fluorene-2,7-dicarboxamide*

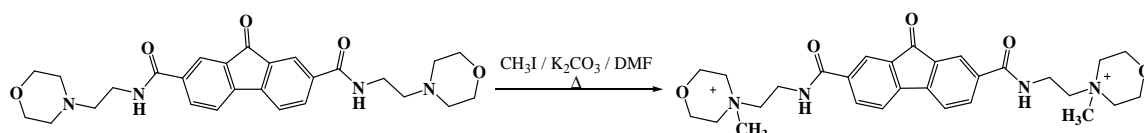


In a flask equipped with a reflux condenser 1g of 9-oxo-9H-fluorene-2,7-dicarbonyl dichloride ( 7.46 mmol) was dissolved 10 ml of chloroform. After vigorous stirring for 3 minute, 2-morpholinopropylamide was added in excess ( 9.84 mmol). The reaction was heated under reflux and monitored by TLC ( eluent: ethyl acetate:hexane 1:1.5). After 2 hours the reaction was completed .and solvent removed under vacuum. A greasy solid was obtain, which was friabilysed in acetone.

The desired pure compound appeared like a yellow crystalline solid.

M.W.: 520.62 g/mol; R.F.: 0.32 ( eluent: ethyl acetate:hexane 1:1,5); M.P.: >250 °C; Yield: 40%

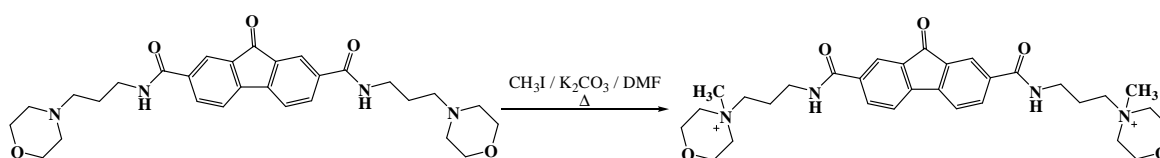
<sup>1</sup>H-NMR (500 MHz, DMSO) δH 1.71 ( m, 4H, CH<sub>2</sub>), 2.37 ( m, 8H, morpholino), 3.31 ( m, 8H, CH<sub>2</sub> morpholino), 3.58 ( m, 8H, CH<sub>2</sub>), 7.98 ( d, 2H, J: 7.5, Ar-CH), 8.12 ( s, 2H, Ar-CH), 8.15 ( d, 2H, J: 8, Ar-CH), 8.71 ( brs, 2H, NH)

**EMAC 2167****4-methyl-4-{2-[(7-{[2-(4-methylmorpholin-4-ium-4-yl)ethyl]carbamoyl}-9-oxo-9H-fluoren-2-yl)formamido]ethyl}morpholin-4-ium**

0.3 g of N2,N7-bis(2-morpholinoethyl)-9-oxo-9H-fluorene-2,7-dicarboxamide ( 0.61 mmol),  $K_2CO_3$  ( 2.4mmol),  $CH_3I$  ( 2.4 mmol) and DMF were introduced in a flask equipped with a reflux condenser. The reaction was heated under reflux and after 3 hours it can be observe the colour changes from yellow to orange. The reaction was monitoreted with TLC ( eluent: ethyl acetate:hexane 1:1.5) and after 4 hours it was completed. At R.T. it can be observed the formation of a crystalline yellow solid. A solid was filtered off and characterised.

M.W.: 522.63 g/mol; R.F.: 0.59 ( eluent: ethyl acetate:hexane 1:1.5); M.P.: >250°C; Yield: 60%

$^1H$ -NMR (400 MHz, DMSO)  $\delta$ H 3.08 ( s, 8H, morpholino), 3.3 ( m, 14H,  $CH_3$  +  $CH_2$  morpholino), 4.00 ( m, 4H,  $CH_2$ ), 4.45 ( m, 4H,  $CH_2$ ), 8.00 ( d, 2H, J: 7.5, Ar-CH), 8.01 ( s, 2H, Ar-CH), 8.13 ( d, 2H, J: 7.5 Ar-CH), NH not detected

**EMAC 2168****4-methyl-4-{3-[(7-{[3-(4-methylmorpholin-4-ium-4-yl)propyl]carbamoyl}-9-oxo-9H-fluoren-2-yl)formamido]propyl}morpholin-4-ium**

N2,N7-bis(2-morpholinopropyl)-9-oxo-9H-fluorene-2,7-dicarboxamide (0.61 mmol, 0.33 g),  $K_2CO_3$  (2.4mmol),  $CH_3I$  (2.4 mmol) and DMF were introduced in a flask equipped with a reflux condenser. The reaction was heated under reflux and after 3 hours it can be observed the colour changes from orange to dark green. The reaction was monitoreted with TLC ( eluent: ethyl acetate:hexane 1:1.5) and after 4 hours it was completed. At R.T.

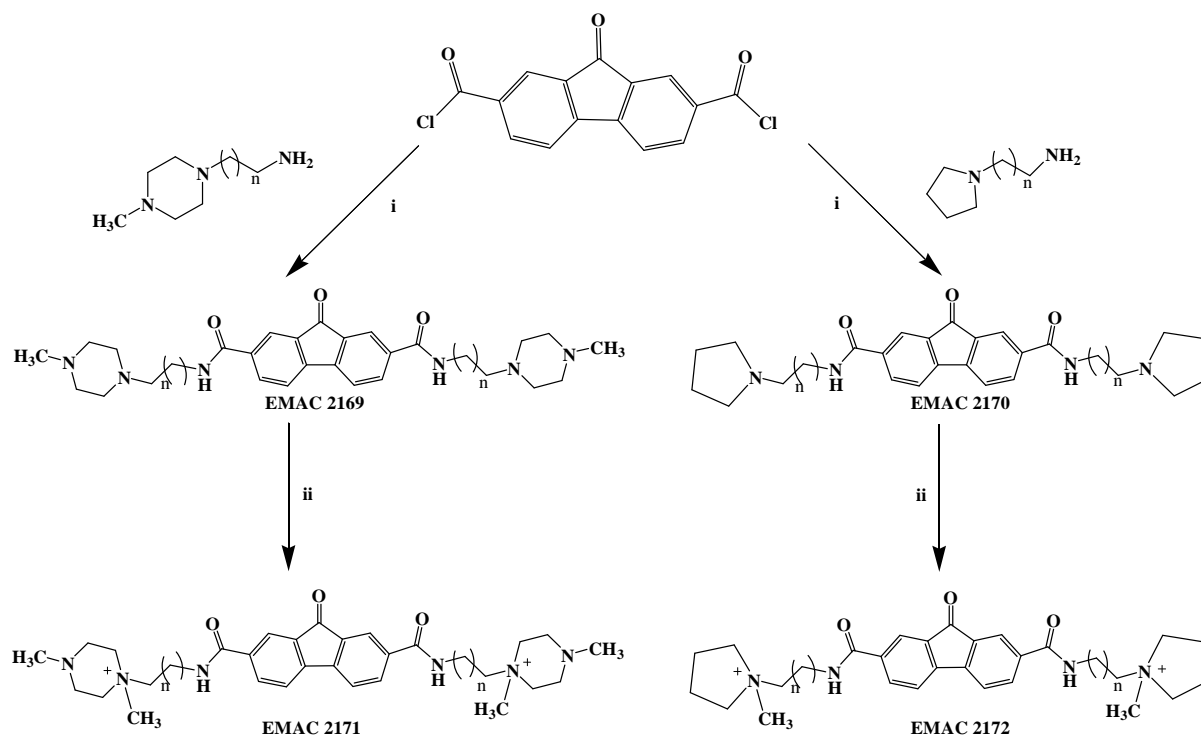
it can be observed the formation of a crystalline yellow solid. The solid was filtered off and characterised.

M.W.: 522.63 g/mol; R.F.: 0.59 ( eluent: ethyl acetate:hexane 1:1.5); M.P.: >250°C; Yield: 60%

<sup>1</sup>H-NMR (500 MHz, DMSO) δH 1.71 ( m, 4H, CH<sub>2</sub>), 2.36 ( m, 8H, morpholino), 3.31 ( m, 14H, CH<sub>3</sub> + CH<sub>2</sub> morpholine), 3.58 ( m, 8H, CH<sub>2</sub>), 7.98 ( d, 2H, J: 7.5, Ar-CH), 8.12 ( s, 2H, Ar-CH), 8.15 ( d, 2H, J: 8, Ar-CH), 8.71 ( brs, 2H, NH)

## 5.1 WORK IN PROGRESS:

**Synthetic scheme:**



n = 1, 2

**Scheme 3.** Synthetic pathway to compounds EMAC 2169-2172. Reagents: (i)  $\text{CHCl}_3$ , reflux condition; (ii)  $\text{CH}_3\text{I}$ ,  $\text{K}_2\text{CO}_3$ , DMF

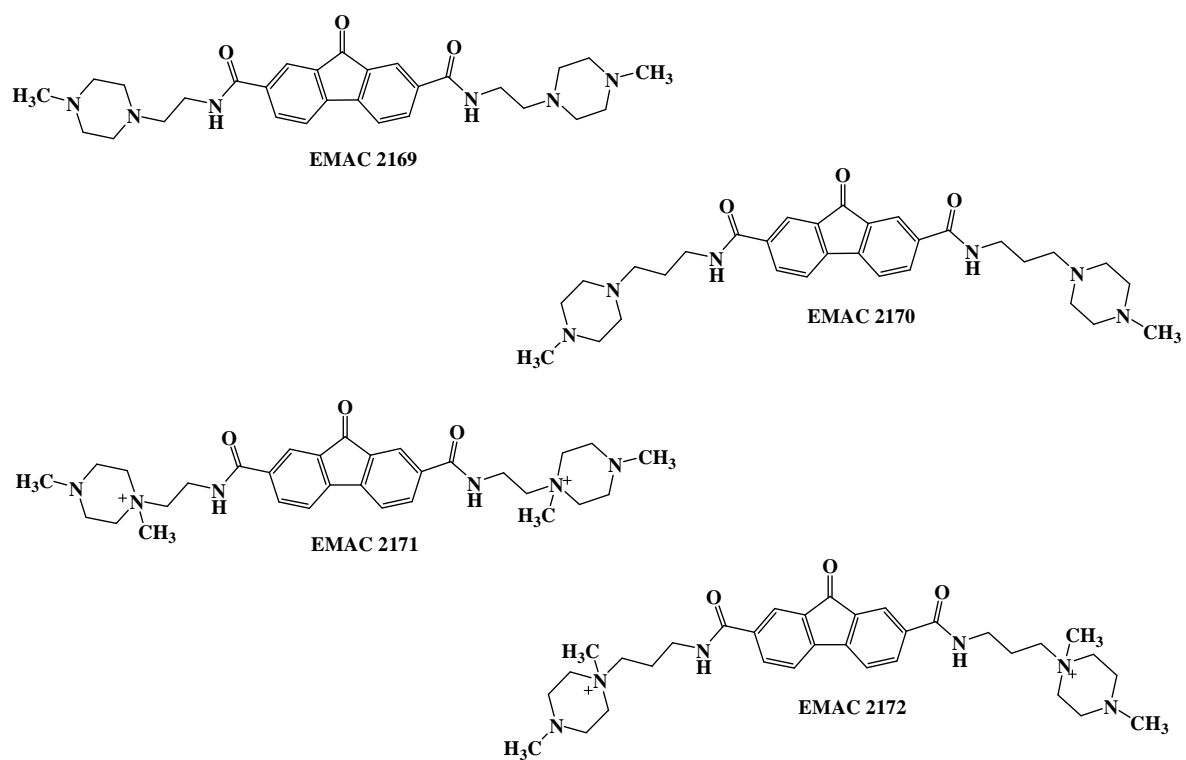
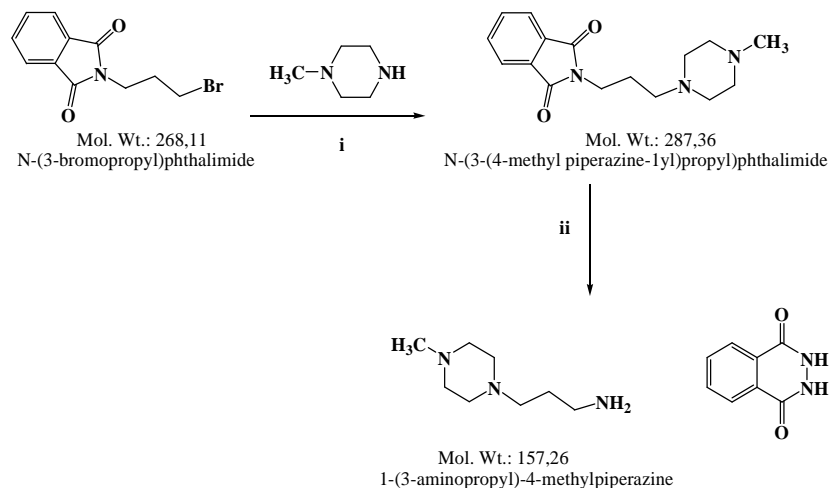


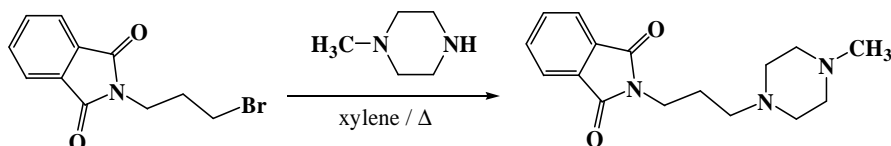
Figure 15. Structure of compounds EMAC 2169-2172

## Synthesis of 1-(3-aminopropyl)-4-methylpiperazine



**Scheme 4:** Synthesis of 1-(3-aminopropyl)-4-methylpiperazine. Reagents: (i) Xylene, reflux condition; (ii) Hydrazine monohydrate, ethanol/methanol, reflux condition

## Synthesis of N-(3-(4-methylpiperazin-1-yl)propyl)phthalimide

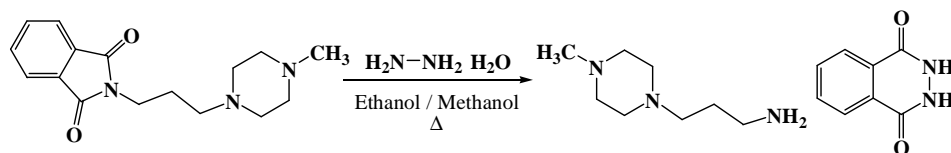


A solution of N-(3-bromopropyl)phthalimide (15 mmol), in xylene (30 ml), was added dropwise to a solution of 1-methylpiperazine (33 mmol), in xylene at 70°C. the mixture was heated under reflux for 20 hours, precipitate was removed by filtration and the filtrate was concentrated. The crude product was purified by silica gel chromatography with  $\text{CH}_2\text{Cl}_2$ :MeOH 9:1 to give the desired pure compound, that appeared as an dark yellow oil.

M.W.: 287.36 g/mol; Yield: 72%

MS (ESI+): 288.17 ( $[\text{M}+\text{H}]^+$ )

### Synthesis of 1-(3-aminopropyl)-4-methylpiperazine



A solution of N-(3-(4-methylpiperazin-1-yl)propyl)phthalimide (10.8 mmol) and hydrazine monohydrate (13 mmol) in ethanol (30 ml) and methanol (30 ml) was refluxed for 4 hours. After cooling to R.T., concentrated HCl (1,2 ml) was added and the mixture heated under reflux for another hours. After removing the solvent, water (50 ml) was added, the mixture stirred and insoluble material removed by filtration. Solid K<sub>2</sub>CO<sub>3</sub> (0.6 eq) and CH<sub>2</sub>Cl<sub>2</sub> (50 ml) was added to the aqueous layer; the mixture was stirred and filtered. The organic layer was washed with water (3x20ml). The combined aqueous layer were washed with ethanol. Water was removed from the organic layer, which were then dried and evaporated to give the pure desired compound as an oil.

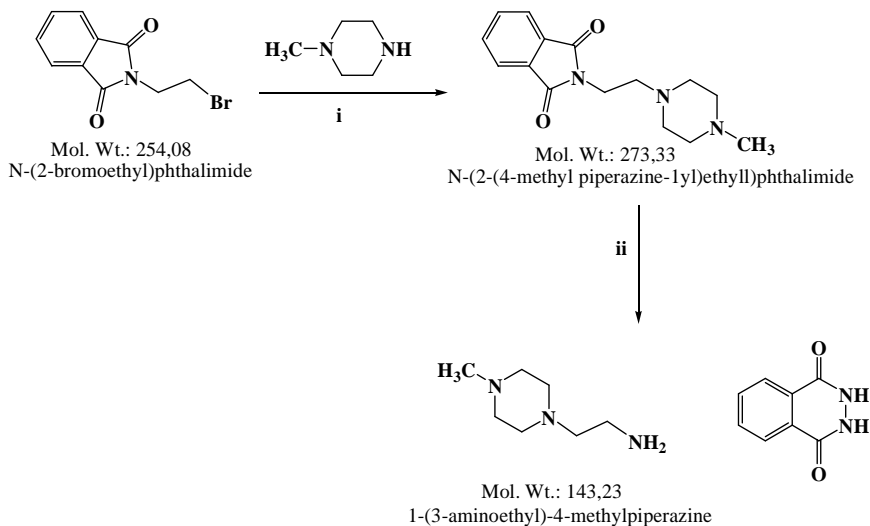
M.W.: 157.26 g/mol; Yield: 39%

MS (ESI+): 158.1 ([M+H]<sup>+</sup>)

The NMR analyses are in progress.

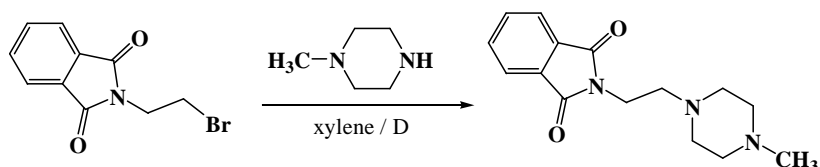


## Synthesis of 1-(3-aminoethyl)-4-methylpiperazine



**Scheme 5:** Synthesis of 1-(3-aminoethyl)-4-methylpiperazine. Reagents: (i) Xylene, reflux condition; (ii) Hydrazine monohydrate, ethanol/methanol, reflux condition

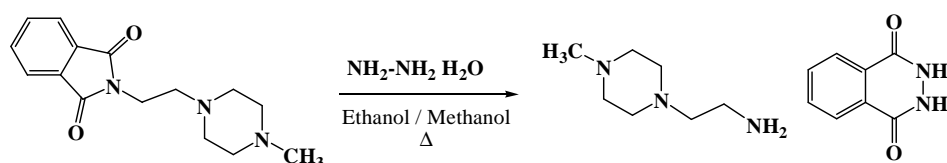
## Synthesis of N-(3-(4-methylpiperazin-1-yl)propyl)phthalimide



A solution of N-(2-bromoethyl)phthalimide ( 15 mmol), in xylene (30 ml), was added dropwise to a solution of 1-methylpiperazine ( 33 mmol), in xylene at 70°C. The mixture was heated under reflux for 20 hours, precipitate was removed by filtration and the filtrate was concentrated. The crude product was purified by silica gel chromatography with  $\text{CH}_2\text{Cl}_2:\text{MeOH}$  9:1 to give the desired pure compound, that appeared as a pale pink solid.

M.W.: 273.33 g/mol; M.P.: 199°-220°C; Yield: 62%  
MS (ESI+): 274.15 ( $[\text{M}+\text{H}]^+$ )

## Synthesis of 1-(2-aminoethyl)-4-methylpiperazine



A solution of N-(2-(4-methylpiperazin-1-yl)ethyl)phthalimide (10.8 mmol) and hydrazine monohydrate (13 mmol) in ethanol (30 ml) and methanol (30 ml) was refluxed for 4 hours. After cooling to R.T., concentrated HCl (1,2 ml) was added and the mixture heated under reflux for another hours. After removing the solvent, water (50 ml) was added, the mixture stirred and insoluble material removed by filtration. Solid K<sub>2</sub>CO<sub>2</sub> (0.6 eq) and CH<sub>2</sub>Cl<sub>2</sub> (50 ml) was added to the aqueous layer; the mixture was stirred and filtered. The organic layer was washed with water (3x20ml). The combined aqueous layer were washed with ethanol. Water was removed from the organic layer, which were then dried and evaporated to give the pure desired compound as a brown yellow solid.

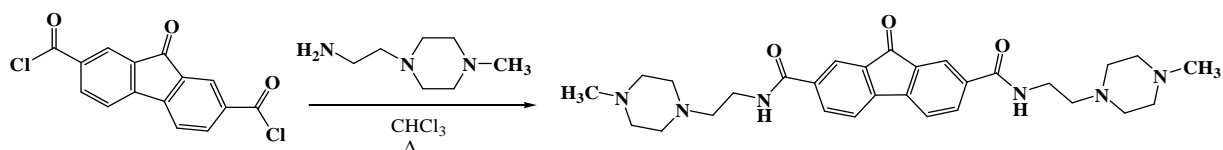
M.W.: 143.23 g/mol; Yield: 34%

MS (ESI+): 144.1 ([M+H]<sup>+</sup>)

The NMR analyses are in progress.

## EMAC 2169

### 2-N,7-N-bis[2-(4-methylpiperazin-1-yl)ethyl]-9-oxo-9H-fluorene-2,7-dicarboxamide



1g of 9-oxo-9H-fluorene-2,7-dicarbonyl dichloride (3.28 mmol) was introduced in a flask equipped with a reflux condenser with 10 ml of chloroform. After stirring for 3 minute, 1-(2-aminoethyl)-4-methylpiperazine was added in excess (9.84 mmol). The reaction was heated under reflux and monitored by TLC (eluent: ethyl acetate:hexane 1:1.5). After 2 hours the reaction was completed. A solid was filtered off and the desired pure compound appeared like a yellowish crystalline solid

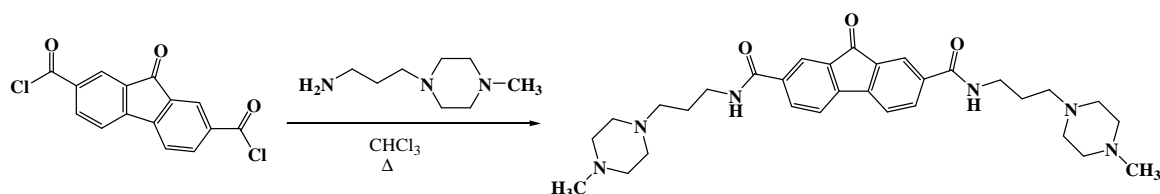
M.W.: 518.65 g/mol; M.P.: >250 °C; Yield: 83%

MS (ESI+): 519.30 ([M+H]<sup>+</sup>)

The NMR analyses are in progress.

#### EMAC 2170

#### 2-N,7-N-bis[3-(4-methylpiperazin-1-yl)propyl]-9-oxo-9H-fluorene-2,7-dicarboxamide



1g of 9-oxo-9H-fluorene-2,7-dicarbonyl dichloride (3.28 mmol) was introduced in a flask equipped with a reflux condenser with 10 ml of chloroform. After stirring for 3 minute, 1-(2-aminoethyl)-4-methylpiperazine was added in excess (9.84 mmol). The reaction was heated under reflux and monitored by TLC (eluent: ethyl acetate:hexane 1:1.5). After 2 hours the reaction was completed. A solid was filtered off and the desired pure compound appeared like a yellowish crystalline solid

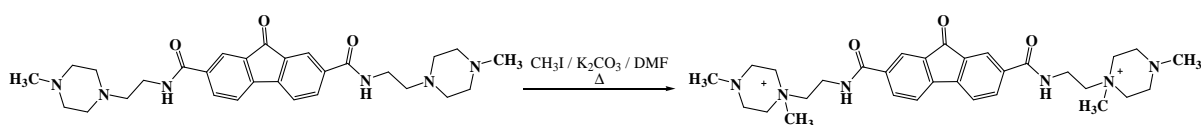
M.W.: 546.7 g/mol; M.P.: >250 °C; Yield: 83%

MS (ESI+): 547.34 ([M+H]<sup>+</sup>)

The NMR analyses are in progress.

#### EMAC 2171

#### 1-{2-[(7-{[2-(1,4-dimethylpiperazin-1-ium-1-yl)ethyl]carbamoyl}-9-oxo-9H-fluoren-2-yl)formamido]ethyl}-1,4-dimethylpiperazin-1-ium



0.32 g of 2-N,7-N-bis[2-(4-methylpiperazin-1-yl)ethyl]-9-oxo-9H-fluorene-2,7-dicarboxamide (0.61 mmol), K<sub>2</sub>CO<sub>3</sub> (2.4mmol), CH<sub>3</sub>I (2.4 mmol) and DMF were introduced in a flask equipped with a reflux condenser. The reaction was heated under reflux and after 3 hours it can be observed the colour changes from yellow to orange. The reaction was monitored with TLC ( eluent: ethyl acetate:hexane 1:1.5) and after 4 hours it was completed. At R.T. it can be observed the formation of a yellow crystalline solid. A solid was filtered off and characterised.

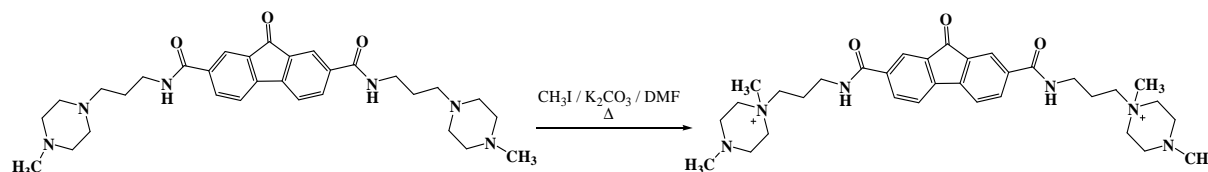
M.W.: 548.72 g/mol; M.P.: >250°C; Yield: 60%

MS (ESI+): 549.35 ([M+H]<sup>+</sup>)

The NMR analyses are in progress.

#### EMAC 2172

#### 1-{3-[(7-{[3-(1,4-dimethylpiperazin-1-ium-1-yl)propyl]carbamoyl}-9-oxo-9H-fluoren-2-yl)formamido]propyl}-1,4-dimethylpiperazin-1-ium



0.33 g of 2-N,7-N-bis[3-(4-methylpiperazin-1-yl)propyl]-9-oxo-9H-fluorene-2,7-dicarboxamide ( 0.61 mmol),  $K_2CO_3$  ( 2.4 mmol),  $CH_3I$  ( 2.4 mmol) and DMF were introduced in a flask equipped with a reflux condenser. The reaction was heated under reflux and after 3 hours it can be observed the colour changes from orange to dark green. The reaction was monitored with TLC ( eluent: ethyl acetate:hexane 1:1.5) and after 4 hours it was completed. At R.T. it can be observed the formation of a yellow crystalline solid. A solid was filtered off and characterised.

M.W.: 576.77 g/mol; M.P.: >250°C; Yield: 70%

MS (ESI+): 577.38 ( $[M+H]^+$ )

The NMR analyses are in progress.

## **5 Acknowledgments**

*This work was supported by Regione Autonoma della Sardegna.*

*I wish to thank Fondazione Banco di Sardegna for founding my Phd grant.*

*I acknowledge Prof. Stefano Alcaro and his group from University of Magna Graecia for their help in the virtual screening investigation and the future computational studies, Prof. Claudia Sissi and his group from University of Padua for the biological investigation and Dr. Giorgia Sarais from University of Cagliari for Mass Spectra measurements.*

## 6 Reference and notes

- [1] Biffi, G.; Tannahill, D.; McCafferty, J.; Balasubramanian, S. Quantitative Visualization of DNA G-Quadruplex Structures in Human Cells. *Nature Chemistry*, **advance online publication**, (2013).
- [2] Huppert, J. L. Hunting G-Quadruplexes. *Biochimie*, **90**, (2008), 1140-1148.
- [3] Sissi, C.; Gatto, B.; Palumbo, M. The Evolving World of Protein-G-Quadruplex Recognition: A Medicinal Chemist's Perspective. *Biochimie*, **93**, (2011), 1219-1230.
- [4] Yang, D.; Okamoto, K. Structural Insights into G-Quadruplexes: Towards New Anticancer Drugs. *Future Med. Chem.*, **2**, (2010), 619-646.
- [5] Aubert, G.; Lansdorp, P. M. Telomeres and Aging. *Physiological Reviews*, **88**, (2008), 557-579.
- [6] Tárkányi, I.; Aradi, J. Pharmacological Intervention Strategies for Affecting Telomerase Activity: Future Prospects to Treat Cancer and Degenerative Disease. *Biochimie*, **90**, (2008), 156-172.
- [7] Pacini, F.; Cantara, S.; Capezzone, M.; Marchisotta, S. Telomerase and the Endocrine System. *Nat Rev Endocrinol*, **7**, (2011), 420-430.
- [8] Brooks, T. A.; Hurley, L. H. The Role of Supercoiling in Transcriptional Control of Myc and Its Importance in Molecular Therapeutics. *Nat Rev Cancer*, **9**, (2009), 849-861.
- [9] Balasubramanian, S.; Hurley, L. H.; Neidle, S. Targeting G-Quadruplexes in Gene Promoters: A Novel Anticancer Strategy? *Nature Reviews. Drug Discovery*, **10**, (2011), 261-275.
- [10] Bugaut, A.; Balasubramanian, S. 5'-Utr Rna G-Quadruplexes: Translation Regulation and Targeting. *Nucleic Acids Research*, **40**, (2012), 4727-4741.
- [11] Dai, J.; Carver, M.; Yang, D. Polymorphism of Human Telomeric Quadruplex Structures. *Biochimie*, **90**, (2008), 1172-1183.
- [12] Parkinson, G. N.; Lee, M. P. H.; Neidle, S. Crystal Structure of Parallel Quadruplexes from Human Telomeric DNA. *Nature*, **417**, (2002), 876-880.
- [13] Wang, Y.; Patel, D. J. Solution Structure of the Human Telomeric Repeat D[Ag<sub>3</sub>(T<sub>2</sub>ag<sub>3</sub>)<sub>3</sub>] G-Tetraplex. *Structure*, **1**, (1993), 263-282.
- [14] Dai, J.; Punchihewa, C.; Ambrus, A.; Chen, D.; Jones, R. A.; Yang, D. Structure of the Intramolecular Human Telomeric G-Quadruplex in Potassium Solution: A Novel Adenine Triple Formation. *Nucleic Acids Research*, **35**, (2007), 2440-2450.
- [15] Dai, J.; Carver, M.; Punchihewa, C.; Jones, R. A.; Yang, D. Structure of the Hybrid-2 Type Intramolecular Human Telomeric G-Quadruplex in K<sup>+</sup> Solution: Insights into Structure Polymorphism of the Human Telomeric Sequence. *Nucleic Acids Research*, **35**, (2007), 4927-4940.

- [16] De Cian, A.; Lacroix, L.; Douarre, C.; Temime-Smaali, N.; Trentesaux, C.; Riou, J.-F.; Mergny, J.-L. Targeting Telomeres and Telomerase. *Biochimie*, **90**, (2008), 131-155.
- [17] Wheelhouse, R. T.; Sun, D.; Han, H.; Han, F. X.; Hurley, L. H. Cationic Porphyrins as Telomerase Inhibitors: The Interaction of Tetra-(N-Methyl-4-Pyridyl)Porphine with Quadruplex DNA. *Journal of the American Chemical Society*, **120**, (1998), 3261-3262.
- [18] Haider, S. M.; Neidle, S.; Parkinson, G. N. A Structural Analysis of G-Quadruplex/Ligand Interactions. *Biochimie*, **93**, (2011), 1239-1251.
- [19] Campbell, N. H.; Parkinson, G. N.; Reszka, A. P.; Neidle, S. Structural Basis of DNA Quadruplex Recognition by an Acridine Drug. *Journal of the American Chemical Society*, **130**, (2008), 6722-6724.
- [20] Cosconati, S.; Marinelli, L.; Trotta, R.; Virno, A.; De Tito, S.; Romagnoli, R.; Pagano, B.; Limongelli, V.; Giancola, C.; Baraldi, P. G.; Mayol, L.; Novellino, E.; Randazzo, A. Structural and Conformational Requisites in DNA Quadruplex Groove Binding: Another Piece to the Puzzle. *Journal of the American Chemical Society*, **132**, (2010), 6425-6433.
- [21] Piazza, A.; Boulé, J.-B.; Lopes, J.; Mingo, K.; Largy, E.; Teulade-Fichou, M.-P.; Nicolas, A. Genetic Instability Triggered by G-Quadruplex Interacting Phen-Dc Compounds in *Saccharomyces Cerevisiae*. *Nucleic Acids Research*, (2010).
- [22] Alcaro, S.; Artese, A.; Iley, J. N.; Maccari, R.; Missailidis, S.; Ortuso, F.; Ottanà, R.; Ragazzon, P.; Vigorita, M. G. Tetraplex DNA Specific Ligands Based on the Fluorenone-Carboxamide Scaffold. *Bioorganic & Medicinal Chemistry Letters*, **17**, (2007), 2509-2514.
- [23] Alcaro, S.; Artese, A.; Iley, J. N.; Missailidis, S.; Ortuso, F.; Parrotta, L.; Pasceri, R.; Paduano, F.; Sissi, C.; Trapasso, F.; Vigorita, M. G. Rational Design, Synthesis, Biophysical and Antiproliferative Evaluation of Fluorenone Derivatives with DNA G-Quadruplex Binding Properties. *ChemMedChem*, **5**, (2010), 575-583.
- [24] Goodford, P. J. A Computational Procedure for Determining Energetically Favorable Binding Sites on Biologically Important Macromolecules. *Journal of Medicinal Chemistry*, **28**, (1985), 849-857.
- [25] Morris, G. M.; Goodsell, D. S.; Halliday, R. S.; Huey, R.; Hart, W. E.; Belew, R. K.; Olson, A. J. Automated Docking Using a Lamarckian Genetic Algorithm and an Empirical Binding Free Energy Function. *Journal of Computational Chemistry*, **19**, (1998), 1639-1662.
- [26] Alcaro, S.; Gasparini, F.; Incani, O.; Mecucci, S.; Misiti, D.; Pierini, M.; Villani, C. A "Quasi-Flexible" Automatic Docking Processing for Studying Stereoselective Recognition Mechanisms. Part I. Protocol Validation. *Journal of Computational Chemistry*, **21**, (2000), 515-530.

- [27] Patel, D. J.; Phan, A. T.; Kuryavyi, V. Human Telomere, Oncogenic Promoter and 5'-Utr G-Quadruplexes: Diverse Higher Order DNA and Rna Targets for Cancer Therapeutics. *Nucleic Acids Research*, **35**, (2007), 7429-7455.
- [28] Ambrus, A.; Chen, D.; Dai, J.; Jones, R. A.; Yang, D. Solution Structure of the Biologically Relevant G-Quadruplex Element in the Human C-Myc Promoter. Implications for G-Quadruplex Stabilization†. *Biochemistry*, **44**, (2005), 2048-2058.